Proceeding of the 18th UIS Congress - Volume IV

Geomorphology

S. 04 - Speleogenesis, geomorphology
S. 12 - Glacier, firn and ice caves

Savoie Mont-Blanc 2022

KARSTOLOGIA 24 Memoirs

Actes du 18ème congrès international de Spéléologie

Proceedings of the 18th International Congress of Speleology

Savoie Mont Blanc 2022

Volume IV / VI

Karstologia-*Mémoires* n°24

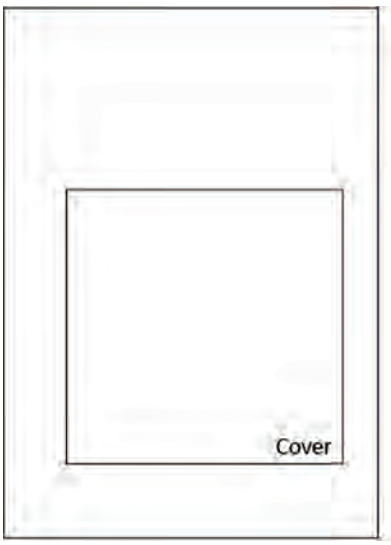

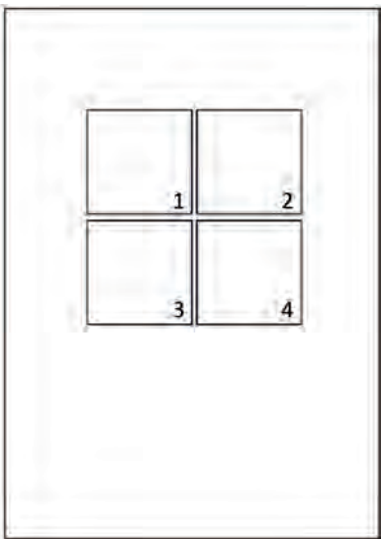

Cover : Gruta Dente de Cao (Mato Grosso do Sul, Brésil). Philippe Crochet
1 : Grotte de la Cocalière (Gard, France), Galerie en trou de serrure. Philippe Crochet
2 : Grotte du Banquier (Hérault, France). Philippe Crochet
3 : Eiskapelle (Bavière, Allemagne). Philippe Crochet
4 : Grotte du Rêve de Blue, Glacier Tempanos, Chili. Bernard Tourte, Centre Terre

Photo-frise sur la tranche, réalisée par Philippe Crochet et Annie Guiraud à la grotte de Saint-Marcel d'Ardèche, mai 2022

Actes du 18ème congrès international de Spéléologie

Proceedings of the 18th International Congress of Speleology

Coordination générale du congrès / *General coordination of the congress*
Yves CONTET

Coordination de la Conférence scientifique / *Coordination of the Scientific Conference*
Christophe GAUCHON

Coordination édition des actes / *Coordination of the edition of the proceedings*
Christophe GAUCHON & Stéphane JAILLET

Comité éditorial de la Conférence scientifique / *Editorial Board of the Scientific Conference*
Christophe GAUCHON (FR), Stéphane JAILLET (FR), Daniel BALLESTEROS (ES), Charlotte HONIAT (FR/AT), Kim GENUITE (FR), Tanguy RACINE (FR/AT)

Fédération Française de Spéléologie

18th INTERNATIONAL CONGRESS SPELEOLOGY SAVOIE MONT BLANC FRANCE 2022

Union Internationale de Spéléologie

Maquette couverture / *Cover design*
Claude BOULIN (Editions Gap)

Coordination des photographies couvertures / *Coordination of the cover photos*
Annie GUIRAUD & Philippe CROCHET

Soutien à l'édition / *Publishing support*

UNIVERSITÉ SAVOIE MONT BLANC

cnrs

Association Française de Karstologie

Volume I. Ecology & Heritage

Volume II. Explorations & History

Volume III. Physical Speleology

Volume IV. Geomorphology

Volume V. Karstic sediment, Palaeontology & Archaeology

Volume VI. Techniques & Societies


01
02
03
04
05
06
07
08
09
10
11
12
13
14
15
16
17
18
19
INTERNATIONAL YEAR
2021
OF CAVES AND KARST
20

SYMPOSIUM 04

Geomorphology and speleogenesis

Coordination: Lionel BARRIQUAND (FR), Laurent BRUXELLES (FR) & Dominic STRATFORD (ZA)

SYMPOSIUM 12

Glacier, firn and ice caves

Coordination: Bulat MAVLYUDOV, Luc MOREAU (FR) & Alessio ROMEO (IT)

Symposium 04

Geomorphology and speleogenesis

Special sessions

Rock-living interaction

Lionel BARRIQUAND (chief) (FR), Laurent BRUXELLES (chief) (FR)

Hypogene karst

Philippe AUDRA (chief) (FR), Alexander KLIMCHOUK (chief) (UA)

Ghost Rock

Laurent BRUXELLES (chief) (FR), Gregory DANDURAND (chief) (FR)

Geomorphology and speleogenesis

Laurent BRUXELLES[1,2], Lionel BARRIQUAND[3] & Dominic STRATFORD[2]

(1) TRACES, UMR 5608 du CNRS, 5 Allées Antonio Machado, 31058 Toulouse, France
(2) GAES, University of the Witwatersrand, Johannesburg, South Africa
(3) Université Savoie-Mont-Blanc, EDYTEM, UMR 5204, F-73376 Le Bourget-du-Lac cedex, France

English

Karstology is a dynamic discipline in constant renewal, nourished by a fundamental approach: fieldwork. Thus, thanks to the unceasing exploration work carried out by cavers and researchers, new and yet fundamental concepts stimulate us to review and reinterpret known features and to identify those that escaped our notice. Throughout the world, this dynamic prevails, as demonstrated by the diverse subjects presented in this symposium.

The pioneers of our discipline first used simple process models to explain the evolution of a landscape or the development of a cavity. Over the years, interpretations have become more complex and new concepts have emerged from the observations made. Sometimes the process is still active. Sometimes it is no longer active and the reading of the morphologies, physico-chemical, mineralogical and isotopic analyses are often the keys that allow a better understanding of the present and past phenomena.

Through this work, new paradigms have appeared in recent years that explore the roles of coverings, tectonics, hypogene karstification, ghost rocks and, more recently, biocorrosion. As these new approaches develop, we must constantly return to the field and revisit the sites we have already visited with new keys to understanding them. This is undoubtedly the sign of a dynamic, evidence-driven discipline, that renews itself through cross-fertilisation of multi-disciplinary concepts and data, and above all, draws on crucial field observations made by speleologists, geomorphologists and geologists. Let us hope that future years will bring us new ways of understanding the formation and evolution of karst.

Our goal is always to establish the most complete inventory possible of the clues that allow us to reconstruct the often complex history of karsts, but our "toolbox" is increasingly rich, as demonstrated by the diversity of the articles that follow in this symposium. Thus, this symposium allows us to review the different morphological and speleogenetic aspects known to date in karst. From the detailed shape of the walls and vaults to the landscape, through the geometry of objects and networks. The study of karst is inherently multi-scalar and interdisciplinary. It is nourished by the interaction between different fields of research, from geomorphology and geology to biology and archaeology, via climatology, aerology and geochemistry. The list of papers of this symposium is a faithful illustration of this richness and of the dynamics of the study of karst. It stimulates many varied discussions that will allow all to acquire new perspectives and appreciation for new evidence of what fascinates us all: the karst!

Français

La karstologie est une discipline dynamique, en constant renouveau et qui se nourrit d'une approche fondamentale : le terrain. Ainsi, grâce au travail d'exploration incessant mené par les spéléologues et de celui des chercheurs *in situ*, des concepts nouveaux et pourtant fondamentaux nous invitent à revoir et à réinterpréter les formes que nous connaissions déjà et même à percevoir celles qui nous avaient échappé. A travers le monde, cette dynamique est forte comme en témoignent les nombreux sujets présentés lors de ce symposium.

Les pionniers de notre discipline ont tout d'abord utilisé des modèles de processus simples pour expliquer l'évolution d'un paysage ou le développement d'une cavité. Avec les années ils se sont complexifiés et les observations réalisées ont permis de mettre en évidence de nouveaux concepts. Quelquefois le processus est encore actif. Quelquefois il ne l'est plus et la lecture des formes, les analyses physico-chimiques, minéralogiques et isotopiques sont bien souvent les seules clés qui permettent de mieux appréhender la succession des phénomènes passés.

Ainsi depuis quelques années de nouveaux paradigmes sont apparus : le rôle des couvertures, la karstification hypogène, la fantômisation ou, plus récemment encore, la biocorrosion. Au fur et à mesure du développement de ces nouvelles approches nous devons sans cesse revenir sur le terrain et revoir les sites déjà parcourus en ayant en tête de nouvelles clés de lecture. C'est sans aucun doute le signe d'une discipline en plein développement, qui sait se renouveler par des approches croisées et qui sait prendre en compte les observations de terrain, celles que nous réalisons tous les jours, spéléologues, géomorphologues et géologues, aussi bien sur terre que sous terre. Rien n'est jamais acquis. Gageons que les années futures nous apporteront encore de nouvelles façons d'appréhender la naissance et l'évolution du karst.

Notre but est toujours d'arriver à établir un état des lieux le plus complet possible des indices permettant de reconstituer l'histoire souvent complexe des karsts mais notre « caisse à outils » est de plus en plus riche comme le démontre la diversité des articles qui suivent. Ainsi ce

symposium permet de faire un point des différents aspects morphologiques et spéléogénétiques connus à ce jour dans le karst. De la forme de détail des parois et des voûtes jusqu'au paysage, en passant par la géométrie des objets et des réseaux. Multiscalaire, l'étude du karst est également éminemment interdisciplinaire. Elle se nourrit de l'interaction entre différents domaines de recherche, partant de la géomorphologie et la géologie jusqu'à la biologie et l'archéologie en passant par la climatologie, l'aérologie et la géochimie. La liste des communications de ce symposium est une fidèle illustration de cette richesse et de la dynamique de l'étude du karst. Il augure de nombreux échanges, très variés, qui permettront à tous d'acquérir de nouvelles grilles de lecture de ce qui nous passionne tous : le karst !

Geomorphology of Ponorul Suspendat Cave, Southern Carpathians: An interplay between thrust tectonics, faulting and karstification

Maria-Laura TÎRLĂ[1,2,3], Alexandru POLOGEA[3], Ovidiu DOLCAN[3] & Gabriel CONSTANTINESCU[3]

(1) Faculty of Geography, University of Bucharest, 1 Nicolae Bălcescu Bv, 010041 Bucharest, Romania, tirla@geo.unibuc.ro (corresponding author)
(2) Research Institute of the University of Bucharest, 90 Panduri Street, 050663 Bucharest, Romania
(3) Silex Brașov Caving Club, 39 Stefan Baciu, 500170 Brașov, Romania, na.pologea@outlook.com, ovidiu_dolcan@yahoo.com, mediator.constantinescu@gmail.com.

Abstract

The Ponorul Suspendat Cave was discovered in 2015 and more than 9 km of passages were surveyed and mapped until present. Plentiful geomorphic evidence of tectonic deformations is exposed in all areas of the cave. We investigated the relationship between cave morphology and geological structure for speleogenetic insights, tectonic evolution and an efficient approach to the forthcoming exploration directions. A supposed link to the Polovragi Cave located 4 km to the south-west could make it the largest karst system in the Southern Carpathians. Structural measurements resulted in two main datasets, resembling early-stage, NE-SW oriented reverse, normal and detachment faults, and late-stage, NW-SE oriented strike-slip faults. The development of vadose canyons and pressure tubes was mainly driven along subsidiary parallel detachment faults. We examined small-scale structures such as calcite-filled tension gashes exposed on the cave walls to infer the vergence of the master (Getic) detachment. Diagnostic morphological features for periodical flooding, rising flow, or supercritical-laminar regime were distinguished. By unravelling the local kinematic fingerprint on the host carbonate rocks, the spatial development of passage network untangles more detailed information on the geological history of the central Southern Carpathians.

Résumé

Géomorphologie de la grotte Ponorul Suspendat, Carpates du Sud : Une interaction entre la tectonique chevauchante, failles et karstification. La grotte de Ponorul Suspendat a été découverte en 2015 et plus de 9 km de galeries ont été explorées et cartographiées jusqu'à présent. Des preuves géomorphologiques abondantes de déformations tectoniques sont visibles dans toutes les zones de la grotte. Nous avons étudié la relation entre la morphologie des grottes et la structure géologique pour gagner des informations spéléogénétiques, ainsi que sur l'évolution tectonique dans le but d'une approche plus efficace pour les futures explorations. Une connexion supposée avec la grotte de Polovragi, située à 4 km au sud-ouest, pourrait former le plus grand système karstique des Carpates Méridionales. Les mesures structurales appartiennent à deux groupes principaux de données, ressemblant à des failles inverses et normales et des détachements à un stade précoce, orientées NE-SO, et à des failles de décrochement à un stade avancé, orientées de manière variable. Nous avons examiné des structures à petite échelle telles que des fentes de tension remplies de calcite pour déduire la direction de la nappe de charriage. Le développement des canyons vadoses et des conduites forcées a été principalement réalisé le long de poussées subsidiaires. Des caractéristiques morphologiques typiques pour le diagnostic des crues périodiques, des crues ascendantes ou du régime supercritique-laminaire ont été mises en évidence. En relevant l'empreinte cinématique locale sur les roches carbonatées, le développement spatial du réseau de galeries apporte des informations plus détaillées sur l'histoire géologique des Carpates Méridionales centrales.

1. Introduction

Cave development is a robust evidence of the geological structure of a region, indicating orientation and frequency of faults and fractures that are not always easily noticeable on outcrops or surface topography. Thrust tectonics complicates even more the groundwater drainage patterns, which tend to track the dislocation planes at various depths. Cerna-Olteț is one of the main karst areas of the Southern Carpathians. Here, the structural framework consists in a highly complex nappe stack, emplaced during the Austrian and "Laramide"/Getic phases of the Alpine orogeny (IANCU *et al.*, 2005). The Danubian Units are the lowest nappe complex, consisting in a granite-metamorphic basement of Neoproterozoic-Cambrian age and Mesozoic sedimentary deposits. The karstifiable rocks consist of Oslea-Polovragi reef limestones of Upper Jurassic-Aptian age, sandwiched between the siliciclastic deposits of Lower Jurassic age at the base and the Turonian-Senonian siliciclastic deposits onto the top. These were overridden by Tithonian-Neocomian carbonatic mylonites of the Severin Nappe and medium grade metamorphism of the Getic Unit, a large crustal nappe of the Southern Carpathians (BANDRABUR & BANDRABUR, 2010).

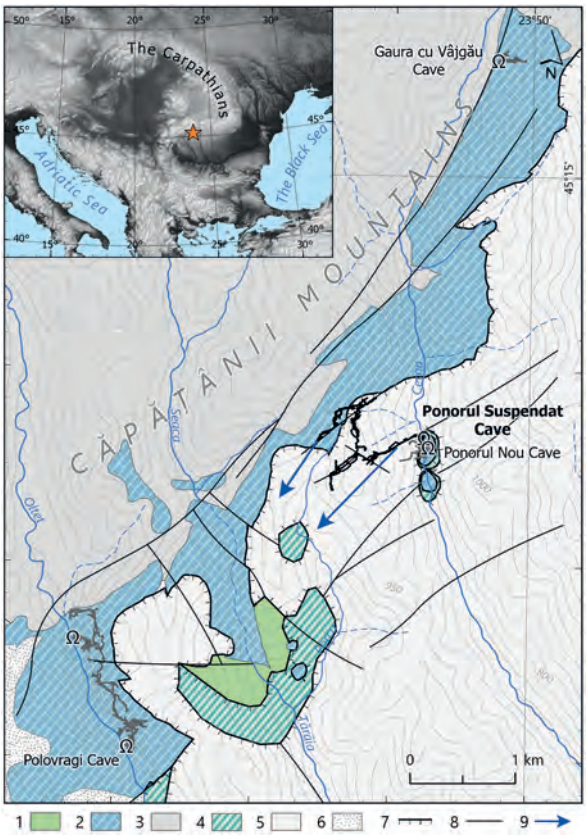

Figure 1: Geologic setting of Ponorul Suspendat Cave. Danubian Units: 1 – carbonatic mylonites (K_2); 2 – limestones (J_3-ap); 3 – granite-metamorphic basement; Severin Unit: 4 – siliciclastic rocks (th-ne); Getic Unit: 5 – metamorphic rocks; 6 – post-tectonic cover; 7 – thrust front; 8 – fault; 9 – groundwater flow direction. Geology modified from BANDRABUR & BANDRABUR (2010).

This architecture has provided conditions for the expansion of karst conduits in non-exposed carbonate rocks. The most striking example is the Ponorul Suspendat Cave (en: The Perched Ponor), discovered in 2015 by members of the Silex Brașov Caving Club in Romania, who have been exploring it continuously ever since (Fig. 1). The most recent achievements (December 2021) raised the total cave development to ~9200 m, a vertical range of 231 m (+38 m; -193 m), and horizontal extent of 1054 m. This makes it the second largest cave in the region, after Polovragi Cave, of 10,793 m in length (DUMITRU & MIHU, 2015). Other important caves in the Cerna basin are Ponorul Nou, of 2940 m in length and Gaura cu Vâjgău, of 2450 m (DOLCAN, 2018). The purpose of this paper is to highlight the role of cave geomorphology and development in archiving rich structural evidence of the major tectonic events that have shaped the Southern Carpathians fold-and-thrust belt over time. The preferred orientations of cave passages are robust evidence that could support the results of earlier dye tracer experiments, which demonstrated the existence of an underground drainage connection between Cerna and Olteț rivers.

2. Materials and methods

Cave surveying using the DistoX2 device and TopoDroid software (running on Android mobile devices) was performed between 2016 and 2021. Some of the passages were surveyed using the DistoX2 continuous scanning mode (10,000-15,000 points per survey day), resulting in better spatial sampling rate and higher model resolution. This permitted an improved graphical representation of cave passages and more accurate morphological inferences.

Post-survey data was processed using Therion (BUDAJ & MUDRÁK, 2008) and other software packages: QGIS, IC Measure, Aven (3D viewer of Survex package). The survey data was exported from TopoDroid, then processed in Therion, producing final cave maps, 2D and 3D models. The cave map was drawn in Therion visual editor (xTherion) using TopoDroid sketches drawn during the survey. Additionally, the final cave map was assembled using the Adobe Illustrator software. We analyzed the geological map sheets published by the Geological Institute of Romania (IGR) to examine and compare the litho-structural features with our findings. The passage network of Polovragi Cave (Fig. 1) was extracted from the base map published on the website of Focul Viu Caving Club in Bucharest.

Structural measurements of thrust and fault planes were recorded underground by using a Freiberger geological compass, then processed in Stereonet *v*11 software (ALLMENDINGER *et al.*, 2012).

3. Cave morphology and structural patterns

Ponorul Suspendat Cave has a typical network pattern, with three key areas distinguished by morphology and orientation: 1) the south-eastern tributary passages; 2) the central collector; 3) the north-western passages (Fig. 2). The cave entrance is located at ~800 m a.s.l. on the right side of Cerna River. The SE passages are vadose and active in the first ~300 m, with a short quasi-cylindrical shaft followed by similar steps that separate tight meanders, and straight parts along subvertical faults and fractures. The morphology suddenly changes to mainly subhorizontal fossil pressure tubes with a dominant NE-SW orientation (~230°), and shorter interconnecting passages shifting to NW-SE (~300°).

The central passage is generally N-S oriented, runs parallel to the major surface drainage network, and maintains at a relatively constant depth of ~-80 m. It describes a zig-zag pattern that matches the orientations of major faults, NW-SE, NNW-SSE and NE-SW. The key aspects of this passage are: i) a complex morphology, where features typical of pressure flow alternate with those of vadose canyons and breakdown; ii) well-developed blind chimneys, ascending galleries and chimney-shafts that interconnect superposed passage levels (Fig. 3); iii) thick silt deposits and passage infills in the central and southern parts; iv) rich speleothem deposits and water-filled pools in the northern part.

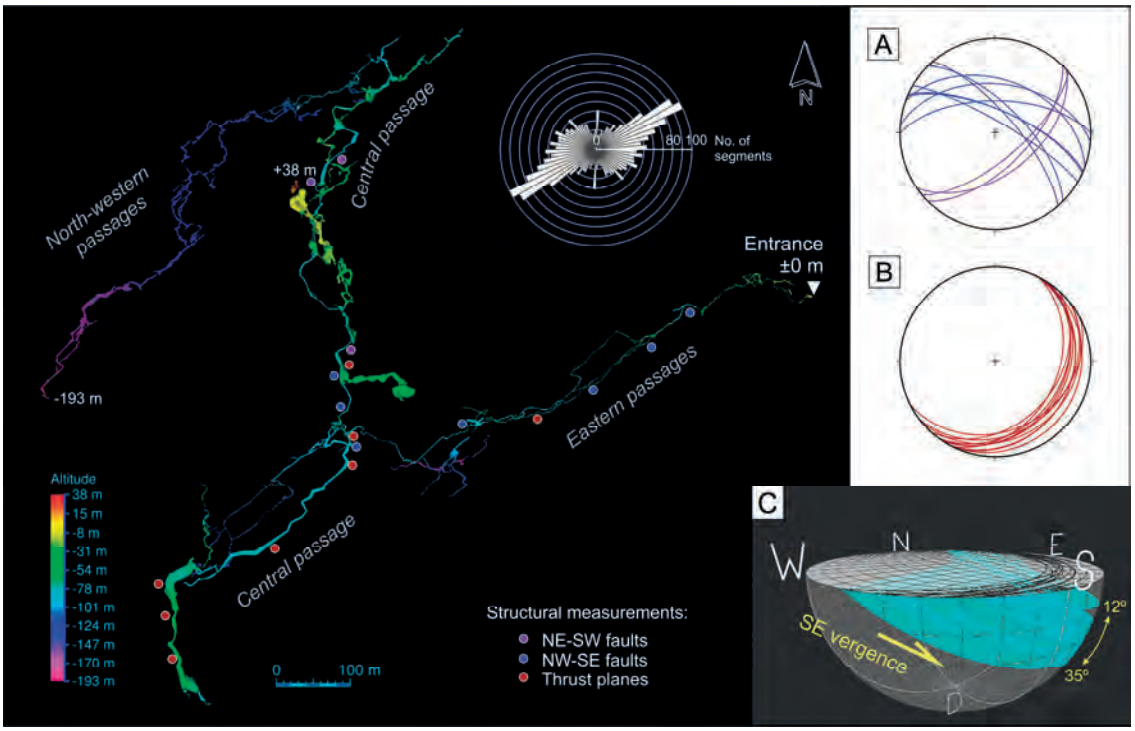

Figure 2: Therion 3D model of Ponorul Suspendat Cave and Stereonet plots of fault and thrust cave measurements: A) normal faults (purple) and strike-slip faults (blue); B) thrust planes (red); C) 3D view of thrust measurements projected in the lower hemisphere (inclination in yellow). The rose diagram shows orientation frequency of passage sectors plotted on a 5° bin width.

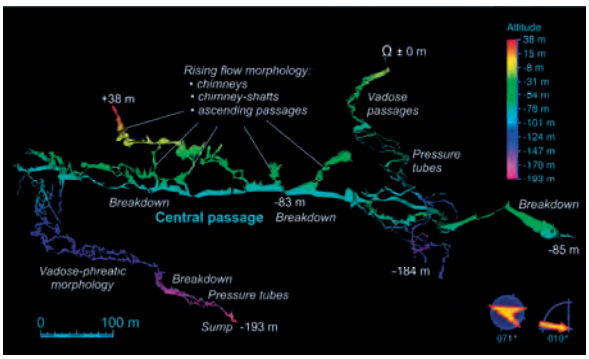

Figure 3: 3D view of cave profile in orthographic projection (Therion), highlighting the major morphological differences.

The north-western passages consist generally of pressure tubes enlarged in vadose conditions. After a rapid descent of -35 m by consecutive shafts, the cave gently dips towards SW at an average angle of 5°. The final tubes, usually flooded, could be accessed, explored and surveyed only during the December 2021 tour. The explored cave ends with a sump at -193 m.

The general preferred orientation of cave passages is NE-SW (62±7° to 242±7°), as shown by frequency data plotted on the rose diagram. The strike and dip of measured fault planes were represented as great circles in stereographic projection (Fig. 2A). In the vertical section, the cave developed mostly on NE-SW striking subsidiary detachment faults that dissect the limestones, with an average inclination of 26° (Fig. 2B, C). The most common brittle shear sense indicators are calcite-filled en-échelon veins, dilational jogs, and sigmoidal shear joints (marked in blue in Fig. 4), exposed on or near the fault plane (in red). All indicate a dominant southeastward detachment vergence, of 136±20°.

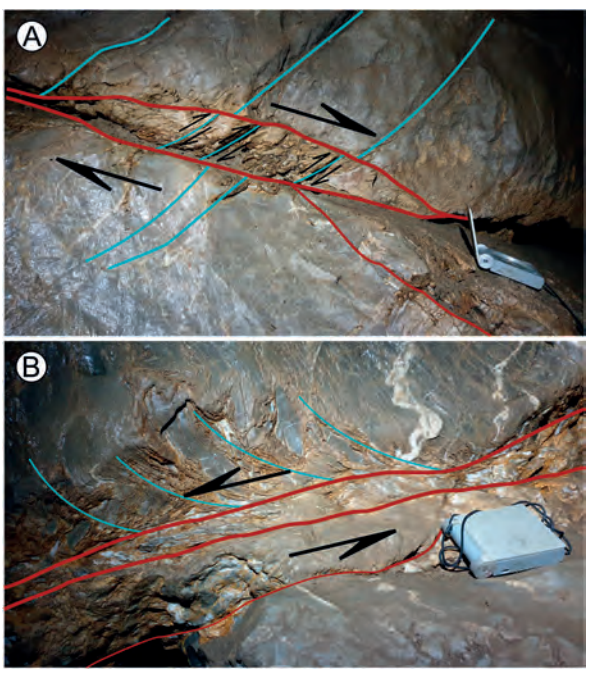

Figure 4: Determining the sense of shear from the curvature of the sigmoidal oblique markers exposed in the central passage (A) and a tributary conduit (B). Compass for scale.

4. Discussions

Ponorul Suspendat Cave developed from north to south by successive subterranean diversions of Cerna River. It is a floodwater cave (PALMER, 2007) fed by sinking streams and diffuse flow, under the strong control of geological structure. The branchwork cave pattern was designed by two intersecting fault sets, oriented NE-SW and NW-SE to NNW-SSE. Subsidiary detachment fault planes have met the ideal conditions for the development of inception horizons, which formed the basis for organizing the main passage network.

The central passage had a complex evolution, initiated in phreatic flow, then dominated by vadose conditions. The chimney-shafts that interconnect the superposed cave levels are diagnostic morphological features for rising flow (KLIMCHOUK, 2009; AUDRA & PALMER, 2011). In the discussed geotectonic setting, these conditions could have probably been forced by base level rise due to local subsidence, such as that related to a possible reactivation of extensional faults. The NW (divergent) and SE (tributary) conduits formed under pressure flow regime at a later stage, by following the preferential direction of NE-SW oriented faults. The morphology of vadose pits and steps in the frontal part shows continuous dissolution and rapid enlargement by permanent supercritical-laminar flow of undersaturated water films, as well as periodical flooding.

The cave passage orientations and the results of our structural measurements suggest the presence of some rather discrete underground connections between the diffuse losses and fossil ponor sinks in Cerna basin and the karstic springs in Olteț basin, as dye tracer experiments had indicated (BANDRABUR & BANDRABUR, 2010).

Cave record of regional geologic history. The NE-SW reverse faults were generated during the Getic compression phase (Maastrichtian), when the Severin-Getic-Supragetic nappe stack was emplaced over the Lower Danubian complex (IANCU *et al.*, 2005). Large-scale orogen-parallel extension in the Eocene lead to exhumation of the Danubian window below the Getic detachment (SCHMID et al., 1998). Results of structural measurements performed on the detachment faults indicate a southeastward vergence, which could be evidence that these low-angle faults are subsidiaries of the Getic detachment. The NW-SE, dominant dextral sets of conjugate faults were produced by the large-scale Middle Sarmatian strike-slip tectonics (MAŢENCO *et al.*, 1997).

5. Conclusion

The karstification pattern and structural details exposed in the morphology of Ponorul Suspendat Cave remarkably highlight the regional tectonic context. Our results bring new evidence on the deformation mechanisms recorded by the sedimentary cover of the Lower Danubian Units during the key tectogenetic events that built the Southern Carpathians orogenic belt.

The overall geomorphology suggests a polygenetic origin of the cave. Further detailed morphological and structural analyses are needed to support these preliminary inferences. The structural data could also be helpful in discovering new exploration pathways, as the potential of this cave in particular, but also of other cavities in the area, is far from being exhausted.

Acknowledgments

We are grateful to all cavers from Silex Brașov Caving Club who explored and surveyed the Ponorul Suspendat Cave and provided the data for this study. Constructive discussions with M. Stoica and H. Mitrofan contributed to disentangling the geologic framework of the area. Suggestions of L. Bruxelles and of an anonymous reviewer were useful in improving the quality of the manuscript.

References

ALLMENDINGER R.W., CARDOZO N., FISHER D. (2012) Structural geology algorithms: Vectors and tensors in structural geology. Cambridge Univ. Press, Cambridge, 313 p.

AUDRA P., PALMER A.N. (2011) The pattern of caves: controls of epigenic speleogenesis. Géomorphologie : Relief, Processus, Environnement, n°17, 359–378.

BANDRABUR G., BANDRABUR R. (2010) Parâng and Căpățânii Mountains. In: Orășeanu, I., Iurkiewicz, A. (Eds.), Karst Hydrogeology of Romania. Belvedere, Oradea, pp. 69–75.

BUDAJ M., MUDRAK S. (2008) Therion – Digital Cave Maps. Spelunca Mémoires, n°33, 138–141.

DOLCAN O. (2018) În căutarea colectorului dintre Cerna și Olteț. Speomond, n°19 (2016–2018), 12–15.

DUMITRU R., MIHU O. (2015) Peștera Polovragi: trecut, prezent și viitor. Speomond, n°18, 27–30.

IANCU V., BERZA T., SEGHEDI A., GHEUCA I., HANN H.-P. (2005) Alpine polyphase tectono-metamorphic evolution of the South Carpathians: A new overview. Tectonophysics, n°410, 337–365.

KLIMCHOUK A. (2009) Morphogenesis of hypogenic caves. Geomorphology, n°106, 100–117.

MAȚENCO L., BERTOTTI G., DINU C., CLOETINGH S. (1997) Tertiary tectonic evolution of the external South Carpathians and the adjacent Moesian platform (Romania). Tectonics, n°16, 896–911.

PALMER A.N. (2007) Cave Geology. Cave Books, Dayton, 454 p.

SCHMID S.M., BERZA T., DIACONESCU V., FROITZHEIM N., FÜGENSCHUH B. (1998) Orogen-parallel extension in the Southern Carpathians. Tectonophysics, n°314, 401–422

A speleogenetic comparison between caves located in two neotectonic grabens in southern Greece

Isidoros KAMPOLIS[1,2] & Kyriaki PAPADOPOULOU-VRYNIOTI[3]

(1) School of Mining & Metallurgical Engineering, Department of Geological Sciences, National Technical University of Athens, 9 Iroon Polytechniou, 15773 Athens, Greece kampolisigeo@gmail.com (corresponding author)
(2) Group of Palaeoenvironment and Ancient Metals Study, Institute for Nanotechnology Nanoscience, National Center for Scientific Research 'Demokritos', 10 Neapoleos, Athens, 15310, Greece
(3) Department of Geography and Climatology, Faculty of Geology Geoenvironment, National Kapodistrian University of Athens, Panepistimioupolis Zografou, Athens, 157 84, Greece papadopoulou@geol.uoa.gr

Abstract

The Corinth and Messiniakos gulfs represent two neotectonic grabens in Greece. The Corinth Gulf is a WNW-ESE bearing asymmetric graben of Late Miocene age separating southern Central Greece from northern Peloponnese. The Tyfion and Kapareli caves are located at the NE border of the Corinth Gulf, about 4 and 7 km from the closest coastline, respectively. On the other hand, the Messiniakos Gulf is an asymmetric graben of Late Miocene age striking NNW-SSE and borders the SW Peloponnese. The composite cave system of Selinitsa-Drakos is 46 km south of Kalamata City on the eastern coast of Messiniakos, 54 m from the sea. In order to compare the speleomorphology with the regional tectonic activity and assess the influence of geodynamics to speleogenesis, the development directions of the aforementioned caves were measured. For Selinitsa-Drakos system, these were extracted from the plan view maps whereas for Tyfion and Kapareli caves, they were measured during their survey. Also, 273 karstic/tectonic directions were measured around the cave entrances. Both cave groups are controlled by the regional tectonic history of the grabens and this can be seen in their development patterns. Finally, a common tectonic history is revealed for the whole area.

1. Introduction

The location of Greece at the European-African subduction zone places the country in one of the most tectonically active areas in the world (TAYMAZ *et al*., 2004). The resultant tectonic deformation of the region in combination with the carbonate outcrops, about 35 % of the total hellenic surface, provides ideal conditions for the genesis of a rich variety of karst landforms both exogenic and endogenic. Among them, caves are the most interesting and spectacular ones. These subterranean environments preserve valuable scientific data for a variety of scientific disciplines like geology, archaeology, palaeontology etc. Moreover, caves are considered significant paleoenvironmental (DELANNOY *et al*., 2009) and palaeoclimatic archives (MCDERMOTT, 2004; FAIRCHILD & BAKER, 2012) and their contribution in unraveling the tectonic history of a region is of high significance, too (HÄUSELMANN *et al*., 1999; KAMPOLIS *et al*., 2020).

In this paper, we highlight the potential of four Greek caves in revealing data regarding the tectonic stress history of the region. This is accomplished by studying their development patterns and comparing them to the prevailing stress directions of the Quaternary period. Two groups of caves are interpreted, situated in two neotectonic grabens of Greece. The first group, including the caves of Tifyon akd Kapareli, lies close to the NE coastline of the Corinth Gulf, whereas the second group comprising the composite Selinitsa-Drakos Cave System is located on the eastern shores of the Messiniakos Gulf. The development patterns of both groups suggest a strong control by the regional neotectonic activity. Also, the dominance of specific tectonic directions on cave patterns provides the ability of relative dating for the different cave sections. Finally, the close proximity of the caves to the sea allows the recording of the environmental changes imposed by the successive sea level changes during the Quaternary.

2. Geotectonic setting

The Corinth Gulf is an active asymmetric graben striking WNW-ESE (Fig. 1). Extension in the area has been established by WNW-ESE normal faults since the Late Miocene (KOKKALAS *et al*., 2006) and the tectonic activity presents a contradicting regime on its borders.

The northern part of the Gulf (central Greece) is under constant subsidence, whereas its southern counterpart (northern Peloponnese) under constant uplift.

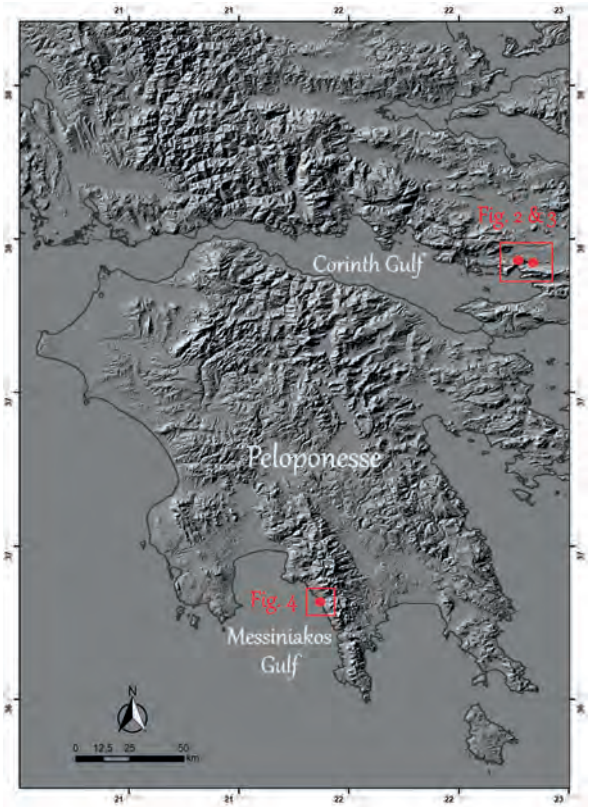

Figure 1: Site map of the studied area. The red squares highlight the location of the caves, whereas the red frames indicate the geographical position of the respective figures.

The area of Tyfion and Kapareli Caves is located at the NE part of the Corinth Gulf. The caves are developed vertically within the Middle-Upper Triassic – Lower Jurassic Limestones and Dolomites of Boeotia Unit. The distance between the shafts is about 8 Km. Tyfion Shaft is a clockwise convolution in plan view and 23 m deep (Fig. 2). Its entrance lies at 611 m altitude in Mavrovouni Mountain and at an uplifted peneplain occupied by large dolines. The Kapareli Shaft presents a counterclockwise convolution in plan view and has a depth of 51 m (Fig. 3). It is located on the southern wall of the Livadostras gorge at 170 m altitude near Kapareli Village.

It is noteworthy to mention that the Tyfion Shaft was found and named for the first time by Isidoros Kampolis during research for new caves back in 2012. The name of the cave derives from the nearby ancient town of Siphai or Tiphai, an ancient harbor at the Corinth Gulf which is occupied by Alyki town, nowadays. The ancient acropolis with the archaeological ruins of the harbor on the coastline witnesses the glamor of this site in ancient times.

The tectonic stress history of the Corinth Gulf is characterized by three phases: a) the younger extension phase accomplished by WNW-ESE to E-W trending normal faults, b) the extensional phase of Quaternary associated with NE-SW normal faults and c) the older extensional phase of Late Pliocene with NW-SE faults (RONTOGIANNI-TSIAMBAOU, 1984).

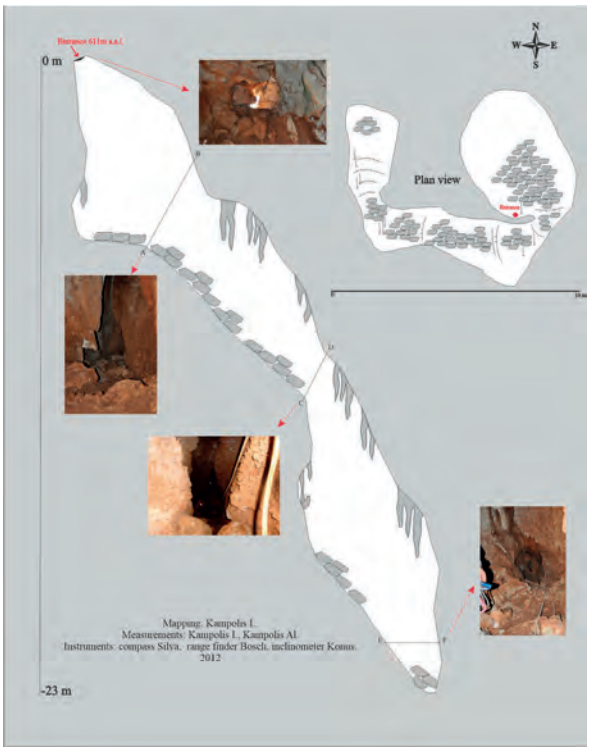

Figure 2: Cross-section and plan view of the Tifyon Shaft.

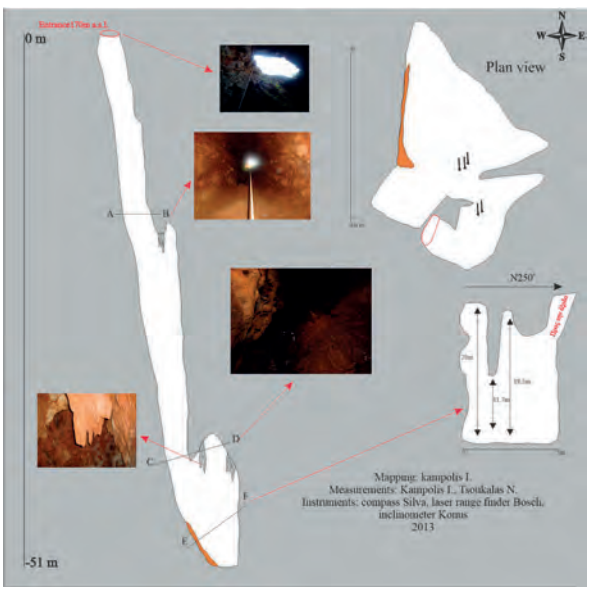

Figure 3: Cross-section and plan view of the Kapareli Shaft.

The Messiniakos Gulf is an asymmetric neotectonic graben of Late Miocene striking NNW-SSE (Fig. 1). It borders SW Peloponnese at a distance of about 50-80 km from the Hellenic trench (PAVLAKIS *et al.*, 1989). Selinitsa-Drakos Cave System (Fig. 4) is located on the eastern shores of the Messiniakos Gulf and comprises the fourth longest cave system in Greece with 4 km length, approximately. The cave system was formed in the Upper Senonian – Upper Eocene Limestones of Mani (Plattenkalk) Unit. It comprises Selinitsa Cave and Drakos Underground River with the former located on the coastline at +18 m and the latter at -10 m, respectively. Both caves began forming without being connected to each other (PAPADOPOULOU-VRYNIOTI &

KAMPOLIS, 2012). Their connection was accomplished through a 28 meter long narrow fissure probably during the Holocene, creating a composite karstic system. The cave system was strongly influenced by the sea level changes of the Late Quaternary (PAPADOPOULOU-VRYNIOTI & KAMPOLIS, 2011; KAMPOLIS *et al*., 2022). More specifically, Selinitsa was occupying the saturated zone as Drakos nowadays, but the cave has been transferred in the unsaturated zone due to the regional tectonic activity.
The tectonic history of Messiniakos Gulf can be classified in two phases: a) the extensional phase of Middle-Late Pleistocene to present with NE-SW faults and b) the Late Pliocene-Early Pleistocene phase with NW-SE normal faults (MERCIER & LALECHOS, 1993).

3. Materials and methods

The speleomorphology of the four caves was assessed based on their respective maps. The cave maps of Selinitsa and Drakos were the outcome of caving activities of SPELEO Caving Club members since 1978. The cave maps of Tifyon and Kapareli Shafts were produced by Isidoros Kampolis with the assistance of Nikolaos Tsoukalas and Alexandros Kampolis. In order to compare the development patterns of the caves with the tectonic lines of the respective areas, we measured the development directions of each cave and produced the respective rose diagrams. The development directions of the Selinitsa-Drakos system were extracted by the plan view maps, whereas the directions of the shafts were measured during their survey. The latter was accomplished with the use of a SILVA compass, a BOSCH laser range finder and a KONUS inclinometer and by following the conventional caving survey method. The field data were introduced in Visual Topo and the speleomorphology of the shafts was reconstructed. Then, the Tifyon and Kapareli cave maps were designed with the use of the CorelDRAW software.
With the aim of revealing the dominant tectonic patterns for each area, we measured 273 tectonic (joints and faults) and karstic directions around the cave entrances. The number of these features in every cave exceeds the value of 50 in order to minimize the statistical error.

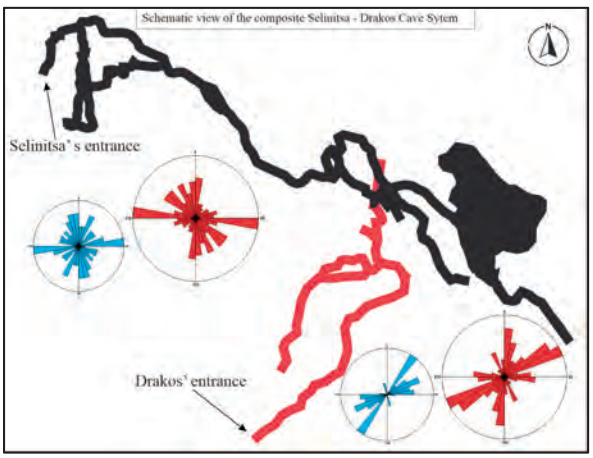

Figure 4: Schematic plan view of the Selinitsa-Drakos Cave System modified after Papadopoulou-Vrynioti and Kampolis (2011). The red rose diagrams correspond to the development directions of the caves, whereas the blue ones correspond to the karstic/tectonic directions of the area. For the interpretation of the rose diagrams see the Discussion and results section.

4. Discussion and results

The comparison of the development directions of the caves (Fig. 5) located at the northeastern Corinth Gulf with the respective tectonic discontinuities (Fig. 6) suggests that speleogenesis in Kapareli and Tifyon Shafts was influenced mainly by the extensional phase of Quaternary established by NE-SW faults. Both caves have been developed along this direction, whereas Kapareli Cave has a dominant NE-SW development. On the other hand, Tyfion Cave presents a dominant WNW-ESE component which is the youngest tectonic fault direction in the area, thus suggesting the younger age of this cave. The depth comparison of these caves also supports this proposal with the deepest cave being the oldest formation. Both caves have passages opened along the older NW-SE Late Pliocene tectonic direction. The tectonic/karstic directions measured on the surface around the entrances present a different pattern in comparison with the caves. At Kapareli Shaft, these features have a dominant WNW-ESE component parallel to the youngest tectonic direction and a secondary one trending NW-SE. A large number of tectonic/karstic features is also parallel to the NE-SW. In the case of Tifyon Shaft, the measured directions on the surface present a dominant NW-SE component along the Late Pliocene tectonic directions and a secondary one along the NE-SW. The former is due to the presence of a large fault zone trending NW-SE.

In the case of Selinitsa-Drakos Cave System, Selinitsa is developed along the Late Pliocene-Early Pleistocene NW-SE tectonic directions whereas Drakos along the NE-SW (to NNE-SSW) directions of Mid-Late Pleistocene (Fig. 4).

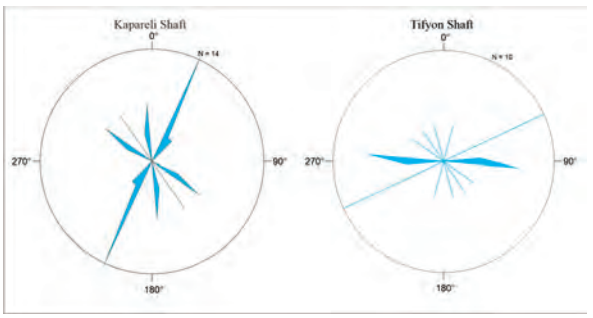

Figure 5: Rose diagrams of the development directions of Kapareli and Tifyon Shafts.

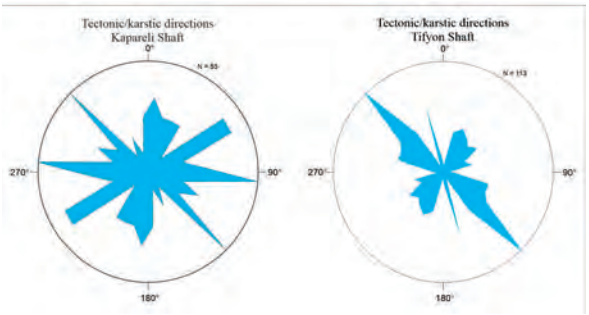

Figure 6: Rose diagrams of the tectonic/karstic directions of Kapareli and Tifyon Shafts.

The respective tectonic/karstic directions follow the same pattern. The observed dominant WNW-ESE development direction of Selinitsa can be attributed to the older Late Pliocene-Early Pleistocene extensional phase. This direction is limited in the rose diagrams of Drakos and underpins the younger age of the cave. Although the gulfs present different current extensional regimes, the extensional phases of Plio-Quaternary have acted in the same directions and have controlled speleogenesis.

Quaternary sea level fluctuations at the gulfs have influenced the caves. The vertical character of the caves at the northern Corinth Gulf, an area of constant subsidence since Miocene, can be explained by the water table dropdown during the glacial periods. During these climatic stages the Corinth Gulf was transforming into a lake. On the other hand, the Selinitsa-Drakos Cave Systen has a development of discrete successive levels corresponding to the sea level stands of the Quaternary.

Acknowledgments

The authors gratefully thank Nikolaos Tsoukalas and Alexandros Kampolis for his assistance during the survey of Kapareli and Tyfion Shafts, respectively. Many thanks are also addressed to our caving colleagues from SPELEO Club for their support during caving fieldtrips and Elefteroudis Kleovoulos for his company at the mountains.

References

DELANNOY J.-J., GAUCHON C., HOBLÉA F., JAILLET S., MAIRE R., PERRETTE Y., PERROUX A.-S., PLOYON E., VANARA N. (2009) Karst: from palaeogeographic archives to environmental indicators. Geomorphologie, 15 (2), 83-94.

FAIRCHILD I. J., BAKER A. (2012) Speleothem Science: From Process to Past Environments. Wiley: Hoboken, N.J.

HÄUSELMANN P., JEANNIN Y. P., BITTERLI TH. (1999) Relationships between karst and tectonics: case-study of the cave system north of Lake Thun (Bern, Switzerland), Geodinamica Acta, 12:6, 377-387.

HEEZEN B. C., EWING M., JOHNSON G., (1966) The Gulf of Corinth Floor. Deep-Sea Research 13, p. 381–411.

KAMPOLIS I., MARI A., KAMPOLIS A. (2020) Lychnospilia or Cave of Pan: An archaeological site with an interesting Quaternary evolution. Bulletin of the Geological Society of Greece, Special Publication No 8, ISBN: 978-960-98709-6-2.

KAMPOLIS I., TRIANTAFYLLIDIS ST., SKLIROS V., KAMPERIS E. (2022) Quaternary evolutionary stages of Selinitsa Cave (SW Peloponnese, Greece) revealing sea level changes based on 3D scanning, geomorphological, biological and sedimentological indicators. Quaternary, 5 (accepted for publication).

MCDERMOTT F. (2004) Palaeo-Climate Reconstruction from Stable Isotope Variations in Speleothems: A Review. Quaternary Science Reviews, 23 (7–8), 901–918.

MERCIER J.L, LALECHOS S. (1993) The Middle-Late Pleistocene NW-SE extension in Southern Peloponnesus and the kinematics of the seismic fault of the 1986 Kalamata earthquake (Greece). Proceedings of the 2nd Congress of the Hellenic Geophysical Union (Seismology), 586-59

PAPADOPOULOU-VRYNIOTI K., KAMPOLIS I. (2011) The "Selinitsa-Drakos" coastal karstic system in the Messinian Mani Peninsula (southwestern Greece) in relation to the terrestrial geoenvironment, Geologica Balcanica 40(1–3), 75–83.

PAPADOPOULOU-VRYNIOTI K., KAMPOLIS I. (2012) Formation and development of a karstic system below and above sea level in Messinian Mani Peninsula (S. Greece), Speleogenesis & Evolution of Karst Aquifers, 12, 17-21 (http://www. speleogenesis.info/content/).

PAVLAKIS P., PAPANIKOLAOU D., CHRONIS G., LYKOUSSIS B., ANAGNOSTOU G. (1989) Geological Structure of Inner Messiniakos Gulf. Pdf. Bull. Geol. Soc. Greece, 3 (XXIII), 333–347.

RONTOGIANNI-TSIAMABASOU Th. (1984) Etude neotectoniique des rivages occidenteaux du canal d' Atalanti (Grèce Centrale). Université de Paris sud Centre d' Osray, Thèse.

TAYMAZ T., TAN O., YOLSAL S. (2004) Active Tectonics of Turkey and Surroundings and Seismic Risk in the Marmara Sea Region. The Proceedings of IWAM04, Mizunami, Japan.

Speleo-morphology and tectonic processes – What can be seen in slowly deforming regions?

Ana MLADENOVIĆ[1,3] & Jelena ĆALIĆ[2,3]

(1) University of Belgrade – Faculty of Mining and Geology, Đušina 7, 11000 Belgrade, Serbia, ana.mladenovic@rgf.bg.ac.rs (corresponding author)
(2) Geographical Institute Jovan Cvijić, Serbian Academy of Sciences and Arts, Đure Jakšića 9, 11000 Belgrade, Serbia, j.calic@gi.sanu.ac.rs
(3) Students' Speleological and Alpinistic Club (ASAK), Studentski trg 16/II, 11000 Belgrade, Serbia

Abstract

There are a lot of methods used to determine tectonic process active in a region, and they vary depending on the purpose of the research. However, a number of them cannot be used in slowly deforming regions, because the effects of active tectonic process on the rocks in such regions could be negligible. This is especially true for the recently active tectonics in such regions, since most of the recently active tectonic structures never reach the surface. Because of that, studying tectonic structures inside karst caves can give valuable information about active tectonic processes. Here, we present evidence about the youngest and recently active faults in the area of the central part of the Carpatho-Balkan orogen, located in Eastern Serbia, based on data from the karst cave Mala Bizdanja. Age of activity of faults mapped inside the cave was determined based on indicators of faults that cut speleothems, forming fault breccias that incorporate broken speleothems, and based on speleogenetic considerations. Also, samples for radiometric dating have been collected, that will help to quantify fault activity rate. Preliminary results show that the research area is characterized by strike-slip tectonics, with recently active NW-SE-trending sinistral faults, suspected to be also seismically active.

Résumé

Spéléo-morphologie et processus tectoniques – Que peut-on voir dans les régions qui se déforment lentement ? Une myriade de méthodes est utilisée pour déterminer un processus tectonique actif dans une région. L'application de chaque méthode dépend de l'objectif de la recherche. Cependant, beaucoup d'entre elles ne peuvent pas être utilisées dans des régions à déformation lente car les effets du processus tectonique actif sur les roches peuvent être négligeables. Cet effet est particulièrement vrai dans les régions qui ont subi une activité tectonique récente, où la plupart des structures actuelles n'atteignent pas la surface. Pour cette raison, l'étude des structures tectoniques à l'intérieur des cavités karstiques peut fournir des informations précieuses sur les processus tectoniques actifs. Ici, nous présentons des preuves sur les failles les plus jeunes et récemment actives dans la partie centrale de l'orogène carpatho-balkanique, située dans l'est de la Serbie, à partir des données obtenues dans la grotte Mala Bizdanja. L'âge d'activité des failles cartographiées à l'intérieur de la cavité a été déterminé sur la base d'indicateurs de failles qui coupent des spéléothèmes, formant des brèches de failles qui incorporent des spéléothèmes brisés, et sur la base de considérations spéléogénétiques. Des échantillons pour datation radiométrique ont également été collectés, ce qui permettra de quantifier le taux d'activité des failles. Les résultats préliminaires montrent que la zone de recherche est caractérisée par une tectonique décrochante, avec des failles sénestres récemment actives orientées NW-SE et proposées comme étant également actives sur le plan sismique.

1. Introduction

Methods to determine tectonic processes in a region vary depending on the purpose of the research but are generally characterized by mapping of tectonic structures and interpreting them in the context of the tectonic process(es) responsible for their activation. However, if one would like to determine recently active tectonic process, available data dramatically decrease, since most of the tectonic structures that are recently active never reach the surface. This is especially true for the regions with slow tectonic deformation, where tectonic deformation does not produce prominent evidence, or if so, they are occasionally eroded. Because of that, studying of tectonic structures inside caves can give valuable information about active tectonic processes.

One of such regions of slow tectonic deformation is located in the central Balkan Peninsula, in the region of Carpatho-Balkan orogen, situated in Eastern Serbia (Fig. 1). This orogen represents the western part of the Carpatho-Balkan orogenic chain, extending in the north to the Romanian Southern Carpathians and in its southeastern part to the Balkan massif in Bulgaria. In its central part, in Eastern Serbia, Carpatho-Balkanides are made up of a system of east-vergent nappes, that have been formed in Early

Cretaceous and were multiplicatively activated during their geological history (SCHMID *et al*. 2020). This activity led to the formation of faults that are favorably oriented in respect to the main thrust system. It is suspected that some of these fault systems are also active in recent times (for discussion see MLADENOVIĆ *et al*. 2019).

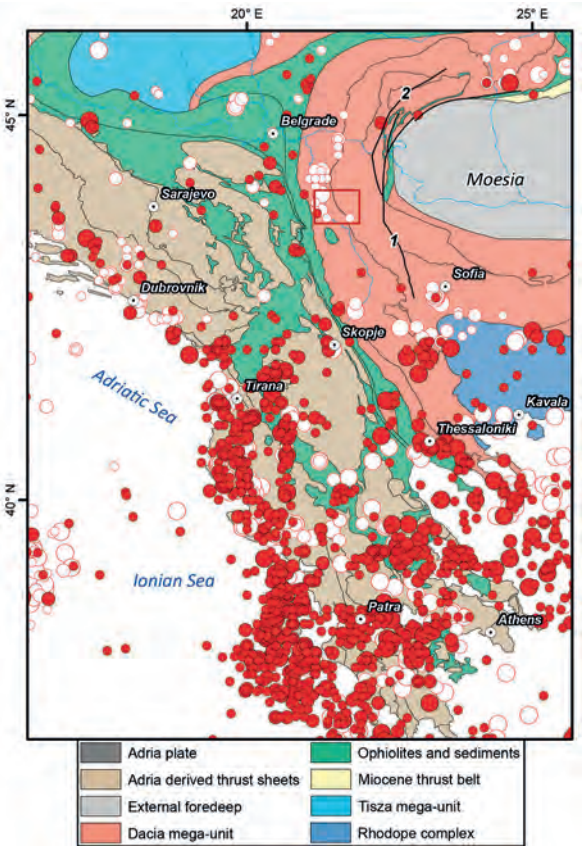

Figure 1: Tectonic map of the wider Balkan Peninsula (after SCHMID et al. 2020), with positions of historical (white circles) and instrumentally located earthquakes (red circles) based on the results of the SHARE project. Immediate research area is marked with red rectangle.

Relatively complex geological structure as well as relatively long time during which the whole area has been exposed on the surface, have both led to the intensive karst process and development of surface and underground karst forms. Because of that, investigation of deformation structures on the field surface is relatively difficult, but investigation of these structures inside the karst caves can give a lot more information.

In this paper, we present evidence about neotectonically active faults that were mapped inside the Mala Bizdanja Cave, situated in the westernmost part of the Carpatho-Balkan orogen (Fig. 2). Vicinity of the research area is characterized by modest seismic activity, and according to earthquake focal mechanisms, recently active tectonic process in the wider area can be characterized as strike-slip, with maximal stress axis oriented NNE–SSW (MLADENOVIĆ *et al*. 2014). The main fault systems that are active in recent times are sinistral faults oriented NW–SE, and dextral faults, generally oriented NE–SW, as well as their secondary structures.

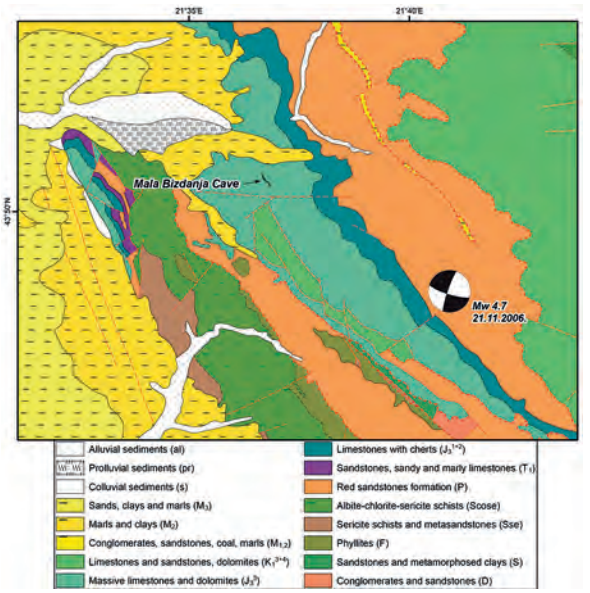

Figure 2: Geological map of the wider research area, based on the General geological map of SFRY.

The Mala Bizdanja Cave is approximately 1 km long, mostly horizontal cave with vertical entrance. It is situated high in the vadose zone, with mild seasonal percolation through the relatively thin overlying caprock. The cave is elongated in the NW–SE direction and located near the suspected seismically active NW–SE-trending sinistral fault (Fig. 2; see also MLADENOVIĆ *et al*. 2014). This cave was extensively explored by members of the Students' Speleological and Alpinistic Club (ASAK) from Belgrade. During these field campaigns, a lot of broken speleothems have been recorded inside the cave, which gave rise to the ideas of tectonic investigation, especially when taking in mind its position in the context of local and regional geology.

2. Methods

Base for tectonic investigations in the Mala Bizdanja Cave was a detailed map of the cave, completed by ASAK team, during numerous field campaigns of topographic surveying of the cave passages. Topographic survey of the cave was performed following standard techniques and using digital compass equipped with laser distance-meter, Leica x310. During these field campaigns, speleologists mapped a lot of broken speleothems, passages guided by structural planes (bedding planes, joints, fault planes). During these investigations, we tried to map not only structures, but also more clear evidence of their neotectonic activity, as well as to try to quantify slip along the supposed active faults. For that reason, we took test sample for U-series radiometric dating to be carried out at the Johannes Gutenberg University in Mainz, Germany.

3. Results and discussion

During tectonic investigations, we succeeded to map a lot of evidence of neotectonic activity inside the Mala Bizdanja Cave, some of which are shown on the Fig. 3.

The most indicative example of the neotectonic activity inside the cave is represented by broken speleothems, as shown on Fig. 3a. Here, the subhorizontal joints developed along the h0l (conjugate joints) systems cut draperies.

Structures shown on Fig. 3b represent fault plane and secondary structures (Riedel shears), along which an extensive fault breccia has been developed. Fault breccias developed on this location, as well as on several other locations inside the cave, often incorporate broken speleothems as clasts inside the tectonic sediment, indicating thus neotectonic activity of these faults.

Fault plane evident on Fig. 3c has well developed striations that indicate two generations of slip along this fault. Older, and less prominent, striations point to reverse slip, which is expected in the research area, most probably active during Oligocene and Miocene complex rotation of the whole area around the rigid Moesian promontory (for detailed discussion see MLADENOVIĆ *et al*. 2019). Clear cross-cutting relationship of the striations along this fault plane indicate that the younger slip along this WNW–ESE-trending fault is sinistral. Although we cannot guarantee for its neotectonic activity, it is evident that this fault belongs to the system of seismically active faults in this area, as shown by the earthquake focal mechanism, presented on the Fig. 2 (also, for detailed discussion on recent tectonic activity in the wider research area see MLADENOVIĆ *et al*. 2014).

Cave passage shown on Fig. 3d is clearly guided by tectonic structures – the main course of the passage is developed along the WNW – ESE-trending fault, and it was widening by mechanical erosion of water running along the Riedel shears related to this fault. According to the orientation of these Riedel shear joints, it can be concluded that the main guiding fault of this passage is also sinistral.

The most promising location for potential radiometric dating of speleothems is shown on the Fig. 3e. This is well developed fault plane trending NNE–SSW, on which striations indicate normal slip. On this location, several "layers" of flowstone are developed. Striations are probably developed on more of these layers, however, we found the youngest ones developed on the second youngest layer of flowstone. Because of that, we sampled the youngest and the second youngest layer for U-series radiometric dating. However, our test samples suffered from low concentrations of uranium, so we were unable to calculate the age of these samples, and hence to try to determine the youngest activity of this fault.

Figure 3: Typical neotectonic elements inside the Mala Bizdanja Cave. See the main text for detailed explanations.

Figure 3f shows cave column that is broken along joints belonging to the h0l system, thus indicating shear along the zone located near the area where the column is located. Although during previous research the shear zone has not been found, it certainly points to the neotectonic activity of this zone.

4. Conclusion and future work

Results of investigation of neotectonically active faults based on tectonic mapping inside the Mala Bizdanja Cave, located in the westernmost part of the Carpatho-Balkan orogen in Eastern Serbia, indicate that neotectonically active faults in the research area most probably belong to the system of WNW–SSE-trending left lateral faults, and NE–SW-trending right lateral faults. This is also in accordance with earthquake focal mechanisms in this area, indicating thus also their recent activity.

Strike-slip tectonic regime in this area most likely result from far-field stress generated by the collision of the Adriatic microplate, the Moesian promontory and the tectonic units in-between. Such stress field is shown to be highly heterogeneous even in this relatively small research area, so local areas of transtension and transpression have also been very important in controlling the recent fault kinematics. The reason for this probably lies in the fact that most of the faults that are active in recent times are reactivated structures, that have been active during previous very intensive periods of tectonic activity.

Future work in this area should consist of more detailed mapping of tectonic structures, and finding locations to sample speleothems for dating, which would certainly be of high importance in determining fault dynamics in this area. Also, it would be useful to map the surface above the cave and try to determine faults and their kinematics also applying this methodology.

Acknowledgments

We gratefully thank members of the Students' Speleological and Alpinistic Club (ASAK) from Belgrade, Serbia, for help during the tectonic investigations.

References

MLADENOVIĆ A., TRIVIĆ B., ANTIĆ M., CVETKOVIĆ V., PAVLOVIĆ R., RADOVANOVIĆ S. and FÜGENSCHUH B. (2014) The recent fault kinematics in the westernmost part of the Getic nappe system (Eastern Serbia): Evidence from fault slip and focal mechanism data. *Geologica Carpathica*, 65/2, 147-161.

MLADENOVIĆ A., ANTIĆ M., TRIVIĆ B. and CVETKOVIĆ V. (2019) Investigating distant effects of the Moesian promontory: brittle tectonics along the western boundary of the Getic unit (East Serbia). *Swiss Journal of Geosciences*, 112, 143-161.

SCHMID S.M., FÜGENSCHUH B., KOUNOV A., MATENCO L., NIEVERGELT P., OBERHÄNSLI R., PLEUGER J., SCHEFER S., SCHUSTER R., TOMLJENOVIĆ B., USTASZEWSKI K. and VAN HINSBERGEN D.J.J. (2020) Tectonic units of the Alpine collision zone between Eastern Alps and western Turkey. *Gondwana Research*, 78, 308-374.

Stylolites control karst formation

Silvana MAGNI[1,2,3]

(1) C.A.R.S, Centro Altamurano Ricerche Speleologiche, 70022 Altamura, Italy
(2) SCR, Speleo Club Ribaldone, 16123, Genua, Italy
(3) University of Barcelona, Department of Mineralogy, Petrology and Applied Geology. Faculty of Earth Sciences, Martí i Franquès s/n. 08028 Barcelona, Spain, magnisilvana@libero.it

Abstract

The dissolution process is a complex phenomenon controlled by several factors (lithology, porosity, stress orientation, environmental conditions, networks of fractures) but compression tectonic structures, like stylolites, have never been taken into consideration. In the karst field, circulation is commonly associated with extensional features (as faults and joints), assuming that there can be no fluid pathway through compression tectonic ones. In this context, stylolites play an important role in fluid circulation during carbonate deformation. Stylolites have an extremely variable shape from the meso- to microscale, with variable porosity and permeability and because of this, they can act as barriers or conduits for flow. The focus of the research is to investigate the starting point of the dissolution and mostly the micro-mechanism that led to the formation of caves. In this research we integrated field work with lab analysis. The field work was carried out in a karst area in the South and North Italy where, using the Caine's method (1996), the permeability of the three fault zones was reconstructed. The lab analyses (chemical, petrographic) were performed on selected samples representative of the 4 main different shapes of stylolites.

Résumé

Les stylolites contrôlent la formation des karsts. Le processus de dissolution est un phénomène complexe contrôlé par plusieurs facteurs (lithologie, porosité, orientation des contraintes, conditions environnementales, réseaux de fractures) mais dans le domaine karstique, les structures tectoniques de compression, comme les stylolites, ne sont jamais prises en compte. Dans le domaine karstique, la circulation est généralement associée à des caractéristiques d'extension (comme des failles et des joints), en supposant qu'il ne peut y avoir de passage de fluide à travers des indices tectoniques de compression. Dans ce contexte, les stylolites jouent un rôle important dans la circulation des fluides lors de la déformation des carbonates. Les stylolites ont une forme extrêmement variable de la méso- à la micro-échelle, avec une porosité et une perméabilité variable et, à cause de cela, ils peuvent agir comme des barrières ou des drains pour l'écoulement. L'objectif de cette recherche est d'étudier le point de départ de la dissolution et principalement les micro-mécanismes qui conduisent à la formation de grottes. Dans cette recherche, nous avons couplé le travail sur le terrain et l'analyse en laboratoire.

1. Introduction

Stylolites are dissolution planar features formed by a pressure solution process that dissolves the soluble particles and leads to an enrichment in insoluble materials along their planes. They are considered as the result of a different solubility within the rock and thus play an important role in fluid circulation in rocks (STOCKDALE, 1943; ROLLAND *et al*., 2014). Inside of stylolites, several insoluble minerals are present such as illite-smectite, pyrite, apatite (PARK, 1968; TOUISSANT, 2018). Consequently, stylolites can modify fluid flow in rocks acting as barriers or channels. Sedimentary stylolites are generally considered to act as horizontal permeability barriers (NELSON, 1981; FINKEL *et al*. 1990; ALSHAR HAM *et al*., 2000), and tectonic ones as a conduit (HEAP *et al*. 2014). The dual behavior of stylolites, conduits minerals but also from the networks of voids that are *vs* barriers, depends not solely on the presence of clay created by the pressure-solution process. Despite this, stylolites have almost never been considered as precursors of karst. On the contrary, due to their role in deformation and permeability change (KOEHN *et al.*, 2016), they can become a key point in understanding karst formation. In fact, stylolites, mostly form in a compressional setting probably by migration of large volumes of water that dissolve the carbonate and leave insoluble materials along the stylolite planes. It is possible that this material influences the solution/precipitation process, providing the starting point for dissolution.

2. Materials and methods

The research work was divided into field work and laboratory analyses. Field research was conducted in two different karst areas: in Apulia (South Italy) and in Verona (North Italy), where we have conducted a detailed structural analysis, using the scanline method. The scanline method followed consists of the use of a scale on the floor and the systematic measurement of all structures of interest (faults, joints and stylolites) that intersect the scale. From the field results, it was clear that the dissolution is more abundant along the stylolites (Fig.1) rather than along joins and faults.

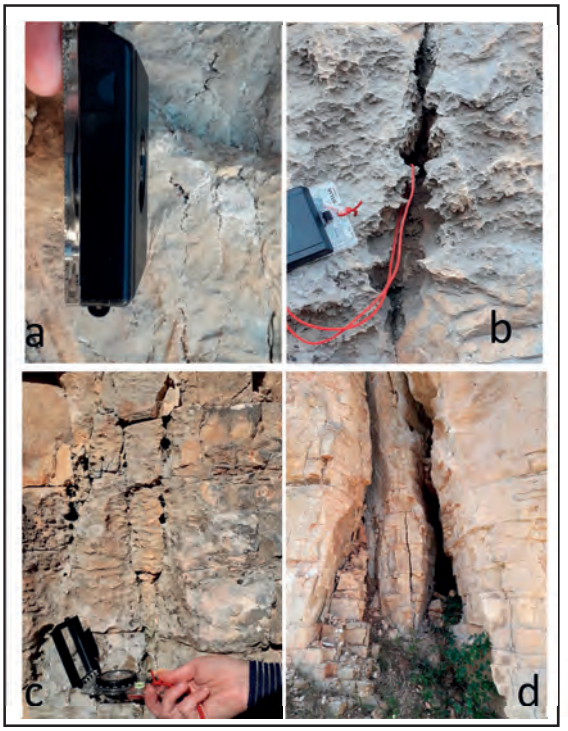

Figure 1: Evolution of stylolites: a) initial stage; b-c) formation of first voids; d) enlargement of stylolite till loss of their original shape making its recognition difficult.

Because of this result, we decided to focus our attention on stylolites and therefore carried out chemical and petrographic analysis on them to characterize the main properties of the insoluble materials and their role in the dissolution process and fluid circulation.

I have performed SEM, FTIR and XRD analysis. XRD and FTIR are the best methods to investigate clay minerals and were carried out, both on the matrix and on insoluble materials.

XRD gives information about mineralogical phases while FTIR helps to characterize which clays are present along stylolitic surfaces.

SEM analysis was performed at very high resolution, helping investigate the size and the distribution of clays and the host rock and moreover of the networks of voids that are important for the fluid circulation.

These analyses were performed on polished thin sections and conducted partially at Mainz and Utrecht University.

The research work initially started in Puglia, but was then extended to Verona as well, to have the possibility of comparing areas with two different geological settings. In both areas, we are relating the direction of the major investigated stylolites with the main karst systems. Despite the stylolites, due to the pressure-solution process and the consequent dissolution, can lose their original shape almost entirely, thus making it difficult to recognize them, through structural techniques, it is still possible to be sure of their presence.

Due to the great variety and complexity of stylolites, we have integrated field work and the laboratory analysis, with the collection of other stylolitic limestones from different geological areas and different countries. This was done because the clays along the stylolithic planes, as well as the variation of the porosity near them, change enormously. Consequently, we have used this approach to increase the certainty of our data and our observations.

3. Results

The scanline method conducted in the field, according to CAINE (1996), allowed both to reconstruct the permeability of the two areas investigated and to evaluate which structures are more subject to the dissolution process or in other words, which act as conductors for fluids.

Against expectations, the data shows that the karst process is more present along the stylolites than joints and faults (Fig. 1). This is consistent with a genesis that involves the dissolution of soluble material and enrichment of insoluble material, finer particle sizes which are more easily eroded, resulting in "expansion" of the vacuum. *In situ*, we have seen, obviously at different sites, various stages related to the process of dissolution along a stylolite, from early stage until the formation of a true cavity. The laboratory analyses, optical, XRD, FTIR and SEM (Fig.2), underline better the reason why this is observed.

In fact, the porosity of the area containing stylolites is always higher than the matrix of the samples.

Despite of the great variety of shape and composition of analyzed stylolites, we have found, from SEM, XRD and FTIR, some common characteristics:

a) the distribution of the voids is highest along the stylolitic surface rather than in the carbonate matrix, which generally has a higher porosity;
b) independently of the matrix composition, Al, Mg, Fe, K are commonly present as insoluble material. It means that a process that forms stylolites accumulates insoluble material therein and evacuates soluble ones;
c) hematite, pyrite and dolomitization processes are also very often found inside of the stylolites, the latter being indicative of a significant increase in porosity following Ca / Mg substitution;
d) kaolinite, montmorillonite and pyrophyllite are the most commonly found minerals.

The nature of stylolite formation (EBNER, 2009a), and the inhomogeneous stress distribution surrounding geometric asperities (ZHOU *et al.,* 2010), results in (1) a complex internal structure that has a higher potential to contain intergranular porosity.

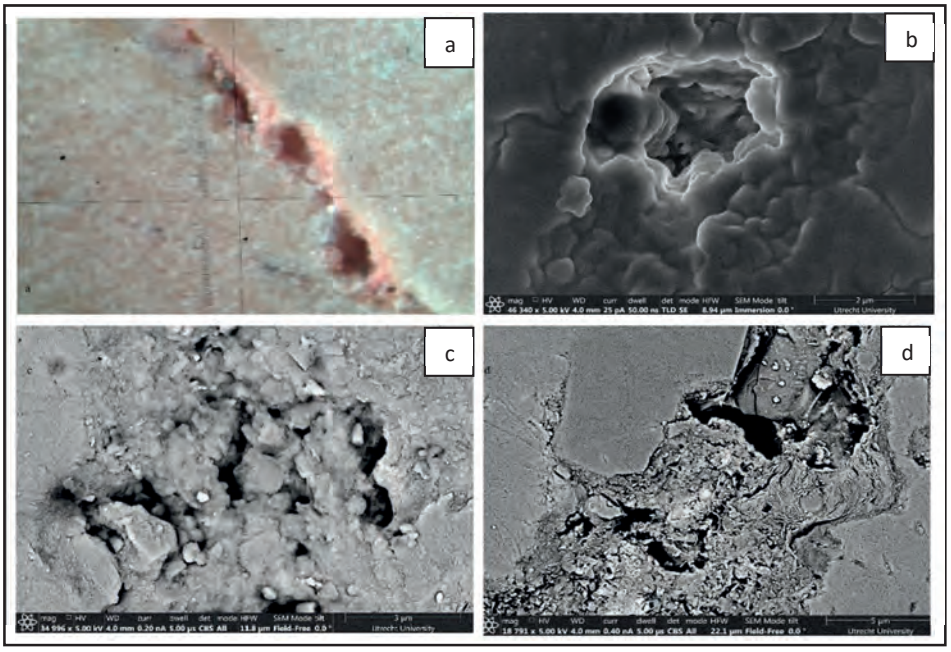

Figure 2: Examples of pores networks in (a) thin section with recrystallized calcite inside of the stylolite and enlargement of voids along stylolitic plane (b-c-d) S.E.M. pictures. (b) Example of voids inside of the stylolite; (c) the pores, sometimes, are even connected between them and (d) they are abundant along the stylolitc surface rather than in the matrix.

4. Discussion

The dissolution process is one of the most studied but at the same time, perhaps one of the most complex phenomena, although it could seem simple.

In the karst field, it is common to consider the extensional structures, as faults and joins for instance, more prone to water circulation and consequently to karst process along them. Conversely, structures as stylolites, formed by a pressure-solution process, then considered contractional features, were never taken in account (MAGNI, 2011,2018)

Despite this, we observed a contrasting picture in both field work and laboratory analyses.

Indeed, in the field, we observed that stylolites are the structures with more, but not exclusively, dissolution along their surface compared with joins and faults.

Even if along the joints the dissolution phenomena has not been observed, we cannot exclude that along them the process does not occur, since they are structures along which water could flow.

The laboratory analyses gave us the possibility to verify whether stylolites can act as conduits or as barriers, and therefore better understand their role as karst precursors.

Specific clays, such as montmorillonite, illite, palygorskite are often present along the stylolite's surface independently from their origin, supporting the idea that there is a fluid circulation along them. Furthermore, we observed the internal reorganization of the crystals along stylolites (Fig.2a), meaning that these crystals are formed directly in the stylolite, most likely due to a circulation of fluids from the outside.

Furthermore, the amount of voids is significantly higher in and around stylolites (Fig.2). Often the pores are mostly present at the contact between insoluble minerals and other grains.

This means that the presence of clay minerals does not prevent the formation of pores and consequently they do not prevent at all the fluid circulation along stylolites.

This could suggest a process for removing the filling material not for dissolving processes but for mechanical processes.

5. Conclusions

Both the field work conducted in Puglia and Verona, and the laboratory analyses, conducted to investigate the distribution of pores and insoluble material along the stylolites, highlight that the role of stylolites in the karst formation must necessarily be re-evaluated, since it is indeed undeniable that they have an important influence in this process (Fig. 3). Evidence such as the formation of new crystals therein and almost rare or completely absent in the matrix, the presence of certain classes of clay minerals, and the distribution of voids, lead us to think that, sometimes, also these structures can act as conductors and therefore could be also be considered a karst precursor. In addition, the direction of the main cavities in the area, matching that of the stylolites, supports this idea.

In summary we can confirm the link between deformation and karst and believe that the phenomenon is not limited by contractional tectonic structures, such as stylolites.

Of course we cannot say that they are always conduits but more reasonably they alternate their behavior from conduits to hydraulic barriers. How and when this can happen is under further investigations.

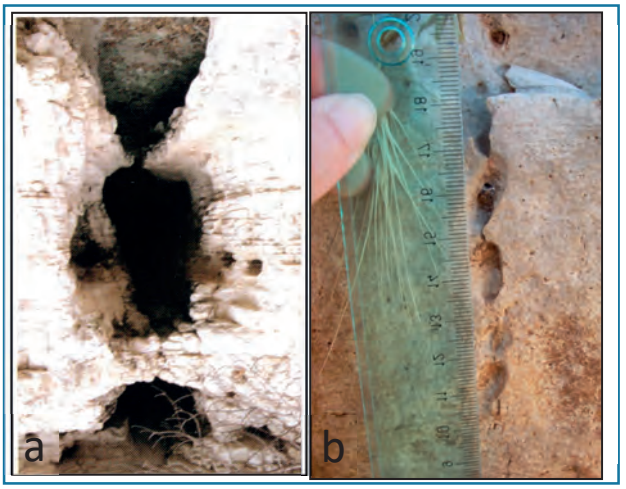

Figure 3: a) tectonic cave (F.Zezza,1999); b) stylolite

Acknowledgments

I want to thank my Supervisors, Juan Diego Martin and Enrique Gomez-Rivas (University of Barcelona). I'm also grateful to Prof. Cees Passchier and Jean Pierre Gratier for the useful and helpful discussions.

References

ALSHARHAN A.; SADD J.L. (2000) Stylolites in Lower Creataceous carbonate reservoirs. U.A.E, Society for Sedimentary Geology Special Publication 69, pp. 185–207.

CAINE J., EVANS J., FORESTER C. (1996) Architecture Fault zone structure and permeability. Geology (11), pp. 1025-1028.

EBNER M., KOEHN D., TOUISSANT R., RENARD F., SCHMITTBUHL J (2009 A) Stress sensitivity of stylolite morphology. Earth and Planetary Science Letters 277(3-4), pp. 94-398.

FINKEL E. A., WILKINSON B. H. (1990) Stylolitization as Source of Cement in Mississippian Salem Limestone, West-Central Indiana. AAPG Bulletin-American Association of Petroleum Geologists, 74(2), pp. 174-186.

HEAP M. J., BAUD P., REUSCHLE' T., MEREDITH P. G. (2014) Stylolites in limestones: Barriers to fluid flow? Geology, 42(1), pp. 51-54.

KOEHN D., ROOD M.P., BEAUDOIN N., CHUNG P., BONS P.D., GOMEZ RIVASE. (2016) A new stylolite classification scheme to estimate compaction and local permeability variations. Sedimentary Geology (346), pp. 60-71.

MAGNI S. (2011) Karst phenomena: new opportunity for development. Proceedings of National Congress of Speleology. Trieste pp. 418-426

MAGNI S. (2011) Karst phenomena: new opportunity for development. Proceedings of National Congress of Speleology. Trieste pp. 418-426

MAGNI S. (2018) Dissolution process: when does the process start? Eurokarst 2018 Besancon: Advances in hydrogeology of Karst and carbonate reservoirs 9Advances in Karst Sciences), pp. 23-29

NELSON R.A. (1981) Significance of fracture sets associated with stylolite zones: Am. Assoc. Petroleum Geologists Bull., 65, pp. 2417–2425.

PARK W. C., SCHOT E. H. (1968) Stylolites: their nature and origin. Journal of sedimentary Petrology 38(1), pp. 175-191.

ROLLAND A., TOUISSANT R., BAUD P., CONIL., LANDREIN P. (2014) Morphological analysis of stylolites for paleostress estimation in limestones, International Journal of Rock Mechanics and Mining Sciences, 67, pp. 212-225.

STOCKDALE P. B. (1943) Stylolites: primary or secondary? J. Sediment. Petrol., 13, pp 3–12.

TOUISSANT R., AHARANOV E., KOEHN D; GRATIER J.P., Ebner M., BONS P. RENARD F., ROLLAND A. (2018) Stylolites: A review Journal of Structural Geology, Elsevier, 114, pp. 163 - 195.

ZHOU X., AYDIN A. (2010) Mechanism of pressure solution seam growth and evolution: Journal of Geophysical Research, 115, p. 1029.

ZEZZA F. (1999) Il carsismo in Puglia. Adda Editore, p.253.

Vertical repetition of structures and cave patterns in the National Park of Ordesa and Monte Perdido (N of Spain) and its relationships with the functioning of recharge in the karstic system

Antonio GONZÁLEZ-RAMÓN[(1)], Jorge JÓDAR[(2)], José María SAMSÓ[(3)], Sergio MARTOS ROSILLO[(1)], Javier HEREDIA[(4)], Ane ZABALETA[(5)], Iñaki ANTIGÜEDAD[(5)], Emilio CUSTODIO[(6,7)] & Luis Javier LAMBÁN[(2)]

(1) Geological and Mining Institute of Spain, Urb. Alcázar del Genil, 4 Edf. Zulema bajo, 18006 Granada, Spain, antonio.gonzalez@igme.es (corresponding author), s.martos@igme.es
(2) Geological and Mining Institute of Spain, C/ Manuel Lasala, 44 - 9º B. 50006 Zaragoza, Spain, j.jodar@igme.es, javier.lamban@igme.es
(3) Consulting Geologist, C/ Mayor 30, 1°. 22700 Jaca, Huésca, Spain. josemsamso@gmail.com
(4) Geological and Mining Institute of Spain, C/ Rios Rosas, 23. 28003. Madrid, Spain. j.heredia@igme.es
(5) Hydro-Environmental Processes Group, Science and Technology Faculty, University of the Basque Country UPV/EHU, Sarriena z/g, 48940 Leioa, Spain. ane.zabaleta@ehu.eus, inaki.antiguedad@ehu.eus
(6) Groundwater Hydrology Group, Department of Civil and Environmental Engineering, Technical University of Catalonia. C/ Jordi Girona, 1 - 3 UPC Campus Nord, Edificio D2. 08034 Barcelona, Spain. emilio.custodio@upc.edu
(7) Spanish Royal Academy of Sciences.

Abstract

The geological disposition and the tectonics of Tertiary carbonates observed in the head of the Arazas river (PNOMP), with overturned folds separated by overthrusts staked in various levels, is reflected in the endokarstic development, with a vertical repetition of cave patterns. The karstic networks are organized in branchwork caves that channel infiltrating water to the collectors, with a water table cave pattern that ends in terminal sumps. Successive collectors have been developed in steps related to synclinal structures, with temporally perched saturated zones caused by the presence of a low permeability base composed of the Marboré sandstones. Tracer tests carried out in the area have shown that all these perched saturated zones are hydrogeologically inter-connected. The monitoring of the temporal evolution of the discharge, temperature and electric conductivity of groundwater allowed studying the recharge and the hydrogeological system dynamics. The preferential snowmelt diffuse recharge in opposition to the fast recharge related with summer storms, is invoked to explain the development of water table caves patterns in epiphreatic galleries, in contrast to looping caves patterns, as would be expected given the characteristics of the aquifer.

1. Introduction

In recent decades, research has shown that the distribution and organization of the explored conduits in a karstic system fall in just a few patterns. They are related to the water-table position and its temporal evolution, the type of aquifer recharge, the density of fractures, the geological structure and, to a lesser extent, with the porosity of the rock (PALMER, 2007; AUDRA & PALMER, 2011).

AUDRA & PALMER (2011; 2015) differentiated two types of epigenic caves in relation to their gallery patterns: looping caves and water-table caves. Shafts and canyons develop in the vadose zone (VZ), but in the deepest zone, the looping caves are characterized by both a permanently saturated phreatic zone and an epiphreatic zone where large water-table variations may occur. The water-table caves (WTC) are associated with a diffuse recharge process. These caves normally present a well-developed epikarst zone associated to an often minor permeability layer over the permeable rocks. In consequence, the WTCs present a complex VZ, with caves of a dominant vertical development that change their inclination to horizontal transects in the deepest zones. They serve as water collectors that guide the drained groundwater to the discharging springs. These springs are permanent with a low variability discharge.

The role of snow accumulation and melting dynamics in the recharge of high mountain karstic aquifers and its relation to the cavern patterns is poorly understood. This is because most of the investigations have been carried out in caves where the recharge areas are below an elevation of 2000 m a.s.l. (HÄUSELMANN, 2019). Most of the caves studied in alpine karst usually present cavern patterns characterized

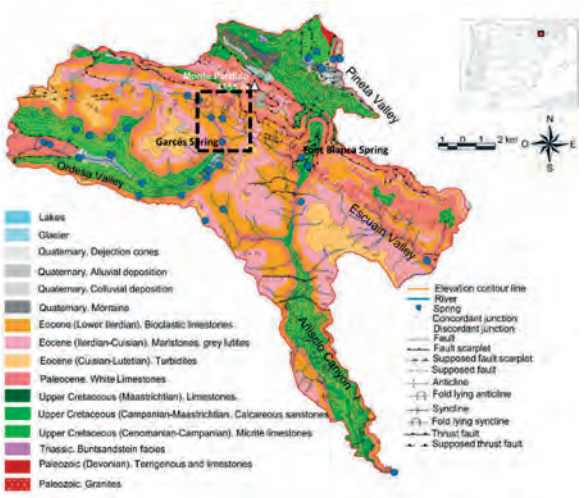

Figure 1: Location, geological map of the PNOMP (modified from LAMBÁN et al., 2015). The black dashed square shows the studied area location.

by a polygenic network of branchwork type in the VZ, and looping caves when the cave reaches the epiphreatic zone.
In the "Parque Nacional de Ordesa y Monte Perdido" (PNOMP; NE Spain) there are a number of karstic systems draining the same hydrogeological basin, where the recharge zone is between 1855 and 3170 m a.s.l. and is normally covered by snow during approximately 8 months of the year (LAMBÁN et al., 2014; JÓDAR et al., 2016). This is a perfect natural laboratory to explore the still unknown relationship between the aquifer recharge processes in alpine environments and the geomorphological pattern of the karstic conduits draining the aquifer, which is the main objective of this study.

The PNOMP is located in the central southern sector of the Pyrenees (Fig. 1). With a WNW-ESE orientation, this mountain range is the highest in the Iberian Peninsula.
The geological structure of the PNOMP is formed by an imbricated group of overthrust sheets and associated folds of carbonate materials. The ages of the materials range from the Upper Cretaceous to the Eocene (Fig. 1).

All the units of the stratigraphic sequence are structured in a set of overturned folds, reverse fault and overthrusts, so that the same structure is repeated several times vertically. Six folded structures can be identified where the karstified carbonates of the Paleocene-Eocene are located. The folds have a vertical N flank that is normally inverted, whereas the S flank gently dips to the N. This disposition allows groundwater storage in the syncline structures due to the rupture of permeability caused by the Sandstones of the Upper Cretaceous (Marboré sandstones).

2. Materials and methods

During this study, a task of information collection has been carried out to integrate all the available information generated by the different speleological groups through the exploration of the different karst systems identified in the study zone. The analysis of all this information yielded a thorough description of six cave systems, namely Marboré, Roya-Cigalois, Fraile-La Tartracina, Sima S-60, Garcés cave and Font Blanca cave (Fig. 2).

On August 5, 2019, members of the Speleological group Otxola and the Geological and Mining Institute of Spain (IGME) conducted a multi-tracer test in the study area. Two fluorometers were installed in sump-1 of the Garcés cave, whose overflow feeds the Garcés Spring (Figs. 2 and 3). A third fluorometer was also installed in the Font Blanca spring (Fig. 2).

To measure the water level (h), temperature (T), and electric conductivity (EC) variations in groundwater along the Garcés karst system, two sensors were installed in sump-1 and sump-3, respectivel.

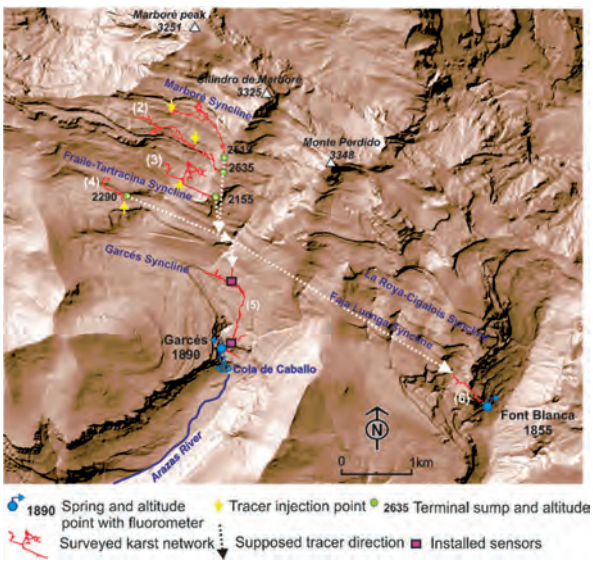

Figure 2: Karstic systems studied. (1) Marboré, (2) La Roya-Cigalois, (3) El Fraile-La Tartracina, (4) S-60, (5) Garcés and (6) Font Blanca

3. Results and discussions

The data recorded by the sensor installed in the Garcés cave allowed observing how recharge controlled the Garcés spring discharge during the period 2018-2019. The water level variations in sump-1 are almost homothetic to those of sump-3 (Fig. 3). This indicates that no significant groundwater contributions fed the system between both control points. From the temporal variation of the hydrometeorological variables five different aquifer recharge stages (Fig. 3) can be inferred when describing the hydrogeological system dynamics during a whole annual cycle:

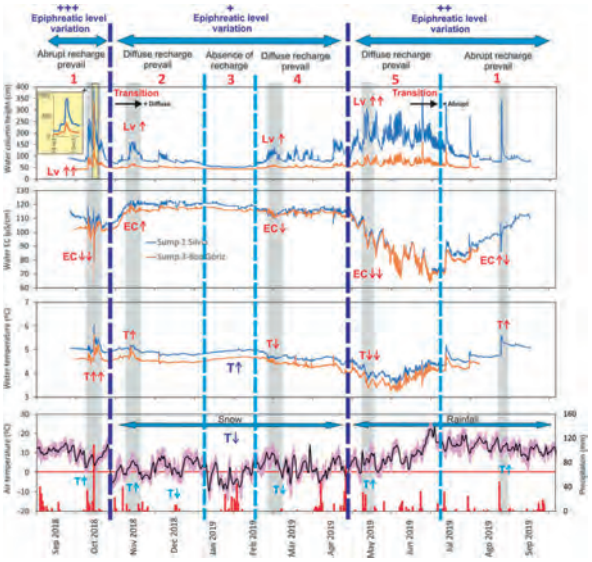

Figure 3: Variation of groundwater level, EC and T observed in the Garcés Cave (Sep-2018 to Sep-2019). For each variable, the upper and lower lines correspond to the time series measured in sump-1 and sump-3, respectively. The lower panel shows the evolution of the daily precipitation and mean atmospheric temperature (meteorological station of Góriz). The shaded strip corresponds to the maximum and minimum daily temperature variations. The details of the different recharge stages (1 to 5) indicated in the figure are explained thoroughly in the text. Gray bars show the different relationships between groundwater level (Lv), EC and T.

Stage 1: The rainfall events generate sudden variations of h, EC and T. Stage 2: Precipitation is mainly as snow. Only a few fast recharge events occur. Stage 3: There is not any fast recharge event entering the system, and the contribution of the in-transit recharge is at most exceedingly small. Stage 4: Precipitation is still solid. Nevertheless, the aquifer recharge process starts, slowly at the beginning and showing a temporal pattern like that of atmospheric temperature. Stage 5: At the beginning, the snowmelt infiltrates through the most conductive karst features. As the contribution of the fast recharge increases in the total system, EC and T decrease as expected. However, once the snowpack covering the study zone disappears, the recharge decreases. The relationship between the climatic seasonal variations and the different types of recharge is summarized in Fig. 4.

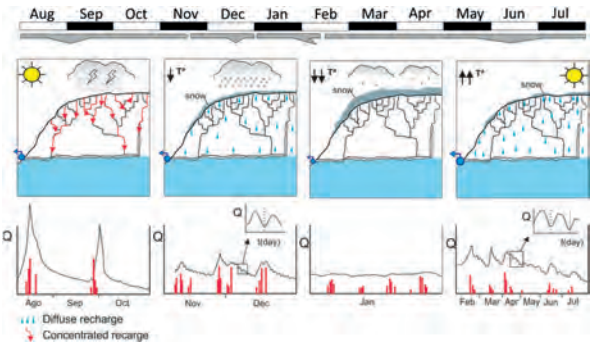

Figure. 4: Schematic conceptual model of recharge observed during the 2018/2019 year in the Garcés karstic system.

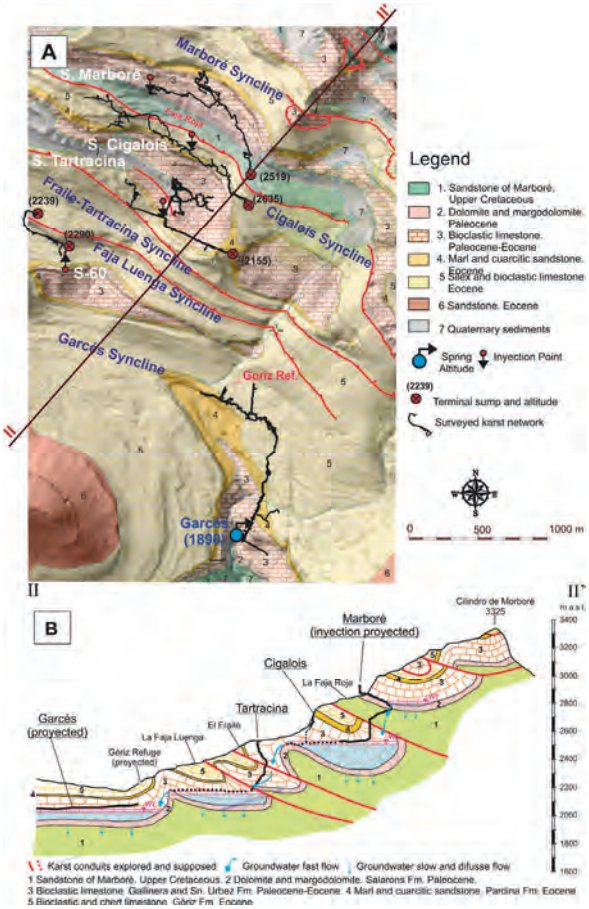

Figure 5: A) Hydrogeological map of the study area. The main mapped cavities and their altitudes are included, as well as the tracer injection points and the main sumps. B) Cross- section with the interpretation of groundwater flow in the system of caves and groundwater storage zones in the synclines. The emplacement of the cross-section is in (A).

The tracer tests for this study were conducted in summer to ensure the system was at the lowest discharge regime. Four tracers (uranine, eosine, amino-G and naphtionate) were injected simultaneously. All of them were detected at the control point of the Garcés system. Thirteen days after injection of the tracers, a rainfall event occurred in the study zone and a new tracer breakthrough was detected in the Garcés cave. Surprisingly, a synchronous tracer breakthrough was detected in the Font Blanca spring (Fig. 2).

The presence of minor permeability sandstone of the Marboré formation at the basis of the Paleocene-Eocene materials, and also of stacked thrust folds separated by both reverse and overthrust faults (Fig. 5), determine the caverning and hence the hydrogeological functioning of the system.

The infiltrated water in the system accumulates in the synclines, which are slowly drained downgradient and flow gently through the epiphreatic zone, enlarging the conduits with a water-table cave pattern. Groundwater flow takes place through the different syncline structures downgradient in line. A given syncline receives drainage

from the immediately previous one at higher elevation and drains immediately to the downflow one, and so on until Faja Luenga syncline, where the groundwater flow seems to divide. One-part flows normally towards the Garcés syncline before reaching the Garcés cave (Fig. 2) and another part moves along the axis of the Faja Luenga syncline towards the Font Blanca spring.

5. Conclusion

The recharge of karst aquifers located in high mountain zones may be controlled by the presence and dynamics of the snowpack during the accretion and snowmelt seasons. Snowmelt produces a steady low-rate infiltration and recharge until the snowpack completely melts. The low recharge rates follow large groundwater level variations, thus favoring the generation of conduits with a water-table cave pattern type.

In the PNOMP, the karstic conduits are staggered with a repetitive pattern, reflecting the complex geological structure of the existing vertically stacked overthrust sheets. A conduit feature connects two consecutive perched saturated zones generated in the inner part of the corresponding syncline structures. The conduit pattern set includes conduits of the branchwork pattern type in the vadose zone and a main water-table cave pattern conduit in epiphreatic zone.

The tracer tests confirmed the hydrogeological connection between all these temporal perched saturated zones, with a short transit time even during the hydrologic low-flow period.

Acknowledgments

This research was undertaken in the framework of the PIRAGUA project. The project EFA210/16 PIRAGUA is co-founded by the European Regional Development Fund (ERDF) through the Interreg V Spain-France-Andorre Programme (POCTEFA 2014-2020) of the European Union. The authors would like to thank the Ordesa and Monte Perdido National Park Direction (Gobierno de Aragón), especially Elena Villagrasa from DGA, Fernando Carmena and Ignacio Gómez from SARGA, the Góriz Mountain Hut Wardens, Marta Quintana, and Sanda Iepure. We are very grateful to G.P. OTXOLA E.T. Speleological Group (Grupo espeleología. Otxola. Espeleologi taldea) for their help in injecting the fluorescent dye tracers during the tracer test campaigns., We also acknowledge both the OTXOLA and SCC (Spéléo Club du Comminges) for providing detailed information of the different karst systems draining the study zone. Meteorological data have been provided by the Spanish Meteorological Agency (AEMET).

References

AUDRA, P., PALMER, A. N., (2011). The pattern of caves: controls of epigenic speleogenesis. Géomorphologie: relief, processus, environnement. 17(4), 359-378.

AUDRA, P., PALMER, A.N., (2015). Research frontiers in speleogenesis. Dominant processes, hydrogeological conditions and resulting cave patterns. Acta Carsologica. 44(3), 315-348.

HÄUSELMANN, P., (2019). Solution caves in regions of high-relief. In: Encyclopedia of Caves (third edition), pp. 943-954. Academic Press.

JÓDAR, J., CUSTODIO, E., LAMBÁN, L. J., MARTOS-ROSILLO, S., HERRERA-LAMELI, C., SAPRIZA-AZURI, G., (2016). Vertical variation in the amplitude of the seasonal isotopic content of rainfall as a tool to jointly estimate the groundwater recharge zone and transit times in the Ordesa and Monte Perdido National Park aquifer system, north-eastern Spain. Science of the total environment. 573, 505-517.

LAMBÁN L.J., JÓDAR, J., CUSTODIO, E., (2014). Caracterización hidrogeoquímica e isotópica del agua subterránea en macizos carbonatados de alta montaña: el Parque Nacional de Ordesa y Monte Perdido (Pirineo Central, España). In: V Congreso Colombiano de Hidrogeología. Medellín, Colombia, pp. 601-608.

PALMER A.N., (2007). Cave Geology. Ed. Cave books, 454 p.

Morphogenesis of the karst system of the Crnopac massif (Velebit, Croatia, Dinaric karst)

Neven BOČIĆ(1), Valerija BUTORAC(2), Teo BARIŠIĆ(3), Mladen KUHTA(4), Darko BAKŠIĆ(5) & Tomislav KUREČIĆ(6)

(1) Faculty of Science, University of Zagreb, Marulićev trg 19, Zagreb, Croatia, nbocic@geog.pmf.hr (corresponding author)
(2) Faculty of Science, University of Zagreb, Marulićev trg 19, Zagreb, Croatia, vbutorac@geog.pmf.hr
(3) Speleological Section HPK Sv. Mihovil, Bana Josipa Jelačića 28, Šibenik, Croatia, teo.barisic@gmail.com
(4) Croatian Geological Survey, Sachsova 2, Zagreb, Croatia, mkuhta@hgi-cgs.hr
(5) Faculty of Forestry and Wood Technology, University of Zagreb, Svetošimunska cesta 23, Zagreb, Croatia, dbaksic@sumfak.hr
(6) Croatian Geological Survey, Sachsova 2, Zagreb, Croatia, tkurecic@hgi-cgs.hr

Abstract

The Crnopac massif is the southernmost part of the Velebit Mountain in Croatia. The aim of this work is to determine the forms, conditions and processes of morphogenesis of this karst system. The emphasis is on the surface and underground geomorphological features. The mapped karst forms of Crnopac include dolines, uvalas, karst towers, dry and blind valleys, and denuded caves. There are more than 300 caves in this area. The longest, Cave System Crnopac (> 55 km), is also the longest cave in the Dinaric karst. The development of the karst system is related to the relative tectonic uplift of the Crnopac massif. This led to a lowering of the level of allogeneic water input into the system and consequently to the formation of lower active conduits. In parallel, denudation of the surface was also active, lowering the level of the surface. Autogenous seepage of meteoric water from the surface led to the formation of vertical channels that intersect inactive channels. Geomorphological indicators suggest that this process did not take place with uniform dynamics.

1. Introduction

The Crnopac massif is a highly karstified area in the southernmost part of the Velebit Mountain in Croatia within the Dinaric karst (Fig. 1). Among the many surface and underground karst forms, the long caves stand out, the longest of which is Cave System Crnopac (hereafter CSC), the longest cave in the Dinaric karst. This area has a long tradition and high intensity of speleological research, especially two decades ago (see more in BARIŠIĆ & BARIŠIĆ, 2022). The aim of this work is to determine the basic forms, conditions and processes of morphogenesis of this complex karst system. In addition to the analysis of geological and climatic conditions, the focus is on the surface and underground geomorphological features. DEM morphometry, geomorphological mapping and speleological data were used for geomorphological analysis. Among the previous geospeleological and karst geomorphological studies, we can single out the following: MALEZ (1965), KUHTA & STROJ (2005), BOČIĆ (2009), MARKOVIĆ et *al*. (2016), TALAJA & KUREČIĆ (2017), CZUPPON et *al*. (2018) and KUREČIĆ et *al*. (2021).

There are three physiographic units. The northernmost is the Gračac karst polje with a ponor zone at the south rim at an elevation of around 550 m a.s.l. The central unit is the Crnopac massif, part of the main ridge of the Velebit Mt. The highest point is at an elevation of 1404 m a.s.l. but the largest and at the same time the most karstified part of Crnopac is at elevations ranging between 900 and 1200 m a.s.l. The southernmost unit is the karst plateau between elevations of 200 to 400 m a.s.l. Sinking water from the Gračac polje flows underground through the Crnopac massif towards the south, to the valleys of the Krupa and Zrmanja river canyons (KUHTA & STROJ, 2005). These karst canyons represent a regional erosion base of the Crnopac area. The elevation of the riverbeds starts at 150 m a.s.l. and then slopes towards the west, i.e., towards the Adriatic Sea. Most of this area has a climate type Cfb (temperate humid with hot summer), but in the south it transitions into climate type Cfa (temperate humid with hot summer) (FILIPČIĆ, 1998).

Geological properties (Figs. 1B and 5) are presented based on IVANOVIĆ et *al.* (1973) and CGS (2009). The structure of the Crnopac massif is dominated by Jurassic and Cretaceous carbonate rocks which are separated by a paleo-relief (unconformable) boundary from overlying Paleogene carbonate (mostly limestone) breccias. These breccias, so-called Jelar deposits (or Velebit breccias), are massive and unbedded and consist of fragments of older carbonate rocks (BAHUN, 1974). They are intensively karstified. To the north is the Gračac karst polje whose bedrock consists of clastic and carbonate rocks (mainly dolomite). Surface water from the wider area of eastern Lika flows through the polje. Along its southern edge, a zone of allogeneic inputs into the karst system of Crnopac has been developed. The low karst plateau, which consists mainly of limestones of the Cretaceous period, lies south of Crnopac.

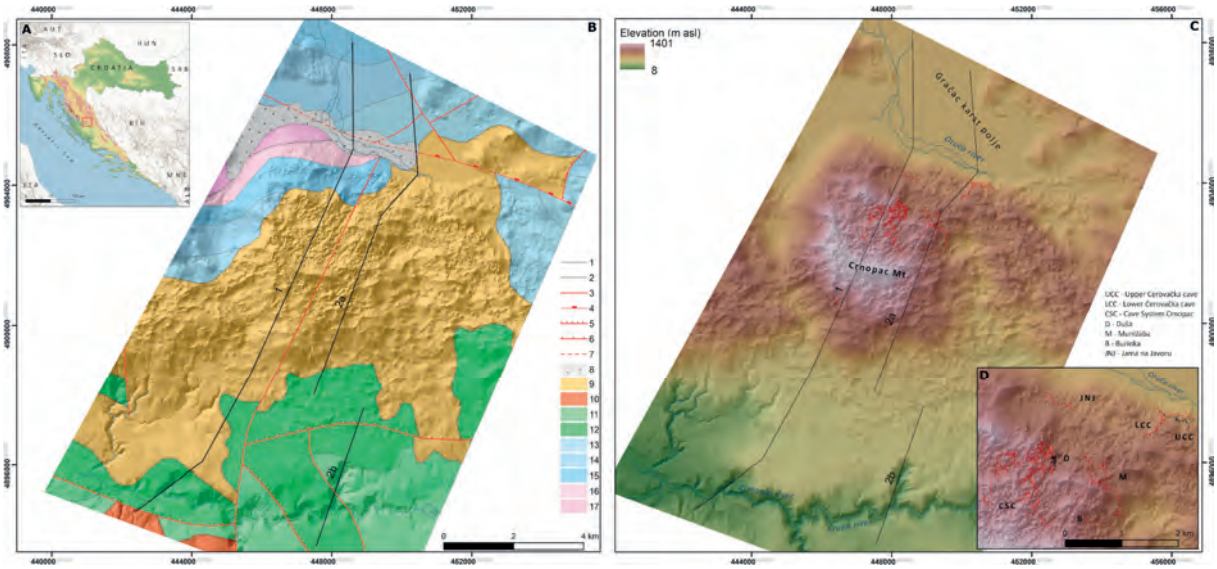

Figure 1: A – Position of Crnopac massif, B - Geological map of the research area (according to CGS 2009, legend: 1 – normal contact, 2 – erosional and/or tectonic-erosional contact, 3 – fault, 4 – relatively lowered block, 5 – reverse fault, 6 – thrust contact, 7 – fault (covered), 8 – alluvial deposits aQ_2, 9 – limestone breccia Pg/Ng, 10 – promina deposits E, Ol, 11 – rudist limestone K_2^{1-6}, 12 – limestone and dolomites K_1, 13 – limestone and dolomites J_3, 14 – thick layered limestone and dolomites J_2, 15 – limestone and dolomites J_1, 16 – dolomites T_3, 17 – carbonate deposits T_2), C- Relief map of research area with cave channels position (in red), D – detail view of the central part of Crnopac area with caves. The straight black lines on map B and C (1, 2a and 2b) indicate the profile lines in Figure 5.

2. Karst geomorphological properties

Surface karst landforms: within the wider research area, three physionomic units stand out (Fig. 2). In the north there is the karst polje (Gračac polje). It is a structural polje representing a hydrogeological barrier with surface drainage and a ponor zone along the southern edge. South of Crnopac there is a large karst plateau (northern fragment of the large North Dalmatian plateau). It is cut by the canyon valley of the Zrmanja River and its tributaries (Krupa and Krnjeza), representing the erosion base of the entire system. Besides less pronounced dolines and shallow uvalas, dry karst valleys are also noticeable in this area.

The Crnopac massif itself is the most karstified part of the researched area. Numerous dolines with narrow rock ridges and karst towers in between have formed here. The doline density reaches values of 100 dol/km^2. Dolines often reach a diameter of 80 meters and more, and their depth can reach several tens of meters. They often have steep, rocky sides. Several deeper karst uvalas have formed in the eastern part of the massif. On the steep northern slopes of Crnopac, above the edge of Gračac polje, several forms resembling karstified blind valleys can be identified, with elevations ranging from 700 to 850 m. Some traces in the relief (e.g. a series of uvalas and karstified valleys) indicate the possibility of surface runoff of water from the Gračac polje zone in the south in the early phase of the formation of Crnopac. Traces of denuded caves were observed in the central part of the Crnopac high plateau.

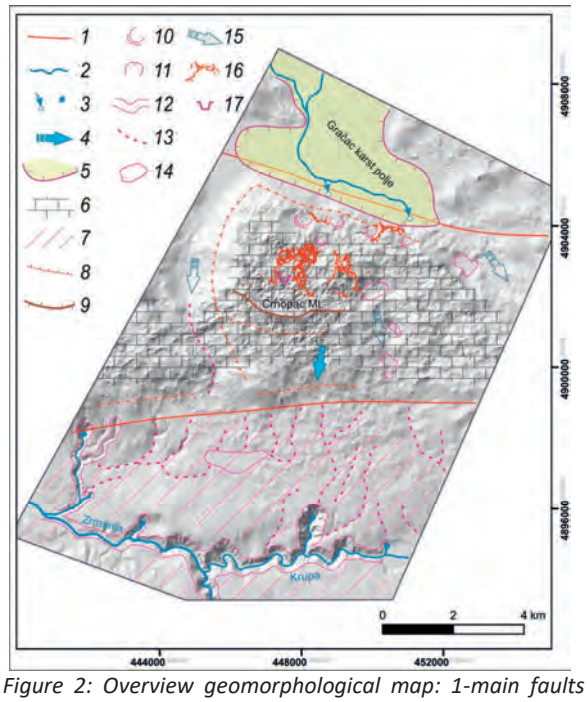

Figure 2: Overview geomorphological map: 1-main faults and lineaments, 2-streams, 3-ponors, springs, 4-general direction of underground runoff, 5-karst polje, 6-highly karstified area, 7-karst plateau, 8-steep slopes, 9-main ridge, 10-assumed blind valleys, 11-pocket valleys, 12-canyons, 13-dry valleys, 14-uvalas, 15-presumed corridors of former surface runoff, 16-cave channels, 17-location of denudated cave.

Caves: the karst of Crnopac is still best recognized by its large caves which number over 300 in this area. The longest is CSC (> 55 km), making it also the longest cave in the Dinaric karst. There are several other large caves whose morphometric characteristics are listed in the table in Figure 3. One of the main characteristics of the larger caves in this area is their morphological complexity. They consist mainly of leveled horizontal passages intersected by vertical or steep vadose channels. The passages of all major caves are characterized by a grouping into several height classes (levels, Fig. 4). The mode of this distribution is at an elevation of 550-650 m (0-100 m above the level of the ponor zone), which includes the lower level of CSC, the main part of Munižaba and most of the passages of Gornja and Donja Cerovačka caves. The next is in the range of 730-830 m (180-280 m above the level of the ponor zone), which includes the upper level of CSC. Other levels are located at elevation of about 670-690 m (120-150 m above the ponor zone; parts of CSC, Gornja Cerovačka and Munižaba) and 430-450 (100-120 m below the ponor zone), which include the passages of the lowest CSC level.

PARAMETER		*CAVES*						
		Cave System Crnopac (CSC)	Munižaba (M)	Upper Cerovačka cave (UCC)	Lower Cerovačka Cave (LCC)	Duša (D)	Jama na Javoru (JNJ)	Burinka (B)
Plan length (m)	Lp	41,996	8,081	3,491	3,704	1,784	1,479	497
Real length (m)	Lr	55,520	9,911	4,035	4,207	2,386	1,653	914
Vertical range (m)	Rv	828	510	224.6	97	318	147	290
Depth (Negative drop) (m)	Dn	828	510	191.4	68.4	318	103	290
Volume (m^3)	V	2,509,556	2,305,038	*No data*	169,691	217,785	350,592	631,227
Extension (m)	Ex	1,593.4	1,366.36	683.82	904.87	363.73	683.60	438.97
Area (minimum rectangle - km^2)	A	2.09	1.08	0.21	0.49	0.06	0.22	0.07
Passage Density (m/km^2)	Den	20,193.8	7,482.4	16,623.8	7,559.2	29,733.3	6,722.7	7,100
Verticality index	Vi	0.01	0.05	0.06	0.02	0.13	0.09	0.32
Horizontality index	Hi	0.76	0.82	0.87	0.88	0.75	0.89	0.54
Linearity index	Li	0.02	0.13	0.16	0.21	0.07	0.40	0.36
Horizontal complexity index	Hci	26.36	5.91	5.11	4.09	4.90	2.16	1.13

Figure 3: Morphometric parameters of the largest caves of the Crnopac area (methodology according PICCINI (2011), prepared on the basis of cave survey data provided by speleological organizations conducting exploration in this area).

3. Morphogenesis of the Crnopac karst system

The most important factor in the speleogenesis of Crnopac is the allogenic input of water into the underground in the ponor zone of Gračac polje. Moreover, the development of the karst system is related to the relative tectonic uplift of the Crnopac massif. This led to a lowering of the level of allogenic water input into the system and consequently to the creation of lower active conduits (Fig. 5). Thus, a pronounced level of cave conduits was created, approximately every 100-200 m in height. We can assume that the main condition for the development of such levels were phases of relative tectonic stagnation. In addition, the amount of sinking water probably had an important influence, which could be controlled by climate changes during the Pleistocene. Lithology may also have played an important role. For example, the highest level of CSC was formed in the zone of paleo-relief contact of Jurassic carbonates and overlying carbonate breccias, but other cave levels are not related to any lithologic contact. Autogenous seepage of meteoric water from the surface has resulted in the formation of vertical channels that intersect inactive conduits. In massive carbonate breccias, these channels are predominantly vertical. In the deeper parts of the CSC, such passages have often developed under the influence of bedding planes within the Jurassic carbonates.

In parallel, denudation of the surface was also active and lowered the surface level. This led to the destruction of the oldest cave levels.

Geomorphological indicators suggest that all these processes did not take place with uniform dynamics. Probably, there were phases of different tectonic activity as well as phases of different intensity of exogenous processes in accordance with climatic fluctuations.

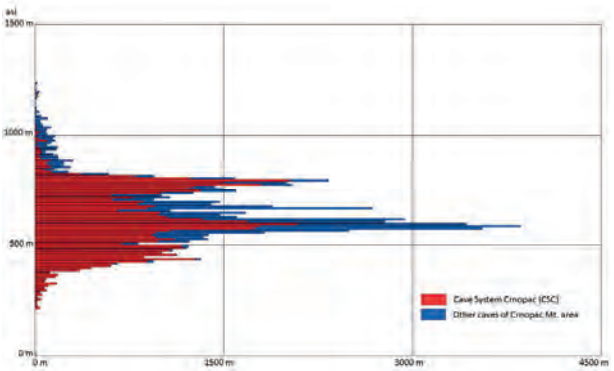

Figure 4: Vertical distribution of cave channels in the area of the Crnopac massif.

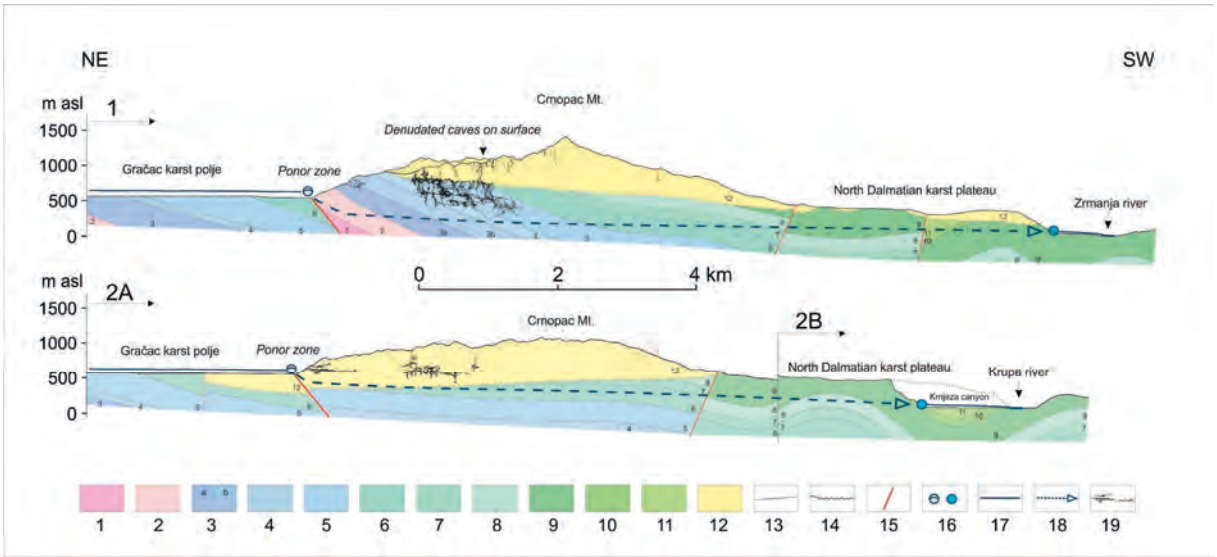

Figure 5: Overview geological profiles of the Crnopac massif. For the position of the profile lines see Figure 1. Profiles are made based on the data presented on the Basic Geological Map 1: 100000, Obrovac sheet (Ivanović et al. 1973), modified. Legend : 1 – clastic deposits $T_3^{1,2}$; 2 – dolomites and limestone $T_3^{2,3}$; 3 – limestone and dolomites J_1^{1-4}; 3a – dolomites and limestone J_1^{1+2}; 3b – lithiotis limestone J_1^3; 4 – spotted limestone and dolomites J_1^{1-4}; 5 – limestone with lenses of dolomites J_2; 6 – limestone and breccia $J_3^{1,2}$; 7 – limestone and dolomites $J_3^{2,3}$; 8 – limestone and breccia $J_3^{2,3}$; 9 – breccia and limestone K_1^2; 10 – breccia and limestone K_2^1; 11 – limestone $K_2^{1,2}$; 12 – limestone breccia Pg, Ng; 13 – normal depositional contact; 14 – erosional (paleo-relief) contact; 15 – fault; 16 – ponor, spring; 17 – surface water stream; 18 – assumed underground flow; 19 – cave channels. Note: geological units in Figure 1 and Figure 5 differ slightly because they are based on different sources, i.e. maps of different scales.

References

BARIŠIĆ, T., BARIŠIĆ, A. (2022) Crnopac Cave System (Jamski sustav Crnopac). 18th Int. Congress of Speleology – SYMPOSIUM 02 – Caving and explorations.

BAHUN S. (1974) Tectonogenesis of Mt. Velebit and the origin of the Jelar deposits [in Croatian]. Geološki vjesnik 27, 35–51.

BOČIĆ N. (2009) Cerovačke caves and other karst phenomena of the Crnopac massif. International interdisciplinary scientific conference Sustainability of Karst Environment Dinaric Karst and other Karst Regions - Excursion guidebook, Gospić, Center for Karst, 12-18.

CGS (2009) Geological Map of the Republic of Croatia, M 1: 300.000. Croatian Geological Survey, Zagreb.

CZUPPON G., BOČIĆ N., BUZJAK N., ÓVÁRI M., MOLNÁR, M. (2018) Monitoring in the Barać and Lower Cerovačka Caves (Croatia) as a Basis for the Characterization of the Climatological and Hydrological Processes that Control Speleothem Formation. Quat. Int. 494, 52–65.

FILIPČIĆ, A. (1998). Klimatska regionalizacija Hrvatske po W. Köppenu za standardno razdoblje 1961.-1990. u odnosu na razdoblje 1931–1960. Acta Geographica Croatica 34, 1–15.

IVANOVIĆ A., SAKAČ K., MARKOVIĆ S., SOKAČ B., ŠUŠNJAR M., NIKLER, L. (1973) Basic Geological Map in scale of 1:100,000 - Sheet Obrovac L33-140. Institut za geološka istraživanja, Zagreb, Savezni geološki institut, Beograd.

KUHTA M., STROJ A. (2005) The Speleogenesis of the Caves in Crnopac Mt. Area. 14th International Congress of Speleology. Proceedings, Athens, Greece, 46–48.

KUREČIĆ T., BOČIĆ N., WACHA L., BAKRAČ K., GRIZELJ A., TRESIĆ PAVIČIĆ D., LÜTHGENS C., SIRONIĆ A., RADOVIĆ S., REDOVNIKOVIĆ L., FIEBIG M. (2021) Changes in Cave Sedimentation Mechanisms During the Late Quaternary: An Example from the Lower Cerovačka Cave, Croatia. Front. Earth Sci. 9:672229. doi: 10.3389/feart.2021.672229

MALEZ M. (1965) Cerovačke pećine [Cerovačke Caves - in Croatian]. Zagreb: Izdanja Speleološkog društva Hrvatske, 1.

MARKOVIĆ J., BOČIĆ N., PAHERNIK M. (2016) Spatial Distribution and Density of Dolines in the Southeastern Velebit Area. Geoadria. 20/1, 1–28.

PICCINI L. (2011) Recent developments on morphometric analysis of karst caves, Acta Carsologica 40 (1), 43-52.

TALAJA M., KUREČIĆ T. (2017). Geological and Geomorphological Observations in the Muda Labudova Pit [in Croatian]. Speleolog. 65 (1), 32–41.

Speleogenesis of juvenile serial sinkhole-resurgence systems in the karsts of the Amazonian side of the Andes Mountains, Peru

Jean-Yves BIGOT[(1)], Jean Loup GUYOT[(2)] & Philippe AUDRA[(3)]

(1) Association française de karstologie (AFK), jeanbigot536@gmail.com (corresponding author)
(2) Groupe Spéléologique Bagnols-Marcoule (GSBM), Bagnols-sur-Cèze, jean-loup.guyot@ird.fr
(3) Polytech'Lab - UPR 7498, Université Côte d'Azur, France, Philippe.AUDRA@univ-cotedazur.fr

Abstract

Serial sinkhole-resurgence systems, crossed by the river, are frequent in Northern Peru. We present here two examples from the Amazonas region, located in the karsts of Cerro Shipago (Utcubamba Prov.) and Soloco (Chachapoyas Prov.). The rivers flowing on the topographical surface sink underground rapidly in less than 10 km distance. The underground segments develop alternatively along dip or joints. They systematically remain at shallow depth. These series of sinkhole-resurgence systems are typical of mountains with high uplift rate and under a wet climate regime. Such karst features correspond to juvenile systems that appear during the first karstification phase of the limestone. Surface runoff occuring on low-permeability covers are gradually captured by sinkholes. Beyond the geological structure, the evolution of these sinkhole-resurgence systems is mainly controlled by surficial dynamic, especially the thickness of low-permeability covers, the topographic gradient and the incision dynamic of the valleys.

Résumé

Spéléogénèse des systèmes juvéniles de type doline-résurgence en série, dans les karsts de la face amazonienne de la Cordillère des Andes, Pérou. Les systèmes perte-résurgence en série, traversés par une même rivière, sont fréquents dans le nord du Pérou. Deux exemples dans la région d'Amazonas sont présentés, situés dans les karsts de Cerro Shipago (Prov. d'Utcubamba) et de Soloco (Prov. de Chachapoyas). Les rivières se perdent parfois jusqu'à trois fois sous terre en seulement 10 km de distance. Les tronçons souterrains se développent tantôt selon le pendage, tantôt selon la fracturation. Dans tous les cas, ces tronçons restent à proximité de la surface, sans pénétration à grande profondeur. Ces systèmes perte-résurgence en série sont typiques des hautes montagnes en forte surrection, bénéficiant de précipitations importantes. Ils correspondent à des réseaux juvéniles apparaissant avec la première karstification d'ensemble des calcaires. Les écoulements de surface soutenus par la présence de couvertures imperméables sont progressivement capturés par des pertes. Au-delà de la structure géologique, l'évolution des systèmes juvéniles de perte-résurgence en série est contrôlée principalement par la dynamique de surface, notamment l'épaisseur des couvertures imperméables, le gradient topographique et la dynamique d'incision des vallées.

Resumen

Espeleogénesis de sistemas juveniles de sumidero-resurgimiento, en los karts de la vertiente amazónica de la Cordillera de los Andes, Perú. Los sistemas de pérdida-resurgencia en serie, cruzados por el mismo río, son comunes en el norte de Perú. Se presentan dos ejemplos en la región Amazonas, ubicados en los karsts de Cerro Shipago (Prov. de Utcubamba) y Soloco (Prov. de Chachapoyas). Los ríos a veces se pierden hasta tres veces bajo tierra en solo 10 km. Los tramos subterráneos se desarrollan a veces según el buzamiento, a veces según la fractura. En todos los casos, estos tramos permanecen próximos a la superficie, sin penetrar a gran profundidad. Estos sistemas de pérdida-resurgencia en serie son típicos de las altas montañas, que se benefician de precipitaciones importantes. Corresponden a redes juveniles que aparecen con la primera karstificación de todas las calizas. Los flujos superficiales, apoyados por la presencia de cubiertas impermeables, son capturados gradualmente por las pérdidas. Más allá de la estructura geológica, la evolución de los sistemas juveniles de pérdida-resurgencia en serie está controlada principalmente por la dinámica de la superficie, incluido la potencia de las cubiertas impermeables, el gradiente topográfico y la dinámica de la incisión del valle.

1. Introduction

Since 2003, the ECA club of Lima (Espeleo-club Andino) and French caving clubs, such as the Bagnols-Marcoule Speleological Group (GSBM), have been exploring continuously the karsts of Northern Peru. During numerous explorations in the Amazonian foothills of the Andes, the frequency of sinkhole-resurgence systems led us to look for the reasons behind the origin of the concentration of such karst phenomena in this area.

Are the series of sinkhole-resurgence systems a main characteristic of the Andino-Amazonian karsts of Peru?
We describe here two examples in the Amazonas Region (Fig. 1), the karsts of Cerro Shipago (Utcubamba) and the massif of Soloco (Chachapoyas), in order to identify similar features and that may provide an explanation for the frequency of these sinkhole-resurgence systems.

2. The slopes of Cerro Shipago

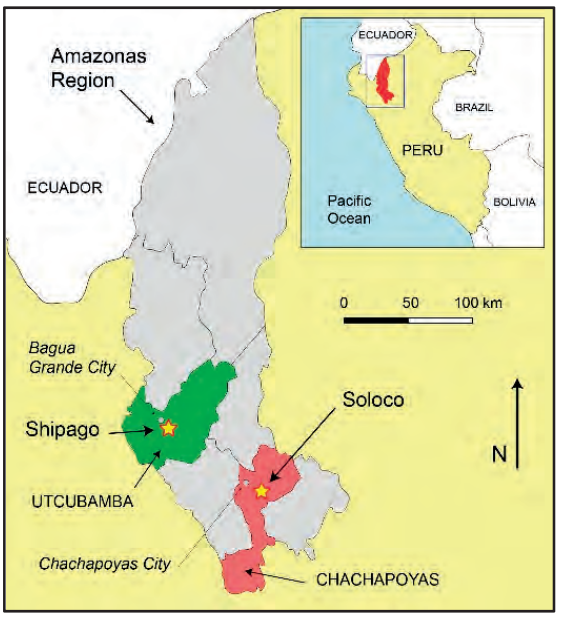

Figure 1: Location of the two provinces of Amazonas Region (Peru) and the sinkhole-resurgence systems of Cerro Shipago (Utcubamba) and Soloco (Chachapoyas).

a) Geological context

Cerro Shipago is one of the highest points (alt. 2849 m) of the limestone massif which extends to the south of the Bagua Grande city, in the Utcubamba Province. The Shipago massif appears as a large anticline fold, with a Permian sandstones core. It is capped by cretaceous series, including limestones, which form a monocline cover on the northern slope of the massif, from its summit to the bottom of the Bagua-Utcubamba syncline valley (alt. 430 m). The cretaceous formation, of several hundred meters thick, displays a steep dip to the north.
The massif is extensively karstified at high altitudes where higher rainfalls are more frequent. Indeed, the longest caves are located above 2000 m. The hilly topography rarely reveals the limestone outcrops, which is covered by thick weathering layers. However, sinkholes (locally called *tragaderos*) capture the streams at the bottom of closed sinks, making the caves active and crossed by streams (Fig. 2).

b) The series of sinkhole-resurgence system of the Río de las Tres Naranjas

The Tragadero del Río de las Tres Naranjas (alt. 2470 m) shows a complete set of passages forming a series of sinkhole-resurgence system of about 250 m in length each (BIGOT, 2019). The system has active and non-active passages over 739 m long and 17 m vertical range.

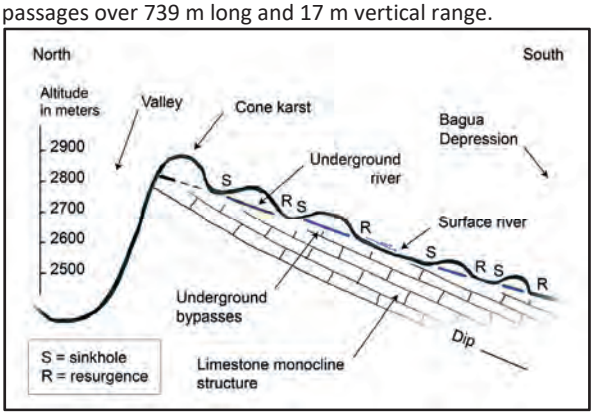

Figure 2: Schematic profile of the Shipago massif showing the shallow development of cave passages as a series of sinkhole-resurgence systems

Such caves are typical contact caves, developed along the dip, following a thin marly layer interbedded in Cretaceous limestones and locally guided by vertical fractures. These sinkhole-resurgence systems do not penetrate deep into the thick limestone and remain at shallow depth, below a thin layer of limestone. These karst systems are probably young, because they are still active.

3. The Soloco area

a) A series of sinkhole-resurgence systems in Soloco area

The series of sinkhole-resurgence systems in this area are extending over a distance of approximately 10 km, from the heights of Ancayrrumo down to the Sonche valley (Fig. 3). From upstream to downstream, segments are: Ancayrrumo-Yacuñahui River, Chaquil-Río Seco, and Salcaquihua River-El Molino. Río Seco Cave is the main the segment, with 2095 m long and 42 m vertical range (-20, +22).

The nearby resurgence of the Río Seco is the largest in the area with an average discharge of about 1.2 m^3/s and a catchment area of about 40 km^2 (GUYOT, 2006). The system is probably fed by the river that sinks into the Tragadero de Chaquil (alt. 2986 m), located 300 m higher and 2.6 km upstream to the south.
Another underground system is developing parallel to Chaquil and Río Seco: the sinkholes of Parjugsha Grande, Parjugsha Alto, and Vaca Negra (Fig. 4). Underground segments were previously partly explored.

b) Hydrogeological and geomorphological context

Caves are developing in the Chambara Fm. limestone of Upper Triassic (BABY, 2006).
The general structure corresponds to a succession of thick limestone stripes between impermeable clastic formations. Sinkholes and resurgences are located at the contact of these formations. As a consequence, the three sinkhole-resurgence systems do not have direct morphological link, apart from the stream that crosses them.

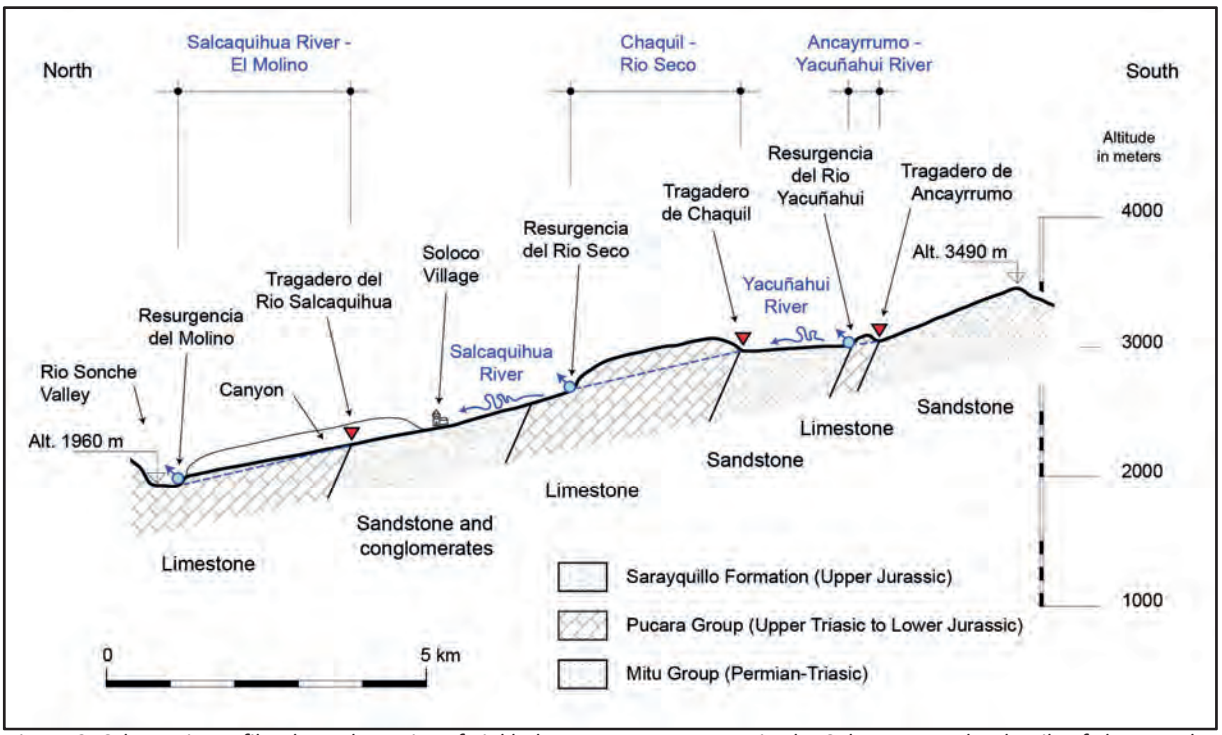

Figure 3: Schematic profile along the series of sinkhole-resurgence systems in the Soloco area. The details of the complex tectonic at the origin of the succession of stripes of the same limestone has not been indicated.

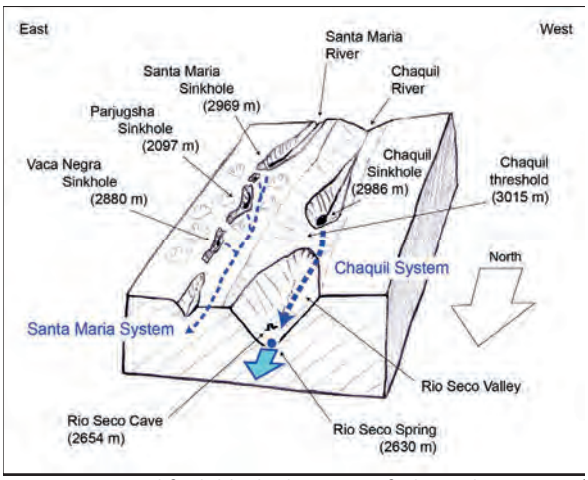

Figure 4: Simplified block diagram of the Soloco massif showing the two parallel underground systems.

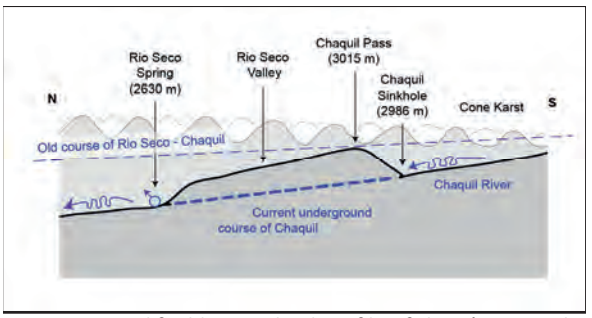

Figure 5: Simplified longitudinal profile of the Río Seco. The pass located at 3015 m attests to the ancient valley of Chaquil whose course has become underground.

The geomorphology of the massif shows that the surface river of Chaquil previously flowed in the Río Seco valley (Fig. 5). The underground captures gradually drained the valley, leaving a threshold upstream, which corresponds to the Chaquil pass (BIGOT, 2013).

4. Discussion and conclusion

In this area of Andino-Amazonia of Northern Peru, most of the caves are characterized by segments of underground bypasses, organized as a series of sinkholes-resurgences along the course of surficial rivers. Some cave waters of streams are crossing limestone stripes and reappear when arriving at the contact of impervious rocks (Soloco area). Others show the same trend even when crossing entirely limestone rocks (Cerro Shipago). In the latter, the cave systems are also guided by a thin marly inception horizon. Here, the underground segments are located along the dip of the limestone strata, locally guided by joints of similar direction as the general gradient. In all the explored caves, caves remain generally at shallow depth below the cone karst landscape. It seems that cave systems with vertical shafts are absent in this area, in opposite to the classical "alpine caves" model, whose caves reach great depth by using succession of fractures (AUDRA et al., 2002).

Such pattern of speleogenesis is typical of the juvenile cave type (AUDRA & PALMER, 2015). It is characteristic of recent karst areas with very fast uplift rates, conducting to important hilly landscapes and significantly eroded under a wet tropical climate such the case of the Amazonian side of the Andean Chain.

Consequently, the hypothesized story behind the karstification, since its early stage to the present-time as seen in both examples here-above, begin with a buried deep limestone which was initially not karstified.

As a consequence, before outcropping, the limestone masses were not karstified, being buried at great depth. This observation is supported by the high runoff largely present at the surface and still eroding or draining the thick weathering covers. Then caves begin to develop from the concentrated input of the streams. Caves follow prominent discontinuities, mainly bedding planes especially when inception horizons are present, fractures parallel to the slope, along the shortest path from sinkhole to resurgence. The resulting pattern shows a rectilinear plan with a moderate and constant slope from sinkhole to resurgence. Caves are always active whereas, abandoned passages are limited to some loops located at a moderate height above the active stream referring thus to their recent abandonment by the drainage system.

In some areas (Soloco), it is possible to follow the evolution stages, from shallow surface valley in the cone karst landscape, to progressive captures in underground segments, then to additional captures toward a new series of sinkhole-resurgence systems, whereas the first series of sinkhole-resurgence gradually tends toward an evolved landscape with large doline fields (Fig. 3, 5).

The new stream captures by sinkhole-resurgence systems are controlled by the dynamic of surface rivers, where those with the largest incision rate are gradually capturing the neighbouring catchment areas.

Finally, we conclude that the early development of underground karst conduits is initially controlled by the landscape characteristics and dynamic: i) the distribution, thickness, and evolution of the weathering covers controls the location of first sinkholes; ii) the topographic gradient controls the slope and extension of juvenile cave systems; iii) the large catchment areas produce surface rivers with higher incision rates that gradually capture the neighbouring catchment areas.

References

AUDRA P. & PALMER A.N. (2015) Research frontiers in speleogenesis. Dominant processes, hydrogeologic conditions and resulting cave pattern. *Acta Carsologica*, vol. 44, n° 3, pp. 315-348. https://ojs.zrc-sazu.si/carsologica/article/view/1960

AUDRA P., QUINIF Y. & ROCHETTE P. (2002) The genesis of the Tennengebirge karst and caves (Salzburg, Austria). *Journal of Cave and Karst Studies*, vol. 64, n° 3, pp. 153-164. https://caves.org/pub/journal/PDF/V64/cave_64-03-fullr.pdf

BABY P. (2006) Géologie des massifs de Soloco. Geología de los macizos de Soloco. *Bull. hors-série du GSBM Spécial* Chachapoyas 2004 & Soloco 2005 et *« Ukupacha » El Mundo Subterraneo*, n° 2, pp. 82-83.

BIGOT J.-Y. (2013) Note géomorphologique sur le massif calcaire de Soloco (Pérou). *Actes de la 22e Rencontre d'Octobre*, La Caunette 2012, *S. C. Paris édit.*, pp. 48-52.

BIGOT J.-Y. (2019) Les systèmes perte-résurgence en série des pentes du Cerro Shipago. *In* Nor Perú 2019. Expédition spéléologique au Pérou du 20 août au 9 octobre 2019. *ECA, GSBM, GS Vulcain, GS Dolomites édit.*, pp. 72-79.

GUYOT J. L. (2006) Hydro-climatologie du massif de Soloco. Hidro-climatología del macizo de Soloco. *Bull. hors-série du GSBM*, Spécial Chachapoyas 2004 & Soloco 2005 et *« Ukupacha » El Mundo Subterraneo*, n° 2, pp. 86-89.

The Peruvian cave files with topographies are available on the website http://www.cuevasdelperu.org

All topographic data and drawings for *TheRíon* are available at https://github.com/robertxa/Mapas_Cavernas_Peru

Geomorphologic presentation of the Iraquara karstic basin Municipio de Iraquara Bahia – Brasil

Gabriel HEZ[1,2,4,5,7] & Claudia SOUSA-LIMA[1,3,6,8]

(1) Sociedade Bahiana de Espeleologia (2) Aventure Grotte et Canyon (3) Universidade Estadual de Feira de Santana
(4) Université Savoie Mont Blanc (5) EDYTEM (6) Gruta de Lapa Doce
(7) Spéléo Club de Villefranche de Conflent (8) Sociedade Nordestina de Espeleologia

Abstract

The Iraquara karst is located in the centre of the Bahia state, in South Sertão. This semi-arid area is covered with a catinga type of vegetation and can be defined as a karstic basin which is lined with quartzite and arenite massifs. The Precambrian limestone in the region which is studied, constitutes a subhorizontal area with altitudes going from 650 to 750 m. The surface we are dealing with is about 800 km^2, and part of it is covered with clayey detritic rock. In some areas we can see lapiaz tables which have often collapsed. The position of the karstic phenomena on the surface (closed valleys, sinkholes, lapiaz) as well as endokarstic phenomena show a conditioning directly in connection with the litho-structural context of the Irece synclinal. A large concentration of sinkholes (several hundreds) and three closed valleys make a remarkable complex of karstic depression. In the downstream part these last ones are ended by large cavities like the Lapa Doce system (see the poster) set by the Agua de Rega closed valleys. These valleys have temporarily slid in a semi-arid climatic context for some 15,000 years. They have created numerous subhorizontal underground complexes which re-emerge at different places as far as several kms south east of the Rio Santo Antonio hydrographic basin. A digging, an aggradation and an incision have been noticed in the paleo drainage. This has happened for a long time according to the dimensions of the galleries and the power of the alluvial deposits which have been noticed. The organisation and the morphology of the galleries can be interpreted according to the structural and lithologic context, allowing the morphogenesis of labyrinths, the morphogenesis of auto-captures and of fracture intensity, and the morphogenesis of all kinds of galleries you can imagine. The vast and deep flooded karst in the Iraquara basin expands around 60 – 120 m in relation with the epikarst level. This karstic aquifer is an important water reserve in South Sertão.

1. A Precambrian sedimentary Basin of south Sertão

Iraquara is located in the northeast of Brazil in the southern part of the Irecê sedimentary basin (Fig. 1), forming a syncline on the São Francisco craton (C.B.P.M, 1993). The limestone fields of the formation Salitre of the Una group grow in the upper Proterozoic, dating from more than a billion to 650 million years. These grey limestones, weakly metamorphic, are thin and laminated with siliceous alternations.

The axis of the syncline in the part studied, is oriented NNW-SSE. The hydrographic organisation of the closed valleys and endokarst is directly related to the litho-structural context and orographic of the Iraquara basin. The dip and fracturing of limestones control morphology and orientation of underground galleries.

Figure 1: Agricultural landscape on the clay detritic cover of the Iraquara basin. In the background, the Chapada Diamantina quartzite mountains (E.R.B., 1979).

2. Geomorphology of a karst basin characterised by closed valleys and hundreds of karstic depressions

The landscape of Iraquara is a karst basin bordered by non-carbonate rocks (IGBE, 1977; VERNIER INDA & BARBOSA, 1978; CRUZ JUNIOR, 1998; INSTITUTO MILITAR, 1980). The limestone bedrock forms a subhorizontal extent with altitudes between 650 and 750 m. Its area of about 1000 km² is partly covered with detritic (clay) rock. Surface karst phenomena are closed valleys, dolines and lapiaz (FERRARI, 1990; HEZ & SOUSA LIMA, 2018). The temporary rivers that feed the karst originate on quartzites and conglomerates (VALLE, 2004). These valleys are cashed from contact with limestones, forming more steep flanks and rocky abrupts. Three closed valleys can be seen on this karst:

- **Agua de Rega valley** (Fig. 2 and 3): 30 km long, it closes at the level of the system of Lapa Doce (HEZ, 2000). The aggradation of the valley is noticeable by the presence of alluvial deposits (LAUREANO *et al*., 2016).
- **Almas valley**: it is organised into seven valleys, and closes at the level of Alto da Cruz.
- **São José Valley**: more modest (5 km), it feeds the Riacho do Gado.

Figure 2: Lapa Doce sinkhole (200 x 100 m). This phenomenon is located at the level of a paleo-meander of the underground river fed by the valley Agua de Rega.

Figure 3: Overlay of the Lapa Doce underground system on aerial photography. We notice the dolines connected with the cavity.

3. Iraquara endokarst: 100 kilometers of subhorizontal galleries

The surveyed cavities highlight the ancient and current underground circulations, between the closed valleys and the Rio Santo Antonio. Currently more than 100 km of galleries have been explored and surveyed. The main paleo-drains are often large, comfortable galleries, filled with fine sediments, abundant and massive carbonate deposits; and sometimes cyclopean screes linked to ceilings collapses and sinkhole openings (Lapa Doce). Ancillary and secondary conduits account for almost 60% of endokarst development. They are characterised by labyrinths dug into large sets of fractures and strata joints. This offers underground landscapes of diaclases and rolling mills. Other ancillary galleries are conducts of catches and self-catches of ancient underground streams. Epiphreatic conducts of large dimensions, more aquatic and less crowded, are often clayey and end on siphons.

Bager, troglobite catfish, are often found there. The drowned karst is spread over several tens of km² and its depth ranges between 60 and 120 m compared to the ground of the epikarst. On the right bank of the Rio Santo Antonio, southeast of the Iraquara basin, lies a karst zone at an average altitude of 670 m. The dolines are aligned north-south and the cavities have the same orientation. Its conduits are epiphreatic galleries (Fig. 4).

Figure 4: Paleo-drain from Lapa da Onça. This cavity, located on the left bank of the Riacho Agua de Rega, 4 km south of Iraquara, retains erosion morphologies characteristic of the slow flow regime, and the stable level of the valley.

4. A large network: the Lapa Doce system

This network offers a development of more than 40 km and represents the major underground system of Iraquara karst. This cavity has more than ten entrances. Lapa Furada, with its arch bridge, is the upstream part of the network, which was the main loss of the Riacho Agua de Rega (LAUREANO *et al*., 2016). This creek has a drainage basin which measures around 600 km². A large conduit follows the paleo-loss, and gives the scope of the old underground watercourses (50 m wide). This can be flooded (h = 30 cm) in the tourist area at the time of heavy precipitation. The majestic sinkhole of Lapa Doce is a hectometric collapse of the second meander of the underground paleo-river, which separates today the network in two parts. Two branches are observable on the left bank of the main gallery: the Téiu gallery and the canyon.

The eight siphons listed in the network are aligned and oriented NNO - SSE, this corresponds to the axis of the synclinal gutter of the Iraquara basin. These views on the karst aquifer would be positioned in the bottom of this gutter for more than 2 km. The siphon of the lake (Fig. 5) was plunged to - 25 m over a distance of 200 m. This area is the deepest part explored in the system: about 90 m from the ground of the epikarst. The downstream of the network ends on a complex of spectacular collapses north of the village from Santa Rita.

The Lapa Doce cave is a horizontal network that has experienced a paragenetic period long proven by forms of ceiling erosion, and a powerful aggradation materialised with about 10 m of fine sediments (LAUREANO, 1998) in several locations in the main galleries (Fig. 6). Racking and morphology incision testify to the decrease of the local base level and/or an uplift of the São Fransisco craton.

Figure 5: Lake Lapa Doce. This view of the aquifer of the Iraquara basin has been plunged to - 25 m over a distance of 200 m.

Figure 6: Santa Rita gallery in Lapa Doce. This fine alluvial deposit in a removal slot, constitutes the memory of the last hydrological functions of the gallery.

References

C.B.P.M. (1993) Stratification, sédimentation et recherches minières du bassin d'Irecê - Salvador.

E.R.B. Companhia de Engenharia Rural da Bahia (1979) Projeto Iraquara, Salvador da Bahia.

CRUZ JUNIOR F.W. (1998) Aspectos geomorfologicos e geoespeleologia do carste da região de Iraquara, centro norte da Chapada Diamantina, Estado da Bahia, dissertaçãtaco de mestrado, Universidade de São Paulo, Instituto de geociencias.

FERRARI J.A. (1990) Interprétation des phénomènes karstiques dans la région d'Iraquara, mestrado à l'Université de Salvador da Bahia.

INSTITUTO MILITAR (1980) Prospec, photographies aériennes au 1/ 25 000.

HEZ G. (2000) Le système souterrain de Lapa Doce, Iraquara, Bahia, Brasil, mémoire de cavité, brevet d'état d'éducateur sportif 1° option spéléologie, Ministère Jeunesse et Sport, Vallon Pont d'Arc.

HEZ G., SOUSA LIMA C. (2018) Présentation géomorphologique du bassin karstique d'Iraquara. Colloque international de karstologie, Karst 2018 Chambéry. Poster.

IGBE (1977) Carte topographique au 1/ 100 000, feuille SD 24 V A1 Seabra.

LAUREANO F.V. (1998) O registro sedimentar clastico associado aos sistemas de Lapa Doce et Torrinha, municipio de Iraquara, Chapada Diamantina, estado de Bahia, dissertação de mestrado, Universidade de São Paulo, Instituto de geosciencias.

LAUREANO F.V., KARMANN I., GRANGER D.E., ALMEIDA R.P., CRUZ F.W., STRICKS N.M., NOVELLO V.F. (2016) Two million years of river and cave aggradation in NE Brazil: Implications for speleogenesis and landscape evolution, Geomorphology 273, 63-77.

VALLE M.A., 2004. Hidrogeoquimica do grupo una (bacias de Irecê e salitre): um exemplo da ação de acido sulfurico no sistema carstico. Tese de doutoramento, Universidade de São Paulo, Instituto de geociencias. 137 p.

VERNIER INDA H.A., BARBOSA J.F., 1978. Notice de la carte géologique de l'état de Bahia, CPM (Coordination de production minéral), Salvador da Bahia.

Fractured speleothems as proxies for cave evolution

Alessia NANNONI[(1)], Marco ANTONELLINI[(2)], Bartolomeo VIGNA[(3)] & Jo DE WAELE[(2)]

(1) Department of Earth Sciences, University of Florence, Via La Pira 4, 50121, Florence, Italy, alessia.nannoni@unifi.it (corresponding author)
(2) Department of Biological, Geological and Environmental Sciences, University of Bologna, Via Zamboni 67, 40126 Bologna, Italy m.antonellini@unibo.it jo.dewaele@unibo.it
(3) Department of Environment, Land and Infrastructure Engineering (DIATI), Polytechnic of Turin, Corso Duca degli Abruzzi 24, 10129 Torino, Italy bartolomeo.vigna@polito.it

Abstract

Several fractured speleothems were studied in the Bossea cave (Piedmont, Italy) to infer the mechanisms that caused the rupture and their relationships with cave speleogenesis. The Bossea cave evolution is strongly controlled by a complex structural setting. It is a contact cave that developed along a detachment between meta-volcanic basement rocks and marbles laying on top. Downward erosion of the strongly deformed meta-volcanics led to the formation of giant halls in the downstream (touristic) part of the cave. The studied speleothems are located on both flanks of this downstream sector. All speleothems show fractures developed in uniaxial compression. Some fractured speleothems also show spalling and uplift of the concretions at the base. The deformation of these speleothems seems to be related to lateral focusing of vertical loads caused by the evolution of the arched cave roof. The sides of the rooms (abutments) are next to the detachment surface where speleothems rest on the highly weathered meta-volcanics, which can deform as the vertical load increases in response to roof collapses carving an arched ceiling profile. The cave ceiling evolution indicates an increasing instability of the downstream sector, a factor that should be considered in this show cave visited by over 30000 tourists every year.

1. Introduction

Broken speleothems are common structures in caves. However, their origin is difficult to infer because many processes may cause their formation (BECKER *et al.*, 2006; GILLI, 2005). Studies carried out in the past 50 years pointed to a co-seismic origin of these features, attempting to use them for neotectonics and paleo-seismological investigations (BRIESTENSKY *et al.*, 2014; FORTI, 2001; PLAN *et al.*, 2010). Other studies demonstrated that some examples interpreted as earthquake-induced were caused by other phenomena (BECKER *et al.*, 2006; GILLI, 2004). Overall, the processes that can lead to speleothem deformation can be divided in two types, speleogenetic and external ones (GILLI, 2004). The former type includes ground failure or creeping of the sediments underlying the speleothems, erosion at the base of the speleothem due to water flow, ice infill creep, rock decompression caused by *in situ* stress reorientation, mechanical failure of jointed blocks, and slope instability. The latter type of processes comprises human activities and active tectonics. Among the speleogenetic processes, mechanical failure is a phenomenon causing the most common cave morphologies, namely collapse or breakdown (FORD & WILLIAMS, 2007). The presence of the cave itself affects stress distribution in the rock surrounding the open passages. The distribution and the magnitude of cave breakdowns depend on many factors (HATZOR *et al.*, 2010): thickness of the rock cover, thickness and homogeneity of the rock layers (e.g. presence of marl layers), span of the opening, intensity of jointing, orientation of discontinuities, shear strength of discontinuities, strength of the intact rock, and groundwater conditions. The local structural setting, by controlling fault and joint distribution, bedding plane orientation and, consequently, water flow organization plays a fundamental role in cave speleogenesis and cave stability.

This contribution presents the first results of the investigation on the relationships between cave speleogenesis and the deformed speleothems found in an alpine cave system whose architecture and evolution are strongly controlled by the local structural setting. Some insights on current cave stability will also be presented. The studied cave, Bossea (NW Italy), is a show cave visited every year by 30,000 tourists and it hosts an underground scientific laboratory that has studied cave hydrology since the late 70s.

2. Geological setting, materials and methods

The Bossea cave (Piedmont, Italy) is a mid-altitude karst system developed in the Ligurian Alps. The surface is characterized by steep SE-facing slopes with bare rock outcrops and a thin soil cover. The development of the cave was strongly controlled by the Alpine tectonics (ANTONELLINI *et al.*, 2019). ENE-WSW striking subvertical faults put laterally in contact blocks of metamorphosed Mesozoic carbonates with the originally underlying metamorphosed Permian volcanoclastic and clastic rocks (quartzite and shale), limiting the areal development of

karstification. The carbonate and the clastic rocks sequence are also tectonically juxtaposed to the meta-volcanoclastics by a detachment (Fig. 1a). The detachment surface is antiformal with a hinge line plunging to ESE with a dip of 10-15°. The sequence made up of marble, quartzite, and shale is isoclinally folded. Consequently, bedding planes are steeply dipping (Fig. 1b). The meta-volcanics are strongly deformed and altered. The cave is 3 km long and is divided into an upstream and a downstream sector. In the former, the underground collector (TM, Fig. 1) flows in a canyon carved in the marble. The latter sector is a show cave and is characterized by large rooms and massive collapses (box in Fig. 1a, Fig. 1c). This part of the cave developed along the detachment surface (contact cave).

Deformed and fractured speleothem (stalagmites, stalactites, and columns) locations and dimensions were mapped inside the cave. Attitude of the fractures cutting the speleothems were measured with a Brunton^{TM} geologic compass. Speleothem's base diameter, relative broken blocks movement, vertical and horizontal displacement along the fracture planes were also measured. The distance between the cave ceiling and the floor was measured at each speleothem location by means of a laser telemeter Leica Disto X. The structural data were plotted by using the Stereonet v.9.3.3 by ALLMENDINGER *et al.* (2012).

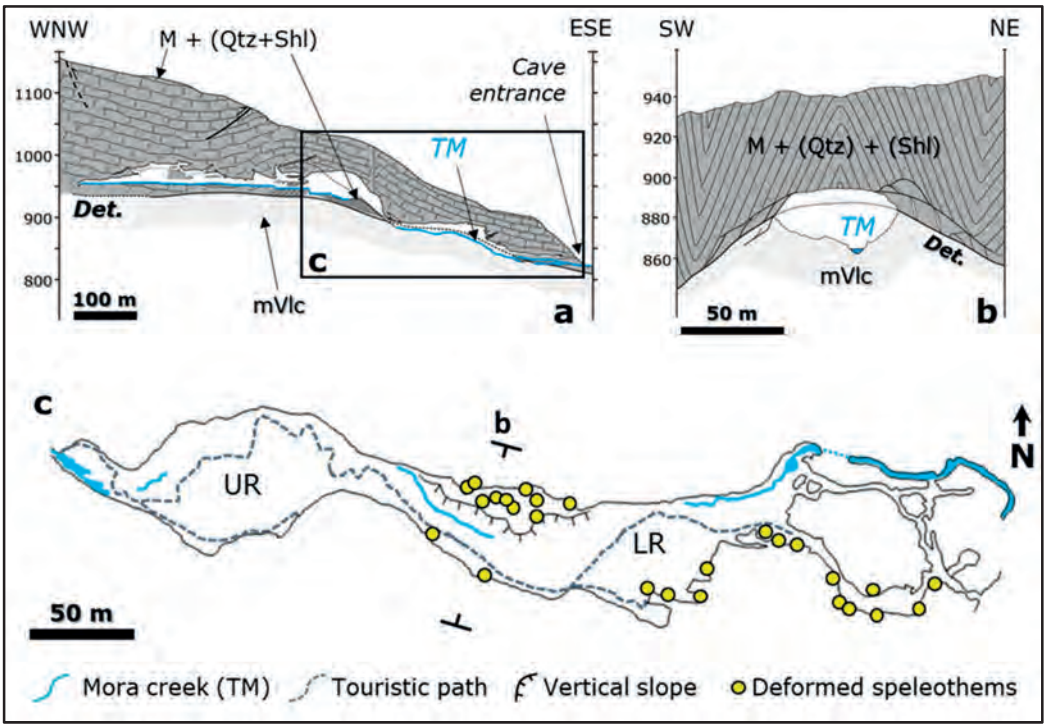

Figure 1: WNW-ESE (a) and SW-NE (b) simplified geological sections of Bossea cave, and plan view of the large rooms sector (c). The location of (b) and (c) are highlighted in (c) and (a), respectively. Labels: Det. = detachment, M = marble, Qtz = quartzite, Shl = shale, mVlc = meta-volcanics, TM = Mora creek, UR = upper room, LR = lower room. Modified after ANTONELLINI et al. (2019).

3. Results

Deformed speleothems are observed on both flanks of the lower part of the cave (i. e. Lower room, LR, and in the entry passage). Fractured concretions were not found nor in the upper room (UR), nor in the upstream part. The direction of displacement of the roof with respect to the speleothems is either northward or southward (Fig. 2a). Most speleothems show fractures that developed in uniaxial compression. These fractures are vertical and aligned with the principal compressional stress at the contact point (Fig. 2b, 2e). The uniaxial compression fractures open up at the roof contact point and propagate downwards. Some fractured speleothems, besides uniaxial compression fractures, show tilting, spalling, and uplift of the concretion at the base (Fig. 2c). Stress concentration at the roof-speleothem contact point caused intense fracturing, crystal cleavage gliding, and re-coloring (Fig. 2d). All speleothem contacts show predominantly contractional deformation (vertical downward) with a subordinate horizontal one (roof top-down). Some large speleothems show, in addition to uniaxial compression fractures, also spoon-shaped high aperture fractures at their base. These speleothems are observed next to steep slopes and rest on the strongly weathered and deformed meta-volcanics (Fig. 2f).

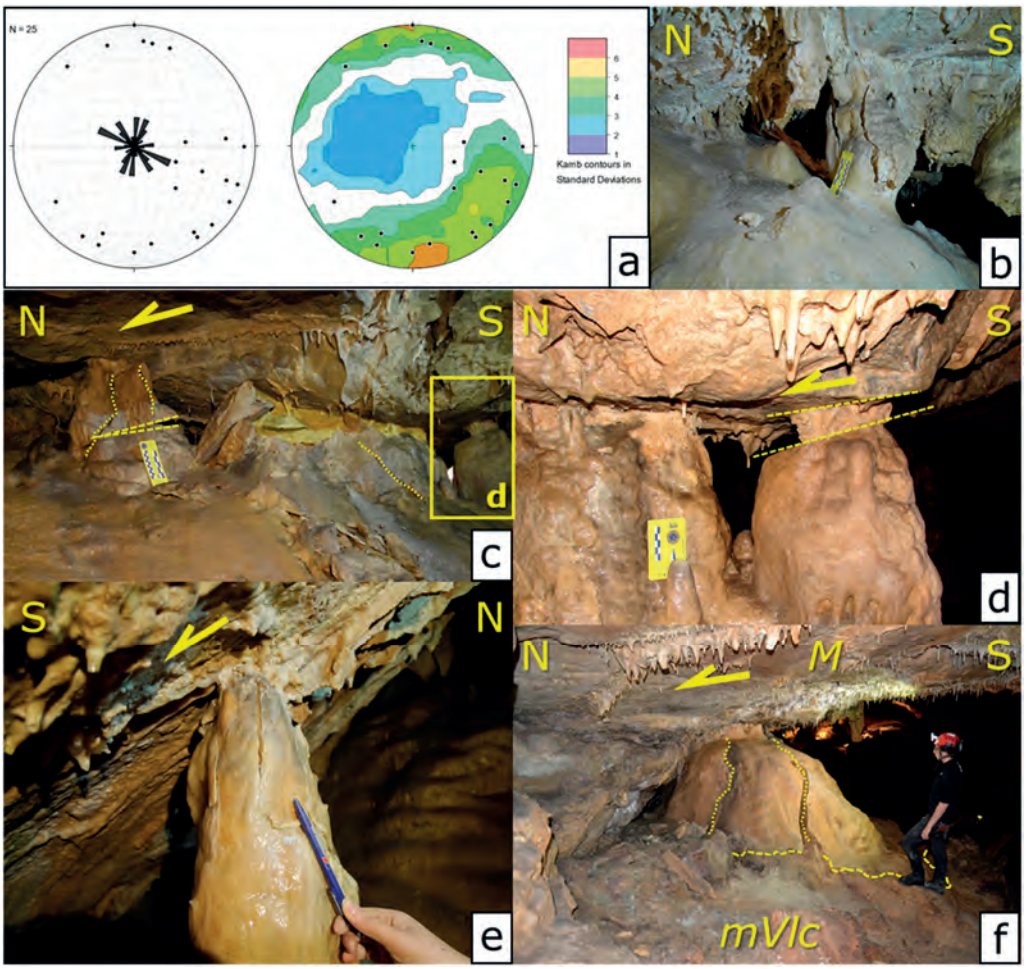

Figure 2: Slip vector diagram reporting the data of the deformed speleothems measured in Bossea cave (a). Morphological features in deformed speleothems: uniaxial compression fractures (b, e), uniaxial fractures and tilting (left column) and extrusion of material (central speleothem, c), calcite re-coloring and possible gliding along cleavage planes (d), high aperture spoon-shaped fracture at the base of a large speleothem (f). Yellow arrows show the roof relative movement with respect to the floor.

4. Discussion

A co-seismic origin for the deformed speleothems observed in the Bossea cave seems unlikely because slip vectors have no uniform orientation. The surface slope above the cave shows no evidence of instability so this factor could be also ruled out. It seems that the ongoing speleogenesis and the local structural setting concur to deform the speleothems. The cave development is progressing by erosion of the metavolcanics and roof collapses. This contributes to form an arched roof in the large rooms of the downstream sector. An arched roof causes the vertical loads to be focused on the abutments at the sides of the rooms. In particular, the gouge zone next to the detachment surface at the sides of the LR where roof and floor meet (Fig. 3b, 3d), represent an important weak element. The speleothems that grow close to the sides can be considered as “abutments or pillars” that deform as the lateral vertical load increases via roof collapse that tends to form an arched profile for the room ceiling. Moreover, these concretions rest on the top of the detachment gouge and highly weathered metavolcanics (Fig. 3e). If the speleothems grow over the metavolcanics on steep lateral slopes under uniaxial compression (load on the abutments due to the arched ceiling), landslides in the soft sediments at the base of these concretions can occur. This latter process is aided by the collapse of jointed strata and duplex blocks from the upper damage zone at the cave roof that contribute to form its arched profile (Fig. 3f). This hypothesis is coherent with the sense of movement of the roof respect to the studied speleothems (top down). Deformed concretions are not present in the UR because (Fig. 3c) the detachment is not outcropping.

The roof profiles of the UR and of the westernmost part of the LR seem less evolved towards an arched shape than the easternmost part of the LR, characterized also by less frequent rockfalls.

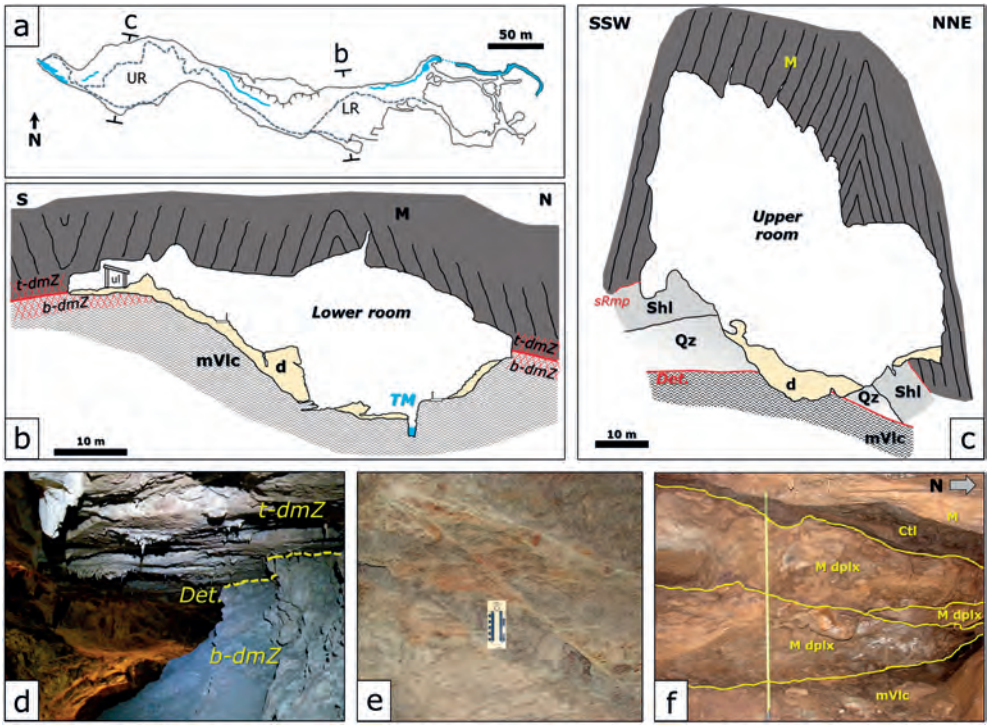

Figure 3: Map view of the LR show cave section (a). Geological cross-section of LR close to the underground scientific lab (ul, b). Geological cross-section UR (c). Outcrop of the detachment and the related damage zones inside the cave (d). Meso-structures of the bottom (e) and the top (f) damage zones. Labels: d = speleothem cover and clastic deposits, sRmp = secondary ramp, M dplx = marble duplex, Ctl = cataclasite. See Fig. 1 for mVlc, Qz, Shl, Det., b/t-dmZ meaning.

5. Conclusions

The investigation of the deformed speleothems of the Bossea cave confirmed the strong relationships between the complex local structural setting and speleogenesis. Overall, the ongoing cave evolution is controlled by important elements such as the detachment zone, the folded stratification, and the different mechanical properties of the rocks. This has implications for cave stability: speleogenesis is ongoing since the cave has not reached a stable roof configuration. The deformed speleothems are evidence of this process rather than an external perturbation (i.e. earthquakes). The cave profile evolution is unique for each sector, because it is strongly related to peculiar structures and morphologies, in fact the deformed speleothems are present in specific sites only.

References

ALLMENDINGER R.W., CARDOZO N., FISHER D. (2012) Structural geology algorithms: Vectors and tensors in structural geology: Cambridge University Press, UK, 302 p.

ANTONELLINI M., NANNONI A., VIGNA B., DE WAELE J. (2019) Structural control on karst water circulation and speleogenesis in a lithological contact zone: The Bossea cave system (Western Alps, Italy). Geomorphology 345, 106832.

BECKER A., DAVENPORT C. A., EICHENBERGER U., GILLI E., JEANNIN P. Y., LACAVE C. (2006) Speleoseismology: a critical perspective. Journal of Seism. 10.3, 371-388.

BRIESTENSKY M., STEMBERK J., ROWBERRY M.D. (2014) The use of damaged speleothems and in situ fault displacement monitoring to characterize active tectonic structures: an example from Západní cave, Czech Republic. Acta Carsologica 43.1, 129-138.

FORD D., WILLIAMS P. (2007) Karst hydrology and geomorphology, Ed. John Wiley & Sons. 562 p.

FORTI P. (2001) Seismotectonic and paleoseismic studies from speleothems: the state of the art. Geologica Belgica 4.3, 175-185.

GILLI E. (2004) Glacial causes of damage and difficulties to use speleothems as palaeoseismic indicators. Geodinamica Acta 17, 229-240.

GILLI E. (2005) Review on the use of natural cave speleothems as palaeoseismic or neotectonics indicators. C.R. Geoscience 337.13, 1208-1215.

HATZOR Y.H., WAINSHTEIN I., MAZOR D.B. (2010) Stability of shallow karstic caverns in blocky rock masses. Int. J. Rock. Mech. & Min. Sciences 47, 1289-1303.

PLAN L., GRASEMANN B., SPÖTL C., DECKER K., BOCH R., KRAMERS J. (2010) Neotectonic extrusion of the Eastern Alps: constraints from U/Th dating of tectonically damaged speleothems. Geology 38, 483-486.

Some indicators of seismic activity in the caves of the Dinaric Karst of Croatia

Davor GARAŠIĆ[(1)] & Mladen GARAŠIĆ[(1,2,3)]

(1) Society for the Research, Surveying and Filming of the Karst Phenomena (DISKF) Zagreb, Nova Ves 66, Croatia
(2) Union Internationale de Speleologie (UIS), Zagreb, Croatia,
(3) Committee for Karst, Croatian Academy of Sciences and Arts (HAZU), Zagreb, Croatia

Abstract

The Dinaric karst is located in a seismically very active area. It is the area of contact between the African geotectonic plate and the Eurasian tectonic plate. The Adriatic plate is the northernmost part of the African plate. In the area of the Adriatic Sea, it subducts under the Dinarides. With such displacement of large tectonic plates, strong earthquakes are a common occurrence. Traces of seismotectonics were discovered in some caves. These traces indicate the possible intensity of the earthquakes from the time when seismology did not exist. Recent measurements of the absolute displacements of parts of the speleothem or even parts of cave channels within the last fifty years may have provided additional information on seismic activity. Special attention was paid to the construction of tunnels, bridges, dams and roads when traces of neotectonic movements were noticed inside the discovered caverns. Examples of the effects of recent earthquakes in some caverns found in tunnels during construction are given. Changes in the movement and amount of groundwater in these places were detected. Such observations significantly help in creating a more realistic interpretation of speleogenesis in certain karst areas within the Dinarides.

1. Introduction

The effects of earthquakes on the terrain surface and in the underground are not the same. There is much evidence that some strong earthquakes recorded on the terrain surface did not cause significant or more noticeable changes in the caves within the earthquake area. On the other hand, in some speleological objects, significant changes were recorded locally in periods when no stronger seismic activity was recorded on the terrain surface. Precise evidence of paleoseismic effects can be observed within caves while on the surface of the terrain it is almost impossible. This suggests the need for more detailed recording and monitoring of earthquakes in selected caves in seismically active areas. Tectonics, along with lithostratigraphic and hydrogeological conditions, is one of the most important factors in speleogenesis, i.e., in the process of cave formation. This means that seismic activity is almost always present in speleogenesis. Recently (2020 - 2021) seismic activity in Croatia increased. A few strong earthquakes (the strongest one with magnitude M=6.3) and thousands of aftershocks occurred. The new measured data, which would be collected underground, could help in better understanding the effects of earthquake waves in different rocks in specific locations.

2. Speleogenesis types - relation to seismic activity

Based on the professional scientific publications in the field of speleology, hydrogeology, engineering seismology, engineering geology and our own experience, it can be concluded that the topic of earthquake effects in speleological objects was not researched much in Croatia (GARAŠIĆ, 1981; GARAŠIĆ & CVIJANOVIĆ, 1985, 1986) and in the world (BECKER H., 1929; BECKER A. et *al*. 2006, 2012; BINI et *al*., 1992; MENICHETTI, 1998; PLAN et *al*., 2005; GILLI, 1999). The reason for this could be found in the relatively small number of recent earthquakes that occurred in areas where conducting speleological research was possible. It is believed that such research would provide significant results only after strong earthquakes with visible effect marks. Such earthquakes are relatively rare and did not occur for a long time before 2020. Thus, this is not the right way of thinking. The effects of tectonic activity, i.e. earthquakes, can be detected within three significant phases of speleogenesis (GARAŠIĆ, 1997, 2007). These effects differ from each other, but are certainly noticeable to those who can distinguish multiple stages of speleogenesis. Speleogenesis in karst areas can be divided into several completely different phases. We will mention only the three most important ones.

The initial stage of speleogenesis is present in easily soluble rocks with smaller fissures and/or fractures. All fractures and fissures were formed by tectonic activity. Active presence of atmospheric and groundwater is one of the key factors of this stage of speleogenesis. There are no secondary sediments and no speleothems. Karstification processes did not reach the depths of less permeable or impermeable rocks in the substrate. There are no visible traces of earthquakes within the speleological objects formed during the initial stage of speleogenesis because of their small size. The effects of earthquakes can only be detected in the primary rocks in which speleogenesis

commenced. These are visible folds, faults or thrust faults formed by tectonics before speleogenesis began. At this stage of speleogenesis, initial sinkholes can be observed on the surface, where the karstification processes are exclusively gravitational.

In the main phase of speleogenesis we are referring to speleological objects in the classical sense of morphology (shape and dimensions). Speleothems are formed here. Fault planes and wide fractures can be observed in cave channels and chambers. Earthquake effects are visible in the form of broken speleothems (Figs. 1, 2, 3, 4, 5) and changes of the underground water flows (direction, flow, turbidity, etc.) (ŠEBELA, 2008; LACAVE et *al*., 2003; FORTI, 1997). Groundwater is always present within this phase of speleogenesis, but locally within the speleological object, deviations in their flows and flow directions are possible.

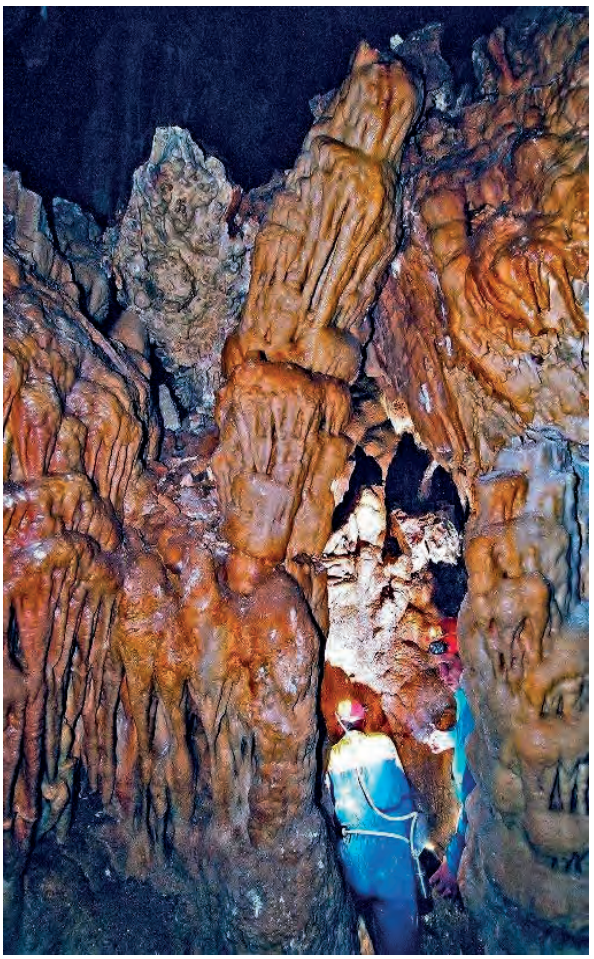

Figure 1: speleothem broken as a result of recent earthquake

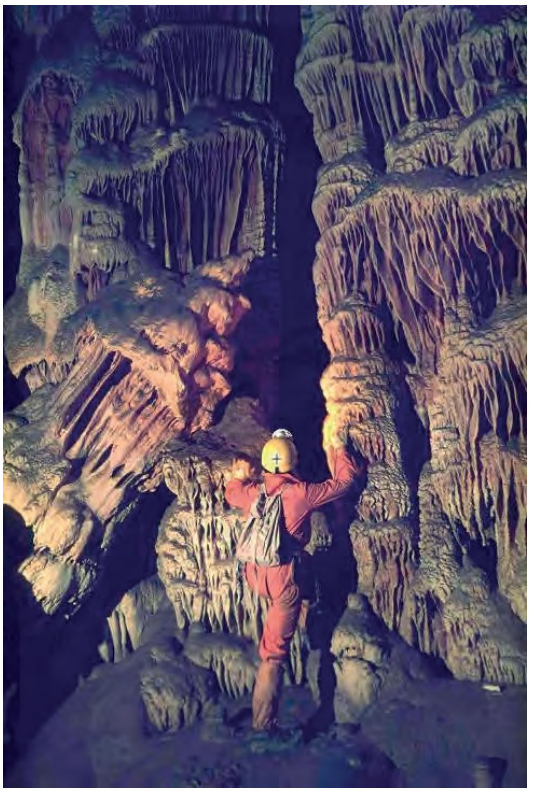

Figure 2: old speleothem broken as a result of active tectonics

Figure 3: vertical and horizontal movement resulting from neo-tectonic activity

The late phase of speleogenesis is related to covered or paleo karst. In this type of area, the occurrence of suffusion

is common. Suffosion sinkholes in the area of paleo karst are directly related to the speleological objects beneath them. It is a regressive and gravitational karstification. Earthquakes can initiate changes in groundwater levels, which can cause the cover material to spill into the speleological objects underneath. The caves are in the fossil phase of speleogenesis (CAMUS et *al*., 2001), but they are not completely filled with material (crystalline, clay etc.). These cavities can be filled with air or water. The material from suffusion sinkholes will eventually fill these cavernous spaces as a secondary deposit. Groundwater is always present in such occurrences.

Figure 4: Coseismic effects in a cave after the strong earthquake of December 29th 2020

It is important to determine the age of seismic movements whose effects were observed underground. The effects of earthquakes vary widely. For example, paleo earthquakes can cause more or less visible changes in speleothems (various deformations). They can even be so strong that they have changed the speleo-morphology, i.e., the shape and orientation of the cave passage.

Neotectonics, new or recent earthquakes can cause collapse of rock creep material within cave channels, collapse of unstable rock blocks, changes in the amount and direction of groundwater, etc. (CRISPIM 1999; DELABY 2001) The cessation or change of further formation of speleothems is particularly noticeable.

On the surface, a series of sinkholes appear on certain paleo-tectonic faults that turn into collapsing valleys. These are mega structures. In neo-tectonic seismic earthquakes, suffosion appears on the surface with still unclear outlines of the final morphology.

Since the effects of earthquakes in speleological objects are more difficult to notice for a large number of scientists and experts from different scientific fields, it would be advisable to install measuring instruments in certain speleological objects of particularly active seismic areas. For the area of operation of the Zagreb earthquakes, it is suggested to place the instruments in Veternica cave or in underground shelters and warehouses near Markuševac. For the area of Petrinja earthquakes, it is suggested to place instruments in a cave near Veliki Šušnjar (GARAŠIĆ & KOVAČEVIĆ, 1991) or in a cave in Velika Gradusa. These are the largest relatively easily accessible underground spaces that could be safe for instruments of various purposes. It is certain that they could measure the absolute displacements of individual rock blocks. Geologists, speleologists, hydrogeologists, seismologists, geotechnicians, etc. should agree on where and what instruments can and should be set up for underground measurements.

Figure 5: speleothem broken after the 2020 earthquake (M=6.3) in the cave (Croatia)

Figure 6: Suffosion in Mečenčani near Petrinja after strong earthquake 29th December 2020

Similar underground laboratories already exist in some active seismic zones in the world (Italy, South Korea, USA, Belgium, etc.). Perhaps it is time to consider one such measurement laboratory in the area of Croatian Karst.

Earthquakes left and are leaving their effects on the surface and in the underground karst. Depending on the dominant degree of speleogenesis (CAMUS et *al*., 2001; CRISPIM, 1999), the effects on the surface of the paleo (covered, older) or neo (recent, present) karst associated with the underground differ. Within speleological objects, we can distinguish the effects of earthquakes on speleothems from those created by altering the complete morphology of channels or even burying them. This may be a locally accelerated transition from the main phase of speleogenesis to the fossil (late) phase of speleogenesis. In these cases, the underground cavities were not completely crystallized or filled with material. Therefore, as a consequence of earthquakes, there is a possibility that the material from newly formed suffusion sinkholes will be deposited in these underground cavities. Similar phenomena were noticed in the area of the Petrinja earthquake (Fig. 6). Data on the effects of earthquakes collected in speleological objects could help provide new insights about the earthquakes (GARASIC, 2021).

References

BECKER H.K. (1929) Höhle und Erdbeben. Mitt. Über Höhlen-u.Karstf. no. 1-4, p. 130-133.

BECKER A., DAVENPORT C., EICHENBERGER U., GILLI E., JEANNIN P., LACAVE C. (2006) Speleoseismology: A critical perspective. Journal of Seismology, vol. 10, no. 3, 371-388.

BECKER A., HAUSELMANN P., EIKENBERG J., GILLI E. (2012) Active tectonics and earthquake destructions in caves of northern and central Switzerland. International Journal of Speleology, 41(1), 35-49.

BINI A., QUINIF Y., SULES O., UGGERI A. (1992) Les mouvements tectoniques récents dans les grottes du Mont Campo dei Fiori (Lombardie, Italie). Karstologia, 19, 1, 23-30.

CAMUS H., SERANNE M., QUINIF Y. (2001) Activité tectoniques récente enregistrée par les spéléothèmes : un contre-exemple sur la faille des Cévennes (sud du Massif Central, Hérault, France). RIVIERA 2000, Tectonique active et géomorphologie, Villefranche-sur-Mer, Revue d'Analyse Spatial-No. Spécial 2001, 53-54, Nice.

CRISPIM J. A. (1999) Seismotectonic versus man-made induced morphological changes in a cave on the Arrábida chain (Portugal). Geodinamica Acta, vol. 12, 3-4, Elsevier, 135-142, Paris.

DELABY S. (2001) Palaeoseismic investigations in Belgian caves. Netherlands Journal of Geosciences / Geologie en Mijnbouw, 80 (3-4):323-332.

FORTI P. (1997) Speleothems and Earthquakes. 284-285, In: Hill, C. & Forti, P., Cave Minerals of the world. Second edition, 463 p., NSS, Huntsville.

GARAŠIĆ M. (1981) Neotectonics in Some of the Speleological Objects in Yugoslavia. Proceedings of the 8th International Congress of Speleology proceedings, Bowling Green, 1981, UIS, 148-149.

GARAŠIĆ M. (1997) Some types of speleogenesis and speleohydrogeology in Dinaric karst area (Croatia, Europe). Proceedings of the 12th International Congress of Speleology. Vol. 1, La Chaux-de-Fonds: UIS, 1997. 147-150.

GARAŠIĆ M. (2007) Some different Types of Speleogenesis in Croatian karst Area. Geophysical Research Abstracts, 9 (2007), EGU,Vienna. 231-238.

GARAŠIĆ M. (2021) The Diraric Karst of Croatia – Speleology and Cave Exploring. pp.I-XXV, 1-437, Springer International Publishing, Cham. https://doi.org/10.1007/978-3-030-80587-6 -

GARAŠIĆ M., CVIJANOVIĆ D. (1985) Speleološke pojave i seizmička aktivnost u krškim poljima. Naš krš, 11 (1985), 18/19; 103-109.

GARAŠIĆ M., CVIJANOVIĆ D. (1986) Speleological phenomena and seismic activity in Dinaric karst area in Yugoslavia. 9. Congresso International de Espeleologia: Procedimento. Vol.1. Barcelona: UIS, 1986. 94-97.

GARAŠIĆ M., KOVAČEVIĆ T. (1991) Speleogeologija Špilje kod Šušnjara - jedinstvenog speleološkog objekta formiranog u laporovitim stijenama (Banija). Spelaeologia Croatica, 2(1991), 31-36.

GILLI E. (1999): Research on the February 18, 1996 earthquake in the caves of Saint-Paul-de-Fenouillet area, (eastern Pyrenees, France). Geodinamica Acta, 12, 3-4, 143-158, Paris.

LACAVE C., EGOZCUE J.J., KOLLER M.G. (2003) Can broken and unbroken speleothems tell us something about seismic history? 12th European Conference on Earthquake Engineering, paper 349, Elsevier.

MENICHETTI M. (1998) Central Italy earthquakes of autumn 1997 and the underground karst features of the area. Speleochronos hors-série, Livre des contributions au colloque "Karst & Tectonics", Han-sur-Lesse, 9-12 mars 1998, 121 p.

PLAN L., SPOTL Ch., GRASEMANN B., DECKER K., OFFENBECHER K.H., WIESMAYER G. (2005) Seismothems caused by neotectonic activity in the Eastern Alps. 14th International Congress of Speleology, 21-28 August 2005, Athens, Final Programme & Abstract Book, 117-118.

ŠEBELA S. (2008) Broken speleothems as indicators of tectonic movements. Acta Carsologica, 37/1, 51-62.

Active water cave Vodna jama v Lozi and Loza Unroofed Cave – a case of morphogenesis in the Slavina Corrosional Plain (SW Slovenia)

Astrid ŠVARA[1,2], Andrej MIHEVC[1] & Nadja ZUPAN HAJNA[1,3]

(1) Karst Research Institute ZRC SAZU, Titov trg 2, 6230 Postojna, Slovenia, astrid.svara@zrc-sazu.si (corresponding author), mihevc@zrc-sazu.si, zupan@zrc-sazu.si.
(2) University of Nova Gorica, Graduate School of Karstology, Vipavska cesta 13, 5000 Nova Gorica, Slovenia.
(3) International Union of Speleology – UIS, Titov trg 2, 6230 Postojna, Slovenia.

Abstract

The Slavina Corrosional Plain is a leveled karst area located between Postojna and Pivka Basin, Karst Plateau, and Vipava Valley, developed in Eocene, Paleocene, and Cretaceous Limestone. The northern part was influenced by allogenic waters, forming a distinctive contact karst geomorphology, among which caves are present, running towards the south. Vodna jama v Lozi is a 7.7 km long active water cave (between 550 m and 470 m a.s.l.). On the surface, an unroofed cave filled with sediments appears (between 630 m and 580 m a.s.l.), named Loza Unroofed Cave. Extending at least 4.3 km on the karst surface, it represents the longest known and studied unroofed cave in Slovenia, classified as a Valuable Natural Feature. The distinctive relict cave channel without a ceiling is up to 10 m deep and 30 m wide. A geomorphological map was produced by LiDAR imaging, cartographic measurements and sediment sampling. The sedimentary methods and X-Ray Diffraction (XRD) were used to determine the origin of sediments. By the analyses, we could prove, that the sediments in the Loza Unroofed Cave were brought into the cave by an allogenic river(s) sinking into the Slavina Corrosional Plain from the North or north-west part of the Postojna Basin. Furthermore, we assume regarding its position, sediment contents, and direction of water flow, to be a precursor of Vodna jama v Lozi, now an active epiphreatic cave about 100 m deeper.

1. Introduction

Geographical, Geological and Hydrological settings

The research area represents an NW part of the Dinaric karst which is the main morphological type of the Dinaric Mountains (MIHEVC & PRELOVŠEK, 2010). The Slavina Corrosional Plain is a karst area with individual peaks from altitude 640 m to 750 m, which on the N borders with the Postojna Basin, with a mean altitude of 550 m. The Postojna Basin comprises of Lower to Middle Eocene flysch rocks and Quaternary alluvium intercalations - river terraces and weathered flysch deposits (MELIK, 1951; PLENIČAR, 1963 and 1970; GOSPODARIČ, 1988). The Slavina Plain is at its contact with the basin developed in Paleocene to Eocene limestones, Cretaceous to Paleocene limestones, and in its main part in Upper Cretaceous limestones (generalized and marked with green color in Fig. 1). From a geological point of view, the Slavina Plain represents the Komen Thrust Sheet predominantly with NW-SE Dinaric and Transverse-Dinaric faulting, common for the structural unit of External Dinarides (PLACER, 2008). The Postojna Basin has impermeable properties with waters gathering in streams and flowing towards its borders. The Rakuljščica Stream has a proven underground water connection from the Sajevče Ponor at the end of the Sajevče Blind Valley (marked with white color in Fig. 1) through the caves Markov spodmol and Vodna jama v Lozi towards the Timava River (HRIBAR *et al.*, 1955), representing the Adriatic Sea Drainage Basin (ARSO, 2020).

Active cave Vodna jama v Lozi and the Loza Unroofed Cave

Due to geological and hydrological settings, contact karst geomorphic features have been forming in the Slavina Plain, along with (epi)phreatic speleological features, influenced by allogenic waters loaded with flysch derived sediments - composed mainly by pebbles, sand, silt, and clay (GOSPODARIČ *et al.*, 1970; MIHEVC, 1991a, 1991b, 1999 and 2006). One of the most representable features is the active cave Vodna jama v Lozi and the denuded cave Loza Unroofed Cave (Fig. 1).

The active water cave Vodna jama v Lozi (Cad. No. 911) is a (sub)horizontal cave, which is through a sump connected to the cave Markov spodmol (Cad. No. 878), together forming a 7.7 km long cave (CAVE REGISTER, 2020). The cave is developed between the approximate elevations of 550 m and 470 m, leaning towards SW. In the cave Markov spodmol, where the (epi)phreatic features are well developed, walls and ceiling are covered with scallops, showing a reworking of a fast river flow (Fig. 2), along with several cave lakes, sumps, and other dissolutional features. This cave is representing an intermittent ponor of the Rakuljščica Stream, today acting as such only at high waters. In the cave, several clastic sediment stacks of mainly channel and slack-water facieses appear. A profile was sampled for the paleomagnetic dating method, which gave an age range of its deposition between 0.78 – 2.58 Ma (ZUPAN HAJNA *et al.*, 2010 and 2020). The continuation part – the active cave

Vodna jama v Lozi is on the other hand represented by many clastic sediment accumulations, affecting the overall appearance of the cave which along with many water sumps and changing stream paths makes it more difficult to research.

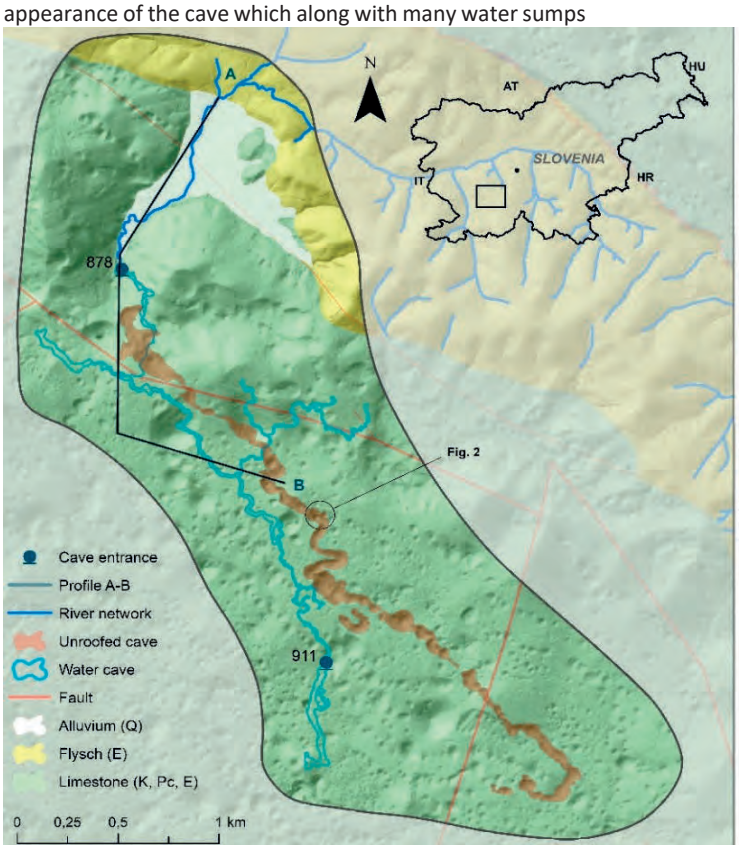

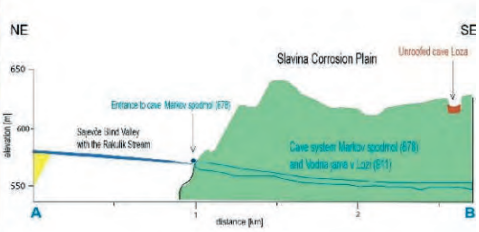

Figure 1: Location of the Loza Unroofed cave and active caves Vodna jama v Lozi (Cad. No. 911) and Markov spodmol (Cad. No. 878), on the Slavina Corrosional Plain, NW Slovenia with locations of Figures 4 and 5. Schematic cross section A-B. Source: GOV (Lidar and OGK geology) and Slovenian Cave Cadaster.

The (sub)horizontal Loza Unroofed Cave has an up to 30 m wide and 10 m deep cave channel, largely filled with allogenic clastic and allochthonous cave sediments. It is exposed on the surface between the elevations of 630 m and 580 m (MIHEVC, 1991a, 1991b, 1999 and 2006). In the approximate vicinity of the denuded cave, a side passage opens with a preserved ceiling. A section of fine clastic sediments was sampled for the paleomagnetic dating method, which revealed its age to be older than 4 Ma (ZUPAN HAJNA *et al.*, 2020).

Figure 2: Scallops in the cave Markov spodmol, showing phreatic genesis (Photo: GEDEI, 2015).

2. Materials and methods

The TTN5 topographic map in scale 1:5000, high-resolution LiDAR map, DMV digital elevation and shaded relief models, from the Slovenian Environmental Agency (ARSO), were used for geomorphological mapping of the research area, along with computer work on ArcMap and Adobe Illustrator software. Reviewing the existing information on cave reports and plans was done in the Slovenian Cave Cadaster at the Karst Research Institute ZRC SAZU in Postojna. Selected allogenic fine-grained sediments (e.g. clay, silt, sand) were sampled by a basic hand/machine drill. The X-ray powder diffraction (XRD) method helped us to determine the mineralogical composition of allochthonous clastic sediments which gave us information about their provenience. Both analyses were performed at the Karst research institute ZRC SAZU in Postojna on the Bruker XRD D2 Phaser system. By observing, mapping, and comparison of the geomorphic cave features in the active and unroofed cave, along with other analyzing methods, a morphogenetic review was made.

3. Results and conclusions

In the active caves Vodna jama v Lozi and Markov spodmol, the known orientation of the scallops, the type of sediment deposition, and the location of the ponor along with the underground river flow, gave us the idea to compare the active caves with the denuded cave in their vicinity, exposed about 100 m above on the surface. The cave Vodna jama v Lozi is represented by quite vast channels and chambers, mainly filled with allogenic sediments (flysch pebbles, sand, silt, and clay). Slack-water sediment facies and cap muds of the latest floodings are mainly covering the variety of depositions, which are in places uncovered by stream incisions. In several higher parts of the cave, stalagmites are deposited on top of the allogenic sediments, which can be inclined due to sediment creeping bellow. The paragenetic overprint is shown by the leveling of the ceiling, in places covered by half-tubes (Fig. 3), anastomoses, and pendants, while on the walls mainly as alluvial notches on several heights.

Figure 3: Half-tubes as paragenetic dissolutional forms in the active cave`s ceiling (Photo: TIČAR, 2020).

The Loza Unroofed Cave has its bottom channel mainly covered by clastic sediments, which are at different depths mixed with flowstone and limestone gravel as chips, derived from the degradation of the cave ceiling and walls due to denudation. In slightly inclined parts of the channel or along channel slopes, small outcrops of flowstone were found, many times easily weathered leaving only small remnants, hard to detect. The channel is frequently meandering and exposing some cave chambers in forms of collapse dolines. In one of them, a cave wall is preserved, with a stalagmite sedimented on top of a flowstone shelf, which was once deposited on top of an allogenic sediment stack/dome (Fig. 4). Along the preserved wall, a slightly tilted up to 3 m high flowstone deposit (stalagmite/stalactite) was observed (Fig. 5).

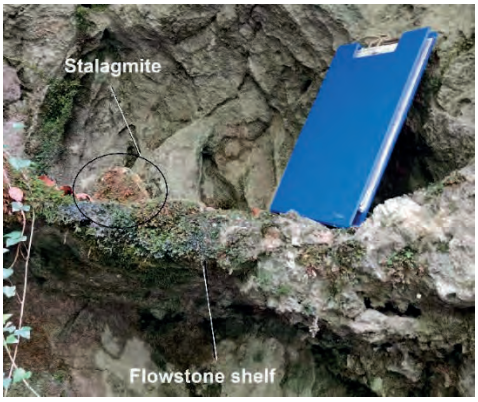

Figure 4: Stalagmite and a flowstone-shelf deposition, preserved in the unroofed cave (Photo: TIČAR, 2020).

Figure 5: Flowstone deposit, preserved in the unroofed cave (Photo: ŠVARA, 2020).

The active cave Vodna jama v Lozi has about 80 m altitude difference in its 7.7 km of length, which shows an average descent of 10.4 m in 1 km of its length, whereas the Loza Unroofed Cave has a 50 m altitude difference in its 4.3 km of length, which represents an average descent of 11.6 m in 1 km of its length. That said, by both representing an approximate descend of 1 m in the length of 100 m which corresponds to a horizontal cave typology, and with both of them generally following a Dinaric NW-SE direction (Fig. 1) along with displaying similar geological and geomorphological features, we can assume, that the unroofed cave is a precursor, a relict passage of the active caves Markov spodmol and Vodna jama v Lozi, formed as (sub)horizontal leveled passages, like others found in similar contact karst areas in its vicinity.

4. Future research

Since the ongoing Ph.D. study will be conducted within this area, many ideas for future research are planned. Hopefully, in the Loza Unroofed Cave, we will manage to conduct further analysis of allogenic sediments covering its bottom channel, comprising of XRD and XRF analysis (giving us more information about the provenience) and electrical resistivity imaging along several cross-sections (giving us exact information on the depth of the sediment cover whereas the total dimensions of the former channel). In the active cave, further studies will comprise of detailed analysis of at least one other sediment profile in the cave Markov spodmol, where sampling for paleomagnetic dating methods and others – if suitable, will be performed). After further analysis, an even clearer picture of the Slavina Corrosional Plain contact karst morphogenesis will appear.

References

ARSO (2020) Drainage Basins.- [Online] Available from http://gis.arso.gov.si/atlasokolja/profile.aspx?id=Atlas_Okolja_AXL@Arso [Accessed on October 24th, 2020].

CAVE REGISTER (2020) Cave Register of the Karst Research Institute ZRC SAZU and Speleological Association of Slovenia. Postojna, Ljubljana.

GEDEI P. (2015) Hlajenje v Markovem spodmolu.- [Online] Available from https://www.petergedei.com/sl/portfolios/hlajenje-v-markovem-spodmolu/[Accessed on December 8th, 2020].

GOSPODARIČ R. (1988) Paleoclimatic record of cave sediments from Postojna karst. Annales de la Société géologique de Belgique 111, pp. 91-95.

GOSPODARIČ R., HABE F., HABIČ P. (1970) Orehovški kras in izvir Korentana. Acta carslogica 5, no°2, pp. 97-108.

HRIBAR F., HABE F., SAVNIK R. (1955) Podzemeljski svet Prestraniškega in Slavenskega ravnika. Acta Carsologica 1, pp. 91-147.

MELIK A. (1951) Pliocenska Pivka. Geografski vestnik 23, no°1, pp. 17-39.

MIHEVC A. (1991a) Morfološke značilnosti ponornega kontaktnega krasa: izbrani primeri iz slovenskega krasa. Master thesis. Faculty of Arts, Department of Geography, Ljubljana, 206p.

MIHEVC A. (1991b) Morfološke značilnosti ponornega kontaktnega krasa v Sloveniji. Geografski vestnik 63, pp. 41-50.

MIHEVC A. (1999) Unroofed caves of Slavenski ravnik. In: Mihevc A. (Ed.) 7th International Karstological School, Classical Karst, Roofless caves. Guide-booklet for the excursions, June 1999, Postojna, Speleological Association of Slovenia and Karst Research Institute ZRC SAZU, pp. 9-14.

MIHEVC A. (2006) Brezstropa jam ana Slavenskem ravniku. In: Boštjančič J. (Ed.) Slavenski zbornik. Slavina. Kulturno društvo Slavina, pp. 27-34.

MIHEVC A., PRELOVŠEK M. (2010) Geographical Position and General Overview. In: Mihevc A., Prelovšek M. & Zupan Hajna N. (Eds.) Introduction to the Dinaric Karst, Collegium Graphicum d.o.o., Ljubljana, pp. 6-8.

PLACER L. (2008) Principles of the tectonic subdivision of Slovenia. Geologija, 51 no°2, pp. 205-217.

PLENIČAR M. (1963) Osnovna geološka karta - tolmač za list Postojna L33-77, Geološki zavod, Ljubljana, 52p.

PLENIČAR M. (1970) Tolmač osnovne geološke karte 1:100.000, List Postojna. Zvezni geološki zavod, Beograd.

ZUPAN HAJNA N., MIHEVC A., PRUNER P., BOSÁK P. (2010) Palaeomagnetic research on karst sediments in Slovenia. International Journal of Speleology, 39 no°2, pp. 47-60.

ZUPAN HAJNA N., BOSÁK P., PRUNER P., MIHEVC A., HERCMAN H., HORÁČEK I. (2020) Karst sediments in Slovenia: Plio-Quaternary multi-proxy records. Quaternary International 546, pp. 4-19.

Fluviokarst on Quaternary eogenetic conglomerates; an example from Slovenia

Matej LIPAR(1) & Mateja FERK(1)

(1) Anton Melik Geographical Institute, Research Centre of the Slovenian Academy of Sciences and Arts, Ljubljana, 1000, Slovenia, matej.lipar@zrc-sazu.si (corresponding author), mateja.ferk@zrc-sazu.si

Abstract

Most of the eogenetic conglomerates in Slovenia are cemented remnants of Quaternary fluvio-glacial deposits. A high proportion of carbonate pebbles made the conglomerate prone to dissolution and karstic development. This includes the development of karst hydrology and geomorphological forms, e.g., dolines, pocket valleys and caves. Udin Boršt, one of the karstified conglomerate terraces in the north-western part of Slovenia, shows the additional development of fluvial geomorphology. Its overall distribution is not even and shows better development of fluvial geomorphology on the eastern/north-eastern side of the terrace. Whilst the first idea that a difference in the amount of percentage carbonate pebbles could cause this phenomenon due to mixing zones of the material from two different valleys, it was later noted that the elevation difference of the underlying impermeable Oligocene clay is the cause for this. We complement this idea that not just the elevation difference, but also the palaeotopography of the underlying clay, promoted the development of fluvial valleys and, in fact, had a predispositional effect on their spatial occurrence.

Résumé

Fluviokarst sur des conglomérats éogénétiques du Quaternaire ; un exemple en Slovénie. La plupart des conglomérats éogénétiques de Slovénie sont des restes cimentés de dépôts fluvio-glaciaires quaternaires. Une proportion élevée de galets de carbonate a rendu le conglomérat sujet à la dissolution et au développement ultérieur du karst. Cela comprend le développement de l'hydrologie karstique et des formes géomorphologiques, par exemple les dolines, les reculées karstiques et les grottes. Udin Boršt, l'une des terrasses de conglomérats du nord-ouest de la Slovénie, montre également le développement de morphologies fluviales. Sa distribution globale n'est pas uniforme et montre un meilleur développement de la géomorphologie fluviale sur le côté est / nord-est de la terrasse. Alors que la première idée selon laquelle une différence dans la quantité en pourcentage de galets de carbonate pourrait amener à ce phénomène en raison du mélange de matériaux issus de deux vallées différentes, il a été noté plus tard que la différence d'élévation de l'argile oligocène imperméable sous-jacente en est la cause principale. Nous aboutissons à cette idée que non seulement la différence d'élévation, mais aussi la paléotopographie de l'argile sous-jacente, a favorisé le développement des vallées fluviales et, en fait, a préparé leur répartition spatiale.

1. Introduction

Quaternary conglomerates in Slovenia reflect periodical deposition of fluvio-glacial material related to glacial and interglacial cycles. Carbonate Mesozoic rocks dominate in the catchments, so conglomerates mostly consist of carbonate pebbles cemented with the calcite. Periodical depositions of the material were followed by fluvial erosion, and consequently the older carbonate sediments appear as isolated terraces.

Karst that evolved on those terraces has been termed as 'conglomerate karst' (HABIČ, 1981; GABROVŠEK, 2005; KRANJC, 2005), 'shallow karst' (ŽLEBNIK, 1978), 'isolated karst' (HABIČ, 1981) and 'eogenetic karst' (LIPAR & FERK, 2011; FERK & LIPAR, 2012), and consists of a variety of karst geomorphological features including dolines, caves, pocket valleys and blind valleys. However, Udin Boršt terrace (Fig. 1) also exhibits fluvial topography, which dominates on its eastern and north-eastern part, expressed with steep valleys and gullies, forming so-called 'fluviokarst'.

The conglomerate of the Udin Boršt terrace was deposited on top of the impermeable Oligocene clay, which slopes down westwards and south-westwards. Consequently, the conglomerate deposits are generally thicker on the south-western part of the terrace, and notably thinner on the north-eastern part; this leads to the conclusion that a thin deposit of conglomerate and relatively shallow occurrence of the Oligocene clay beneath the conglomerate on the north-eastern part caused predominantly fluvial geomorphological regime. However, the question is whether these fluvial valleys could have been additionally influenced by the (palaeo)topography of the Oligocene clay that was present prior to deposition of the fluvio-glacial sediment (i.e., present day conglomerate). This paper illustrates the initial approach of field work mapping of the clay exposures and construction of the cross-section of the valley-ridge system in the north-eastern part of the terrace (Fig. 1).

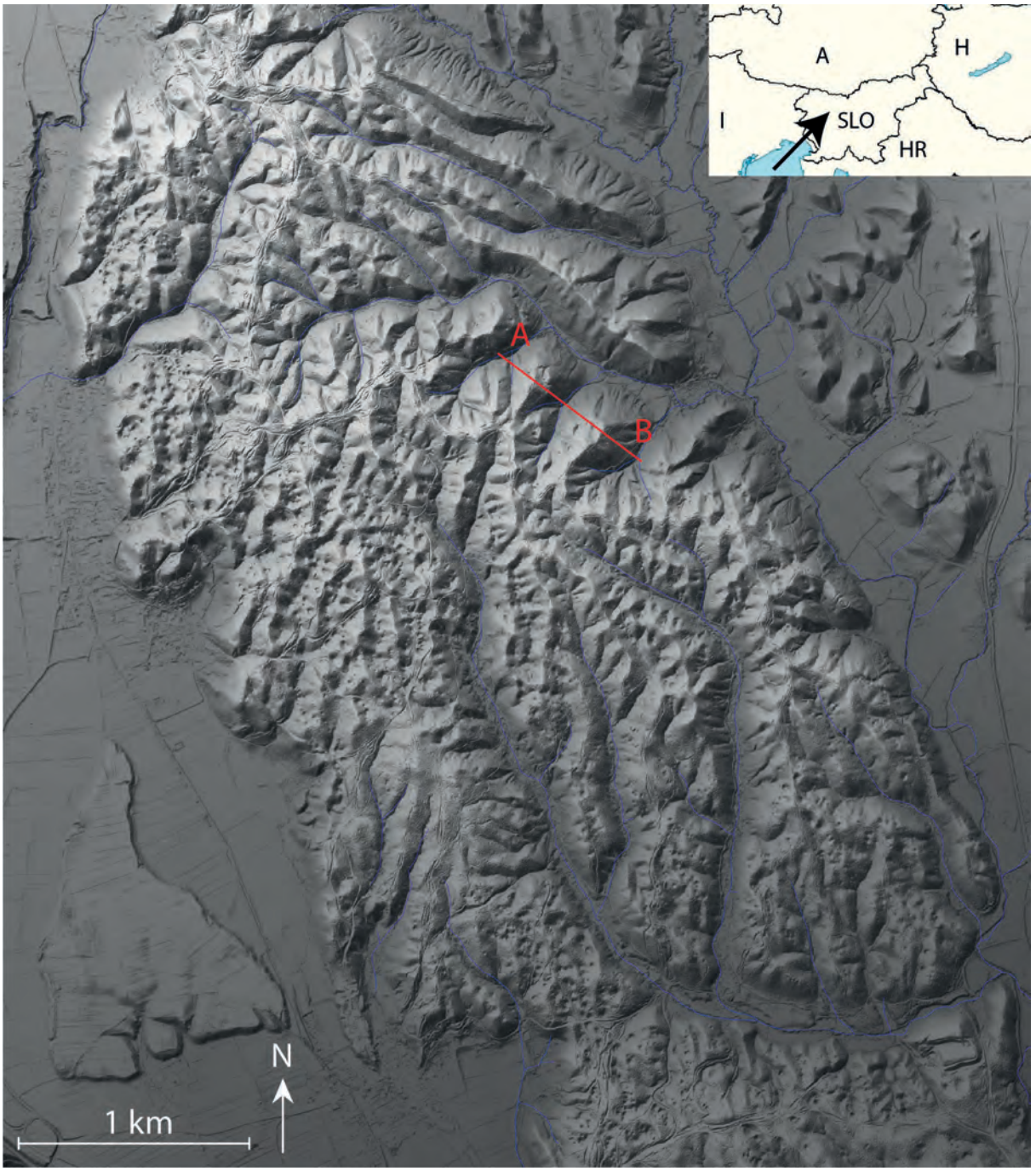

Figure 1: Digital elevation model based on LiDAR (source: ARSO, 2015) of the Udin Boršt terrace. Note the predominant fluvial geomorphology on its northeastern part and predominant karst topography on its southwestern part. A – B cross-section is shown in Fig. 3.

2. Materials and methods

Field work was conducted throughout the Udin Boršt terrace to map the exposures of Oligocene clay and Quaternary conglomerate. In several occasions, we used a hand drill to check for the Oligocene clay beneath the soil and residual sediment cover. Mapping was performed using SWMaps software on field, and then exported into Global Mapper software. Due to large errors in GPS elevation points from field, we adopted LiDAR data elevations to all the points for consistency and small error.

3. Results

The outcrops of the Oligocene clay and conglomerates have been mapped over the whole Udin Boršt terrace, but comparing the elevations of the exposed clay in relation to conglomerate around the whole terrace is problematic because the terrace has experienced neotectonic movement (MIHEVC *et al.*, 2015). We have therefore focused on a small section of the northeastern part of Udin Boršt (A – B cross-section in Fig. 1).

The exposure of the clay is, similarly to most of the valleys in Udin Boršt, restricted mostly to the floors of the valleys by on-going creek erosion (Fig. 2A). The lower parts of valley slopes are mostly covered by colluvium, but in places just above the colluvium, clay exposures were observed at the contact with the conglomerate, which is usually also seen as a steeper slope or a cliff-face. Springs are common at these contacts (Fig. 2B).

As the palaeotopography of the clay behind/underneath the conglomerate could not be observed, the overall topography of the clay within the valley floors could still be simply the result of the erosion postdating the deposition of the conglomerate. This led to the additional surveying of the ridges on both sides of the valley by sampling sediment up to 4 m in depth at multiple points with a hand-drill. We successfully found one occurrence of the clay 3 m deep underneath the soil and residual sediment that was left over after the denudation of the conglomerate on one of the valley ridges (Fig. 2C, Fig. 3).

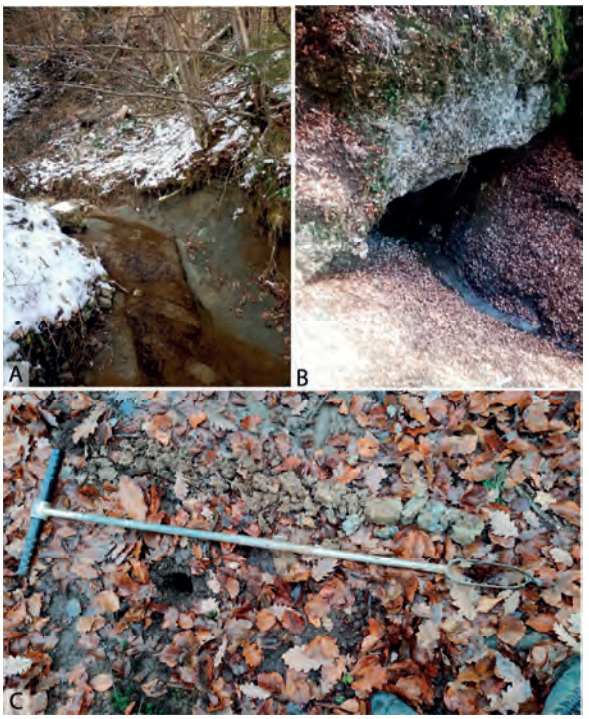

Figure 2: Oligocene clay exposures: (A) – exposure of the clay at the bottom of the valleys by creek erosion; (B) – exposure of the clay at the contact with the upper lying conglomerate (note that these sections usually represent karst springs); (C) – clay occurrence underneath the soil and residual material on the ridge.

4. Discussion

Since conglomerate exposures were mapped in lower elevations on the valley slopes, the occurrence of the clay at higher elevations relative to the conglomerates in the same valley system confirms the presence of the palaeotopography of the clay. The 'palaeoridge' of the clay is illustrated as the ridge on the right hand-side in Fig. 3. Clear contacts of conglomerate and clay were found on both sides of the ridge, whilst the residual scattered non-carbonate pebbles within the loamy sediment at the drilling point on top of the ridge indicates the presence of conglomerate even above this point. MIHEVC *et al.* (2015) published a burial age of 1.86 Ma for the conglomerate of Udin Boršt, which represents enough formation-time for the great amount of non-carbonate residual material found on top of the ridge.

Furthermore, the Oligocene clay 'palaeoridge' within the present-day conglomerate ridge sparks the possibility that at least some present-day valleys can be re-activated palaeovalleys originating in the Oligocene clay before the initial burying by fluvio-glacial material. This suggests that occurrence and direction of particular valleys within the fluviokarst system of Udin Boršt was not led only by the shallow depth of the Oligocene clay on its eastern and north-eastern part, but also by its previous topography. Furthermore, the palaeotopography could partly explain the focusing of underground water in otherwise porous conglomerates with prevailing matrix porosity, and could therefore represent a complex and unique type of a 'fluviokarst' (for other processes that form fluviokarst see, e.g., FORD & WILLIAMS (2007)). The simplified proposed process suggests that the buried palaeovalleys collect and redirect underground water flow and cause (sub)vertical jointing of the conglomerate, which later evolves into present-day fluvial valleys. At the same time, the water still flows underground where the conglomerate is present and subsequently causes the formation of small caves at discharge points at the conglomerate-clay contact.

Nevertheless, a single find of the clay on the top of the ridge currently demonstrates only the possibility of the overall palaeotopographical influence. Further multiple-method approaches are necessary for detailed reconstruction of the palaeotopography, so that the pilot study within this paper can be developed to explain the Earth processes and their timing to form fluviokarst on
Quaternary carbonate conglomerates.

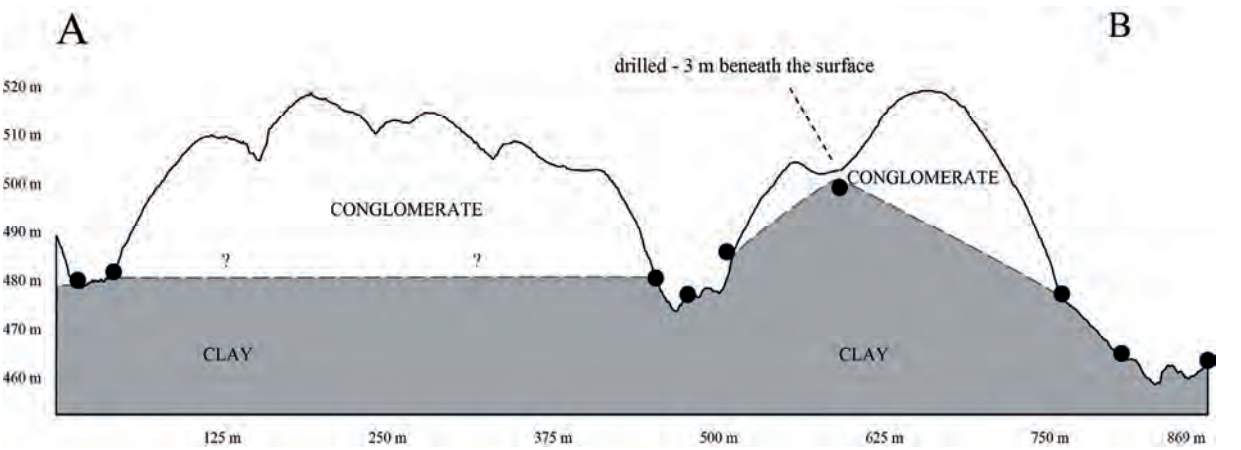

Figure 3: Cross-section (see Fig. 1 for location) of the fluvial valley within the conglomerate terrace. Black dots are locations of mapped clay on the field.

5. Conclusion

Field investigation of the impermeable Oligocene clay exposures confirmed the presence of its palaeotopography prior to fluvio-glacial material deposition (forming present carbonate conglomerate) and possible influence on later development of fluviokarst. Geomorphological features in the area therefore depend on several different components, including the depth of the conglomerate above the Oligocene clay, surface water seepage paths along fractures, horizontal and vertical contacts between karst and clay material, and the direction of groundwater flow which depends on the palaeotopography of the area.

Acknowledgments

The research on eogenetic conglomerates is funded by the Slovenian Research Agency research core funding Geography of Slovenia (P6-0101), Infrastructure Programme (I0-0031), fundamental research project Geomorphological peculiarities of AEOLianite KARST and their palaeoclimatic significance (N1-0162) and bilateral project Geomorphological characteristics on eogenetic carbonate rocks in Slovenia and United States of America (BI-US/19-21-005).

References

ARSO (2015) Online repository of LiDAR data (gis.arso.gov.si/). Slovenian Environment Agency.

FERK M., LIPAR M. (2012) Eogenetske jame v pleistocenskem karbonatnem konglomeratu v Sloveniji (Eogenetic caves in Pleistocene carbonate conglomerate in Slovenia). Acta geographica Slovenica, 52(1), 7-33.

FORD D., WILLIAMS P. (2007) Karst geomorphology and hydrology. John Wiley & Sons Ltd, Chichester, England, 562 p.

GABROVSEK F. (2005) Jame v konglomeratu: primer Udin Boršta, Slovenia (Caves in conglomerate: case of Udin Boršt, Slovenia). Acta Carsologica, 34(2), 507-519.

HABIČ P. (1981) Tipi krasa na Gorenjskem (Karst types in Upper Carniola). 12th meeting of the Slovene geographers. Geographical Society of Slovenia, Ljubljana, pp. 78-88.

KRANJC A. (2005) Conglomerate Karst in Slovenia : History of Cave Knowledge and Research of Udin Boršt (Gorenjsko). Acta Carsologica, 34(2), 521-532.

LIPAR M., FERK M. (2011) Eogenetic caves in conglomerate: an example from Udin Boršt, Slovenia. International Journal of Speleology, 40(1), 53-64.

MIHEVC A., BAVEC M., HÄUSELMANN P., FIEBIG M. (2015) Dating of the Udin Boršt conglomerate terrace and implication for tectonic uplift in the northern part of the Ljubljana Basin (Slovenia). Acta Carsologica, 44(2), 169-176.

ŽLEBNIK L. (1978) Kras na konglomeratnih terasah ob Zgornji Savi in njenih pretokih (Karstification of conglomeratic terraces along the Upper Sava River and tributaries). Geologija, 21, 89-9.

The lost river of Ingleborough

Aaron CAMPION

4 Fitzroy Street, Hull, City of Kingston Upon Hull, HU5 1LL, United Kingdom

Abstract

Newby Moss, on the southern slopes of Ingleborough Hill, covers an extensive area of the Yorkshire Dales where sinking streams and karst features can be found in abundance. However, unlike adjacent area of Gaping Gill, no extensive cave system has been discovered. By undertaking an artificial water tracing, this study has used methods that have provided good evidence to support the hypothesis that an extensive cave system exists beneath Newby Moss. Surface mapping has revealed information about subsurface structure and geology, water tracing has confirmed hydrological connections, and water chemistry reveals dissolution consistent with continuous cave development.

1. Introduction

The limestone area of the Yorkshire Dales is well known for its spectacular karst features including an abundance of caves and potholes which attract tourist from all over the world to visit its national park. Ingleborough Hill, an iconic landmark with its flat-topped summit visible from all directions is one of the famous Yorkshire three Peaks that rises to 723 metres from extensive areas of limestone pavement and till cover where many sink holes and pothole entrances are located (RODGERS *et al*., 2011). The Gaping Gill system, located on the SE slopes of Ingleborough, provides access to an extensive network of large cave passages.

Whilst this system has many explored passages connecting to form a master cave (BECK, 1984), the area due south of Ingleborough Hill, Newby Moss, has karst features and an extensive catchment but very little-known horizontal passage or master cave. It has many deep vertical pothole entrances which all terminate in obstructions or flooded passages (BROOK *et al*., 1991). Many have speculated the existence of an underground system stretching from the western flanks of Newby Moss to Moses Well, over 4km in distance with a potential elevation of 240m making the deepest traversable system in the Yorkshire Dales (HEAP, 1964; ACLAND & WILCOCK, 1969; DRACUP, 1969; WALTHAM, 1990; WILCOCK, 1991; NUNWICK & YEADON, 2000; PEARSON, 2018). However, despite speculative attempts over many years to unlock the underground secrets of the area, exploration of Newby Moss has not revealed the long-dreamt master cave.

2. Geology and glacial history

The bedrock of the area primarily consists of Palaeozoic rocks and younger millstone grits (Fig. 1). The carboniferous limestone where caves are formed is in the Great Scar Limestone which is approximately 200m thick. They are 95% calcium carbonate, massively formed and fine-grained with significant shell and crinoidal fragments (WALTHAM, 2013).

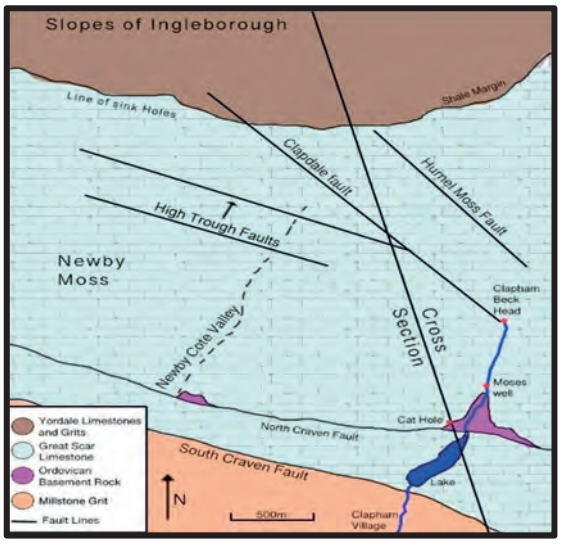

Figure 1: Plan view of the area without the drift cover. The North and South Craven Faults and minor faults that will have influenced the drainage, direction, and development of caves in the area. (WALTHAM, 2017; BRITISH GEOLOGICAL SURVEY, 1997).

In the Yorkshire Dales, cave development took place during warm interglacial episodes, by rapidly melting glaciers following successive glaciations that have exposed the limestone. Most of the landscape is the result of the Devensian ice retreat which played an important part in both the development and destruction of caves. On Newby Moss, located in the protected lee of Ingleborough Hill, there has been minor glacial erosion and very little shale retreat which makes the likelihood of both active and fossil caves beneath the surface likely. It is significant that all the known caves with large passages are located at the southern side of Ingleborough Hill where the limestone has been exposed over a very long period (WALTHAM, 2012).

2. Method

The method chosen to test the sites on Newby Moss was to use a fluorocapteur of activated charcoal to absorb traces of sodium fluorescein (Colour index Acid Yellow 73, known as uranine, CAS No.518-47-8). Sodium fluorescein was chosen because it is not toxic, has a high fluorescence intensity and a low detection limit (GOLDSCHEIDER *et al.,* 2008 in HARRISON, 2013). The difficulty was deciding on the quantity to be used. It was agreed with the landowner, the Environment Agency and the Natural, England that the quantity used would be below the visible threshold in the valley so no visual pollution would result. The following equation was used to calculate the amount.

$$M - a(LQC)b$$

"Where M is the mass of tracer injected (grams), *a* is the empirical coefficient, *b* is an exponent that is unity in most cases, Q is the discharge at the spring where the tracer emerges(m^3/s), L is the distance between input and output points, and C is the peak tracer concentration at the resurgence (g/m^3)" (WORTHINGTON & SMART, 2003 in HARRISON, 2013). It was decided that the coefficient 'a' was presumed to be 19 and a peak concentration of approximately 200ppb, just at the detectable range in the field (HARRISON, 2013; HARDWICK, 2019). Over a period of one month 150 grams of tracer was introduced into each of the six sinking streams.

The fluorocapteurs were placed in the resurgences before the tracer was injected into the sink holes (Fig. 2). The activated carbon was kept separate from the fluorescein and placing the fluorocapteurs was undertaken on a different day to inputting the artificial tracer to ensure there was no chance of cross contamination. A background test was conducted with trial fluorocapteurs to try and eliminate any colouration from organic material in the sinking streams. The water sinking from the shale boundary in the dales has high organic loads which may fluoresce at similar frequencies as fluorescein (GUNN & KELLY, 2017).

The activated charcoal used comprised 25. grams of granular activated charcoal (18 x 16 mesh) contained in fluorocapteurs, nylon pop socks tethered with strong nylon cord placed below the stream surface in flowing but not turbulent sections of the resurgences. Where this was not possible, the fluorocapteurs were placed inside a section of black motorcycle inner tube which permitted flow through but not exposure to daylight which might lead to photo decay of the tracer.

After removal from the field site the samples were labelled and isolated in a sealable plastic bag, dark container. The procedure of eluting the charcoal was carried out as soon as possible after removal to minimise any organic growth on the charcoal or photo decay of the fluorescein traces. The samples were washed to remove any organic debris and air dried. The eluent used was an equal mixture of de-ionised water and iso-2-propanol alcohol, 10 ml of each. 1.0 gram of potassium hydroxide flakes was then dissolved in the mixture. Eluting was done by adding 7.5 grams of the charcoal sample to 20 ml of the eluent in a 140ml Pyrex beaker, the mixture was then heated on a portable hot plate, allowed to boil for 1 minute and then cool in subdued light (Hardwick, 2019). The solution with charcoal was kept in darkness then observed at 15-minute intervals by shining a LED torch at 90 degrees (Fig. 3) to the viewing angle to establish whether there was evidence of fluorescence (ALEY, 2002).

3. Results

Testing of the seven sinking streams revealed the following results these can be seen below in figure 2.

DATE TESTED IN AUGUST	SINKING STREAM	FALL TO Moses Well	RESURGENCE, POSITIVE, NEGATIVE, VARIABLE.			
			Clapham Beck Head	Cat Hole	Moses Well	Newby cote spring
10.	Fluted Hole	269	*Variable*	*Negative*	*Positive*	*Variable*
24	Grey Wife Hole	221	*Positive*	*Negative*	*Variable*	*Positive*
01	Newby Moss Cave	218	*Positive*	*Variable*	*Variable*	*Not tested*
13	P2A	248	*Variable*	*Variable*	*Positive*	*Variable*
20	P2B	245	*Positive*	*Negative*	*Variable*	*Variable*
29	Hurnel Ridge Sink	169	*Negative*	*Negative*	*Positive*	*Positive*
08	Pillar Holes	248	*Variable*	*Variable*	*Positive*	*Variable*

Figure 2: Results from seven sink holes using artificial tracer after eluting the tracer from the carbon fluorocapteurs and conducting a visual test. The term variable indicates where test was neither negative or positive and therefore, inconclusive.

Unfortunately, it was not possible to fully complete a comprehensive laboratory testing of the samples using a spectrofluorometer.

Figure 3: Demonstrates a strong positive trace after elution by shining a LED light in a dark room at rightangles, four days after the tracer was introduced to Fluted Hole.

The results from the artificial tracer testing demonstrates that Newby Moss underground flow is not constrained to the Newby Moss area alone shows that sink holes northeast of the Clapdale Fault also flow to Clapham Beck Cave (Fig. 4). Equally, sink holes southwest of the Clapdale Fault; Pillar Holes, Fluted Hole and P2A, whilst having a strong positive result in Moses Well have some albeit restricted flow towards Clapham Beck Head.

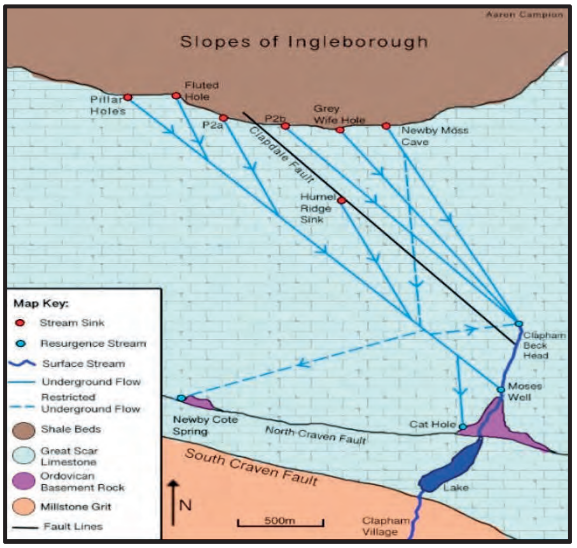

Figure 4: Shows direction of flow from sinking streams to resurgences confirmed by the artificial tracer exercise. These sites had never previously been tested. The restricted flows are confirmed by the variable results from the eluting exercise.

4. Conductivity, pH, and temperature measurements

The lower temperature of Moses Well water reflects the longer time the water was in residency compared to the water in Clapham Beck Head. The higher values at Cat Hole may be due to the extremely slow- moving discharge, the water having an opportunity to warm up in the ambient temperature just inside the cave entrance. The conductivity and pH of the water resurging at valley level was considerably higher than the water sinking high on the fell. Similarly, higher water temperatures were recorded at recharge compared to water temperatures at the resurgences. Despite some of the variables discussed above, the data demonstrates that high levels of dissolution exist in the cave water when it reaches Moses Well and Cat Hole resurgences (Fig. 5).

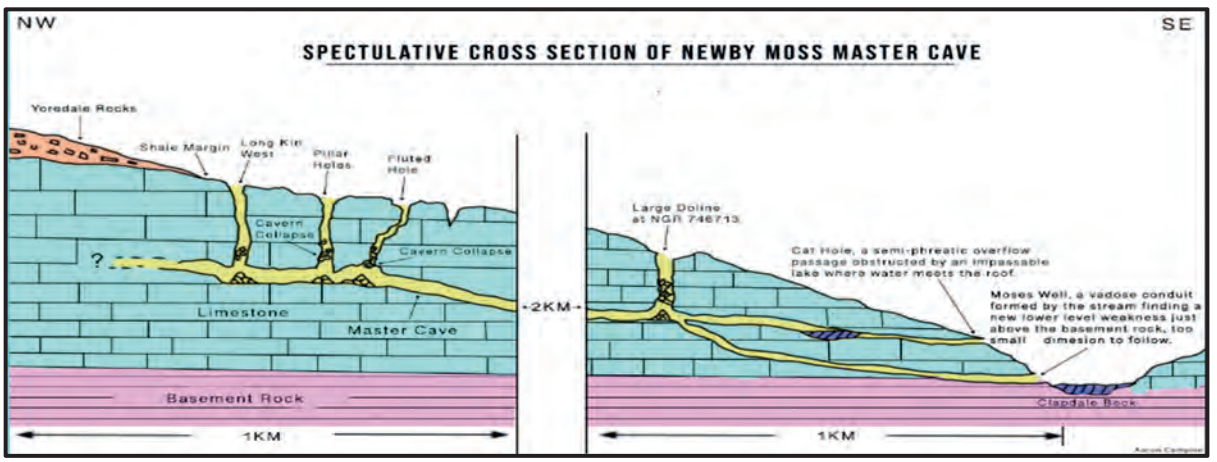

Figure 5: Speculative cave system approximately 4 km in length with a vertical range of 222 Metres from Long Kin West to Moses Well.

5. Conclusion

There is therefore considerable evidence to suggest that an extensive cave system exists beneath Newby Moss on the Southern slopes of Ingleborough. Mapping has shown that Newby Moss has the advantage of being in the protected lee of Ingleborough Hill, where there has been only minor glacial erosion, and very little shale retreat which makes the

likelihood of both active and fossil caves beneath the surface likely.

Evidence from water samples indicate that high levels of carbonation taking place between the stream sinks on the fells and the discharges in the valley. The sinking streams provide a source of allogenic recharge percolation and the continual through the soils continuous autogenic recharge, both of which will play a major part in the continuing development of underground conduits and cave passages. The water discharging from Moses Well and Cat Hole compared to Clapham Beck Head shows a longer residency period in the system beneath Newby Moss allowing considerable opportunity for dissolution of the bedrock. Comprehensive artificial tracer testing was able to demonstrate positive hydrological connections between the main sinking streams on Newby Moss and the valley resurgences.

Building on the knowledge of this study will hopefully lead to further work to assist those who continue the tradition of exploration and scientific enquiry of caves. In the fullness of time, the hard work of explorers will help unravel the secrets of the cave system beneath Newby Moss and finally reveal what PEARSON (2018) has aptly described as the 'Lost River of Ingleborough'.

Bibliography

ACLAND E.F.D. & WILCOCK J. (1969) The Eastern Edge of Newby Moss and Grey Wife Hole. *Kendal Caving Club,* 4, 28-30.

ALEY T. (2002) *Ozark Underground Laboratory's Groundwater Tracing Handbook* [booklet]. Ozark Underground Laboratory.

BECK H.M. (1984) *Gaping Gill 150 years of exploration*, Robert Hale, London.

BENSLEY B. & CAMPION G. (2005) Newby Moss Cave. *Yorkshire Ramblers Club Bulletin, 24 Winter 2005*, 26-28.

BRITISH GEOLOGICAL SURVEY (2020) [Geology of Britain Viewer] 1:50:000. Available online: http://mapapps.bgs.ac.uk/geologyofbritain/home.html?location=clapham [Accessed 29/01/20].

BROOK A., GRIFFITHS J & LONG M.H. (1991) *Northern Caves 2: The Three Peaks.* Clapham, The Dalesman.

CARTER W.L. & CASH W. (1904) Proceedings of the Yorkshire Geological and Polytechnic Society. *The underground waters of Northwest Yorkshire,* II, Leeds: Chorley & Pickersgill.

DRACUP C. (1969) Newby Moss Pot. *Gritstone Club*, 3-8.

DONNAN W. H. (1952) Some notes on discharge measurements in small streams. *Newsletter Cave Research Group,* 40, 7-15.

FIELD M.S., WILHELM R.G., QUINLAN J. F. & ALY T. J. (1995) An assessment of the potential adverse properties of fluorescent tracer dyes used for groundwater tracing. *Environmental monitoring and assessment,* 38, 75-96.

FORD D. & WILLIAMS P. (2007) *Karst Hydrology and Geomorphology.* Chichester: Wiley & Sons.

GUNN J. & KELLY J.T. (2017) Underground flow-paths in the Malham Karst, England: Part 1, artificial tracer experiments. *Cave and Karst Science,* 44 (1), 5-16.

HARDWICK P. (2019) *Water tracing: a guide for cavers.* BCRA, Limestone Research and Consultancy ltd.

HARRISON T. (2013) Underground watercourses beneath the Swaledale/Wensleydale surface watershed. Yorkshire Dales UK: a review and extension of tracer dye-test data. *Cave and Karst Science,* 40(2), 62-72.

HEAP D. (1964) *Potholing: Beneath the Northern Pennines.* London: Routledge and Kegan Paul.

KASS W. (1998) *Tracing technique in geohydrology.* Rotterdam, Balkema.

MITCHELL W. (2013) Glaciation and Quaternary evolution. In Waltham, T. & Lowe, D. *Caves and Karst of the Yorkshire Dales.* Nottingham: British Cave Research Association, 29-64.

NUNWICK M. & YEADON J. (2000) The Health Farm on Newby Moss. *Descent,* 156, 28-30.

PEARSON F. (2018) Long Kin West and the lost river of Ingleborough. *Descent,* 264 October/November 19-23.

PITTY A. F. (1968) Some notes on the use of calcium hardness measurements in studies of cave hydrology. *Symposium on Cave Hydrology and Water-tracing,* 10(2), 115-120.

RODGERS P. C., STRAUGHTON E.A., WINCHESTER A.J.L. & PIERACCINI M. (2011) *Contested Common Ground Environmental Governance Past and Present.* London: Earthscan.

SMART P.L. & LAIDLAW I.M.S. (1977) An evaluation of some fluorescent dyes for water tracing. *Water Resources,* 13, 15-23.

SMART C. & SIMPSON B. (2002) Detection of fluorescent compounds in the environment using granular activated charcoal detectors. *Environmental Geology,* 42, 538-545.

WALTHAM T & DAVIES M. (1987) *Caves and Karst of the Yorkshire Dales: A field guide.* Sherwood Press, BCRA.

WALTHAM T. & LONG H. (2011) Limestone plateaus of the Yorkshire Dales glaciokarst. *Cave and Karst Science,* 38, 68-70

WALTHAM T. & MURPHY P. (2013) Cave geomorphology. In Waltham T. & Lowe D. (ed) *Caves and Karst of the Yorkshire Dales*. Nottingham, British Cave Research Association, I, 117-146.

WALTHAM T. & BROOK G. (2017) Caves of Ingleborough. In Waltham T. & Lowe D. (ed) *Caves and Karst of the Yorkshire Dales*. Nottingham, British Cave Research Association, II, 349-362.

WILCOCK J. (2002) The Science of Dowsing for Caves. *Caves & Caving,* 92, 33-37.

YEADON G. (1971) Another 12 months on Newby Moss. *Kendal Caving Club,* 6, 57-58.

L'âge des gorges de l'Ardèche révélé par la « rivière souterraine fossile de Saint-Remèze » et données nouvelles sur les remplissages tortoniens

Jacques MARTINI

Saint-Remèze, France. Email : jacquesmartini07@orange.fr

Résumé

Cette note fait office d'addenda à un article publié par l'auteur en 2019 : discussions et controverses sur l'âge du creusement des gorges de l'Ardèche en fonction de l'évolution d'une rivière souterraine fossile et de la géomorphologie régionale ; découverte d'un petit remplissage karstique fossilifère de l'âge de la limite mio-pliocène, contenant des molaires tortoniennes remaniées. Des hypothèses sur l'évolution du karst à cette époque sont proposées.

Abstract

The age of the Ardèche River Gorges revealed by the "Saint-Remèze fossil underground river": new data on Tortonian fillings. This article is dealing with two topics concerning the Saint-Remèze karst. The first one is treating the genesis of the Saint Remèze fossil undergound river and of the Ardèche River Gorges, for which some authors advocate a formation almost entirely during the Salinity Crisis. The validity of this model is debated by the author. The second topic deals with a new fossiliferous karst filling, contemporary with the Miocene-Pliocene boundary, but which revealed reworked Tortonian rodent molars. Hypotheses are proposed about the local karst evolution during this last stage.

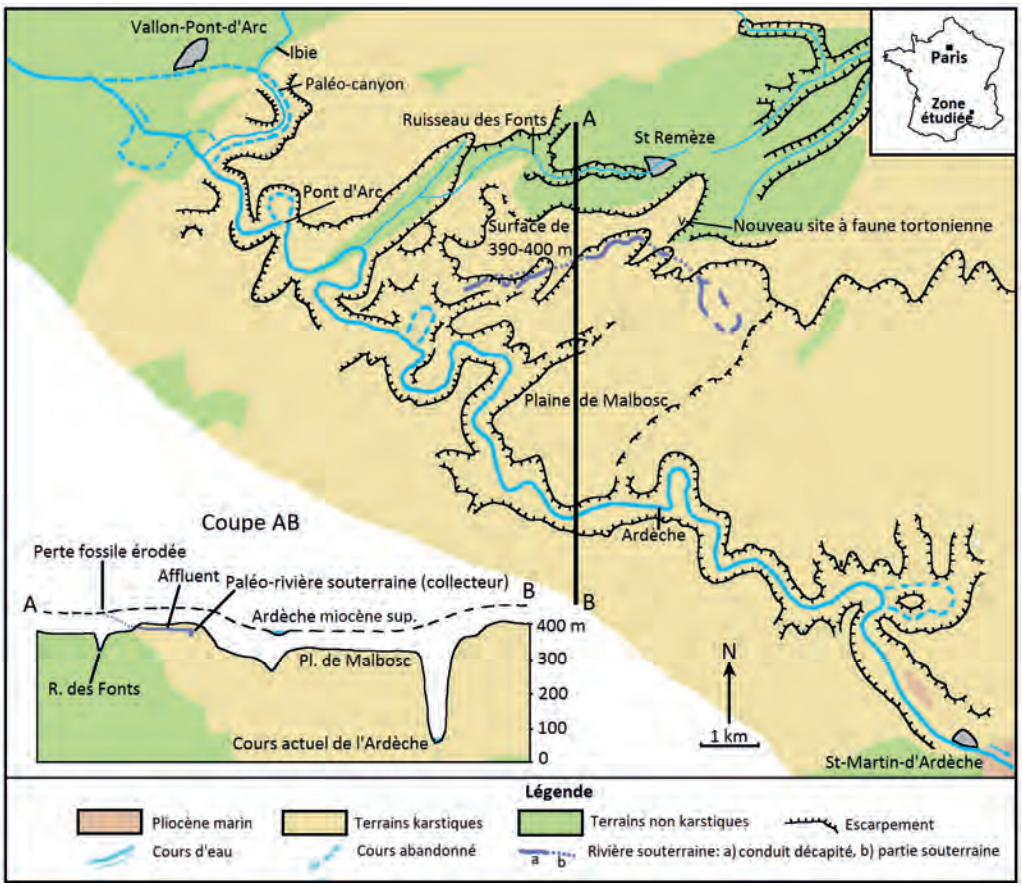

Figure 1 : Contexte géologique, géomorphologique et topographique des gorges de l'Ardèche.

1. Introduction, la « rivière souterraine fossile de Saint-Remèze »

Cette ancienne rivière souterraine du Sud de la France (Fig. 1) est principalement représentée par des segments d'une galerie fossile décapitée, observée sur une longueur de 5,2 km et à altitude constante, ce qui suggère le contrôle par un ancien niveau hydrostatique. Elle a été alimentée par une perte partielle de l'Ardèche, alors que cette dernière coulait 305 m plus haut que son cours actuel (Fig. 2). À la fin de sa période active, après un petit abaissement de l'Ardèche, elle n'avait plus été alimentée que pendant les crues par des eaux boueuses, chargées d'alluvions, qui ont progressivement colmaté le conduit. Le présent article fait office d'addenda à une récente publication (MARTINI 2019) et traite de deux sujets distincts : premièrement de l'âge de la formation des gorges de l'Ardèche, lequel a été discuté par les partisans d'une genèse presque entièrement messinienne et par ceux en faveur d'une formation échelonnée de la fin du Miocène à actuellement, et deuxièmement d'une nouvelle occurrence renfermant des fossiles tortoniens remaniés.

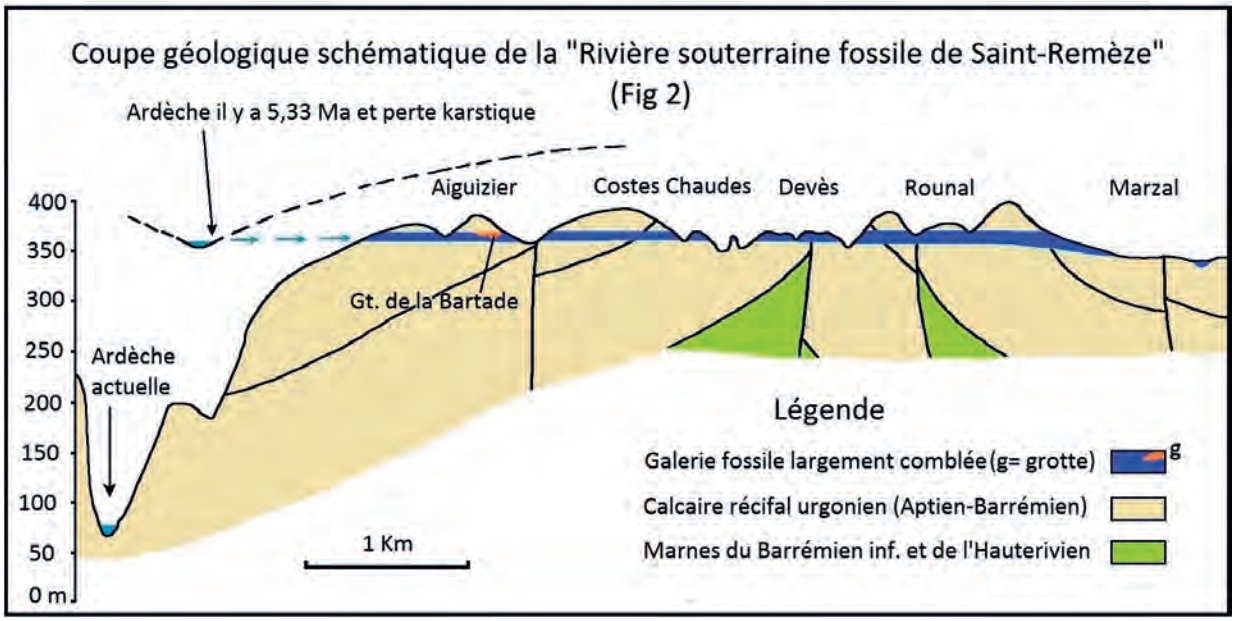

Figure 2 : Coupe géologique de la rivière souterraine fossile et des gorges de l'Ardèche.

2. La chronologie de la formation des gorges de l'Ardèche

La phase finale de la genèse de la rivière souterraine fossile a été datée par la paléontologie comme proche de la limite mio-pliocène, soit 5,33 Ma, (MARTINI 2019). Ces données ont permis de comprendre le déroulement du creusement des gorges. Comme 5,33 Ma représente l'âge de l'assèchement de la perte alimentant la rivière souterraine et aussi celui de la remise en eau de la Méditerranée, il est apparu, que le creusement des gorges avait débuté au Messinien (Fig. 3). En effet le front du cycle d'érosion avait simultanément atteint la sortie des gorges et la perte de la rivière souterraine. Comme il s'est avéré, qu'un peu plus du tiers des gorges a été creusé au Messinien, en amont de la perte le reste de la glyptogenèse ne pouvait être que pliocène et quaternaire.

Cependant ce modèle s'oppose en partie à celui de MOCOCHAIN et *al* 2009, qui a été inspiré par un cours abandonné de l'Ardèche, perché à environ 20 m au-dessus de son cours actif virtuel et actuellement emprunté par l'Ibie (Fig.1). Ce dernier renferme des reliques alluviales, que ces auteurs estimèrent pliocènes, lesquelles auraient rempli un paléo-canyon, qui serait donc messinien. Par sa situation à l'entrée des gorges, ils en déduisirent, que ces dernières ont été presqu'entièrement creusées encore au Miocène. Mais on se heurte à des problèmes. L'âge pliocène du remplissage ne semble pas fermement établi, car ce dernier ne renferme pas les caractéristiques d'un environnement marin, alors que les gorges auraient été transformées en une ria à partir de la limite mio-pliocène. Cependant, d'après ces auteurs, les influences marines ont été réelles, mais ne sont pas exprimées à cause de la nature grossière du gravier. Pourtant, l'unique affleurement de Pliocène marin, situé dans les gorges peu avant leur sortie (Fig. 1 et 3, cité dans MARTINI 2019), n'est pas conglomératique, mais présente son faciès argileux marin typique. Néanmoins, comme ces auteurs estiment que les alluvions avaient complètement rempli le paléo-canyon, elles seraient quand même pliocènes. Cette preuve d'un complet remplissage alluvial semble également fragile, car les témoins alluvionnaires sont réduits à des poches karstiques dispersées. Il faut aussi remarquer, que si ce paléo-canyon était messinien, en aval de ce dernier on devrait observer un lit actuel sur le Pliocène, lequel aurait pu être argileux à graveleux. Mais dans les gorges le lit repose sur calcaire urgonien. Donc on ne peut pas écarter leur origine par érosion et redistribution de ces graviers à partir des terrasses pléistocènes. Ainsi, il

apparaît que ces graviers ne peuvent pas constituer une preuve axiomatique en faveur d'un âge de formation presque entièrement messinien.

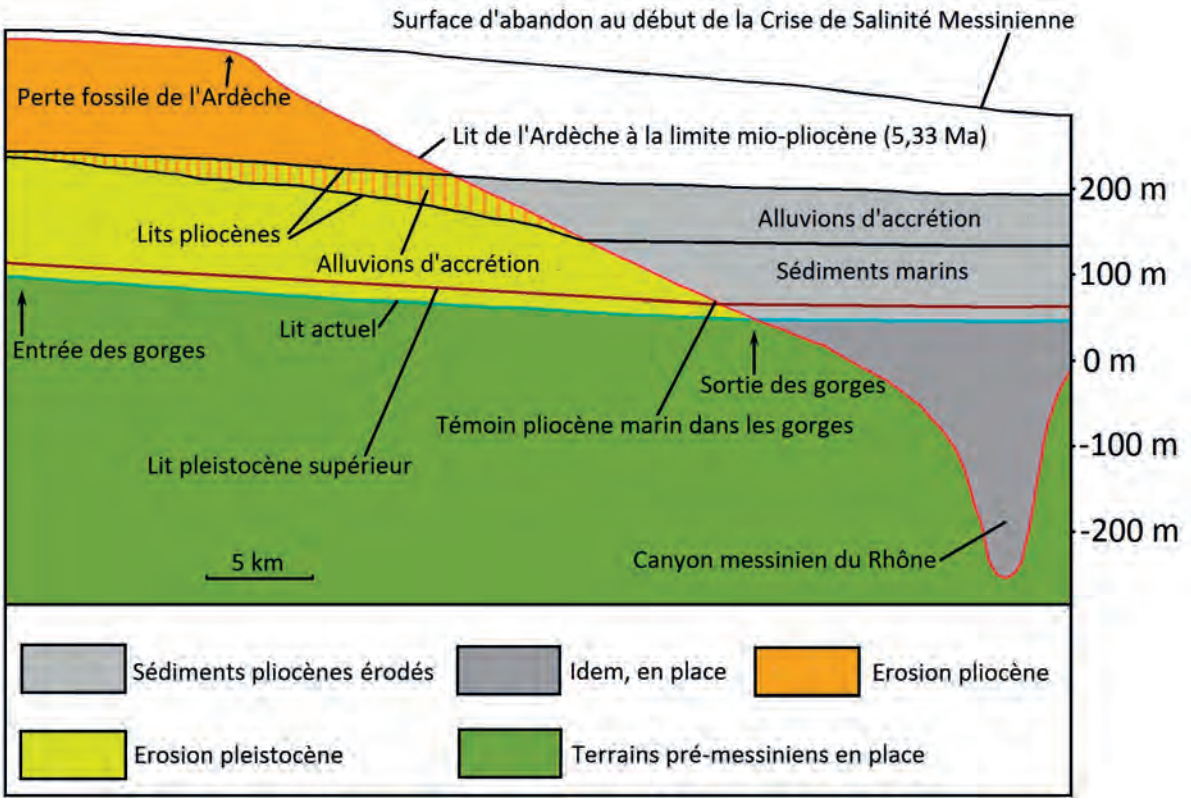

Figure 3 : Diagramme des phases de creusement des gorges de l'Ardèche.

Afin de déterminer lequel de ces deux âges s'avère possible, avec l'aide de la géomorphologie observée, on peut construire un profil du lit, que l'Ardèche a été forcée d'adopter. Le fond de ce paléo-canyon passait à l'altitude de 100 m et à environ 20 m au-dessus de son cours actif, une valeur estimée par extrapolation à partir de la confluence de l'Ibie avec l'Ardèche. Comme son fond ne surmontait que de peu ce cours extrapolé, en aval le lit fossile doit avoir reposé sur calcaire urgonien pour toute la longueur des gorges. En effet, comme le lit actuel est rocheux, avec un gradient de 1,0 m/km, le lit fossile sus-jacent n'a pu dévier de cette valeur que de quelques dixièmes de mètres. Si l'évolution de l'Ardèche est interprétée en fonction de ce lit virtuel, il apparaît qu'une grande épaisseur de calcaire devait avoir été érodée, puisqu'il ne restait que 20 m à enlever au-dessus du lit actuel. On peut en conclure, que la formation des gorges était presque achevée. Donc il s'avère logique d'attribuer un âge pléistocène supérieur à ce lit (Fig. 3). S'il était messinien, ces 20 m restants auraient représenté une érosion pliocène-quaternaire d'une minceur surprenante. Donc il semble que le paléo-canyon n'a pas été abandonné au Messinien, mais beaucoup plus tardivement.

D'autres faits confortent ce modèle pléistocène supérieur. À la sortie des gorges, ce lit virtuel reposait encore sur l'Urgonien. Mais un peu plus en aval, il a dû atteindre les sédiments pliocènes, qui renferment un réel lit messinien sous leur base. Si ce lit pléistocène supérieur était encore miocène, il devrait se poursuivre par ce lit fossile, car il ne pourrait pas reposer sur des terrains plus jeunes que lui. Le gradient de ce lit fossile a été estimé à 14 m/km, soit celui d'une droite synchrone de 5,33 Ma, reliant la perte à la sortie des gorges (MARTINI 2019). Mais à sa « jonction » avec ce lit messinien fossile, il se produit une rupture de pente suggérant qu'il s'agit plutôt d'un recoupement de deux lits d'âges différents. Si le paléo-canyon était messinien, une intersection de lits devrait s'observer à l'entrée des gorges, mais pas à leur sortie. Alternativement on pourrait supposer qu'en amont de cette dernière, l'Ardèche aurait amplifié sa vitesse d'érosion, afin d'abaisser le gradient de son lit de 14 à 1 m/km. Cette solution est absurde, à moins d'admettre que l'Ardèche a bénéficié d'un temps plus long pour aplanir son lit. C'est très probablement ce qui s'est produit. Cependant pas seulement pendant la crise de salinité messinienne (une partie de 0,63 Ma), mais surtout lors du Pliocène et du Quaternaire (5,33 Ma). Toutefois ce temps a été amoindri par des périodes d'accrétion (Fig. 3), mais compensé par des allongements : alors que la vitesse d'érosion de la rivière chutait progressivement en fonction de la décroissance du gradient de son lit, soit un déclin de 14 à 1 m/km, le temps s'accroissait (temps = partie érodée /vitesse d'érosion). Pour aplanir son lit encore au Messinien, la contribution de l'érosion pliocène-quaternaire aurait été de nouveau très sous-estimée : il serait surprenant, que durant 5,33 Ma, l'Ardèche ait presque cessé de couler. Le fait que le lit

reposant sur le Pliocène ne soit pas remonté de la sortie des gorges jusqu'au paléo-canyon, incite à penser, sans calculs sophistiqués, que l'âge de ce dernier ne peut pas être messinien. Néanmoins, si à l'avenir des preuves nouvelles en faveur d'une genèse principalement messinienne auront été mises en évidence, l'auteur de ces lignes sera amené à modifier ses opinions.

3. Un nouveau remplissage karstique à faune tortonienne

En 2020 l'auteur a investigué une occurrence fossilifère située à environ 500 m au NE du site de Rounal I (Fig. 1, 2). Elle consiste en fragments épierrés de grès mature et de spéléothèmes, épars sur un périmètre restreint, traversé par un chemin important. Le gisement en place n'a pas été excavé, mais pourrait être associé à une petite doline. Le grès n'a livré que 7 molaires déterminables : $1M_1$ d'*Apodemus dominans*, $2M_1$ d'*A. gorafensis-jeanteti* et $1M_2$ d'*Occitanomys* cf *adroveri* ; cette association suggère une faune proche de la limite faunistique MN 13-14, donc de l'âge de la limite mio-pliocène communément rencontrée dans les remplissages karstiques des environs de Saint-Remèze ; les 3 autres molaires consistent en $1M^1$ d'*Hispanomys mediterraneus* , $1M^2$ et $1M^3$ de *Progonomys* cf *cathalae*; ces deux dernières molaires, d'après leurs tailles relativement grandes, peuvent appartenir à la même espèce que celle rencontrée à Rounal 1 et dans les gisements 2 et 4 des Arredons, c'est à dire à "*P.* cf. *cathalae*", une forme distincte de l'espèce type. Ces 3 molaires suggèrent la zone MN 10 (Tortonien moyen). Cette faune a été remaniée dans la première, soit celle de la limite MN13-14, car le grès est très riche en magnétite fine, d'origine basaltique (voir MARTINI 2019 pour la signification stratigraphique de ce minéral).

À remarquer que cette nouvelle occurrence, renfermant des molaires tortoniennes, augmente son nombre de 3 à 4 sur le territoire communal, ce qui pourrait plus fermement suggérer une décroissance d'activité karstique locale à cette époque. En plus, l'altitude de ces poches est voisine de celles associées à la limite mio-pliocène, bien que la différence d'âge des fossiles s'élève à environ 4 Ma. Cependant, il faut considérer qu'ailleurs d'autres cas de karsts à développement apparemment ralentis ont été observés, également basés sur la paléontologie. Par exemple l'étude des gisements de la surface d'érosion des Corbières, dans l'extrême Sud de la France, située dans des conditions climatiques et géologiques comparables, a suggéré que cette dernière est restée inchangée pendant plus de 20 Ma (CLAUZON 1990). Pour le karst de Saint-Remèze, il a été proposé (MARTINI 2019), que ce ralentissement apparent serait dû au développement de conditions crypto-karstiques en relation avec des recouvrements intermittents par les ultimes dépôts alluviaux du bassin molassique local à la fin du Miocène. Les affleurements auraient été érodés, mais après pédogenèse, auraient représenté la source du matériel détritique mature des remplissages karstiques de Saint-Remèze.

Références

CLAUZON G. (1990). Restitution de l'évolution géodynamique néogène du bassin du Roussillon et de l'unité adjacente des Corbières d'après les données écostratigraphiques et paléogéographiques. *Paléobiologie continentale, Montpellier*, XVII, 125-155.

MARTINI J. (2019). Données nouvelles sur la « rivière souterraine fossile de Saint-Remèze » : modèles spéléogéniques et évolution morphologique régionale du Sud-Ardèche au Néogène supérieur. *Karstologia* n° 74, 15-30.

MOCOCHAIN L., AUDRA P., CLAUZON G., BELLIER O., BIGOT J.-Y., PARIZE O. and MONTEIL P. (2009). The effect of river dynamics induced by the Messinian Salinity Crisis on landscape and caves: example of the Lower Ardèche River (mid Rhône valley). *Geomorphology*, 116 (1), 46-61.

Géomorphologie des vides et remplissages de la grotte touristique de Saint-Marcel d'Ardèche (France) : Construction de clés de lecture comme support de médiation scientifique

France DUBICH, Elodie LECORNU, Jean-Jacques DELANNOY & Stéphane JAILLET

Laboratoire EDYTEM, Université Savoie Mont Blanc, CNRS, Avenue de la Mer Caspienne, 73376 Le Bourget du Lac (France)

Résumé

La grotte de Saint-Marcel d'Ardèche a fait l'objet de nombreuses recherches spéléogénétiques et paléogéographiques associées à la crise messino-pliocène. Si ces travaux ont fait l'objet de publications, ils ne se sont guère adressés au public qui visite la partie touristique de la grotte et les premiers systèmes spéléologiques. C'est dans cet esprit que cette communication est faite. Elle s'appuie sur ce contexte karstogène déjà bien connu tout en s'appuyant sur les indices et arguments spéléologiques présents dans la partie touristique de la grotte. Les observations de terrain (cartes et coupes géomorphologiques, photos commentées) ont été réalisées (i) à l'échelle des principaux vides souterrains (morphologies d'emboîtement et dépôts endokarstiques) et (ii) à plus haute résolution sur les dépôts carbonatés, spécifiquement le gour de la galerie Boas. Les résultats de l'étude visent à proposer (i) une reconstruction de l'évolution spéléogénique de la section touristique, (ii) une chronologie relative de la mise en place du gour en fonction des variations hydro-climatiques et (iii) une suggestion des morphologies particulières associées aux gours. Au final, les données acquises fournissent aux visiteurs des clés de lecture et élargissent le discours de médiation tel que voulu par la société de gestion.

Abstract

Geomorphology of emptiness and cave deposits of the touristic cave of Saint-Marcel d'Ardèche (Ardèche France). Construction of reading keys as a support for scientific mediation. The cave of Saint-Marcel d'Ardèche has been the subject of numerous speleogenetic and palaeogeographic research associated with the Messino-Pliocene eustatic crisis. If these works have been the subject of publications, they hardly have been directed towards the public who visit the tourist part of the cave and the first speleological systems. It is in this spirit that this communication is made. It is based on this already well-known karstogenic context while relying on clues and speleogenic arguments present in the tourist part of the cave. Field observations (geomorphological maps and cross sections, commented photos) were made (i) at the scale of the main underground voids (interlocking morphologies and endokarstic deposits) and (ii) at a higher resolution on carbonate deposits, specifically the gour in the Boas Gallery. The results of the study aim to propose (i) a reconstruction of the speleogenic evolution of the tourist section, (ii) a relative chronology of the setting up of the gour according to hydro-climatic variations and (iii) a suggestion of the particular morphologies associated with the gours. In the end, the data acquired provides visitors with reading keys and broadens the mediation discourse as intended by the management company.

1. Introduction

À l'image de nombreuses cavités du sud Ardèche, la grotte de Saint-Marcel-d'Ardèche (France) a fait l'objet de plusieurs recherches sur sa spéléogenèse. Celles-ci ont révélé des morphologies souterraines spécifiques témoignant d'un ancien fonctionnement paragénétique lié à la crise eustatique messino-pliocène (DELANNOY *et al.*, 2007 ; MOCCOCHAIN *et al.*, 2007, 2008 ; JAILLET *et al.*, 2007 ; SADIER *et al.*, 2007). Toutefois, en-dehors des recherches visant à définir le contexte paléogéographique régional, aucune recherche géomorphologique dédiée à l'évolution spéléogénique tout en proposant un focus sur des dépôts carbonatés inactifs n'a été réalisée. C'est face à ce manque d'informations et à la demande de la société de gestion de la grotte de Saint-Marcel-d'Ardèche que ce travail s'est conduit.

Ainsi l'accent est mis sur la lecture spéléogénique et la reconstitution des événements à l'origine de la facture des paysages souterrains actuels ; (i) à l'échelle de la partie aménagée et (ii) à plus haute résolution sur les dépôts carbonatés inactifs (gours) de la galerie des Boas. Ce secteur, en dehors de la partie touristique, a été préféré pour ses emboitement de plusieurs générations de gours permettant une lecture fine de leur morphogénèse.

Avec comme point de départ un contexte karstogénique déjà reconnu, cette étude vise, à partir d'indices et

raisonnements spéléogéniques, à retrouver les principaux témoins de l'évolution géomorphologique de la cavité.
Pour ce faire, les observations de terrain sont reportées sur des cartes et coupes géomorphologiques ainsi que des photos commentées. Les différents résultats aspirent à proposer (i) une chronologie relative de l'évolution géomorphologique de la galerie touristique, (ii) une seconde chronologie relative recentrée sur les gours afin de suivre les variations des paléo-écoulements, (iii) accompagnée d'une description des amorces de gours particulières. *In fine*, les données acquises et supports de réflexion sont transmis à la société de gestion de la cavité et constituent une base de médiation touristique.

2. Méthode et résultats

Le choix des supports de réflexion s'est fait de façon à ce qu'ils conviennent aux relevés de terrain et à la reconstitution géomorphologique des espaces étudiés, tout en étant suffisamment clairs et visuels en vue d'une médiation scientifique par la société de gestion de la cavité. Pour cela, le choix s'est porté sur la réalisation (i) d'une cartographie géomorphologique (galerie des Boas) élaborée à partir d'un fond 3D, (ii) de coupes géomorphologiques au sein des différents secteurs de la partie touristique et enfin (iii) de photographies commentées. La légende de la carte et des coupes géomorphologiques s'est inspirée de celles utilisées à la grotte Chauvet (DELLANOY *et al*., 2020) ou encore à l'Aven d'Orgnac (JAILLET *et al.,* 2007) et a évolué en fonction des besoins de représentation.
La réalisation des coupes géomorphologiques, transversales et longitudinales, au sein des différents secteurs de la cavité a permis de construire une chronologie relative de chacun d'entre eux et a mis en avant une analogie des mémoires souterraines de la partie touristique.

Genèse et évolution géomorphologie de la galerie touristique :
Dans un premier temps, l'ancien fonctionnement paragénétique et le creusement *per ascensum* des réseaux souterrains se lisent dans l'ensemble des galeries étudiées, au travers des banquettes limites, vagues d'érosion, coupoles de voûte et de paroi de même que par la présence de nombreux placages d'argiles (Figure 1.2). Ces morphologies sont les témoins de la hausse du niveau de base due à la transgression pliocène et à l'aggradation continentale. Par la suite, l'abaissement du niveau de base instaure une nouvelle dynamique souterraine avec l'apparition d'écoulements en surface libre. Mise en place vers la fin du Pliocène, début du Quaternaire, cette dynamique a permis le décolmatage progressif, parfois partiel, des galeries de la grotte. Ainsi, le remaniement des argiles paragénétiques laisse place à d'imposants volumes souterrains en proie aux réajustements mécaniques. De cette façon, le toit des galeries se relève à mesure que les phénomènes gravitaires ont lieu (Figure 1.3). Suite à ces évènements, des blocs effondrés, en amas ou isolés, sont encore visibles au sein des différents secteurs visités. Les dépôts carbonatés, très présents dans le paysage souterrain, se mettent majoritairement en place à la suite des réajustements mécaniques. Toutefois, une première période de formation a pu se dérouler de manière conjointe à la période de détente mécanique, notamment dans le secteur de la Salle de la Cathédrale (Figure 2). Enfin, des ruissellements incrustants se développent à partir des spéléothèmes et entraînent la formation de gours, caractéristiques des paysages souterrains de la grotte étudiée.

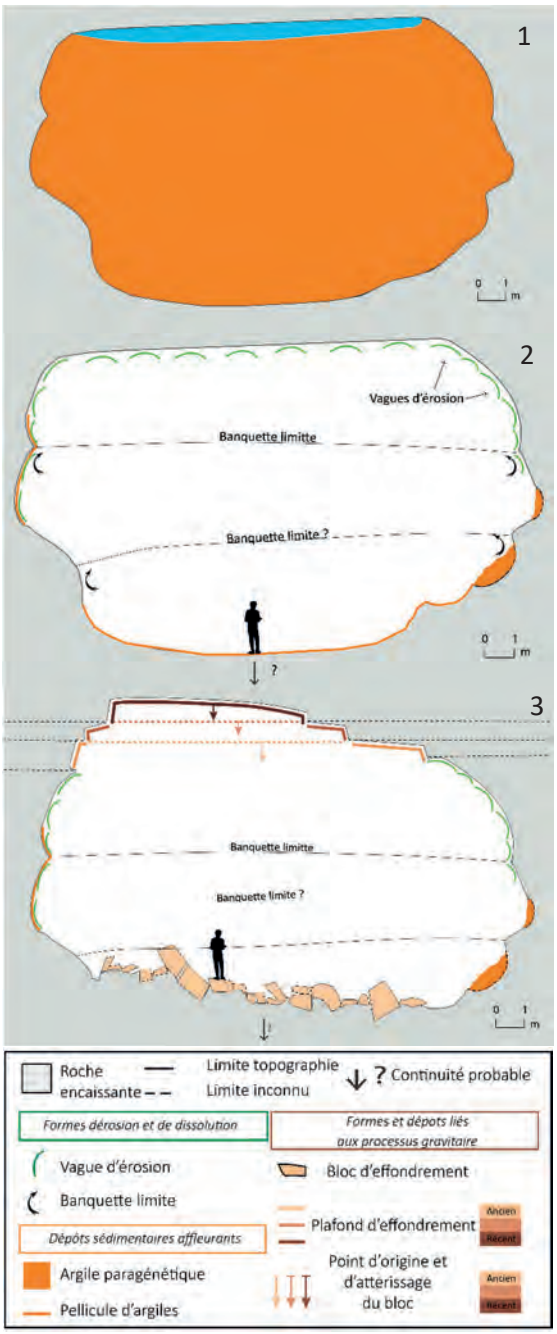

Figure 1 : Coupe géomorphologique évolutive de la galerie des Peintres, Dubich F.

Figure 2 : Illustration d'un bloc effondré au bas de la salle de la Cathédrale, Dubich F. L'imbrication des différentes morphologies présentes sur ce bloc effondré a permis de consolider la chronologie de la salle de la Cathédrale. En vert et orange sont représentés une vague d'érosion et un dépôt d'argile, tous deux constituant une archive du creusement paragénétique de la cavité. Le violet clair, retrace les coulées stalagmitiques développées antérieurement à la chute du bloc. Enfin, le violet foncé souligne la trace d'un ancien niveau d'eau, lié au fonctionnement des gours de la salle avant son aménagement.

Morphochronologie des ruissellements incrustants ; les gours de la galerie des Boas :

La dernière phase d'évolution de la grotte de Saint-Marcel d'Ardèche a généré des dépôts carbonatés, dont la majorité sont des gours. De morphologies et d'âges différents, ces spéléothèmes sont comparables à des barrages issus d'écoulements laminaires fins (GEZE, 1973 ; CHOPPY, 1985 ; SALOMON, 2000 ; GILLI, 2011). Leur formation résulte de la mise en relation de trois facteurs principaux : le débit de l'écoulement, le pourcentage de la pente et la rugosité du sol (DELANNOY et *al*., 2013). La prédominance d'un ou plusieurs de ces facteurs s'enregistre dans la morphologie et l'emboîtement des gours.

En début de croissance, la morphologie et quelquefois l'orientation d'un gour sont davantage influencées par la rugosité. Dans la galerie des Boas et plus généralement dans le réseau 1 de la grotte de Saint-Marcel d'Ardèche, deux rugosités se distinguent ; (i) une forte concentration d'amorces de stalagmites actives et (ii) des fissures encroûtées renflées de quelques centimètres.

Les premières morphologies de gours, centimétriques et assez distinctes entre elles, s'harmonisent durant leur développement. Dans le même temps, le nombre de gours actifs diminue progressivement. La pente et les variations d'intensité de l'écoulement en sont les principaux responsables. Le premier conditionne le sens principal du concrétionnement (horizontal en faible pente et vertical en pente prononcée) et le second provoque l'ennoiement ou l'assèchement de certains gours produisant alors plusieurs générations de gours actifs.

Construire une chronologie relative des dynamiques des paléo-écoulements passe par la recherche des principales générations de gours en s'appuyant sur des clés de lecture morphologiques. La hauteur, l'orientation et l'état de conservation des gours, ajoutés à des dépôts de calcite linéaire correspondant à des paléo-niveaux d'eau, constituent les principaux indices morphologiques recensés et employés.

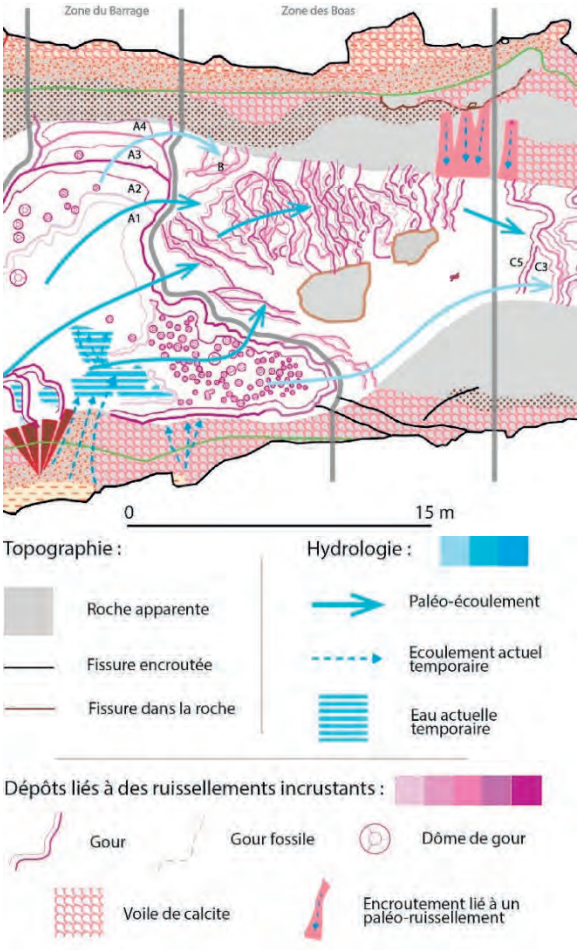

Figure 3 : Variation d'intensité du principal paléo-écoulement de la galerie des Boas, Lecornu E.

Au total cinq générations de gours (violet clair la plus ancienne et violet foncé la plus récente) recouvrent le sol de la galerie des Boas (Figure 3). La dernière génération en activité (« génération 5 »), définit à l'échelle de la galerie par les gours les plus haut, limite l'utilisation des clés de lecture morphologiques. Semblables à des obstacles, les gours de « génération 5 » empêchent parfois la mise en relation entre gours de générations plus anciennes. De ce fait, la galerie est dissociée en quatre secteurs (Coude, Barrage, Boas, Replat) où des chronologies relatives distinctes sont construites pour les générations anciennes (Figure 3).
Concernant le principal apport en eau alimentant les quatre secteurs de la galerie des Boas, les gours nommés « A » soulignent une hausse de l'intensité de son écoulement occasionnant une avancée progradante des gours de la zone du Barrage (Figure 3). Le paléo-écoulement alimente alors l'ensemble des gours présents dans la galerie. L'orientation et l'âge des gours « B » (« génération 3 »), ainsi que la réorientation du gours « C3 » en « C5 » attestent d'une baisse de l'intensité de ce même écoulement au niveau du gour A2 redevenu un gour de « génération 5 » (Figure 3). Ainsi, le paléo-écoulement se concentre au centre de la galerie en provoquant l'ennoiement et l'assèchement de certains gours (Figure 3, flèche bleu modéré).

3. Conclusion

L'analogie et l'imbrication géométrique des morphologies et formations observées, aussi bien dans la partie touristique que la galerie des Boas, ont permis de déduire les principales étapes de développement et de l'évolution de la cavité donnant lieu à la chronologie relative suivante ;

1. Un fonctionnement paragénétique lié à la transgression pliocène.
2. Un abaissement du niveau de base à la fin du Pliocène permettant le décolmatage des argiles par des écoulements en surface libre.
3. Des réajustements mécaniques apparaissent en raison du retrait des argiles.
4. Une phase de concrétionnement issue de ruissellements incrustants, dont la temporalité s'avère relativement longue comme en témoigne la richesse des spéléothèmes.

Ces étapes, illustrées sur différents supports (Figures 1, 2 et 3) rassemblent l'ensemble des clés de lecture sur lesquelles s'est basée cette chronologie. Ils sont un support de médiation facilement abordable et transmis aux gestionnaires de la cavité.

Références bibliographiques :

CHOPPY J. (1985) Dictionnaire de spéléologie physique et karstologie, *Phénomènes karstiques*, Série 9, 148 p.

DELANNOY J-J., GAUCHON C. et JAILLET S. (2007) *L'Aven d'Orgnac, valorisation touristique, apports scientifiques*, Collection Edytem, Cahiers de Géographie n° 5, 184 p.

DELANNOY J-J., CLAUDE M., HUGUET D. et JAILLET S. (2013) *Carnet des faciès de l'anamorphose de la grotte Chauvet Pont d'Arc*, Collection Edytem, 119 p.

DELANNOY J-J., DEBARD E., FERRIER C., KERVAZO B., JAILLETS., PERRETTE Y., PERROUX A-S. et SADIER B. (2020) La carte intégrée des sols : principes et sémiologie. In *Atlas de la grotte Chauvet-Pont d'Arc* (sous la dir. Delannoy et Geneste) 45-83.

DUBICH F. (2019) *La grotte touristique de Saint-Marcel d'Ardèche ; Approche géomorphologique et reconstitution spéléogénique*, Mémoire de Master 1, Université Savoie Mont-Blanc.

GEZE B. (1973) Lexique des termes français de spéléologie physique et de karstologie. *Annales de spéléologie*, Tome 28, Fasc. 1, 20 p.

GILLI E. (2011) *Karstologie : karsts, grottes et sources*, Dunod, Paris, 244 p.

JAILLET S., DELANNOY J-J., BERSIHAND J-L., NOURY M., SADIER B. et TOCINO S. (2007) L'aven d'Orgnac : un grand réseau paragénétique, étude spéléogénétique des grands volumes karstifiés. In : Collection EDYTEM. Cahiers de géographie, numéro 5. *L'aven d'Orgnac, Valorisation touristique, apports scientifiques*, 56-77.

LECORNU E. (2019) *Analyse morphogénique et morphochronologique de gours : Le cas de la galerie des Boas dans la Grotte de St-Marcel (Ardèche, France)*, Mémoire de Master 1 Université de Savoie Mont-Blanc, 76 p.

MOCOCHAIN L. (2007) *Les manifestations géodynamiques - externes et internes- de la crise de salinité messinienne sur une plateforme carbonatée péri-méditerranéenne : le karst de la Basse Ardèche (Moyenne vallée du Rhône ; France)*, Thèse de Doctorat en Géographie sous la direction de Mireille Lippmann-Provansal et de Olivier Bellier, Université Aix-Marseille I.

MOCOCHAIN L. et BIGOT J-Y. (2008) Géomorphologie : Les origines de la grotte de Saint-Marcel, *La grotte de Saint-Marcel*, 182-201.

SADIER B., PERROUX A-S., PERETTE Y., DELANNOY J-J., QUINIF Y. et KAUFMANN O. (2007) *L'aven d'Orgnac, étude des remplissages, mémoires des dynamiques spéléogéniques post paragénétiques*. Cahier de géographie - collection EDYTEM, n° 5, pp. 79-98.

SALOMON J-N. (2000) *Précis de Karstologie*, Scieteren, 285 p.

The karst geomorphology of the Boukadir region (Chelif – Algeria)

Meriem Lina MOULANA[1,2], Aurélia HUBERT[1], Mostefa GUENDOUZ[2], Camille EK[1] & Bernard COLLIGNON[3]

(1) Department of Geography, University of Liege, Quartier Village 4, clos Mercator 3, 4000 Liège, Belgium, ml.moulana@uliege.be (corresponding author), aurelia.ferrari@uliege.be & camille.ek@uliege.be
(2) Faculty of Earth Sciences, Geographical and Territorial Planning, University of Science and Technology Houari Boumediene, (USTHB), El Alia, BP 32, Bab Ezzouar, 16111 Algiers, Algeria, mguendouzdz@yahoo.fr
(3) HYDROCONSEIL, 198, chemin d'Avignon - 84470 Châteauneuf-de-Gadagne, France, collignon@hydroconseil.com

Abstract

In June 1988, in the region of Boukadir, northwestern Algeria, a large collapse 60 m in diameter and 35 m deep occurred in the National Road RN 4. This region was not considered as strongly exposed to a geotechnical karst hazard. However, this collapse sinkhole suggests that there are large underground cavities under the Quaternary alluvium of the Boukadir plain, at an altitude near or lower than the present sea level. Geological analysis reveals that the Lithothamnium limestones outcropping on the northern Ouarsenis piedmont extend under the Quaternary alluvium. The surface karstic morphology is not spectacular because of the friable nature of this carbonate platform, but a deep collapse sinkhole called "Bir Djeneb" or "Puits du Diable" was evidenced. The underground voids below the plain could be the result of the base level drop during the Messinian Salinity Crisis (MSC) which let an imprint on the marginal platforms of the Mediterranean Basin.

Résumé

Deux dolines d'effondrement dans la région de Boukadir (Algérie). En juin 1988, dans la région de Boukadir, au nord-ouest de l'Algérie, un large effondrement de 60 m de diamètre et 35 m de profondeur s'est produit sur la RN 4. Cette région n'était pas considérée comme fortement exposée à l'aléa géotechnique typique du karst. Ce gouffre d'effondrement suggère cependant qu'il existe de grands vides souterrains sous les alluvions quaternaires de la plaine de Boukadir à une altitude proche ou inférieure à celle de la mer. L'analyse géologique révèle que les calcaires à Lithothamnium qui affleurent sur le piémont nord des Ouarsenis se prolongent sous les alluvions quaternaires. La morphologie karstique de surface n'est pas spectaculaire à cause de la nature friable de cette plateforme carbonatée, mais une profonde doline d'effondrement y a été mise en évidence, « Bir Djeneb » ou « Puits du Diable ». Les vides souterrains sous la plaine pourraient être le résultat de l'abaissement généralisé des niveaux de base pendant la crise de salinité messinienne (MSC), qui a laissé son empreinte sur les plates-formes marginales du bassin méditerranéen.

1. Introduction

Karstic carbonate landscapes are directly linked to climate and relief. These two variables offer large variations in Algeria (COLLIGNON, 1991).

Knowledge in Algeria about karstic landscape is restricted, though their study is important for several reasons. This study focuses on the marginal Messinian carbonate platform outcropping (Fig. 1), in the northern piedmont of Ouarsenis mountains. It is in the Boukadir region, northwest of Algeria, on the southern edge of the 20 km wide lower Chelif plain crossed by the Chelif River. There is a lack of knowledge in karst geomorphology about this carbonate platform. On June 16th, 1988, a large collapse pit occurred about 1 km north of the Ouarsenis piedmont, in the Chelif Basin (OURABIA & BENNALLAL, 1989). It broke the national road RN4 that connects the Capital Algiers to the city of Oran in west. At the level of the foothills, there is another large collapse sinkhole perched high up called "Bir Djeneb" or "Puits du Diable". The aim of this paper is to unravel processes that lead to the formation of these collapse sinkholes, by combining geology, speleology, and geomorphology.

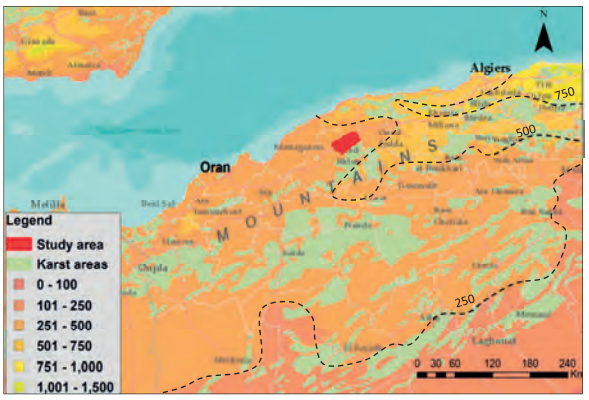

Figure 1: Karstic areas of Algeria and the study area. Mean annual rainfall (mm/year). Esri Copyright © 1995–2022 Esri.

2. Materials and methods

The geology is studied by analysing the lithological characteristics of this region, the drilling made by the Central Laboratory for Public Works (LCTP) on 20-05-1989, and the geological cross section drawn by SCET-AGRI (1985). The speleological study is based on the report of BIREBENT (1947), entitled *Speleology of Algeria: Inventory*, where the author made an inventory of the caves of the regions. The geomorphological analysis is based on field work, Google Earth images, and aerial photographs.

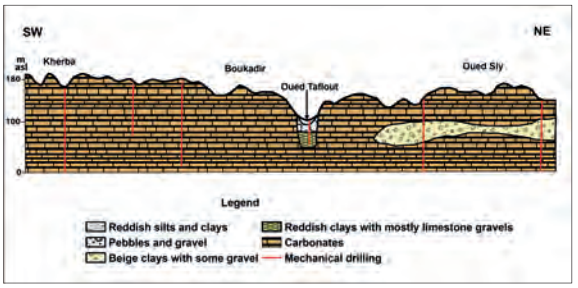

Figure 2: Reinterpreted geological cross-section based on 6 mechanical drill cores parallel to the piedmont and across Oued Taflout (SCET-ARGI, 1985). The section shows a ~ 70 m deep Messinian incision at the location of Oued Taflout filled first by ~40 m of clay and then by coarser alluvial deposits.

3. Results

3.1. Geology

The Ouarsenis piedmont is composed of Messinian carbonates outcropping in the form of a large monoclinal slab, south of the Chelif valley (Boukadir region). It is composed of 3 main geological units. The basal up to 500 m thick Tortonian to Messinian blue marls are overlain by two Messinian bioclastic carbonate units having low dips (NEURDIN- TRESCARTES, 1992; MOULANA *et al*., 2021). The lower bioclastic carbonate unit is an up to 70 m thick heterogeneous bioclastic carbonate unit. It is overlain by the upper unit comprising at least 80 m of homogeneous Lithothamnium carbonate packstones. In the Chelif Plain, the S1 drill hole reveals that the top unit is a 22.5 m thick alluvial formation composed of clayey silty and sandy conglomerate and corresponds to the Quaternary surface aquifer. Then, unit 2 is a 26.2 m thick layer of brown clay. It corresponds to a Pliocene aquiclude that separates the alluvial aquifer from the limestone aquifer which starts at the depth of 61 m. The geological cross-section (SCET-ARGI, 1985) parallel to the piedmont and across Oued Taflout, evidenced a 70 m deep incision in the carbonate at the level of the present river Oued Taflout (Fig. 2). The incision is filled by a basal brown clay unit, then by an alluvium unit. The top layer consists in silt and red clay.

3.2. Speleology

BIREBENT (1947) describes five caves in the carbonate massif of the piedmont of the Ouarsenis. Bir Djeneb is the most considerable karstic feature of the studied area (Fig. 3). Located 5.5 km SW of Boukadir. It is a cylindrical pit about 20 m in diameter and 63 m deep (Fig. 3). It is dug mainly in the soft Messinian carbonate. At the top, colluvium is made of pebbles with little matrix outcrops and below more clay-rich sediments. In the bottom, a narrow conduit in the lower bioclastic carbonate unit about 3 m in diameter goes down with a faint slope to 73 m deep. The bottom of the main shaft is made of scree. The latter ends to a second pit, much smaller than the first one, 5 m deep and 3 m in diameter. In 2021, a new exploration evidenced the continuous infilling of the pit that reaches the depth of 53m.

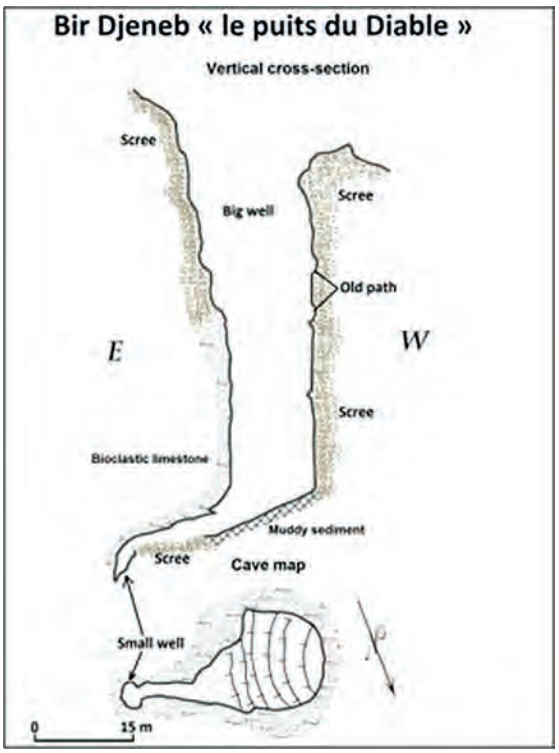

Figure 3: Map and cross-section of Bir Djeneb cave, northern Ouarsenis piedmont; after BIREBENT (1947), modified.

3.3. Geomorphology

The geomorphological analysis reveals that the most frequent karstic dissolution features are small shelter-caves; they are more frequent in the lower bioclastic carbonate unit than in the upper Lithothamnium unit. Their interior is composed of pinkish white tuffaceous limestones, and their external roof is composed of a thin layer of hard and compact limestones. We also notice the occurrence of landslides in association with shelter-caves hanging on the steep valley walls high above the present riverbed due to the breaking of their roof (Fig. 4). We observed few vertical swallow holes dug in the top calcrete in the east. Some rare ponors are evidenced. A few large resurgences, in the west end of our study area are distinguished.

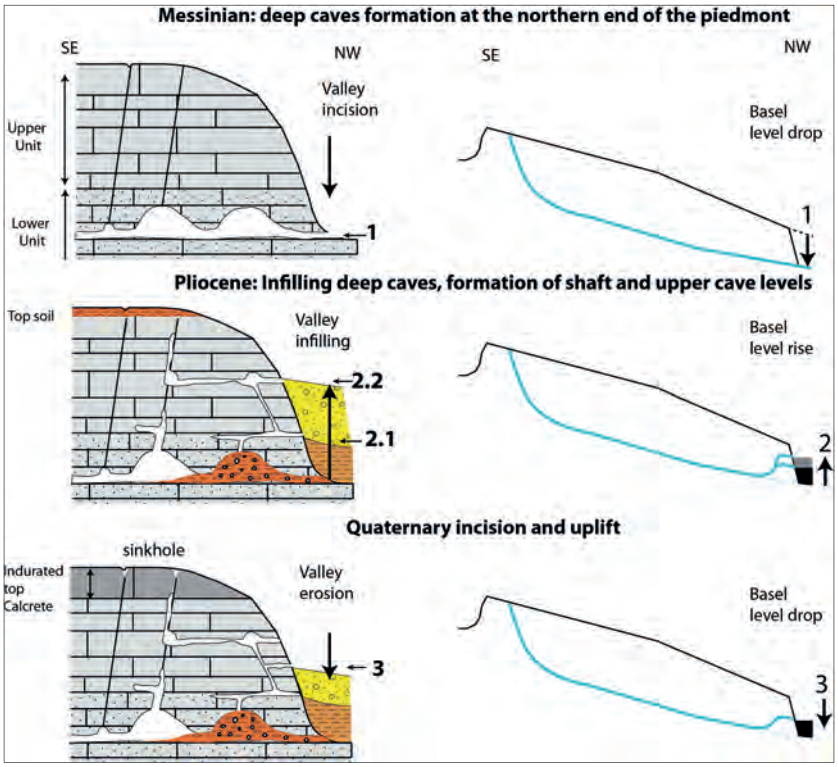

Figure 4: Drawing of the northern piedmont of the Ouarsenis representing. 1. Valley incision and deep void formation during the Messinian Salinity Crisis (MSC). 2 Infilling of deep caves and formation of shafts during the Pliocene. The clay-rich infill is evidenced in Figure 2 in caves and valleys and is followed by a valley alluvium infill. 3. Tectonic uplift and lowering of the base level during the Quaternary leading to river incision.

4. Discussion

The results of the geological and the geomorphological analyses show that the current surface weathering and the deep active karstification are relatively limited. Infiltration is restricted by the present-day top calcrete. However, caves and shelter-caves resulting partly from river incision imply a sizable karstic network (or endokarst).

The 35 m deep 1988 collapse occurred through a thick pile of sediments. The beds of the collapsed terrain are unconsolidated and made of relatively insoluble material. They are not karstic, but we infer that the phenomenon is fully karstic. Messinian carbonates, that outcrop 1.5 km more to the south, lie at 61 m depth and a gigantic void must have existed in this formation to let the place for a falling in of at least 95 000 cubic meters. In addition of the RN4 shaft, there exist another imprint of an active karstification of the Messinian carbonates: “Bir Djeneb”. This collapse shaft suggests that the piezometric base level was quite deeper than the present one. The last possible occurrence of such low base level is during the Messinian itself. Indeed, during this period, the climate was hot and dry (FAUQUETTE *et al.*, 2006), so a strong evaporation occurred, triggering a fall of the Mediterranean Sea level to about -1500 m (RYAN, 1976). Around the Mediterranean Sea, rivers cut deep canyons to adapt to this low base level (CLAUZON, 1982; JULIAN & NICOD, 1984; BINI, 1994; BOURILLOT *et al.*, 2010; KRIJGSMAN *et al.*, 2018). It is considered here that the large underground cavities at Boukadir along the southern margin of the Chelif valley were formed during this MSC, even though the collapse sinkhole of Bir Djeneb, has no simple link with the eustatic variations.

5. Conclusion

The karst pattern in the investigated carbonates is relatively undeveloped. The high porosity of the Lithothamnium carbonates favours diffuse infiltration rather than the widening of fractures, which reduces localized dissolution and flow, and impedes the development of large caves. Boukadir karsts are characterized by a low present-day activity. The endokarst is relatively poorly developed whereas the epikarst is prevalent and characterized by shelter caves. The large voids deep below the present-day base-level on the southern edge of the Chelif Plain are inferred to be a paleokarst related to the Messinian Salinity Crisis who lowered the Mediterranean Sea level. These are responsible for the collapse hole of RN4, in 1988, which has a convergence of forms with the collapse sinkhole of Bir Djeneb (collapse sinkhole of a few tens of meters) (Fig. 5). However, the link of Bir Djeneb with the MSC, is not evident. The genetic relation of the two holes thus remains problematic.

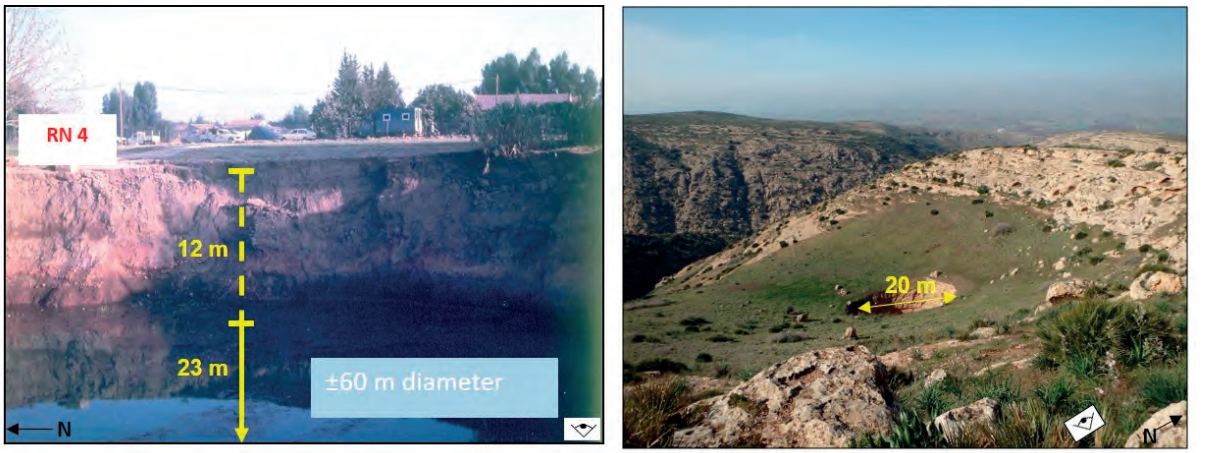

Figure 5: The 2 major sinkholes in the study area. Left: the 1988 RN4 sinkhole in the Chelif Basin 500 m from the carbonate piedmont (Photo taken by Pr. Mostefa GUENDOUZ on 16/06/1988). Water table is 12 m below the level of the road. Right: The Bir Djeneb in the carbonate Ouarsenis Mts.

Acknowledgments

The authors gratefully thank Dr. Sebastien DOUTRELOUP for his contribution in climate analysis.

References

BINI A. (1994) Rapports entre la karstification périméditerranéenne et la crise de salinité du Messinien. *Karstologia*, 23, 33-53.

BIREBENT J. (1947) *Spéléologie de l'Algérie : Inventaire*. Agence Nationale des Ressources Hydraulique. Alger, le 1er décembre 1947. Rapport.

BOURILLOT R., VENNIN E., ROUCHY J.-M., BLANC-VALLERON M.-M., CARUSO A. & DURLET C. (2010) The end of the Messinian salinity crisis in the western Mediterranean: Insights from the carbonate platforms of south-eastern Spain. *Sedimentary Geology*, 229(4), 224-253.

CLAUZON G., SUC J.-P., GAUTIER F., BERGER A. & LOUTRE M.-F. (1996) Alternate interpretation of the Messinian salinity crisis: Controversy resolved? *Geology*, 24(4), 363-366.

COLLIGNON B. (1991) Les principaux karsts d'Algérie. Quelques éléments de synthèse, *actes du 9ème Congrès National de la SSS*, Akten des, 9.

FAUQUETTE S., SUC J.P., ADELE BERTINI A., POPESCU S.M., WARNY S., BACHIRI TAOUFIQ N., PEREZ VILLA M.J., CHIKHI H., FEDDI N., SUBALLY D., CLAUZON G. and FERRIER J. (2006) How much did climate force the Messinian salinity crisis? Quantified climatic conditions from pollen records in the Mediterranean region. *Palaeogeography, Palaeoclimatology, Palaeoecology*, 238(1-4), 281-301.

JULIAN M. & NICOD J. (1984) Paléokarsts et paléo-géomorphologie néogènes des Alpes Occidentales et régions adjacentes. *Karstologia*, 4(1), 11-18.

KRIJGSMAN W., CAPELLA W., SIMON D., HILGEN F. J., KOUWENHOVEN T. J., MEIJER P. T.... & FLECKER R. (2018) The Gibraltar corridor: Watergate of the Messinian salinity crisis. *Marine Geology*, 403, 238-246.

LCTP (1989) *Effondrement de la RN4. Oued Sly (Boukadir) Chlef*. Laboratoire Central des Travaux Publics d'Alger. Rapport.

MOULANA M. L, HUBERT-FERRARI A, GUENDOUZ M, EL OUAHABI M, BOUTALEB A & BOULVAIN F (2021) Contribution to the sedimentology of the Messinian Limestones of Boukadir (Chelif Basin-Algeria); *Geologica Belgica*. 24/1-2 : 85-104. DOI : 10.20341/gb.2021.002.

NEURDIN-TRESCARTES J. (1992) *Le remplissage sédimentaire du bassin néogène du Chelif, modèle de référence de bassins intramontagneux* (Doctoral dissertation, Pau).

RYAN W. B. (1976) Quantitative evaluation of the depth of the western Mediterranean before, during and after the Late Miocene salinity crisis. *Sedimentology*, 23(6), 791-813.

Scet – Argi (1). (1985) *Hydrologie – Hydrogéologie et bilan des ressources, Étude du réaménagement et de l'extension du périmètre du moyen Chéliff* : Rap A1.1. 2. Pub. Ministère de l'Hydraulique. 72 p.

L'endokarst témoin de l'évolution complexe du paysage régional en milieu tropical : l'exemple du Curral das Pedras (Minas Gerais, Brésil)

Joël RODET[(1)], Frederico A.A. GONÇALVES[(2)] & Luc WILLEMS[(3)]

(1) Centre Normand d'Etude du Karst (CNEK) & Université de Rouen-Normandie, UMR 6143, M2C CNRS, bât. Blondel, place Emile Blondel, 76821 Mont Saint Aignan, France, joel.rodet@univ-rouen.fr (corresponding author)
(2) Universidade Federal de Minas Gerais, Departamento de Geografia-IGC, Belo Horizonte, Minas Gerais, Brasil, faagoncalves@gmail.com
(3) Université de Liège, Département de Géologie ; Haute Ecole Charlemagne, 4540 Amay, Belgique lucwillems65@googlemail.com

Résumé

Les grandes étendues de haut plateau qui entourent la vallée du Rio São Francisco dans sa traversée de l'État de Minas Gerais, sont réputées stables depuis le Cénozoïque sous l'influence du climat tropical à saison sèche. Cependant, les systèmes karstiques gardent des traces remarquables d'une évolution plus complexe qu'envisagée, des systèmes morphologiques régionaux. C'est le cas pour le système souterrain semi-actif du Curral de Pedras, installé dans les calcaires Bambuí du Néoprotérozoïque. L'étude de son endokarst démontre la succession de deux axes de drainage, le plus ancien vers la vallée du Rio Jequitai, le plus récent vers la vallée affluente du Riacho Fundo. La réduction importante du bassin d'alimentation sous l'effet de l'incision des affluents du Rio Jequitai qui isole le Curral de Pedras, est responsable de la perte de flux qui désormais se limite à la saison des pluies. Cette évolution est favorable au développement de petits poljés au détriment des drains souterrains. Ces mêmes poljés, résiduels et inactifs pour la plupart, sont effacés peu à peu par l'érosion superficielle.

Abstract

The endokarst as a witness of the complex evolution of a regional landscape in a tropical environment: the example of Curral das Pedras (Minas Gerais, Brazil). The endokarst as indicator of the complex evolution of the regional landscape under tropical climate: the example of the Curral de Pedras site (Mina Gerais, Brazil). The large expanses of high plateau that surround the Rio São Francisco valley as it crosses the state of Minas Gerais, have been known to be stable since the Cenozoic under the influence of the tropical climate in the dry season. However, karstic systems keep remarkable traces of a more complex than expected evolution of regional morphological systems. This is the case for the semi-active underground system of Curral de Pedras, installed in Bambuí limestones of the Neoproterozoic. The study of its endokarst shows the succession of two drainage axes, the oldest towards the valley of the Rio Jequitai, the more recent towards the tributary valley of the Riacho Fundo. The significant reduction in the supply basin under the effect of the incision of the tributaries of the Rio Jequitai which isolates the Curral de Pedras, is responsible for the loss of flow which is now limited to the rainy season. This development is favorable to the development of small poljes to the detriment of underground drains. These same poljes, residual and inactive for the most part, are gradually erased by surface erosion.

1. Introduction

En rive droite du cours moyen du Rio São Francisco, les formations carbonatées néoprotérozoïques occupent de vastes étendues. En rive droite de son affluent, le Rio Jequitai, à mi-distance entre les villes de Pirapora et Montes Claros (Minas Gerais), la région du Curral de Pedras (Fig. 1) se caractérise par la présence de plusieurs affleurements calcaires que l'incision des vallées a isolés au sommet des collines, leur conférant une morphologie tabulaire. Ces secteurs développent de grandes surfaces lapiazées, interrompues ponctuellement par des gouffres et des fentes. Des parois rocheuses qui peuvent atteindre 40 m de hauteur, des dolines, des poljés, des cavités, des abris sous-roche, des canyons, des avens participent de la diversité de ces paysages karstiques.

Ces massifs sont constitués de dépôts carbonatés intercalés de pélites, attribués à la Formation Lagoa do Jacaré, du Groupe Bambuí (Néoprotérozoïque) et datés de 635 à 541 Ma. De par leur moindre sensibilité aux agents d'altération, les niveaux de pélites, qui constituent localement une couverture meuble, sont responsables de la suspension des systèmes karstiques dans le haut des massifs (RODET, 2012). Les zones de calcaire sont de morphologie plutôt plane, alors que les zones à pélites offrent des versants pentus, parfois supérieurs à 40°. Le tout se développe entre 500 m d'altitude auprès du Rio Jequitai et

1000 m au sommet des collines. Dès la fin des années 2000, nous nous sommes intéressés à ce secteur qui a révélé ses spécificités : karst suspendu 200 m au-dessus des drainages épigés actuels, petits poljés fonctionnels, organisation labyrinthique des réseaux souterrains, paléo-gradients hydrauliques successifs d'orientation différente, etc. (GONÇALVES, 2013).

2. Un labyrinthe, du poljé à l'introduction

Le secteur du Curral das Pedras offre un passage de la couverture à forêt sèche au lapiaz à *tsingy*, c'est-à-dire aux arêtes étroites et hautes, extrêmement coupantes, comme on en observe classiquement dans les pitons résiduels calcaires des zones tropicales. Cette transition se caractérise par le développement de micro-poljés dès le contact formations meubles / calcaire, et où le substrat carbonaté récemment découvert, offre une empreinte cryptokarstique. Ceci signifie que le niveau de base est haut perché et qu'il limite l'enfouissement des eaux dans le massif.

Figure 1 : Situation de la zone d'étude

Parmi cette dizaine de poljés, le plus important semble être celui de la Lagoinha, constituée d'une dépression à fond plat qui naît au contact avec la couverture boisée. Les trois autres côtés buttent sur de petites falaises, percées de dix porches karstiques donnant accès à un réseau spéléologique labyrinthique. Le fond plat de la dépression permet de la définir comme poljé, comme le confirment les entailles périphériques sur les parois des falaises et des blocs isolés. Durant la saison des pluies (octobre/avril), le poljé offre une nappe d'ennoiement qui pénètre loin dans le réseau souterrain.

Figure 2 : Vue panoramique du labyrinthe souterrain du Curral de Pedras.

Le poljé donne accès à un développement souterrain labyrinthique (Fig. 2), peu organisé et sans drain collecteur véritable. On y observe de nombreuses formes surimposées induites par de légères variations du niveau de base (Fig. 4). La faible épaisseur du toit calcaire favorise le recoupement par les avens et les rainures du lapiaz, du réseau endokarstique (Fig. 6) et contribue fortement à son fonctionnement en résurgence. De ce fait, le réseau souterrain (Fig. 3) travaille en inversac, selon les apports hydriques, par le poljé ou par les drains.

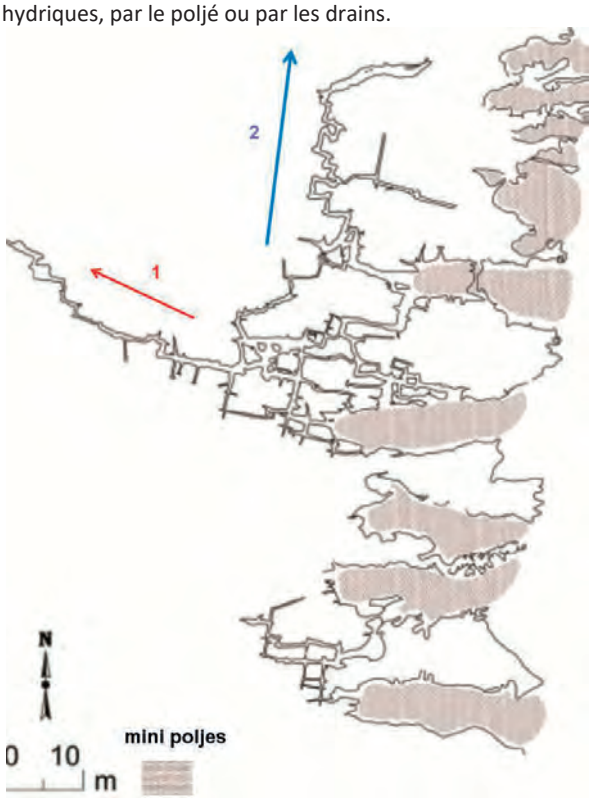

Figure 3 : Topographie du réseau karstique du Curral de Pedras

Ce mécanisme se répète malgré des modifications du niveau de base comme le montrent les exemples de certains poljés. Dans la petite dépression de la Lapa do Sol, la plus au sud, nous observons le même mécanisme, avec une dénivellation légèrement supérieure entre les deux principaux niveaux de base, le plus récent étant imprimé dans le plus ancien. De plus le fond de plusieurs poljés est percé d'une perte ou sumidouro.

Mais le drainage souterrain ne se limite pas au rôle de réservoir. Il offre une certaine organisation spatiale plus complexe en reliant plusieurs poljés, comme celui de la Lagoinha à celui du Mandacaru. Une évolution plus récente a transformé en perte, la partie proche de la zone boisée de ces poljés, dégageant alors un seuil rocheux entre les deux parties (GONÇALVES et *al*., 2013).

À l'approche du versant, le gradient hydraulique intervient plus franchement et permet finalement de percer le niveau

lithologique imperméabilisant. Ceci explique la gradation des stades d'évolution identifiables dans les différentes parties du réseau karstique.
On peut envisager que les poljés ne se soient développés que relativement récemment, quand l'épaisseur de calcaire au-dessus du niveau de base a été suffisamment réduite, gommant les témoins d'un endokarst supérieur. Cette évolution expliquerait la localisation des poljés au contact de la couverture boisée. Les poljés semblent s'être développés aux dépends d'un réseau karstique inférieur (Fig. 4) installé sur le niveau de base à pélites. Plus loin, lorsque l'épaisseur de calcaire devient plus importante, c'est le drainage souterrain labyrinthique qui l'emporte (Cavalo Marinho), mais il ne semble pas que le karst atteigne une organisation poussée, mature. C'est ce que semble illustrer le karst labyrinthique observé dans et autour de la Lapa da Passagem, appartenant à un autre système du Curral de Pedras, comparable semble-t-il.

3. Un karst suspendu par la lithologie

Figure 4 : À gauche, drains coalescents légèrement étagés ; à droite, paléo-drain recoupé par l'évolution du poljé

Il est possible que le développement des mini-poljés résulte directement des conditions hydroclimatiques réduisant les périodes de drainage à la saison des pluies, caractérisée par des précipitations soudaines et importantes. La zone de contact entre la couverture boisée et le lapiaz, dont le drainage souterrain est encombré notamment de dépôts calcitiques, se transforme alors en zone de stockage des eaux provenant tant de la couverture boisée que du lapiaz lui-même. Ce régime erratique ne permet pas l'établissement d'un drainage régulier qui pourrait réaliser une évacuation calibrée, voire transpercer le niveau pélitique et relier le développement karstique au niveau de base actuel. Il en résulte un endokarst labyrinthique, sans organisation et surtout suspendu 200 m au-dessus des vallées voisines (GONÇALVES et *al.*, 2017). Les anciens drains sont remodelés par les phases d'ennoiement (Fig. 4). C'est ainsi qu'on observe des coups de gouge sur des parois de galerie, là où aucune circulation rapide ne peut s'établir. Il s'agit de paléoformes résiduelles épargnées jusqu'alors par les phases fonctionnelles.

4. Un karst témoin de l'évolution régionale

L'isolement du système par l'évolution du relief (creusement des vallées affluentes du Rio Jequitai) réduit sérieusement le bassin d'alimentation du karst du Curral de Pedras. La saisonnalité climatique renforce cet impact en générant une phase sèche de plus en plus importante et donc une réduction de l'adaptation du système à l'évolution topographique.

Le paysage géomorphologique de la région du Curral de Pedras est caractérisé par le développement de deux surfaces planes d'érosion avec des pentes inférieures à 10°, définissant des compartiments altimétriques distincts. La transition entre ces deux surfaces se réalise par une dénivellation abrupte, de près de 200 m, avec des pentes mesurées à 40°. Il est probable que la réalisation de la surface supérieure se soit poursuivie entre le Miocène moyen et le Pliocène supérieur, lorsqu'un probable soulèvement a marqué une interruption entre sa réalisation et le début de l'incision de l'actuel surface inférieure. Cette interprétation chronologique repose surtout sur des relevés de terrain et ceux extraits du Deep Sea Drilling Project (DSDP) selon lesquels à partir du Pliocène supérieur, on note une croissance rapide du taux d'accumulation sédimentaire dans les bassins océaniques profonds (GONÇALVES, 2013).

Cette croissance serait une réponse à l'intensification de la dénudation continentale associée au soulèvement du Pliocène (VALADÃO, 1998). Il est fort probable que la karstification du Curral de Pedras remonte au Miocène supérieur, période pendant laquelle la paléogéographie du Curral de Pedras était vraisemblablement associée à une surface plane plus étendue. Au Pliocène inférieur, le début de l'incision du réseau hydrologique, illustrant un abaissement du niveau de base, entraîne un gradient hydraulique jusqu'alors inexistant.

Figure 5 : Micro-hum dans le poljé actif de Lagoinha.

Avec le développement de l'incision, les premières formes de restitution ont du apparaître. Ainsi le système karstique déjà soumis à des conditions phréatiques, est impacté par les conséquences de l'établissement de conditions épigées. La réponse du karst à ces phases d'incision semble être l'établissement et la mutation des gradients de drainage, d'abord vers l'ouest (axe 1, flèche rouge, de la figure 3) puis vers le nord (axe 2, flèche bleue, de la figure 3).
Probablement ces conditions ont fait qu'au fur et à mesure du développement des processus de l'incision, plusieurs secteurs du réseau karstique reconnu ont été contrôlés par une dynamique vadose (Fig. 6). Cette évolution est responsable de la modification partielle de la morphologie jusqu'alors soumise à une dynamique phréatique. Cette phase se traduit par une morphologie marquée par une incision verticale de certains conduits au profil en trou de serrure dans le secteur ouest du Curral de Pedras 1 (Fig. 4).

5. Conclusion

Un système karstique est toujours un témoin de l'évolution régionale. Dans le cadre du cours moyen du rio São Francisco, l'incision du réseau hydrographique est assurément l'évènement géomorphologique majeur des plateaux de cette région. Heureusement, le karst conserve les épisodes marquants que l'érosion superficielle gomme. En cela, le réseau karstique du Curral de Pedras se révèle un témoin pertinent de cette longue évolution. La variation de l'axe principal de drainage de l'ouest pour le nord (fig. 3) souligne une modification importante du relief dans un contexte continental réputé pour son apparente stabilité. Rapportées à l'échelle du bassin du rio São Francisco, ces modifications sont plutôt légères, mais localement, les incisions des affluents du São Francisco ont entraîné la partition des plateaux calcaires et la réduction drastique des bassins d'alimentation, portant les systèmes karstiques à l'indigence hydrique et à l'inadaption des réseaux au cadre morphoclimatique actuel, et donc à leur fossilisation.

Figure 6 : Plafond résiduel de l'ancien collecteur orienté vers le Riacho Fundo (axe 2 de la figure 3).

Références

GONÇALVES F.A.A. (2013) Morfodinâmica e morfogênese de um carste suspenso e evolução geomorfológica de longo termo: uma aproximação baseada no caso do setor oeste do Curral de Pedras I / Jequitai-MG. Mestrado de Geografia, IGC/UFMG : 162 p.

GONÇALVES F.A.A., MAGALHAES JÚNIOR A. P. and RODET J. (2013) Contribution to the study about the Brasilian Karstic areas: the geomorphological cartography as a subsidy to the analysis of the evolution of the karst in the karstic region of Currais de Pedras (KRCP). "Geomorphology and sustainability" - 8th IAG International Conference on Geomorphology, Paris, 27-31 august 2013, Abstract Volume: 330.

GONÇALVES F. A. A., RODET J. e MAGALHÃES JÚNIOR A. P. (2017) Carste suspenso e geomorfologia de longo termo. A região cárstica dos Currais de Pedras, Jequitaí, Minas Gerais (Brasil). Revista Brasileira de Geomorfologia, 18 (2) : 279-294 [2236-5664]

RODET J. (2012) Prémices d'une approche géoarchéologique et karstologique de la région de Jequitaí (Minas Gerais, Brésil) - Primícias de uma abordagem geoarqueológica e carstológica da região de Jequitaí (Minas Gerais, Brasil). Carso Brasiliensis, n° 2 : 58 p. [978-2-9506258-5-4].

VALADÃO R. C. (1998) Evolução de longo-termo do relevo doBrasil oriental: desnudação, superfícies de aplainamento esoerguimentos crustais. Thèse de doctorat, Universidade Federal da Bahia, Salvador :242 p.

Late Quaternary evolution of the Ardèche river. Study of the karst-river relationships based on an integrated topographical approach.

Kim GENUITE[(1)], Stéphane JAILLET[(1)], Jean-Jacques DELANNOY [(1)], Jean-Jacques BAHAIN[(2)], Pierre VOINCHET[(2)], Edwige PONS-BRANCHU[(3)], André REVIL[(1)] & Marceau GRESSE[(4)]

(1) UMR 5204 EDYTEM, University of Savoie Mont Blanc / CNRS, Le Bourget du Lac CEDEX, France, kim.genuite@gmail.com (corresponding author), jean-jacques.delannoy@univ-smb.fr, stephane.jaillet@univ-smb.fr
(2) UMR 7194 HNHP / CNRS, Paris, bahain.mnhn.fr, pvoinch.mnhn.fr
(3) UMR 8212, LSCE / CNRS, Paris. edwige.pons-branchu@lsce.ipsl.fr
(4) marceau.gresse@gmail.com, University of Tokyo, Tokyo, Japan.

Abstract

The Ardèche river canyon (Ardèche, France) is famous for its deep ingrown meanders and represents one of the most touristic assets of the region. It is also a central place of Upper Palaeolithic occupancy with numerous caves containing some of the most ancient and impressive rock art ever discovered like in the Chauvet cave, located at the canyon entrance, whose artwork was dated more than 36 ka cal BP. However, the Late Quaternary river remains poorly constrained as almost no absolute dating studies were conducted on the alluvial deposits. We conducted an integrated geomorphological approach based on 3D topographical surveys in the Ardèche river deposits, inside and outside the cave systems. The construction of an integrated 3D model allowed the comparison and discussion of the relative chronology of alluvial and cave deposits by positioning them on an accurate altitudinal grid, yielding evolution model for the Ardèche valley spanning the Middle to Late Quaternary.

1. Introduction

The Ardèche valley is known for its many sites of high landscape and heritage value (UNESCO listed site of the Chauvet cave, Grand site de France du Pont d'Arc, biological reserve of the Gorges de l'Ardèche). In the lower valley, the Gorges de l'Ardèche, with their many steep meanders, offer attractive landscapes from a tourist point of view (DUVAL, 2008) because they offer many remarkable topographical points, including the abandoned meander of the Combe d'Arc. In the latter, located at the entrance to the Ardèche gorges, the river has cut through the peduncle forming a natural arch whose vault reaches more than 30 m in height: the Pont d'Arc. Here, the topographical and landscape design still preserves intact the evidence of the morphological evolution of the watercourse during the progressive incision of the Ardèche valley (GENUITE *et al*., 2019) (Fig. 1). At different altitudinal levels, above the current course of the river, other forms are also visible in the landscape, and bear witness to the ancient passage of the course of the Ardèche. These paleo-forms, abandoned meanders, paleo-valleys, and ancient river deposits (alluvial terraces) can provide information on the geodynamic history of the river as it evolves over time and as such are relevant markers for understanding the evolution of the valley over long time periods (on the scale of several million years). Some of these markers have been extensively studied, such as the Miocene palaeo-valley of the Ardèche, near Aubenas, fossilised under the basaltic lava of the Coirons, or the Miocene and Pliocene erosion surfaces visible on the plateau of the Ardèche gorges (MARTINI, 2005; MOCOCHAIN et *al*., 2009; TASSY et *al*., 2013; SADIER, 2013). From a speleogenetic perspective, high-level cave drains have been studied and were attributed mostly to Miocene and Pliocene (MOCOCHAIN et *al*., 2009; TASSY et *al*., 2013; SADIER, 2013). Nevertheless, little work has focused on the fluvial and endokarstic geodynamics of the intermediate morphological levels of the Plio-Pleistocene (AUDRA et *al*., 2001).

This work is based on topographical analysis based on cave and canyon surveys, with geomorphological observations on both environments. It focuses on the lower levels, between 0 and + 45 m above the current river level. It aims to propose a relative chronological model of the river evolution constrained both by fluvial and endokarstic observations.

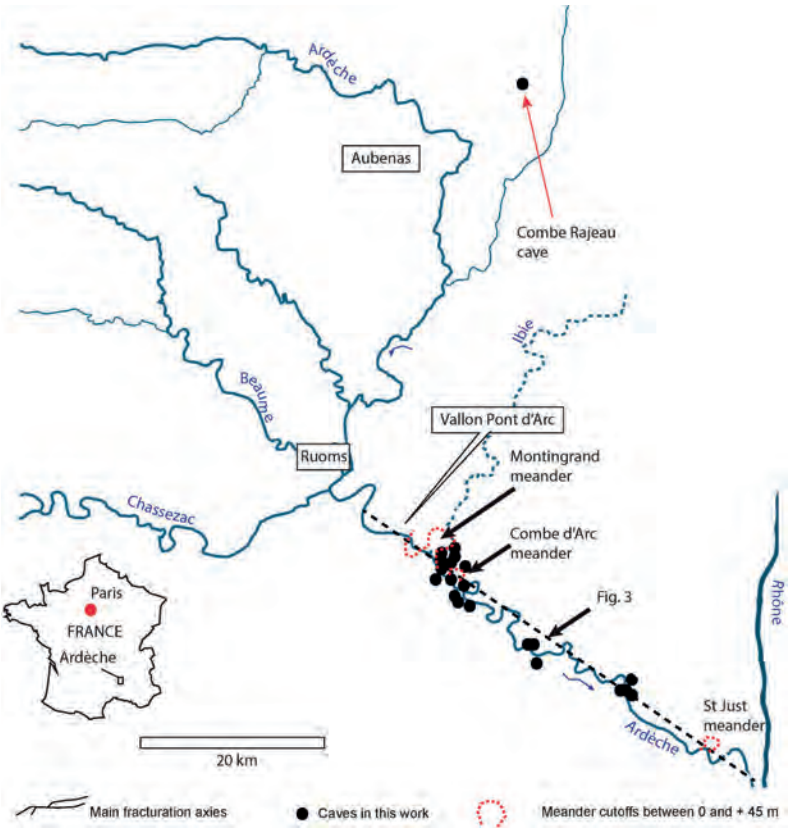

Figure 1: Location map of the Ardèche river catchment. Caves referenced in this work are represented by black dots and meander cutoffs by dashed red lines. Caves location: synthesis from MONNEY (2012) and courtesy of CDS07.

2. Site settings and methods

The topographic and geomorphological analysis alluvial and endokarstic morphologies, carried out using GIS topographic analysis tools and 3D modelling, allows the different shapes to be precisely positioned in space. The altitudinal correlation (in height in relation to the current watercourse) of the fluvial deposits, characterising the former base levels of the Ardèche valley, with morphological and structural features still visible in the relief, offers a key to understanding the history of the landscapes of the Ardèche on the Quaternary scale.
The Ardèche valley has several abandoned meanders still visible in the relief. These are only preserved in the carbonate rocks along the middle and lower Ardèche valley, at different altitudinal levels.

In order to compare the external morphological features with the cave levels, cave surveys were conducted and collected at the entrance of the Ardèche gorges and replaced in a high-resolution 3D topography of the river surroundings (GENUITE et *al*., 2019).
For the Ardèche gorges entrance, some cave surveys previously conducted with *Visualtopo* software, were implemented along the external topography with the *3DReshaper* software modeller. Caves were positioned according to their entrance point GPS coordinates (Cave entrance database access: courtesy of CDS 07). The following caves could be extracted as 3D models and added to the Ardèche gorges topography: the Chauvet cave, Foussoubie, Châtaigniers, Spectaclan, Chasserou, Déroc, Nouvelle and Marteau caves. For the other caves, located down the river, when 3D data was not available, only topographical cross sections were considered.

Alluvial deposits altitudes were checked by hand-held kinematic PPK differential GPS tracking. Polygons representing the deposit extensions were digitised under GIS software (QGIS 7.8.3) using both the photogrammetric 3D model for the Ardèche gorges area (GENUITE et *al*., 2018), and the 5 m IGN DEM for the remaining of the Ardèche watershed (Fig. 2). Differential GPS points and polygon traces were projected orthogonally to the river main trunk (Ardèche river) following DELMAS et *al*. (2018) method description (Fig. 2c and Fig. 3).

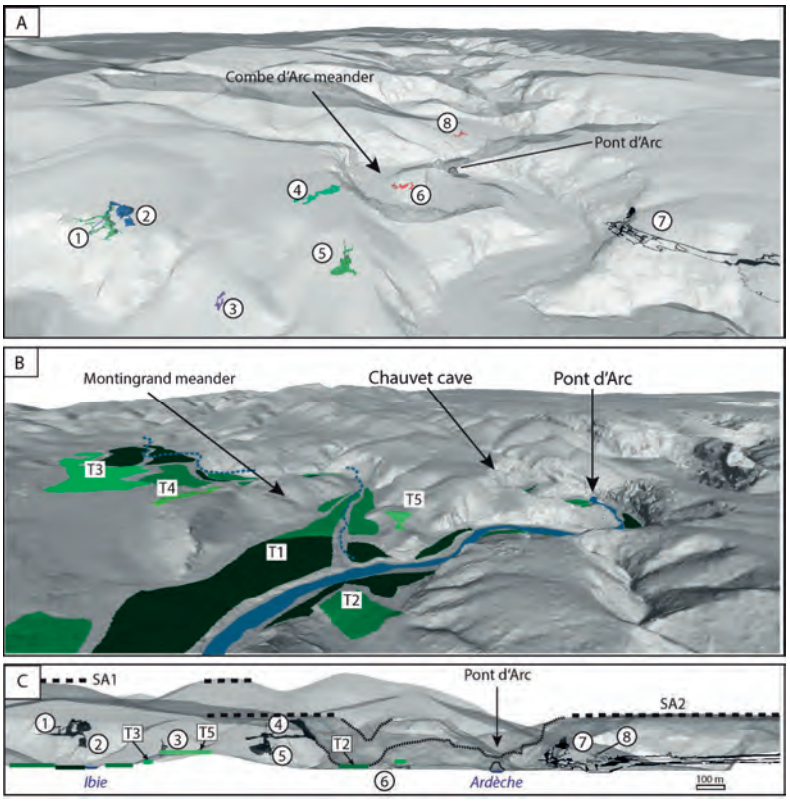

Figure 2: 3D modelling steps, from cave and river survey (a), to geomorphological mapping (b), and large-scale cross-sections (c). Ardèche river surveys and geomorphological mapping from from GENUITE et al. (2018, 2019) and GENUITE (2019). 1. Chasserou cave, 2. Déroc cave, 3. Nouvelle, 4. Chauvet, 5. Marteau, 6. Châtaigniers, 7. Foussoubie, 8. Spectaclan. Chauvet and Foussoubie cave synthetic surveys: SADIER 2013. Other cave surveys: courtesy of Philippe MONTEIL.

3. Preliminary results and interpretations

The integrated geomorphological analysis based on a 3D model of the site and its surroundings enabled the reconstruction of some steps in the river landscape evolution. The topographic observations and pointing carried out in the field and reported on the 3D topographic model make it possible to discuss the layering and evolution of the watercourse during its incision. While most of the caves referenced here were studied for their archaeological contents, more are in the pipeline for integration in this model. If the T5 level (+ 70 m) was attributed to the Bruhnes/Matuyama paleomagnetic reversal by AUDRA et *al*. (2001) from the Combe Rajeau Cave deposits, the lower terrasses absolute chronology is still in process. For the T4 level (+ 45 m), at the entrance of the Ardèche gorges, Mézelet PC du Maquis, Points, Cloches and Figuier caves correspond to that level. It is also the case for Spectaclan, Foussoubie and Châtaigniers cave drains that also reach the same height above the talweg. (Fig. 3). For the T3 level (+ 30 m), Huguenots, Colombier, Tunnels, Midroï, 2 Ouvertures caves correspond to that level. For the T2 level (+ 15 m), few caves correspond to that height inside the Ardèche gorges, for example the Ebbou and the Huchard cave. A few cave outputs also reach the same height than the T1 level (+ 8 m) such as Gigogne output, in the middle of the Ardèche gorges. Between T1 and T4 levels, meander cutoffs are also visible in the external landscape. The Montingrand meander presents an abandonment surface between + 30 and + 45 m, while the Combe d'Arc one is close to the + 15 one. At the end of the Ardèche gorges, a meander cutoff is also visible inside the T1 level, near St Just d'Ardèche. While this last one is made of sediments, the other ones are ancient, entrenched meanders, inside the limestone bedrock.

The numerous correspondences between alluvial deposits and cave levels, especially T4 and T3, are particularly interesting. Those pose the question of a potential low altitude speleogenesis linked to the Quaternary fluvial evolution of the Ardèche river. It is however less clear for the T1 and T2 levels (respectively + 8 m and + 15 m). The entrenched paleo meanders at the beginning of the Ardèche gorges are all below the Middle Pleistocene level, which is materialised on Fig. 3 by the T5 level, based on the assumption of AUDRA et *al*. (2001). Those meanders represent important landscape changes during this period, hence an active bedrock erosion and landscape evolution of the river from the middle to upper Palaeolithic period. Some of the caves at those altitudes host fluvial sediments from the Ardèche river (GENUITE et *al.*, 2019) and could thus be related to one of the low altitude fluvial deposits. Such observations provide new insights for future works to date cave sediments and to understand shared processes between river and cave dynamics.

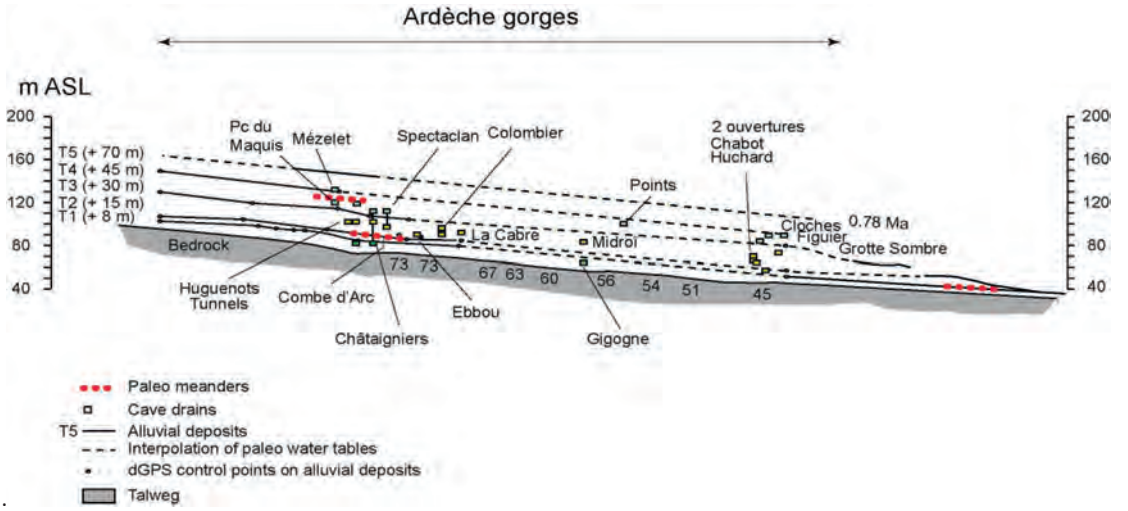

Figure 3: Cross-section of the Ardèche gorges. T1 to T5 fluvial levels are compared with cave altitudes along the Ardèche gorges course.

4. Conclusions

This study highlights the synchronous development of cave systems with river incision dynamics in the lower Ardèche valley during the Quaternary. It also demonstrates the need to investigate karst-river dynamics through an integrated 3D topographical approach in both environments (caves and rivers). Such an approach provides a solid basis for discussing spatial relationships which are key to understanding the response of cave systems (speleogenesis and sediment deposition) to regional dynamics involving large-scale processes such as the valley evolution.

Acknowledgements

The authors would like to thank Judicaël ARNAUD for opening us some of the Ardèche speleological documentation (CDS07) and Philippe MONTEIL who agreed to give us some of his cave surveys that are visible in Fig. 2.

References

DELMAS M., CALVET M., GUNNELL Y., VOINCHE, P., MANEL C., BRAUCHER R., TISSOUX H., BAHAIN J.-J., PERRENOUD C., SAOS T. (2018) Terrestrial 10Be and electron spin resonance dating of fluvial terraces quantifies quaternary tectonic uplift gradients in the eastern Pyrenees. Quaternary Science Reviews 193, 188–211. https://doi.org/10.1016/j.quascirev.2018.06.001

GENUITE K., DELANNOY JEAN-JACQUES, JAILLET S, (2018) Reconstitution des paléogéographies karstiques par l'approche cartographique 3D : Application au Pont d'Arc et à la Combe d'Arc (Ardèche, France). KARSTOLOGIA 67, 1–10.

GENUITE K., DELANNOY J.-J., JAILLET S., ARNAUD J., BERTHET J., GENUITE P. (2019) Le Pont d'Arc et la grotte des Châtaigniers (Gorges de l'Ardèche, France), indicateurs des processus du recoupement du méandre de la Combe d'Arc. Géomorphologie : relief, processus, environnement 25, 57–68. https://doi.org/10.4000/geomorphologie.12830

MARTINI J. (2005) Etude des paléokarsts des environs de Saint-Remèze (Ardèche, France) : mise en évidence d'une rivière souterraine fossilisée durant la crise de salinité messinienne. Karstologia 1–18.

MOCOCHAIN L., AUDRA P., CLAUZON G., BELLIER O., BIGOT J.-Y., PARIZE O., MONTEIL P. (2009) The effect of river dynamics induced by the Messinian Salinity Crisis on karst landscape and caves: Example of the Lower Ardèche river (mid Rhône valley). Geomorphology, Recent developments in surface and subsurface karst geomorphology 106, 46–61. https://doi.org/10.1016/j.geomorph.2008.09.021

MONNEY J. (2012) Et si d'un paysage l'on contait passé. Tissu de sens et grottes ornées le long des gorges de l'Ardèche. edytem 13, 21–42. https://doi.org/10.3406/edyte.2012.1203

SADIER B. (2013) 3D et géomorphologie karstique : La grotte Chauvet et les cavités des Gorges de l'Ardèche 478p.

TASSY A., MOCOCHAIN L., BELLIER O., BRAUCHER R., GATTACCECA J., BOURLÈS D. (2013) Coupling cosmogenic dating and magnetostratigraphy to constrain the chronological evolution of peri-Mediterranean karsts during the Messinian and the Pliocene: Example of Ardèche Valley, Southern France. Geomorphology 189, 81–92. https://doi.org/10.1016/j.geomorph.2013.01.019

Unravelling speleogenetic histories from the residence of Gods. A geomorphologic approach to understand speleogenesis in the foothills of Mount Olympus, Greece.

Christos PENNOS[1,2], Michael STYLLAS[3] & Yorgos SOTIRIADIS[2,4]

(1) Department of Earth Science, University of Bergen, 5020 Bergen, Norway, pennos4@gmail.com
(2) Proteas Caving Club, Grigoriou Lampraki 7, 55337 Thessaloniki, Greece
(3) Ecole Polytechnique Fédérale de Lausanne, Stream Biofilm and Ecosystem Laboratory, 1015, Lausanne, Switzerland. mstyllas@gmail.com
(4) Department of Geography, Aegean University, 81100 Mytilene, Greece, yorgossotiriadis@gmail.com

Abstract

We present new evidence that explains the speleogenetic setting under which the formation of caves in a high porosity host rock has been taking place. These caves are forming inside partially consolidated carbonate conglomerate that comprises an extensive lithified alluvial fan field in the foothills of Mount Olympus in Greece. We perform macro-morphological analysis of four caves that we explore through high detailed 3D surveys and couple our findings with a geomorphologic surveys of the alluvial fans. Our results suggest that the formation of these small caves is controlled by the combination of local climatic conditions and high relief of the host landforms, which has resulted in a shallow interbedded vadose zone. Our study demonstrates that the interplay between climate and landscape evolution was the key factor that controlled the formation of these caves.

1. Introduction

Mountain fronts in arid and semi-arid regions like the ones around the Mediterranean are often characterized by the presence of alluvial fans (KELLER & PINTER, 2002). These formations are considered as the endpoints of a source-to-sink system, where sediment is eroded from the mountainous area and is transported and deposited in the mountain front forming a cone-like shaped body (KELLER & PINTER, 2002). The link between the source and the sink is the rivers that efficiently erode and transport the material. Rivers are extremely sensible to climate variations over time, and hence their deposits are ideal to study any changes in these driving mechanisms. In carbonate mountainous areas with high erosion rates and sediment production, alluvial fans are usually built up by matrix-supported conglomerates composed of variable amounts of carbonate clasts (e.g., limestone, dolomite and marble) and fine clastic material. When the alluvial fans are entirely made of carbonate clasts it is common that the matrix is calcite, and the entire formation acts as a pure carbonate rock (Ford & Williams, 2007). Mount Olympus in Greece is built up by a 3000m sequence of metacarbonates that are exposed in the form of a tectonic window along its frontal fault of NNW – SSE direction (SMITH et *al*., 1997). The calcareous texture of basement rocks, along with intense faulting, high Pleistocene uplift rates (c. 1.6 mm/yr, NANCE, 2010) three major phases of glaciation and deglaciation episodes over the past 300 ka BP (SMITH et *al*., 1997, STYLLAS et *al*., 2015; STYLLAS et *al*., 2018), have resulted to the formation of a dramatic landscape curved by a steep fluvial network. The steep drainage system is responsible for transporting large amounts of sediment to the mountain front forming an extensive network of alluvial fans. Since their deposition, these alluvial fans have been subjected to the percolation of Ca-rich waters during the deglaciation phase. This initially resulted to their lithified structure and in a second stage, to the development of surface karstic formations and caves.

2. Materials and methods

We identified and explored in detail 4 caves (Fig. 1) through extensive fieldwork across the foothills of Mount Olympus close to Vrontou village. We used the DistoX (HEEB, 2010) data acquisition array to construct the cave survey and we followed the survey method of a centre line with vertical cross-sections along the direction of the survey. Survey stations were set at every 1 m to 3 m along the galleries and cross-sectional shots were made at <10° intervals. In this way, the dimensions and the shape of the cave passages are described in detail. The acquired data were processed using the Therion software package (BUDAJ & MUDRÁK, 2008) to produce the cave maps. The cave surveys were imported in a GIS database, to further investigate their spatial arrangement in relation to the bedrock and to any prominent geological formations.

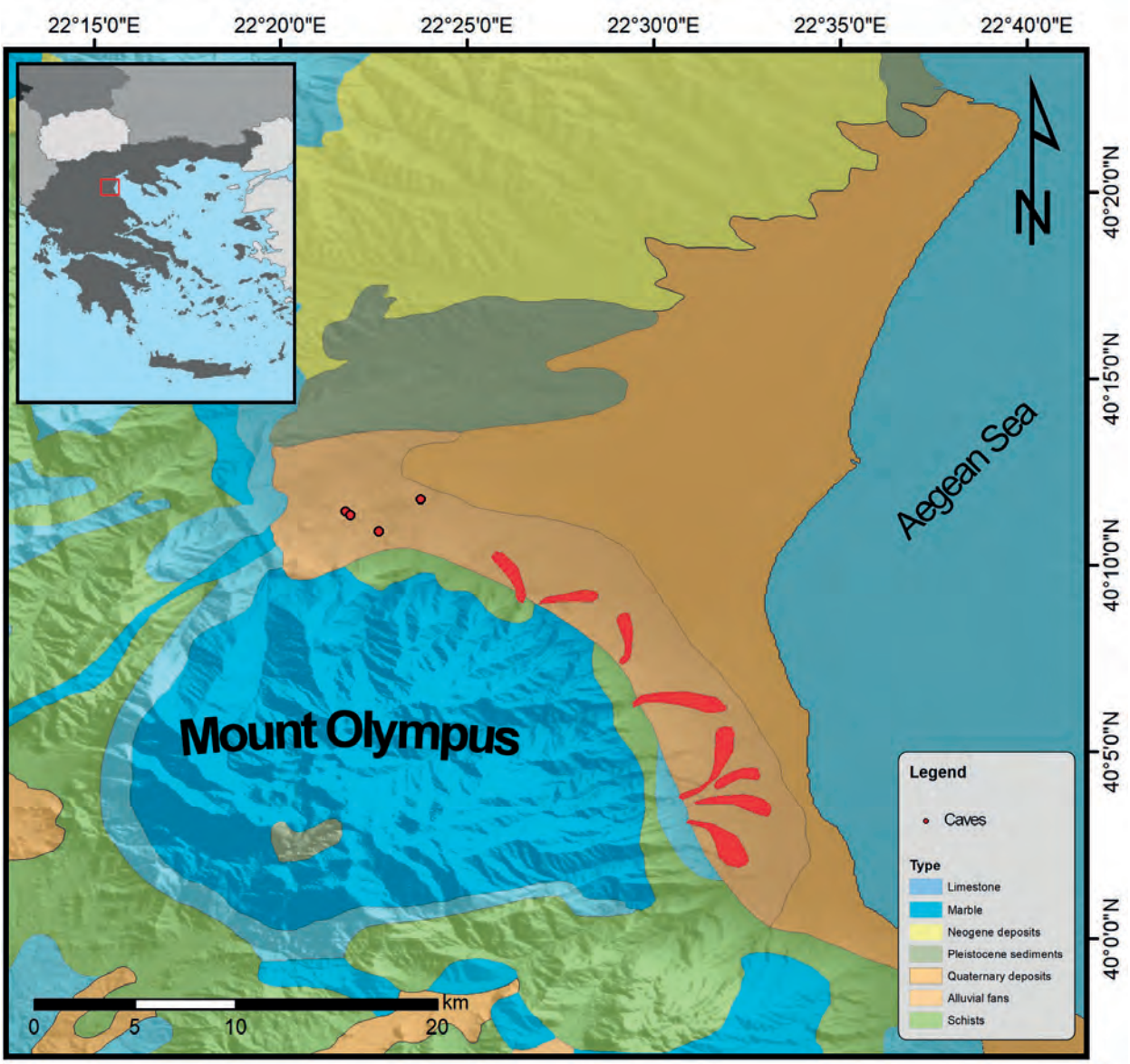

Figure 1: Geological map of the broader area

3. Results

The cave surveys showed that the length of the caves (Fig. 2) varies from 28 to 82 m. They are formed in a conglomerate host rock that consists of large limestone clasts connected by a homogenous calcite matrix (Fig. 3). The homogenous bedrock is interrupted by thin layers of fine material. The cave corridors present a canyon-like shape in cross section (Fig. 4) following an almost vertically dipping guiding discontinuity. All caves are forming with their main development axis striking towards SSE and present similar vertical extent ranging from 25 to 32 m. In Saki Chorafi cave, the deepest chamber is formed inside very fine reddish mud.

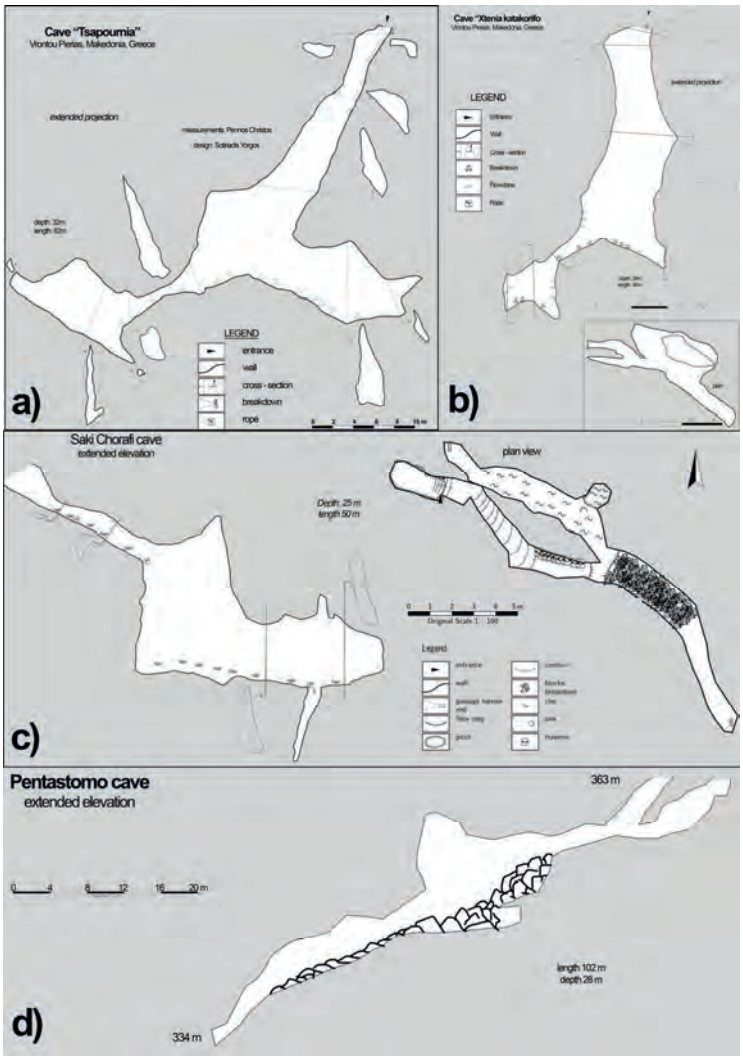

Figure 2: a) Cave surveys a) Tsapournia cave, b) Xtenia cave, c) Saki Chorafi cave and d) Pentastomo cave.

Figure 3: View of the host rock from Pentastomo cave. Red rectangles show the areas where the conglomerate is exposed. This is the typical setting for all the caves.

Figure 4. View from the corridor in Tsapournia cave depicting the characteristic morphology.

4. Discussion

Our results show that all four caves are formed by aggressive solutions percolating into the lithified alluvial fan deposits. The guiding fracture for all the caves is a surface that runs from NNW to SSE. Cave formation stops at almost the same depth for all caves (25-32 m below surface). Based on the above we suggest a plausible scenario describing the speleogenetic conditions under which the caves were formed. Following the deposition of the alluvial fans, the Quaternary deformation extensive brittle tectonics (NANCE et *al*., 2010), resulted to the formation of discontinuities in NNW - SSE direction, along the direction of Mount Olympus main frontal fault (SMITH et *al*., 1997, NANCE et *al*., 2010). During the mid to late Quaternary deglaciation episodes MIS 7, MIS 5 and MIS 1 (SMITH et *al*., 1997, STYLLAS et *al*., 2018), aggressive unsaturated glacially derived solutions were flowing on the surface of the alluvial fan, using tectonic striations as the main pathways to percolate the alluvial fan mass. The solutions rapidly dissolved the carbonate matrix, but the dissolution of the marble clasts was considerably slower. This explains the presence of boulders and pebbles on the cave floor. Even though the vadose zone is quite deep in the area (the caves are formed in the apex of the fans) dissolution halts approximately 30 m below surface. Although the dissolution terminus layer is not observed in all caves, we believe that it comprises a laterally extensive layer of fine sediment, formed during periods of low energy fluvial activity, when the local drainage system was depositing fine material on top of the older alluvial fans.

5. Conclusions

Our study shows that the formation of the caves in the foothills of Mount Olympus can be attributed to the deglaciation conditions that first resulted in a very active fluvial setting that transported and deposited the alluvial fans and in second stage (most likely during early Holocene) relished great amounts of unsaturated water that efficiently dissolved the carbonate formations. Equally important was the role of active tectonics forming the main conduits for the water to enter the mass of the alluvial fans. Finally, a more comprehensive study of the caves in the area in relation to the fluvial geomorphology alongside with chronological constraints is needed to understand the speleogenetic conditions in the area.

Acknowledgments

We gratefully thank the members of the Proteas caving club for their help during fieldwork. We also thank Aristeidis Zacharis for providing us photos from Pentastomo cave.

References

BUDAJ M., MUDRAK S. (2008) Therion: Digital cave maps, in Proceedings 4th European Speleological Congress 2008, 6.

FORD D., WILLIAMS P. (2007) Karst Hydrogeology and Geomorphology, in John Wiley & Sons Ltd, T. A., Southern Gate, Chichester, West Sussex PO19 8SQ, England, ed.

HEEB B. (2010) A general calibration algorithm for 3-axis compass/clinometer devices: Cave Radio and Electronics Group Journal, v. 73.

KELLER E. A., PINTER N. (2002) Active Tectonics: Earthquakes, Uplift, and Landscape.

NANCE R. D. (2010) Neogene–Recent extension on the eastern flank of Mount Olympus, Greece: Tectonophysics, 488, 1-4, 282-292.

SMITH G.W., NANCE R.D., GENES A.N. (1997) Quaternary glacial history of Mount Olympus, Greece. Geol. Soc. Amer. Bull. 109, 809–824.

STYLLAS M. N., SCHIMMELPFENNIG I., BENEDETTI L., GHILARDI M., AUMAITRE G., BOURLES D., KEDDADOUCHE K. (2018) Late-glacial and Holocene history of the northeast Mediterranean mountains - New insights from in situ -produced 36 Cl - based cosmic ray exposure dating of paleo-glacier deposits on Mount Olympus, Greece: Quaternary Science Reviews, 193, 244-265.

STYLLAS M. N., SCHIMMELPFENNIG I., GHILARDI M., BENEDETTI L. (2015) Geomorphologic and paleoclimatic evidence of Holocene glaciation on Mount Olympus, Greece: The Holocene.

Advances in the speleogenetic characterization of the flank margin caves from Cozumel island, México

Hugo E. SALGADO-GARRIDO[1,2], Salvador TREJO-PELAYO[1,2], Rafael LÓPEZ-MARTÍNEZ[2,3], Ricardo BARRAGÁN[2,3], German YAÑEZ[4] & Luis MEJÍA-ORTÍZ[5]

1 Postgraduate in Earth Sciences. National Autonomous University of Mexico (UNAM). 6 04510, Mexico City, Mexico. hugoe1617@gmail.com (corresponding author); salvador.trejo.p@gmail.com
2 Karst and Carbonates Laboratory. Institute of Geology. National Autonomous University of Mexico (UNAM). 04510, Mexico City, Mexico. ralopezm@geologia.unam.mx
3 Institute of Geology. National Autonomous University of Mexico (UNAM). 04510, 10 Mexico City, Mexico dirigl@unam.mx
4 Círculo Espeleológico del Mayab A.C., Isla Cozumel, Quintana Roo, México. yanez.cave@gmail.com
5 Biospeleology and Carcinology laboratory, Universidad de Quintana Roo, División de Desarrollo Sustentable, Av. Andrés Quintana Roo s/n, Cozumel 77600, Quintana Roo, Mexico. luismejia@uqroo.edu.mx

Abstract

The Cozumel island is composed of young carbonate rocks and represents an excellent example of a simple carbonate island. The karst evolution and geomorphological configuration of the island are related to coastal processes, glacioeustatic changes, and dissolution within the mixing zone. Solutional structures like caves have been documented but poorly studied in the area. Though, a precise speleogenetic characterization of some karst structures will help to elucidate the island's evolution. We describe flank margin caves and banana holes from Cozumel island according to their morphologies and the depositional environment of the host rock. Caves are mainly developed in rocks belonging to the ancient lagoon, strand plains, sand cays, and low-lying islands. The classical flank margin caves are located within the restricted lagoon facies or facies zone (FZ) 8 of Wilson's (1975) model. In contrast, the banana holes are preferentially distributed in the transitional zone between the open lagoon and platform margin (FZ 6-7). This finding suggests that flank margin caves could be related to the last highstand MIS 5e and the then the oldest caves from the island. Simultaneously, the banana holes are associated with strand plain progradation during the subsequent regressive stage and the increase of the Cozumel island area.

Résumé

Progrès dans la caractérisation des grottes de marge de biseau salé à partir de l'île Cozumel, Mexique. L'île Cozumel est composée de roches carbonatées récentes et offre un très bon exemple d'île calcaire simple. L'évolution du karst et la configuration géomorphologique de l'île sont liées aux processus littoraux, aux variations glacio-eustatiques et à la dissolution dans la zone de mélange. Des grottes étaient connues dans cette zone, mais pas réellement étudiées, de telle sorte qu'une caractérisation spéléogénétique précise des structures du karst était nécessaire pour éclairer l'évolution de l'île. Nous décrivons les grottes de marge de flanc et les trous « banane » en fonction de leurs morphologies et de l'environnement sédimentaire. Les grottes se développent principalement dans les roches appartenant à l'ancien lagon, aux plaines de sable, aux cayes de sable et aux îles basses. Les grottes classiques de marge de biseau salé sont situées dans le faciès lagunaire restreint ou zone de faciès (FZ) 8 du modèle de Wilson (1975). En revanche, les trous « banane » sont localisés de préférence dans la zone de transition entre la lagune ouverte et la marge de plate-forme (FZ 6-7). Cette constatation suggère que les grottes de marge de biseau salé pourraient être liées au dernier highstand MIS 5e et qu'elles sont alors les plus anciennes grottes de l'île. Simultanément, les trous « banane » sont associés à la progradation de la plaine de flanc pendant le stade régressif ultérieur et à l'augmentation de la superficie de l'île de Cozumel.

1. Introduction

Cozumel Island has ubiquitous coastal karst features, including caves due to its geological and geographical specific conditions, combining physical, biological, and chemical processes. These conditions triggered intense speleological exploration on the island and the study of organisms inhabiting the anchialine systems (*e.g.* MEJÍA-ORTÍZ et *al*. 2007, YAÑEZ et *al*. 2007). However, karst morphology has been poorly studied.

In Cozumel, the karst morphologies and erosional features have been influenced by the marine environment since its formation. Currently, the island's border displays morphologies caused by sea-water action, including the wave zone, splash, and spray marine (*e.g.,* sea caves, karrenfields mixed with biokarst features among others). Also, are documented wind (tafoni) and mixing corrosion (inlets) morphologies. All these karst features decrease in abundance to the island's center.

Towards the center, the dissolution structures such as cenotes and solution pans, locally named "aguadas or "rejolladas" are most evident, even increasing in size (YAÑEZ

et *al*., 2007; MEJÍA-ORTÍZ et *al*., 2007). KELLEY et *al.,* (2006) suggest the ancient flank margin cave (FMC) process, probably related to the FMC's in the Bahamas archipelago. Some explorations draft the cave maps related to sinkholes with similar FMC morphologies.

The FMC morphology was first described in the Bahamas archipelago; subsequently, MYLROIE and CAREW (1990 and 1995) encompass the speleogenetical theory of FMC linked to mixing solution of freshwater and seawater, forming the cavities at the margins of freshwater lens related to the sea-level position. The mixing solution is considered the primary process to the dissolution of $CaCO_3$ in these types of environments (MYLROIE and MYLROIE 2007). Nonetheless, the organic matter catchment leads to rich sulphuric acid-aggressive solutions to play a special role in speleogenesis (BOTTRELL et *al*., 1993, MYLROIE and MYLROIE 2007). Recently other research favors the oxidation of organic matter and preferential contribution of CO_2 for the generation of similar morphologies (GULLEY et *al.,* 2016). This discovery shed new light on the discussion about the primary process involved in the dissolution in these karst environments.

During the last two decades, advances in recognition of the FMC occurs throughout the world. Specifically on islands with young and mature carbonates like Bahamas, Bermuda, Isla Mona, Sicily, Sardinia, and regions with greater geological complexity such as Mariana islands. These morphologies have been summarized in the carbonate island karst model (CIKM) (MYLROIE and MYLROIE 2007).

It is accepted that flank margin speleogenesis is associated with sea-level changes, especially with the last highstand (MYLROIE and MYLROIE 2007). In some regions, they are recognized as index markers of sea-level position (VAN HENGSTUM et *al.,* 2015). This work aims to characterize the flank margin morphologies in Cozumel island as a key to understand its geomorphological evolution throughout the Quaternary.

2. Study area, materials and methods

The island of Cozumel is located in the northeastern Yucatan peninsula (20°16'12" and 20°35'15"N and between 87°01'48" and 86°43'48"W) comprising an area of 482 km^2 (MEJÍA- ORTÍZ et *al*. 2007) (Fig.1).

Cozumel displays an average altitude of 5m asl (meters above sea level), with a maximun of 15m asl (FRAUSTO-MARTÍNEZ et *al*. 2018).

The island is part of a set of isolated carbonate platforms that extends from Belize to Mexico (Gischler and Lomando 1999, 2000), developed on a horst-block section of the northeastern fault affecting the continental margin (WARD 1997).

The geology and stratigraphy of the Cozumel are correlated with the continental part of the Yucatan peninsula (WARD 1997) with the presence of the Carrillo Puerto Formation (Miocene-Pliocene) overlayed by subtidal carbonate sands, deposited during the Pleistocene and Holocene (SPAW 1978, WARD 1997, SALGADO-GARRIDO et *al*., *in review*). Among these deposits, the occurrence of pedogenetic carbonates called calcretes or caliches has been widely recognized (WARD 1997, VALERA-FERNÁNDEZ et *al.,* 2020). The most well-known are the caliches 1 and 2, corresponding to the last lowstands sea-level of isotopic marine stages (MIS) 6 and 4.

Cave morphologies were described according to MYLROIE and CAREW (1990 and 1995) and PALMER (2007) from visual inspection and cave topographies. Rock samples were analyzed in thin sections under a petrographic microscope Olympus BX51.

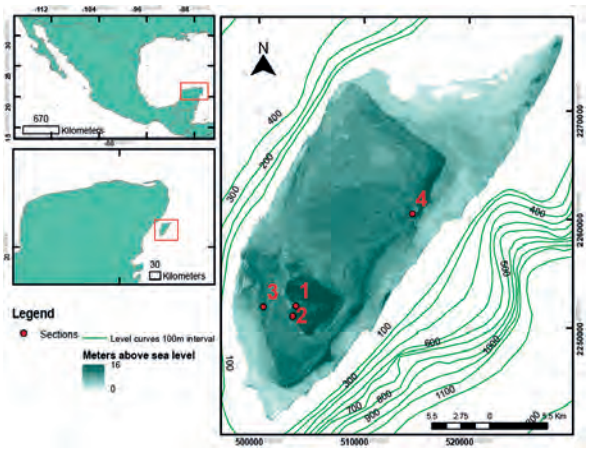

Figure 1. Location of the studied caves. 1. Nohoch Hool cave. 2. Cenote Chempita. 3 Cedral area (Aktun Balam cave). 4. Cantera Transversal and Murciélagos caves.

Photomicrographs were taken using the Image-Pro Plus v.5.1.1 software. Samples were classified following DUNHAM (1969) and EMBRY and KLOVAN (1971) criterias while Facies Zones (F.Z.) by FLÜGEL (2010).

3. Results and discussions

Flank margin caves usually occur on the center of the island (Fig. 1), with an altitude between 5-6m asl. They are generally documented in flat areas, at the average height of the island.

These caves are characterized by lenticular to oval cameras with round and smooth walls. Ceilings are usually near flat with little copulas ending in blind passages. Stand out the lack of fluvial sediments, scallops, or large debris collapses. Some residual structures, like pillars, are commonly documented.

The clear FMC development is delimited to the Pleistocene carbonate sands, bounded by the caliche 1 and 2 and related to (MIS) 6 and 4, respectively (SALGADO-GARRIDO et *al., in review*). Petrographic analysis evidenced three facies association for the host rocks of FMC. The first one corresponding to F.Z. 8 or platform interior restricted lagoon. This facies is composed of highly weathered massive calcarenites with wackestone-packstone of peloids and coated bioclast (Fig. 2 a,c). The F.Z. 8 are present in the Nohoch Hool cave and the upper level of the Cenote Chempita.

The second facies zone F.Z. 7 (platform open marine) comprises grainstone of peloids, ooids, and aggregated grains associated with a decrease of coated bioclast (Fig.2 b, d). In some parts display low to high angle cross-stratification, herringbone stratification, and bioturbation.
The F.Z. 7 are documented in Murcielagos, Cantera Transversal caves, and Aktun Balam cave.
The third facies zone F.Z. 6 are sand shoals meteorically affected overlying the previous 7 and 8 zones.
The FMC morphologies are consequence of mixing waters, consider as a sub-category of hypogenic caves, due as they do not directly relate to surface hydrological processes (PALMER 2007, MYLROIE and MYLROIE 2007). Their formation occurs without a direct input, and they do not develop real conduits. In that sense, their morphology of "phreatic conduits" is reached by the conjunction of isolated chambers and could be organized in spongiform patterns (PALMER, 2007).
Like other carbonate islands (*e.g.,* Bahamas, Bermuda, Isla Mona Island, Mariana Islands) in Cozumel island, FMC are restricted to the freshwater lens position. This fact points to the FMC as a precise proxy for the detection of past sea levels.
Flan Margin Caves on the island of Cozumel appears at an altitude of 5-6 masl. They are developed on carbonate sandstones deposited during the last MIS 5e highstand (SPAW 1978, SALGADO-GARRIDO et *al., in review*). As previously suggested, these deposits can be correlated with similar ones from the Bahamas (KELLEY et *al.,* 2006). Nonetheless, FMC of Cozumel occurs on sediments deposited on subtidal environments, while in the Bahamas on eolian and subtidal deposits.
FMC are currently divided into two types: Classical FMC, which requires a pre-existing rock for its development, and the syngenetic FMC, which has been named Banana Holes in the Bahamas archipelago (PACE et *al.,* 1993; HARRIS et *al.,* 1995, MYLROIE and MYLROIE, 2017). In Cozumel, the classic FMC appear in the center of the island (Fig. 1, 2). This part corresponds to the flanks of the protected lagoon facies proposed by SALGADO-GARRIDO et *al.* (*in review*).
Recently, a lagoon environment has been proposed below the highest landform (16m asl) of Cozumel, whose origin and the other more elevated areas are associated with the cay islands formations during MIS 5e. These cay islands acquire a similar morphology like an atoll during the last highstand sea-level (SALGADO-GARRIDO et *al., in review*).
The micritic texture founded in Nohoch Hool cave walls and the upper part of the Cenote Chempita suggests partial protection and low energy of the depositional environment interpreted as a protected lagoon.
Within these environments, the dissolution occurs by mixing of the meteoric waters from ancient cays and the saltwater, favoring the generation of flank margin morphologies.

On the other hand, the syngenetic FMC or Banana Holes appear in the progradation of the ancient strandplains (F.Z. 7) (Fig. 1, 2). The Banana Holes corresponds to caves of the Cedral community (*e.g.* Aktun Balam) on the west side of the island while in the north, on Murcielagos and Cantera Transversal. Sedimentary structures and microfacies of these zones are similar to those found in the Bahamas, associated with FMC (PACE et *al.* 1993, MYLROIE and MYLROIE 2017).
On the other hand, the development of Banana Holes is restricted to the areas belonging to the ancient strand plains or coastline progradation.
According to those above mentioned, we suggest that the classical FMC development corresponds to the maximum sea-level peak during MIS 5e when the first cay islands were established. After that, the subsequent sea-level drop triggers the strandplain progradation and the formation of the syngenetic Banana Holes.

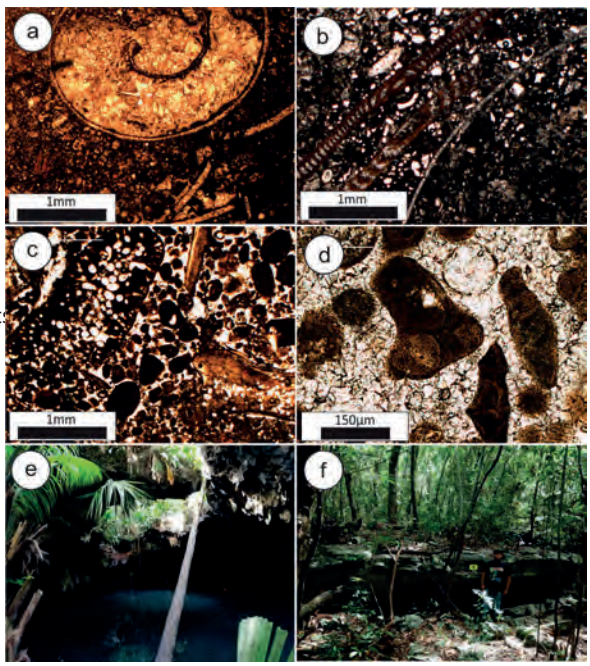

Figure 2. Microfacies of the host rock and Cave features. Microfacies (a-d): a) Cenote Chempita b) Nohoch Hool cave. Wackestone-packstone textures with peloids, mollusks and foraminifera bioclasts, correspondig to F.Z. 8 or protected lagoon. c) Cantera Transversal cave. d) Aktun Balam cave. Grainstone textures with peloids, ooids, biolcasts and aggregated grains corrsponding to F.Z. 7 platform open marine. Cave features (e-f): e) Chempita cenote, above of water table representing FMC. f) Murcielagos cave represent the Banana Hole.

4. Conclusion

Two different FMC were identified, the classic FMC and Banana Holes. The first one, located in the center of the island, evolved during the last highstand sea-level and can be correlated with similar caves in the Caribbean region.

The second one is considered as a syngenetic structure evolving with the strandplain progradation. More work is needed to better comprehend flank margin caves in the Cozumel and their relationship with the sea-level variations, but the evidence points to a very precise proxy for its determination.

Acknowledgments

We acknowledge the financial support by National Council of Science and Technology (CONACytT) for the fellowship of PhD studies and grant PAPIIT IN113020. We thank the support of Sara Grisset, Orlando Gutiérrez, Lourdes Rodríguez, and Jaime Díaz during field sessions as well as for obtaining the thin sections. Special thanks to Emilio Novelo Flores and Mariano Dzay, the commissioners of the Villa Cozumel ejido, and the Fidel Ladron de Guevara of the Wild Tours Cozumel for providing access to the area and hospitality

References

BOTTRELL S.H., CAREW J.L. and MYLROIE J.E. (1993) Bacterial sulphate reduction in flank margin environments: Evidence from Sulphur isotopes, in White B., ed., *Proceedings of the 6th Symposium on the Geology of the Bahamas*, Port Charlotte, Florida, Bahamian Field Station, p. 17–21.

DUNHAM R. (1962) Classification of carbonate rocks according to depositional texture. iI Ham W (ed) Classification of Carbonate Rocks: *American Association of Petroleum Geologists*, Memoir 1: 108-121.

EMBRY A. and KLOVAN J. (1971) A late Devonian reef tract on Northeastern Banks Island Northwest Territories: *Bulletin of Canadian Petroleum Geologist*, 19: 730-781.

FLÜGEL E. (2010) *Microfacies of carbonate rocks analysis, Interpretation and application*: Springer-Verlag Berlin, 984p.

FRAUSTO-MARTÍNEZ O., ZAPI SALAZAR A. and COLIN-OLIVARES O. (2018) *Identification of Karst Forms Using LiDAR Technology: Cozumel Island, Mexico, Trends in Geomatics - An Earth Science Perspective*, Rifaat Abdalla, IntechOpen.

GISCHLER E. and LOMANDO A.J. (1999) Recent Sedimentary facies of isolated carbonate platforms, Belize-Yucatan system, Central America. *J. Sediment Res.*, 69: 747-763.

GISCHLER E. and LOMANDO A.J. (2000) Isolated carbonate platform of Belize, Central America: sedimentary facies, late Quaternary history and controlling factors. In Salaco E, Skelton PW, Palmer TJ (eds) *Carbonate platforms systems: components and interactions*. Geol. Soc. Spec. Publ, 178: 135-146.

GULLEY J.D., MARTIN J.B. and BROWN A. (2016) Organic carbon inputs, common ions and degassing: rethinking mixing dissolution in coastal eogenetic carbonate aquifers. *Earth Surface Processes and Landforms* 41(14):2098-2110.

HARRIS J.G., MYLROIE J.E. and CAREW J.L. (1995) Banana holes: Unique karst features of the Bahamas. *Carbonates and Evaporites*. 10(2): 215-224.

KELLEY K.N., MYLROIE J.E., MYLROIE J.R., MOORE C., COLLINS L., ERSEK L., LASCU I., ROTH M., MOORE P., PASSION R. and SHAW C. (2006) Eolianites and karst development in the Mayan Riviera, Mexico. *Speleogenesis and Evolution of Karst Aquifers*, Issue 11.

MEJÍA-ORTÍZ L.M., YAÑEZ G., LÓPEZ-MEJÍA M., ZARZA-GONZÁLEZ E. (2007) Cenotes (anchialine caves) on Cozumel island, Quintana Roo, México. *Journal of Cave and Karst Studies*, 69 (2): 250-255.

MYLROIE J.E., CAREW J.L (1990) The flank margin model for dissolution cave development in carbonate platforms. *Earth Surface Processes and Landforms*. 15:413-424.

MYLROIE J.E. and CAREW J.L (1995) Geology and karst geomorphology of San Salvador Island, Bahamas. *Carbonates and Evaporites* 10(2):193-206.

MYLROIE J.R. and MYLROIE J.E. (2007) Development of the carbonate island karst model. *Journal of Cave and Karst Studies*. 69(1):59-75.

MYLROIE J.E. and MYLROIE J.R. (2017) Bahamian flank margin cave as hypogene caves, in Klimchouk A., Palmer A.N., De Waele J., Auler A. S. and Audra P. eds. *Hypogene karst regions and caves of the world*. Springer International Publishing. pp 757-767.

PACE M.C., MYLROIE J.E. and CAREW J.L. (1993) Petrographic analysis of vertical dissolution features on San Salvador Island, Bahamas, in White B. ed. *Proceedings of the 6th Symposium on the Geology of the Bahamas*. pp. 109-123.

PALMER A.N. (2007) *Cave geology*. Cave Books 454p.

SALGADO-GARRIDO H. E., VALERA-FERNÁNDEZ D., TREJO-PELAYO S., SOLLEIRO-REBOLLEDO E., LÓPEZ-MARTÍNEZ R., BARRAGÁN R., YAÑEZ G., CORCHO-ALVARADO J. A., RÖLLIN S. and MEJÍA-ORTÍZ L. M. (In review) Sedimentary evolution of the island of Cozumel, Mexico, led by Quaternary sea-level changes. Microfacies and radiometric evidence. *Facies*.

SPAW R.H. (1978) Late Pleistocene stratigraphy and geologic development of Cozumel island, Quintana Roo, México. *Trans. Gulf Coast Assoc. Geol. Soc.*, 28: 601-620.

VALERA-FERNÁNDEZ D., CABADAS-BÁEZ H., SOLLEIRO-REBOLLEDO E., LANDA-ARREGUÍN F. and SEDOV S. (2020) Pedogenic carbonate crusts (calcretes) in karstic landscapes as archives for paleoenvironmental reconstructions: a case study from Yucatan Peninsula, Mexico. *Catena* (in press).

VAN HENGSTUM P.J., RICHARDS D.A., ONAC B.P. and DORALE J.A. (2015) Coastal caves and sinkholes. In: Shennan I., Long A.J. and Horton B.P. eds. *Handbook of sea-level research*. Jhon Wiley & Sons, pp. 83-103.

WARD W.C. (1997) Geology of coastal island northeastern Yucatan Peninsula perspective. In Vacher HL, Quinn TM eds. Geology and Hydrogeology of carbonates islands. *Developments in Sedimentology*, 275-198.

YAÑEZ-MENDOZA G., ZARZA-GONZÁLEZ E., MEJÍA-ORTÍZ L.M. (2007) Sistemas anquihalinos. In: Mejía-Ortiz L.M., ed. *Biodiversidad acuática de la Isla de Cozumel*. México: Universidad de Quintana Roo-CONABIO; 2007. 49–70.

New insights on the Carburangeli Cave speleogenesis: a flank margin cave in Northern Sicily (Italy)

Giuliana MADONIA[(1)], Giuseppe RIOLO[(1)], Cipriano DI MAGGIO[(1)], Rosario DI PIETRO[(2)], Ilenia M. D'ANGELI[(3)], Jo DE WAELE[(3)] & Marco VATTANO[(1,4)]

(1) Dipartimento di Scienze della Terra e del Mare, Università di Palermo, giuliana.madonia@unipa.it (corresponding author), cipriano.dimaggio@unipa.it, marco.vattano@unipa.it
(2) Legambiente Sicilia – Riserva Naturale Grotta di Carburangeli, Italy
(3) Dipartimento di Scienze Biologiche, Geologiche e Ambientali, Università di Bologna, jo.dewaele@unibo.it, dangeli.ilenia89@gmail.com
(4) Ass. Nat. Speleologica "Le Taddarite" - Italy

Abstract

Flank margin caves form in coastal regions by mixing dissolution. Their development is controlled by the position of the fresh-salt water mixing boundary, which in turn, is related to sea-level position. They are characterized by a typical cave pattern and cave-wall morphologies and represent good indicators of past sea levels.
This contribution shows the results of recent studies conducted in the Carburangeli Cave, a small sub-horizontal cavity developed in Northern Sicily, close to Palermo. This cave was firstly known for paleontological and archaeological findings and for these reasons, along with its speleological and biological interest, a Nature Reserve has been instituted by the Sicilian government, and the cave was put under the management of "Legambiente Sicilia".
Carburangeli Cave opens on a marine palaeocliff at 22 m a.s.l., roughly 500 m far from the coastline, and is partially developed in Mesozoic limestone and in the overlying Pleistocene calcarenites. Its position, pattern, peculiar morphologies, lack of turbulent-flow wall sculptures and alluvial/colluvial sediments suggest an origin controlled by coastal mixing processes giving also important information on the Upper Pleistocene sea level and coastline position in this Northern sector of Sicily.

1. Introduction

Flank margin caves are peculiar dissolution caves which develop along many carbonate coastal regions. These caves form by mixing dissolution processes in the distal margin of the freshwater lens, under the flank of the enclosing landmass (MYLROIE & CAREW, 1990). Their development is controlled by the position of the fresh-salt water mixing boundary, which in turn, is connected to sea-level position.
The first studies demonstrated flank margin caves to be typical cavities of diagenetically immature young carbonates (MYLROIE & CAREW, 1990; FRANK *et al*., 1998; MYLROIE & MYLROIE, 2013). High primary porosity of these rocks favours diffuse flow and the formation of irregular globular rooms, dead-end passages, phreatic, slow-flow morphologies.
Nevertheless, more recent publications have reported flank margin caves to develop also in diagenetically mature carbonate rocks (MYLROIE *et al*., 2008; OTONIČAR *et al*., 2010; RUGGIERI & DE WAELE, 2014; D'ANGELI *et al*., 2015; ARRIOLABENGOA *et al*., 2017). In these rocks primary porosity is often insignificant and water flow is controlled mainly by joints, faults, and bedding planes (PALMER, 1991; FORD & WILLIAMS, 2007), therefore, cave pattern and morphologies of flank margin caves result strictly influenced by discontinuity planes.
This contribution shows the results of recent geomorphological studies carried out in the Carburangeli Cave, a small sub-horizontal cavity developed in Northern Sicily, close to Palermo (Fig. 1). The palaeontological and archaeological importance, along with the speleological and biological interest of this site has allowed its classification as a regional Nature Reserve instituted by the Sicilian government, and the cave was put under the management of "Legambiente Sicilia".

2. Materials and methods

A geomorphological study has been carried out in the Carburangeli Cave to identify its pattern and the main dissolution/erosion and depositional features. Preliminary palaeontological and mineralogical analyses have been performed on cave sediments and bedrock samples of different areas in the cave.

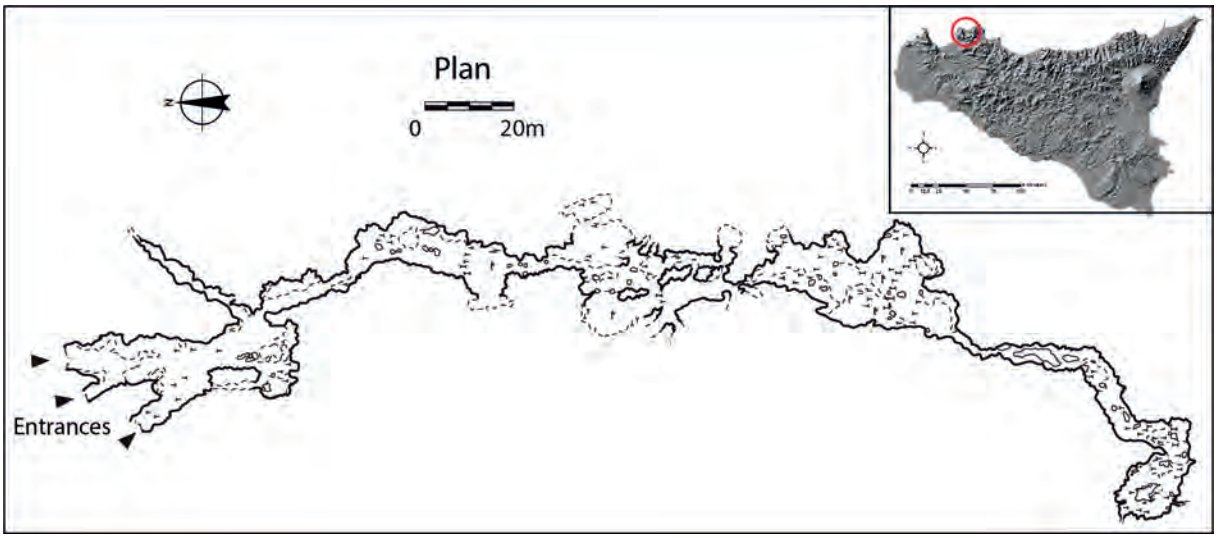

Figure 1: Plan view and location of the Carburangeli Cave (modified from: archive of Carburangeli Cave Nature Reserve).

3. Results

The Carburangeli Cave opens at the foot of a marine palaeocliff at 22 m a.s.l., roughly 500 m far from the current coastline (Fig. 2A). The cave develops horizontally for about 400 m in the N-S direction, only a few meters below the external surface (Fig. 1). From the entrance area to about 300 m from the entrance, the cave is carved in Calabrian marine calcarenites and conglomerates, whilst the innermost sector is hosted in Lower Jurassic-Triassic limestones and dolomitic limestones.
The cave morphology is different in the two host rocks. In the porous and permeable Calabrian calcarenites and conglomerates the cavity consists of wider than high irregular chambers with a flat roof connected by narrow galleries (Fig. 2B, 2C), dead-end passages, characterized mainly by phreatic, slow-flow features such as wall and ceiling cusps, intricate dissolutional wall sculptures, small phreatic tubes, pillars, ceiling pockets and spongework (Fig. 2D). In the entrance area the cuspate morphologies occur both on the ceiling and on the floor (Fig. 2B). The ceiling and walls show very weathered surfaces caused by condensation-corrosion processes.

The morphology varies radically in the telogenetic Mesozoic carbonate rock, where the cave is articulated along a narrow passage, which is clearly developed along a discontinuity plain. In this sector bedrock pendants, small phreatic tubes and curvilinear bedrock surfaces have been observed (Fig. 2E). The cavity ends with a breakdown chamber where collapse deposits obliterate the early morphologies.
The cave communicates to the outside through three openings, the largest of which shows a well pronounced intertidal wall notch, clearly visible also in the first room of the cavity (Fig. 2A, 2B), and in the deeper parts of the cave where the contact between the Pleistocene calcarenites and the Mesozoic limestones is recognizable. The marine influence is testified also by numerous distinct *Lithophaga litophaga* boreholes which cut mainly the Mesozoic carbonate bedrock (Fig. 2F). The cave lacks high flow velocity features, such as scallops or similar flow marks on the walls.

Cave deposits consist of different kinds of carbonate vadose speleothems (Fig. 2C), which often obliterate pattern and erosion features, and great amounts of physical deposits localized on the floor and locally in the wall niches.
The mineralogical and palaeontological composition of the physical deposits vary in relation to the cave area where they occur. In the entrance area the deposits unfortunately appear highly reworked as they were removed and studied during several palaeontological and archaeological excavation campaigns between the end of the 19th and the beginning of the 20th century. These investigations revealed the presence of important Upper Palaeolithic vertebrate fossils, and remains of meals and artifacts dating back to the Palaeolithic and the Bronze Age (GEMMELLARO, 1886; BURGIO & DI PATTI, 2001).

In some wall niches a more preserved aeolian deposit consisting mainly of quartz grains has been discovered.
In the middle part of the cave, sedimentary cave deposits can reach thickness up to about 50 cm. They are made of coarse sands and fine gravels and are composed mainly of calcite with small amounts of quartz and halite. At places phosphate has been found. Palaeontological analysis reported the presence of foraminifera, such as *Elphidium Crispum, Rosalina sp., Ammonia Beccarii,* and remains of echinoids and bryozoans. Bat bone fragments also occur.
In the inner area, where the cave is carved in the Mesozoic limestones, red and brown sterile silty sediments infill some wall niches.

Stream-laid sediments and other types of fluvial features have not been recognised.

Figure 2: Typical morphologies in the Carburangeli Cave. A) Entrance of the Carburangeli Cave carved in Pleistocene calcarenites, exposed by sea-cliff retreat. A distinct horizontal marine wall notch on the left of the entrance is visible. B) Cusp morphologies on the roof and floor in the first chamber, near the entrance. The wall notch is well distinguishable. C) A classical chamber with flat roof developed in the calcarenite rock, characterized by great amounts of vadose carbonate speleothems. D) Some phreatic, slow-flow features developed in the calcarenite. E) Pendants and small phreatic tubes developed in the Mesozoic carbonate bedrock. F) Lithophaga litophaga *boreholes cut in the Mesozoic carbonates*.

4. Discussions and Conclusions

Geographic position, sub-horizontal setting, presence of low galleries with a flat roof and developed in width rather than in height (at least along the calcarenite level), occurrence of phreatic, slow-flow features, and lack of fluvial deposits clearly indicate the Carburangeli Cave to be a flank margin cave controlled by coastal mixing processes. These caves

form along the distal margin of the freshwater lens, whose position is closely tied to the sea level at the time of cave formation. Here the maximum dissolution occurs by freshwater mixing, organic decay, and enhanced lens flow velocities (MYLROIE J.E. & MYLROIE J.R., 2007).

Carburangeli Cave began to form during a sea level highstand. In this phase, the first phreatic voids formed as cavities with poor connection with the exterior environment. In the Quaternary bedrock, given the high porosity of the calcarenites and conglomerates, water was able to dissolve the rock in all directions, creating large and rather low rooms shaped by typical phreatic features; in the Mesozoic carbonate level, on the other hand, the dissolution processes acted along preferential discontinuity planes with a N-S direction, generating rather narrow passages more developed in height, as joints provided preferential flow paths in the fresh-water lens, and therefore mixing environments (MYLROIE *et al.*, 2008).

After a first phase of phreatic void formation by mixing water, the cave was breached and intercepted by marine erosional processes and sea-cliff retreat. Preliminary analyses of sediments did not allow to discriminate whether they are marine deposits formed during this phase or are the weathered product of the original rock, as they show similar features to those of the Pleistocene host rock. Analysis of some morphologies, like the marine wall notch and *lithophaga* boreholes, confirm anyway that the cave was intercepted by sea water.

By relating the altitude at which the cave develops with the heights of the internal margins of the marine terraces (DI MAGGIO, 2000), the Carburangeli Cave most likely formed during the MIS 5e sea level highstand. The cave appears to be the result of a single sea-level highstand phase, as such its pattern and morphologies do not seem overprinted by successive phreatic conditions.

Following the relative lowering of the sea level, the cavity passed to continental conditions, as evidenced by the likely aeolian sediments, and the great amounts of speleothems.

Condensation-corrosion processes and vadose speleothem formation mainly characterise the current speleogenetic phase.

Acknowledgments

We gratefully thank prof. E. Di Stefano for the help with the palaeontological analysis.

References

ARRIOLABENGOA M., D'ANGELI I.M., DE WAELE J., PARISE M., RUGGIERI R., SANNA L., MADONIA G., VATTANO M. (2017) Flank Margin Caves in Telogenetic Limestones in Italy. In: Moore K., White S. (Eds), Proceedings of the 17th International Congress of Speleology, July 22–28, Sydney, NSW Australia, 1, 289-292.

BURGIO V., DI PATTI C. (2001) Aspetti paleontologici della Grotta di Carburangeli. Naturalista siciliano, S. 4, 25, (suppl.), 351-360.

D'ANGELI I.M., SANNA L., CALZONI C., DE WAELE J. (2015) Uplifted flank margin caves in telogenetic limestones in the Gulf of Orosei (Central-East Sardinia—Italy) and their palaeogeographic significance. Geomorphology, 231, 202-211.

DI MAGGIO C. (2000) Morphostructural aspects of the central northern sector of Palermo Mountains (Sicily). Mem. Soc. Geol. It., 55, 353-361

FORD D.C., WILLIAMS P.W. (2007) Karst Hydrology and Geomorphology. Wiley, 561pp.

FRANK E.F., MYLROIE J.E., TROESTER J., ALEXANDER E.C., CAREW J.L. (1998) Karst development and speleogenesis, Isla de Mona, Puerto Rico. Journal of Cave and Karst Studies, 60, 2, 73-83.

GEMMELLARO G.G. (1886) Sulla Grotta di Carburangeli. Nuova grotta ad ossame e armi di pietra dei dintorni della Grazia di Carini. Giorn. di Sc. Nat. ed Econom., 1, 1-12.

MYLROIE, J.E., CAREW, J.L. (1990) The flank margin model for dissolution cave development in carbonate platforms. Earth Surf. Process. Landf. 15, 413–424.

MYLROIE J.E., MYLROIE J.R. (2007) Development of the carbonate island karst model. Journal of Cave and Karst Studies 69, 59 - 75

MYLROIE, J.E., MYLROIE, J.R. (2013) Flank margin caves in carbonate islands and the effects of sea level. In: Shroder, J. (Editor in Chief), Frumkin, A. (Ed.), Treatise on Geomorphology, 6, Karst Geomorphology, 351–362.

MYLROIE J.E., MYLROIE J.R., NELSON C.S. (2008). Flank margin cave development in telogenetic limestones of New Zealand. Acta Carsologica, 37(1), 15-40.

OTONIČAR B., BUZIJAK N., MYLROIE J.E., MYLROIE J.R. (2010) Flank margin cave development in carbonate talus breccia facies: an example from Cres Island, Croatia. Acta Carsologica, 39, 79–91.

RUGGIERI, R., DE WAELE, J. (2014). Lower - to Middle Pleistocene flank margin caves at Custonaci (Trapani, NW Sicily) and their relation with past sea levels. Acta Carsologica 43 (1), 11–22.

Relationship between marine planation surfaces and speleogenesis in Boca de Jaruco (Mayabeque-Cuba). Preliminary results

Vladimir OTERO-COLLAZO[(1)], Antonio GONZÁLEZ-RAMÓN[(2)], Leslie MOLERIO-LEÓN[(3,4)], Oriol CHAVEZ-BONORA[(4)] & Mariam ALONSO-MARTÍNEZ[(5)]

(1) Grupo Ciro Berrios, Sociedad Espeleológica de Cuba. vlado6208@nauta.cu
(2) Geological and Mining Institute of Spain, Urb. Alcázar del Genil, 4 Edf. Zulema bajo, 18006 Granada, Spain, antonio.gonzalez@igme.es. Asociación Espeleológica Velezana, C/ Levante, 1, Vélez Rubio-Almería, Spain.
(3) Inversiones Gamma, S.A. Apartado 6246, CP 10600, Habana 6, La Habana, Cuba. especialistaprincipal@gmail.com
(4) Grupo Martel, Sociedad Espeleológica de Cuba
(5) Sociedad de Ciencias Espeleológicas Alfonso Antxia. Bilbao- Bizkaia, Spain. alonso.mariam@gmail.com

Abstract

Close to the mouth of the Jaruco River, almost 30 km East of La Habana, Cuba, three marine planation surfaces built of reefal limestone (Middle Miocene to Upper Pleistocene) are developed. Eighteen caves concentrated in a 3 km^2 territory have been explored. Five of them have been recently resurveyed and studied. Three of them reach the local water table whose altitude and mineralization shows the seawater influence almost 1.5 km inland. Cave morphology, sediments and speleothems sustain a hypothesis of an origin and evolution linked to the modifications of the coastal line and to the formation of the marine erosion surfaces. The evolutionary scheme comprises a first episode of void development below the water table related with the mixing of different mineralization waters, a possible neotectonic uplift that dewatered those voids followed by a second episode of void development at a lower depth together with an intense hypogenic corrosional process accompanied by a residual *terra rossa* sediments filling of the voids. A large breakdown process took place and one or several speleothem generations are recorded in the upper cave levels.

1. Introduction

On the north coast of the island, between Havana and Matanzas, numerous caves with different characteristic features appear (flank margin caves, abrasive -marine- caves, spring caves -some of them below sea level- mixed epigenetic-hypogenetic caves: MOLERIO-LEÓN, 2013; DE WAELLE *et al.*, 2018) (Fig. 1) are developed over a series of coastal reef limestone platforms.

Figure 1: Location of the study area.

Boca de Jaruco is one of those areas (Fig. 1), where different generations of Cuban speleologists have been locating, exploring and documenting a huge number of caves in which these hypogenic morphologies have been observed. Currently 18 cavities are known, concentrated in a small surface of only 3 km^2 (OTERO-COLLAZO & ZALDIVAR 1986).

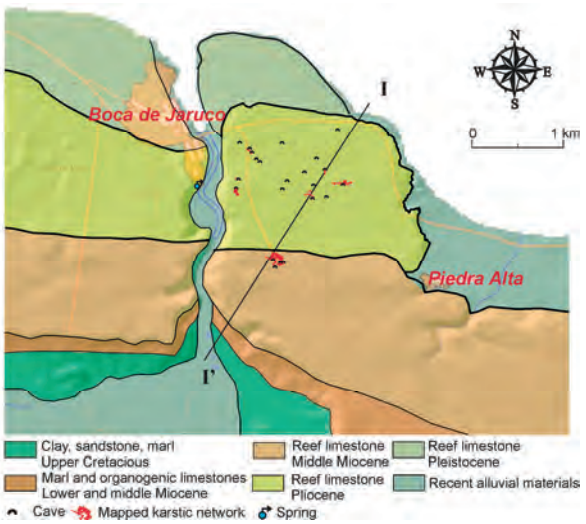

Figure 2: Geological map of the Boca de Jaruco karst. The black line corresponds to the trace of the section in Fig. 7.

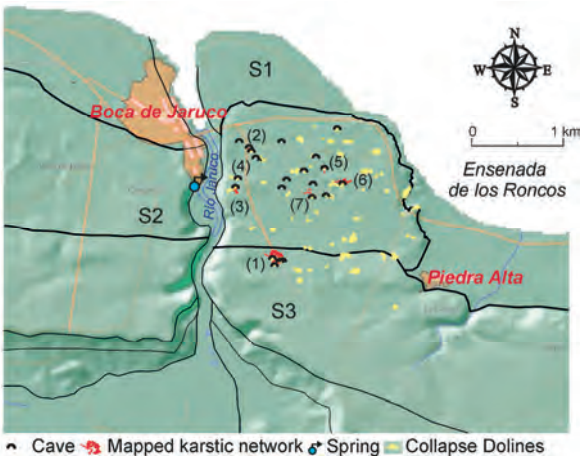

Figure 3: Relationship between sinkholes, caves and marine erosion surfaces (S1, S2 and S3). (1) Cinco Cuevas, (2) Cueva de la H, (3) Don Martín, (4) Las Muelas, (5) Aura, (6) Vapor, (7) El Cable.

The main goal of the Cuban-Spanish campaigns carried out between 2019 and 2020 was to study these morphologies, propose the possible mechanisms of development and evolution of this very particular set of caves. The substrate is made up of marly limestones and marls from the Lower and Middle Miocene and Eocene. Finally, the sequence lies on Upper Cretaceous flyschoid materials (Fig. 2 and 7). The geomorphological element defining the area is the Coastal Plain, whose width varies between 1 and 3 km (ITURRALDE-VINENT, 1985). Three main surfaces above sea level are recognized in the area (S1, S2 and S3 in Fig. 3) (ACEVEDO-GONZÁLEZ, 1967; MOLERIO-LEÓN, 1978).
The landscape is characterized by the presence of a dense lapiaz (locally known as “diente de perro”, v.gr. "dog's tooth"). Another characteristic feature is the sinking (swallow) sinkholes or small dolines, which are easily recognized as the points where the largest trees are concentrated. The entrances of most cavities are typically open in these sinkholes (MAGAZ, 2017) (Fig. 3).

2. Materials and methods

A precise mapping has been carried out in five of the most important caves, which has included a three-dimensional model for each one. Surveying was done with a modified Leica Disto X310 laser meter, which allows distance, direction and inclination to be measured in a single shot. The data obtained has been processed with the Therion software, which offers many possibilities, including a 3-D representation of the surveyed galleries.
Most of the topographic work has been carried out in Cinco Cuevas, by far the most developed of the group of caves in the area. Work has also been done on Cueva de la H, Don Martín, Las Muelas and El Aura. Likewise, other cavities were visited, such as Vaho and El Cable (Fig. 3), for the completion of observations and collection of water samples. Only three of the known caves reach the aquifer water table: the aforementioned Cinco Cuevas, El Cable and El Aura. These three caves are aligned in a SW-NE direction, closer to the coastline from Cinco Cuevas towards Aura. This fact allowed the study of the physicochemical characteristics of the water stored at different points and its variation depending on its proximity to the sea, with which the aquifer is in contact. In situ measurements were made of the water Specific Electrical Conductivity of (EC), temperature (T°C) and pH. Water samples were collected for physico-chemical and isotopic analysis.
The physico-chemical data obtained are under study and will not be included in this contribution, which focuses exclusively on the morphology of the cavities and their relationship with the aquifer in which they have formed and with the coastline, but there have allowed us to understand the relationships between the caves and the sea.

3. Results

The complete Cinco Cuevas map shows us a distribution of conduits that does not fit easily with predetermined directions due to fracturing (Fig. 4). A complexity of superimposed galleries with labyrinthic layouts is observed, strongly modified by collapse structures that have generated spacious rooms with domed morphology, such as the Sala de la Claraboya (Skylight Room) or the Sala de los Murciélagos (Bats Room). The extraction of guano, mostly mixed with red decalcification clays (*terra rossa*), has been of great importance. In many sites the effect of former mining works for guano extraction emptied the filling sediments and produced vertical slopes in the walls allowing to study local stratigraphy.

Several stratigraphic sections were documented in different places. The sedimentary column begins with a fill of between 1 and 5 m of *terra rossa*, generally mixed with guano. In some zones, a thin detrital layer formed by very fine sands with current marks is observed on the upper part. The sequence seems to be fossilized by roof collapses in many places. When no collapses appear, the sequence is covered by carbonate crusts where stalagmites and columns grow. Speleothemic growth is also observed over the collapsed blocks, but never below them.
Speleothems are well developed in the upper levels of the cave. One or more generations were identified with not current calcite deposition. The active speleothems of recent age are scarce and of little development.

Where the walls and ceilings have not been modified by collapses or speleothem coatings, dissolution morphologies are observed, congruent with condensation-corrosion processes in the presence of CO_2 in the cave atmosphere (Fig. 6). We interpret that these processes were very active at a certain moment in the geological history of the cavity and are responsible for the *terra rossa* filling, which is especially important in the upper area of the cavity.

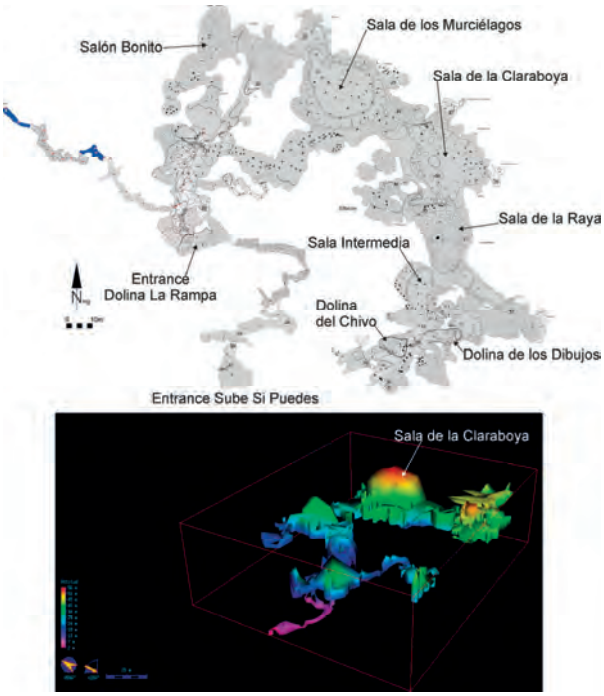

Figure 4: Topographic map and three-dimensional model of Cinco Cuevas.

Figure 6: Corrosive morphologies in the walls of the deepest part of the cinco cuevas.

In Cinco Cuevas there are two well differentiated main cavern levels, although some minor ones can be distinguished. The highest level is characterized by a further development of labyrinthine galleries, large halls with huge collapse structures, and sequences of *terra rossa* fillings covered by speleothems. The lower level appears from 20 m a.s.l. (Fig. 5). In this area, there are no caving fillings, and the walls are only modified by corrosive morphologies (Fig. 6) similar to those associated to solution in mixing zones as described by Palmer (1990). Flank margin caves has been identified at the Eastern Cliff known as Punta Jijira coexisting with typical marinaes (abrasive) caves.

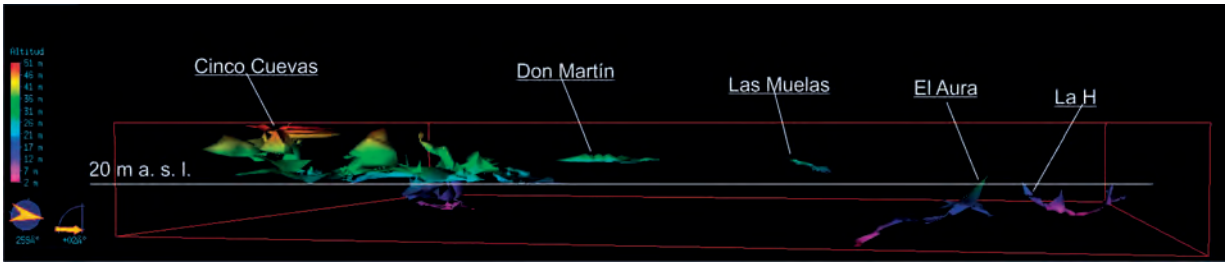

Figure 5: 3D model of the set of surveyed caves. The 20 m elevation marks the level that differentiates two main cave areas, possibly of different ages. The horizontal scale has been modified for comparison of the dimensions of the different caves.

4. Discussions and conclusions

Accordingly, the following preliminar speleogenetic evolution of the set of cavities can be summarized in five stages:

1) A first episode of void generation in a mixing zone possibly occurred during the Lower Pleistocene or late Pliocene. This episode must have occurred with a part of the emerged outcrop (S3). This favored the mixing of fresh-salt water generated by the protocave. 2) A drop in the water table (tectonic uplift?) that leaves the previously generated voids, at least partially, out of the water. 3) New generation of voids in a mixing zone below the 20 m elevation, accompanied by an intense subaerial corrosion process produced an important filling of residual dissolution clays (*terra rossa*) in the upper area of the cave and solutional morphologies in walls and ceilings have been identified. Whether or not are consequence of the development of flank margin cave is really premature at this stage of the study. 4) Generalized collapses that enlarge the voids forming the great rooms of Cinco Cuevas contributing to the opening or widening of connections with surface. 5) Finally, especially humid phases generated a great caving growth in the highest areas of the cave covering both the collapsed blocks and the terra rossa fillings.

In all these processes, the initial generation of voids certainly occurred in the mixing zone of fresh water and salt water (interface zone). From the physical-chemical data obtained in the 2020 campaign, it is known that the interface can currently go inland more than 1.5 km (Fig. 7). After the decrease in the piezometric level, the voids formed by chemical dissolution in the phreatic zone are enlarged in a subaerial environment (during cold periods?) by condensation-corrosion. The residue from these processes

produced decalcification clay fillings. The progressive growth of the holes produced roof instabilities in some areas of the cave permitting roof collapses. During the hot and humid stages of the Middle and Upper Pleistocene was produced the speleothemic fill that covers both the collapses and the *terra rossa*. In a final stage, the rupture of speleothems occures, possibly due to settling of the soil due to subsidence in the lower levels, without excluding the eventual contribution from seismicity as pointed out by MOLERIO-LEÓN (2018).

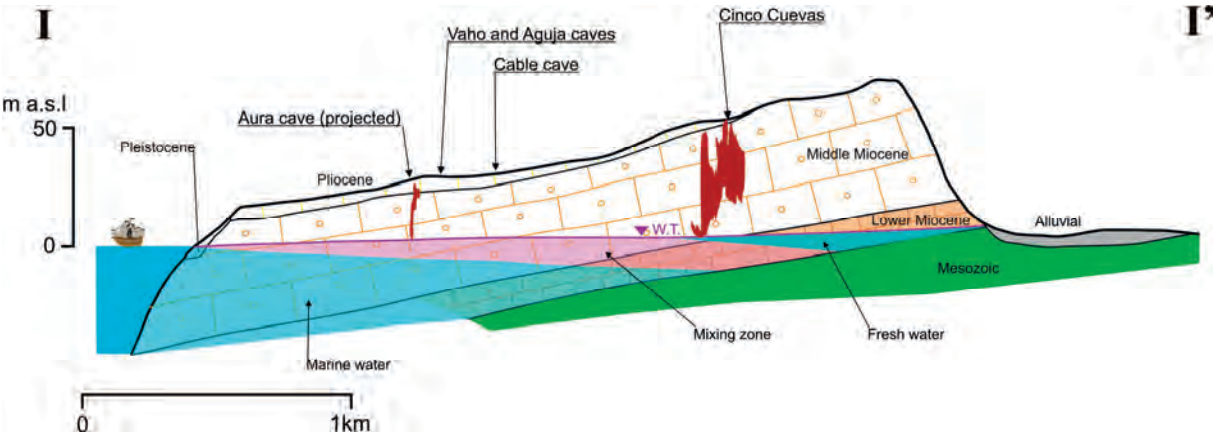

Figure 7: Schematic hydrogeological section of the study area with location of some of the caves and the different types of waters that appear in the aquifer deduced from the EC measurements carried out. Its trace can be seen on the map in Fig. 2.

Acknowledgments

These works have been carried out within the framework of the collaboration between the Ciro Berrios and Martel caving groups of the Cuban Speleological Society, the Alfonso Antxia Speleological Sciences Society and the Velezana Speleological Association with the collaboration of Inversiones Gamma S.A. and the Geological and Mining Institute of Spain. We would also like to thank anonymous reviewers for their constructive comments and suggestions, which led to a substantial improvement of the paper.

References

ACEVEDO GONZÁLEZ, M. (1967). Estudio espeleológico de la cueva el Vaho o Bao. Boca de Jaruco. *Habana. Rev. Serie Ciencias Biológicas*. Fasc. 1. Vol. 1, n° 5. J.

DE WAELE, J., D'ANGELI, I. M., BONTOGNALI, T., TUCCIMEI, P., SCHOLZ, D., JOCHUM, K. P., ... & TISATO, N. (2018). Speleothems in a north Cuban cave register sea-level changes and Pleistocene uplift rates. *Earth Surface Processes and Landforms*, 43(11), 2313-2326.

ITURRALDE VINENT M. (1985). Algunos aspectos geomorfológicos del territorio de las provincias de La Habana. En: *Contribución a la geología de las provincias de La Habana y ciudad de La Habana*. Instituto de Geología y Paleontología. Academia de Ciencias de Cuba.

MAGAZ GARCÍA A.R. (2017). *Geomorfología de Cuba*. Amazon Books, Kindley editions. 377 p.

MOLERIO LEÓN, L. F. (1978). Sobre la Edad de las Superficies de Erosión de Boca de Jaruco. *Voluntad Hidráulica*, La Habana. XV (45), 32-34.

MOLERIO LEÓN L. F. (2013). *Evidencias de carsificación y cavernamiento mixto epi-hipogenético en la Cobertura Neoautóctona de la Franja de Crudos Pesados del Norte de La Habana-Matanzas*. Mapping Latino, 2.

MOLERIO LEÓN L. F. (2018) Cronoestratigrafía relativa de eventos paleosísmicos en el tercio inferior del Río Jaruco, Cuba occidental. *Gota a Gota* n°15, 93-96.

OTERO COLLAZO V. y ZALDIVAR CHATELOIN B. (1986). Notas preliminares geoespeleológicas de Boca de Jaruco. 2da *Jornada Científica Provincial*. Ciudad de La Habana

Anthropogenic salt karst in Germany

Manfred KUPETZ

Verband der deutschen Höhlen- und Karstforscher e.V. VdHK, Schulweg 1a, D-03055 Cottbus, Germany. manfred.kupetz@t-online.de

Abstract

According to FULDA (1912), caves created by dissolving of halite layers within anhydrite rock in the area of the Mansfeld Syncline (Mansfeld copper shale district, Saxony-Anhalt, Germany) are named Mansfelder Schlotten of Ottoschächter type (anhydrite-chloride karst or chloride karst). These caves have no entrances. They were discovered by subsurface copper mining or by exploration drillings. This paper presents four examples of these salt caves unknown so far. The caves are recorded in an unpublished geological cross section by Wolfgang Blei in 1959/1960. Their location is the historical copper shale subsurface mining near Paul Shaft (in 1951 renamed into Otto Brosowski Shaft) about 8 km north of the city of Eisleben. The caves are not accessible anymore. This paper describes speleogenetic features of Ottoschächter cave type for the first time in an international context. The caves were formed by dissolution of halite layers intercalated between anhydrite rock of Werra Formation (Zechstein, Permian). The caves occur at a depth between 280 and 440 m below surface within a tectonic fault zone. Speleogenesis was driven by a groundwater flow into artificially drained mining cavities. For this reason, the Mansfelder Schlotten of Ottoschächter type can be associated with mining-induced salt karst speleogenesis (anthropogenic karst).

Résumé

Un karst salin d'origine anthropique en Allemagne. Selon FULDA (1912), les Mansfelder Schlotten vom Ottoschächter Typ sont des cavernes formées par la dissolution de sel gemme dans des roches anhydrites (karst de sel anhydrite ou karst de sulfate-chlorure) dans le Mansfelder Mulde (Mansfelder Kupferschieferrevier, Saxe-Anhalt, Allemagne). Ces grottes sont sans entrée naturelle. Elles ont été découvertes lors de l'extraction souterraine de minerai de cuivre ou lors de forages d'exploration. Quatre dômes de sel de ce type, inconnus jusqu'alors, sont décrits. Elles ont été documentées dans une carte géologique souterraine inédite près du Paul-Schacht (rebaptisé Otto-Brosowski-Schacht en 1951) à environ 8 km au nord d'Eisleben dans la Mansfelder Mulde par Wolfgang Blei en 1959/1960. Ainsi, il est possible pour la première fois dans un contexte international de décrire en détail les grottes, qui ne sont plus accessibles aujourd'hui, d'un point de vue spéléogénétique. Elles ont été formées par la dissolution du sel gemme de la Werra, dans la séquence anhydrite de la Werra (z1 : séquence de la Werra, Zechstein, Permien) dans les zones tectoniques d'extension à proximité des failles et des flexions de fractures. Elles se trouvent à une profondeur comprise entre 280 et 440 m sous la surface. Leur genèse a été causée par l'eau qui s'écoulait des couches rocheuses supérieures dans un champ de mine souterrain qui avait été drainé par le pompage des eaux souterraines. Les évents de type Ottoschächter peuvent donc être considérés comme des karsts salins anthropogènes induits par l'exploitation minière.

Kurzfassung

Ein anthropogener Salzkarst in Deutschland. Als Mansfelder Schlotten vom Ottoschächter Typ werden nach FULDA (1912) Höhlenräume bezeichnet, die durch die Auflösung von Steinsalzkörpern in Anhydritgesteinen (Anhydrit-Steinsalz-Karst bzw. Sulfat-Chlorid-Karst) in der Mansfelder Mulde (Mansfelder Kupferschieferrevier, Sachsen-Anhalt, Deutschland) entstanden sind. Diese Höhlen sind von Natur aus eingangslos. Sie wurden nur durch den untertägigen Kupferschieferschieferbergbau zugänglich oder in geologischen Erkundungsbohrungen angetroffen. Es werden vier bisher unbekannte Schlotten dieses Typs beschrieben. Sie wurden in einer bisher unveröffentlichten geologischen Untertagekartierung in der Nähe des Paul-Schachts (1951 in Otto-Brosowski-Schacht umbenannt) ca. 8 km nördlich von Eisleben in der Mansfelder Mulde von Wolfgang Blei 1959/1960 dokumentiert. Damit ist es erstmals in internationalem Kontext möglich, die heute nicht mehr zugänglichen Schotten vom Ottoschächter Typ aus speläogenetischer Sicht detailliert zu beschreiben. Sie bildeten sich durch Auflösung von Werra-Steinsalz, einer Einlagerung innerhalb der Werraanhydrit-Folge (z1: Werra-Folge, Zechstein, Perm), in tektonischen Dehnungszonen im Bereich von Bruchstörungen und Flexuren etwa in einer Tiefe zwischen 280 und 440 m unter Erdoberfläche. Ursache ihrer Genese war aus höherliegenden Gebirgsschichten nachfließendes Wasser in ein gesümpftes, d.h. durch Abpumpen des Grundwassers trockengelegtes untertägiges Bergwerksfeld. Die Schlotten vom Ottoschächter Typ können daher als bergbaulich induzierter, d.h. anthropogener Salzkarst angesprochen werden.

Introduction

Caves of the Mansdelder Schlotten type (KUPETZ & KNOLLE 2015; a.o.) exist in the fringes of the Harz and Kyffhäuser mountains and in two southeastern geological basin structures (Mansfelder and Sangerhäuser Mulde). They are mostly deep phreatic, hypogene entrance-less caves. Their cave rocks are usually calcium sulphate rocks, mostly

anhydrite rock and rarely also anhydrite rock secondarily changed into gypsum from the Permian (Zechstein). They were discovered in historical times through underground mining for copper ore, the so-called Kupferschiefer (copper slate). Since time immemorial, they have been referred to as Mansfeld Schlotten or simply Schlotten. In an unpublished graduation thesis as a mining engineer (perhaps comparable with recent Bachelor's thesis), the later famous German mining officer and salt geologist Ernst Fulda described the Mannsfelder Schlotten. He distinguished between the Wimmelburg type (anhydrite caves) and the Ottoschächter type (salt caves). The most common type is the Wimmelburg type (KEMPE 1996; KUPETZ & KNOLLE, 2015; a.o.). The salt caves occur only very rarely and are no longer accessible because mining has ceased. There are no known published descriptions. They are only mentioned and mapped in some unpublished mining reports.

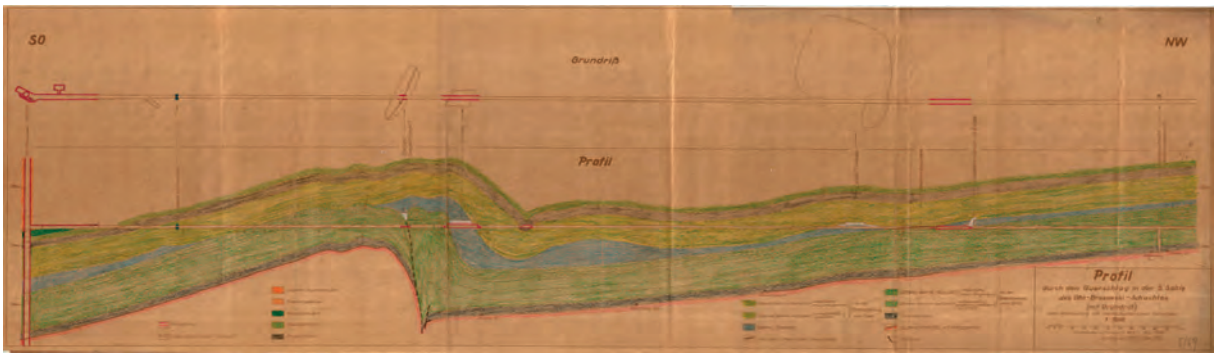

Figure 1: Geological cross section showing four anthropogenic salt caves in the Otto-Brosowski Shaft (formerly Paul Shaft) near Eisleben, author Wolfgang Blei 1959/1960, hand-drawn manuscript coloured with coloured pencils, size 29 x 104 cm. Note: The name Ottoschächter Schlotten refers to the Otto Shafts 10 km away, not to the Otto-Brosowski Shaft!

Figure 2 (left): Section of Jung's cross section with salt caves no. 8 (Zeppelin Hall) and no. 9 (Schlotte without name), compare with Fig. 4.

Figure 3: Section of Jung's profile showing the salt caves no. 10 (Big Schlotte) and no. 11 (Schlotte at water inrush from September, 17th 1958), compare with Fig. 4.

The most significant document on the speleological character of the Ottoschächter Schlotten is a manuscript of a geological cross section through four of these caves by the

exploration geologist Wolfgang Blei, found in the early 1990s (Fig. 1, 2 and 3). This document was the occasion for a summary treatment of this type of vent in the context of the monograph on the Mansfeld vents in the journal "Karst und Höhle" (KUPETZ 2021 i.pr.), which is currently in print.

Currently, a total of 12 salt caves are known (Fig. 4). They are small-scale caves with mostly only a few hundred m³ volume. The volume of the smallest is estimated at 20 – 40 m³, that of the largest around 3000 – 5000 m³. They are located at depths between 280 and 440 m.

No.	Name	Size (LxWxH) [m x m x m]	Volume, app. [m³]	Cave morphology, remarks	Depths [m] ***	Reference
1	Schlotte, 2nd ground of Otto-Schacht (Shaft)	unknown	unknown	unknown	-	FULDA (1912)
2	Schlotte, 3rd ground Otto-Schacht (Shaft)	(10 ?) x 5 x 6	(?) 300	trianglular cross section with flat halt bottom	-282	FULDA (1912), STOLBERG (1943)
3	Schlotte, 4th ground Otto-Schachts (Shaft)	unknown	unknown	unknown	-310	FULDA (1912, STOLBERG (1943)
4	Schlotte in borehole no. 38 near village Heiligenthal	unknown	unknown	6 m high cave chamber within a halit layer	-426	FULDA (1912) STOLBERG (1943)
5	Schlotte, 5th ground near Graf-Hohenthal-Schacht (Shaft)	unknown	unknown	konkav-lendeshaped cross section at a tectonic rupture structure	-344	FULDA (1912) STOLBERG (1943)
6	Schlotte, 5th ground Pauls-Schacht, crosscut (Querschlag)	unknown	unknown	two cave chambers	437, 5	FULDA (1912) STOLBERG (1943)
7	Mansfeld borehole no. 61 near Bennungen	unknown	unknown	7 m high cave chamber within a halit	-276	STOLBERG (1943)
8	Schlotte Zeppelinhalle (Zeppelin Hall)*	50 x 10,0 - 13,5 x 7 - 8	2000	trianglular cross section with horizontal ceiling and downward directed trialgule tip	-424	BLEI (1959/1960)
9	Schlotte without name *	20 x 13 x 3	800	trapezoid outline with flat bottom and horizontal ceiling within halit	-430	BLEI (1959/1960)
10	Große Schlotte *(Big Schlotte)	90 x 80 x 0,5-10	3000 - 5000	circular chamber with cross section in shape of a overturned watchglass and horizontal ceiling	-431	BLEI (1959/1960)
11	Schlotte at water inrush at from September, 17th 1958 *	2 - 3 x 2 - 3 x 6	20 - 40	cone-shaped blind pocket with circular cross section, formed in halit and upward directed into anhydrite layer	-436	BLEI (1959/1960)
12	Schlotte, 7th ground **, in the sense of LATK (2003): Zeppelinhalle	210 x 35 x ?	unknown	chamber with lanceolate-shaped bottom	ca. -555	BRAETZSCH (1959) SCHUBERT et *al*. (1960) LATK (2003)

* in the 5th ground crosscut in the Otto-Brosowski-Schacht (Paul Schacht)
** Otto-Brosowski-Schacht (Paul-Schacht)
*** below earth´s surface

Figure 4: The currently known Ottoschächter type Schlotten (salt caves) in the Mansfeld Syncline.

For the speleogenetic interpretation of the salt caves, evaluable information is only available from the four objects at the Otto-Brosowski-Schacht (Fig. 4, no. 8-11). The following explanations therefore only refers to these. The most important aspects are their tectonic position, the speleogenic water inflow and the question whether they are phreatic or vadose caves.

Tectonically, the salt caves are located at a complicated rupture-tectonic fault zone (flower structure, and wrenchfault; Fig. 5). This has caused processes of salt flow with salt pillow formation. The caves are located in

tectonically stressed salt layers. Due to mining, the groundwater was lowered over a wide area. After the subsidence, the caves did not yet exist. They were only formed in later times by karst water with a high salt dissolving capacity, which flowed in as fresh water from the overburden through permeable fracture faults.

There are two types of cavities with different genesis:

1. solution caves with a horizontal ceiling, formed by stagnant or very slow flowing water (Fig. 4 no. 8 and 9),
2. cone shaped blind pocket scouring by vertically inflowing water (Fig. 4 no. 11).

In case of mining water subsidence, they would be interpreted as vadose cave formations. According to the above explanations, however, the Ottoschächter Schlotten are neither of phreatic nor of vadose cave genesis in the sense of natural karst processes. Without mining water drainage, the Ottoschächter Schlotten could not have been formed at all. A characterisation as an “anthropogenically influenced cave" is therefore also inappropriate. Rather, they are “anthropogenically induced caves”. Detailed explanations will be published in KUPETZ (2021, i.pr.).

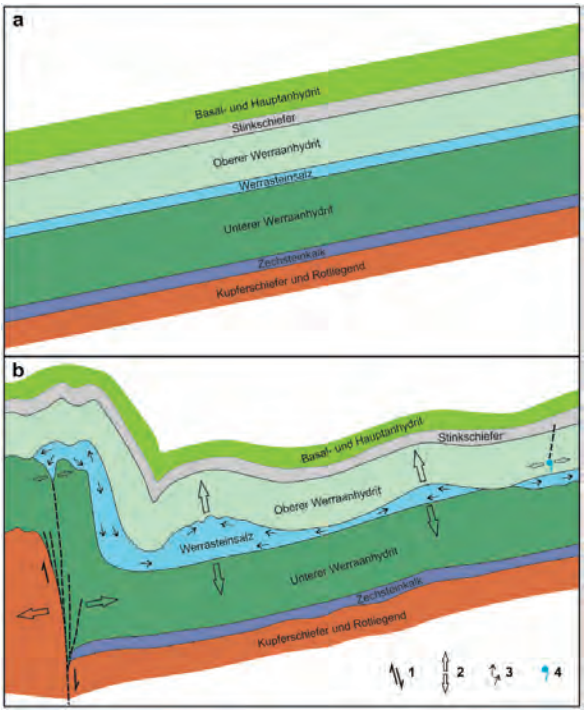

Figure. 5: Fracture-tectonic situation and tectonopastic flow of rock salt in the area of the four salt caves at the Otto Brosowski Shaft, brown: sandstones and conglomerates, green and greenish colours: anhydrite rocks, light blue: rock salt, 1 - fracture-tectonic movements, 2 - direction of minimum principal stress σ1, 3 - direction of salt flow, 4 - source.

Acknowledgments

I would like to thank the Lausitzer und Mitteldeutsche Bergbau-Verwaltungsgesellschaft mbH (LMBV), i.e. Frank Naundorf and Sven Bauer, for historical information, the Landesamt für Geologie Sachsen-Anhalt (LAGB), i.e. Konrad Schuberth, as well as Michael K. Brust, Dr. Friedhart Knolle and Almut Kupetz for discussions on this topic and technical support.

References

BLEI W. (1959/1960) Profil durch den Querschlag in der 5. Sohle des Otto-Brosowski-Schachtes 1959/ 1960. – *Archiv Lausitzer und Mitteldeutschen Bergbau-Verwaltungsgesellschaft mbH (LMBV)*, unpublished sheet, 1 p.

BLEI W. (1961) *Die Tektonik der Mansfelder Mulde. – Unveröff*. Maschinenmanuskript, Neumark, unpublished, 96 p.

BRAETZSCH (1959) [Red.] Bericht über den Wassereinbruch im VEB Kupferbergbau Otto Brosowski am 17.9.1958. *VEB Kupferbergbau Otto Brosowski Eisleben*, 10. Februar 1959, unpublished, 68 + 2 p.

FULDA E. (1912) *Die Verbreitung und Entstehung der Schlotten in der Mansfelder Mulde*. – Bergreferendarsarbeit, unpublished, 39 p.

KEMPE S. (1996) Gypsum karst of Germany. *Intern. J. Speleology*, 25, 3-4, 209-224.

KUPETZ M. (2021i.pr) Bergbaulich induzierter (anthropogener) Salzkarst – die Schlotten vom Ottoschächter Typ im Grubengebäude des Otto-Brosowski-Schachts (ehem. Paul-Schacht). *Karst und Höhle 2018-2021*, 228-241.

KUPETZ M., KNOLLE F. (2015) Die Mansfelder Schlotten – Verbreitung und Genese der größten mitteleuropäischen Anhydrit-Schichtgrenzhöhlen. *Z. Dt. Ges. Geowiss.*, 166, 327-339.

LATK M. (2013) Der katastrophale Wassereinbruch von 1958 auf dem Otto-Brosowski-Schacht. www.vmbh-mansfelder-land.de/artikel/bergbau-huettenwesen/Wassereinbruch-OBS-2013.pdf

SCHUBERT H., BUSCH W., HETZER H. (1960) Der Wassereinbruch vom 17. September 1958 im Mansfelder Kupferschieferbergbau. *Freiberger Forsch. Heft A*, 176, 41-51.

STOLBERG F. (1942) Die Mansfelder Schlotten. *Z. Karst- u. Höhlenkunde* 1942/1943, 11.

Large barrage-type tufa deposits in the karst of Northwest Namibia a preliminary evaluation of their occurrence, hydrology and caves

Dr Mark E. TRINGHAM

Gloucester Speleological Soc., University of Bristol Spelaeological Soc. Malvern, WR136QN UK. mtringham@btinternet.com

Abstract

The extensive Proterozoic dolomite and limestone karst in Kunene Province Northwest Namibia has been explored by international speleological expeditions, most recently in 2015 & 2018. These discovered some new hypogenic caves of modest length (<350m), but with very large passage and chamber sizes. Some large barrage-type tufa deposits were also found on the karst surface in the same region and these are up to 140m in height. More than 16 major tufa deposits have so far been recorded in this area, some of which are newly reported and initial ideas developed on their genesis. The tufas act as a local aquifer and they contain some caves of modest size. It is recommended to evaluate the tufas more thoroughly and help preserve them as an important ecological and tourism resource.

Résumé

Grands barrages de tuf dans le karst du nord-ouest de la Namibie : évaluation préliminaire de leur présence, de leur hydrologie et de leurs grottes. De grandes zones karstiques présentes dans les calcaires dolomitiques d'âge protérozoïque ont fait l'objet d'explorations par une équipe spéléologique internationale, notamment entre 2015 et 2018. Elles ont permis la découverte de cavités hypogéniques de dimension modeste (< 350 m), possédant des salles et des passages très larges. En surface, de grands barrages en tuf atteignant 140 m de hauteur ont été repérés. Au total, 16 barrages ont été localisés, dont certains pour la première fois. Leur genèse est expliquée. Leur grande taille permet de renfermer un aquifère local et l'on y retrouve des cavités de taille modeste. Une étude plus détaillée de ces travertins serait nécessaire d'autant qu'ils constituent une ressource écologique et un potentiel touristique important.

1. Introduction

Tufa deposits are a type of karst feature of significant scientific interest because of their geology, hydrology and their relationship to changes in paleoclimate. Tufa is a type of freshwater limestone with a soft porous texture composed of microcrystalline calcite. Tufa commonly incorporates stream debris such as cobbles and boulders of older rocks and forms a sedimentary breccia or conglomerate. It can also incorporate plant and animal remains as well as archaeological remains.

Tufa is found downstream from some karstic springs where the water is laden with calcium bicarbonate and is deposited in a range of environments including perched spring lines, barrages, stream channels, marshes, and lakes. Tufa deposition can occur due to warming of the spring water, evaporation, or loss of carbon dioxide during aeration or photosynthesis.

During the Anglo-French expedition of 2015 a major tufa deposit was visited near the village of Otjimatemba. Then the 2018 speleological expedition team visited further tufa deposits at Okomutati and Ekoto (Fig. 1). Also one tufa cave called Okombeiza was explored and surveyed.

Besides these four tufa outcrops visited more than ten others of significant size were found in the same karstic region using Google Earth images. A comprehensive literature search indicated that although tufa deposits have been studied and reported upon from elsewhere in Namibia and South Africa, the ones in Kaokoland had only received preliminary attention before.

2. Study methods

A preliminary study was made for these tufas using field observations and photographs looking at lithology, the tufa body geometries, searching for and surveying the caves, locating water sinks and springs and observing modern fauna. This was followed post-expedition by integration and mapping using satellite Google Earth images to obtain physical measurements of the tufa body dimensions, get perspective views and find out the geological setting and stream catchment area dimensions. A literature search was also conducted to fit these deposits into their global context.

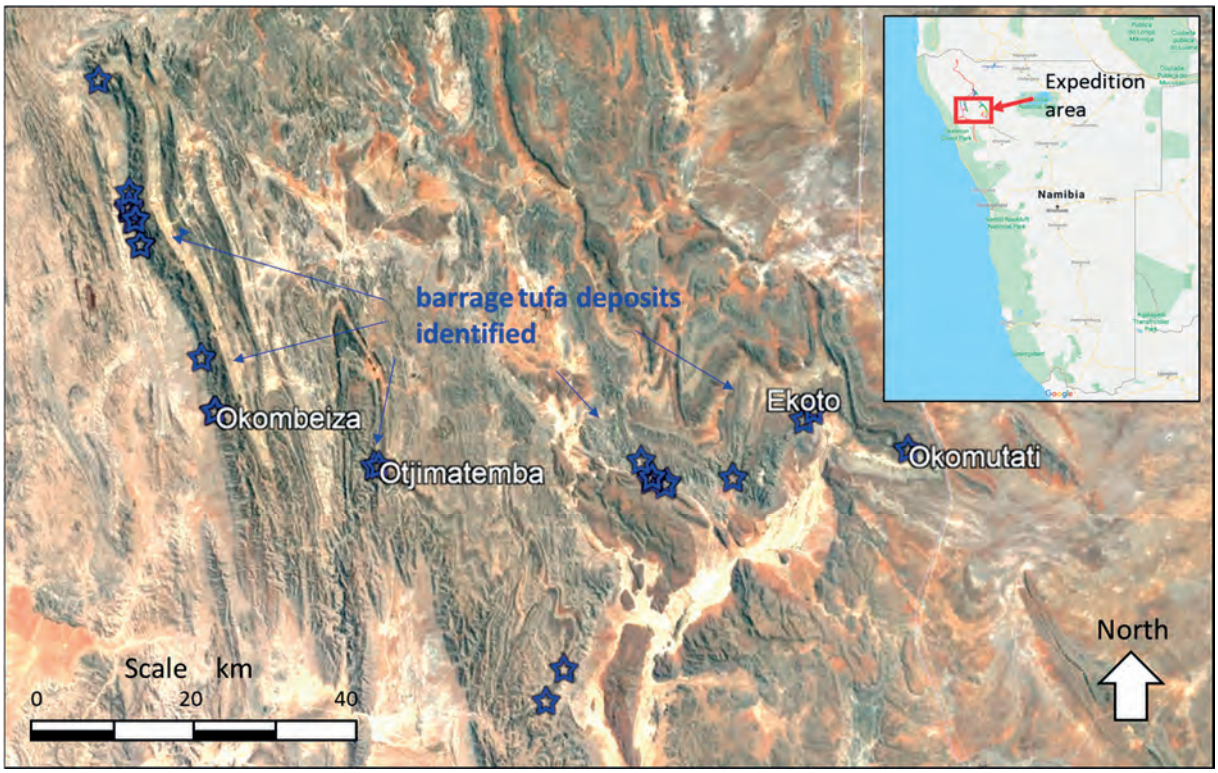

Figure 1: Google Earth Map showing the tufa deposit locations with index map highlighting the expedition area

3. Results

a) The Okomutati Tufa Barrage

This comprises a fan-shaped cascade/barrage deposit located at the mouth of a side-valley. It has a spectacular cliff line 50m high in total with three steps and a talus slope around. At the apex of the fan there is a water well with a pump, just up from the expedition camp. There is a network of 3 dry distributary channels, 2 of which run southwards to the cliff edge, while the 3rd deflects around the western side of the deposit. Three tufa lobes are evident and there is a marked colour change between the middle and top one, with grey more compact tufa limestone below and reddish stained creamy limestone above.

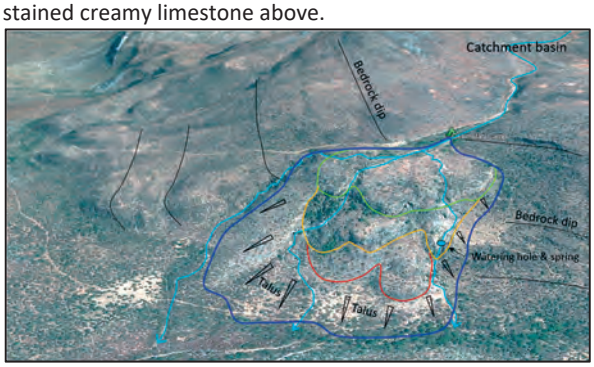

Figure 2: Google earth perspective view of the Okomutati tufa looking NE showing the 3 tufa lobes, fringing talus slope and surrounding topography and bedrock structure.

The catchment area upstream is just over 10^2 km extent with dolomite and subordinate limestone the main rock types, providing surface and ground water laden with calcium and magnesium.

Figure 3: Dried out calcite rimstone pools formed in the stream bed near the cliff edge

In the middle tufa lobe, a small spring occurs with natural pools and a main watering hole and this was flowing at about 2 litres/minute when the team visited. The spring and pools attract a wide variety of wildlife and the team saw baboons and kudu for example and were told that elephants visit the watering hole too. PICKFORD (pers. comm. email Oct. 2020) reported finding fossilised snails in a calcrete layer on top of the Okomutati tufa during a 2017 palaeontological expedition.

b) The Ekoto Tufa Barrage

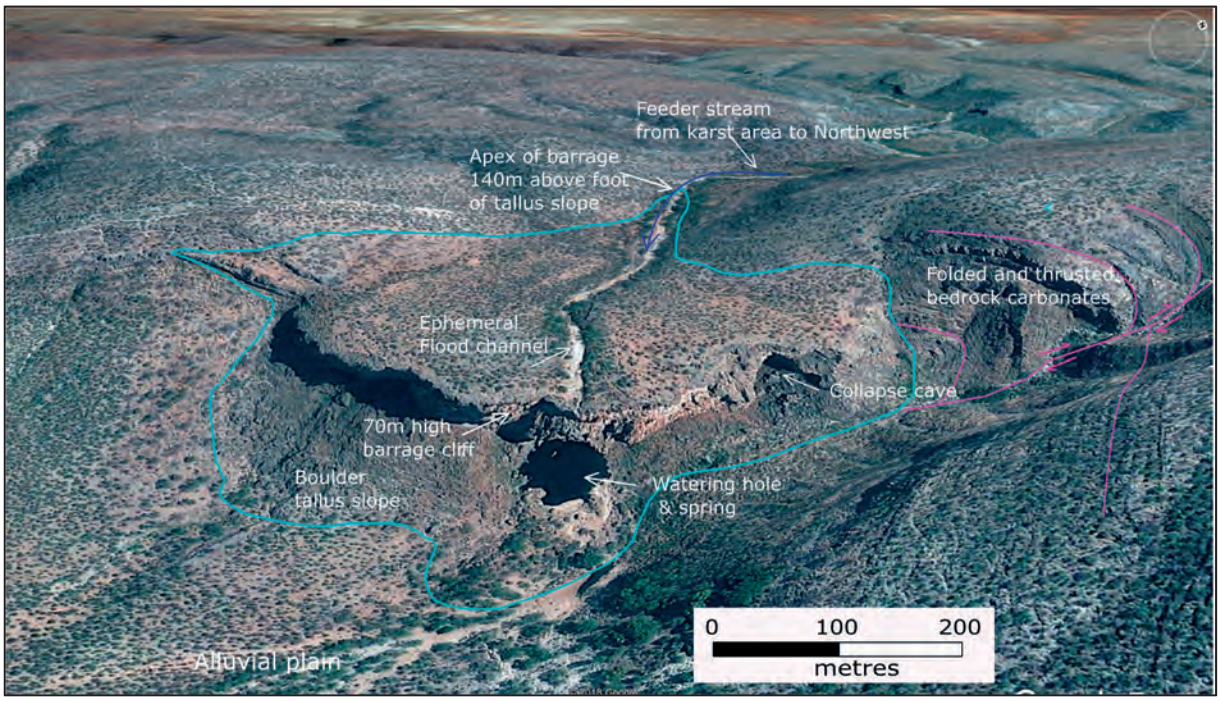

Figure 4: Google earth perspective view of the Ekoto tufa looking NW and showing the dimensions and main features present.

Figure 5: The Ekoto barrage tufa cliff seen in the distance with Ekoto village

This deposit is located close to Ekoto village where a side valley joins a main valley in an analogous geographical position to the Okomutati example. It is represented by a high tufa cliff which dominates the surrounding terrain and is visible from many kilometres away. The cliff is part of a single 140m thick barrage type tufa deposit, which ranks among the tallest such features known world-wide. Besides its major geological significance, the cool spring and watering hole at the foot of the cliff form an important resource for wildlife.

The tufa deposit here has a clear barrage shape with a 70m high and 650m wide cliff, a talus boulder slope below and a ramp shaped surface above. On the surface of the barrage there is an ephemeral stream channel. Directly below where the stream channel reaches the cliff there is a large pool presumably eroded out by strong scouring action at times of flood, but this pool is also spring fed during normal dry periods. The cliff face is vertical to overhanging with a myriad of tufa flowstone sheets, curtains, stalactites and caves. This irregular cliff face has attracted a parakeet colony, while the watering hole attracts wildlife such as antelopes and elephants. Towards the northeast end of the cliff a large cave archway 50m wide and 20m high has formed, likely by upward roof collapse.

Figure 6: The 70m high tufa cliff with pool below

Because the tufa barrage is porous and permeable in times of low stream flow all the water seeps through the stream bed into it rather than going down the stream channel to the cliff line. So the tufa forms a local aquifer available to feed the watering hole at the base of the cliff. The bedrock below and behind the tufa comprises a strongly folded Neoproterozoic sedimentary sequence of carbonates and shales, with dolomite the dominant rock type. The stream valleys feeding the Ekoto tufa have a catchment area of more than 200 km².

c) Ondimba ja Okombeiza

This cave is located in a fan shaped tufa deposit around 25m thick. A spacious entrance chamber has a gently sloping floor with dusty guano and small boulders with animal footprints including leopard.

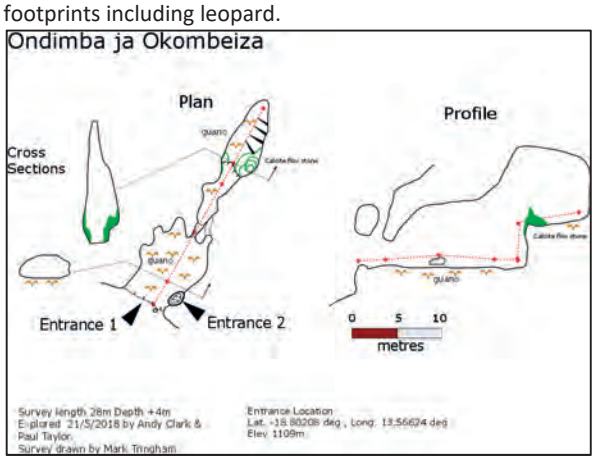

Figure 6: Okombeiza tufa cave plan and profile

After the entrance chamber the cave narrows into a high rift passage with a short bridge and bone strewn floor and then a 4m climb up with a lot of calcite flowstone and stalagmite formations. The cave terminates after a total length of 28m at a calcite blockage. This cave is the only significant one found in tufa by this expedition, other tufas examined containing only modest rock shelters and overhangs.

Figure 7: View of the entrance part of Okombeiza.

4. Discussion

Within the Kunene region several other similarly shaped but smaller tufa barrages occur and these include either single or multiple lobate barrages. They mostly have formed where tributary valleys join a main valley like the Okomutati and Ekoto examples described above. A comparison to published examples from elsewhere in Africa, such as described by VILES et *al* (2007), FORD & PEDLEY (1996) and MARKER (1988), shows that the ones here are relatively major deposits with an interesting geology to unravel. Like many of the others they also commonly share a polyphase history likely spanning several pluvial phases through the Pleistocene and perhaps even earlier, as deduced from their fossil content and other aspects by PICKFORD et *al* (2016). The tufas show evidence for only minor contemporary deposition. The lack of long caves in these tufas is probably related to their extreme porosity and permeabilty causing void spaces to be quickly choked by calcite speleothems.

5. Conclusion

The numerous and large tufa barrage deposits in the subject area merit further comprehensive and integrated study. They additionally require special protection from quarrying or other unsustainable exploitation so that their geological and ecological value can be maintained for the benefit of wildlife and local and scientific communities. They also have significant potential for tourism because of their scenic value, geology and potential for wildlife-watching.

Acknowledgments

I gratefully thank IRDNC (Institute for Rural Development and Nature Conservation) in Namibia for facilitating the 2015 and 2018 speleological expeditions. Also I thank Martin Pickford and the Geological Survey of Namibia for their discussions.

References

FORD T.D. & PEDLEY H.M. (1996), A review of tufa and travertine deposits of the world. Earth Science Reviews 41, pp 117-175.

MARKER M.E. (1988), Tufa deposits of southern Africa: A review. In: K. Heine (Ed.) Paleoecology of Africa and the surrounding islands, Vol. 19. Balkema, Rotterdam, pp. 377 – 389.

PICKFORD M., MOCKE H., SENUT B., SEGALEN L. & MEIN P. (2016), Fossiliferous Plio-Pleistocene Cascade Tufas of Kaokoland, Namibia. In Communications of the Geological Survey of Namibia Vol. 17 pp. 85-112.

VILES H.A., TAYLOR M.P., NICOLL K. & NEUMANN S. (2007), Facies evidence of hydroclimatic regime shifts in tufa depositional sequences from the arid Naukluft Mountains, Namibia. Sedimentary Geology 195 pp 39-53.

Identification of calcareous tufa in northeast of the state of Goiás, Brazil

Leonardo MENDES[(1)], Adivane NOGUEIRA[(2)], Dandara CALDEIRA[(3)] & Rogério UAGODA[(4)]

(1) Laboratório de Geografia Física, ICC Norte, Bloco 23, Campus Darcy Ribeiro, Brasília, Brazil, lchaves21@gmail.com (corresponding author)
(2) Laboratório de Geografia Física, ICC Norte, Bloco 23, Campus Darcy Ribeiro, Brasília, Brazil, adinogueira2010@hotmail.com
(3) Laboratório de Geografia Física, ICC Norte, Bloco 23, Campus Darcy Ribeiro, Brasília, Brazil, dandara.caldeira2014@gmail.com
(4) Laboratório de Geografia Física, ICC Norte, Bloco 23, Campus Darcy Ribeiro, Brasília, Brazil, rogeriouagoda@unb.br

Abstract

Studies in calcareous tufas are of great importance for the development of paleoenvironmental reconstructions and understanding of the landscape dynamics. As features originated from areas of occurrence of carbonate rocks, these concretions solidify in different forms and facies, due to the conditions provided by the environment in which they develop. This research seeks to map and describe the calcareous tufa formations in the northeastern portion of the state of Goiás, Brazil. Some areas of occurrence were identified through field work, involving description and extraction of outcrops. Thus, the carbonate deposits were spatialized with the registration of coordinates, inserting them in a Geographic Information System (GIS) environment, using the QGIS v.3.16.3 with GRASS v.7.8.5 software (v.10.6.1). In this sense, the faciological description of the testimonies was possible to be realized, associating them with depositional environments, identifying cascade, waterfall, dam and inter-dam pool tufas, correlated to the facies typology. In addition, cartographic materials of the spatial distribution of such features were generated, in which certain linearity of the occurrence of outcrops, including in areas without active drainage, was found.

1. Introduction

Over high porosity and solubility rocks, karstic terrains develop and are known for being systems of constant interaction between water and the geological environment. The northeastern portion of the state of Goiás, Brazil, is encompassed by three main geological groups (Bambuí, Areado and Urucuia), associated with the Sanfranciscana Basin. The Lagoa do Jacaré formation, which belongs to the Bambuí, has pelite-carbonated outcrops linked to the regressive erosion of the Serra Geral do Goiás (W-E).

Thus, exuberant features such as caves, lapiaz, sinkholes, tufas and travertines appears, generating rich and complex landscapes, which can be considered both open and closed systems (TRAVASSOS, 2019). Typical features of karst areas, such as tufas, occur near or in the bed of rivers that, at any moment, were in direct contact with carbonate rocks. Carbonate deposits are the result of the interaction between CO_2-rich waters and carbonate rocks. The supersaturation benefits the precipitation of calcite, a chemical precipitation mineral that constantly occurs in karstic areas (HILL; FORTI, 1997). The reprecipitation of calcite can be indicated by the equation:

$$Ca^{+2} + 2\,HCO^{-}_{3} \leftrightarrow CaCO_3\downarrow + H_2O + CO_2\,(g)\uparrow$$

(Calcium carbonate precipitation equation)

A study by FORD & PEDLEY (1996) demonstrated that the formation of tufas is linked to climatic periods of great humidity and heat. However, other studies have recognized tufa formations in different environments, such as humid tropical (CARTHEW et *al.*, 2006) and semi-arid (MOEYERSONS et *al.*, 2006; ORDÓÑEZ et *al*., 2005).

For interpretation about fossil tufas, environmental models are used, since weathering and burial complicate the stratigraphic and geomorphic characterization, influenced by biological and climatic aspects (CARTHEW et *al.*, 2006; PEDLEY, 2003). These environmental models are understood as conceptual representations, as they have the morphological characterization of the deposit, association of facies and sedimentation environments (PEDLEY, 1990). The need to use models related to regions with similar climatic factors is emphasized.

Calcareous tufas are extremely fragile, as their formation and conservation directly depend on the use of land throughout their area of influence. Thus, considering that the studied area stands out for agricultural production, the conservation of these features can be directly affected, even before they are properly studied to understand different perspectives (climatic, tectonic and anthropic) (FORD & WILLIAMS, 2007; CAPEZZUOLI et *al*., 2014; MIRAGAYA, 2014; DABKOWSKI, 2020). Therefore, works containing mappings for the spatialization of these outcrops, as well as the development of scientific research on karst landscapes, are extremely important, as they foment conservation and greater understanding of the dynamics of such rich and vulnerable areas.

2. Materials and methods

This study sought to map and characterize the sedimentation environments of calcareous tufas in the northeastern portion of the state of Goiás, Brazil. In this way, a field visit was carried out during the first half of the second semester of 2021, aiming to verify the areas with occurrence of the features and the prior recognition of the characteristics of depositional environments. In order to verify the internal biological content as well as to carry out further analysis, it was necessary to extract samples from the cores.

In the field work, some testimonies were measured in terms of height and width, with coordinates recorded using the Avenza Maps application on an Android device. Photographs were also stored from available cameras. These cartographic and image data were inserted in a GIS environment (QGIS v.3.16.3 with GRASS v.7.8.5), generating the spatialization of the observed features. Other data, such as hydrography and contours (30 meters), were extracted, respectively, from the State Geoinformation System (SIEG) and the Alos PALSAR Digital Elevation Model. (DEM) of the Shuttle Radar Topography Mission (SRTM) project, both acquired from the United States Geological Survey (USGS). The satellite image applied comes from the Google Satellite Plug-in, available within the aforementioned GIS.

The characterization, both in field and in the observations of the samples in the laboratory, were based on the calcareous tufa model for tropical regions influenced by monsoonal systems (CARTHEW et *al*., 2006). In this way, aspects such as form, biological material, mineral and the place of deposition were considered in the context of the associated hydrography.

3. Results

The mapping procedure demonstrated the occurrence of fourteen points with tufa outcrops, being identified in the rivers and streams Ventura (area 1), Barreiro (area 2) Chumbada (area 3), and São Vidal (area 4). The highest concentration of occurrences, according to this survey, occurs in the pelite-carbonated Lagoa do Jacaré Formation, which belongs to the Bambuí Group (Fig.1A).

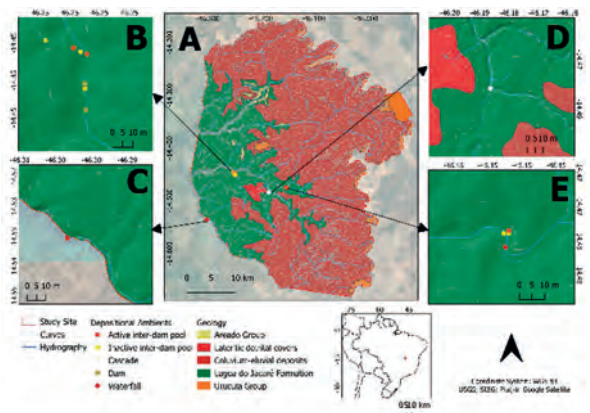

Figure 1: A) Spatialization of features; B) Barreiro tufa; C) São Vidal tufa; D) Chumbado tufa; E) Ventura tufa.

Through the characterization, it is possible to establish a classification of the types of tufas, which are cascade, waterfall, inter-dam pool and dam. In addition, the classification also encompassed the presence or absence of water activity, as shown in Figure 1 A, B, C, D, E. In relation to the different depositional environments related to the tufa genesis, in area 1, linked to Ventura, waterfall tufas were analyzed in areas of water spraying, where there was an association of the outcrops with bryophytes (Fig.2A) and inter-dam pool, in an area with undergrowth vegetation, such as ferns. Also, tufas with low or no activity were identified (Fig.2B,C) in an area associated with what was the drainage gutter in ancient times. Due to the proximity of the inter-dam pool area, at a lower ground level, it is inferred that it is part of a system of small waterfalls/cascades. This characteristic is combined with dense laminations in the formation of tufas (Fig.2D). As observed in the field, there is a large transport of leaves by rivers, a fact that justifies the marking of incrustations of these in the deposits (Fig.2E).

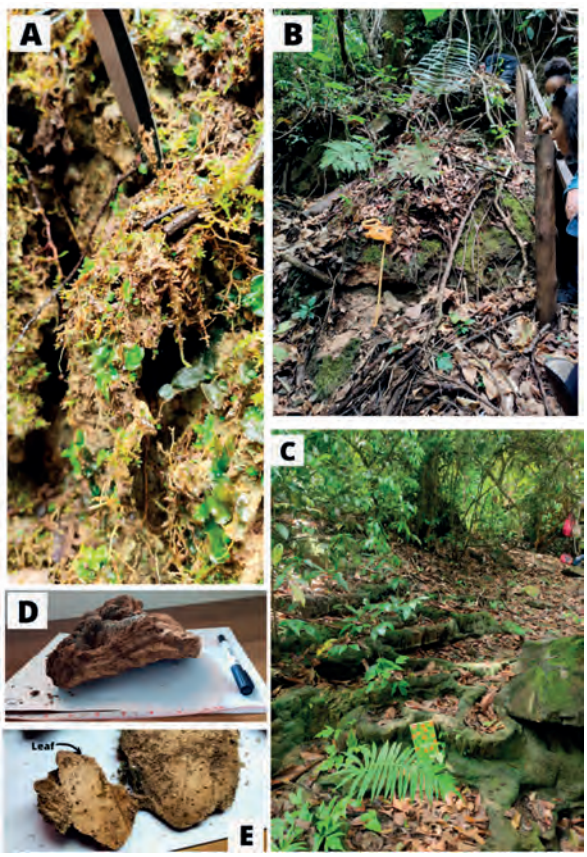

Figure 2: A) Funil Waterfall Tufa; B/C) Inter-dam pool tufa; D) Tufa with dense lamination; E) Leaf incrustation on calcareous tufa.

The area 2, linked to the Barreiro stream, presented dam tufas (Fig.3A) and an inter-dam pool with stromatolites at the bottom, in a 7-meter U shape, allowing the formation of two pool levels, one measuring 1.70m and the other, 2m wide (Fig.3B, D). Its structure shows leaf incrustations. A little further down the same river, there were inactive tufas (Fig.3C) of inter-dam pool, possibly forming a foregone large waterfall with a height of 1.93m.

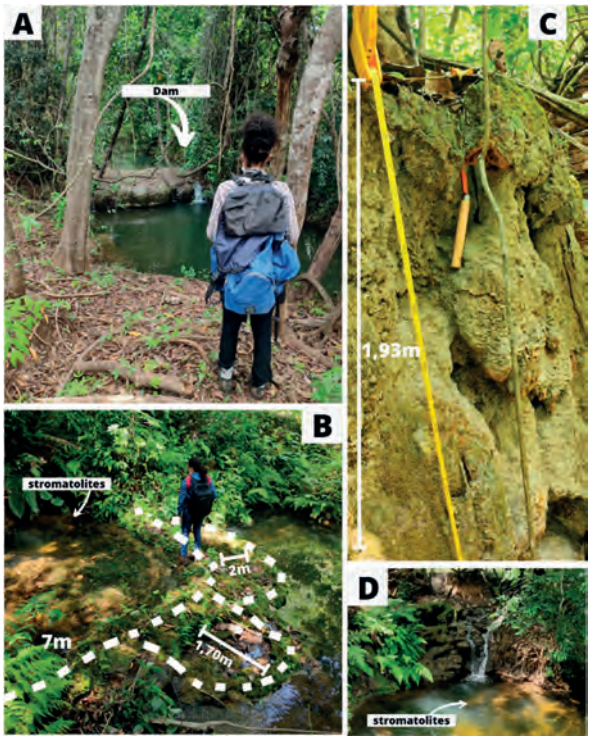

Figure 3: A) Dam tufa; B/D) Active inter-dam pool tufa with stromatolites; C) Inactive inter-dam pool tufa formation, possibly an ancient cascade/waterfall.

The Chumbada stream area (area 4) has an environment of tufa formation related to cascades (Fig.4A, B). As in the previous cases, the transport of leaves through the river is intense, with the possibility that these plant structures may come to act as supports for calcite. However, no fossil records were found in the collected core. The dimension of the outcrop is 1.70m width by 2.20m height. It is evident that the forming river is in full activity.

Figure 4: A) Cascade tufa formation; B) Outcrop measured.

Finally, in São Vidal stream (area 4), the outcrops originate from an active waterfall of large dimensions (Fig.5A). Thus, the type of formation environment is predominantly waterfall. The outcrop of the specific extractions, which is 4.17 meters high, is located on the right bank of the waterfall and has a flow variation during the seasons of the year (Fig.5B, C).

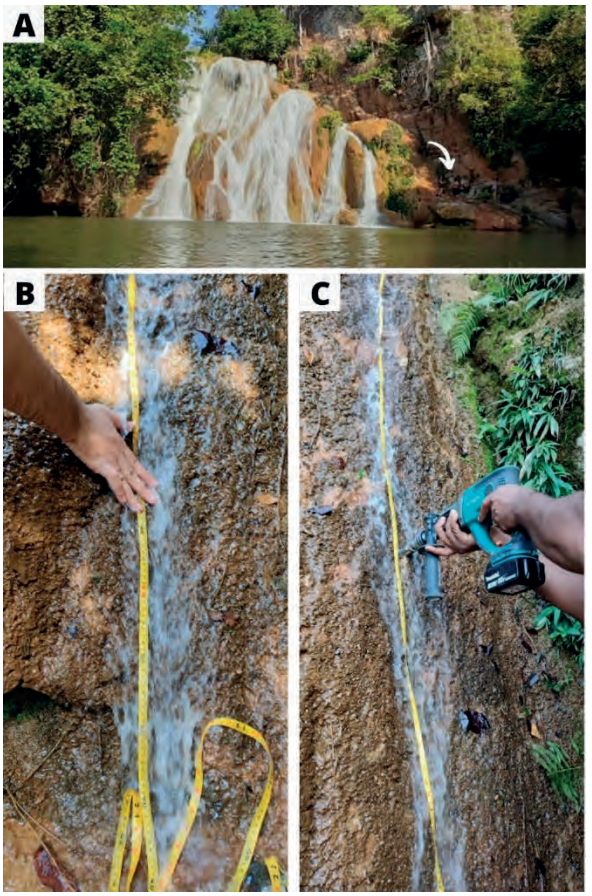

Figure 5: A) Paraíso do Cerrado Waterfall tufa; B) Paraíso do Cerrado tufa outcrop; C) Tufa extraction process.

4. Discussions

The calcareous tufas of northeastern Goiás in Brazil can be a source of information on climate history correlated by monsoons. It is observed that there is a great variety of types of tufas in active and inactive places, however, well preserved.

The mapping of the tufas allows to observe their distribution in the study area, with a concentration of outcrops in the Barreiro stream, with morphology of altimetric variation along the hydrography, favoring the occurrence of tufa formation of waterfalls, as well as slower flows in flat terrain, with a predominance of dams. The concentration of abandoned outcrops on the edge of the river allows us to deduce that there was a time when the riverbed expanded due to an increase of water flow or that they are products of a river direction change.

Among the types of sedimentation environments, inter dam pool is the most prevalent type, occurring between two types of sedimentation ambients (dam and pool) observed in the field with frequency.

5. Conclusion

The study showed that the concentrations of calcareous tufa outcrops are associated with the Lagoa do Jacaré Formation, belonging to the Bambuí Group. There is a variation of types of environments in which they appear. This identification and the general characterization of the testimonies demonstrates the potential use for several environmental studies. For this reason, the importance of conserving these carbonate concretions is emphasized, regarding the anthropogenic pressure that directly affects their formation process.

Acknowledgments

The authors would like to thank the Postgraduate Program in Geography and the Postgraduate Program in Applied Geosciences, both at the University of Brasília (UnB). To CAPES, CNPq, the Postgraduate Deanship of UnB and also the funding obtained by TCCE 01/2018 Vale/ICMBio. We would like to thank Paulo Éder Gouveia e Adelaine Morais Nogueira for supporting during field works.

References

CAPEZZUOLI E., GANDIN A., PEDLEY M. (2014) Decoding tufa and travertine (fresh water carbonates) in the sedimentary record: The state of the art. Sedimentology, vol 61, n°1, 1–21.

CARTHEW K. D., TAYLOR, M. P., DRYSDALE R. N. (2006) An environmental model of fluvial tufas in the monsoonal tropics, Barkly karst, northern Australia. Geomorphology, vol 73, n°1–2, 78–100.

DABKOWSKI J. (2020) The late-Holocene tufa decline in Europe: Myth or reality? Quaternary Science Reviews, v. 230.

FORD D., WILLIAMS P. (2007) Karst Hydrogeology and Geomorphology. 2. ed. Chichester: Wiley.

FORD T. D., PEDLEY H. M. (1996) A review of tufa and travertine deposits of the world. Earth-Science Reviews, vol 41, n°3–4, 117–175.

HILL C. A., FORTI P. (1997) Cave minerals of the world. National Speleological Society, p.463.

MIRAGAYA J. F. G. (2014) O desempenho da economia na Região Centro-Oeste. Um olhar territorial para o desenvolvimento: Centro-Oeste, 424–453,

MOEYERSONS J. et *al*. (2006) Age and backfill/overfill stratigraphy of two tufa dams, Tigray Highlands, Ethiopia: Evidence for Late Pleistocene and Holocene wet conditions. Palaeogeography, Palaeoclimatology, Palaeoecology, vol 230, n°1–2, 165–181.

ORDÓÑEZ S., GONZÁLEZ M, J. A., GARCÍA DEL CURA, M. A., PEDLEY H. M., (2005) Temperate and semi-arid tufas in the Pleistocene to Recent fluvial barrage system in the Mediterranean area: The Ruidera Lakes Natural Park (Central Spain). Geomorphology, [S. l.], vol 69, n°1–4, 332–350.

PEDLEY H. M., (1990) Classification and environmental models of cool freshwater tufas. Sedimentary Geology, vol 68, n°1–2, 143–154.

TRAVASSOS L. E. P., (2019) Princípios de Carstologia e Geomorfologia Cárstica. Brasília: Instituto Chico Mendes de Conservação da Biodiversidade,

PEDLEY M., GONZÁLEZ MARTÍN J. A., ORDÓNEZ DELGADO S., GARCÍA DEL CURA M. A., (2003) Sedimentology of quaternary perched springline and paludal tufas: Criteria for recognition, with examples from Guadalajara Province, Spain. Sedimentology, vol 50, n°1, 23–44.

New chronological constraints on the intrakarstic fluvio-glacial fan of the cave Sous-les-Sangles (Bas-Bugey, France)

Stéphane JAILLET[(1)] & Edwige PONS-BRANCHU[(2)]

(1) Laboratoire EDYTEM, Université Savoie Mont Blanc, CNRS, Pôle Montagne, 73 376 Le Bourget-du-Lac, stephane.jaillet@univ-smb.fr (corresponding author)
(2) Laboratoire des Sciences du Climat et de l'Environnement, LSCE/IPSL, CEA-CNRS-UVSQ, Université Paris-Saclay, F-91191 Gif-sur-Yvette, France

Abstract

The age of the Last Glacial Maximum extension of the French north-western Alps is still under discussion. Lateral to the ancient glacial valleys, karstic galleries functionned as glacial sinkholes during the glacial retreat phases and are thus relevant recorders of these glacial phases. In the Bas-Bugey (Ain, France), the cave Sous-les-Sangles hosts a remarkable laminated detrital sequence associated with an ancient position of the Isère glacier in the "Cluse des Hôpitaux". Several U/Th alpha dates undertaken 20 years ago are revised here. Five new U/Th ICP-MS dates on speleothems frame the detrital complex, providing a terminus post quem (TPQ) and a terminus ante quem (TAQ) to this glacial invasion. The TPQ is dated 87.3 ± 3.9 ka (MIS 5.b.c) and the TAQ is dated 11.6 ± 4.3 ka (MIS 1). The laminated detrital sequence is thus better constrained and the glacial invasion could have only been deposited during MIS 4 (locally Würm II, first max) or MIS 2 (Last Glacial Maximum or locally Würm IV) stages. The cave Sous-les-Sangles has a strategic position to constrain maximum glacial extension during the last cold stages of the Quaternary in the French Alps.

Résumé

Nouvelles contraintes chronologiques sur le cône fluvio-glaciaire intrakarstique de la grotte Sous-les-Sangles (Bas-Bugey, France). L'âge de la dernière extension maximale glaciaire des Alpes nord-occidentales françaises est toujours discutée. En position latérale aux anciennes vallées glaciaires, des conduits karstiques ont fonctionné en pertes juxtaglaciaires durant les phases de retrait glaciaire et constituent des enregistreurs pertinents de ces phases glaciaires. Dans le Bas-Bugey (Ain, France), la grotte Sous-les-Sangles abrite une remarquable séquence détritique laminées associée à une position du glacier de l'Isère dans la cluse des Hôpitaux. Des datations entreprises il y a 20 ans (U/Th alpha) sont ici révisées. Cinq nouvelles dates U/Th MC-ICP-MS ont été entreprises sur des spéléothèmes encadrant l'ensemble détritique offrant un terminus post quem et un terminus ante quem à cette invasion glaciaire. Le TPQ est daté à 87,3 ± 3,9 ka (MIS 5) et le TAQ est daté à 11.6 ± 4.3 ka (MIS 1). La série détritique laminée est ainsi mieux contrainte et l'invasion glaciaire ne peut se situer que dans les stades MIS 4 (localement Würm ancien) ou MIS 2 (localement Würm récent). La grotte Sous-les-Sangles confirme sa position stratégique pour contraindre l'extension maximale glaciaire au cours des derniers stades froids du Quaternaire.

1. Introduction

The latest maximum glacial extension of the French north-western Alps (Würm) is still under discussion. Does it rather correspond to the ancient Würm (MIS 4) or to the recent Würm (MIS 2)? Lateral to the former glacial valleys, karstic galleries functionned in juxtaposed sinkholes. They are relevant recorders of these phases. South of the Jura, the Bas-Bugey is in a strategic position to record the French Alps glaciers maximum extension and the glacial retreat. The "Cluse des Hôpitaux" is an important valley currently drained by two diverging rivers. During the last glacial maximum, the cluse was invaded by a diffluence of the Isère glacier. The Upper Kimmeridgian limestone karst recorded this invasion. On the surface, the remains of the maximum glacial extension consist of till belts recognised at around 900 to 950 m above sea level (asl) in the Innimond sector and at around 850 to 900 m asl in the Ordonnaz sector (Kerrien *et al.*, 1990). The origin of these the Bas-Bugey glacial overflows has long been attributed to the Rhône (Kerrien *et al.*, 1990) and finally to Isère on the basis of petrographic analysis (Coutterand, 2010). In this sector, where glacial records are remarkable, an important karst develops: the Burbanche karst system (22 km) on the southern edge of the "Cluse des Hôpitaux" (Chirol, 1985; Chirolet Hugon, 2010; Hugon, 2013) (Fig. 1). We chose to analyse an exceptional sedimentary deposit at the Sous-les-Sangles cave (Fig. 2). It has already been the subject of extensive studies (Sbai *et al.*, 1995; Lignier *et al.*, 2002), but the precise chronology of the deposit remains to be established. This is the subject of this note.

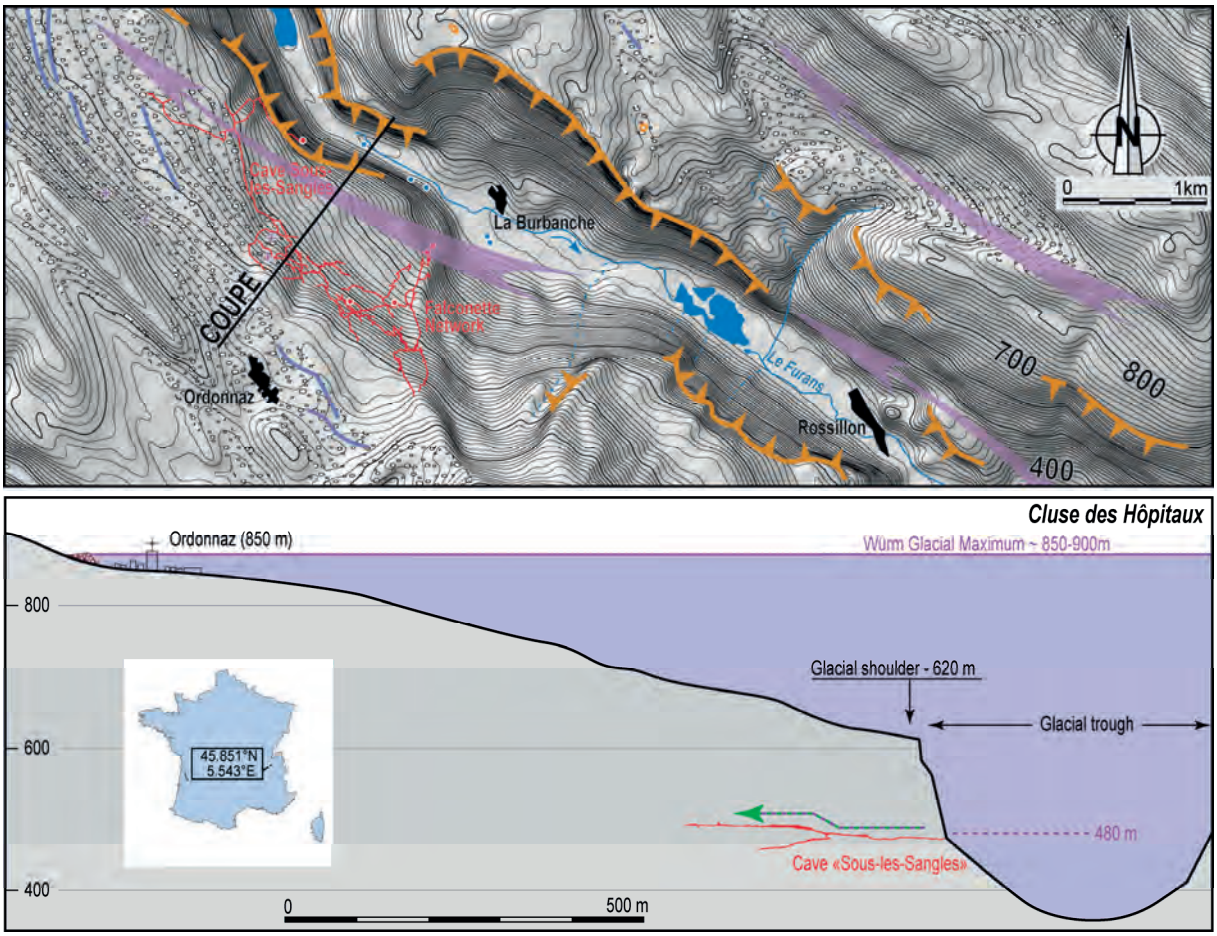

Figure 1: Location of the Sous-les-Sangles cave (plan and section) in the Bas-Bugey. Note the position of the horizontal cave in relation to the WGM (Würm Glacial Maximum) extension.

2. The karstic filling of the Sous-les-Sangles cave

At 475 m asl, the Sous-les-Sangles cave is a horizontal gallery developing in the lower third of the southern slope of the cluse. Underground, three major sedimentary formations have been identified (Fig. 3) (Lignier *et al*., 2002): (i) at the base, a morainal and fluvio-glacial filling composed of (I_{1-2}) dark, greenish, stratified sands, rich in quartz, mostly unworn (Sbai *et al*., 1995), covered in discordance by a coarser set (G_2) composed of decimetric blocks with a poorly sorted matrix. On top, a coarser sandy series (I_{2-3}), less stratified and partially channelled, lies in discordance (Lignier *et al*., 2002); (ii) on this set rests the sequence (G_3), composed of millimetre to multi-centimetre alternation of carbonate silts and clear clays over a thickness of more than 3 m: the Boulevarve. A detailed analysis of the laminations made it possible to propose a period of 350 years (Lignier *et al.*, 2002) for the setting. Closer to the entrance of the cavity, a set of clear morainic debris (iii) is identified in the "la Plage" sector (Lignier *et al*. 2002). This material has been largely reworked and washed away by the suffosion operation in the "La Plage" sector. In addition to these three types of deposits, there are also pre- and post-glacial speleothems. The cave was about 350 m below the surface of the glacier during its maximum extension. Under such a thickness, hydrological circulations are limited to the upper third of the ice mass or within the upper 100 to 150 m (Bini *et al*., 1998; Irvine-Fynn *et al.*, 2017). Considering these elements, juxta-glacial hydrological penetration is likely to occur when the ice surface is around 550 m, i.e. more than 250 m below the WGM line, i.e. well after the WGM.

Figure 2: The G_3 karstic infill is a 3 m thick sequence composed of millimetre to multi-centimetre alternation of carbonated silts and clear clays.

3. Contemporary filling of deglaciation

We propose the following deglaciation and endokarstic sedimentation scenario:

- **At the WGM (Würm Glacial Maximum)**, the glacial surface is at 850 m asl (Kerrien *et al.*, 1990). Underground, the drain is flooded but does not experience significant hydrological circulation. On the other hand, sedimentary sets at the bottom of galleries are already present (I_{1-2} and G_2 in particular, Lignier *et al*. 2002). These are intra-karstic fluvio-glacial cones dating from a previous glacial phase (Würm possible).
- **During a phase of retreat**, the ice surface stabilises at around 550 m. The sub-glacial flows are then around 480 m and allow hydrological exchanges with the karst in a juxta-glacial sinkholes position. The penetration of large water flow, carrying a fine detrital load and richly carbonated, leads to the sedimentation of the filling (G_3). Such a mechanism presupposes a certain equilibrium, an outlet downstream and a certain duration. These circulations are conditioned by the cavity altitude and therefore provide information on the glacial surface altitude, which itself give information on the glacier spatial extension.
- The further lowering of the ice surface ended this equilibrium **and the sedimentation stopped**. At the cave entrance, surface circulation can be lost underground with poorly sorted fluvio-glacial material. This coarser material indicates an increased hydrological competence, which can be attributed to a stronger hydraulic gradient. The proximity of the glacier front during the retreat dynamics may explain this temporary hydraulic gradient increase and thus in the importance of the water flows.
- Finally, **the glacier disappears** and the cavity recovers its hydrological functioning, still known today, with partial incision of the sedimentary deposits. Speleothems are set up and seal these sedimentary deposits in their partially dismantled state.

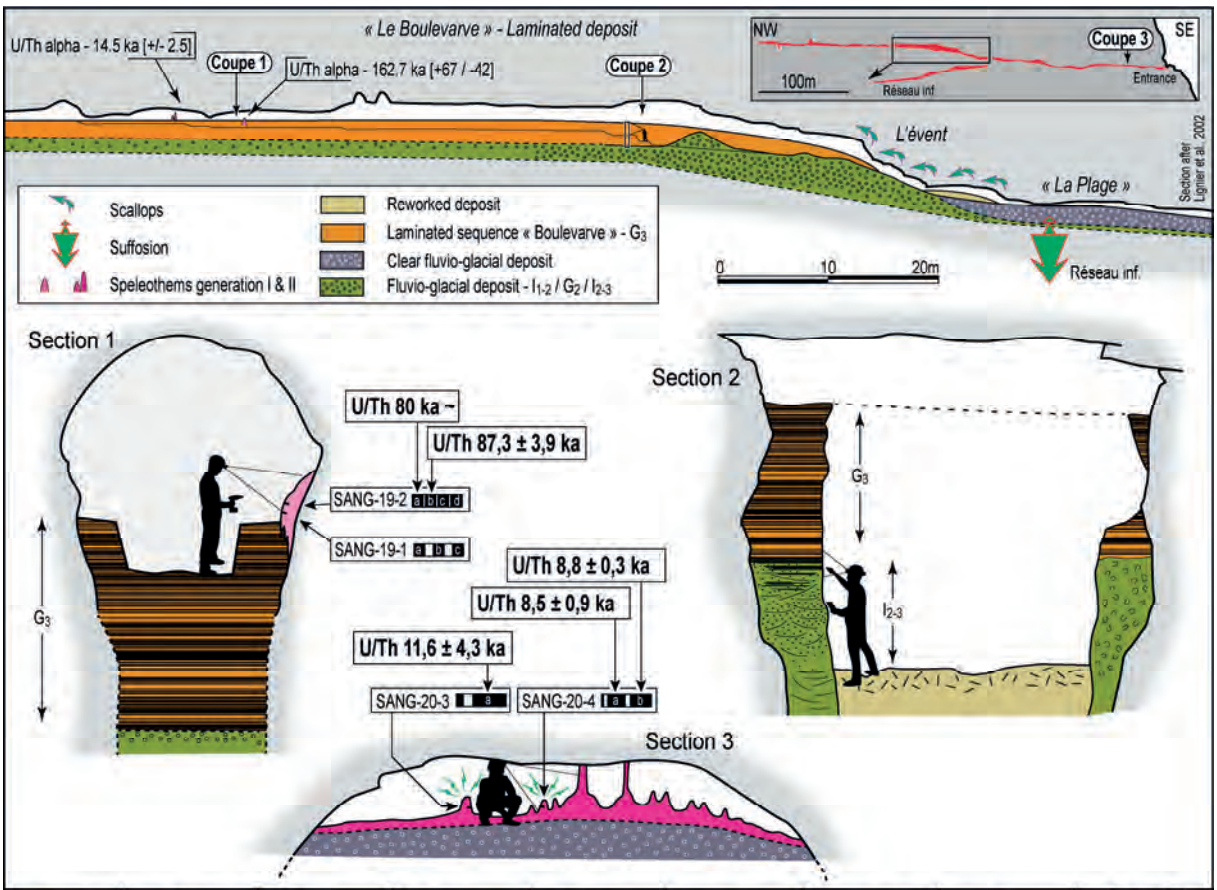

Sample	[^{238}U] ppm		[^{232}Th] ppb		δ^{234}U M (‰)		(^{230}Th/^{238}U)		(^{230}Th/^{232}Th)		Age (ka) 2019		δ^{234}U T		Age cor (ka) before 2019/2020	
SANG-19-2-a	0,125	0,00	43,27	0,51	340,64	5,63					~ 90				~ 80	
SANG-19-2-b	0,139	0,00	23,45	0,19	306,63	4,75	0,7736	0,00	13,98	0,03	93,55	0,9	392,5	7,4	87,32	3,87
SANG-20-4-b	0,273	0,002	3,05	0,02	430,66	2,55	0,1156	0,0007	32,22	0,18	9,17	0,07	441,5	2,6	8,76	0,27
SANG-20-4-a	0,255	0,002	11,42	0,09	437,34	3,26	0,1271	0,0008	8,84	0,06	10,06	0,09	447,9	3,5	8,46	0,89
SANG-20-3-b	0,216	0,002	51,59	0,42	368,70	2,18	0,2331	0,0008	3,04	0,01	20,22	0,11	381,0	5,1	11,60	4,29

Figure 3: Synthetic section of the cave Sous-les-Sangles with location of the studied sections. Table of the 5 U/Th dates with U and Th contents, activity ratios and ages. Raw ages were corrected ("Age cor" column) assuming a ^{230}Th/^{232}Th activity ratio for the detrital phase of 1.5 ± 50%. The data obtained show that the sedimentary ensemble belongs to the MIS 4, 3 or 2 stage.

4. New U/Th dates

For this reconstruction, we propose chronological constraints. U/Th dating (alpha method, Quinif, 1987) had made it possible to propose two dates framing the sequence and gave the following ages: 162.7 ka (+67 / -42) for a flowstone sealed by the G_3 deposit and 14.5 ka (+/- 2.5) for a stalagmite covering the G_3 deposit (Lignier *et al*., 2002). We have chosen to reuse these dates and supplement them with new analysis. For this purpose, three sections were invested. Section 1 is in line with the flowstone already dated. Analyses were performed at LSCE using a MC-ICP-MS and following the protocol described in Pons-Branchu et al., 2014. Two micro cores (SANG 19-1 and SANG 19-2) were dated, with for sample 2, an age of 87.3 ± 3.9 ka and a second age of approximately 80 ka. Near the entrance (section 3), two stalagmites (SANG 20-3 and SANG 20-4) were likewise cored and delivered the following Holocene ages: 11.6 ± 4.3 ka, 8.5 ± 0.9 ka, 8.8 ± 0.3 ka (Fig. 3). The speleothems SANG 20-3 and SANG 20-4 are shocked (fig. 4), i.e. they are marked by pebble impacts associated with the evacuation of clasts by flood waters. These impacts can only be identified on one side of the stalagmites and are evidence of the clean-up phase (coarse fillings with hydrological and sedimentary circulation) from the interior of the karst towards the valley. It is therefore not possible for glacial material to penetrate after the stalagmites establishment. These dates are terminus post quem and ante quem of the G_3 detrital sequence penetration. Consequently, the last glacial phase responsible for this detritic invasion took place at MIS stages 4, 3 or 2. Unfortunately, as it stands, it is not possible to distinguish between ancient Würm and recent Würm or even to correctly link this sequence to one of the stages of the glacial retreat. However, it has been possible to better constrain the relationship between the glacial dynamics in the valley and the invasion of sediments. The filling of the Sous-les-Sangles cave is an eloquent case that deserves further study. OSL analyses are planned to directly date the detrital deposits.

Figure 4: Micro-core drilling of the SANG 20-04 speleothem. Note the shocks (white dots in the green circle) showing the evacuation of the pebbles after growth.

References

BINI A., TOGNINI P., ZUCCOLI L. (1998) Rapport entre karst et glaciers durant les glaciations dans les vallées préalpines du sud des Alpes. *Karstologia*, 32, 7-26.

CHIROL B. (1985) Contribution à l'inventaire spéléologique de l'Ain, Jura méridional. *Spéléo01*, CDS Ain, 425 p.

CHIROL B., HUGON B. (2010) Le système Plaine du Bief – Falconnette – Source de la Burbanche (Jura méridional). *Grottes et Karsts de France*. Karstologia Mémoires n°10 (Audra dir.), pp.188-189.

COUTTERAND S. (2010) *Étude géomorphologique des flux glaciaires dans les Alpes nord-occidentales au Pléistocène Récent. Du maximum de la dernière glaciation aux premières étapes de la déglaciation*. Thèse, Université de Savoie, Chambéry, 468 p.

HUGON B. (2013) Réseau de la Falconette. Nouveau joyau du massif du Bugey, la Burbache, Ain. *SpéléoMagazine* n°82, topo HT, pp. 20-25.

KERRIEN Y., JUVENTI G., LORENCHET DE MONTJAMONT M., MONTJUVENT G., GAILLARD C. (1990) *Carte géologique de la France (1/50.000), feuille Belley* (700), Orléans, BRGM, Notice explicative par Kerrien Y., Montjuvent G., Combier J., Gaillard C., Girel J., Laurent R., Lorenchet de Montjamont M., 73p.

IRVINE-FYNN T., HUBBARD B. (2017) Glacier Hydrology and Runoff. *The International Encyclopaedia of Geography*, 18 p.

LIGNIER V., DESMET M. (2002) Les archives sédimentaires quaternaires de la grotte Sous les Sangles (Bas-Bugey, Jura méridional, France) ; indices paléo-climatiques et sismo-tectoniques. *Karstologia*, 39, 27-46.

PONS-BRANCHU E., DOUVILLE E., ROY-BARMAN M., DUMONT E., BRANCHU E., THIL F., FRANK N., BORDIER L. AND BORST W. (2014). A geochemical perspective on Parisian urban history based on U-Th dating, laminae counting and yttrium and REE concentrations of recent carbonates in underground aqueducts. *Quaternary Geochronology* 24, 44-53

SBAI A., EK C., DROUIN P., CHIROL B., ARIAGNO J.-C., PELISSON A., QUINIF Y. (1995) Les remplissages karstiques de la grotte Sous-les-Sangles : Sédimentologie et évolution spéléomorphologique d'une grotte du Jura méridional (France). *Quaternaire*, vol. 6, n°1, pp. 35-45.

The caves of Hellfjell, Norway, and their speleogenesis

Trevor FAULKNER

GEES, University of Birmingham, Edgbaston, Birmingham, B15 2TT, UK. e-mail: trevor@marblecaves.org.uk

Abstract

About 60 karst caves occur in semi-circular marble outcrops on Hellfjell and in linear outcrops east of Mosjøen, south Nordland, Norway. The cave passages lie within 30 m of the overlying surface and only a few have higher and older levels leading to palaeo resurgences. Most therefore unlikely survived the typical 40 m erosion of the Weichselian glaciation. Instead, most were initiated during the last deglaciation, forming by dissolution of conduit walls by meltwaters flowing from submerging ice-dammed lakes along fractures created by isostatic rebound during ice thinning. As deglaciation proceeded, dry-land catchment areas and flow rates increased as the lake meltwaters migrated from supraglacial streams into englacial conduits and finally into subglacial waterways towards the sea. Most caves later enlarged by vadose and sump dissolution in the Holocene. Caves with relict upper levels probably formed during the previous deglaciation. A seaway existed between Vefsnfjord and Elsfjord, as the ice margin retreated, and lower altitude caves that had just been formed were flooded, before early Holocene isostatic uplift raised them above sea level.

1. Introduction

Semi-circular outcrops of mica schist and metamorphic calcitic limestones of the Helgeland Nappe Complex in the Scandinavian Caledonides surround the southern part of the large unforested granite pluton of Hellfjell (809 m a.s.l.) in an anticlinal formation (Fig. 1). They contain an interesting set of c. 20 marble caves on the forested southern slopes. These range from 90–334 m a.s.l., with lengths up to 386 m and a total passage length of c. 1400 m, within 9 local areas containing c. 40 more caves, mainly east of Mosjøen in Vefsndal (FAULKNER, 2019). Their deglacial speleogenesis depended on a complex interplay among ice melting down from summits and retreating back from the coast, land uplift, seismic fracture creation, flowing ice dammed lakes, and marine incursion.

L Length (m); VR Vertical Range (m); XS mean Cross-Section (m^2); Vol Volume (m^3); A Altitude (m a.s.l.).

2. The longer caves on Hellfjell

Dripsteinhola / Loop Cave

L 386 VR 23 XS 4.8 Vol 1853 A 337 (Dripsteinhola entrance)

A small stream sinks into the highest marble band at the head of the dry Bergdal in Area 3, below the entrance to Loop Cave (Fig. 2). The Entrance Chamber is littered with blocks of mica schist, which forms its floor (Fig. 3). Meander Passage descends to a junction with the Main Tunnel. The stream enters and leaves through sumps in Wet Passage, near the Cross Roads. A draughting crawl leads to the short Dripsteinhola entrance shaft that is just 2 m below the ridge top. Most of this cave formed phreatically, from passage morphology, roof pendants, pillars and oxbows.

The Subway / Snowmelt Sink Cave

L 209 VR 12 XS 3.2 Vol 424 A 327

A stream from Hjortdal sinks into Snowmelt Sink Cave at a 5m-deep blind gully, 180 m SE of Dripsteinhola, but in the next marble band (Fig. 4). The relict Subway on the north bank descends with a sloping wall of mica schist. This forms the floor after a bend and reaches the stream at a sump, near the Six Ways junction. Scallop Passage becomes choked, but instead wet crawls lead to the sink entrance.

Engåselvgrotta

L 254 VR 9 XS 2.1 Vol 533 A 295 (Upper Entrances)

The First (impenetrable) Engåselv Rising from Bergdal and Hjortdal is from the lower edge of the second marble band (Fig. 2). The stream later sinks inside the Upper Entrance chamber to Engåselvgrotta near the edge of a wide marble band, but is not seen again until near the Lower Entrances (Fig. 5). A T-junction leads to the Link Crawl, the only known connection to the Middle Entrances and the rest of the cave. Chest Jam Rift leads into four large sub-parallel strike-aligned passages that connect to the Lower Entrances, below which the Engåselv resurges.

Høgligrotta L 248 VR 38 XS c. 6.3 Vol c. 1320 A 90

Høgligrotta in Area 4 is in a continuation of the narrow lowest marble band from Rokåsen, 5 km to the west. The distinctive noisy Doorway Entrance bounded by fractures is in a cliff 6m above a road (Fig. 6). It enters a larger passage with a view down into a roaring streamway. The passage swings east, passing descents on the left into the streamway, which sumps upstream. Crawls lead to the base of the smooth steeply-sloping Black Dyke Aven, where the Top Entrance is in a doline 50 m north of the Doorway. The cave carries the stream Grøftremelv from another doline, c. 100m farther north. Downstream, the passage descends steeply, becoming larger below the Roaring Pitch. It lowers over sediment to a choke, after the water flows down tiny slots to an impenetrable rising c. 160m away and c. 13 m lower.

3. Speleogenesis

The eastward back-wasting deglaciation of the Weichselian ice sheet as the depressed land uplifted isostatically was accompanied by coastal marine incursion. Lines connecting places with equal amounts of relative isostatic uplift since the end of the Younger Dryas (YD) period, 10,000 ^{14}C years BP (11,703±4 cal. a before 1950), are YD isobases (Fig. 1). They are roughly parallel to the coast, and increase eastwards at c. 1 m per km. Local sea-level curve shapes for YD isobases up to 185 m were estimated by FAULKNER (2018) from an assumed sea level curve for Velfjord, 60 km to the SW (FAULKNER & HUNT, 2009).

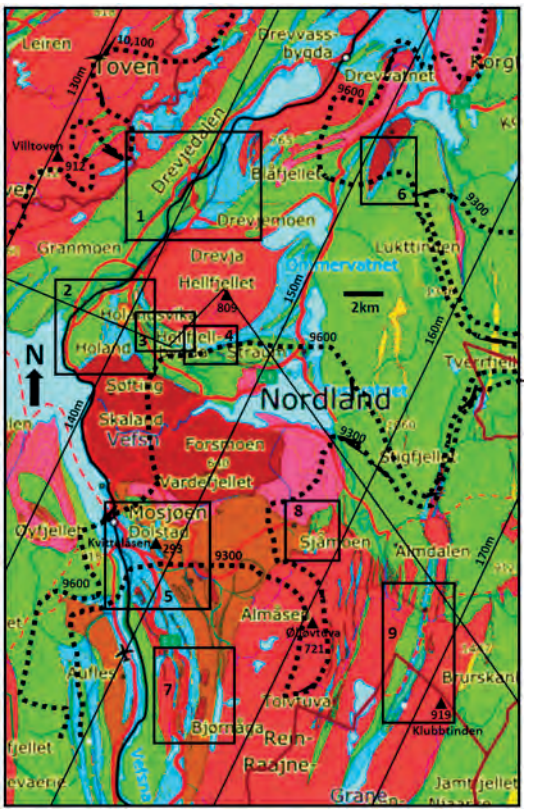

Figure 1: Hellfjell geology, showing: cave areas; YD isobases at 10 m intervals, from SØRENSEN et al. (1987) *(straight lines); Weichselian ice margin retreat stages, from BERGSTRØM (1995), with ages in ^{14}C years BP (dotted lines); and the profile via Hellfjell used in Fig. 7. Blue: marble. Green: mica schist. Other colours: igneous. Red lines: roads.*

Marine incursion up to the marine limit occurred at Hellfjell near the start of the Holocene. It has receded ever since, with continuing uplift. Inland encroachment can be derived from the YD isobase and the eastward recession of the western ice margin, as also shown on Fig. 1. The sea in Vefsnfjord inundated Drevjedal on the 140 m YD isobase to an altitude of 140 m at 10.0 ^{14}C ka BP. This incursion must have initially created a steep marine ice cliff where it melted the tidewater glacier, which was then still >300 m thick. Because the col at its north end is 110 m a.s.l., the whole valley was submerged and there was a direct sea connection between Vefsnfjord and Elsfjord to the north until c. 9.5 ^{14}C ka BP, when uplift rose the col above the sea.

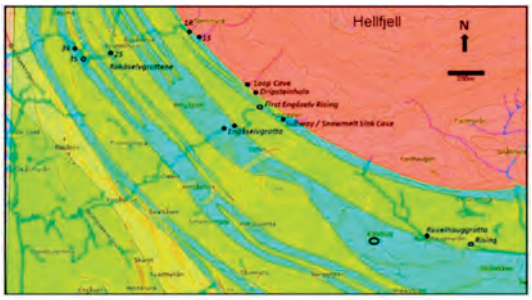

Figure 2: Hellfjell. Green: marble Yellow: schist Pink: granite.

Figure 3: Dripsteinhola / Loop Cave survey.

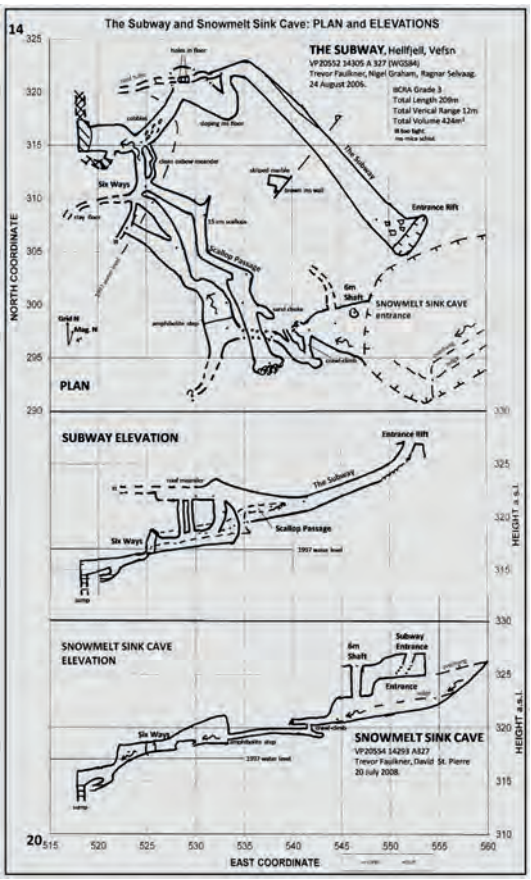

Figure 4: The Subway / Snowmelt Sink Cave survey.

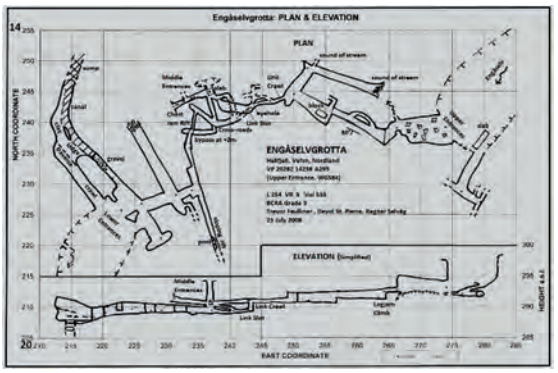

Figure 5: Engåselvgrotta survey

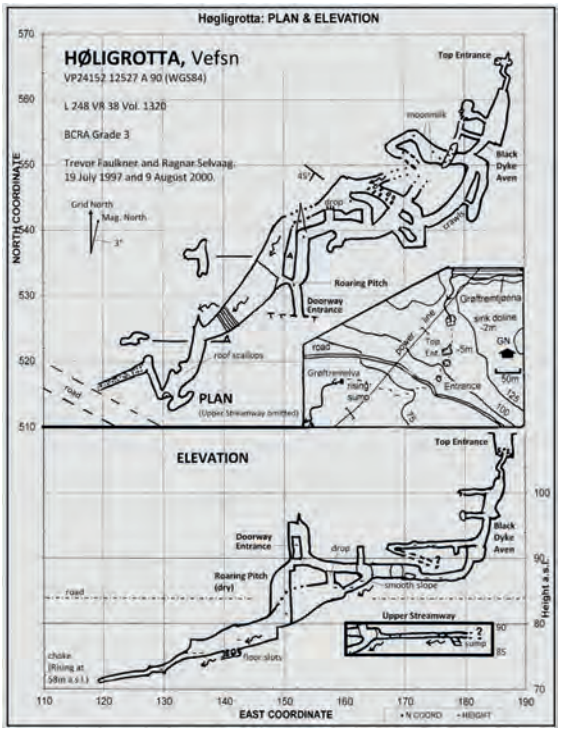

Figure 6: Høgligrotta survey

Contemporaneously with coastal back-wasting, the ice sheet melted by down-wasting onto the summits and later into the valleys. This necessarily created ice-dammed lakes (IDLs) around cold-based nunataks each summer, as plotted by FAULKNER (2005), from a formula derived from GRØNLIE (1975). Some IDLs grew to several 10s of km^2, with depths of several 100 m. It could take many 100s of years for them and the ice surface to lower past a point (such as a fracture entrance) in the mountains. The eastward and downward deglaciations are indicated in Fig. 7. This shows the local ice height and eastern margin at various times along a profile via the Hellfjell summit (Fig. 1), and as plotted against the YD isobase. It also shows the vertical extents of the 9 cave areas, discussed in more detail by FAULKNER (2019).

Caves in central Scandinavia commonly formed by dissolution by meltwaters flowing from submerging IDLs along fractures created by isostatic rebound during ice thinning (FAULKNER, 2006a; 2006b; 2008). The IDLs were initially static, but with downwasting, dry-land catchment areas and flows from the lakes increased. As well as flowing away as supraglacial streams on the distal side of overflowing lakes, the water could also flow out through the ice in englacial conduits, and later in subglacial waterways along warm-based Nye channels on the beds of the present surface streams towards the sea. Suitable fractures in marble beneath an IDL were inundated with flowing aggressive meltwater and enlarged by dissolution to create conduits up to 2 m in diameter within c. 1000 calendar years (FAULKNER (2006b). Wall scallops of length 3–20 cm that point downstream or to palaeo outlets record turbulent dissolutional flow speeds, as do deposited clastic sediments.

The deglaciation of Hellfjell is considered from Figs. 1 and 7. The summit of Hellfjell emerged as a nunatak at 10.9 ka, so that the caves in area 3 at c. 300 m a.s.l. near the 141 m YD isobase were submerged by an IDL on its southern side for c. 1 ka (c. 1700 cal. a), until c. 9.9 ka. This provided the time needed to form the phreatic passages with mean diameters ≤2.5 m in the three surveyed cave systems. The submersion of Høgligrotta at 90 m a.s.l. near the 144 m YD isobase continued until c. 9.6 ka, when the sea at 120 m a.s.l. forced the ice margin to retreat past the cave and its IDL must have collapsed at a jökulhlaup. This duration of 1.3 ka (1900 cal. a) gave time to form its phreatic parts prior to Holocene vadose entrenchment. However, the four cave surveys show relict upper levels that probably led to resurgences that were active during the MIS5e interglacial. The Doorway Entrance obviously functioned as a resurgence before the Roaring Pitch and lower passage formed. The higher levels in these caves were therefore likely formed by similar deglacial processes at the end of the MIS6 glaciation.

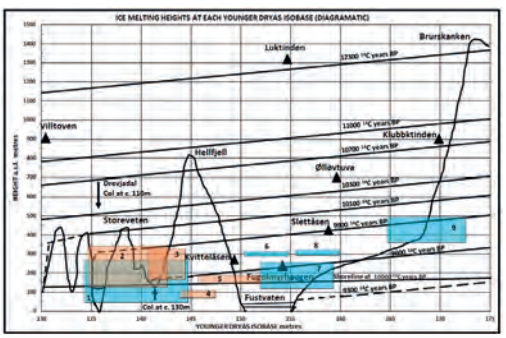

Figure 7: Ice sheet heights at various times along the profile in Fig. 1 plotted against the YD isobase, with several relevant summits included. The marine terminating western extremities of the later decaying ice sheet are shown by steep dashed ice cliff lines. The vertical extents of nine cave areas are shown in shaded boxes. 3 = Hellfjell. 4 = Høgli.

Its Top Entrance is only 109 m a.s.l., so the sea completely flooded Høgligrotta after its ice collapse. Marine abrasion might have shortened the Doorway Entrance as the sea fell to the 58 m altitude of its choked rising at 9.0 ka. The sea melted the ice south of Mosjøen at 9.3 ka, to inundate Vefsndal, where marine shells were found in raised beaches (GRØNLIE, 1975). He showed that melting was complete at 9.08 ka at 133 m a.s.l. at the 200 m YD isobase: the sea melted the tidewater glacier from one side, whilst ablation melted the remnant ice away on the other side. Between the 150–157 m YD isobases, the sea flooded to altitudes of 100–107 m, below the known karst caves in most areas. Although

there are no reports of marine shells in any of the lower caves in areas 1, 2 or 4, they can be anticipated in places protected from springmelt floods, as in Neptune's Cave in Velfjord (FAULKNER & HUNT, 2009).

Several surveys show entrances that are enlarged in width and height, compared with internal passages. These cannot be explained by collapse from simple frost heave, because fallen blocks would remain on the floor, and they are not tapering or are too high for marine abrasion. They therefore likely enlarged by freeze-thaw cycles and outward block pushing as an IDL descended past them during deglaciation, as discussed further by FAULKNER (2018). From Fig. 7, the ice sheet surface and its IDLs lowered by c. 100 m in 200 ^{14}C years, i.e., by c. 0.33 m cal. a^{-1}. With a typical winter ice lid 1.4 m-thick, a 2 m-high entrance would be in contact with ice during the period that such an IDL lowered 3.4 m, i.e., c. 10 years. The entrance enlargements are ≥3 m, suggesting widening of each wall at >0.15 m per year.

The deglacial chronology for the other cave areas was discussed by FAULKNER (2019). Small caves in the west of area 1 were likely created when water flowed through them from an IDL that survived for only 0.2 ka. Kumragrotta in the east of area 1 was probably submerged for 1 ka. A small phreatic roof level in a cave in area 2 was probably initiated whilst supplied from an IDL for 0.5 ka. Small caves in area 5 were probably submerged for only 0.3 ka before emerging above water level. Luktindgrotta (L 611 VR 65 XS 6.0 Vol 3666 A 302), near the 152m YD isobase in area 6, is the longest and most voluminous cave in the whole area. It formed below an IDL on the west side of Luktinden (A 1346), so that phreatic water flow started at c. 12.3 ka, when the ice margin was still west of adjacent coastal islands. The IDL lowered below the cave at 9.7 ka, giving a possible phreatic dissolution time of 2.6 ka (c. 3000 cal. a), easily providing the time needed to form the upper phreatic levels in the cave. Holocene entrenchment subsequently created a large vadose streamway. Small caves in area 7 were flooded for maximum times of 0.3–0.4 ka. Other small caves in area 8 are in a wide marshy area that is distant from local summits, so that their submerging IDL formed late in the sequence and lasted for only 0.3 ka. Ten caves in area 9, many with XS = c. 2 m^2, were probably initiated below an IDL on the western side of Klubbtinden that flooded them for 0.9 ka.

From this discussion, there is a trend of increasing cave L, XS and Vol with increasing time submerged by an IDL. This database is too small to propose precise empirical laws. However, some observations are relevant for deglacial phreatic dissolution, despite several complicating factors, including any MIS5e origin, entrance enlargement, and Holocene entrenchment with vadose passage dimensions related to catchment area (FAULKNER, 2009). There is a probabilistic relationship between explored length and mean cross-section, from the size of the human body and the time needed for any excavation. It seems that caves are only explorable, with XS ≥1 m^2, if they were submerged for at least 0.2 ka. Submersion for 1.3 ka created Høgligrotta, giving a mean radius increase rate of c. 1 mm a^{-1}. Luktindgrotta was submerged for 2.6 ka, giving a mean radius increase rate of c. 0.5 mm a^{-1}. Both these required dissolution rates seem reasonable in high-flow aggressive meltwater (FAULKNER, 2006b). Future study with a larger database should be able to distinguish between phreatic and vadose enlargement rates.

Each glaciation typically removes 40 m of bedrock from the upper and outer parts of caves (FAULKNER, 2008), so there were probably 'cave passages in the sky' above the existing caves. The survey elevations show that all these passages occur within 30m of the surface and only a few caves have higher levels leading to palaeo resurgences. This suggests that most of the passages were initiated during the last deglaciation. Following the FAULKNER (2009) hydrological classification, most are Combination caves, with relict phreatic levels above active vadose parts. Although no local relict vadose passages are known, shallow vadose streamways below relict phreatic levels probably existed in MIS5e, before being removed. An example of Weichselian entrance shortening prior to marine abrasion is provided by the Høgligrotta Doorway Entrance, which probably functioned as a resurgence during the MIS6 deglaciation and throughout MIS5e.

References

BERGSTRØM B. (1995) ELSFJORD. Kvartaergeologisk kart 1927 III. 1:50,000. Norges Geologiske Undersøkelse.

FAULKNER T.L. (2005) Cave inception and development in Caledonide metacarbonate rocks. PhD Thesis. Huddersfield.

FAULKNER T. (2006a) Tectonic inception in Caledonide marbles. Acta Carsologica, 35 (1), 7–21.

FAULKNER T. (2006b) Limestone dissolution in phreatic conditions at maximum rates and in pure, cold, water. Cave and Karst Science, 33 (1), 11–20.

FAULKNER T. (2008) The top-down, middle-outwards, model of cave development in Central Scandinavian marbles. Cave and Karst Science, 34 (1), 3-16.

FAULKNER T. (2009) Relationships between cave dimensions and catchment areas in Central Scandinavia: implications for speleogenesis. Cave and Karst Science, 36 (1), 11-20.

FAULKNER T. (2018) The ages of the Scandinavian caves. Norsk Grotteblad, (70), 15-33, 40.

FAULKNER T. (2019) The caves of Hellfjell and eastern Vefsn. Norsk Grotteblad, (72), 18-43.

FAULKNER T.L. and HUNT C.O. (2009) Holocene deposits from Neptune's Cave, Norway: environmental interpretation and relation to the deglacial and emergence history of the Velfjord–Tosenfjord area. Boreas, 38, 691-704.

GRØNLIE A. (1975) Geologien i Vefsnbygdene. Vefsn Bygdebok 1975, 417–483.

SØRENSEN R., BAKKELID S. and TORP B. (1987) Land Uplift. 1:5000000. Nasjonalatlas for Norge. Statens kartverk.

The future of Quaternary geomorphology lies underground

Trevor FAULKNER

GEES, University of Birmingham, Edgbaston, Birmingham, B15 2TT, UK. e-mail: trevor@marblecaves.org.uk

Abstract

Little detail is known about the Quaternary evolution of upland Britain and Ireland. Multiple glaciations shaped the landscapes, but the maximum extent of the last British-Irish Ice Sheet is still being clarified, and its verticality is poorly constrained in space and time. Almost nothing is known about earlier upland glaciations, because surface evidence was reworked. Help is at hand, by studying karst caves. Caves have a special 'museum' property to preserve evidence of palaeo-environments, from their location, morphology, hydrology, dimensions and contents. Caves develop at successively lower levels during each deglaciation, as recharge and discharge points follow glacially-eroded valleys downwards. Phreatic passage diameters and vadose canyon entrenchments record timescales, perhaps confirmed by sediment dates. Using integrated studies of 'museum' attributes and working backwards in time and upwards in elevation, cave history, the varying glacial, deglacial and interglacial climate regimes, and the uplift and erosion of the local topography, can be deduced, and extrapolated beyond the immediate karst area. Partial successes with this approach include landscapes in Wales, Yorkshire and Norway. Resolution of these histories requires a holistic multi-disciplinary collaboration among geological, geomorphological, sedimentological, glaciological, hydrological, climatological, seismological and speleological communities.

1. The geomorphological problem

Little is known about the detailed Quaternary evolution of upland Britain (Fig. 1), Ireland and other glaciated northern environments. What were: The horizontal and vertical extents of icesheets during each glaciation? The erosion rates of summits and valley floors? The relationships to relative sea levels and the isostatic responses during each deglaciation? How much land lost by erosion was then elevated above sea level during each succeeding interglacial? What effects did seismic and aseismic tectonic movements have on the landscapes? This knowledge is challenging to obtain from surface observations, because each glaciation reworks or destroys previous evidence.

2. Present knowledge

Glaciological events in Britain and Ireland since the Last Glacial Maximum (LGM) are partly known. The global LGM occurred c. 26,000 years ago, when eustatic sea level was lower by c. 130 m (PU CLARK *et al.,* 2009). The development of the British-Irish Ice Sheet (BIIS) around the time of its local LGM was asynchronous, with an early build up in Scotland, followed by later extensions and growths southwards that covered all Ireland and Wales and most of England, with ice streams that flowed 'down' the Irish and North Seas (CD CLARK *et al*., 2012). The oscillations between the LGM and the Younger Dryas Stadial are still being investigated (Fig. 2). Little is published about glacial initiation at Marine Isotope Stage (MIS) 5d, although more is known about its onset in Norway (LUNDQVIST, 1986). Earlier glacial extremities have only been studied in England far from the upland areas.

There is more knowledge of the horizontal extents of the Fennoscandian Ice Sheet (FIS; OLSEN *et al*., 2013) and the Laurentide Ice Sheet (LIS; Quaternary Science Reviews, 5, 1986) for the last few glaciations. These were much larger than the BIIS and easier to model from deep sea sediments. Their oscillations after each local LGM commonly occurred before the ice margins retreated to the present coastlines, giving less terrestrial ambiguity. Their detailed landscape changes caused by each previous glaciation remain unknown, but the total erosional effect of *all* the FIS glaciations has been estimated (LIDMAR-BERGSTRÖM, 1997). The smaller BIIS, in warmer latitudes, was much more dynamic in space and time and more difficult to decipher.

Figure 1: Suilven, viewed from Stac Pollaidh in Assynt, Scotland, an area with karst caves.

Later glaciations in N. Europe, including the BIIS, were reviewed by BOSE *et al.* (2012). SIMMS (2004) discussed erosion and isostasy in Ireland, distinguishing between mechanical erosion of siliciclastic rocks and chemical dissolution of limestones. The question remains: how did the local landscapes evolve before the LGM, during the first 99% of the Quaternary, from 2.6–0.026 million years ago? Study of pre-LGM upland geomorphology appears to be 'stuck'.

3. A karst geomorphological approach

Geomorphological history of glaciated northern uplands can be improved from evidence in local or adjacent limestone caves. These act as 'museums' of previous environments, from their location, hydrology, morphology, dimensions, and chemical, clastic and archaeological contents.

Figure 2: Lacustrine deposits under till, Glen Findhorn.

Location, hydrology, morphology, dimensions

Cave location relative to present fluvial drainage is key. Streams in vadose passages and sumps are commonly continuing to enlarge passages in harmony with erosion of the local landscape. Whilst streams are flowing in steep topography, they are likely to be sufficiently dilute, turbulent, and flowing fast enough, for dissolution to be beyond the chemical breakthrough point where unsedimented floor lowering and wall retreat rate are maximised for the ambient temperature and P_{CO2}. This is c. 1 mm per year at 10°C with 1% P_{CO2} (PALMER, 1991). During floods, dissolution might obey the Fast Rate Law (KAUFMANN & DREYBRODT, 2007) and be supplemented by significant mechanical erosion, increasing enlargement rates by an order of magnitude. The duration of this latest phase can be estimated from the local annual precipitation, its seasonality, and the size of the relevant catchment area, using dissolution rates for relatively low temperature and P_{CO2} (FAULKNER, 2006). Hydrological parameters might be deducible from the lengths of wall scallops (FAULKNER, 2013a). In vadose passages, dissolution rates can be checked against passage depth and width (CHECKLEY & FAULKNER, 2014). It can be estimated if an active passage enlarged in the Holocene, or if it started prior to that, if phreatic, or in a previous interglacial, if vadose. Relict vadose passages could have been active earlier in the Holocene, or if at high levels, during a previous interglacial, when catchment areas and sink entrances were higher, prior to glacial erosion.

Relict phreatic caves high above a valley floor, such as Victoria Cave in Yorkshire (Figs. 3 and 4), are unrelated to Holocene hydrology. However, they formed and enlarged under phreatic hydraulic control, when filled by flowing water. The last opportunity for this in glaciated landscapes was during the last deglaciation, when submerged by an ice-dammed lake as the ice down-wasted (FAULKNER, 2008). Several narrow spillways above Victoria Cave and along the southern edge of the limestone (Fig. 5) show where lake water jökulhlaups burst through the ice sheet that continued to the south (MURPHY *et al.,* 2015). Fig. 6 shows an enigmatic feature at Gully Cave, Giggleswick Scar, Yorkshire. The only conceivable explanation is that water from an ice-dammed lake sank into an inception fracture to initiate the cave. Flow was forced upwards from the initial phreatic conduit in the roof, to create rising cupolas in the limestone cliff and a moulin in the continuing ice sheet, which had previously sealed the cliff edge.

Figure 3: A distant view of Victoria Cave, Yorkshire, UK, high on the far hillside.

Figure 4: The excavated entrance to Victoria Cave.

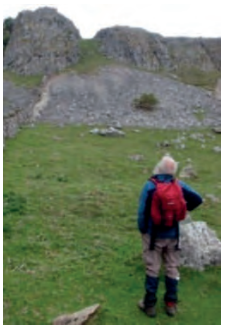

Figure 5: A spillway on the southern edge of the Yorkshire karst. Figure 6: Rising cupolas above the relict phreatic conduit at the entrance to Gully Cave, Yorkshire Dales.

Figure 7: Scallop size records the last dissolutional phreatic flow regime during deglaciation in Elgfjellhola, Norway. Isostatic uplift then caused cm-scale tectonic movement that can be observed around the passage circumference, including where it displaced the wall scallop. Glove for scale.

Both deglacial and interglacial phreatic enlargement opportunities were necessarily available during previous

glacial cycles. They could also occur at the start of each interstadial, dependent on the extent of local downwasting. Surface evidence of these occasions is extremely rare, but might be retained in underground deposits (see below). Sharp slickensides record neotectonic movements after passages enlarged to present sizes (Fig. 7). In central Scandinavia, probably all phreatic caves record a tectonic movement, but none that are mainly vadose. Relating movement to a known seismic event gives the latest time that the passage drained, probably at an ice dam collapse.

Contents

The ages of contents place constraints on passage formation. Their composition provides information about the external environment when deposited. Commonly, internal deposits are younger than the containing passage and most chemical deposits formed after the passage drained. Speleothems can be dated. Trace elements elucidate the contemporary local environment. Corroded large speleothems could indicate dissolution when submerged during a subsequent deglaciation. Speleothem 'straws' would probably not survive dissolution and mechanical erosion by flooding, and therefore formed in the Holocene. Allogenic clastic deposits can commonly also be dated and provide more external information. For example, Broadway in County Pot, Yorkshire, contains stacked sediment layers, including flowstone above rounded cobbles (FAULKNER, 2016), which indicate multiple deposition events, probably related to cycles of glaciation, deglaciation and interglaciation.

Various layered stalagmite and clastic deposits In Victoria Cave represent all the glacial cycles back to before 600 ka in MIS15 (LUNDBERG *et al*., 2010), so that a large passage (Fig. 4) must have existed before then. The deposits' presence hints that the cave was not subject to interglacial flows since, otherwise they could have been washed away. MIS8 is represented only by a hiatus in speleothem deposition between MIS9 and 7, rather than by a significant clay layer. This shows that MIS8 ice was thinner or absent in Yorkshire, and perhaps in Britain, when compared with ice from MIS14 to MIS2. The absence of large mammal deposits during some interglacials suggests that the entrance was sporadically blocked by scree. An elephant tooth and other interglacial mammal remains preserved in the short relict Joint Mitnor Cave, S. Devon, UK (WILMUT *et al*., 2014, p. 106) suggests that it has been relict since MIS5e.

Deducing the timescales

The evolutionary history of multi-level caves in glaciated areas can commonly be estimated, even before dating internal deposits. Glaciation modified the local landscape, caves and hydrology by the erosional deepening and widening of glacial valleys and by removing upper passages and entrance areas. Deglacial seismicity created deeper fractures that allowed new passages to form at lower levels (FAULKNER, 2008). Hence, cave and surface evolution can be deduced by considering the external and internal hydrology and cave configuration at each interglacial, by working backwards in time and upwards in elevation. The dimensions of the active vadose canyons and active phreatic sumps can indicate their age after inception, with suitable wall scallops confirming estimated flow rates and flow speeds. Where the cave has keyhole morphology, with relict phreatic passages or levels above an active streamway, this next higher level probably formed during the last deglaciation. Any relict vadose passages might have formed in the previous interglacial. Higher relict phreatic passages and levels could have formed during the deglaciation before that. This reasoning can be applied up to the highest levels in the cave, where higher entrances commonly indicate earlier sinks and resurgences. Because each passage level was submerged by flowing water during each subsequent deglaciation, higher conduits tend to increase in diameter. However, where the surface was more protected, such as under cold-based ice at high altitude, cave hydrology could stay more constant, and the same phreatic conduits could just increase in size.

Integrated studies of karst cave development and the glacial impact on the local topography are needed to deduce these timescales. This requires a holistic multi-disciplinary collaboration among geological, geomorphological, sedimentological, glaciological, hydrological, climatological, seismological and speleological communities. For safety and conservation, collaborating teams of researchers and cave explorers are needed. Most disciplines reside in university departments, which might be unaware of the opportunities available from speleological science. Nevertheless, contacts between university and local caving clubs ought to initiate from the academic side, to ensure that relevant scientific projects are specified, implemented and suitably reported.

Recent applications

Several examples with similar methodologies correlated cave and local topographical evolution. WALTHAM *et al.* (2010) used information from several long caves in Kingsdale, Yorkshire, to equate the formation of surviving high-level passage fragments to the Anglian MIS12 glaciation. WALTHAM & LONG (2011) deduced from erosion rates and isostasy that the age of exposure of the cavernous Great Scar Limestone was c. 1.3 Ma. SIMMS & FARRANT (2011) and FARRANT & SIMMS (2011) studied landscape evolution in SE Wales. They showed that Ogof Draenen, with >70 km of passages, had at least four development phases. It comprises essentially three long separate stacked systems that individually drained southwards, northwards, then southwards again, in response to fluvial and glacial incisions of the valleys at each end. FARRANT *et al.* (2013) showed that thick fine-grained sediments in the cave derived from glacial meltwater, probably after MIS12, 10 or 6. FAULKNER (2013b) showed that Toerfjellhola in Norway probably started as two separate high-level palaeocaves after MIS12, which became connected by a common flow route during MIS5e. COOPER & MYLROIE (2015) interpreted the effect of glaciation on speleogenesis in the NE United States and HARMAND *et al. (*2017) concentrated on fluvial evolution and karstification south of the major icesheets. VERESS *et al.* (2019) have recently presented a review of global glaciokarst knowledge. WESTAWAY (2020) inferred the uplift history of the English Peak District from cave deposits and levels.

4. The future vision

Digital technology now produces custom-made maps. A future aim would create maps and Digital Elevation Models for the Earth's upland surface as it was in previous interglacials, at scales up to 1:50,000. The first issues would be of glaciated karst areas in the MIS5e (Eemian) interglacial, followed by maps to represent MIS7e, MIS9, MIS11 etc. This would permit better understandings of how the many long and complex cave systems in Britain, Ireland and elsewhere developed relative to the glacial erosion and uplift of the local landscape. Clearly, this information becomes more tenuous with age, and initial maps of earlier interglacials would only be feasible at smaller scales. However, with refinement, both the timescale and physical resolution should increase. A coupled aim should be to produce geological maps that represent the lithology exposed at the surface during previous interglacials.

Acknowledgement

The International Union for Quaternary Research is thanked for providing the opportunity to present the poster, as now expanded in this paper, at the XX INQUA Congress in Dublin, 25–31 July 2019.

References

BOSE M., LÜTHGENS C., LEE J.R. and ROSE J. (2012) Quaternary glaciations of N. Europe. *Quaternary Science Reviews*, 44, 1–25.

CHECKLEY D. and FAULKNER T. (2014) Scallop measurement in a 10m-high vadose canyon in Pool Sink, Easegill Cave System, Yorkshire Dales, UK and a hypothetical post-deglacial canyon entrenchment timescale. *Cave and Karst Science*, 41 (2), 76-83.

CLARK C. D. and 4 others. (2012) Pattern and timing of retreat of the last British-Irish Ice Sheet. *Quaternary Science Reviews*, 44, 112-146.

CLARK P.U. and 8 others. (2009) The Last Glacial Maximum. *Science*, 325, 710-714.

COOPER M.P. and MYLROIE J.E. (2015) *Glaciation and Speleogenesis: Interpretations from NE USA*. Springer.

FARRANT A.R. and SIMMS M.J. (2011) Ogof Draenen: speleogenesis of a hydrological see-saw from the karst of South Wales. *Cave and Karst Science*, 38 (1), 31-52.

FARRANT A.R., SIMMS M.J. and NOBLE S.R. (2013) Subterranean glacial spillways: an example from the karst of S. Wales, UK. *16th International Congress of Speleology Proceedings*, Vol. 3, 42-47.

FAULKNER T. (2006) Limestone dissolution in phreatic conditions at maximum rates and in pure, cold, water. *Cave and Karst Science*, 33 (1), 11–20.

FAULKNER T. (2008) The top-down, middle-outwards, model of cave development in central Scandinavian marbles. *Cave and Karst Science*, 34 (1), 3-16.

FAULKNER T. (2013a) Speleogenesis and scallop formation and demise under hydraulic control and other recharge regimes. *Cave and Karst Science*, 40 (3), 114-132.

FAULKNER T. (2013b) A methodology to estimate the age of caves in northern latitudes, using Toerfjellhola in Norway as an example. *16th International Speleological Congress Proceedings*, Vol. 3, 342-348.

FAULKNER T. (2016) Cave Science Field Meeting: Barbon and Easegill, UK. [In 2011]. BCRA Annual Review for 2015, 35-37.

HARMAND D. and 8 others. (2017) Relationships between fluvial evolution and karstification related to climatic, tectonic and eustatic forcing in temperate regions. *Quaternary Science Reviews*, 166, 38-56.

KAUFMANN G. and DREYBRODT W. (2007) Calcite dissolution kinetics in the system CaCO3–H2O–CO2 at high under-saturation. *Geochimica et Cosmochimica Acta*, 71, 1398–1410.

LIDMAR-BERGSTRÖM K. (1997) A long-term perspective on glacial erosion. *Earth Surface Processes and Landforms*, 22, 297–306.

LUNDBERG J., LORD T.C.and MURPHY P.J. (2010) Thermal ionization mass spectrometer U-Th dates on Pleistocene speleothems from Victoria Cave, North Yorkshire, UK: Implications for paleoenvironment and stratigraphy over multiple glacial cycles. *Geosphere*, 6 (4), 379-395.

LUNDQVIST J. (1986) Late Weichselian glaciation and deglaciation in Scandinavia. *Quaternary Science Reviews*, 5, 269–292.

MURPHY P.J., FAULKNER T.L., LORD T.C. and THORP, J. (2015) The caves of Giggleswick Scar - examples of deglacial speleogenesis? *Cave and Karst Science*, 42 (1), 42–53.

OLSEN L., FREDIN O.and OLESEN O. (2013) *Quaternary Geology of Norway. Norges Geologiske Undersøkelse*. Special Publication 13.

PALMER A.N. (1991) Origin and Morphology of limestone caves. *Geological Society of America Bulletin*, 103, 1–21.

SIMMS M.J. (2004) Tortoises and hares: dissolution, erosion and isostasy in landscape evolution. *Earth Surface Processes and Landforms*, 29, 477-494.

SIMMS M.J. and FARRANT A.R. (2011) Landscape evolution in southeast Wales: evidence from aquifer geometry and surface topography associated with the Ogof Draenen cave system. *Cave and Karst Science*, 38 (1), 7-16.

VERESS M. and 5 others. (2019) *Glaciokarsts*. Springer Geography.

WALTHAM T. and LONG H. (2011) Limestone plateaus of the Yorks. Dales glaciokarst. *Cave and Karst Science* 38 (2),65-70.

WALTHAM T., MURPHY P. and BATTY A. (2010) Kingsdale: evolution of a Yorkshire Dale. *Proceedings of the Yorkshire Geological Society*, 58 (2), 95-105.

WESTAWAY R. (2020) Late Cenozoic uplift history of the Peak District, central England, inferred from dated cave deposits and integrated with regional drainage development: A review and synthesis. *Quaternary International* 546, 20-41.

WILMUT J., PROCTOR C. and JEAN D. (2014) *Exploring the limestones of south Devon*. William Pengelly Cave Studies Trust.

Why there are probably caves beneath the Norwegian Sea

Trevor FAULKNER

GEES, University of Birmingham, Edgbaston, Birmingham, B15 2TT, UK. e-mail: trevor@marblecaves.org.uk

Abstract

Norway has many littoral caves at various heights a.s.l., whose ages depend on the effects of glaciations and deglaciations on local sea levels. The height that the sea rose above present sea level in the early Holocene is the deglaciation marine limit (DML), which increased inland to a maximum of 163 m. Huge coastal caves above the local DML were formed during a glacial onset, when icesheets expanded rapidly, depressing the land ahead of the falling eustatic sea level. Their sizes were increased by upward stoping by rising sea levels. The glaciation marine limit was >120 m higher than the DML. Whilst Scandinavia was depressed isostatically, large forebulge areas, including around the Scottish islands of Shetland and St. Kilda uplifted, as local sea level also fell. This process reversed during deglaciations. During parts of both episodes, forebulge islands were surrounded by unfrozen sea water, so that small coastal caves could form during glacial onset. Larger caves formed during deglaciation, some continuing to exist b.s.l. at St. Kilda, and probably beneath Norwegian islands west of the hinge line.

1. Introduction

Norway has >300 littoral (coastal sea) caves at various heights above sea level (a.s.l), formed in schists, granites and other lithologies, some being huge (SJÖBERG, 1988). Their formation depended mainly on marine abrasion at the contemporary sea level. This was governed by the extent of glaciation during the Quaternary, when Scandinavian karst areas were sculpted by large strongly erosive icesheets (FAULKNER, 2017). Additionally, several well-known karst caves are actually hybrid, having entrances enlarged by marine abrasion (FAULKNER, 2005a). This paper discusses the age and formation of Norwegian littoral caves and considers the probability that some exist below sea level.

2. The formation of littoral caves

Norwegian glaciations started at the summits and spread westwards on to the continental shelf. Deglaciations started both by downwasting inland and by backwasting eastward margin retreats via the strandflat. Both processes started at high relative sea levels, because local isostatic depression exceeded falls in eustatic sea level throughout glaciation. The eastward retreat after the Last Glacial Maximum (LGM) was mapped by ANDERSEN & KARLSEN (1986), starting at 19,000 ^{14}C years BP from the NW extremity of the Lofoten Islands. VORREN *et al*. (2015) confirmed that this retreat from the continental shelf, which is <20 km wide locally (Fig. 1), started at c. 22.2 cal. ka BP. It reached inland Norway during the warm Bølling Interstadial after 13,500 ^{14}C years BP (14,692±4 cal. a B2k), when the sea flooded the depressed coastal areas and attacked the continuing ice cliff.

Younger Dryas isobases and marine limits

With less ice, the land rose rapidly in the early Holocene. YD isobases record equal amounts of uplift relative to present local sea level since the end of the Younger Dryas stadial, 10,000 ^{14}C years BP (11,703±4 cal. a B2k). SØRENSEN *et al*. (1987) mapped land uplift with linear isobases parallel to the northern coast (Fig. 1). The hinge line at a YD isobase of 0 m went from the western tip of Norway to Vesterålen. Earlier, the ice was thicker and the hinge line lay farther west. The maximum height that the sea reached inland is the local *deglaciation marine limit* (DML). This increased eastwards, peaking at 163 m at the 170 m YD isobase at 9890 ^{14}C years BP (Faulkner, 2018). It then reduced to 133 m at the 200 m YD isobase at 9080 ^{14}C years BP (Grønlie, 1975). Marine incursion was controlled by competition between uplift and the position of the ice margin. Thus, the 146m YD isobase sea level curve for Velfjord, derived by FAULKNER & HUNT (2009) and FAULKNER (2012), shows that all places to the east below a present 146 m altitude were inundated by the sea at the start of the Holocene, *providing that the ice had melted by then at that location*.

Valley glacier and mountain icesheet expansions at glacial *onsets* and glacial stadials depressed the land. This caused a rising local sea level ahead of the falling eustatic level, as at the Weichselian onset, when "*depression extended ahead of the ice margin*" (LUNDQVIST, 1986: p. 288) in the rapid Herning stadial at Marine Isotope Stage (MIS) 5d (115–100 ka). There is therefore another limit, the *glaciation marine limit* (GML), which is the maximum elevation that the sea reached inland before freezing or meeting an ice margin. OLSEN *et al*. (2001) found evidence of marine-influenced sediments dated from 35–24 ^{14}C ka BP at 260 m a.s.l. in north central Norway, at the 210 m YD isobase. This pre-LGM marine incursion was 120 m above the equivalent local DML, at an altitude that would have occurred there during deglaciation at 12,700 ^{14}C years BP without persisting ice. However, MANGERUD (1991) concluded that the MIS5d glaciation was as extensive as in the YD. Eustatic sea level was also probably higher, according to CREVELING *et al*. (2017). Thus, it probably caused the Weichselian GML at a height >120 m above the DML, during a high local sea level.

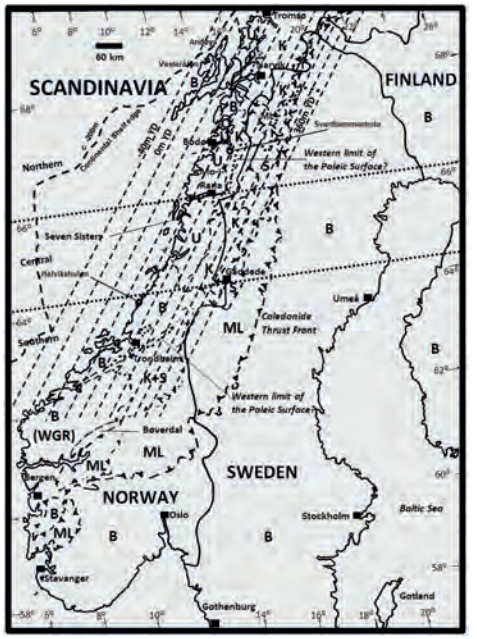

Figure 1: YD isobases at 40 m intervals (SORENSEN, 1987).

Shorelines

The amount of isostatic uplift produced by the denudation of mountains alone is a matter of continuing research, with views expressed that the equivalent of 70–85 % of lost land becomes elevated above sea level (WALTHAM & LONG, 2011). The YD and other conjectured shorelines are plotted against YD isobases in Fig. 2, together with the vertical ranges of some large karst and non-karst cave entrances. The main shorelines shown are those formed: a) after the onset of each major glaciation, when the new ice sheet was as extensive as at the YD and local sea level was rising; b) at the start of each interglacial, when the melting ice sheet was as extensive as at the end of the YD and local sea level was falling; and c) late in each interglacial, when ice was restricted to mountain glaciers and local and eustatic sea levels were almost static. For each stage, shorelines at the 150 m YD isobase are separated by 30 m of erosional uplift, assuming that a mean of 40 m of bedrock was removed at each of the last few glacial cycles. On this reconstruction, early interglacial shorelines coincide with the shoreline of the next but one major glacial onset at the 150 m YD isobase.

Icesheets flowing westwards smoothly eroded the eastern stoss slopes and caused ice plucking on the western lee slopes, causing coastline retreat. Each interglacial marine incursion then consolidated the process, creating the Norwegian strandflat (Fig. 3), which is commonly ≥25 km wide and within ±50 m of present sea level. It is commonly assumed that it formed primarily during the Quaternary, giving an average western cliff retreat rate ≥1 km per 100 ka. Retreats were probably much greater in each later more severe glaciation, when each hinge line retreat probably represents c. 15 m of YD isobases, from Fig. 2, a distance of c. 15 km due east. Glacial erosion along the northern and southern slopes of fjords and islands probably equalled the assumed minimum depth of valley deepening per 100 ka glacial cycle, giving a minimum rate of 40 m for the later retreats of cliffs aligned E–W. A hiatus in continuous sea level change can be observed as a raised beach, shoreline, terrace or platform (Fig. 4). Any that are now below sea level can be detected as submerged platforms.

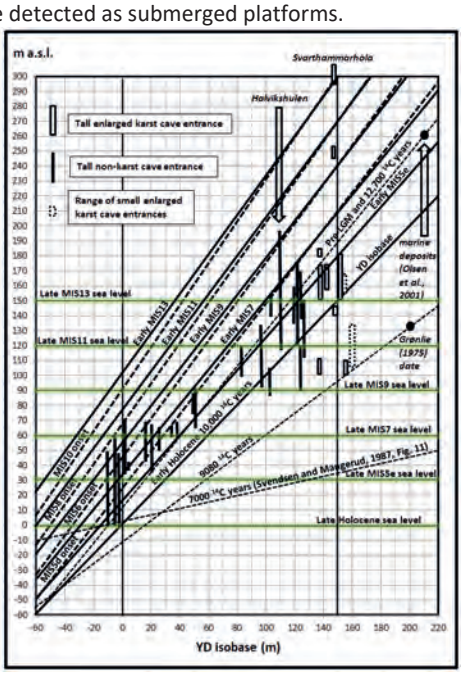

Figure 2: Conjectural shorelines plotted against YD isobases, showing the vertical ranges of large karst and non-karst cave entrances. Late interglacial: dotted. Early interglacial: solid. Glacial onsets: heavy dashed. Others: light dashed.

Figure 3: The Norwegian strandflat. Photo from the internet.

Formation mechanisms

The formation and demise of Norwegian littoral caves depend on competing processes. When not glaciated, the enclosing cliff is eroded by both marine abrasion and winter ice wedging, so that a cave only lengthens relative to cliff retreat if along a weak zone roughly orthogonal to the coast. Caves formed, and karst cave entrances modified, by the sea commonly taper both horizontally and vertically, showing the inward reducing power of marine abrasion (FAULKNER, 2005a). Lengths and entrance widths mainly depend on the time spent in the tidal range. Without ice wedging, the largest and longest caves should occur on coasts that face the open sea. Once a cave starts to form, ice-wedging accelerates enlargement by the spalling of the roof and walls. Collapse debris occupies c. 40 % more space than the original bedrock, but is partly removed by abrasion, tidal changes and movement outwards by ice as it expands prior to melting. These processes persist as long as the sea remains unfrozen in summer and is at the level of the cave or above it. Caves on islands facing north, south or east or farther inland along fjords in sheltered locations should be influenced more by ice wedging than by direct marine abrasion, resulting in narrower and shorter caves.

Figure 4: Two raised platforms viewed from the raised littoral cave Uamh nan Calman on the island of Lismore, Scotland.

Figure 5: Halvikshulen. Figures for scale. Photo from the internet.

Littoral cave classes

FAULKNER (2005a) estimated when >51 karst caves near the north central Norway coast became uncovered by the last ice sheet and how long they remained submerged by the sea. Five with enlarged entrances are above the local DML, as are seven in northern Norway (FAULKNER, 2018). Marine influences are demonstrated by enlarged entrances, non-laminated sand (FAULKNER, 2005b), holes bored by marine molluscs (FAULKNER, 2012), or shell deposits and barnacles attached to walls and roofs (FAULKNER & HUNT, 2009). Following diagrams by FAULKNER (2005a) of entrances enlarged by falling or rising sea levels, FAULKNER (2018) divided coastal caves into three classes:

1 Those below the DML and formed only during the Weichselian deglaciation with a *falling* local sea level, which typically have roof heights ≤5 m.
2 Those above the DML and formed during the onset of a glaciation or glacial stadial with a *rising* sea level, which have roof heights >>5 m.
3 Those below the DML, which were formed as class 2, but enlarged further during deglaciation.

Tall and wide non-karstic littoral cave entrances on the Norwegian coast and islands were described by HOLTEDAHL (1984), MØLLER (1985), and SJÖBERG (1988). Many roofs are well above the local DML, so they predate the Weichselian deglaciation as class 2 caves. Upward stoping by rising sea levels enlarged them during one or more glacial or stadial onsets, assisted by megatides caused by gravitational attraction from icesheets, when oceanic volume was smaller (VELAY-VITOW & PELTIER, 2020). Most cave floors listed by SJÖBERG (1988) descend deeper below collapsed rocks at the entrance, demonstrating that upward stoping by ice wedging continues when above sea level, and that bedrock floor altitudes are difficult to determine. Those entrances >>5 m high with floors below the local DML and any that are entirely below it also predate deglaciation, but were probably slightly enlarged by later deglacial marine abrasion and ice wedging as class 3 coastal caves, when the sea level fell past them.

If the shorelines in Fig. 2 are correct, the north-facing upper entrance to the hybrid karst cave Svarthammarhola at the end of Saltfjord at the 148 m YD isobase in northern Norway (Fig. 1), with its 311 m roof altitude, enlarged at the MIS10 onset or earlier. This was when it was greatly depressed isostatically, being 50 km inland from the present main coastline. The largest littoral cave in Europe is Halvikshulen (Figs. 1 and 5), near the 110 m YD isobase north of Trondheim. Its 78 m-high entrance, which spans 117–195 m a.s.l., is 340 m long and 250 m wide (SJÖBERG, 1988). Its roof is 65 m above the local DML, which is just 5 m above the assumed sea level at the MIS6 glacial onset, giving its youngest age of formation. Other tall caves were formed at or before MIS5d and some hybrid entrances enlarged before the LGM. Only the latest ages can be given, because the caves could have formed as the sea rose past them during an earlier glacial onset, with later enlargements until the latest glaciation that could raise sea level high enough. From Fig. 2, there were 17 main climatic episodes, from early MIS13 to the late Holocene, during which littoral caves could form or be enlarged. Eastward coastal cliff retreats per glacial cycle estimated above greatly exceed the length of any Scandinavian coastal cave. This suggests that even long class 2 caves can only survive succeeding major glaciations in positions well-protected from glacial plucking. Hence, the surviving tall caves facing west were much longer earlier in the Weichselian glaciation and are unlikely to predate most of it. Indeed, the protected entrances of most tall class 2 caves do face north or south. SVENDSEN & MANGERUD (1987) gave deglacial sea level curves extending inland near Trondheim for 155 km, which FAULKNER (2005a) interpreted for the 15–150m YD isobases farther north. Local sea level fell at 6.5–0.3 cm per year after 12 ka ^{14}C BP, taking 77–1667 years to fall 5 m. These seem reasonable timescales to erode class 1 caves. Those older and smaller are at higher YD isobases and elevations and those initiated later at low isobases and elevations are longer and wider.

Forebulge areas and submerged caves

A large forebulge area (Fig. 6) extended beyond the varying hinge line, towards the continental shelf during glaciation (FJELDSKAAR, 1994). Another lay around the Scottish islands Shetland and St. Kilda. Whilst Scotland and Scandinavia were depressed by 1–3 km of ice, the Scottish forebulge uplifted below ≤300 m of ice on these islands, whilst eustatic sea level also fell. This antiphase process reversed during deglaciations. The forebulge depressed farther below present sea level at each interglacial, as the successively lighter main landmasses rose higher after each glacial denudation and Shetland lowered in altitude, as shown by flooded valleys (called voes; FLINN, 1964). MYKURA (1976) reported the occurrence of offshore submerged platforms of probable earlier erosion surfaces, perhaps glacially-assisted, at depths of 9, 24, 45 and 82 m. These might correspond to local sea levels at MIS5e, 7, 9 and 11.

Although submerged sea caves are still unknown at Shetland, many huge tidal range littoral caves and geos occur on its NW coast. Calder's Geo Cave is 122 m long, 107 m wide, c. 8 m high and the largest natural chamber in Britain (DIXON, 2018). It shows that huge class 1 caves could form in interglacials when not protected by a strandflat. However, many submerged sea caves have been found by recreational divers at St. Kilda. This has no elevated littoral caves and a wave-cut platform 40-50 m b.s.l., as investigated by HARRIES *et al*. (2018). The caves variously extend to 180 m in length, with some class 2 roof heights being 25 m a.s.l., with some passage floors descending to 50 m b.s.l. Shorter partly submerged littoral caves on the island of North Rona extend to 65 m in length and 10 m in depth. The submerged

littoral caves at these islands within forebulge areas confirm their formation when mainland areas were glaciated. Class 2 initiation probably occurred early in interglacials during rising relative sea levels. Enlargement then continued during the interglacial, as sea level became almost static, until after the next glacial onset, when sea levels fell again. In Norway, the coasts and some small offshore islands at Lofoten and Vesterålen extend westwards into the YD forebulge area to the -20 m YD isobase (Fig. 1). Hence, class 1 caves could form at these places during uplift at glacial onset. Class 2 caves could form there during depression at early deglaciation. Shorelines were lower and the small islands larger when surrounded by unfrozen sea water at both times. These caves should continue to exist below present sea level, although some will be covered by soft sediments.

Figure 6: Forebulge areas

3. Conclusion

Littoral caves can only form when or if they are in the tidal range, they are not covered by ice, and their cave lengthening rate is greater than the cliff retreat rate. Competitions at all glacial stages among eustatic sea level, local isostasy and the ice margin determine the local relative sea level, showing that littoral caves can now occur above or below present sea level. Thus, there is a high probability that littoral caves continue to exist beneath the Norwegian Sea.

References

ANDERSEN B.G. and KARLSEN M. (1986) Glacial chronology – recession of the ice margin. 1:5000000. Nasjonalatlas for Norge. Kartblad 2.3.4. Statens kartverk.

CREVELING J.R., MITROVICA J.X., CLARK P.U., WAELBROECK C. and PICO T. (2017) Predicted bounds on peak global mean sea level during marine isotope stages 5a and 5c. Quaternary Science Reviews 163, 193-208.

DIXON K. (2018) Big! Descent 265, 33-35.

FAULKNER T. (2005a) Modification of cave entrances in Norway by marine action. 14th International Speleological Congress Proceedings, Athens. Paper O-69, 259-263.

FAULKNER T. (2005b) Nordlysgrotta og Marimyntgrotta. Norsk Grotteblad (45) 23–28.

FAULKNER T. (2012) Marin påvirkning og grottene ved Aunhatten og Langskjellighatten, Brønnøy. Norsk Grotteblad (58) 11-22, 48-49.

FAULKNER T. (2017) Are there any pre-Quaternary caves in Scandinavia? 17th International Speleological Congress. Proceedings Volume 2, 263-268 (Ed 1) or 269-274 (Ed 2).

FAULKNER T. (2018) The ages of the Norwegian caves. Norsk Grotteblad 70, 15-33, 40.

FAULKNER T.L. and HUNT C.O. (2009) Holocene deposits from Neptune's Cave, Nordland, Norway: environmental interpretation and relation to the deglacial and emergence history of the Velfjord–Tosenfjord area. Boreas 38 691-704.

FJELDSKAAR W. (1994) The amplitude and decay of the glacial forebulge in Fennoscandia. Norsk Geologisk Tidsskrift 74 (1) 2–8.

FLINN D. (1964) Coastal and submarine features around the Shetland Islands. Proc. of the Geol. Assoc. 75 (3) 321-339.

GRØNLIE A. (1975) Geologien I Vefsnbygdene. Vefsn Bygdebok 1975, 417–483.

HARRIES D.B. and 5 others. (2018) The establishment of site condition monitoring of the sea caves of the St. Kilda and North Rona Special Area of Conservation. Scottish Nat. Her. Res Report 1044. 213pp.

HOLTEDAHL H. (1984). High Pre-Late Weichselian sea-formed caves and other marine features on the Møre-Romsdal coast, W. Norway. Norsk Geol. Tidsskrift, 64, 75-85.

LUNDQVIST J. (1986) Late Weichselian glaciation and deglaciation in Scandinavia. Quaternary Sci. Rev. 5 269–292.

MANGERUD J. (1991) The Last Ice Age in Scandinavia. Striae 34, 15–30.

MØLLER J.J. (1985) Coastal caves and their relation to early postglacial shore levels in Lofoten and Vesterålen, north Norway. Norges Geol. Undersøkelse Bulletin 400 51–65.

MYKURA W. (1976) British Regional Geology: Orkney and Shetland. HMSO. 149pp.

OLSEN L., SVEIAN H. and BERGSTRØM B. (2001) Rapid adjustments of the western part of the Scandinavian Ice Sheet during the Mid and Late Weichselian - a new model. Norsk Geologisk Tidsskrift 81 93–118.

SJÖBERG R. (1988) Coastal Caves Indicating Preglacial Morphology in Norway. Cave Science 15 (3) 99–103.

SVENDSEN J.I. and MANGERUD J. (1987). Late Weichselian and Holocene sea-level history for a cross-section of western Norway. Journal of Quaternary Science 2 113–132.

SØRENSEN R., BAKKELID S. and TORP B. (1987) Land Uplift. 1:5000000. Nasjonalatlas for Norge. Statens kartverk.

VELAY-VITOW J. and PELTIER W.R. (2020) Out of the Ice Age: Megatides of the Arctic Ocean and the Bølling-Allerød, YD Transition. Geophysical Res. Letters 47 (23) 10 p.

VORREN T.O., RYDNINGEN T.A., BAETEN N.J. and LABERG J.S. (2015) Chronology and extent of the Lofoten–Vesterålen sector of the Scandinavian Ice Sheet from 26–16 cal. ka BP. Boreas 44, 445-458.

WALTHAM T. and LONG H. (2011) Limestone plateaus of the Yorkshire Dales glaciokarst. Cave & Karst Science 3 (2) 65-70.

The high-flow low-storage extreme in marble aquifers

Trevor FAULKNER

GEES, University of Birmingham, Edgbaston, Birmingham, B15 2TT, UK. e-mail: trevor@marblecaves.org.uk

Abstract

High grade marbles have negligible primary porosities after limestone metamorphism. Nevertheless, there are >2800 marble caves in Scandinavia, Scotland and North America. About a third consist of shallow vadose passages without pre-Holocene speleothems, which could not have survived the last glaciation. They therefore formed during the Holocene. However, other caves in Norway clearly pre-date the Holocene or survived several glaciations. These were initiated by phreatic 'pure' water flows from ice-dammed lakes through neotectonic fractures that were opened by isostatic rebound during deglaciation, many passages being horizontal even in vertical and angled foliations. Some flow routes were short enough and fractures wide enough for fast flow rates (shown by small sizes of later wall scallops) during tectonic inception to be immediately beyond rates required for chemical breakthrough or even for the Fast Rate Law. This was despite the absence of vegetation, resulting in little CO_2 in pure glacial meltwater. Phreatic passages enlarged at fast rates to ≤2 m diameter in the typical 1000 years duration of deglacial water flow, possibly followed by vadose entrenchment in the succeeding interglacial. The resulting marble aquifers have high flow rates and low storage capacity.

1. Main study area: central Scandinavia

Central Scandinavia comprises four allochthons of Caledonide nappe complexes in an area of c. 40,000 km^2. Metamorphic grades decline from amphibolite to greenschist facies eastwards, as the nappes are descended from the Helgeland Nappe Complex in Norway in the Uppermost Allochthon to the narrow Lowest Allochthon in Sweden, which overlies older crystalline basement. There are >1000 marble outcrops, commonly forming linear stripe karsts with lengths up to 53 km and widths from 3 to 3000 m (Fig. 1), containing >1000 caves. These commonly occur in groups along the outcrops at altitudes that appear randomly distributed. The area experienced multiple large Quaternary glaciations. These were likely warm-based most of the time, causing large-scale erosion of deep glacial valleys. There is no evidence of any existing pre-Quaternary caves. Toerfjellhola is perhaps the oldest cave in the area, probably dating from MIS12 (FAULKNER, 2013a).

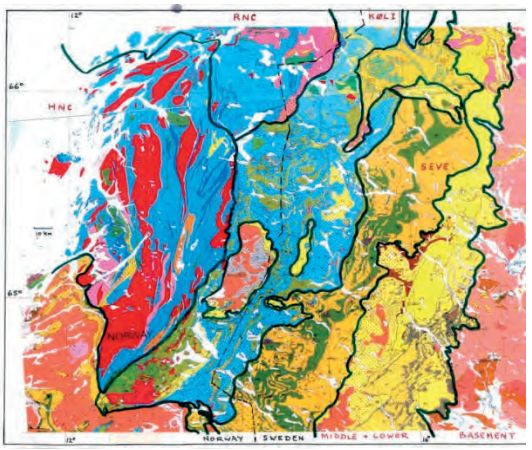

Figure 1: Central Scandinavia lithology and structure. Marble outcrops are shown in dark blue.

2. The cave inception problem

Aquifers in amphibolite-grade marbles in the mountainous Uppermost Allochthon (at least) are unlike those in sedimentary limestones. Negligible primary porosity and widely-spaced fractures produce zero matrix storage and no watertables. Metamorphism and folding removed the sedimentary bedding planes and much of the marble is vertically foliated or steeply inclined. Hence, speleogenesis is not explicable by the Inception Horizon Hypothesis (LOWE & GUNN, 1997) and there is no evidence of any hypogenic origin. However, there are several clues to the local speleogenetic processes. Long and deep caves are rare. The longest cave, c. 6 km, is Korallgrottan in Sweden in the lower metamorphic grade Upper Allochthon (ISACSSON, 1989) and the deepest, 180m, is Ytterlihullet in Norway (HEAP, 1975; FAULKNER, 2008a). However, the mean cave length is only 85m and the mean depth is only 9 m (FAULKNER, 2009a). Because these caves are epigean (Fig. 2), all except Ytterlihullet remaining within 55 m of the surface, this suggests that they evolved synchronously with the glacial topography. Many relict phreatic caves exist in 'impossible' situations, high on the sides of glacial valleys, without any present catchment area. Rather than being formed before the Quaternary glaciations, each of which removed up to 40 m of bedrock, and then being truncated by them, this suggests that they formed during periods of deglaciation. Enlargements during warm-based glaciation when submerged by subglacial lakes are unlikely, because such lakes would be slow moving and unaggressive, becoming saturated with calcite if overlying marble. The absence of relict vadose caves and the presence of only few large speleothems and few relict vadose passages suggest that most caves are relatively young.

3. The formation of neotectonic fractures

Despite crystalline 'hard rocks' in silicate lithologies being non-karstic and without effective primary porosity, they host millions of wells and boreholes world-wide with significant hydraulic yields. The fast flow rates through their fractures and the flow distances involved show that if some had formed in limestones, they could dissolve the limestone at a fast rate beyond that of the chemical breakthrough point determined by PALMER (1991), as discussed by FAULKNER, 2007a). It therefore follows that water flowing through newly-created fractures in crystalline metamorphic limestones could immediately dissolve the marble under a pre- or post-chemical breakthrough regime, as proposed in the Tectonic Inception Hypothesis (FAULKNER, 2006a).

Figure 2: The resurgence entrance to Eiterådalgrotta.

Figure 3: Deformed sediments on the Swedish High Coast.

Ice c. 3 km thick melted away at the end of the Weichselian glaciation. This caused rapid isostatic rebound that peaked at c. 0.5 m per year at the Baltic coast during the early Holocene (MÖRNER, 2003) and produced steep sea level curves at the Norwegian coast (SVENDSEN & MANGERUD, 1987). The rapid uplift created large earthquakes up to Magnitude 8, as evidenced by many examples of screes, rock splitting, soft sediment deformation (Fig. 3), mega-slides, talus (Fig. 4) and talus caves on the Swedish High Coast (MÖRNER & SJÖBERG, 2018). DEHLS *et al*. (2000) showed the widespread extent of neotectonic activity in Scandinavia. In Norway, 54 neotectonic movements were reported in non-karstic bedrocks by OLESEN *et al*. (2004). Additionally, FAULKNER (2005) recorded 56 seismic or aseismic centimetre-scale neotectonic movements in karst caves and outcrops in the Norwegian part of the study area (Figs. 5–9), when large blocks of marble shook and moved to slightly different positions. Holocene neotectonic displacements seen in phreatic passages were subsequent to the movement that created the same or a different inception fracture during deglaciation.

Figure 4: Talus created by the seismic 'blowing-up' of a hilltop roche moutonée above Boda Cave in Sweden.

Figure 5: Horizontal and near-vertical tectonic movements in Marimyntgrotta, north central Norway.

The distance of cave passages from the surface is not greater than one-eighth the depth of the local glacial valley in central Scandinavia (Fig. 10, from FAULKNER, 2007b). This applies in all Caledonide terranes, except in some deeper caves in northern Norway that were probably initiated along fractures created by long-range plate tectonics. Thus, caves formed along neotectonic fractures created during deglaciation that were deeper in steep topography, where seismic acceleration was greatest.

Figure 6: Horizontal opening of the base of a phreatic passage in Cliff Cave, north central Norway.

4. Deglaciation

The availability of water to submerge neotectonic fractures was investigated by deriving the deglaciation of the whole study area from basic principles at nine-time steps (FAULKNER, 2005). The decaying Weichselian icesheet necessarily generated sequences of ice-dammed lakes (IDLs; DAHL *et al.,* 1997), as occur in the mountains of SE Greenland at present (*Google Earth*). Study area analysis showed that all inland fractures and pre-existing caves were submerged by an IDL, typically for c. 1000 years, as the icesheet lowered by down-wasting. IDLs around nunataks at high levels were initially static, with pure meltwater. As the icesheets and IDLs lowered, catchment areas increased in size. Water was sucked via the fractures and out into supraglacial streams and englacial and subglacial channels in the ice (FAULKNER, 2021). By the time the IDLs lowered into valley bottoms, the inflowing streams carried significant sediments, leaving surface deposits with horizontal laminations that probably represent varves in some places (LUNDQVIST, 1972: Fig. 2).

Figure 7: Shattering at Cliff Cave entrance. Figure for scale.

Figure 8: Rotational tectonic movement in Beehive Cave.

Limestone dissolves in dilute flowing water, even when at 0°C with only atmospheric CO_2, at a 'normal' estimated maximum dissolution rate of 0.35 mm per year (FAULKNER, 2006b). This applies if the flow rate is high enough and the calcite concentration is low enough so that the chemical breakthrough point is exceeded (PALMER, 1991). However, the diameter of many phreatic passages in the study area is c. 2 m (Fig. 11), suggesting a radius increased of c. 1 mm per year for c. 1000 years. When water is <20 % saturated with calcite, as in meltwater, a Fast Rate Law applies that raises the dissolution rate by an order of magnitude (KAUFMANN & DREYBRODT, 2007). A rigorous treatment of the submergence timescales and phreatic passage sizes in the study area could thus provide the first practical support for the truth of the Fast Rate Law. However, the flows were turbulent, also causing mechanical erosion of mica schist and other impurities in the marble conduit walls. The present high speeds of flows through some local cave passages are shown by the small sizes of wall scallops (FAULKNER, 2013b) in Fig. 12. Thus, where vadose flows and phreatic flows through sumps continued in interglacials, high flow rates in relatively short conduits, even with low CO_2 above the tree line, could also cause dissolution and mechanical erosion at high rates.

Figure 9: Marble block moved after smoothing by glacial erosion on Elgfjell, north central Norway.

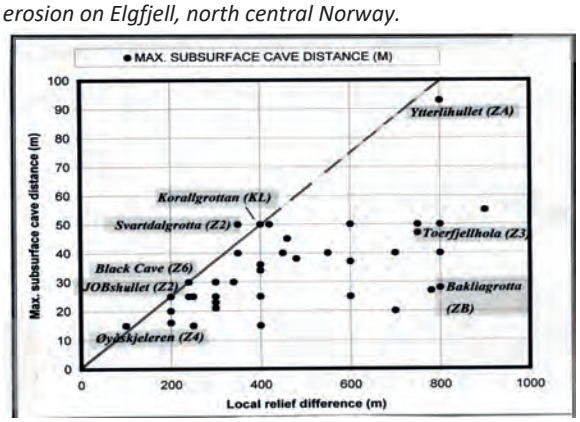

Figure 10: The sub-surface cave distance of caves in central Scandinavia plotted against the local relief difference.

Figure 11: 2 m-diameter phreatic passage in Jegerhullet, Norway, with a Holocene neotectonic movement.

5. Summary

Relict phreatic passages in marble caves in the non-Arctic Caledonides of New England (FAULKNER, 2009b; COOPER & MYLROIE (2015), Ireland, Scotland and Scandinavia (FAULKNER, 2009c) were formed along tectonic inception fractures created by deglacial earthquakes after rapid isostatic rebound. Ice-dammed lakes submerged marble karsts, allowing fast dissolution with turbulent flow, probably invoking the Fast Rate Law. The caves evolved and were removed during a 4-stage process that repeated during each glacial cycle (FAULKNER, 2008b). With open passages but negligible porosities and relatively low fracture densities in high- grade marbles, these aquifers respond rapidly after heavy rainfall (Fig. 13), but their low storage capacity allows floods to dissipate in a few hours.

Figure 13: High flow in Kvannlihola 2 in vertical stripe karst.

Figure 12: Longer scallops in the phreatic part of Fasett Resurgence Cave, Norway, indicate a deglacial flow speed of c. 1.1 ms^{-1}. Shorter scallops in the vadose part indicate a springmelt speed of c. 2.5 ms^{-1}. Photo by Alan Marshall.

References

COOPER M.P. and MYLROIE J.E. (2015) Glaciation and Speleogenesis: Interpretations from the Northeastern United States. Springer. 142 p.

DAHL R., SVEIAN H. and THORESEN M.K. (1997) Nord Trøndelag og Forsen: Geologi og Landscap. Norges Geologiske Undersøkelse. 137pp.

DEHLS J.F. and 5 others (2000) 1:3000000 Neotectonic map: Norway and adjacent areas. Geol. Survey of Norway.

FAULKNER T.L. (2005) Cave inception and development in Caledonide metacarbonate rocks. PhD. Huddersfield.

FAULKNER T. (2006a) Tectonic inception in Caledonide marbles. Acta Carsologica 35 (1) 7–21.

FAULKNER T. (2006b) Limestone dissolution in phreatic conditions at maximum rates and in pure, cold, water. Cave and Karst Science 33 (1) 11–20.

FAULKNER T. (2007a) The hydrogeology of crystalline rocks as supporting evidence for tectonic inception in some epigean endokarsts. Cave and Karst Science 33 (2) 55-64.

FAULKNER T. (2007b) The one-eighth relationship that constrains deglacial seismicity and cave development in Caledonide marbles. Acta Carsologica 36 (2) 195-202.

FAULKNER T. (2008a) Tilbake til Bryggfjelldalen. Norsk Grotteblad (50) 14-24, 36-37, 66-67.

FAULKNER T. (2008b) The top-down, middle-outwards, model of cave development in central Scandinavian marbles. Cave and Karst Science 34 (1) 3-16.

FAULKNER T. (2009a) Relationships between cave dimensions and local catchment areas in Central Scandinavia: implications for speleogenesis. Cave and Karst Science 36 (1) 11-20.

FAULKNER T. (2009b) Speleogenesis of the New England marble caves. 15th Int. Spel. Congress Proc., 2, 855-862.

FAULKNER T. (2009c) The general model of cave development in the metalimestones of the Caledonide terranes. 15th Intl. Spel. Congress Proc., Vol. 2, 863-870.

FAULKNER T. (2013a) A methodology to estimate the age of caves in northern latitudes, using Toerfjellhola in Norway as an example. 16th Int. Spel. Congress Proc., 3, 342-348.

FAULKNER T. (2013b) Speleogenesis and scallop formation and demise under hydraulic control and other recharge regimes. Cave and Karst Science 40 (3) 113-132.

FAULKNER T. (2021) Englacial conduits and crevasses in the artificial tunnel inside Langjökull glacier, Iceland. 18th International Speleological Congress Proceedings.

HEAP D. (1975) William Hulme Grammar School Report of Expedition to Nordland 1974. 27pp.

ISACSSON G. (1989) Cave deposits during glaciations and interglacials - an example from the Korallgrottan in Middle Sweden. 10th Intl. Spel. Congress Proceedings 217–218.

KAUFMANN G. and DREYBRODT W. (2007) Calcite dissolution kinetics in CaCO3–H2O–CO2 at high under-saturation. Geochimica et Cosmochimica Acta 71, 1398–1410.

LOWE D.J. and GUNN J. (1997) Carbonate Speleogenesis: An Inception Horizon Hypothesis. Acta Carso. 26/2 457–488.

LUNDQVIST J. (1972) Ice-lake types and deglaciation pattern along the Scand. mountain range. Boreas 1, 27–54.

MÖRNER N-A. (Ed.) (2003) Paleoseismicity of Sweden: a novel paradigm. Stockholm University. 320pp.

MÖRNER N-A. and SJÖBERG R. (2018) Merging the concepts of pseudo-karst and paleoseismicity in Sweden: A unified theory on the formation of fractures, fracture caves, and angular block heads. Int. Jnl. of Speleology 47 (3) 393-405.

OLESEN O. and 9 others. (2004) Neotectonic deformation in Norway and its implications: a review. Norwegian Journal of Geology 84 3–34.

PALMER A.N. (1991) Origin and Morphology of limestone caves. Geological Society of America Bulletin 103 1–21.

SVENDSEN J.I. and MANGERUD J. (1987) Late Weichselian and Holocene sea-level history for a cross-section of western Norway. Journal of Quaternary Science 2 113–132.

Neogene caves reactivated in Quaternary: Niaux-Lombrives-Sabart (Ariège, Pyrénées, France)

Patrick SORRIAUX[(1)], Hubert CAMUS[(2)], Ludovic MOCOCHAIN[(3)], Philippe AUDRA[(4)] & Philipp HÄUSELMANN[(5)]

(1) Route de Surba, lieu-dit La Pesse, 09400 Bédeilhac, France, psorriaux@gmail.com
(2) CENOTE, 1 chemin de Valdegour, Nîmes 30000, France, camus.hubert@cenote.fr
(3) 125 rue de Salados, 05230 Chorges, France, ludomocochain@gmail.com
(4) University Côte d'Azur, Polytech'Lab - UPR 7498, Nice, France, Philippe.AUDRA@univ-cotedazur.fr
(5) Swiss Institute for Speleology and Karst Studies SISKA, Serre 68, 2301 La Chaux-de-Fonds, Suisse, praezis@speleo.ch

Abstract

The Niaux-Lombrives-Sabart cave system is located in the south of France in the Pyrénées. Several filling sequences date from ancient warm periods and more recent cold periods associated with the last glaciations. The meltwater from these glaciers only reactivated an already largely organized cave system. Several activity periods are well supported by U/Th dating of flowstones between 450,000 years and the Holocene. On the basis of recently published ^{26}Al / ^{10}Be cosmogenic dates in the oldest fluvio-karstic formation, it can be shown that the cave was traversed by a powerful river between 8 and 3 million years ago making successive underground oxbows. An ancient level of the Ariège valley at 650 m, only 170 m above its current position, can be attributed fairly precisely to the Upper Miocene-Pliocene.

Résumé

Réactivation d'un karst Néogène pendant le Quaternaire : Niaux-Lombrives-Sabart (Ariège, Pyrénées, France). Le réseau de Niaux-Lombrives-Sabart est situé au sud de la France, dans les Pyrénées. Plusieurs séquences de remplissages témoignent de périodes anciennes chaudes et de périodes plus récentes froides associées aux dernières glaciations. Les eaux de fonte de ces glaciers n'ont fait que réactiver un système karstique déjà en grande partie organisé. Plusieurs périodes d'activité sont bien calées par la datation U/Th des planchers stalagmitiques entre 450 000 ans et l'Holocène. Sur la base de datations cosmogéniques $^{26}Al/^{10}Be$ dans la formation fluvio-karstique la plus ancienne (récemment publiées), on peut montrer que le karst a été parcouru par une puissante rivière entre 8 et 3 millions d'années, constituant plusieurs boucles de recoupement souterrain. On daterait assez précisément du Miocène supérieur-Pliocène un ancien niveau de la vallée de l'Ariège à 650 m, seulement 170 m au-dessus de sa position actuelle.

1. Introduction

The Niaux-Lombrives-Sabart (NLS) cave system develops in the massif of Cap de la Lesse (1189 m) in the southern part of the Tarascon-sur-Ariège basin (Ariège, Pyrénées). More than 14 km of passages are known, from 3 interconnected caves (Fig. 1): the prehistoric Niaux Cave (678 m asl.), Sabart Cave (563 m asl.) in the Vicdessos valley, and Lombrives Cave (605 m asl.) in the Ariège valley. The system is organized in 3 main cave levels: the main drain between Niaux and Lombrives (650-700 m), an intermediate level (about 600 m), and the lower passages of Lombrives and Sabart (550 m). A series of vertical shafts in Lombrives Cave connects the 650-700 m and 550 m levels. The massif is in a favorable location at the confluence of two valleys, the Ariège and the Vicdessos, which allowed to record several karst phases related to the evolution of both valleys, following the uplift of the Pyrénées along the Cenozoic (CALVET & GUNNELL, 2008; MONOD *et al.*, 2016) and the successive rejuvenation of the cave system following glacial advances during the Quaternary (MARTEL, 1908; RENAULT, 1970; SORRIAUX, 1981, 1982; BAKALOWICZ *et al.*, 1984; SORRIAUX *et al.*, 2016).

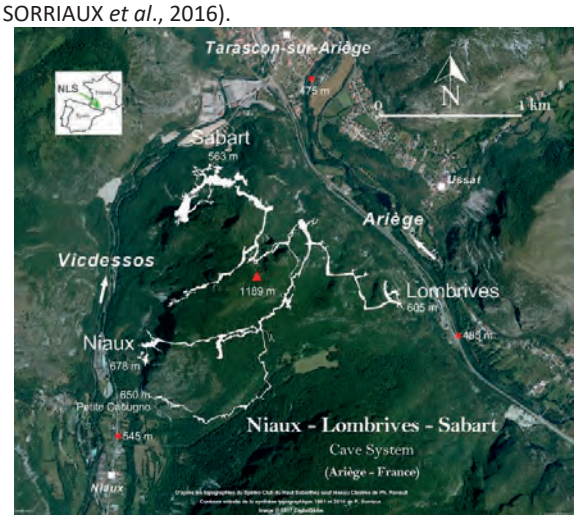

Figure 1: plan view of Niaux-Lombrives-Sabart cave system (Ariège, Pyrénées).

2. Morpho-sedimentary evolution of the cave system during the Quaternary

During each glaciation, the whole cave system could have been entirely flooded. However, the last Würm glaciation is responsible for the most fresh and widespread morphological and sedimentary witnesses (SORRIAUX, 1982; SORRIAUX *et al*., 2016). The reconstruction of paleo-flows has been mainly established using erosional features and sedimentary structures. Glacially induced flow in the caves was mainly controlled by the advances and relative position of glaciers in both valleys. When the ice cap was higher than 1000 m asl. during MIS 4 (70 ka), flow was directed from Ariège valley to Vicdessos valley across the upper cave level. Around MIS 2 (29 ka), underground flows gradually abandoned the Niaux branch to be eventually entirely diverted through the Lombrives shafts toward Sabart. At the end of deglaciation, underground flows were probably limited to the lower levels of Lombrives and Sabart, originating from Ariège valley and using a currently obstructed sink.

The oldest recorded glaciations correspond to MIS 6 and 8 (Fig. 2), and possibly MIS 14 or 16 (SORRIAUX *et al*., 2016). They apparently left a minor impact on the caves. Even with a complete ice capping, the reactivation of the whole cave system did not occur, and only limited and discontinuous deposits were left. Such a situation is well established through the recent studies of glacio-karsts, which show that reactivation can only occur in case of coincidence between surface glacial meltwater flow and potential areas of underground capture (BINI *et al*., 1998; HÄUSELMANN *et al*., 2008).

The definitive draining of the system has been dated to about 19 ka, corresponding to the generalized retreat of the glaciers in both valleys (SORRIAUX 1982, 2016). Paleogeographic reconstructions show that at the ultimate advance stage, the Ariège glacier shortly went further than the Tarascon basin, but the Vicdessos valley was already deglaciated and flooded by a proximal lake due to the downstream dam of Ariège glacier. This lake extended up to 580 m asl., 100 m below the Niaux Cave entrance (DELMAS, 2009; DELMAS *et al*, 2011, 2012).

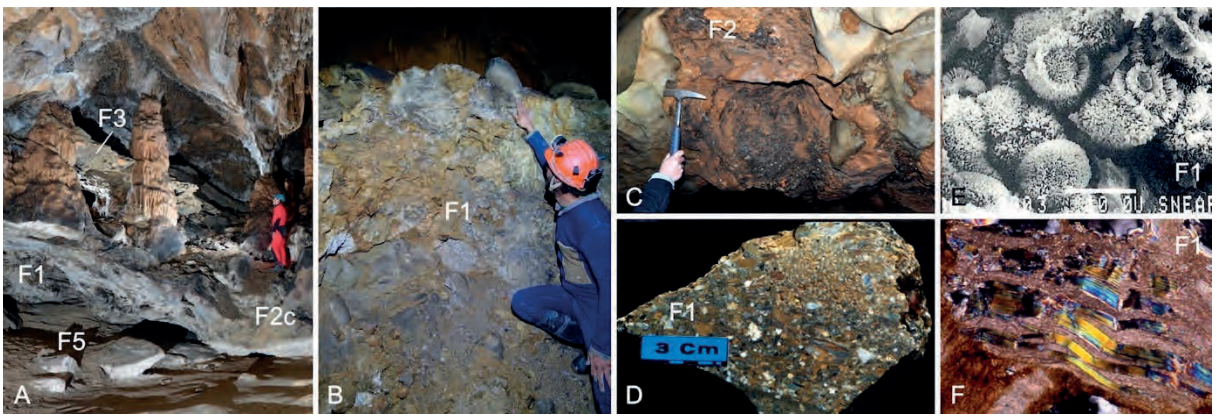

Figure 2: A: the reference site in Niaux Cave. Pillars of the « Calcite Complex » (F2c) are buried under a conglomerate (F3) corresponding to a pre-würmian MIS 8 glacial phase. In the lower part of the picture, the sands (F5) correspond to the main würmian glacial phase (MIS 4 to 2), which reactivated the cave system between 90 et 20 ka. B: The Lombrives Alluvial Fm. (F1) in Lombrives Cave. C: Red argillite facies with ferruginous gravels, from the Red Fm. (F2). D: slice of sandstone from the Lombrives Alluvial Fm. (F1). E: SEM image showing goethite spherulites in F1. F: thin section showing epigenesis of calcite after mica in F1.

3. Old sedimentary remnants of non-glacial origin

The oldest identified deposits correspond to the Lombrives Alluvial Fm. (F1). These are conglomerates and allogenic sandstones grading up gradually to argillites with pebbles, then to hardened lacustrine clays (Red Fm. F2). The whole formation constitutes an aggradation sequence as a morpho-sedimentary response to a baselevel rise. When entirely preserved, its thickness is up to 10 m in the 650 m asl. gallery level of Lombrives Cave close to the Garrigou shaft (Fig. 3), and it can be tracked along 1.5 km. It is strongly weathered with intense carbonate diagenesis. Sandstones are reddish, and we can observe epigenesis of calcite after phyllosilicate minerals (Fig. 2). The clay content is characterized by an association of kaolinite, smectite, and interstratified I/S, C/V, and C/S originating from *in situ* weathering of illites and chlorites, suggesting a non-glacial origin of these sediments. Regarding their chronology, first paleomagnetism measures already suggested an age >780 ka for the F2 Red Fm. (BAKALOWICZ *et al*., 1984). Recent $^{26}Al/^{10}Be$ cosmonuclide dating of the F1 Lombrives Alluvial Fm. yielded several ages comprised between 8 and 3 Ma (SARTÉGOU *et al*., 2020). Their interpretation remains difficult due to the numerous reworkings and inheritages inside the caves, and we know that burial ages have to be taken carefully in caves where filling are polyphasic (CALVET *et al*., 2018). Anyway, we observe a convergence of 9 ages between 8 and 3 Ma in the F1 Lombrives Alluvial Fm., where the morpho-sedimentary setting is rather well constrained. Moreover, 4 ages around 3.5 Ma characterize the upper part of the formation, giving a reliable, more recent age limit.

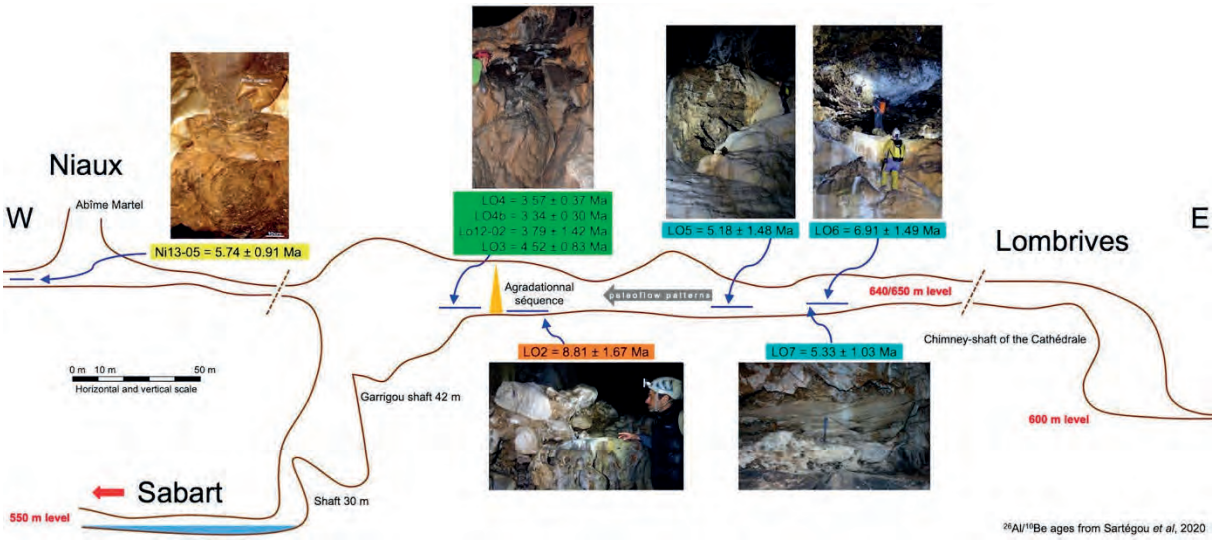

Figure 3: synthetic profile of the passage between Niaux and Lombrives caves, showing the location of the main sites of the Lombrives Alluvial Formation (F1).

4. Speleogenesis of the cave system

This dating series of the F1 Lombrives Alluvial Fm. shows that the cave system was crossed by a powerful river between 8 and 3 Ma, entering the cave at 650 m asl. This means that the valley floor of the Ariège was 170 m above its current position during the Mio-Pliocene, which is in accordance with new data on Neogene paleo-surface geodynamics (MONOD *et al*, 2016). The wide range of ages would show a dynamic fluvio-karst which would integrate several overlapping sedimentary units concordant with successive underground oxbows developed between the entrance zone of Lombrives Cave and the Garrigou shaft.
The organization of the system with underground oxbows is controlled by the aggradation in the valley. They correspond to successive self-capture footpaths between sinks and resurgences along the left bank of Ariège River. The conditions for an underground connection between both Ariège and Vicdessos valleys occurred according to the differential aggradation of these valleys. Regarding the dynamic of a self-capture, the development of an underground oxbow starts with the establishment of an autochthonous drainage from the karst plateau toward the valley floor. When aggradation filling starts in the valley, some sinkholes can appear upstream, they then connect to the autochthonous underground flow path and eventually use its downstream part towards the outlet (MOCOCHAIN *et al*, 2006). In the course of aggradation, several underground oxbows can succeed each other or work simultaneously, and propagate deep inside the karst massif. Such a dynamic setting occurred at the Mio-Pliocene transition until the effects of the first glaciations in the valleys at the onset of Plio-Quaternary. When the valley incision continued, the fluvial cave sediments that partly filled the passages were washed away. Some abandoned drains still harbor these old fluvial deposits, whereas the new flows reuse the reopened passages. The latter still harbor million-years old reworked sediments.

The review of the ages of the fluvial deposits involves therefore several evolution stages: (i) a first incision phase of the Ariège and Vicdessos valleys allows to establish a first underground connection prior to 8 Ma; (ii) an aggradation phase in the valleys allows the development of successive underground oxbows, with fluvial transit, between 8 and 3 Ma; (iii): an incision phase, or rather some baselevel oscillations, cause cave sediment remobilisation and reopening of these oxbows. This timing is rather well constrained between 780 and 19 ka. The lowermost reopened level corresponds to the Lombrives/Sabart lower level at about 550 m asl., which is 70 m above the current Ariège valley floor. Therefore, the karst records mainly a fluvial aggradation phase which would correspond to the most stable and favorable situation between 5 and 3 Ma.

5. Conclusions

The sediments preserved in the passages of the Niaux-Lombrives-Sabart (NLS) cave system show the complexity of the evolution of this Pyrenean karstic cave system and provide some clues for the interpretation of its speleogenesis. Even if the morpho-sedimentary traces of the youngest glaciation are widespread in the system, the meltwater flows only reactivated an old cave system, already well-organized, and whose morphological characteristics and origin can now be assigned to the incision of the old miocene paleo-surfaces. The last glaciers only reused pre-existing morphologies very similar to the current landscape and did not contribute to a significant additional incision. This landscape is almost entirely inherited of the old Mio-Pliocene phases, and the karst

alone has preserved its precious morpho-sedimentary record. Field work is still in progress in order to better understand the fluvial processes, both in valleys and underground, that led to the underground connections and oxbows. The study of the transport conditions of the sediments brought in and exported from the caves during the pre-glacial and Quaternary period is still to be refined.

Acknowledgements

We thank Catherine Blasco, the manager of Lombrives Cave, the Operating Service of the Ariège Touristic Sites (SESTA) led by Pascal Alard, Jacques Azéma (responsible of the site of the prehistoric Niaux Cave), Yanik Le Guillou from the Culture Affairs Direction of the Midi-Pyrénées region (DRAC/SRA, Occitanie), and friends of Spéléo-Club du Haut Sabarthez who were always helpful for the access to the caves.

References

AUDRA P., BINI A., GABROVSEK FR., HÄUSELMANN PH., HOBLEA F., JEANNIN P.-Y., KUNAVER J., MONBARON, M., ŠUSTERSIC FR., TOGNINI P., TRIMMEL H. & WILDBERGER A. (2006) Cave genesis in the Alps between the Miocene and today: a review. *Zeitschrift für Geomorphologie*, t. 50, n° 2, 153–176.

BAKALOWICZ M., SORRIAUX P. and FORD D.C. (1984) Quaternary glacial events in the Pyrenees from U–series dating of speleothems in the Niaux–Lombrives–Sabart caves, Ariège, France. *Norsk Geografisk Tidsskrift*, 38, 193-197.

BINI A., TOGNINI P. et ZUCCOLO L. (1998) Rapport entre karst et glaciers durant les glaciations dans les vallées préalpines du sud des Alpes. *Karstologia*, 32, 7–26.

CALVET M. and GUNNELL Y. (2008) Planar landforms as markers of denudation chronology: an inversion of East Pyrenean tectonics based on landscape and sedimentary basin analysis. In: GALLAGHER K., JONES S.J., WAINWRIGHT J. (eds), *Landscape Evolution*, Geological Society Special Publications, London, 296, 147-166.

CALVET M., BRAUCHER R., SORRIAUX P., HEZ G. et GUNNELL Y. (2018) De la difficulté de dater les réseaux karstiques étagés. Poster KARST 2018 *Colloque International de Karstologie*, Chambéry 17 juin au 1 juillet 2018.

DELMAS M., (2009) *Chronologie et impact géomorphologique des glaciations quaternaires dans l'est des Pyrénées*. Thèse de Doctorat, Université Paris 1 Panthéon-Sorbonne, Paris, 529 p.

DELMAS M., CALVET M., GUNNELL M., BRAUCHER R. and BOURLÈS D., (2011) Palaeogeography and 10Be exposure-age chronology of Middle and Late Pleistocene glacier systems in the northern Pyrenees: implications for reconstructing regional palaeoclimates. *Palaeogeography, Palaeoclimatology, Palaeoecology*, 305, 109-122.

DELMAS M., CALVET M., GUNNELL Y., BRAUCHER R. et BOURLÈS D. (2012) Les glaciations quaternaires dans les Pyrénées ariégeoises : approche historiographique, données paléogéographiques et chronologiques nouvelles. *Quaternaire*, 23, 61–85.

HÄUSELMANN Ph., LAURITZEN S.E., JEANNIN P.Y. and MONBARON M. (2008) Glacier advances during the last 400 ka as evidenced in St Beatus Caves (BE, Switzerland). *Quaternary International* 189, 173-189.

MARTEL É.-A. (1908) Cavernes de Tarascon-sur-Ariège. *Spelunca*, Bulletin & Mémoires de la Société de Spéléologie, 54, VII, 47 p.

MOCOCHAIN L., BIGOT J.-Y., CLAUZON G., FAVERJON M. et BRUNET P. (2006) La grotte de Saint-Marcel (Ardèche) : un référentiel pour l'évolution des endokarsts méditerranéens depuis 6 Ma. *Karstologia*, 48, 33–50.

MONOD B., REGARD V., CARCONE J., WYNS R. and CHRISTOPHOUL F. (2016) Postorogenic planar palaeosurfaces of the central Pyrenees: weathering and neotectonic records. *C. R. Geoscience* 348, 184–193.

RENAULT Ph. (1970) *Excursion dans les grottes de Niaux et de Lombrives*, réunion intergroupe sur les remplissages karstiques de l'Association des Sédimentologistes Français, 20 - 21 Novembre 1970 à Foix, 14 p.

SARTEGOU A., BLARD P.-H., BRAUCHER R., BOURLÈS D, SORRIAUX P., ZIMMERMANN L., LAFFITTE A., TIBARI B., LEANNY L., GUILLOU V., BOURDET A. and ASTER Team (2020) Late Cenozoic evolution of the Ariège River valley (Pyrenees) constrained by cosmogenic 26Al/10Be and 10Be/21Ne dating of cave sediments. *Geomorphology* 371 (2020).

SORRIAUX P. (1982) *Contribution à l'étude de la sédimentation en milieu karstique. Le système de Niaux-Lombrives-Sabart (Pyrénées Ariégeoises)*. Thèse de doctorat de 3° cycle, Univ. Paul Sabatier de Toulouse et Laboratoire Souterrain de Moulis CNRS, 255 p.

SORRIAUX P., DELMAS M., CALVET M., GUNNELL Y., DURAND N. et PONS-BRANCHU E. (2016) Relations entre karst et glaciers depuis 450 ka dans les grottes de Niaux-Lombrives-Sabart (Pyrénées ariégeoises). Nouvelles datations U/Th dans la grotte de Niaux. *Karstologia*, 67, 3-16.

Speleogenesis and geomorphology of caves in conglomerate rocks in the Eastern Sayan

Anatoliy BULYCHOV

Cave conservancy of Hawaï

Abstract

Big Oreshnaya and Badjeiskaya caves in conglomerates (Siberia, Manskiy trough, Narva's suite) are unique as their length is about 50 km and 10 km respectively, while in general, there is no significant development of caves in such rocks. The reasons for the local karstification of the Narva's suite conglomerates are high porosity and fracturing of the rocks, high content of limestone and dolomite pebbles, boulders of gravelite rocks with quartz-calcite-dolomite filler, and the location of the cave massif which is favorable for infiltration and discharge of ground waters. The length of the passages in Big Oreshnaya cave is increasing year by year. Our geomorphological observations show the presence of large linear faults, which played an obvious role in karstogenesis, and the presence of signs of a near-surface cave level, which has not been discovered yet.

1. Introduction. Badjeiskiy site of Manskiy trough

The area of Manskiy trough (East Sayan) represents a part of a large synclinorium. The layer of conglomerates 2000m thick belongs to Narva's suite of lower Ordovician and covers 132 km² but the karst area occupies only 36 km² (TSYKIN 2004).

The rocks correspond to calcareous-dolomitic clays and marls, in which caves are not developed (TSYKIN 1990), and Narva's conglomerates which contain large cavities, undoubtedly of karst origin (TSYKINA & TSYKIN 1971). This is due to the structure of the rock, consisting of debris and cement, where dissolution of any of the components leads to a selective loss of strength. The cement of the rock has a high porosity, which is exemplified by intensive dripping from dead-end domed tubes. The rock composing boulders is fine-grained and crossed by 2-3 systems of fractures.

2. Geology of Big Oreshnaya and Badjeiskaya caves

The site with the largest caves is subject to tectonic fragmentation. In the caves, there are interlayer fracturing, and a network of faults. The conglomerate layers dip south-west-ward with an inclination from 45 to sometimes 80°. The entrances to the caves are located at an altitude of 600 m, relative elevations are up to 250 m. The relief of the surface is formed by erosion and denudation. Karst is heavily turfed and poorly expressed on insignificant fragments of the flatten surfaces.

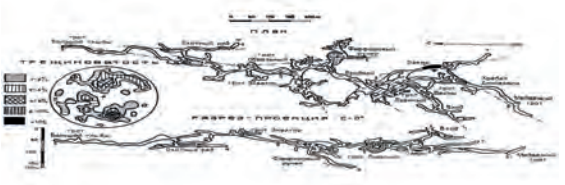

Figure1: Badjeiskaya cave (by Burmak I., Krasnoyarsk)

The main elements of the cave system are galleries of vaulted and triangular cross-sections 4-15 m wide, 2-30 m high, passages and squeezes with blocky and loamy deposits. Isometric rooms sometimes reach more than 30 m in diameter. Genesis of voids is erosional and tectonic-denudational with accumulation of loam and blocks of debris. Occasionally in the rooms, there are snow-white and reddish stalactites, stalagmites, draperies and cascades. Vertical shafts and chimneys with a depth of 6-40 m, elliptical and slit-shaped, connect the underlying and overlying parts of the cave system.

The main factor of the dynamic system is corrosion due to condensation, infiltration of water and transfer of water vapor, so Badjeiskaya and Big Oreshnaya caves are still developing (new systems and rooms that were either impossible to get into 45 years ago or that were dug open). The presence of calcium bicarbonate in water vapor is evidenced by numerous exudates: spherulites, grains, flowers, and the Crystals Gallery, discovered in 1978, all consist of crystalline sheaf-like aggregates. The number of luminescent moon-milk in «Galaxy way» and in «Siberian system» has increased. Moon-milk is probably a white cement of vein calcite with 88Sr impurities (TSYKIN & TSYKINA 1978).

Permanent watercourses have little flow rate (up to 3.5 l/sec). Most of the streams are cut into loams, but the Porcelain Creek in Badjeiskaya and the streams in the rooms of Dreams, Mazodrom, Adventure, Columnar in Big Oreshnaya are cut into the bedrock. Temporary streams are intensively eroding in vertical cracks. Active infiltration of karst waters is represented by intense dripping.

Permanent small lakes were formed by the clogging of the bottom of rooms or galleries with loam. Large lakes are located at the lower levels of the caves, but their drainage towards the surface was not found.

The deposits are represented by loams, consisting of sandy, silty and clayey particles interspersed with pebbles. The clay mineral is represented by hydromica (TSYKIN 1985). The accumulation of loams continues in the passages along their longitudinal axis in the form of swelling.

The morphology of the area shows that Badjeiskaya cave (Fig. 1) was opened by a nival-corrosive shaft (23 m deep) and developed initially at the same level (the impressive volumes of the Broadway gallery are about 0.5 km long), Big Oreshnaya was opened by slope denudation and developed simultaneously at different levels.

3. History of speleogenesis

Speleogenesis at the initial stage is associated with the formation of a Miocene peneplain (TSYKIN 1990) and occurred due to the structural factors of rocks with selective high water permeability.

In the Neogene, the conglomerate was saturated with water. As the neotectonic uplift increased and karst discharge decreased, the water saturation of the speleosystem dwindled. Fluctuations in climatic conditions significantly influenced the formation of karst waters. In the caves, the pluvial of the Middle-Upper Pleistocene can be traced by following the tracks of lake levels and relics of thick drip crusts.

At the contemporary (Late Quaternary) stage of speleogenesis, the leading factor is the complex denudation and development of cave systems along tectonic faults.

From the main entrance, Big Oreshnaya cave is 155 meters deep. The bottom sump is 35 m deep. The highest point of the cave (system “Zastrem”) is situated 44 meters above the main entrance. So the recent amplitude of Big Oreshnaya cave is 234 m. The total volume of voids is estimated to be over 400 000m^3. All separate parts and systems of the cave are mapped carefully and appear to be more than 60km totally. But it is still difficult to synthetize all of them to a general map (BOULYTCHOV 1999, Fig. 2), so an accomplished map doesn’t exist completely yet. Persistent efforts to perform the entire map are being continued. Young cavers have been working a lot last 20 years but mostly digging a loam in narrows or excavating in breakdowns, and they have succeeded to discover new systems. But the mapping is hardly being done.

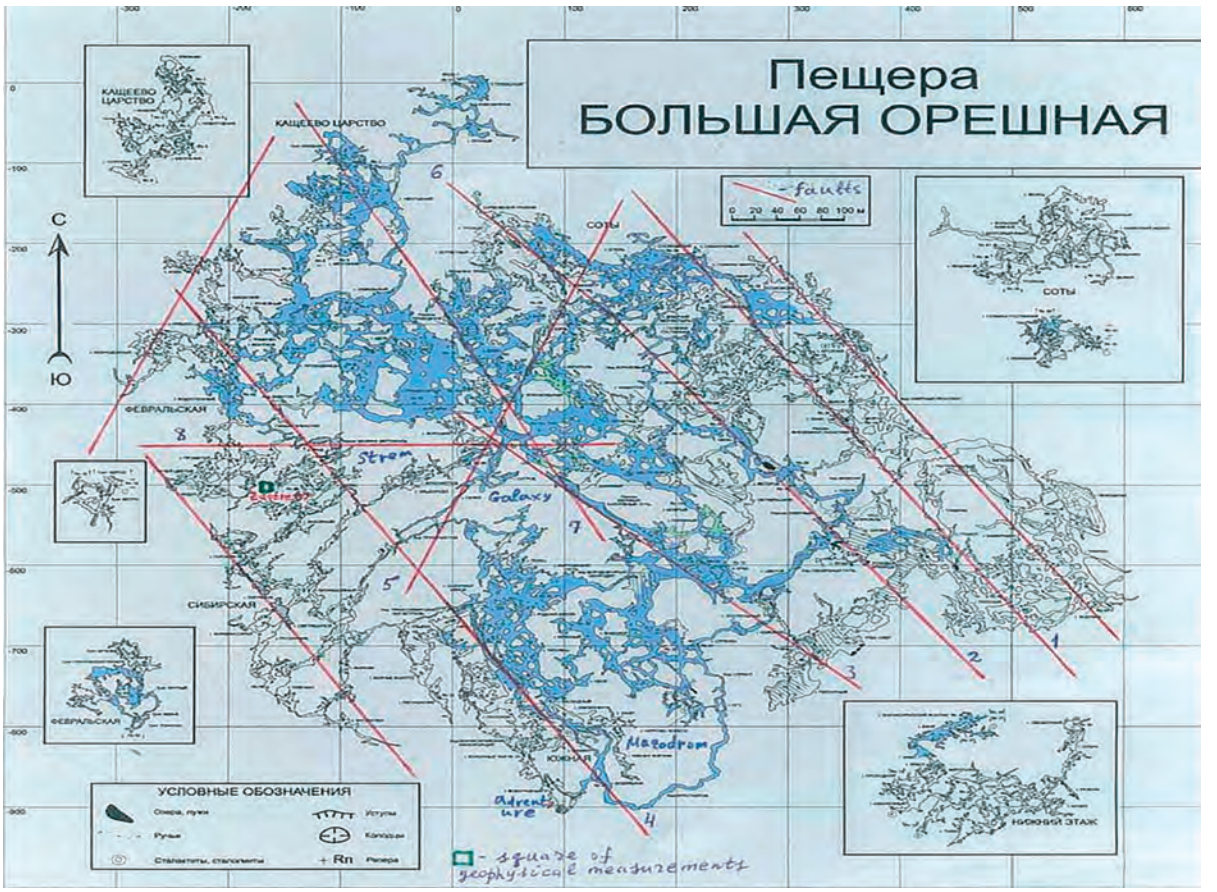

Figure 2: Preliminary map of Big Oreshnaya cave and deduced faults, along which the cave is developed

4. Geomorphological and geophysical observations

After our discovery of Siberian, Lotos and Strem systems where we had to free climb up 70 m vertical and overhanging walls (BULYCHOV & SOROKINA 2017), we proposed to search on the upper part of the mountain where Big Oreshnaya cave is developed. This prompted us to carry out seismic-electrical (BOULYTCHOV 1997, BOULYTCHOV 2000, SOROKINA & BOULYTCHOV 2001) measurements on the surface near the top of the mountain on a relatively flat area. As a result of processing the geophysical data, emptinesses were recorded at depths of 3-8 m. It gave enthusiasm to squeeze through a breakdown in the Strem system upwards to discover Zastrem system which appeared to be very close to the surface (3-5 m but totally blocked by calcite-cemented boulders).

The assumption about the possible continuation of the cave along the upper horizons led to the search for fragments of ancient alignment surfaces near the top of the mountain and in the direction of the significant Rucheinaya cave, which has been very actively extended towards Big Oreshnaya cave the last year. By means of deciphering aerial photographs, signs of destroyed peneplains and faults were deduced (Fig. 3).

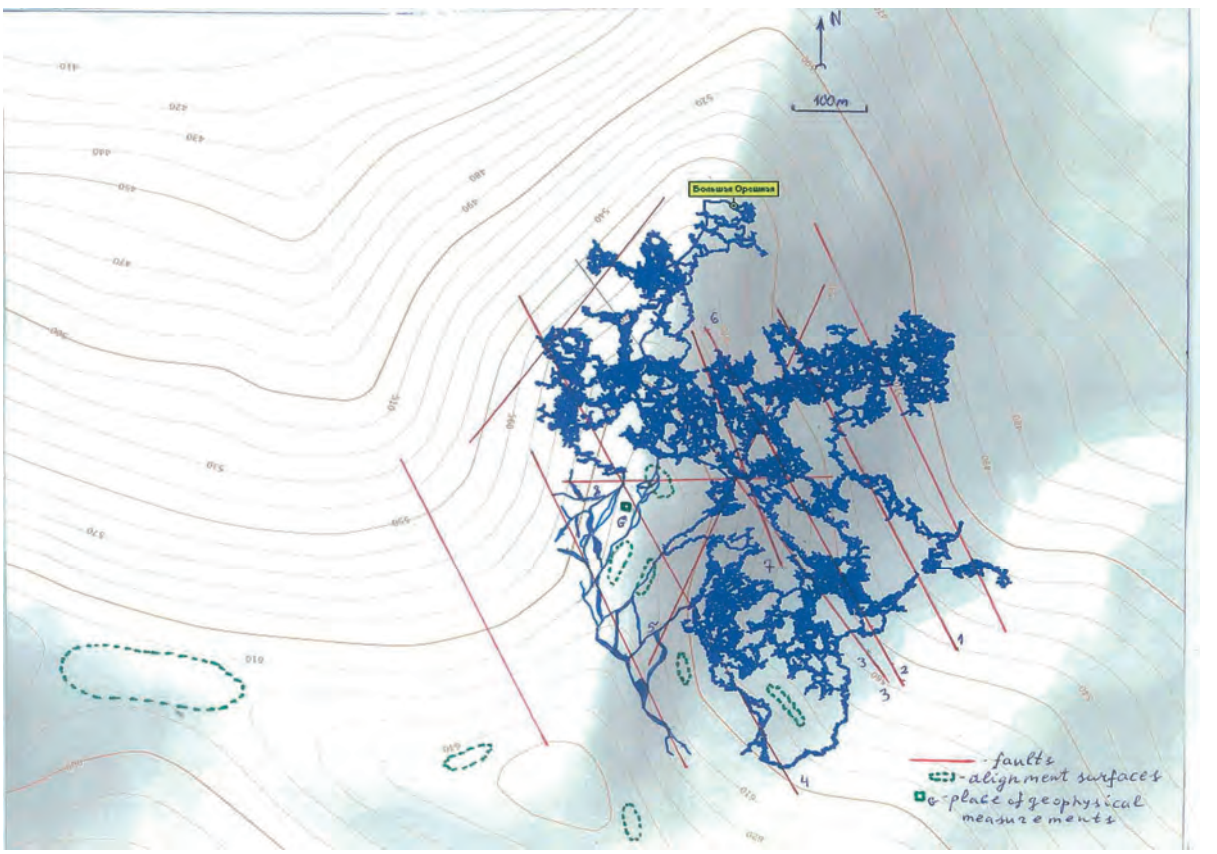

Figure 3: Deciphered faults and projection of the map of Big Oreshnaya cave to the surface.

5. Discussion

It is clearly seen (Fig. 3) that Big Oreshnaya cave is developed in a block bound by a network of faults, which is geomorphologically expressed by a sharp bend of the horizontal lines in the massif. Moreover, it was possible to clearly identify faults to the west of the main massif of the cave, along which the cavers have not yet found anything.
The assumption about the existence of a continuation of the cave is strengthened by the identified fragments of the peneplains located on the surface near the top of the mountain, and the deciphered faults to the west of the main massif of the cave.

Careful analysis of aerial photographs through high-resolution optical binoculars did not allow to identify geomorphological signs of faults and karst forms further to the west towards Rucheinaya cave, which is about 1.5 km away.
Since we have already discovered a very significant extension of the cave in the upper part of the Vertical fault, there is reason to try our luck to make new discoveries in the upper parts of other faults.

6. Conclusions

The study of the data obtained allowed us to infer the following conclusions:

- perspective for the development of Big Oreshnaya cave along upper levels storeys is quite possible (especially to the West towards Rucheinaya cave);
- a connection with Rucheinaya cave (Fig. 4), according to geomorphological analysis, is unlikely;
- the discovery of new systems should be attempted by climbing the walls (Fig. 2, 3) of faults (2- Ozerny, 5- Kolokolny, 7- Prohodnoy, 3- Convict, 4- NSU, 1- Extraterrestrial Galaxy, 6- Surdovsky, 8- Vertical, another part) from the bottom up, followed by the excavation of clay plugs or squeeze in the breakdowns, as well as by means of excavation at the base of the fault zones.

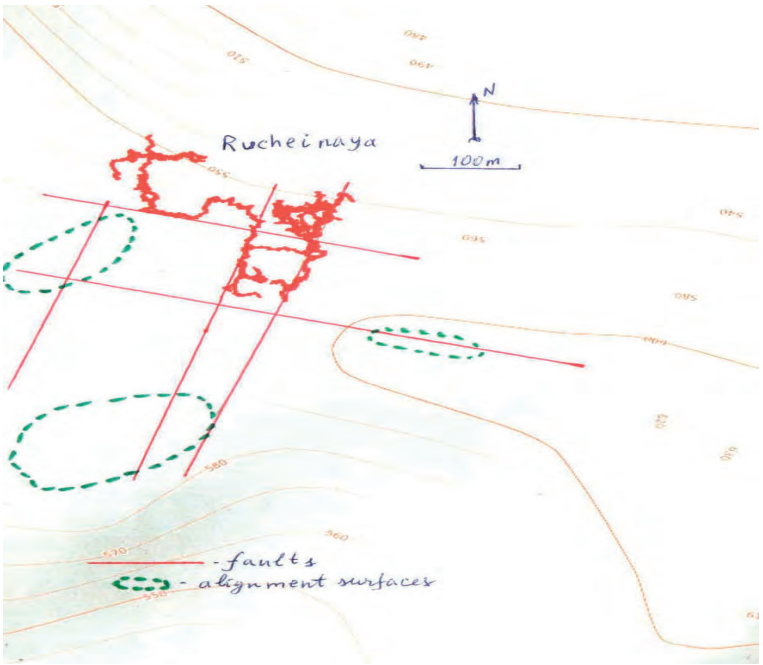

Figure4: *Deciphered faults and projection of the map of Rucheinaya cave to the surface.*

Acknowledgments

I would like to express my gratitude to Artem Barinov (Krasnoyarsk Speleo Club) for the scheme of projection of the Big Oreshnaya cave to the surface.

A separate profound reverence to my fellow colleagues, our fraternity of speleologists for the 45-year practice of joint exploration of the Big Oreshnaya and nearby caves of the Badjeiskiy site: Denis Rogozin, Alexey Zhdanov, Sergei Shundeev, Vasily Shcherbakov ...

References

BOULYTCHOV A.A. (1997) Geophysically predicted and discovered large cave emptinesses in Siberia. *Proceedings of the 12-th International Congress of Speleology*, La-Chaux-de-Fonds, Switzerland, v.5, 89-92.

BOULYTCHOV A.A. (1999) Kektash - the deepest cave of Siberia and Big Oreshnaya - the longest one. *Stalactite*, Bern, Switzerland, n° 49, 1, 47-48.

BOULYTCHOV A.A. (2000) Seismic-electric effect method on guided and reflected waves. *Physics and Chemistry of the Earth*, Journal of EGS, v.25, No 4, 333-336.

BULYCHOV A.A., SOROKINA T.V. (2017) Multi-faceted training of caver-explorer. *Proceedings of the 17-th International Congress of Speleology*, Sydney, Australia, v.1, 278-284.

SOROKINA T.V., BOULYTCHOV A.A. (2001) Seismic-electric benchmarking of shallow subsurface horizons and dome cavities. *Extended abstracts of EAGE*, Amsterdam, Netherlands, v.2, P133.

TSYKINA Z.L., TSYKIN R.A. (1971) Badjeiskie conglomerate caves, *Caves*, Perm, edition 10-11.

TSYKIN R.A. (1985) *Deposits and minerals of karst*, Science, Novosibirsk, 165 p.

TSYKIN R.A. (1990) *Karst of Siberia*, Krasnoyarsk, 154 p.

TSYKIN R.A. (2004) *Karst-speleological regions and caves of Krasnoyarsk district*, Krasnoyarsk, 129 p.

TSYKIN R.A., TSYKINA Z.L. (1978) *Karst of eastern part of Altai-Sayan folded region and its related minerals*, Science, Novosibirsk, 104 p.

Nerochytical Speleogenesis (NERO), mobil CO_2 as a drive for karstification

Harald SCHERZER[(1)], Holger CLASS[(2)], Bettina STRAUCH[(3)], Martin ZIMMER[(3)] & Andreas LAENGE[(4)]

(1) Hoehlen- und Heimatverein Laichingen, Muehlaeckerstr. 2, D-72660 Beuren.
(2) Universitaet Stuttgart, Institut für Wasser- und Umweltsystemmodellierung, Pfaffenwaldring 61, D-70569 Stuttgart.
(3) Helmholz-Zentrum Potsdam, Telegrafenberg, D-14473 Potsdam.
(4) Arge Hoehle und Karst Grabenstetten, Boesmannstr. 9/1, D-72762 Reutlingen

Abstract

This very young thesis is so simple that it is hard to imagine that it is new and that no one had this idea before. The thesis applies to the Green Karst only. It promises to be an essential addition to the understanding of karstification.
NERO assumes that CO_2 not only participates passively in the water cycle, but also has an independent, in-depth mobility (Greek: nerochytis = sink). NERO could be highly relevant to karstification.
CO_2 has a higher specific density than air. Carbonated water has a higher specific density than non-carbonated water. Overall, CO_2 has an in-depth mobility vector.
The NERO thesis means turning the focus away from only the water cycle and towards both, water cycle and cave-air CO_2 mobility. There are stations and transitions: the soil, the gaseous transition from the soil to the vadose zone, the vadose zone with cave-air ventilation, density-driven dissolution at the karst water level, the phreatic zone and the karst spring.
The NERO thesis offers a new approach to understanding cave formation in the Green Karst: At the karst water level, water is enriched with additional CO_2 from the cave air. In the following new solubility arises. Subterranean waterways with their typically round, phreatic wall and ceiling shapes can be understood as a result of that process. Perhaps even giant halls can be explained by this process (SCHERZER et *al*. 2017, 2020).

The NERO processes and NERO stations in detail (Fig. 1)

The CO_2-rich biologically active soil:

Soil slows infiltration and water absorbs CO_2 and dissolves lime within hours until it is saturated. This process leads to near-surface lime solution (denudation) but probably not to large cavities at great depth.

In *early* summer, when the weather is warm and *humid* plants grow and the CO_2 production in the soil is high. Dissolved inorganic carbon dissolves lime just beneath the soil.

In *late* summer, when the weather is warm and *dry* the crop is harvested. The soil has shrinkage cracks and the pores are filled with air rich in gaseous CO_2.

Data from eddy covariance measuring stations from Hohenheim University have so far not been able to prove this process.

NERO assumes that gaseous soil CO_2 will sink into the vadose zone following gravity and summer ventilation.

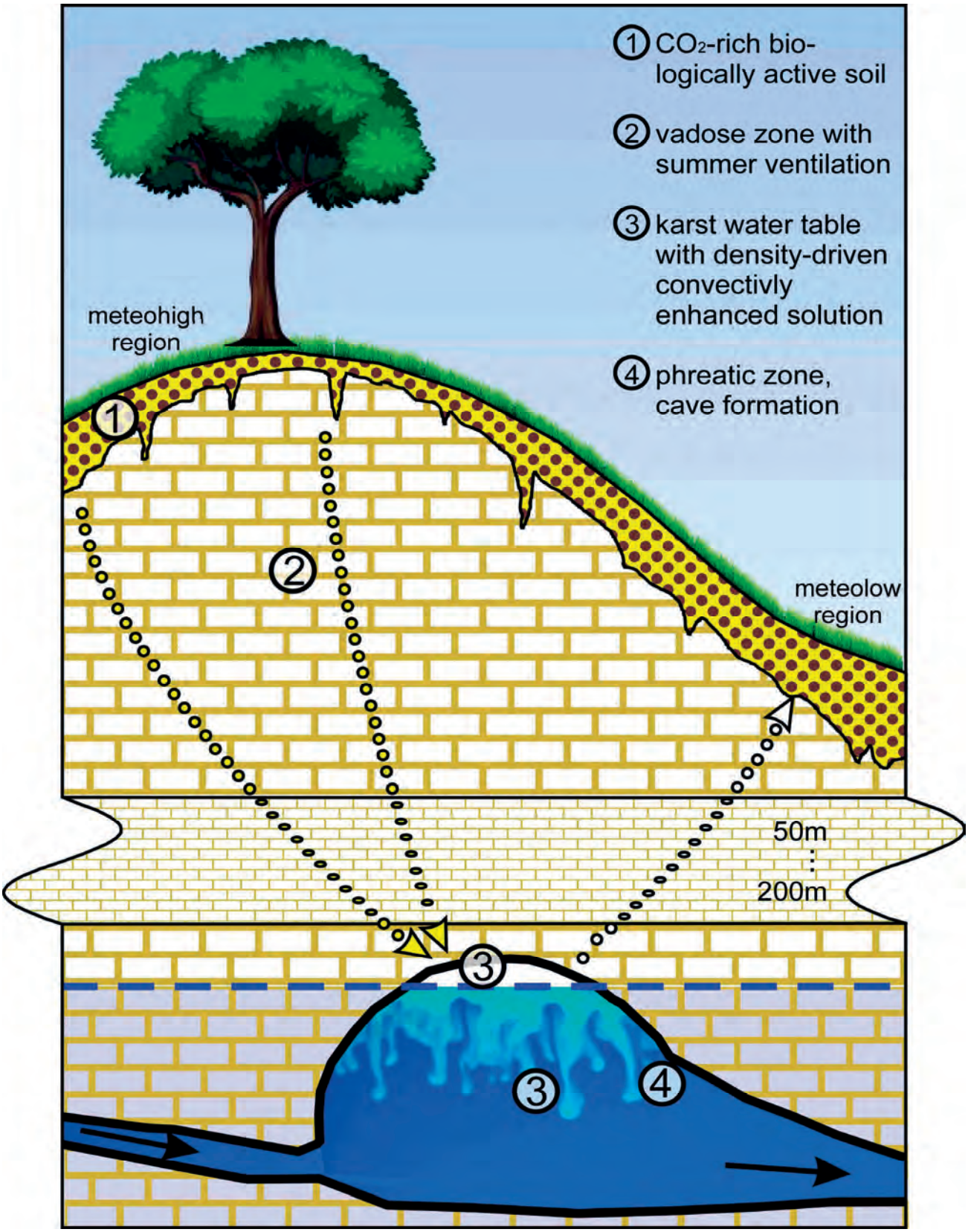

Figure 1: The NERO processes and NERO Stations

The vadose zone with summer ventilation:

The NERO thesis states that summer ventilation transports gaseous CO_2 into the depths. This transport comes from meteo-high parts of the landscape. It does not affect large amounts of water. It is reinforced by the high density of the CO_2 it contains.

Furthermore, the atmospheric air pressure increases with depth and CO_2 partial pressure as well. Ventilation and increase in the partial pressure of CO_2, both lead to additional dissolving power in the phreatic zone.
Long-term measurements of CO_2 in cave air in deep shafts and in water caves far behind siphons have begun.

Density-driven and convectively enhanced dissolution at the karst water table:

The NERO thesis states that CO_2 from air passes quickly and easily into karst water. Density-driven and convectively enhanced dissolution is the assumed physical process.

In an experiment in a Swabian cave CO_2 transfer from cave air into water was observed (Fig. 2). In a water-filled column, open at the top, measurable CO_2 dissolved from cave-air into the columns water. In an air-filled bell at the bottom of the column the CO_2 value rises (CLASS et *al*. 2020, 2021). The picture shows sketch, photo with black column in the background and CO_2-readings.

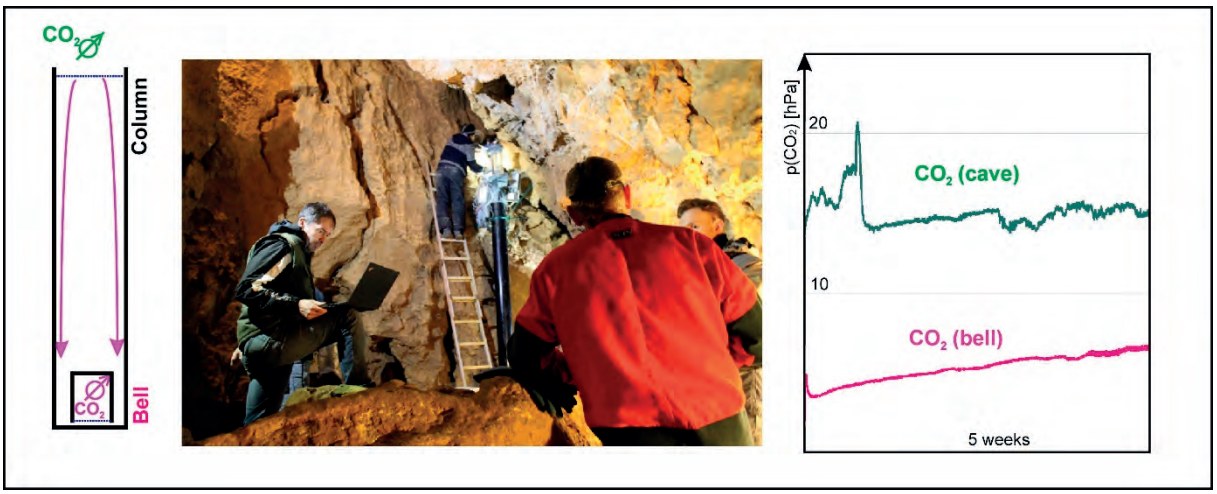

Figure 2: the experiment in a swabian cave.

In another experiment in the laboratory, CO_2 transfer from air to water was observed (Fig. 3). In a water-filled glass cuvette with pH indicator color and with superimposed air containing CO_2, density-driven and convectively enhanced dissolution was visually observed. The pictures below show experimental setup, cuvette-photo and numerical model.

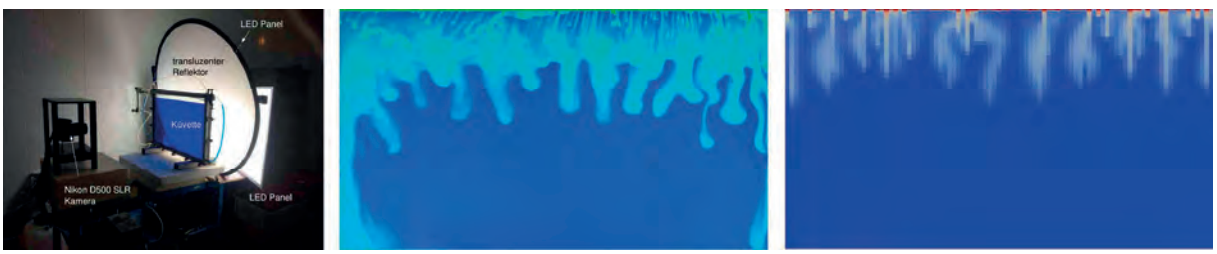

Figure 3: Experiment in the laboratory.

Phreatic zone and karst spring:

The age of the water in springs of the Green Karst is often many years to many decades.

The content of dissolved lime in cave rivers and karst springs are constant and high.
It looks like the karst water level is acting as a CO_2 trap. It seems to absorb CO_2 easily, but it does not release it again.

Excursus on CCS technology:

Carbon Capture and Storage CCS is a technology that captures CO_2 from power plant exhaust gases and injects it into underground aquifers. This CO_2 goes into solution through density-driven and convectively enhanced dissolution. This process is well known and can be grasped with numerical models. CCS-Experts from the University of Stuttgart are leaders in the working group NERO.

Excursus on climate change:

If the thesis proves to be correct and if CO_2 actually has a great tendency to sink and to be stable in aqueous solution then this could easily be used to counteract climate change.

The atmosphere is the wrong place to dispose CO_2
The disposal of CO_2 in the underground or in the deep sea could be better. It does not come up again and does not lead to acidification of the upper sea water layers!

Refercences

CLASS H., BUERKLE P., SAUERBORN T., TROETSCHLER O., STRAUCH B. and ZIMMER M. (2021). On the role of density-driven dissolution of CO_2 in phreatic karst systems, *Water Resources Research* 2021 10.1029/2021WR030912.

CLASS H., WEISHAUPT K. and TROETSCHLER O. (2020). Experimental and simulation study on validating a numerical model for CO_2 density-driven dissolution in water, *Water 2020* 12(3):738, doi:10.3390/w12030738.

SCHERZER H., CLASS H. et. al. (2017). Konvektiver Vertikaltransport von geloestem CO_2 – ein Antrieb fuer Verkarstung in der phreatischen Zone im bedeckten Karst. *Laichinger Hoehlenfreund* 52:29-35.

SCHERZER H. und CLASS H. (2020). Versenkung von CO_2 aus der vadosen Zone in das Karstwasser der phreatischen Zone, Stand der Forschung 2020. *Laichinger Hoehlenfreund* 55.

Modeling the evolution of cave passage cross-sections: Understanding drivers of passage shape

Matthew COVINGTON[1,2], Max COOPER[1] & Franci GABROVŠEK[2]

(1) University of Arkansas, Fayetteville, AR, USA, mcoving@uark.edu (corresponding author)
(2) Karst Research Institute ZRC SAZU

Abstract

Caves preserve complex forms that often tell stories about past conditions and the processes that formed a given passage. To more quantitatively understand the formation of passage morphologies, we develop a speleogenetic model that enables the simulation of the evolution of cave passage cross-sectional shape. We begin with the simulation of single cross-sections and explore scaling relationships between equilibrium passage width and its controls, examining both vadose conditions and phreatic conditions with sediment load, where paragenesis can occur. Simulations with asymmetric shear stress distributions are compared against observed patterns of cave scallops to attempt to provide quantitative constraints on erosion mechanisms. Finally, we use a multi-cross section model to simulate simultaneous evolution of slope and passage shape along a single conduit. This model incorporates CO_2 exchange between air and water as well as cave ventilation processes. We show that patterns of cave ventilation, via their influence on dissolved CO_2, can drive changes in passage cross-section and slope.

1. Introduction

It has long been recognized by speleologists, that cave passage cross-sectional shapes provide important information about the conditions under which a cave passage developed (BRETZ, 1942; FORD and WILLIAMS, 1989; LAURITZEN and LUNDBERG, 2000; PALMER, 2007). In particular, passage shapes often indicate whether a passage developed under phreatic or vadose conditions. However, passage shapes also contain substantially more information about paleo-discharges, sediment loads, perturbations to changes in tectonic uplift, and the response to the development of new cave levels. To enable a more quantitative understanding of the drivers of passage shape, we have developed a new model for simulating the evolution of cave passage cross-sections. Here we provide a high-level overview of several applications of this model.

2. Model description

One of the first obstacles to developing a model of cave cross-section evolution is determining how to estimate wall dissolution rates under turbulent flow conditions as a function of wall shear stress. When taken at face value, available models of calcite dissolution under turbulent flow predict that dissolution rates should be surface-reaction rate limited, and therefore independent of wall shear stress, under most turbulent flow conditions (COVINGTON, 2014). However, field observations of scallops and channel cross-sections suggest that this is incorrect (COVINGTON, 2014; COOPER & COVINGTON, 2020), and that dissolution rates do vary with wall shear stress.

To sidestep this problem, we employ a generic erosion rule, where erosion rate at each point on the wall scales with a power law of boundary shear stress at that point,

$$E = K\tau_b^a,$$

where E is erosion rate, K is a rock erodibility parameter, and τ_b is the boundary shear stress. This approach is motivated by prior studies of bedrock channel erosion, which note that such an erosion rule can approximate different erosional processes using different values of the exponent, a, in the power law (WHIPPLE et al. 2000).

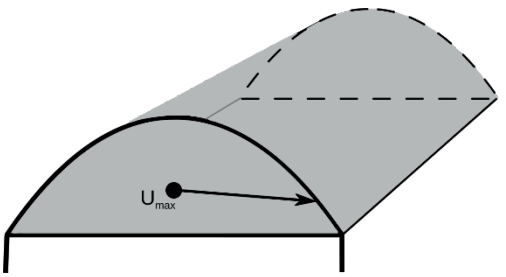

Figure 1: Schematic of a cave passage cross-section with velocity profiles calculated from a maximum velocity point (U_{max}) located at the centroid of the cross-section.

This approach can also approximate chemical erosion processes, where a value of a=1/2 represents transport-limited dissolution, a value of a=0 represents surface-reaction rate-limited dissolution, and intermediate values represent mixed kinetics (COOPER & COVINGTON, 2020). For chemical erosion, K is a function of stream chemistry, and rock chemical composition, rather than rock mechanical properties.

To estimate boundary shear stress along the passage wall, we implement a modified version of an algorithm developed by WOBUS et *al.* (2006) to estimate boundary shear stress

within open channels. The details of our implementation are provided in COOPER & COVINGTON (2020), and the code is available on *Github*. In summary, the algorithm assumes that a maximum velocity point is located at the centroid of the passage cross-section under phreatic conditions and the center of the free surface under vadose conditions. Estimation of boundary shear stress is then made by assuming that velocity profiles follow the law of the wall between this maximum velocity point and the wall (Fig. 1). Closure is provided by requiring force balance between drag and acceleration forces on the column of water.

3. Applications of the cross-section model

Our first application of the model explored the evolution of single passage cross-sections and incorporated a prescription for sediment transport to enable simulation of passage evolution via paragenesis. In this work we find that passage cross-sections only reach equilibrium widths if erosion rates vary as a function of boundary shear stress.

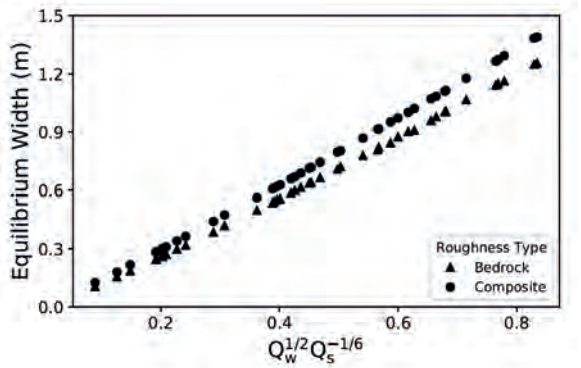

Figure 2: Scaling relationship between equilibrium passage width under paragenetic conditions and the discharge of water (Q_w) and sediment (Q_s). Symbols indicate different prescriptions for wall roughness (modified from COOPER & COVINGTON, 2020).

Since many natural cave streams have channels that incise with relatively constant widths, this provides further evidence that transport impacts local erosion rates within natural cave streams. We also find that paragenetic passages reach an equilibrium width that is primarily a function of discharge and sediment supply rate (Fig. 2), where width scales with the square root of discharge and the negative 1/6th power of sediment supply rate. This relationship can be predicted from simple analytical considerations (*COOPER & COVINGTON, 2020)*.

Field observations of scalloped meandering passages in Copperhead Cave, Arkansas, USA, formed in limestone, and Parks Ranch Cave, New Mexico, USA, formed in gypsum, indicate that the angle of channel incision (Fig. 3A) is correlated to the contrast in boundary shear stress recorded in scallop sizes on opposite walls (Fig. 4). We modified the model to enable situations with contrasting shear stress, as would be expected within a meander bend, by shifting the maximum velocity position horizontally towards one wall (Fig. 3B). Within these model runs, we can examine how incision angle relates to the contrast in boundary shear stresses on the two walls (COOPER, 2018).

We find that this relationship depends on the erosion exponent, *a* (Fig. 4). Consequently, it may be possible to distinguish the importance of different erosion regimes by examining these relationships in the field, with a=1/2 indicating transport-limited erosion, a<1/2 indicating influence of surface reaction rates, and a>1/2 indicating influence of mechanical processes. Currently, there is too

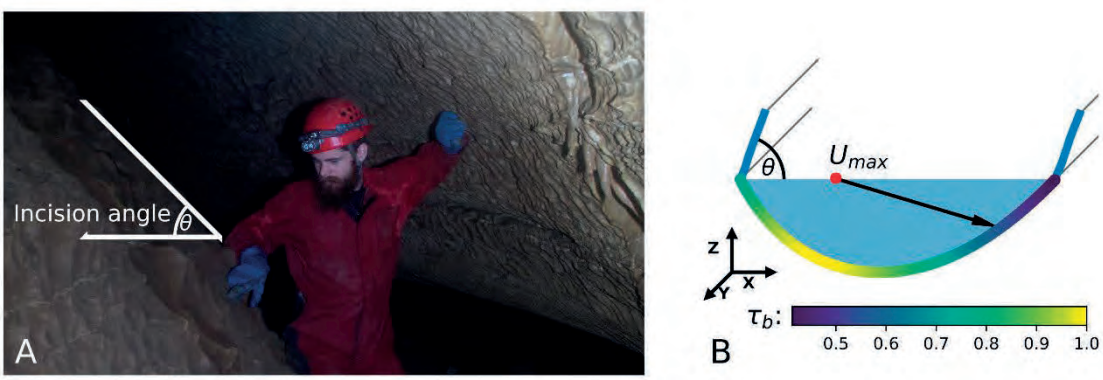

Figure 3: A) Channel incision angle from horizontal (θ) within a meandering vadose canyon. Contrast in wall shear stresses is estimated by comparing scallop sizes on opposite walls. B) A modification of the cross-section model where the maximum velocity position can be offset from the center of the passage, resulting in shear stress that is higher on one wall than the other. Shear stress contrasts can be compared against channel incision angle within the model. After COOPER (2018).

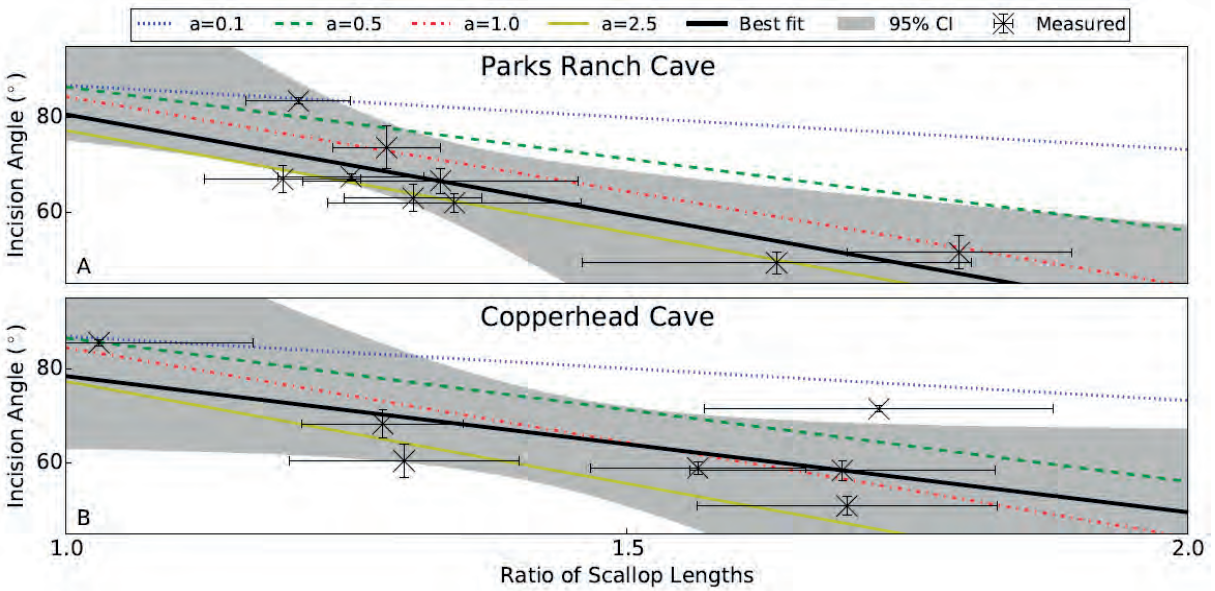

Figure 4: Channel incision angles as a function of the ratio in scallop lengths on opposite walls at sites within Parks Ranch cave (top) and Copperhead Cave (bottom). Black line indicates best fit to data and the other lines indicate model results using different values of the erosion exponent, a. After COOPER (2018).

much noise within the data to distinguish these various cases (Fig. 4). However, surprisingly, the data from Parks Ranch Cave, which is in gypsum, are more consistent with mechanical erosion than chemical erosion.

In a final application of the model, we extend the single-cross section into a multi-cross-section model, incorporating a steady flow solver. We also calculate CO_2 transport and exchange with an air phase, where air transport of CO_2 is driven by chimney effect airflow. The incorporation of CO_2 dynamics was motivated by field observations that CO_2 exchange can drive the spatial (COVINGTON et *al*. 2013) and temporal (COVINGTON et *al*., 2021) variation in cave stream dissolution rates. Preliminary results, comparing two paired simulations with and without CO_2 dynamics (Fig. 5), suggest that feedback mechanisms produced by CO_2 lead to substantial adjustments in channel slope and width.

The model we have developed can be used to explore a wide variety of questions about the relationships between cave passage shapes and the processes that form them. Here we only present some initial results. In future work, we plan to continue exploring these threads to develop a broader quantitative framework for interpreting cave passage shapes.

References

BRETZ J.H. (1942) Vadose and phreatic features of limestone caverns.*The Journal of Geology*, *50*(6), 675-811.

COOPER M.P. (2018) Speleogenesis in Turbulent Flow. *University of Arkansas,* PhD dissertation.

COOPER M.P., COVINGTON M.D. (2020) Modeling cave cross-section evolution including sediment transport and paragenesis. *Earth Surface Processes and Landforms*, *45*(11), 2588-2602.

COVINGTON M.D., PRELOVŠEK M., GABROVŠEK F. (2013) Influence of CO_2 dynamics on the longitudinal variation of incision rates in soluble bedrock channels: feedback mechanisms. *Geomorphology*, 186, 85-95.

COVINGTON M.D., (2014) Calcite dissolution under turbulent flow conditions: a remaining conundrum. *Acta Carsologica, 43*(1), 195-202.

COVINGTON M.D., KNIERIM K.J., YOUNG H.A., RODRIGUEZ J., GNOZA H. (2021) The impact of ventilation patterns on calcite dissolution rates within karst conduits. *Journal of Hydrology,* 593, 125824.

FORD D., WILLIAMS P. (1989) Karst geomorphology and hydrology, Ed. Unwin Hyman Ltd. London, 601 p.

LAURITZEN S.E. LUNDBERG J., (2000) Solutional and erosional morphology. *Speleogenesis: Evolution of Karst Aquifers, National Speleological Society, Huntsville*, 408-426.

PALMER A.N. (2007) Cave Geology. *Dayton, OH: Cave Books*.

WHIPPLE K.X., HANCOCK G.S., ANDERSON R.S. (2000) River incision into bedrock: Mechanics and relative efficacy of plucking, abrasion, and cavitation. *Geological Society of America Bulletin*, *112*(3), 490-503.

WOBUS C.W., TUCKER G.E., ANDERSON R.S. (2006) Self-formed bedrock channels. *Geophysical Research Letters*, *33*(18).

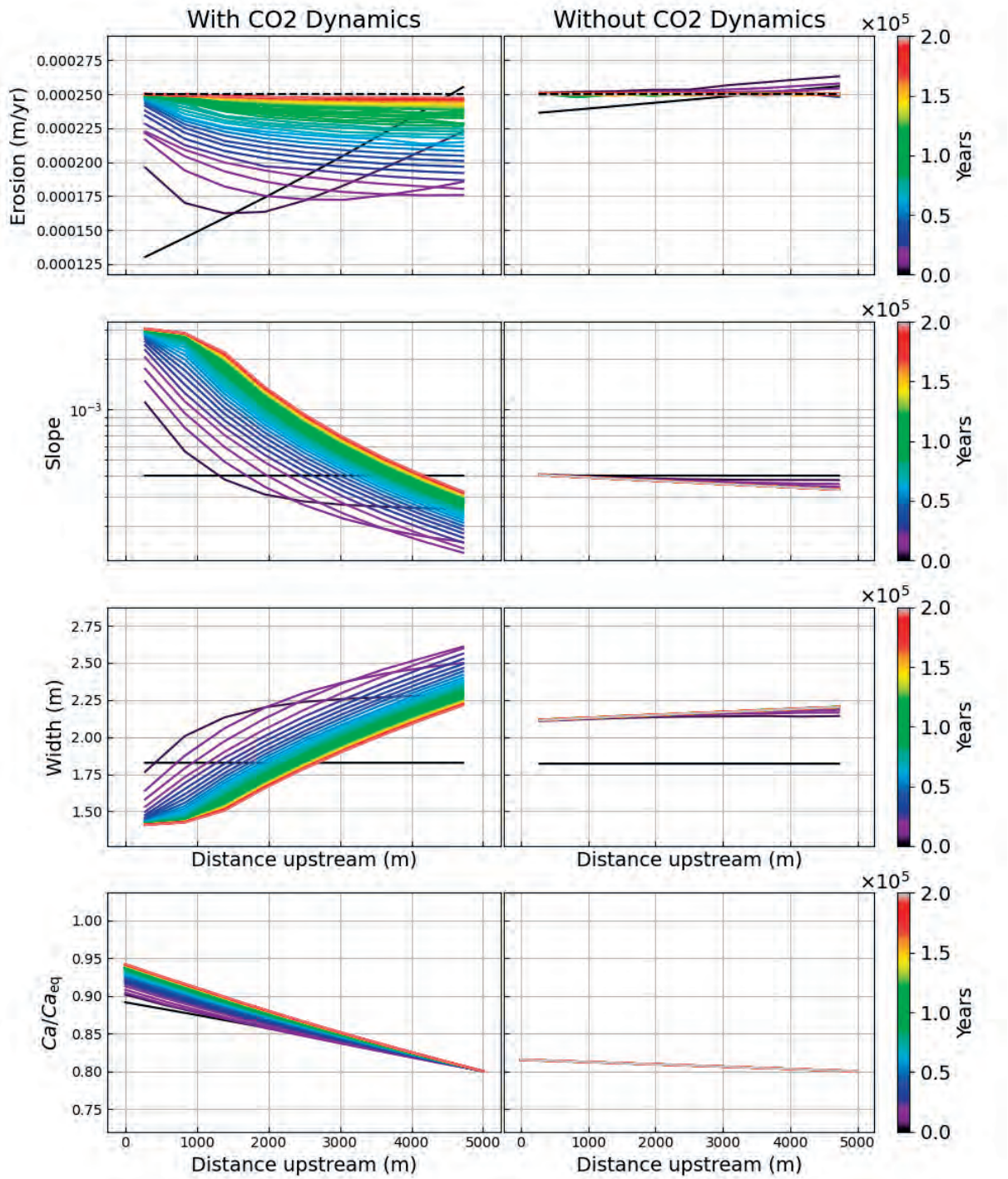

Figure 5: Channel erosion rate (first row), slope (second row), width (third row), and saturation ratio (fourth row) as a function of distance upstream from a spring. Each line represents a snapshot in time, with color indicating years since the start of the simulation. The left column presents results for a simulation that includes CO_2 dynamics, and the right column excludes CO_2 dynamics. Both channels are subjected to a constant rate of base level fall (0.25 mm/yr) and gradually approach an equilibrium state where erosion rates are equal to uplift (dashed line). For the case with CO_2 dynamics, equilibrium morphologies downstream steepen and narrow in order to compensate for the reduced aggressivity (fourth row) that results from CO_2 degassing. Effectively, to keep up with erosion rates within the upstream reach, which has higher pCO_2, the downstream portion of the channel has to locally increase the shear stress.

Intensity of chemical corrosion on limestone plates at two localities in the Slovak Karst (Slovakia)

Alena GESSERT, Zdenko HOCHMUTH & Mária SCHWARZOVA

Institute of Geography, Faculty of Natural Sciences, P.J.Šafárik Univerisity, Jesenná 5, Košice, Slovakia,
alena.gessert@upjs.sk, zdenko.hochmuth@upjs.sk, maria.schwarzova@student.upjs.sk

Abstract

Chemical corrosion in karst is one of the basic processes of karst relief formation. Based on measurable results of weight loss on two types of limestone plates, we monitor the intensity of chemical corrosion in two areas of the Slovak Karst (Silica Plateau and Jasov Plateau), that are situated in the most developed plateau like karst area of Slovakia. In each locality, we placed 3 sets of plates at a depth of 50 cm, 20 cm and on the soil surface, which are constructed of two different types of limestone (local limestone and standardized plates used for similar research in IRCK Guilin, China). The research began in December 2016 and continues to this day, with drying and weighing of the samples taking place every 3 months. The smallest weight loss was recorded on samples placed on the surface (in both locations). During the whole duration of the experiment (2016-2019) the chemical corrosion on standardized plates was of 4,78 mg/year/cm2 in average on the Jasov Plateau (J0, J20, J50) and of 3,06 mg/year/cm2 on the Silica Plateau (S0, S20, S50).

1. Introduction

Chemical corrosion in karst is one of the basic processes of karst relief formation. The relief is being shaped, which is still taking place today, with different intensity under different physical-geographical and geological conditions – especially climate conditions, amount of precipitation and its chemistry, average temperature, CO_2 amount, chemical reaction of soil and rock properties. That is why chemical corrosion has been the object of study in various karst areas for many decades, as evidenced by previously published works.

GAMS (1966, 1981, 1985) and PULINA (1974) were among the pioneers in the study of the degree of denudation and its factors in world literature. Both dealt with chemical denudation in different climatic zones and tried to compare them with each other. Based on their results, a basic overview of the degree of chemical denudation on the earth's surface was created. The limestone plate method applied in the past, mainly by Gams and later taken over by the Karst Commission of the International Speleological Union, is also used for its measurement.
KLIMCHOUK *et al.* (1996) monitored chemical denudation limestone plates on three sites in Europe - Ukraine, Spain, Italy. Factors influencing the rate of chemical denudation in the Austrian Alps were studied by PLAN (2005), who performed a chemical analysis of limestone plates from the area and calculated the value of limestone solubility. CO_2 as one of the main factors influencing the dissolution rate of carbonate rocks was addressed by ZHANG (2011) in three karst basins in China. He came to the clear result that the highest value of CO_2 and thus denudation was recorded in the forest soil. KRKLEC *et al.* (2013) studied the development of microscopic forms of carbonate weathering by a combination of methods (quantitative analysis of weight loss of "standard" tablets and qualitative analysis of weathered surfaces with colored acetate peels and imaging by scanning electron microscopy). The influence of denudation factors by the limestone tablet method in China was investigated by SHAO et *al.* (2020) at 30 test sites. The results showed that the effect of precipitation on platelet solubility is more significant than the effect of temperature. PRELOVŠEK (2012) studied the dynamics of karst denudation in several Slovenian caves through several methods (including limestone tablets).
In Slovakia, the topic of chemical denudation is also considered to be one of the basic ones for understanding the functioning of the karst system, and therefore in the past this process was studied by several methods. The most important research results are summarized in the work of DROPPA (1976, 2012) from several karst areas of Slovakia. Based on quantitative methods in several localities, ŠAVRNOCH (1978) explained the extent and importance of chemical denudation. SLÁDEK (2014), HOCHMUTH & VADELOVÁ (2010) dealt with this topic in two karst areas of Slovakia (Slovak karst and Slovak Paradise) and compared their results with MATSUKURU & HIROSIHO (2010) from tropical climate of Japan. SLÁDEK (2014) studied the influence of the content of the dolomite component in the limestones of the eastern part of the Slovak Karst on the process of karst corrosion in the area of one of our research sites.

The area of the Slovak Karst is the most typical plain karst area in Slovakia, characterized by a nappe structure (Silica nappe) and the extensive occurrence of relatively pure Wetterstein limestones. The plains are richly permeated by

all types of karst forms. We decided to sample in two different parts of the study area, the easternmost and the westernmost plateaus (Fig. 1). Because of previous geomorphological and speleological studies in the area our starting hypothesis was that the corrosion should be higher in the western part of the Slovak karst.

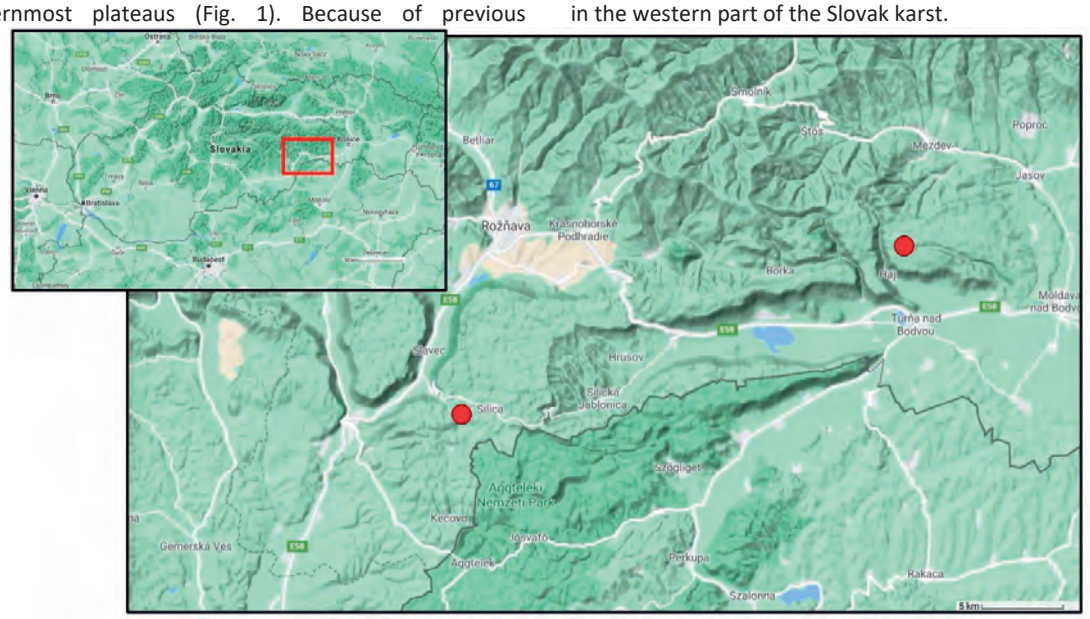

Figure 1: Position of Slovakia and samples position (maps.google.sk, modified).

2. Methodology

For the research of chemical corrosion, we chose two sites (Fig. 2) that are considered different in terms of location and degree of karstification (Silica Plateau - west, Jasov Plateau – east of the Slovak karst). Before placing the samples, we analyzed the chemical composition of standardized and local limestone plates (the limestone comes from Silica Plateau) by atomic absorption spectrometry in the laboratory of the Chemical Institute (Faculty of Natural Sciences, U.P.J. Šafárik University, Košice).

	Jasov Plateau	Silica Plateau
Altitude (m a.s.l.)	575	519
Position	Flat surface	Flat surface
Rainfall (mm/year)	700-800	600-700
Evapotranspiration (mm/year)	400-500	500-600
Soil reaction (pH)	8,01	7,09
Soil type	Rendzina	Rendzina
Vegetation	Beech/Oak forest	Beech/Oak forest

Figure 2: Experimental sites comparison.

Limestone plates (Fig. 3) weighing 11-13 g were placed at three different depths - on the soil surface, at a depth of 20 cm and at a depth of 50 cm. At each horizon, 3 control plates are placed from two different types of limestone, namely standardized plates supplied by IRCK in Guilin (China) and later local limestone, 18 plates in total at each site). Standardized plates were placed on experimental sites right at the beginning of the measurements (December 2016), and from 26.9.2018 onwards local limestone plates were added to them. This was done under the assumption that corrosion data based on the measurements of the standardized plates will be different from the local ones, which come from the given area and the rocks originated in local conditions.

The principle of the limestone plates method is to measure the weight loss of plates over a period of time during which they are stored in the terrain (on the surface, buried in the soil, etc.) where they are affected by rainwater seeping into the soil and many other factors. The plates were then dug out in a 3-month cycle, transported to laboratories of the Chemical Institute and Geographical Institute of UPJŠ, dried at 80 degrees for 8 h and weighed to the nearest 10 µg on KERN ABT-NM high-precision analytical scales

In the following paragraph, we present the results from a closed period of 3 years (from December 2016 – December 2019), but the research is still ongoing.

Figure 3: Limestone plates at a depth of 50 cm.

3. Results

The results of our research are clearly summarized in the following tables and graphs. Measurements show an apparent weight loss at all samples of both sites of varying intensity.

As we expected, the smallest weight loss was recorded on samples placed on the surface (in both locations). During the whole duration of the experiment (2016-2019) it was on standardized plates on the Jasov Plateau (J0, J20, J50) an average of 0.47% and on the Silica Plateau (S0, S20, S50) 0.49%. The highest mass loss was recorded in the Jasov Plateau at a depth of 50 cm by 3.40%, but on the Silica Plateau at a depth of 20 cm and 3.62% (at a depth of 50 cm it was 2.62%). When comparing the results measured on our local plates (from 26.9.2018) there are no significant differences. More interesting results will certainly be obtained after a longer observation time. The average results from the whole experiment period are shown in the following Figure 4 and for individual measurements of standardized plates in Figure 5.

Samples	Standardized plates (mg/year/cm^2)	Local plates (mg/year/cm^2)
J50	5.2639	2.7426
J20	4.3353	2.4910
J0	0.7432	0.8459
S50	4.1228	3,.2319
S20	5.6168	2.4034
S0	0.5674	0.4682

Figure 4: Average chemical corrosion at different depths.

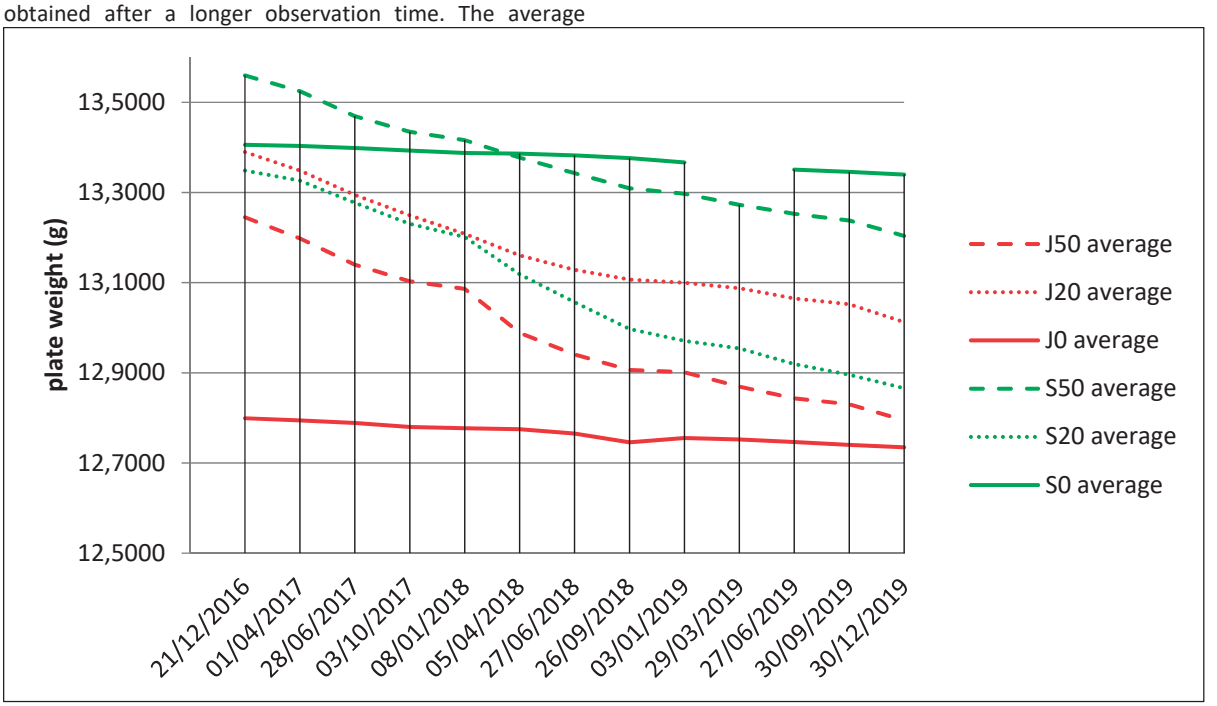

Figure 5: Measurement results for standardized plates during the period 2006-2019.

4. Discussion and conclusions

There may be several reasons for the differences in corrosion intensity, requiring further observations. The measured results between standardized and local plates cannot be compared at this stage of the research and only fundamental differences can be deduced, as they were not located at experimental sites for the same time.

One of the most important factors affecting the intensity of corrosion is the amount of precipitation in the area and the value of runoff. Both sites are situated at similar altitude and relief conditions, so these are not the decisive factor. The quality of the limestone plate, its purity and porosity allow faster dissolution.

As stated in the methodology, we have chemical analyses of both types of plates (listed in Fig. 6). At this stage of the research (similarly to the case mentioned above), it is not yet possible to evaluate the degree of influence of this factor on our results. For the period during which the plates were buried in the soil together (26.9.2018-30.12.2019), we do not register significant differences in the measured value of corrosion area. Differences in corrosion between the standard and local tablets are also significant. This may be due to the elevated amount of $MgCO_3$ in the local rock, 0.937% higher than in the standard plates.

As mentioned above, karst denudation (corrosion) research has been carried out in several regions in the past. This paper does not allow a detailed comparison of our and other sites, so we have selected only a few. Our results are similar to other studies from Low Tatra and Slovak paradise region

in Slovakia (DROPPA, 1976, HOCHMUTH & VADELOVÁ, 2010), measured corrosion is 3,469-5,505 mg / year / cm^2 respectively 2,914 mg / year / cm^2.

Component	Standardized plate	Local plate
$CaCO_3$	97%	98%
$MgCO_3$	0,310%	0,937%
Fe_2O_3	0,10%	0,257%
Mn	0,002%	0,003%
Other	2,586%	0,803%

Figure 6: Simplified chemical analyses of limestone plates.

The proximal area of Austrian Alps was examined by PLAN (2005), who reported a denudation rate of about 30-40 mg / year / cm^2. This area receives a total annual precipitation of 2100 mm.

The depth of the root system, chemical and isotope composition of precipitation, the chemical and physical properties of the soil and, last but not least, the CO_2 content of the soil affect the intensity of corrosion in the forested area. We plan to study and evaluate the impact of all these factors in the next phase of our research.
The results measured at studied sites compare well and do not show any significant differences.

Acknowledgment

We gratefully thank Rastislav Serbin from the Chemical Institute (P.J.Šafárik University) and Gabriela Fabriciová from Physical Institute (P.J.Šafárik University) for help with chemical analyses and measurements. We would like to thank you also to the members of Speleoklub UPJŠ for the help with excavating of the samples.
This research was supported by VEGA 1/0798/20 "Synergistic use of multiple sources of data from remote sensing of the Earth in the research of the country" and KEGA 016UPJŠ-4/2021 "International year of caves and karst – explore, understand and protect".

References

DROPPA, A. (1976) Corrosion intensity of karst streams in the Demänovská dolina Valley. Slovenský kras, 14, 3-30 (in Slovak).

DROPPA, A. (2012) Corrosive effect of karst streams on the northern side of the Low Tatras. In: Slovenský kras 51, Suppl. 1, 100 p. (in Slovak).

GAMS, I. (1966) Corrosion factors and dynamics of Slovenian Dinaric karst rocks. Geogr. Vestnik 38, Ljubljana (in Slovenian).

GAMS, I. (1981) Comparative research of limestones solution by means of standard tablets (Second preliminary report of the commission of karst, denudation, ISU). Proceedings of 8th International Congress of Speleology, 1, 273-275.

GAMS, I. (1985) International comparative measurements of surface solution by means of standard limestone tablets. Razprave IV. razreda SAZU – Zborník I. Rakov. XXVI. Ljubljana, 361–386.

HOCHMUTH, Z., VADELOVÁ, Z. (2010) Research of kvantitative aspects of the karst rocks surface corrosion in Slovak Karst and Slovak Paradise. Slovenský kras, 48, 2, 239-250 (in Slovak).

KLIMCHOUK, A., CUCCHI, F., CALAFORRA, J., M., AKSEM, S., FINOCCHIARO, F., FORTI, P. (1996) Dissolution of gypsum from field observations. International Journal of Speleology, 25: 37-48.

KRKLEC, K., MARJANAC, T., DRAŽEN, P. (2013) Analysis of "standard" (Lipica) limestone tablets and their weathering by carbonate staining and SEM imaging, a case study on the Vis Island, Croatia. Acta Carsologica, 42, 1, 135-142.

KRKLEC, K., DOMÍNGUEZ-VILLAR, D., PERICA, D. (2021) Use of rock tablet method to measure rock weathering and landscape denudation. Earth-Science Reviews 212, 103449.

MATSUKURA, Y., HIROSE, A. (2000) Five years measurements of rock tablet weathering on forced hillslope in a humid temperate region. Eng Geol, 55, 1, 69-76.

PLAN, L. (2005) Factors controlling carbonate dissolution rates quantified in a field test in Austrian Alps. Geomorphology, 68, 3, 201-212.

PRELOVŠEK, M. 2012. The dynamics of the present-day speleogenetic processes in the stream caves of Slovenia. Carsologica 15, Postojna-Ljubljana. 156 p.

PULINA, M. (1974) Chemical denudation in the areas of carbonate karst. Prace geograficzne 105, 159 p. (in Polish).

SHAO, M., ZHANG, L., LIU, P., CAO, J. (2020) Infuential factors and spatial suitability of the method of limestone. Carbonates and Evaporites, 35:85.

SLÁDEK, I. (2014) Preliminary Research Results of the Influence of the Dolomite Component Content in Limestone in the Eastern Part of the Slovak Karst on the Process of Karst Corrosion. Geographia Cassoviensis, 8, 2, 173-180.

ŠAVRNOCH, J. (1978) Kvantitative methods of the karst denudation research. Slovenský kras, 9, 1, 18-25 (in Slovak).

Estimation de paléodébits dans une cavité du karst alpin : la galerie Isa du gouffre de la Petite Marielle (massif de Platé, Haute-Savoie, Alpes externes, France)

Philippe MONTEIL & Malo COURTIER

Césame : Centre Éclaireur de Spéléologie et d'Archéologie de Mézelet.

Résumé

Sur le bassin versant de la Flaine (Haute-Savoie), à 2300 m d'altitude, à proximité de trois grands bassins versants du Massif de Platé, le gouffre de la Petite Marielle est situé à la limite amont du réseau de grottes de la Tête des Vers (environ 10 km pour -7,47 m de dénivelé). Ce gouffre peut être l'entrée d'un système de plus de 1 000 mètres de profondeur. C'est aussi le plus haut de ce massif avec un développement important et une profondeur supérieure à - 300 m permet de traverser les différentes couches géologiques du massif. En plus de l'exploration et de la topographie, nous nous sommes intéressés aux remplissages et aux vagues d'érosion observés dans une partie d'une galerie : la Galerie Isa. Cet article traite d'une étude statistique de la taille des vagues d'érosion observables dans une portion de cette galerie afin d'estimer les paléo-écoulements et la taille du paléo-bassin versant.

Abstract

Estimation of paleoflow rates in an alpine karst cave: the gallery Isa in the abyss of the Petite Marielle (Platé massif, Haute-Savoie, France). On the Flaine watershed (Haute-Savoie), at 2300 m above sea level, near three large watershed of the Massif de Platé, the abyss of the Petite Marielle is located on the upstream limit of Tête des Vers cave system (about 10 km for -7,47 m of difference in height). This abyss may be the entrance of more 1,000 meters deep. It is also the highest of this massif with significant development and a depth higher than – 300 m allows to cross the different geological layers of the massif. In addition to the exploration and topography, we were interested in the fillings and erosion waves observed in a portion of a gallery: la Galerie Isa. This article deals with a statistical study of the size of the erosion waves observable in a portion of this gallery in order to estimate paleo flows and the size of paleo watershed.

1. Introduction

Dans le présent article, nous exposons une estimation de paléo-débits fondée sur la mesure des vagues d'érosion (ou coups de gouge) d'après la méthode présentée par Didier CAIHLOL (2011).

Nous avons appliqué cette approche à un conduit actuellement totalement fossile : la galerie Isa se développant vers l'altitude de 2210-2220 m dans le gouffre de la Petite Marielle dont l'entrée s'ouvre à 2300 m d'altitude au cœur du massif de Platé dans les Alpes externes en Haute-Savoie (Fig. 1). Nous ne disposions pas d'autres informations sur cette cavité que celles publiées par Richard MAIRE (1984). Aussi nous avons relevé la topographie lors de l'exploration.

2. Situation géographique et contexte géologique du gouffre de la petite Marielle

Le gouffre de la Petite Marielle possède à ce jour un développement de 750 m et une profondeur de 300 m nous permettant de traverser les trois principales couches karstifiables de la série crétacée du massif. L'entrée de cette cavité est aussi l'une des plus élevées du bassin versant de Flaine et occupe une position très marginale en limite du bassin versant de la Combe de Platé (Fig. 1).

Notons qu'elle constitue probablement l'une des branches se rattachant aux extrêmes amonts (alt. 1895 m) du réseau de la Tête des Verds qui se développe sur environ 10 km pour -747 m de profondeur (BUGNET, 1985). À ce titre, la Petite Marielle pourrait constituer l'entrée d'un réseau spéléologique de plus de 1000 m de profondeur.

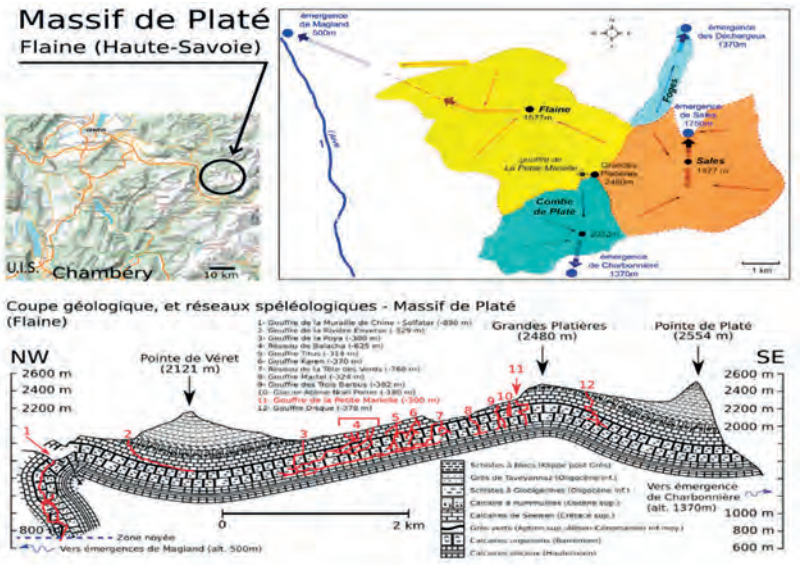

Figure 1 : Situation, contexte du gouffre de la Petite Marielle et coupe (Philippe MONTEIL, et Dominique MONTEIL d'après Richard MAIRE, 1990 et Michel DELAMETTE).

3. Choix du site, des mesures et contraintes : la galerie Isa

La galerie Isa se présente comme un étage horizontal fossile intermédiaire recoupé par quatre conduits verticaux distincts. Elle s'oriente sur l'axe de fracturation principal (70° Nord) et présente un profil en « montagnes russes » caractéristique d'un conduit épiphréatique (AUDRA et PALMER, 2015) Le choix de la section étudiée a été dicté par la qualité des vagues d'érosion. Elle se localise après la partie sommitale de la galerie Isa, juste en amont du P10 qui donne accès au Méandre des 3M. Celui-ci se développe sur la « couche à orbitolines », formation marno-calcaire qui se situe dans les 2/3 supérieurs des calcaires urgoniens. Ce méandre donne accès à la suite du gouffre jusqu'à -300 m (Fig. 2).

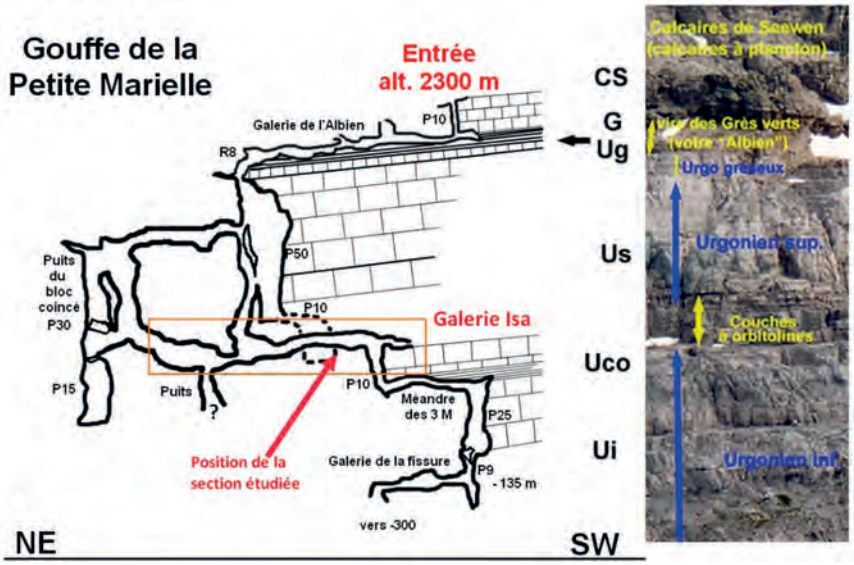

Figure 2 : Coupe du gouffre de la Petite Marielle (dessin Philippe MONTEIL – Stratigraphie d'après Michel DELAMETTE).

4. Méthode de travail, choix des approximations et estimations des débits

Pour la section étudiée (Fig. 2 et 3), nous avons retenu de bas en haut, trois sections (A, B, C) de forme elliptique au-dessus de la quatrième (D) de forme rectangulaire (fig. 4). Les mesures des longueurs de ces différentes sections ont été effectuées sur place au lasermètre (Disto X). Pour la mesure des vagues d'érosion, compte tenu des conditions topographiques locales, nous les avons effectuées à partir de documents photographiques observés sur écran d'ordinateur.

Sur chacune des photographies, une règle était maintenue le plus possible parallèle à la paroi et pour le repérage des différentes photographies, le cadrage insérait un repère fixe. Le manque de recul pour les prises de vue (notamment pour la section D) ne nous a pas permis de prendre toutes les photos de face. À partir de l'étude statistique de ces mesures, nous avons estimé la vitesse à l'aide de l'abaque de CURL (1974) selon la méthodologie proposée par Didier CAIHLOL (2011). Les coups de gouges renseignent sur la vitesse à proximité de la paroi, là où il y a le plus de frottements et donc là où la vitesse de la lame d'eau est la plus lente. C'est

pourquoi habituellement nous affectons cette vitesse avec un coefficient de rugosité supérieur à l'unité. Dans le présent article, nous avons basé notre réflexion sur une hypothèse basse, aussi nous avons choisi la valeur 1 pour ce coefficient comme si la vitesse de la lame d'eau était celle de la vitesse contre la paroi. Concernant les sections et pour prendre en compte les erreurs de forme et de mesure, nous avons estimé une erreur de 5 % sur les mesures de longueur et négligé les erreurs sur les angles (ceux-ci étant mesurés avec un Disto X et utilisés uniquement pour le calcul des longueurs projetées). Pour les lames d'eau considérées, nous avons appliqué un coefficient de 0,9 sur les sections elliptiques calculées (soit une estimation de 10 % inférieure). Cela donne donc en moyenne des surfaces pour les lames d'eau de 0,34 m² pour la A ; 0,17 m² pour la B ; 0,15 m² pour la C et 0,16 m² pour la D.

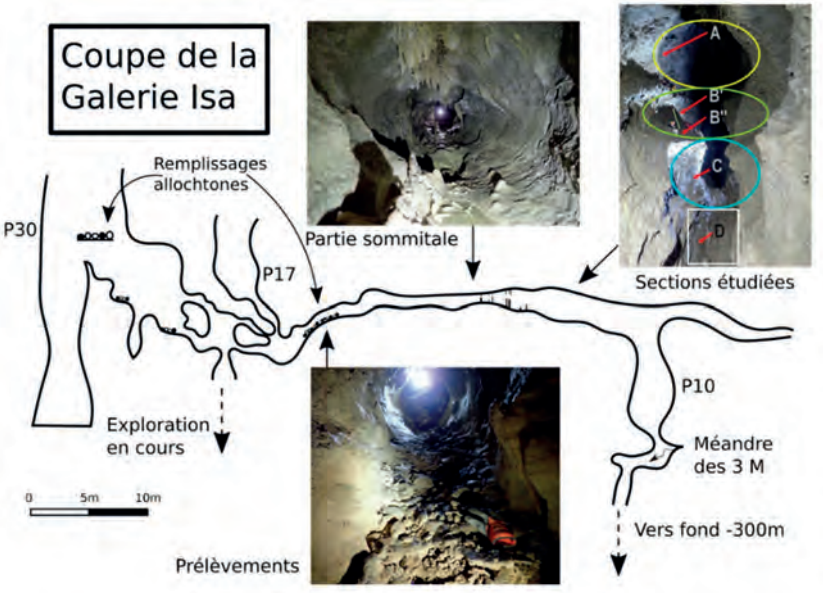

Figure 3 : Coupe de la galerie Isa (dessin et photos Philippe MONTEIL).

Le calcul des longueurs des vagues d'érosion s'est fait à partir de la visualisation à l'écran de quelques relevés photographiques. L'échelle étant déterminée par la taille des éléments photographiés : règle, Disto X, carnet, canards. Nous n'avons pas tenu compte d'effet de perspective. La couverture photographique de la zone, nous a permis d'effectuer entre 20 et 35 mesures pour chaque section (soit plus de 100 mesures). On peut remarquer que la répartition des tailles de ces vagues d'érosion justifie bien la distinction de nos quatre sections comme correspondant à quatre creusements différents (ce qui semble aussi s'observer sur la partie sommitale de la galerie, Fig. 3). Pour l'approximation des vitesses d'écoulement au contact de la paroi, nous avons utilisé la droite correspondant à une température d'eau de 5 °C dans l'abaque de CURL. Ces vitesses sont donc sous-évaluées car, compte tenu de l'altitude du conduit, la température de l'eau était probablement plus faible. Pour nous éviter la multiplication des erreurs de lecture graphique nous avons déterminé la fonction réciproque associée à la droite du diagramme de CURL (v(x) = exp(((b-log(x)/a)*ln(10)) avec a = 0,97 et b =2,50). Ainsi nous déterminons une vitesse pour chacune des vagues d'érosion et nous calculons les indicateurs statistiques des vitesses (Fig. 4).

Vitesse L/s	A	B	C	D
min	74	92	45	39
Q1	83	146	60	52
Me	102	167	110	71
Q3	121	205	126	88
max	189	341	187	128
moyenne	106	177	103	70
Ecart-type	29	53	41	25

Figure 4 : Étude statistique des vitesses.

En considérant les différentes lames d'eau déterminées précédemment et les vitesses moyennes obtenues après mesures et calculs via l'abaque de CURL, nous obtenons ainsi les valeurs des débits (Fig. 5).

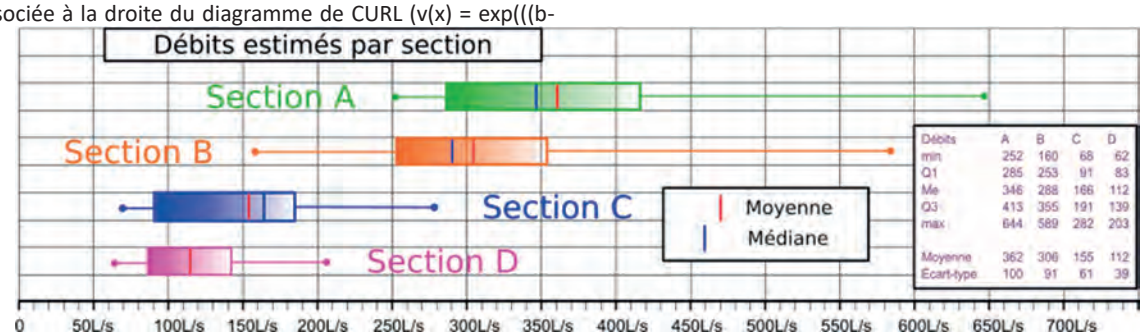

Figure 5 : Estimation des paléo-débits (dessin Philippe MONTEIL).

5. Passage des paléo-débits estimés au dimensionnement du paléo-bassin versant

La position du gouffre en limite amont du bassin-versant karstique de Flaine nous autorise à partir des paléo-débits une approche de la taille du bassin versant associé. Cette estimation est forcément minimale car nous n'avons pas pris en compte d'éventuelles pertes hydrologiques en amont (quid du P30 sur la coupe fig. 3 - effet de seuil ?), ni l'existence d'autres drains éventuels à cette altitude. Aussi compte tenu des valeurs minimales estimées pour les lames d'eau (0,34 m² pour la section A et 0,16 m² pour la section D) et en prenant 68 l/s/km² comme valeur du débit spécifique (donné par Richard MAIRE, 1990), nous arrivons à une superficie minimale approximative de 5,3 km² pour la section A à 1,6 km² pour la section D. Ces estimations minimales nous conduisent à étendre l'aire d'alimentation en direction du Sud.

Ces estimations ne prennent pas en compte les augmentations de débits en cours lors des épisodes glaciaires. Elles pourraient être revue largement à la baisse. Mais une première approche pétrographique des galets prélevés juste en amont de la zone d'étude (Fig. 2 et Fig. 3) nous indique que ces remplissages allochtones, parfois scellés sous de la calcite, proviennent en partie de la série cénozoïque sus-jacente à la cavité, mais aussi des Grès de Taveynnaz et de l'olistostrome sommital de la Pointe de Platé (données communiquées par Michel DELAMETTE voir KINDLER, 1990). Ce qui corrobore nos estimations de superficie, car ce secteur appartient actuellement aux bassins versants de la combe de Platé et de Sales (Fig. 1). Il faut donc nécessairement envisager une karstification antérieure au décapage des couvertures sus-jacentes et étendre plus au sud les limites d'un paléo-bassin de Flaine.

6. Conclusion

Dans cette étude, nous avons minimisé les indicateurs (sections, vitesses) pour ne pas surévaluer les débits. Un travail de mesures des vagues d'érosion sur place au pied à coulisse et une analyse hydrodynamique plus éclairée permettraient d'affiner ces valeurs pour obtenir des vitesses d'écoulement plus précises (et certainement plus élevées) que celles adoptées.

Toutefois, telle quelle, cette étude de la taille des vagues d'érosion, croisée avec celle des remplissages allochtones, permet une estimation quantitative de l'extension des anciens bassins versants dont l'endokarst garde une partie de la mémoire.

Il reste à élargir cette approche à quelques cavités avoisinantes, et à placer un cadre chronologique en s'appuyant sur des datations U-Th de concrétions et les données existantes (MAIRE, 1990) pour aboutir à une meilleure compréhension de l'histoire paléo-hydrogéologique du massif.

Remerciements

De grands mercis à Michel DELAMETTE pour son soutien, ses conseils, ses relectures et les précisions qu'il nous a apportées ; à David CANTALUPI pour son regard critique et sa connaissance du terrain ; à Didier CAIHLOL pour ses remarques et ses réactions encourageantes et à Dominique MONTEIL pour son aide et ses conseils en D.A.O.

Références bibliographiques

AUDRA P. and PALMER A. N., 2015 - Research frontiers in speleogenesis. Dominant processes, hydro-geological conditions and resulting cave patterns, Acta Carstologica 44/3, Postojna 2015, p. 315-348.

BUGNET M., 1985 - Réseau de la tête des Verds, Spéléo Dossier n°19, p. 14-22.

CAIHLOL D., 2011 – Analyse croisée débits / vagues d'érosion du moulin de Vogüé (Ardèche), Karstologia n°57, p. 28-32.

CANTALUPI D., CHARLETTY C. et PATRICK N., 2018 – Explorations et connaissances spéléologiques sur le karst de Flaine (Platé, Haute-Savoie, France). Bilan 2017, Karstologia mémoires n°20, Karst 2018 p. 193-204.

CURL R. L., 1974 – Deducing flow velocity in cave conduits from scallops, The NSS Bulletin vol.36, n°2, p. 1-5.

KINDLER P., 1990 - Géologie du sommet de la Pointe-de-Platé (Domaine helvétique, Haute-Savoie, France) ; Calcaires paléocènes et faciès chaotiques - Eclogae geol. Helv. 83/1, p. 7-19.

MAIRE R., 1984 – Un exemple de karst haut-alpin du Haut-Giffre et de Suisse occidentale, Karstologia n°3, p. 25-33.

MAIRE R., 1990 – La haute montagne calcaire, Karstologia Mémoires n°3, 710 p.

L'origine des puits : du cryptokarst à l'aven

Joël RODET

Centre Normand d'Etude du Karst (CNEK)& UMR6143 M2C CNRS, Université de Rouen-Normandie, bât. Blondel, place Emile Blondel, 76821 Mont Saint Aignan, France, joel.rodet@univ-rouen.fr

Résumé

Le puits, élément emblématique de la spéléologie, est un phénomène associé à la notion de karst d'introduction, guidé par la force gravitaire terrestre contrariée par la structure de l'encaissant. C'est aussi le fruit d'une évolution complexe issue d'une succession de stades dans le déroulé des processus d'altération sous couverture meuble regroupés sous le vocable de cryptokarst. Cette couverture peut être une langue glaciaire. Se développent alors des formes subverticales issues de la couverture d'altération qui progressent vers le bas comme des racines, les solution-pipes des Anglo-Saxons. L'altération périphérique par sa forte composition argileuse favorise la descente par à-coups du saprolite qui encombre la forme. La trépanation d'un vide basal permet la vidange des altérites et le modelage par l'hydrodynamique subverticale de ce qui devient un puits. Cet hydrodynamisme prend sa pleine dimension une fois établie la liaison entre karst d'introduction et karst de restitution. La morphologie pariétale se transforme alors, passant de parois à alvéoles à parois à cannelures subverticales, voire en puits en éteignoir. La disparition de la couverture en surface réduit puis supprime le bassin d'alimentation et le puits se fossilise tandis que se développe un lapiaz. Ceci explique l'ouverture d'avens au milieu des rainures des surfaces nues.

Abstract

The origin of wells: from cryptokarst to sinkhole. The origin of potholes: from the cryptokarst to the shaft. The shaft or pothole, symbol of caving, is a feature associated to the concept of input karst, guided by the earth gravity upset by the structure of the substratum. It is also the fruit of a complex evolution of several stages within the development of weathering processes under cover named "cryptokarst". The cover can be a glacier. Subvertical forms then develop from the weathering blanket which progress downwards like roots, the solution-pipes of the Anglo-Saxons. The trepanation of a basal vacuum allows the emptying of alterites and the subvertical hydrodynamic modelling of what becomes a shaft. This hydrodynamics takes on its full dimension once the connection between introduction karst and return karst is established. The parietal morphology then changes, going from cell walls to subvertical fluted walls, or even into a snuffer well. The disappearance of the surface cover reduces then removes the supply basin and the well fossilizes as a lapiaz develops. This explains the opening of avens in the middle of the grooves of the bare surfaces.

1. Introduction

Une des grandes interrogations en karstologie est de comprendre l'incidence des formes d'introduction sur le fonctionnement du système karstique. Certains n'ont vu, dans les irrégularités qui crénellent le contact entre le substrat (Fig. 1) et sa couverture meuble, qu'une simple impression d'une altération limitée à l'interface et résultant de l'érosion superficielle. D'autres les ont classées un peu hâtivement dans les formes exokarstiques.

Cependant, dès les années 1970, nous avons montré que ces irrégularités se prolongent parfois très profondément dans le massif, sur plusieurs dizaines de mètres de dénivellation, venant déstabiliser les établissements anthropiques souterrains qui ont eu la malchance de les recouper (RODET, 1981). Ces irrégularités soulignent l'activité d'un des agents les plus importants dans l'établissement du système karstique. Il s'agit des formes d'introduction, sans lesquelles l'endokarst serait fortement réduit (RODET, 2014).

Figure 1 : Série de racines du manteau d'altération à Tancarville (Normandie, France).

2. D'une couverture-écran…

Le manteau d'altération est constitué de saprolithes ou résidus d'altération du toit d'un encaissant solubilisable, qui coiffe le substrat. Parfois, ce manteau est couvert par des dépôts et/ou des apports exogènes plus récents que le substrat, fréquemment des sables et des lœss éoliens, des dépôts fluviatiles ou marins, souvent de forme résiduelle. Dans la craie du bassin de Paris qui fournit des exemples parmi les plus spectaculaires, le manteau est constitué des

résidus de l'encaissant, à savoir des argiles et des silex (le *Clay with flints/CWF* des Anglais). Ce manteau est observable sur les formations calcaires Bambuí du karst de Lagoa Santa (MG, Brésil), sous climat tropical.

Figure 2 : Plafond de carrière recoupant des racines du manteau d'altération sans influence tectonique (Visée, Belgique).

Les études réalisées *in situ* ont montré le processus d'imperméabilisation du toit du substrat (RODET et *al*., 2009), responsable du développement d'un aquifère suspendu dans le manteau d'altération (BROWN et *al*., 2008). Les qualités géochimiques des eaux de cet aquifère suspendu sont celles d'eaux saturées, proches de celles des eaux de l'aquifère de la craie. Toujours en Normandie, où ces aspects ont été étudiés, ces eaux peuvent être définies comme des eaux de nappe, alors qu'elles se concentrent dans les altérites, à savoir dans un encaissant décarbonaté, et plutôt siliceux (BROWN et *al*., 2010). Il est vraisemblable que ces eaux acquièrent leur minéralisation au contact de l'écran. Rappelons que sur le site de Fécamp (Normandie, France), 80 % de l'altération de l'encaissant du système karstique se réalise dans cette zone d'introduction (LACROIX et *al*., 2002).

Cet écran n'a pas la même qualité partout. Il peut présenter des manques, qui comme les trous d'une passoire, laissent passer l'eau en la concentrant. Ce mécanisme de concentration est responsable de la karstification de l'encaissant. C'est la naissance des racines du manteau d'altération (ou RMA), c'est-à-dire de ces fronts d'altération individualisés qui se démarquent visuellement par une progression plus rapide que le front généralisé lui-même, réalisant les indentations basales de ce dernier (Fig. 1). En conséquence, l'installation des RMA ne dépend pas du réseau tectonique du substrat ou de la sensibilité plus ou moins forte à l'altération de ce dernier, mais très clairement des conditions de l'interface à tendance imperméable qui le couvre (Fig. 2). Si des fissures se situent à l'aplomb des trous d'introduction, elles peuvent faciliter le développement des RMA, surtout dans les encaissants à très faible porosité.

3. …À la racine du manteau d'altération

Figure 3 : Détail du contact entre l'encaissant carbonaté et le cortège d'altérites, montrant le film argileux de dissolution (Normandie, France)

Une fois amorcée, la racine du manteau d'altération (RMA) ne peut que s'approfondir si elle reçoit son alimentation hydrique. En fait, elle est l'expression la plus visuelle des processus d'altération dans un karst d'introduction. Les variations lithologiques ont un impact certain si elles offrent des contrastes forts et épais. Dans un continuum carbonaté, les petites variations de faciès ne sont généralement que faiblement exprimées, et logiquement les RMA tendent à rejoindre leur niveau de base lithologique et/ou hydrologique. Dans des ensembles assez denses, certaines RMA peuvent cesser de progresser vers le bas : le plus souvent c'est parce que leur alimentation a été capturée par l'amplification de l'ouverture sommitale des RMA dominantes. Le littoral de la Normandie crayeuse offre de très nombreux exemples, en particulier dans la région d'Etretat où les RMA sont les plus fortement établies, la largeur des entonnoirs atteint 14 m (COSTA et *al*., 2006), alors que leur diamètre se réduit généralement entre 1 et 3 m dans leur partie profonde. De nombreuses RMA atteignent l'aquifère et alimentent les drains karstiques de restitution, ce que ne montre pas forcément le front de falaises, les drains n'étant pas toujours exactement verticaux en raison des variations lithologiques du massif carbonaté. Au contact avec le niveau de base, les RMA qui n'ont pas épuisé leur potentiel géochimique agressif, peuvent évoluer latéralement, en offrant des ouvertures basales (RODET, 2014).

Dans son évolution, la RMA finit par offrir un espace vide, par digestion plus ou moins avancée de l'altérite, que les matériaux de couverture vont remplir. La RMA est avant tout un milieu d'altération dont les zones les plus actives sont (1) prioritairement le fond ou cul, en fait le front de progression, par progradation subverticale, et (2) d'une façon moindre, la périphérie de la forme au contact avec l'encaissant (Fig. 3). Cette seconde partie est importante dans la progression verticale de la racine car, en produisant essentiellement des argiles, elle facilite la descente saccadée de matériaux, malgré la rugosité du contact, dès lors que ces argiles connaissent des alternances de

dessiccation et d'humidification. Le cœur de la forme accueille les produits de la surface, plus mobiles que les argiles, notamment les lœss quaternaires des plateaux périglaciaires de Normandie, en raison des effets de l'indice de rugosité.

Figure 4 : Stock résiduel d'altérites accompagnant une morphologie en alvéoles des parois verticales.

4. La trépanation et l'hydrodynamisme

Dans cette progression, la RMA peut être amenée à recouper un drain de restitution. Il s'agit d'une trépanation dont la réalisation est presque toujours soudaine, par rupture de la cloison qui isole les deux drains. La RMA, de par sa dimension verticale, concentre une force potentielle énorme, et globalement elle domine la dynamique lors de la trépanation, en envahissant le drain de restitution et en injectant les produits qu'elle contient, d'autant plus mobiles qu'ils seront imbibés d'eau. Il s'agit donc d'un événement soudain, catastrophique, impliquant des masses solides, liquides et visqueuses propulsées par la hauteur, de plusieurs dizaines de mètres, de la colonne d'altération [BAUER, 1989 ; MAIRE, 1990 : p. 531-533]. La trépanation peut se réaliser à n'importe quel moment, et les indices annonciateurs sont peu étudiés. Suintements et fissures « fraîches » sur la paroi peuvent prévenir d'une rupture imminente de la cloison.

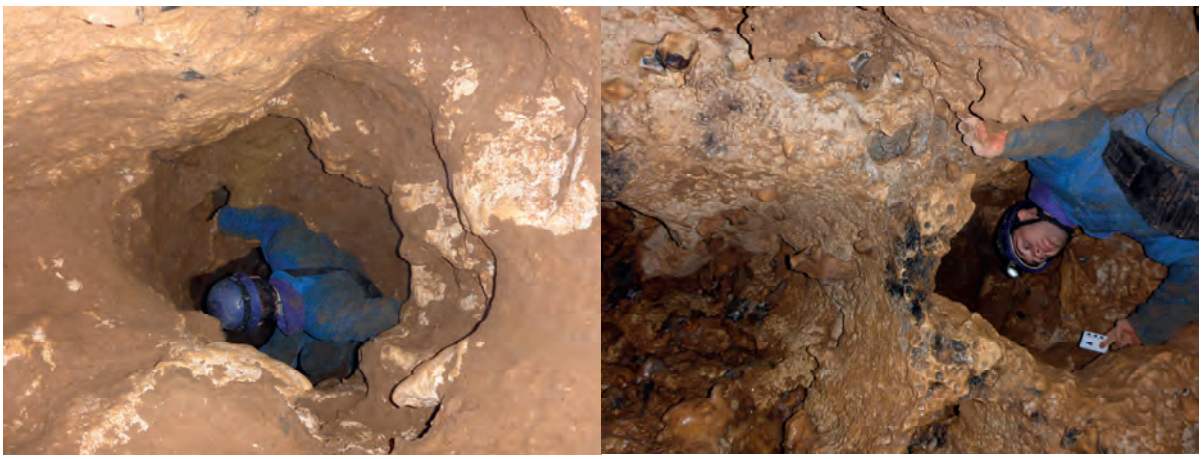

Figure 5 : Un cas un peu particulier : à la base d'une racine du manteau d'altération, partiellement dégagée de ses altérites (à gauche), on pénètre dans une cheminée d'équilibre sans comblement (à droite). On peut en déduire qu'une phase d'ennoiement du drain basal, en développant la cheminée, est responsable de la trépanation d'une Racine du Manteau d'Altérations, plus ancienne et fossile car sinon les altérites auraient envahi la cheminée.

Les incidences de ces évènements catastrophiques sur les RMA sont conséquentes. Le départ des produits d'altération laisse apparaître la morphologie d'altération de contact, généralement un ensemble d'alvéoles centimétriques, ovalisées en disposition subhorizontale (Fig. 4). Avec le départ du produit d'altération, la RMA se vidange et libère un espace vide dans lequel les eaux vont chuter, usant les parois en s'écoulant et formant peu à peu des rainures et cannelures subverticales (Fig. 5). C'est la naissance du gouffre et du puits des cavités verticales dans lesquelles les formes d'altération géochimiques sont gommées par les morphologies d'écoulement physique (Fig. 6). À échéance, toute trace d'altération devrait être gommée (RODET, 2017a, 2017b).

5. Conclusions

Figure 6 : Racine du manteau d'altération transformée en puits, avec ses cannelures subverticales qui gomment peu à peu les alvéoles de contact avec les altérites.

L'aven est assurément l'élément karstique le plus mystérieux en raison des difficultés d'exploration résultant de sa verticalité. Cette dimension est l'objectif majeur de l'activité spéléologique qui s'exprime dans la recherche de la dénivellation la plus importante possible dans le réseau souterrain, mais aussi dans la profondeur du puits lui-même. Cette forme offre une large gamme morphologique qui reflète la diversité de son évolution, fortement encadrée par les conditions locales d'ordre structural, géomorphologique et climatique. La genèse de cette forme fondamentale est restée largement sous-étudiée, en raison du paradigme « classique » du karst élaboré grâce à la solution de continuité hydrologique qu'offriraient tous les réseaux souterrains en raison des discontinuités lithologiques et tectoniques. La nouvelle approche (DUBOIS et *al*., 2014) qui insiste sur l'importance primordiale des phases géochimiques, permet de reclassifier les puits comme fruit des phénomènes de dissolution verticale dont tous les massifs karstifiés présentent des exemples surprenants. Tout comme pour les drains subhorizontaux, les phases primokarstiques préfigurent les formes verticales dont l'évolution finale est le puits en éteignoir (Fig. 7). C'est la succession spatiale des secteurs verticaux et des secteurs horizontaux qui fait la richesse et la variété spectaculaire de l'endokarst. Cette évolution explique la présence de l'aven, fruit de la concentration des eaux, au cœur d'un lapiaz au bassin d'alimentation très diffus.

Figure 7 : Puits en éteignoir, ouvert dans les grès (Paraná, Brésil).

Références

BAUER J. (1989) Achama Lecia : les causes de l'accident. *Bull. de l'ARSIP*, 16 : 192-194.

BROWN J., DUPONT J.-P., RODET J., MOTELAY A., LAIGNEL B., MASSEI N. and JARDANI A. (2008) Role of superficial formations in the recharge processes of a chalk karstified aquifer. *33td International Geological Congress*, Oslo, 6-14 août 2008.

BROWN J., DUPONT J.-P., RODET J. and JARDANI A. (2010) Hydrological function of the karst mantle in the karstogenesis and recharge processes of the chalk limestone aquifer of the West Paris Basin (Upper-Normandy, France). *23e RST*, Bordeaux : 45.

COSTA S., LAIGNEL B., HAUCHARD E. et DELAHAYE D. (2006) Facteurs de répartition des entonnoirs de dissolution dans les craies du littoral du Nord-Ouest du bassin de Paris. *Zeitschrift für Geomorphologie*, 1 (50) : p. 95-116.

DUBOIS C., QUINIF Y., BAELE J.-M., BARRIQUAND J., BARRIQUAND L., BINI A., BRUXELLES L., DANDURAND G., HAVRON C., KAUFMANN O., LANS B., MAIRE R., MARTIN J., RODET J., ROWBERRY M.D., TOGNINI P. and VERGARI A. (2014) The process of ghost-rock karstification and its role in the formation of cave systems. *Earth-Science Reviews*, 131: 116-148.

LACROIX M., RODET J., WANG H.Q., LAIGNEL B. and DUPONT J.-P. (2002) Microgranulometric approach to a chalk karst, western Paris Basin. *Geomorphology*, **44** : 1-17.

MAIRE R. (1990) *La haute montagne calcaire, karsts, cavités, remplissages, Quaternaire, paléoclimats*. Karstologia-Mémoires, n° 3 : 731 p.

RODET J. (1981) *Contribution à l'étude du karst de la craie : l'exemple normand et quelques comparaisons*. PhD Université de Paris I "Panthéon - Sorbonne": 427 p.

RODET J. (2014) The primokarst, former stages of karstification, or how solution caves can born. *Geologica Belgica*, **17** (1): 58-65.

RODET J. (2017a). The cave: a result of a long evolution named karstification, a conceptual approch. *25th International Karstological School "Classical Karst"*, 19-23 june 2017: p. 48-49

RODET J. (2017b). La grotte, fruit d'une longue gestation appelée karstification. *Karstologia*, 69 : 57-64.

RODET J., BROWN J., DUPONT J.-P. (2009) Development and function of a perched aquifer in the covering layers of the chalk limestones in the Paris Basin. *Proceedings of the 15th ICS*, Kerrville (Texas, USA): 1662-1666.

Assessment of Soil Losses by Erosion in a Karst Environment in the Cerrado Biome of Brazil

André Silva TAVARES[(1)] & Rogério Soares UAGODA[(2)]

(1) University of Brasília, Darcy Ribeiro Campus, 70910-900 Brasília-DF, Brazil, andresttavares@gmail.com
(2) University of Brasília, Darcy Ribeiro Campus, 70910-900 Brasília-DF, Brazil, rogeriouagoda@unb.br (corresponding author)

Abstract

This work aimed to estimate the volume of soil losses due to water erosion in a watershed dominated by karst features, which results in the quantity of sediment directed to the caves in the region. The Corrente river watershed is located in the Northeast region of the State of Goiás, Brazil. Through the Erosion Potential Method (EPM) applied in the Geographic Information System, soil losses were quantified for the year 2021. The estimated average soil loss was 26.41 to/ha/year-1, with a maximum flow of 10,689,083.57 to/year-1 in the watershed outlet. The limits of the catchment, producing sediments to the caves were obtained, which allowed extracting an average estimate of transported sediments in these karst regions.

Résumé

Évaluation des pertes de sol par érosion dans un environnement karstique du biome de Cerrado au Brésil. Ce travail vise à estimer le volume des pertes de sol dues à l'érosion hydrique dans un bassin hydrographique dominé par des caractéristiques karstiques, ce traduisant par la quantité de sédiments dirigée vers les grottes de la région. Le bassin hydrographique de la rivière Corrente est situé dans la région nord-est de l'État de Goiás, au Brésil. Grâce à la méthode d'érosion potentielle (EPM) appliquée dans un système d'information géographique, les pertes de sol ont été quantifiées pour l'année 2021. La perte de sol moyenne estimée est de 26,41 to/ha/an^{-1}, avec un débit maximum de 10 689 083,57 to/an^{-1} à l'exutoire du bassin versant. A partir des limites des micro-bassins versants, ou zones productrices de sédiments, des zones de convergence vers les grottes ont été obtenues, ce qui a permis d'extraire une estimation moyenne des sédiments transportés dans ces régions karstiques.

Resumo

Avaliação das Perdas de Solo por Erosão num Ambiente de Carso no Bioma do Cerrado do Brasil. Esse trabalho visou estimar o volume das perdas de solo por erosão hídrica em uma bacia hidrográfica dominada por feições cársticas, que resulta no quantitativo de sedimentos direcionados para as cavernas da região. A bacia hidrográfica do rio Corrente está localizada na região Nordeste do Estado de Goiás, Brasil. Por meio do Método de Erosão Potencial (EPM) aplicado em Sistema de Informação Geográfica, foram quantificadas as perdas de solo para o ano de 2021. A perda de solo média estimada foi de 26,41 to/ha/year^{-1}, com vazão máxima de 10.689.083,57 to/year^{-1} no exutório da bacia. A partir dos limites das micro-watersheds, ou áreas produtoras de sedimentos, foram obtidas áreas de convergência para as cavernas, que permitiu extrair uma estimativa média de sedimentos transportados nessas regiões cársticas.

1. Introduction

In Brazil, karst landscapes make up between 5 and 7% of the territory, and yet studies on hydrology and karst sedimentology are scarce (KARMANN, 2016). However, the karst evolution processes through superficial and underground flow networks carry relevant information about the type, quantity and quality of the transported material, revealing aspects of the functioning of the karst aquifer in the transport of sediments.

It is known that the degree of development of the karst relief forms varies according to the characteristics of the climate, vegetation and the type of source material. The characteristics of forms, surface and underground, have already been widely elucidated in the literature (PALMER, 1984; JENNINGS, 1985; FORD & WILLIAMS, 2007; HARDT, 2011).

In Brazil, the karst relief gains special importance in the Cerrado biome, where native vegetation is the most affected by suppression among other biomes in Brazil. Allied to this, the deficiency of phosphorus and other nutrient minerals in some soils does not favor forest development and allows the origin of landscapes consisting mainly of pastures with sparse trees (BRECKLE, 2002). As a result, erosive processes become more and more intensified during rainfall, contributing to a large volume of sediment that is transported to underground channels and karst galleries.

The sources and types of detritus sediments are varied, as the material is pedogenized on the surface, or alluvial sediments, or epiphreatic mud, or insoluble residues, or suspended solids and organic deposits. Deposition zones are seen in widened fractures, abysses, sinks, internal subsidence, flooded gallery networks and back-flooding (LAUREANO & KARMANN, 2013). These zones of autochthonous and allochthonous sediment transport can imply high speeds and rise of the water table, which can promote rapid flooding above the vadose zone (CALDEIRA *et al*., 2019). Thus, the preservation of speleological heritage

involves the need to delimit the areas that produce sediment, since inadequate land management and the replacement of native vegetation accelerate erosion processes, increasing the amount of sediment in rivers and caves.

Therefore, in order to assess soil loss and sediment production due to water erosion, this study used a watershed dominated by karst features in the Brazilian Cerrado biome, in which an extremely active process of underground karstification and relief dissection occurs. To quantify the sediments directed to the caves, the Erosion Potential Method (EPM) was used, which quantifies the loss of soil by erosion.

2. Materials and methods

The Corrente River watershed (3,824 km2) belongs to the Tocantins River basin, located in the northeast of the State of Goiás, Brazil. The upper portion (Highlands) is formed by sandstones (Urucuia Group) that constitute unconsolidated siliciclastic sediments, while the lower portion (Karst Terrains) has pellitic rocks intercalated with carbonates (Bambuí Group). The area with densification of karstic features acts as recharge areas through fractures and large convections distributed in sinks and underground flows. About 47 cavities with perennial flows were identified (Fig. 1). The climate is tropical with dry winter (Aw), with an average of 1,165 mm/year^{-1} (CARDOSO *et al*., 2014).

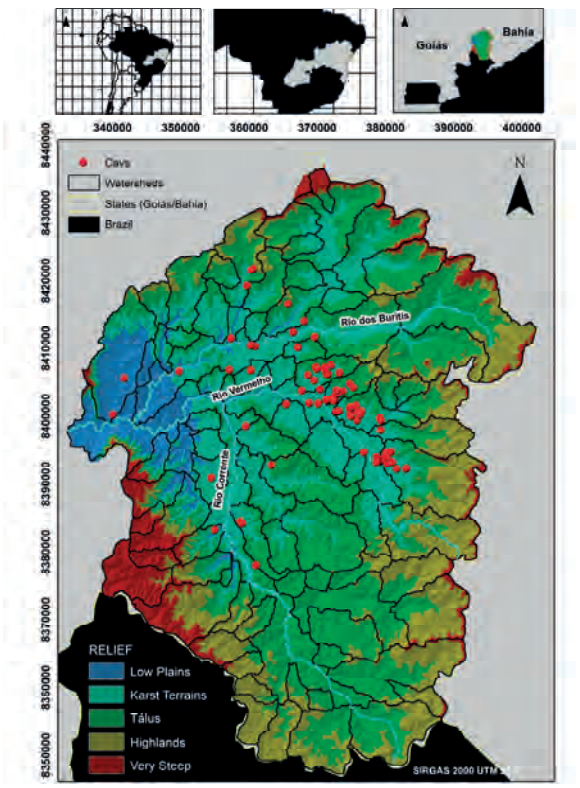

Figure 1: Stream river basin and mapped caves.

Between the domain of carbonates and siliciclastic sediments, karstic depressions occur with intensified erosive processes, from which there is capture of surface runoff by fractures or collapsed sinks, generating the accumulation of sediments in some caves above the base level.

- Erosion Potential Method (EPM)

The EPM is an empirically-based model that estimates soil loss and the determinants of water erosion intensity, which directly affect soil loss rates at the scale of watersheds, such as soil slope, soil strength, erosive features, land use and management, air temperature and precipitation (GAVRILOVIC, 1988).

Soil loss (Wyr) in the EPM model is estimated by Equation 1.

$$W_{yr} = T * H_{yr} * \pi * \sqrt[3]{Z^3} \qquad \text{Eq. 1}$$

Where: Wyr = total sediment production (m^3 yr^{-1}); T = temperature coefficient (dimensionless); Hyr = mean precipitation (mm year^{-1}); π = 3.14; Z = erosion coefficient (dimensionless).

The temperature coefficient (T) is calculated according to Equation 2.

$$T = \sqrt[2]{\frac{t_0}{10}} + 0{,}1 \qquad \text{Eq. 2}$$

Where: T = temperature coefficient (dimensionless); t_0 = mean air temperature (°C year^{-1}).

The erosion coefficient (Z) is obtained by Equation 3:

$$Z = Y * X_a * (\varphi + \sqrt[2]{I_{sr}}) \qquad \text{Eq. 3}$$

Where: Y = soil resistance to water erosion (dimensionless); Xa = land use and management (dimensionless); φ = degree of erosion features in the soil (dimensionless); Isr = mean slope of the watershed (%).

The Z coefficient values are classified according to the degree of erosion intensity (Fig. 2).

Categories	Erosion intensity	Erosion Coefficient (Z)	Average of Z
I	Very severe	Z > 1.0	Z = 1.25
II	Severe	0.71 < Z < 1.00	Z = 0.85
III	Moderate	0.41 < Z < 0.70	Z = 0.55
IV	Weak	0.20 < Z < 0.40	Z = 0.30
V	Very weak	Z < 0.19	Z = 0.10

Figure 2: The degree of erosion intensity (Z)

In the ENVI 5.3 program, land use and land cover were classified using the OBIA (Object-Based Image Analysis) method. The method is based on the segmentation of matrix images, where samples are defined for training in supervised machine learning, based on the Support Vector Machine model, a non-probabilistic linear binary algorithm (COHENCA & CARVALHO, 2015). LandSat 8 satellite images (OLI sensor) were used.

Through temporal series of rainfall stations, the average rainfall and temperature of the last 30 years was established, using the inverse distance weighting (IDW) method, which interpolates and gathers the areas of influence of each station from the polygons of Thiessen. Soils were classified based on the Brazilian Soil Classification System (EMBRAPA, 2018). Digital images from the Alos satellite (Palsar sensor) with 12.5 meters of spatial resolution were used for the relief classes. In addition to results obtained in the analyzes published by Nunes (2020).

3. Results

The predominant phytophysiognomy is field/pasture (56.67%), followed by Cerrado (21.40%), dense forest (10.98%), agricultural culture (7.60%), exposed soil (2.83%) and water bodies (0.49%). The dominant soils were Quartzarenic Neosols (38.51%), followed by Red-Yellow Latosols (29.47%), Chernosols (24.46%) and Cambisols (7.54%). The steepest slopes are located near the springs and dissected canyons. However, flat to smooth sloping areas (0-8%) are predominant, with an average slope of 5.6%. The average soil loss for the year 2021 in the Corrente River watershed was 26.41 to/ha/year^{-1}.

Figure 3 highlights the micro-watersheds that act as producers of sediments that converge to the caves. The caves with perennial courses are accumulated in the karst areas of the Vermelho River, more specifically, in the Extrema, Serragem and Ventura micro-watersheds, which contribute to a sediment production in the scale of 33.66, 19.45 and 35.22 to/ ha/year^{-1}, respectively.

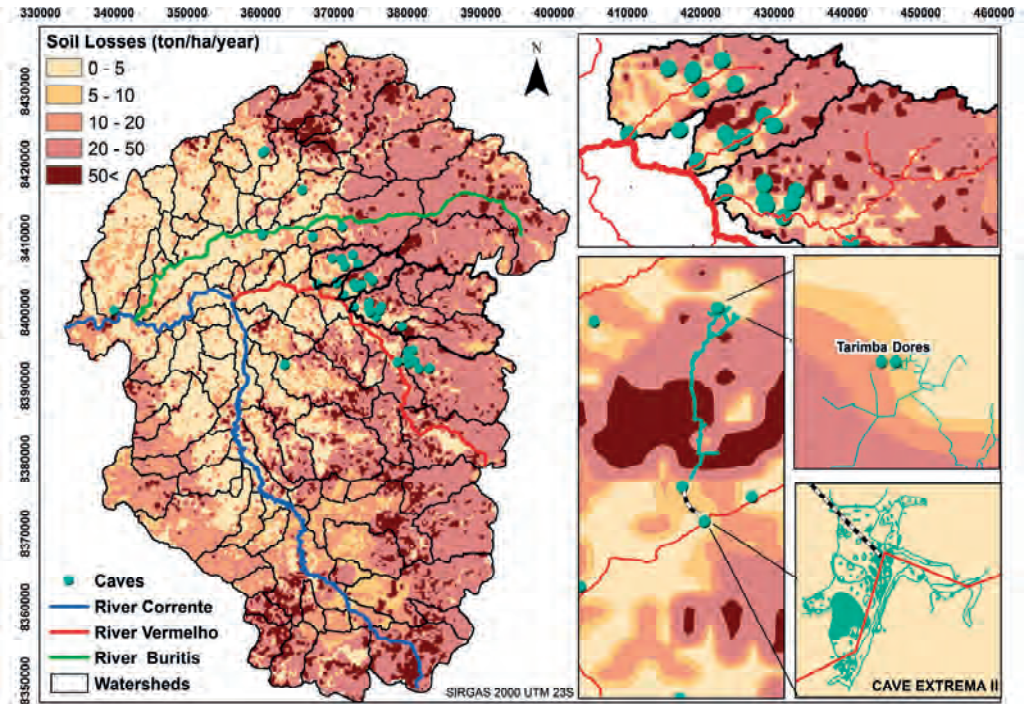

Figure 3: Soil losses by erosion in the Corrente River watershed and in the karst areas.

4. Discussions

In the watershed of the River Corrente, the cretaceous sediments of the Urucuia Group (upper), which would cover the Bambuí Group (lower), are found inside caves, guided by networks of conduits and fractures. The morphology of the transition from sandstones to carbonates occurs through abrupt breaks, in the form of steep slopes, with the presence of erosion in an advanced stage. Part of these structures are related to karstification, which in this situation is expressed externally in the form of sinkholes.

Cave Extrema III, for example, receives volumes of sediment in the scale of 33.12 to/ha/year^{-1}, originating from surface and underground flows associated with sinkholes and adjacent caves, such as coming from the Tarimba cave.

As the study is carried out in a covered karst, the hypothesis is that the underlying karst system works as an inducer of superficial erosion processes, that is, the opening of sinkholes or sinks leads to a rearrangement of the balance profile of rivers and, consequently, expands the erosive capacity of captured surfaces. The absence of conservation practices in land use can increase this process, both with the increase in the sediment load in the suppression of native vegetation, and with the abstraction of water from aquifers, which tends to make karst systems more unstable.

In Figure 4, the estimated values of sediments transported in caves of perennial flows are highlighted, according to the related micro-watershed.

	Micro-Watershed			Soil loss average (to/ ha/ year^{-1})		
	Extrema	**Serragem**	**Ventura**	**Extrema**	**Serragem**	**Ventura**
Caves	Ponte de terra	Meândrica	Cachoeira do Funil	0,38	12,32	0,25
	Extrema I	Lapa I	Corredeiras	0,38	1,33	67,13
	Esperança	Ana Paula I	Pasto	2,28	0,5	56,38
	Extrema II	Judite	Porcos	0,23	0,35	16,14
	Extrema III	Dores	Marimbondos	33,12	2,36	11,88
	Vila Nova	Tarimba	Associação II	0,43	2,36	1,27
		Serragem II	Desgosto		10,49	1,62
		Penhasco			10,34	

Figure 4: Average estimate of sediment transport to the caves.

5. Conclusion

Through the estimation of soil loss in the watershed scale, it was possible to evaluate the spatial dynamics of the sediment producing areas, allowing to highlight the transport potential of these materials in karstic micro-watersheds. From there, such units can be investigated and monitored to better assess the causes and effects that are still little known. The karst region in this research is managed by an important Conservation Unit for the preservation of the region's speleological heritage.

Acknowledgments

The authors thank the Chico Mendes Institute for Biodiversity Conservation (ICMBio), National Water Agency (ANA), National Center for Research and Conservation of Caves (CECAV) and "Coordenação de Aperfeiçoamento de Pessoal de Nível Superior – Brasil" This study was financed in part by CAPES – Finance Code 001.

References

BRECKLE, S.W. (2002) Walter's Vegetation of the Earth: The Ecological Systems of the Geo-Biosphere, Springer Berlin Heidelberg, ed. 4, 527 p.

CALDEIRA, D.M.V.S.; Uagoda, R. and Nogueira, A.M. (2019) Dinâmica dos sedimentos clásticos cavernícolas: Potencialidade para estudo paleoambientes no Brasil. *Espaço & Geografia*, n°22 (1), 153-189.

CARDOSO, M.R.D.; Marcuzzo, F.F.N. and Barros, J.R. (2014) Classificação climática de Köppen-Geiger para o Estado de Goiás e o Distrito Federal. *Acta Geográfica*, 8(16), 40-55.

COHENCA D., CARVALHO, R. (2015) Comparação de métodos de classificação OBIA, Máxima Verossimilhança e Distância Mínima em imagem OLI/Landsat-8 em área de alta diversidade de uso do solo. *Anais* XVII Simpósio Brasileiro de Sensoriamento Remoto, João Pessoa-PB, Brasil, 1035-1042.

EMBRAPA - Empresa Brasileira de Pesquisa Agropecuária (2018) Sistema Brasileiro de Classificação de Solos. Brasília, 4. ed.356 p.

FORD, D.; WILLIAMS, P. (2007) Karst Hydrogeology and Geomorphology. Wiley: Chichester, 562 p.

GAVRILOVIC, Z. (1988). The use of empirical method (Erosion Potential Method) for calculating sediment production and transportation in unstudied or torrential streams. In: White, W.R. (ed.), International Conference on River Regime; Chichester, 411–422.

HARDT, R. Da Carstificação em Arenitos: Aproximação com o suporte de geotecnologias. Tese (doutorado). 224f. Universidade Estadual Paulista, Instituto de Geociências e Ciências Exatas. Rio Claro - SP, 2011.

JENNINGS, J.N. (1985) Karst Geomorphology. Oxford: Basil Blackwell, 293 p.

KARMANN, I. (2016) Carste e cavernas no Brasil: distribuição, dinâmica atual e registros sedimentares, breve histórico e análise crítica das pesquisas realizadas no âmbito do IGc USP. Livre Docência em Espeleologia. Instituto de Geociência. Universidade de São Paulo, 62 p.

LAUREANO, F. V. KARMANN, I. (2013) Sedimentos clásticos em sistemas de cavernas e suas contribuições em estudos geomorfológicos: uma revisão. *Revista Brasileira de Geomorfologia*, (14) 23-33.

NUNES, J.G.S. (2020) Mapeamento de solos através de técnicas diretas e indiretas na APA Nascentes Do Rio Vermelho, Mambaí-GO. Dissertação, Universidade de Brasília, 110 p.

PALMER, A.N. (1984) Geomorphic interpretation of karst features. In: Lafleur, R.G. Groundwater as a Geomorphic Agent. Boston: Allen and Unwin, 173-209

A major paleokarst horizon found within a modern cave in NE India; the Pielkhlieng Pouk-Krem Sakwa System, Meghalaya.

Dr Mark E. TRINGHAM

Gloucester Speleological Soc., University of Bristol Spelaeological Soc. Malvern, WR136QN UK. mtringham@btinternet.com

Abstract

The Paleocene to Eocene rocks exposed in Meghalaya comprise a ~400m thick interlayered sandstone and limestone sequence. Cave systems totalling over 500km occur mostly in the Lakadong and Prang Limestone Members. One such cave is the 20km long PP-KS System. Exploration here over the last decade has found a wide variety of paleokarst features present including a pinnacle epikarst on the top surface of the limestone with sandstone and coals infilling around pinnacle towers. Also, within the upper part of the limestone, large ball-shaped sandstone bodies occur interpreted as pit and cavern infills. Results show that the Late Paleocene stratigraphical sequence probably contains a significant unconformity during which the Lakadong Limestone was exposed and karstified during a period of relative sea level fall with later sandstone deposition. This unconformity horizon has formed a major focus for new cave formation and underground drainage.

Résumé

Un horizon paléokarstique majeur découvert dans une grotte du NE de l'Inde : le système de Pielkhlieng Pouk-Krem, Meghalaya. Les roches du Paléocène-Éocène exposées à Meghalaya comprennent une séquence de grès et de calcaire intercalés de 400 m d'épaisseur. Des systèmes de grottes totalisant plus de 500 km se développent principalement dans les calcaires de Lakadong et Prang. L'une de ces grottes est le système PP-KS, long de 20 km. L'exploration, au cours de la dernière décennie, a permis de mettre en évidence une grande variété de caractéristiques paléokarstiques y compris un épikarst à "pinacle" sur la surface supérieure du calcaire, avec un remplissage de grès et des charbons autour des pinacles. La partie supérieure du calcaire contient également de grands blocs de grès en forme de boule interprétés comme des remplissages des puits et cavernes. Les résultats montrent que la séquence stratigraphique probablement du Paléocène supérieur contient une discordance significative au cours de laquelle le calcaire de Lakadong a été exposé et karstifié pendant une période de baisse relative du niveau de la mer avec un dépôt ultérieur de grès. L'horizon de cette discordance a constitué un axe majeur pour la formation de nouvelles grottes et le drainage souterrain.

1. Introduction

Expedition caving in Meghalaya (Fig. 1) has provided many scientific discoveries on cave biology, geology, hydrology and speleogenesis, as described for example by ARBENZ (2021). The majority of the caves are formed in the Eocene aged Prang Limestone, but others are formed in the Late Paleocene Lakadong Limestone, as well as in early Paleocene and Late Cretaceous sandstones and calcarenites (Fig. 2). Near the village of Sakwa (Fig. 1) the major cave system of Pielkhlieng Pouk-Krem Sakwa (PP-KS) is mostly developed in the Lakadong Limestone, but with some upper parts extending into overlying sandstone formations. During the exploration and surveying of this cave system many spectacular and unusual geological features were noticed which are interpreted as a major paleokarst developed during the late Paleocene at an unconformable contact between the two lithologies.

Figure 1: Topographic and Google Earth Maps showing the Meghalaya study location in Northeast India.

2. Study methods

Geological observations were mostly integral to the original cave exploration and surveying, conducted from about 2007 until 2018. Notes and photographs were recorded and the stratigraphical setting of the cave systems compared to the published literature. The PP-KS system was first explored from a large resurgence at its southern downstream end starting in 1998 and this was initially joined up with two sinkhole entrances located around 4km to the north.

During this phase explorers noticed that sandstone and coal seams formed the cave roof in some places, while in other parts the cave was formed entirely in limestone. Krem Sakwa initially received little attention, but in 2017 it had a major exploration break-through at a short dig and it was then quickly joined up with the overall cave system. The Krem Sakwa part of the system showed the interpreted paleokarst characteristics particularly well.

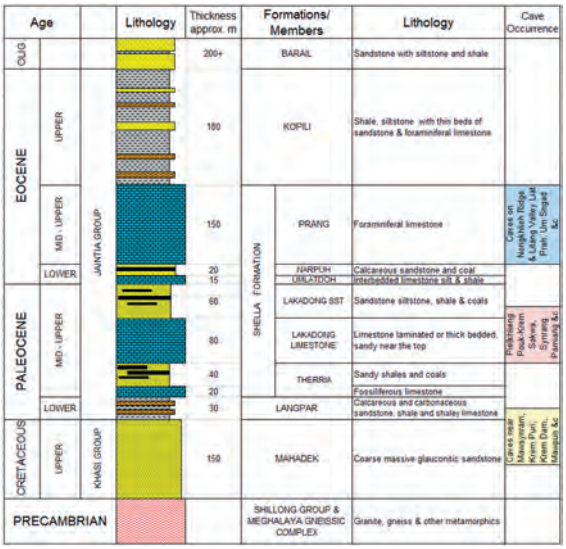

Figure 2: Stratigraphical summary chart Sakwa region.

3. Results

Observations show that the limestone pinnacles mostly have steep to overhanging sides and sharp tops, although in some areas they are broader with flatter tops. In dry areas of the cave the limestone-sandstone contact is associated with gypsum crusts and red hematite staining (Fig. 6), while in wet areas the sandstone mostly has a shiny dark brown weathered surface, likely composed of goethite (Fig. 3). The sandstone bedding onlaps the limestone pinnacles, and in many pits the nearby sandstone bedding is contorted and broken with evidence of flowage and differential compaction. The overlying sandstone and coal layers are seen to become more regular and parallel not far above the pinnacle tops.

Figure 3: An example limestone tower (grey) with sandstone infilling around (dark brown) seen in Krem Sakwa.

The plan of the PP-KS system and neighbouring caves summarises where the interpreted unconformity and paleokarst has been found, with a special concentration in Krem Sakwa (Fig. 4).

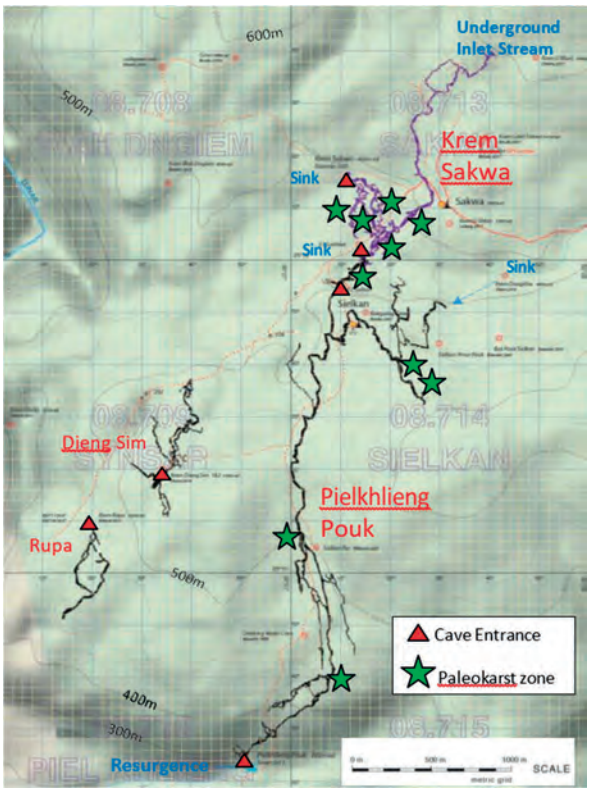

Figure 4: Plan of Pielkhlieng Pouk-Krem Sakwa and neighbouring caves. Adapted from ARBENZ (2021).

Within some parts of Krem Sakwa, a dense network of cave passages have formed with sandstone pits 10's of metres wide with encircling cave passages in the surrounding limestone, giving an unusual very crinkled shape in plan view (Fig. 5).

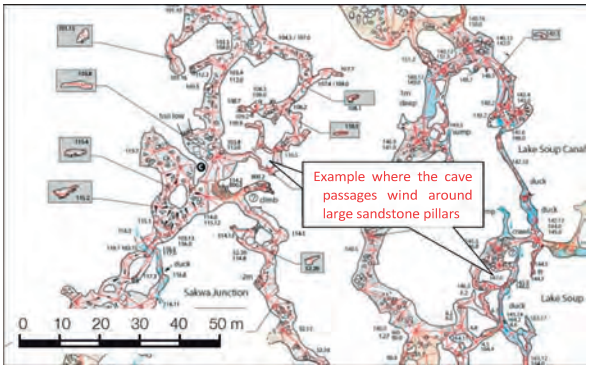

Figure 5: Detailed cave plan in part of Krem Sakwa showing crinkled passage form (Survey drawn by T. Arbenz).

Figure 6: The unconformity in a dry part of Peilkhlieng Pouk, with abundant white gypsum and red hematite staining (photo by C Howes).

The ball-like sandstone masses seem to occur in one area about 400m wide in the southern part of Krem Sakwa. The individual balls generally range in diameter from around 1m to 5m (Fig. 7) and they are more resistant to erosion than the surrounding limestone and hence stick out from the passage walls and roof. Many have been eroded out and remain as large fallen boulders in the streamway.
In the upstream part of Krem Sakwa silty and dolomitic interbeds occur in the limestone forming prominent ledges and cascades and these resistant layers likely inhibited paleokarst formation during the Paleocene, leaving a relatively smooth and planar contact between the limestone and sandstone.

Figure 7: Sandstone balls seen in the walls and ceiling of the Krem Sakwa streamway (photo by M. Burkey)

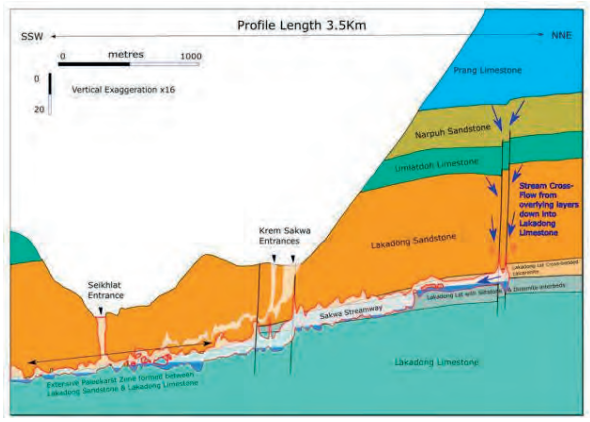

Figure 8: Profile showing the Krem Sakwa entrances and streamway and geological interpretation. The main paleokarst zone occupies ~3km shown on left and centre of the profile.

4. Discussions

In Krem Sakwa all the cave passages discovered to date have formed at or just below the limestone/sandstone contact (Fig. 8) and later upward 'stoping' collapse has in many places concealed the limestone completely so that the passages have the false appearance of being solely formed in sandstone. However, in Pielkhlieng Pouk the underground river has in many places eroded large canyon passages 30m or more deeper into the Lakadong Limestone but with the roof level in many places still at or close to the paleokarst horizon.
The obvious interpretation is that these masses are previous shallow caves associated with the paleokarst erosion which were rapidly infilled by sand at the start of Lakadong Sandstone deposition. The bulbous shapes likely indicate that limestone solution continued at the porous and permeable sandstone margin even after a paleocave had been filled in, perhaps enhanced by acidic ground-water circulating around the freshly buried humic layers a few metres above. However because the sandstone and coal layers become regular and parallel within a few metres above the pinnacle tops a deep endokarst origin seems unlikely.
The paleokarst horizon has provided the focus for recent cave formation and development. Presumably a 'ready-made' inception horizon was present along which meteoric waters could more easily pass to rejuvenate the erosion surface and form the modern day Lakadong Limestone/Sandstone cave systems. The pyritic nature of the sandstones has also made it likely that permeating groundwaters became acidic so that solution at the interface between the sandstone and limestone was enhanced.

Besides the cave exposures studied, during this evaluation the same stratigraphical contact was also examined on the

surface at Kurtinsiang near Mawsynram, just over 90Km to the West of Sakwa. Here the top of the Lakadong Limestone was found to have similar looking paleokarst pinnacles and ball-like sandstone masses present (Fig. 9). Therefore the unconformity and the paleokarst are clearly extensive regional features, rather than just being a local curiosity.

While earlier publications by SAMANTA & RAYCHAUDHURI (1983) and GARG *et al.* (2000) record this stratigraphical interval as conformable, the paleokarst features found show that a significant unconformity likely occurs between the Lakadong Limestone and Lakadong Sandstone. This must have involved a relative sea-level fall, limestone lithification and karstification, followed by inundation beneath sandy and coaly fluvial and swamp deposits. The timing of this probably corresponds to a globally recognized period of sea level fall between 55 and 53.2 Ma ago in the late Paleocene.

Figure 9: Quarry outcrop at Kurtinsiang showing pinnacle topography and sandstone infill on the top surface of the Lakadong Limestone.

5. Conclusion

Paleokarst phenomena are quite commonly found in the geological record and described in the literature, but the occurrence of sandstone-filled paleokarsts is relatively rare and not so well understood as breccia or shale filled ones. Further work is recommended to give a more detailed surface and subsurface evaluation in caves and quarries in the region between Sakwa and Kurtinsiang to provide further details for this interesting stratigraphical horizon and determine more fully its role in cave inception and development. The possibility for the observed phenomena to be formed in the subsurface rather than predominantly as an epikarst also needs consideration.

Acknowledgments

The author gratefully acknowledges support received from fellow cavers during the expedition cave exploration, surveying and photography and support of the Caving in the Abode of Clouds Project supported by the Meghalaya Adventurers Association, The Government of India Tourist Office and the State of Meghalaya State Tourisn Department.

References

ARBENZ T. (Ed. 2021) Cave Pearls of Meghalaya. A cave inventory covering the Jaintia Hills, Meghalaya, India. Vol. 3. South Shnongrim and the Um Thloo Cave System, Sielkan/Sakwa and the Pielkhlieng Pouk Cave System. Emetstrasse 34, 4713 Matzendorf, Switzerland.

GARG R., KHOWAJA-ATEEQUZZAMAN (2000) Dinoflagellate cysts from the Lakadong Sandstone, Cherrapunji area; biostratigraphical and palaeo-environmental significance and relevance to sea level changes in the Upper Palaeocene of the Khasi Hills, South Shillong Plateau, India. Palaeobotanist 49, pp 461-484.

SAMANTA B.K. & RAYCHAUDHURI A.K. (1983) A revised lithostratigraphical classification of the Cretaceous-Lower Tertiary shelf sediments of the Eastern Khasi and Jaintia Hills, Meghalaya. Quart. Jour. Geol. Min. Met. Soc. India, Vol. 55, No. 3, pp.101-129.

Structural control on the geomorphology of karst depressions and caves in the Burren, Ireland

Robert A. WATSON[(1)], Simone FIASCHI[(1)], Eoghan P. HOLOHAN[(2)] & John WALSH[(2)]

(1) School of Earth Sciences, robt.watson225@gmail.com, University College Dublin – Irlande
(2) Irish Centre for Research in Applied Geosciences (iCRAG), School of Earth Sciences, University College Dublin – Irlande

Abstract

The Burren in Co. Clare, Western Ireland, is world-renowned for its distinctive karst landscape of terraces, bare-rock pavements, clints and grykes. The Burren comprises a Lower Carboniferous limestone sequence within which there is a vertically-persistent suite of calcite and silica-rich veins. These veins are visible in aerial imagery as roughly N-S orientated lineaments, and they have been recently recognised as key structural controls on groundwater flow and on cave passages, of which over 60 km have been mapped. Our work examined the evidence for similar structural control on the Burren's surface karst features. High-resolution optical aerial imagery and associated digital surface models were acquired for the Burren's entire 250 km2 area in 2017. We have used these data, complemented by fieldwork, to develop an updated landform map and a revised morphological framework for the Burren's surface karst features. Over 2500 karst depressions were newly recorded, representing a 25-fold increase on the 109 dolines in an existing national database. Our new data demonstrate that the vein-associated lineaments are indeed a key control on the morphology and distribution of most of the newly mapped Burren dolines.

The paleocaves of Pierre-Saint-Martin/Larra massif (France/Spain). Mapping and diagnostic

Benjamin LANS[(1)], Richard MAIRE[(2)], Yves QUINIF[(3)] & Michel DOUAT[(4)]

(1) TRACES, UMR 5608 du CNRS, Université Jean Jaurès, 5 allées Antonio Machado, 31058 Toulouse, France. Email : benjamin.lans@gmail.com
(2) PASSAGES, UMR 5319 du CNRS, Université Bordeaux-Montaigne, 12 Esplanade des Antilles, 33607 Pessac cedex, France.
(3) Service de Géologie fondamentale et appliquée, Faculté Polytechnique, Université de Mons, Rue de Houdain, 9, 7000-Mons, Belgium
(4) ARSIP (Association pour la Recherche Spéléologique Internationale à la Pierre Saint Martin), France

Abstract

The Pyrenean Pierre-Saint-Martin/Larra massif presents more than 465 km of surveyed caves. But at the surface of this well-known karstic mountain area, we can observe "cemeteries" of unroofed and open-air palaeocaves, due to the erosion/dissolution of cretaceous limestones since the Mio-Pliocene. An accurate mapping of these palaeocaves is actually done by remote sensing, in addition to essential field work. Indeed, walls and ground of palaeocaves have not the same micro-topographic characteristics (e.g. roughness) than the surrounding limestone. Those small differences are detected and quantified on the very high-density LIDAR full cover. Moreover, palaeo-speleothems can be detected and localized by the mean of spectral indices analysis, on very high resolution orthophotography and satellite imagery. Some palaeo-galleries have a development of several hundred meters, and show ancient stalagmitic massifs. The first U/Th dating indicate ages older than 400 000 years. An illustration is given by the Lepineux pit, which is extended at the surface by unroofed palaeo-pits, presenting old concretions. Those palaeo-speleothems situated at the surface indicate a pre-ice age, when the entire massif was at a lower elevation, with a forest and a pedologic cover, very favourable to the concretion formation.

Karst Development on the Southern Peninsula of Haiti

Patricia KAMBESIS

Center for Human GeoEnvironmental Studies, Western Kentucky University – United States

Abstract

In the Republic of Haiti's southern peninsula, the mountains making up the backbone of the region are predominantly limestone interspersed with some volcanics and small coastal plains. Coastal areas consist of uplifted reef terraces that also occur on small islands off the coast. The mountainous areas of the region are dominated by fluvial karst consisting of spectacular cone karst, deep sinkholes, sinking streams, caves, and resurgences that emerge along river beds and the fringing coastal plains. The uplifted reef terraces reflect changes in sea level during the Pleistocene and have been karstified by coastal mixing zones resulting in flank margin caves. Wave action on the southern coasts and islands resulted in littoral cave development as well as overprinting of littoral process on flank margin caves. The first documented modern cave explorations were undertaken in the early nineteen eighties and the late nineteen nineties respectively. More systematic and detailed studies on the caves and karst of Haiti were initiated in 2007. The results of that work show that a complex interplay of geology and speleogenetic processes have shaped the physical expressions of cave and karst development on the southern peninsula of Haiti.

Entangling the influence of the last deglaciation on a complex cave system: Grønli-Seter cave system, Northern Norway

Rannveig SKOGLUND[(1)], Stein-Erik LAURITZEN[(2,3,4)], Sara SKUTLABERG & Hilde HESTANGEN

(1) Department of Geography, rannveig.skoglund@uib.no, University of Bergen – Norvège
(2) Earth Science, Bergen University – Norvège
(3) SapienCe (Centre for Early Sapience Behaviour), University of Bergen – Norvège
(4) Centre for Ecological and Evolutionary Synthesis (CEES), Department of Biosciences, University of Oslo, 0316 Oslo – Norvège

Abstract

Pleistocene glaciations had a strong influence on landscape and cave development in high latitudes. Fjords, U-shaped valleys, glacial troughs and hanging valleys are typical glacial erosion features in a landscape shaped by continental glaciations. While glaciofluvial terraces, deltas and marine deposits witness shifting base levels during the deglaciation and the Holocene, glacial cycles induce repeated changes in the hydraulic regime, sediment availability and base level in adjacent caves. Grønli-Seter cave system comprises more than 8 km of passages with maze sections and trunk passages forming phreatic loops. The cave system is situated close to the interface between the calcite marble and the overlying mica schist. Scallops in the cave walls demonstrate an ascending water flow, evidence of subglacial speleogenesis under a topographically guided valley or outlet glacier. However, thorough inspections of the cave morphology, including meso- and microforms, and sediment facies, indicate several hydrological phases, from stagnant conditions identified by clay cap mud to excessive flow rates identified by boulders imbricated in a rising setting. Linking cave morphology and deposits to shifting base levels during the last deglaciation and the Holocene may provide new insight into how previous deglaciations and interglacials influenced the caves system.

Symposium 04 – special session

Hypogene karst

Introduction to Hypogene karsts session

Philippe AUDRA

Univ. Côte d'Azur, France

English

Previously limited to a few emblematic exotic cases, such as the hydrothermal caves of Budapest, the mine-caves associated with mineralizations in Central Asia, a few sulfuric caves such as Lower Kane Caves in Wyoming, and of course Lechuguilla Cave in New Mexico, to which were added the giant gypsum labyrinths in Ukraine, formed by upflows, the identification and characterization of hypogenic speleogenesis has made a considerable jump forward in the last two decades.

Since these pioneering works, the conceptual synthesis of our Ukrainian colleague A. Klimchouk, *Hypogene Speleogenesis*, published in 2007, has prompted a re-examination of the origin of many caves, finally leading to the recognition that, on a global scale, about 10-15% of them are partly or entirely of hypogenic origin. The magnitude of the cases identified led to the publication ten years later, under the direction of the same author, of a monumental synthesis, *Hypogene karst regions and caves of the world*, which illustrates the ubiquity of hypogenic caves, the diversity of processes, and the resulting specific morphologies and mineralogies.

This session presents some works illustrating the principal areas of current investigations:

- the origin of the sources of aggressiveness (magmatic and volcanic, thermochemical sulfate reduction (TSR), oxidation of diffuse sulfides, cooling of hydrothermal upflows, mixing of different waters including marine and continental, carbonic degassing, hydrocarbon leakages…);
- the expression contexts integrating geodynamic aspects, regional hydrogeology, local structural and petrographic characteristics;
- morphologies of networks and conduits, including in active and subaqueous cavities, specific mineralizations resulting from hypogenic speleogenesis processes;
- analytical, hydrochemical and especially isotopic approaches to precisely characterize the processes, which sometimes follow one another over complex cycles;
- geochemical and morphometric modeling to better constrain the action of the processes and their morphological role;
- finally, these hypogenic caves play a role as a record of past landscape evolution, and have sometimes even been the driving force behind major morphogenic processes such as the entrenchment of canyons, and make it possible to approach chronological aspects over extended periods of time, or sometimes flash times due to the rapidity of sulfuric corrosion processes (SAS).

The case studies presented, from most continents, reflect the problematics of this field, which has now reached scientific maturity in the short time since the beginning of the 20th Century, both from a conceptual point of view and by using the most effective methods, and which concerns a significant part of the study of karsts and cavities, with major operational implications.

Français

Auparavant limitée à quelques cas exotiques emblématiques, telles que les cavités hydrothermales de Budapest, les grottes-mines associées à des minéralisations d'Asie centrale, quelques cavités sulfuriques comme Lower Kane Caves dans le Wyoming, et bien sûr Lechuguilla au Nouveau-Mexique, auxquelles s'ajoutaient les labyrinthes géants de gypse en Ukraine, formés par des flux ascendants, l'identification et la caractérisation de la spéléogenèse hypogène à fait un bond considérable ces deux dernières décennies.

Depuis ces travaux précurseurs, la synthèse conceptuelle de notre collègue ukrainien A. Klimchouk, *Hypogene Speleogenesis*, parue en 2007, a suscité un réexamen de l'origine de nombre de cavités, aboutissant finalement à la reconnaissance qu'à l'échelle de la Planète, environ 10-15% d'entre elles sont partiellement ou totalement d'origine hypogène. L'ampleur des cas identifiés a conduit à la publication dix ans plus tard, sous la direction du même auteur, d'une synthèse monumentale, *Hypogene karst regions and caves of the world*, qui illustre l'ubiquité des cavités hypogènes, la diversités des processus, et les morphologies et minéralogies spécifiques résultantes.

Cette session présente quelques travaux illustrant les principaux domaines d'investigation actuels :

- l'origine des sources d'agressivité (magmatique et volcanique, réduction thermochimique des sulfates enfouis (TSR), oxydation des sulfures diffus, refroidissement des remontées hydrothermales, mélanges d'eaux de nature différente y compris marine et continentales, dégazage carbonique, fuites d'hydrocarbures, etc.) ;
- les contextes d'expression intégrant les aspects géodynamiques, l'hydrogéologie régionale, les caractéristiques structurales et pétrographiques locales ;
- les morphologies des réseaux et des conduits, y compris dans les cavités actives et subaquatiques, les minéralisations spécifiques résultants des processus de spéléogenèse hypogène ;
- les approches analytiques, hydrochimiques et notamment isotopiques permettant de caractériser précisément les processus, qui se sont parfois succédés sur des cycles complexes ;

- les modélisations géochimiques et morphométriques permettant de mieux contraindre l'action des processus et leur rôle morphologique ;
- enfin, ces cavités hypogène jouent un rôle d'enregistreur des évolutions paysagères passées, parfois même ont été moteurs des grands processus morphogéniques comme le creusement de canyons, et permettent d'aborder les aspect chronologiques, sur des temps longs, ou parfois des temps-éclairs dues à la rapidité des processus de corrosion sulfuriques (SAS).

Les cas d'étude présentés, issus de la plupart des continents, reflètent les problématiques de ce domaine ayant atteint en peu de temps de ce début du XIX^{e} siècle une maturité scientifique, tant du point de vue conceptuel que des méthodes employées les plus performantes, et qui concerne une part significative de l'étude des karsts et des cavités, avec des implications opérationnelles majeures.

Aziza cave, Photo M. Renda

Dissolution-corrosion measurements with limestone and gypsum tablets in active sulphuric acid caves of southern Italy

Ilenia M. D'ANGELI[(1)], Mario PARISE[(2)], Marco VATTANO[(3)], Giuliana MADONIA[(3)] & Jo DE WAELE[(1)]

(1) Dipartimento di Scienze Biologiche, Geologiche e Ambientali, Università di Bologna, jo.dewaele@unibo.it (corresponding author), dangeli.ilenia89@gmail.com
(2) Dipartimento di Scienze della Terra e Geoambientali, Università di Bari, mario.parise@uniba.it
(3) Dipartimento di Scienze della Terra e del Mare, Università di Palermo, marco.vattano@unipa.it, giuliana.madonia@unipa.it.

Abstract

Dissolution-corrosion (DC) represents an important factor for speleogenesis, and can be measured monitoring weight variation over time of carbonate and gypsum tablets exposed in underground environments. The oxidation of H2S produces H2SO4, which in carbonate host rock induces the surface of carbonate tablets to be rapidly corroded by sulphuric acid, whereby CaCO3 is replaced by CaSO4·2H2O, producing a significant weight gain. We describe preliminary results of DC monitoring in four still-active SAS systems, including Ninfe Cave and Terme Sibarite (Calabria), Fetida Cave (Apulia), and Acqua Fitusa Spring Cave (Sicily). The tablets have been set inside the caves, in three different conditions of exposure (i.e. underwater, air, interface zone) in the winter 2015-2016 to monitor DC in five years. The results show how the condition of exposure is an important control for the behaviour of weight variation. Tablets set underwater displayed significant weight loss during the first period of exposure, whereas those located at the interface zone exhibited a tendency of weight variation significantly dependent on time, and tablets in air showed weight gain.

1. Introduction

Dissolution-corrosion (DC) represents the key process to understand the speleogenesis and evolution of karst systems (GABROVŠEK & PERIC, 2006). Generally, in caves, geomorphological changes are slow and invisible, but observable over long time scales (PRELOVŠEK, 2012).

DC rates can be measured using: 1) micro-erosion meter (MEM) (HIGH & HANNA, 1970; MIHEVC, 2001) or Traversing micro-erosion meter (TMEM) (TRUDGILL *et al.*, 1981), 2) rock tablets (SWEETING, 1979), and 3) hydrogeological methods (CORBEL, 1959; PULINA & SAURO, 1993; FORD & WILLIAMS, 2007).

Rock tablets measure the weight loss throughout cave exposure. Weight loss/gain is calculated using a weight scale, and it is more precise than micrometer measurements. Since the size of the exposed surface is known, it is possible to convert weight loss into metric units, comparable to MEM measurements and hydrogeological balance calculations.

For sulphuric acid caves the most important factor is the oxidation of H_2S into H_2SO_4, which immediately tends to corrode carbonate rocks both underwater or in aerate conditions. In aerate conditions, calcium carbonate ($CaCO_3$) is replaced by gypsum ($CaSO_4 \cdot 2H_2O$), the most common secondary mineral in sulphuric acid speleogenetic (SAS) caves. In addition, active sulphuric acid caves are influenced by microbiological extremophiles which colonize waters, walls and ceilings (D'ANGELI et al. 2019b).

The study of DC rate in still-active SAS caves can give significant information on the evaluation of the different stages of cave formation, and to correlate them with landscape evolution (GALDENZI *et al.*, 1997; MARIANI *et al.*, 2007; GALDENZI, 2012).

Italy hosts 25% of the SAS caves known worldwide, and several of them are still-active (D'ANGELI *et al.*, 2019). Investigations on DC rates began in the winter 2015-2016, and are still ongoing in the following SAS caves of southern Italy (Fig. 1): 1) Ninfe Cave (Cerchiara di Calabria) and Terme Sibarite (Cassano allo Ionio) in Calabria; 2) Fetida Cave (Santa Cesarea Terme) in Apulia; 3) Acqua Fitusa Spring Cave (San Giovanni Gemini) in Sicily. The preliminary results of our DC monitoring are shown in this work.

Figure 1: Study area displaying caves location.

2. Materials and methods

Limestone, marble and gypsum tablets (7x4x1 cm with an initial mean weight of 74 g) were produced and placed in several locations of the caves (Fig. 2) to observe eventual differences in DC rate in various environmental conditions: 1) underwater (10-20 cm below water table); 2) at the water-air interface; 3) in the cave atmosphere (Fig. 2). In each site, we placed 2 tablets each per lithology: a) selenitic gypsum (G); b) Istria limestone (I); c) Carrara marble (M); and for Fetida and Acqua Fitusa Spring caves, also host rock which are, respectively, d) Altamura limestone (C) and Rudist breccias member of the Crisanti Formation (B).

In Fetida Cave the experiment started in October 2015 and it is still ongoing. Here two sites were monitored, both located in the innermost portion (B1 and B2), where we observe evidences of rising sulphidic waters (B1). In addition, in B2, three limestone tables were set horizontally in aerate conditions to observe possible changes of DC rate due to space orientation of the exposed surface.

In Fitusa, Terme Sibarite, and Ninfe caves the experiments started at the beginning of January 2016 and are still ongoing. Here the tablets were placed in a single site. In Acqua Fitusa Spring Cave, tablets were placed in the lower still-active level, where the sulphidic water table is currently located (Fig. 2E). In the Terme Sibarite Cave, tablets were placed in a small water body (Fig. 2B), and in Ninfe Cave in the innermost zone (Fig. 2A).

In all these locations, we also carried out water sampling. Water parameters (pH, T, EC) were measured using the multiparameter sensor Hanna HI991001, and in each location two samples (250 ml) were collected, one of which was acidified with 65% HNO_3. Water samples were analyzed in the laboratories of Politecnico di Torino. The saturation analysis showed (following Debye-Hückel equation) the index for calcite to be slightly undersaturated in almost all the locations, excluding Ninfe Cave which was oversaturated. Saturation index for dolomite was close to the equilibrium state, and for gypsum was undersaturated.

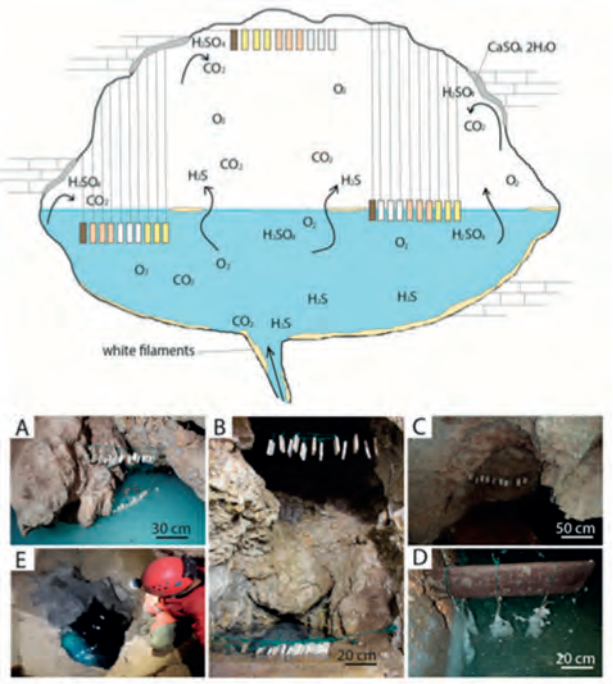

Figure 2: Sketch showing how tablets were placed in a cross-section. Pictures: A) Ninfe Cave; B) Terme SIbarite; C and D) Fetida Cave; E) Acqua Fitusa Spring *Cave.*

3. Results

Gypsum tablets showed different rates of dissolution depending on environmental conditions (i.e. underwater, interface water-air, air). In Fetida Cave (B1 and B2) gypsum weight loss reached a mean of 92% in 33 days in underwater conditions, and 60% at the interface. In aerate conditions the dissolution was slower: as a matter of fact, we observed 0.49% in 601 days of exposure.

In Terme Sibarite, in 2 days we recorded weight loss of 59 and 35%, respectively underwater and at the interface, whereas in Ninfe Cave in 10 days the loss reached 36% underwater and 5% at the interface.

In Acqua Fitusa Spring Cave, gypsum tablets after 40 days totally disappeared (100%), whilst at the interface and in aerate conditions they showed values of 72 and 0.9% respectively.

Significant is the weight variation of carbonate limestones in Fetida Cave (Fig. 3A-B). The DC in B1 (Fig. 3A) exhibited higher values than in B2 (Fig. 3B); the weight loss reached 7% in 837 days of exposure. In B1, DC underwater is higher during the first part of the monitoring, whilst after 582 days in the cave an inversion of tendency was visible, and weight loss at the interface became higher.

Tablets in aerate conditions showed an initial weight loss, followed by weight gain. In B2, DC at the interface was higher than underwater, and this tendency was quite stable over time. In aerate conditions, tablets set horizontally (Ch) showed a significant weight loss in the first part of the monitoring, followed by weight gain. The general behaviour for the tablets in air, both horizontally and vertically oriented was similar; however, those horizontally oriented showed a higher weight loss (see cyan line in Fig. 3B). The weight variation observed in Terme Sibarite (Fig. 3C) exhibited higher values of DC underwater. In Ninfe Cave (Fig. 3D) the dissolution of marble was faster with respect to Istria limestone, both underwater and at the interface. In Acqua Fitusa Spring Cave the Carrara marble was the only lithology showing a certain degree of DC, which was exclusively visible at the interface zone (Fig. 3E). In Terme Sibarite, Ninfe Cave, and Acqua Fitusa Spring Cave it was difficult to observe weight variation in aerate conditions.

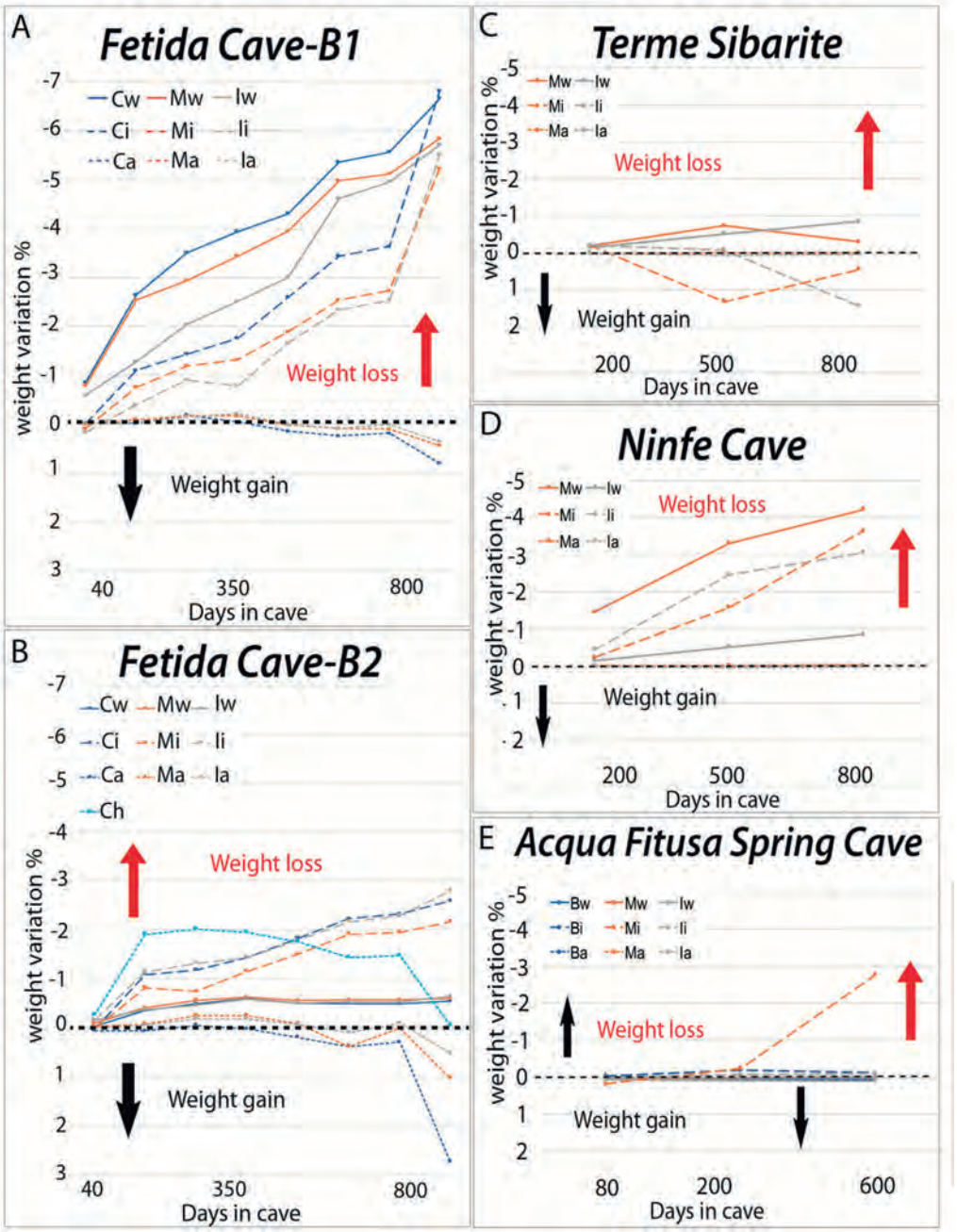

Figure 3: Weight variation (%) of tablets over time (days of exposure in cave), in A) Fetida Cave, monitoring site B1 (close to a sulphidic spring); B) Fetida Cave, monitoring site B2 (in the innermost portion of the cave); C) Terme Sibarite; D) Ninfe Cave; E) Acqua Fitusa Spring Cave. "C" means Altamura limestone and "B" Rudist breccias member of the Crisanti Formation (both host-rocks), "M" Carrara Marble, "I" Istria limestone, whereas "w" means underwater, "I" interface, and "a" air, "h" means horizontally oriented (cyan colour). Colours and lines help to discriminate lithologies (blue, orange, grey) and environmental conditions of exposure (continuous line means underwater, dashed line interface, dotted line air). Red arrow shows the area of weight loss and the black line the weight gain area.

4. Discussion and Conclusions

Field monitoring of DC and laboratory measurement of weight variation showed interesting results, demonstrating the importance of environmental parameters, essential key factors for the weight loss/gain. Overall, the gypsum tablets underwater and at the interface were easily dissolved, especially due to the undersaturation of water solution with respect to gypsum. As a matter of fact, the weight loss in aerate conditions was significantly lower.

In Calabria and Sicily, the DC rate seems to be controlled by lithology, and the weight loss of marble is favoured with respect to the other lithologies. In Terme Sibarite and in

Ninfe Cave, the dissolution is faster underwater, whereas in *Acqua Fitusa Spring* Cave it was faster at the interface.
The investigations carried out in Fetida Cave demonstrated the DC to have a different behaviour as a function of the vicinity to the sulphidic spring (located in B1). The average value of weight loss reached 7% close to the sulphidic spring (B1). In the first stages of monitoring (before 582 days of exposure), DC underwater was faster, whilst after day 582, DC became higher at the interface. On the contrary, in B2, located in the innermost portion of the cave, the higher DC was observed at the interface throughout the whole exposure. Overall, in aerate conditions it is possible to observe an initial weight loss, followed by weight gain. This behaviour is linked to the interaction of H_2SO_4 with the external surface of tablets, which tends to dissolve carbonate producing weight loss. Then the dissolved ion of carbonate (CO_3^{2-}) is replaced with SO_4^{2-} inducing the precipitation of gypsum ($CaSO_4 \cdot H_2O$), and subsequent weight gain of the tablet.
Significant is the weight loss observed on the horizontally oriented tablets in B2. From Figure 3B it is possible to observe how a few months after the exposure, the weight loss reached an average of 2%, due to the falling of gypsum moonmilk (pH 0-1) from the upper surface of tablets. After moonmilk removal, the weight variation exhibited the same tendency of the vertically oriented tablets (in aerate conditions).
The field monitoring of DC and weight loss/gain in the aforementioned systems will end in 2021, and final results will allow to clarify these preliminary outcomes.

Acknowledgments

Thanks to all the people who helped us during the field monitoring and documenting the cave environments. In particular, we thank Orlando Lacarbonara, Rosangela Addesso, Isabella Serena Liso, Luca Pisano, Marianna Mazzei. Thanks to Sergio Pispico to Santa Cesarea Terme spa director. Thanks to Giuseppe Martire, Carlo Forace, to the "Associazione Speleologica Liocorno" and to Terme Sibarite spa director. Thanks to Antonio Cesarini, and to the whole caving group of "Serra del Gufo".
Thanks to the members of the "Le Taddarite" of Palermo speleological association.
Thanks to Bartolomeo Vigna and Adriano Fiorucci from Politecnico di Torino for the geochemical analysis of water samples. Ilenia D'Angeli thanks the "Lions Club Megaride" (district 108 YA) and the "Stazione Zoologica Anton Dohrn" for the financial support in the framework of the "Paolo Brancaccio" award.

References

CORBEL, J. (1959). Erosion en terrain calcaire. Annales de Géographie, 68, 97-120.

D'ANGELI IM., PARISE M., VATTANO M., MADONIA G., GALDENZI S., DE WAELE J., (2019) Sulfuric acid caves of Italy: A review. Geomorphology, 333, 105-122.

D'ANGELI IM, GHEZZI D., LEUKO S., FIRRINCIELI A., PARISE M., FIORUCCI A., VIGNA B., ADDESSO R., BALDANTONI D., CARBONE C., MILLER AZ., JURADO V., SAIZ-JIMENEZ C., DE WAELE J., CAPPELLETTI M., (2019b) Geomicrobiology of a seawater-influences active sulfuric acid cave. PLoS ONE, 14(8): e0220706.

FORD D., WILLIAMS P., (2007) Karst hydrogeology and geomorphology. John Wiley & Sons, 562 p.

GABROVŠEK F., PERIC B. (2006) Monitoring the flood pulses in the epiphreatic zone of karst aquifer. Acta Carsologica, 35(1), 35-45.

GALDENZI S. (2012) Corrosion of limestone tablets in sulfidic ground-water: measurements and speleogenetic implications. International Journal of Speleology, 41(3), 149-159.

GALDENZI S., MENICHETTI M., FORTI P. (1997) La corrosione di placchette calcaree ad opera di acque sulfuree: dati sperimentali in ambiente ipogeo. In: P.Y. JEANNIN (Ed.), Proceedings of the 12th International Congress of Speleology, La Chaux-de-Fonds, 1, 187-190.

HIGH C.J., HANNA K. (1970) A method for the direct measurement of erosion on rock surface. British Geomorphological Research Group, Technical Bulletin 5.

MARIANI S., MANIERO M., BARCHI M., VAN DER BORG K., VONHOF H., MONTANARI A. (2007). Use of the speleogenetic data to evaluate Holocene uplifting and tilting: an example from the Frasassi anticline (northeastern Apennines, Italy), Earth Planetary Science Letters, 257(1-2), 313-328.

MIHEVC A., (2001) Speleogeneza Divakega krasa. Zalozba ZRC, Ljubljana, 148 p. šGypsum caves as indicators of climate-driven river incision and aggradation in a rapidly uplifting region. Geology, 43, 539-542.

PULINA M., SAURO U. (1993) Modello dell'erosione chimica potenziale di rocce carbonatiche in Italia. Memorie della Società Geologica Italiana, 313-323.

PRELOVŠEK M. (2012) The dynamics of the present-day speleogenetic processes in the stream caves of Slovenia. Carsologia, 15, 152 p.

SWEETING M.M. (1979) Solution and erosion in the karst of Melinau limestone in Gunung Mulu national park, Sarawak, Borneo. Proceeding of the 4th International Congress of Speleolgy in Yugoslavia. Lubljana, 227-232.

TRUDGILL, S., HIGH, C.J., HANNA, F.K. (1981). Improvements to the micro-erosion meter. British Geomorphological Research Group Technical Bulletin, 29, 3-17.

Point distribution statistics of mesoscale dissolutional forms in caves: the analysis of feeder landmarks

Georgios LAZARIDIS[(1)], Despina DORA[(2)] & Konstantinos VOUVALIDIS[(3)]

(1) Aristotle Univeristy of Thessaloniki, School of Geology, Thessaloniki, 54124, Greece, geolaz@geo.auth.gr (corresponding author)
(2) Aristotle Univeristy of Thessaloniki, School of Geology, Thessaloniki, 54124, Greece, despdora@geo.auth.gr
(3) Aristotle Univeristy of Thessaloniki, School of Geology, Thessaloniki, 54124, Greece, vouval@geo.auth.gr

Abstract

In this work, the distribution of feeders is statistically investigated. Feeders are conduits that represent basal input points in hypogene speleogenesis. These forms may be clustered or overdispersed. Their "random or systematic" distribution is already discussed by KLIMCHOUK in "Morphogenesis of hypogenic caves" (2009), who provides two excellent examples of maps with feeder locations from the Ozerna Cave (Ukraine) and Coffee Cave (USA). The first cave seems to follow a "random" pattern (207 feeders), whereas the second cave shows two distinct clusters (129 feeders). Another example comes from the underwater cave Ordinskaya in Russia (SIVINSKIH, 2009). Using this dataset, two-dimensional landmarks are created for the feeders. Nearest-neighbor analysis is used to test the distribution. The results are similar in all caves, where there is statistically significant clustering of feeders. Directional data from the previous analysis are further tested to investigate whether they are randomly distributed. Furthermore, the datasets compared with a random point pattern with Correlation Length Analysis. These results can be used on modeling hypogene caves; to investigate new questions such as what causes point clustering etc. Points and landmarks have not been extensively used in cave morphometry, but it can be suggested that there is a good potential to provide useful information.

1. Introduction

Cave morphometrics use a number of parameters in order to compare and characterize caves' shapes, dimensions and patterns (KLIMCHOUK, 2004). The parameters are obtained from the quantification of shapes and the geometry of all those cave features derived from speleogenetic processes. Analysis and comparison of shapes are tools for identification and categorization of features, but they are also tools of decoding formation mechanisms. PICCINI (2011) suggested that morphometric indices could be used to classify caves based on their genetic category.

This research is being introduced to the use of landmarks in the field of cave morphometrics. Landmarks are Cartesian coordinates representing points in 2 or 3 dimensions which can be used for the location of these points in space and their graphic representation. As landmarks are representing points, their graphical display will reflect their spatial distribution and the dataset of points can be further investigated in terms of their distribution pattern.

Spatial distribution analysis has been used before in the wider field of cave research (SHOFNER *et al.*, 2001; WEINER *et al.*, 2002; BALDINI *et al.*, 2006; FERNANDEZ-CORTES *et al.*, 2006; CAI *et al.*, 2009; PERRETTE & JAILLET, 2010; ZHOU *et al.*, 2017; PRELOVŠEK *et al.,* 2018) and much lesser in the field of karst morphometry (*e.g.* DENIZMAN, 2003; VERBOVSEK, 2007), but statistical analysis of spatial distributions is an underdeveloped area within cave morphometrics.

This study applies a solid statistical analysis to the spatial distribution of feeders from hypogene caves. Feeders are morphological features developed by dissolution in hypogene speleogenesis. They are conduits through which fluids rise from the source aquifer and thus they represent basal input points. These forms may be clustered or overdispersed. Their "random or systematic" distribution is already mentioned by KLIMCHOUK (2009). Feeders define the distribution and geometry of cave passages (FRUMKIN, 2009). The consolidation of the statistical analysis of the spatial distribution with the use of landmarks in the methods of cave morphometry is discussed, but also their potential to describe, differentiate and maybe interpret cave types and features.

2. Methods

Definitions of point distribution pattern can be found in DAVIS (1986): **Uniform** point pattern means that their density in any subarea is equal to the density of points in all other subareas (same size and shape assumed). A **regular** point pattern appears when the distance between a point i and a point j lying in the specified direction from i, is the

same for all pairs of points i and j. A regular pattern is also uniform, but the converse may not be true. **Random** pattern is defined when any subarea is as likely to contain a point as any other subarea (same size assumed) regardless of its location. In such a random pattern the placement of a point is not related to the placement of any other point. In a **clustered** pattern of points, the probability of a point placement is inversely related to the distances of preexisting points. KLIMCHOUK (2009) provides two excellent examples of partial maps with feeder locations from the Ozerna Cave (Ukraine) and Coffee Cave (New Mexico, USA). The first cave seems to follow a "random" pattern, whereas the second cave shows two distinct clusters, the west and northeast one. Furthermore, Coffee Cave feeders consist of those developed at the lower level and those at the upper levels (STAFFORD *et al.*, 2008) and they are also examined separately. Note that, although feeders smaller than 10 cm are abundant in the cave, they are not surveyed due to map scale (STAFFORD *et al.*, 2008). Another example comes from the underwater cave Ordinskaya in Russia (SIVINSKIH, 2009). Using these maps, two-dimensional landmarks are created for the feeders with the use of TPS software. These landmarks represent not georeferenced points that are in scale (in meters). Feeder density is drawn in Kernel density maps. In general, the size of the feeders is small compared with the distance between them, allowing them to be approximated as points. To test the spatial distribution of feeders, nearest-neighbor analysis is used. The null hypothesis of randomly and independently positioned points, the so-called Poisson pattern, is tested. The R, nearest-neighbor statistic (index) is estimated as the ratio of mean nearest-neighbor distance to the mean expected distance for the Poisson pattern. Values range from 0 for all points coinciding to 2.15 for a hexagonal array of maximally dispersed points. The Poisson pattern corresponds to R=1. Donelly's edge correction is used. The area is estimated by a convex hull method that corresponds to the smallest convex polygon enclosing the points. Directional data from nearest-neighbor analysis are further tested to investigate whether they are uniformly distributed, or preferred orientations can be assumed. A combination of Rayleigh's and Chi-square tests are used. Correlation length analysis is used to investigate the spatial distribution of the point patterns at different scales. Analyses were performed in PAST 4.04 (HAMMER *et al.*, 2001), with a level of significance set at α=0.05.

3. Results

Landmarks extracted from the mapped caves are shown in scatter diagrams (Fig. 1). In total, 207, 129 and 157 landmarks were created for the Ozerna Cave, Coffee Cave and Ordinskaya Cave, respectively. Regarding the nearest-neighbor analysis the following results are derived. In Ozerna Cave the area of the partial map is estimated by the algorithm to be 0.062 km^2. This represents about 8% of the cave (the area of the polygon cave field is estimated to be 0.74 km^2 in KLIMCHOUK, 2006). Mean feeder density in that area is 0.0033. The mean nearest-neighbor distance is 7.95 m for the feeders in Ozerna Cave. The expected nearest-neighbor distance for a Poisson pattern is 9.05 m. Therefore, the R-value is 0.88 indicating a statistically significant clustering of feeders (p[random]=1.8×10^{-4}). Coffee Cave is represented by an area of 0.072 km^2 and a mean density of 0.0018. The R-value is 0.60 indicating a statistically significant clustering of points with a mean nearest-neighbor distance of 7.53 m (p[random]=1.8×10^{-15}). The same results are extracted when testing separately the distribution of feeders in the lower and upper levels of the cave. However, mean density in the lower level is more than three times lower than that of the upper one. Similarly, in Ordinskaya Cave the mean nearest-neighbor distance is 18.83 m, mean density is 0.0006 and the area is 0.26 km^2. The R-value is 0.88 due to statistically significant clustering (p[random]=0.006).

Directional data from the previous analysis are subjected to further analysis in order to investigate if the directions are randomly distributed. In both Ozerna Cave and Ordinskaya Cave a null hypothesis of uniform distribution cannot be rejected, indicating that preferred directions are not statistically significant. This is not true for Coffee Cave, where the existence of two or more preferred directions is statistically significant. However, when the levels are tested individually random directions cannot be rejected.
Furthermore, comparison of the data sets with a random point pattern is done with Correlation Length Analysis. In Ozerna Cave and Ordinskaya Cave the possibility of random distribution is rejected, whereas it is statistically significant for Coffee Cave in total and when the two levels are separately tested.

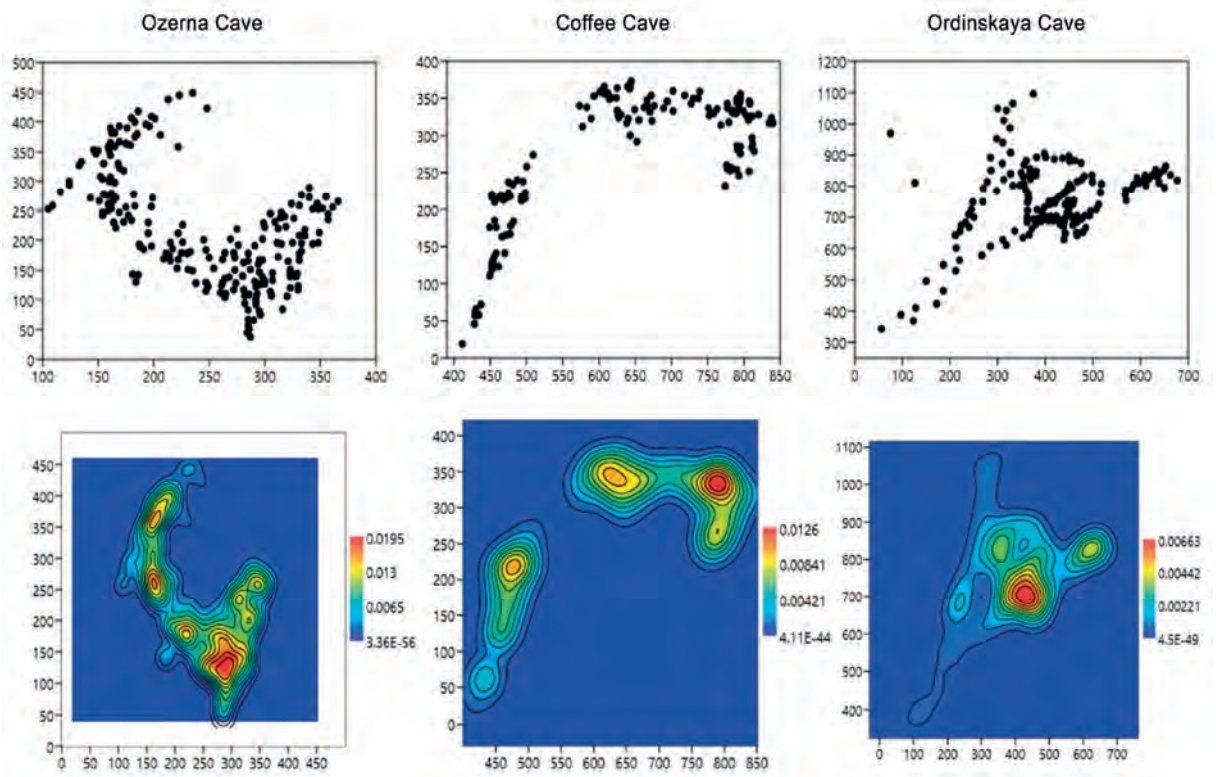

Figure 1: Scatter diagrams and kernel density maps of feeder landmarks in Ozerna Cave, Coffee Cave and Ordinskaya Cave. Data extracted from maps published by KLIMCHOUK (2009) and SIVINSKIH (2009).

4. Discussion and conclusion

Nearest-neighbor analysis uses distances between closest points instead of the number of points in subareas and this produces results that are independent of scale. Regarding the scale, however, at least in one of the examined cases (Coffee Cave, STAFFORD *et al.*, 2008) smallest in size feeders have been excluded from the survey. The nearest-neighbor index (R) that is calculated can be compared from area to area (FORD, 2003). The clustered pattern of feeder distribution indicates that they are more likely to be formed in the vicinity of others. This, however, does not exclude their formation in new locations.

Directional statistics are used to examine possible alignments of points. Such alignment detections may reflect some relation with underlying features such as tectonic discontinuities (HAMMER, 2009). Analysis of feeders supports a random distribution that means there is no preferred direction for their development, even though passages are developed mainly along tectonic discontinuities. In the case of Coffee Cave two or more preferred directions indicate that in none of the examined cases there is a dominating direction. In total, no single fracture set guides the distribution of feeders.

Controls other than fracture geometry may be responsible for the distribution of feeders. In general, lithological, and hydrological criteria also play a key role in the formation of caves. Since there is no reference from the examined caves as well as from field work in Greek hypogene caves (*e.g.* LAZARIDIS, 2017) of any specific observation for lithological control that favors the feeders' formation, the hydrological control is suggested to be the dominant factor. This could be related to the locations of early communication among the various aquifers during the transverse-hypogene speleogenesis.

Points have not been extensively used earlier in cave morphometry, but it can be suggested that there is a good potential to describe, differentiate and maybe interpret cave types and features. The use of landmarks provides the advantage that they can be extracted from any cave map even without georeference (*e.g.* old cave surveys) and the nearest-neighbor analysis can be applied directly on such data sets.

References

BALDINI J. U., BALDINI L. M., MCDERMOTT F., CLIPSON N. (2006) Carbon dioxide sources, sinks, and spatial variability in shallow temperate zone caves: evidence from Ballynamintra Cave, Ireland. Journal of Cave and Karst Studies, 68(1), 4-11.

CAI B. G., SHEN L. M., ZHENG W., LI K. P., BAI Y. Z., DONG, C. Z. (2009) Spatial distribution and diurnal variation in CO_2 concentration, temperature and relative humidity of the cave air-A case study from Water Cave, Benxi, Liaoning. China, 4.

DAVIS J.C. (1986) Statistics and Data Analysis in Geology. John Wiley & Sons, New York.

DENIZMAN C. A. N. (2003) Morphometric and spatial distribution parameters of karstic depressions, Lower Suwannee River Basin, Florida. Journal of cave and karst studies, 65(1), 29-35.

FERNANDEZ-CORTES A., CALAFORRA J. M., SANCHEZ-MARTOS F. (2006) Spatiotemporal analysis of air conditions as a tool for the environmental management of a show cave (Cueva del Agua, Spain). Atmospheric Environment, 40(38), 7378-7394.

FORD R.L. (2003) Nearest-neighbor analysis and karst geomorphology: an introduction to spatial statistics: Geological Society of America Abstracts with Programs, v. 35, no. 6, p. 46.

FRUMKIN A. (2009) Active hypogene speleogenesis and the groundwater systems around the edges of anticlinal ridges. Hypogene Speleogenesis 137-149.

HAMMER Ø. (2009) New methods for the statistical analysis of point alignments. Computers & Geosciences 35:659-666.

HAMMER Ø., HARPER D. A., RYAN P. (2001) PAST: Paleontological Statistics Software Package for Education and Data Analysis Palaeontologia Electronica, 4(1), 1-9.

KLIMCHOUK A. (2009) Morphogenesis of hypogenic caves. Geomorphology, 106(1-2), 100-117.

KLIMCHOUK A. B., FORD D. C., PALMER A. N., DREYBRODT W., MIICKE B., VOLKER R., ... ZUPAN HAJNA N. (2004) Morphometry of caves. Journal of Geology, 6(2), 675-811.

LAZARIDIS G. (2017) Hypogene Speleogenesis in Greece. In A. Klimchouk, A. N. Palmer, J. De Waele, A. S. Auler & P. Audra (Eds.), Hypogene Karst Regions and Caves of the World (pp. 225-239): Springer.

MITTEROECKER P., GUNZ P. (2009) Advances in geometric morphometrics. Evolutionary biology, 36(2), 235-247.

PERRETTE Y., JAILLET S. (2010) Spatial distribution of soda straws growth rates of the Coufin Cave (Vercors, France). International Journal of Speleology, 39(2), 2.

PICCINI L. (2011) Recent developments on morphometric analysis of karst caves. Acta Carsologica, 40(1).

PRELOVŠEK M., ŠEBELA S., TURK J. (2018) Carbon dioxide in Postojna Cave (Slovenia): spatial distribution, seasonal dynamics and evaluation of plausible sources and sinks. Environmental earth sciences, 77(7), 1-15.

STAFFORD K. W., LAND L., KLIMCHOUK A. (2008) Hypogenic speleogenesis within seven rivers evaporites: Coffee Cave, Eddy County, New Mexico. Journal of Cave and Karst Studies, v. 70, no. 1, p. 47–61.

SHOFNER G. A., MILLS H. H., DUKE J. E. (2001) A simple map index of karstification and its relationship to sinkhole and cave distribution in Tennessee. Journal of Cave and Karst Studies, 63(2), 67-75.

SIVINSKIH P. (2009) Features of geological conditions of the Ordinskaya underwater cave, fore-Urals, Russia. Hypogene Speleogenesis 267-269.

VERBOVŠEK T. (2007) Fractal analysis of the distribution of cave lengths in Slovenia. Acta Carsologica, 36(3).

WEBSTER M. A. R. K., SHEETS H. D. (2010) A practical introduction to landmark-based geometric morphometrics. The paleontological society papers, 16, 163-188.

WEINER S., GOLDBERG P., BAR-YOSEF O. (2002) Three-dimensional distribution of minerals in the sediments of Hayonim Cave, Israel: diagenetic processes and archaeological implications. Journal of Archaeological Science, 29(11), 1289-1308.

ZHOU Z., ZHANG S., XIONG K., LI B., TIAN Z., CHEN Q., ... XIAO S. (2017) The spatial distribution and factors affecting karst cave development in Guizhou Province. Journal of Geographical Sciences, 27(8), 1011-1024.

Sulphur stable isotope signatures from sulphuric acid caves of Italy

Ilenia M. D'ANGELI(1), Stefano M., BERNASCONI(2), Cristina CARBONE(3), Mario PARISE(4), Giuliana MADONIA(5), Marco VATTANO(5), Jo DE WAELE(1)

(1) Dipartimento di Scienze Biologiche, Geologiche e Ambientali, Università di Bologna, jo.dewaele@unibo.it (corresponding author), dangeli.ilenia89@gmail.com
(2) Geological Institute, ETH Zürich, stefano.bernasconi@erdw.ethz.ch
(3) Dipartimento di Scienze della Terra, dell'Ambiente e della Vita, cristina.carbone@unige.it
(4) Dipartimento di Scienze della Terra e Geoambientali, Università di Bari, mario.parise@uniba.it
(5) Dipartimento di Scienze della Terra e del Mare, Università di Palermo, marco.vattano@unipa.it, giuliana.madonia@unipa.it.

Abstract

The study of sulphur stable isotope signatures in Sulphuric Acid Speleogenetic (SAS) caves gave rise to interesting information on both H_2S sources and reactions involved in the sulphur cycle. In general, the stable isotope geochemistry of gypsum, sulphur and other sulphate by-products found in underground SAS environments, provides the most robust evidence of present-time and past SAS processes. Chemical signatures during sulphuric acid weathering can be influenced by microbial sulphate reduction (MSR) and/or thermochemical sulphate reduction (TSR). Studies on S isotope fractionation revealed large fractionations during MSR (from -30‰ to -70‰) with typical 34S-depleted sulphides, whereas TSR shows smaller variations or no fractionation (δ34S values of SAS by-products due to TSR are more or less similar to the original source of reduced sulphur). In the last two decades, the investigation on SAS caves around the world increased and produced interesting results. Italy hosts 25% of the worldwide known SAS caves, which are mainly located along the Apennine Chain, but also in Apulia, Sicily and Sardinia. In this contribution, we will report the new results from the study of the sulphur stable isotopes of sulphate and sulphur by-products found in 18 SAS systems in Italy.

1. Introduction

Chemical signatures of sulphuric acid speleogenesis in inactive-fossil caves are mainly preserved in the stable isotopes of sulphur, which can give important information regarding both the H_2S sources and involved reactions in the sulphur cycle.

In general, sulphur stable isotope investigations of gypsum and sulphur, found as by-products in underground environments, represent the most robust evidence of past SAS processes. Sulphur has four stable isotopes in nature (^{32}S, ^{33}S, ^{34}S and ^{36}S), but only ^{32}S (95%) and ^{34}S (4.2%) have mostly been used, mainly because the other two isotopes account for less than 1% (ECKARDT, 2001; CANFIELD, 2001). Nevertheless, some authors proved ^{33}S to represent a valuable tool in unravelling complex biogeochemical sulphur cycling processes (CANFIELD *et al.*, 2010; ZERKLE *et al.,* 2010).

In general, the isotopic composition of geological samples is expressed in $\delta^{34}S$, the ratio of ^{34}S and ^{32}S in ‰, normalized to the universal standard (Cañon Diablo Troilite: CDT), and the average values of $\delta^{34}S$ observed can vary significantly from -70 to +35 ‰.

One of the most striking chemical signatures of SAS is the often very negative value of $\delta^{34}S$ (down to -25‰) of gypsum which indicates that sulphate was produced by oxidation of sulphide produced by MSR (microbial sulphate reduction). These low $\delta^{34}S$ values were the first compelling evidence for the implication of hydrocarbons in the origin of H_2S in the Guadalupe Mountains in New Mexico (HILL, 1981). There, the hydrocarbons of the Delaware Basin provided the electrons for microbial sulphate reduction of the Castile Formation evaporites, demonstrated by a $\delta^{34}S$ shift from around +10‰ of these Permian gypsum deposits to around −20‰ for the H_2S (HILL, 1987, 1990).

Studies on S isotope fractionation during S oxidation have shown that the $\delta^{34}S$ shift can be very small, producing no fractionation at high T (OHMOTO & RYE, 1979) or small fractionation at low T (FRY *et al.*, 1988). This means that the $\delta^{34}S$ values of SAS minerals (e.g., gypsum, Al-Fe-sulphates) due to TSR (thermochemical sulfate reduction) are more or less similar to that of the original source of reduced sulphur (BOTTRELL *et al*., 2001; SEAL, 2006). Nevertheless, as in the case of Cerna Valley (Romania), the wide range of $\delta^{34}S$ values have been proven to derive both from TSR of sedimentary sulfates and their reaction with methane, produced by microbial decay of nearby coal deposits (ONAC *et al.,* 2011).

On the contrary, sulphate reducing microbes preferentially use ^{32}S for their metabolic reactions and produce ^{34}S-depleted H_2S (STRAUSS, 1997), causing $\delta^{34}S$ values of sulphides to shift by as much as -70‰ (BRUNNER & BERNASCONI, 2005).

In general, the final $\delta^{34}S$ value depends on the initial isotopic signature of the sulphur source and many other factors such as e.g. sulfate reduction rate and concentrations of reactants. Similar to the Guadalupe Mountains (SPIRAKIS & CUNNINGHAM, 1992), low sulphur isotopic compositions of

gypsum have been found in Villa Luz Cave (Mexico) where H_2S most probably derives from microbial reduction of evaporites using electrons of hydrocarbons coming from the nearby oil fields (HOSE *et al.,* 2000). Further, $\delta^{34}S$ values of gypsum in Kraushöhle (Austria) (PUCHELT & BLUM, 1989; PLAN *et al.,* 2012) and Montecchio (Tuscany, Italy) (PICCINI *et al.,* 2015) are very low deriving from the fractionation of Triassic evaporites, due to microbial reduction and successive oxidation.

Recently, interesting investigations on sulphur isotopes have been carried out in some Italian SAS systems such as Frasassi (ZERKLE *et al.,* 2016) and Calabrian caves (GALDENZI & MARUOKA, 2019). They found sulphide $\delta^{34}S$ values ranging between -21 and -13‰, whilst sulphate $\delta^{34}S$ ranged between +16 and +23‰, demonstrating the deep-seated Triassic evaporites of the Burano Formation (15 to 17 ‰) to play an important role as dominant source of sulphate (GALDENZI & MENICHETTI, 1995).

During the last five years SAS by-products have been collected in several still-active and fossil cave systems in Italy, including Monte Cucco (MC), Acquasanta Terme (AT), Cavallone-Bove (CB), Capo Palinuro (CP), Monte Sellaro (MS), Cassano allo Ionio (CI), Santa Cesarea Terme (SCT), Acqua Mintina (AM), Acqua Fitusa (AF) caves (Fig. 1, to which the labels are referred). In addition, the sulphur isotope composition of bitumen (Maiella Mts., Abruzzo), Messinian and Triassic gypsum deposits have been investigated.

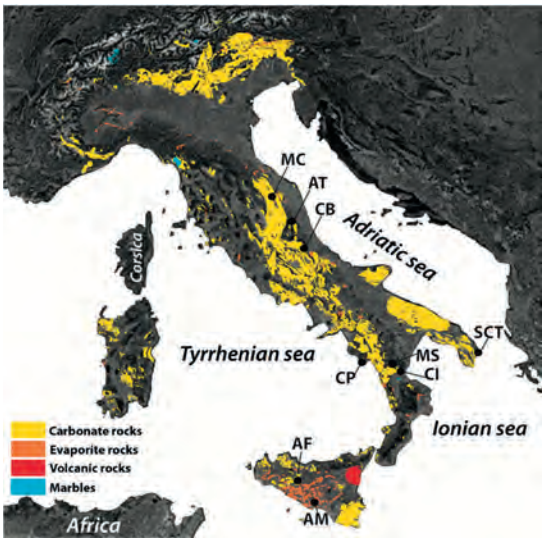

Figure 1: Study area displaying caves location. MC Monte Cucco (Umbria), AT Acquasanta Terme (Marche), CB Cavallone-Bove (Abruzzo), CP Capo Palinuro (Campania), MS Monte Sellaro (Calabria), CI Cassano allo Ionio (Calabria), SCT Santa Cesarea Terme (Apulia), AM Acqua Mintina (Sicily), AF Acqua Fitusa (Sicily).

2. Materials and methods

SAS minerals were collected directly in the field from broken pieces of deposits or provided by collections of the Circolo Speleologico Idrogeologico Friulano as in the case of Capo Palinuro.

A total of 91 mineralogical samples coming from Santa Cesarea Terme (7), Acqua Mintina (10), Acqua Fitusa (10), Cavallone-Bove system (17), Cassano allo Ionio (15), Capo Palinuro (4), Monte Cucco (17), Acquasanta Terme (3), Monte Sellaro (2), Messinian evaporite (1) and Triassic evaporite (1) and bitumen from Majella Massif (4) were powdered and analyzed at ETH Zurich to study ^{34}S stable isotopes. Of these 91 samples (excluded 4 samples of bitumen, 1 sample of Messinian and Triassic evaporites), 49 were constituted by gypsum (the most common by-product in SAS environment and observable in all the systems described in this paper), 16 by alunite (AM, CB, MC), 7 by sulphur (SCT, AM, CI, CP, MC, AS), 7 by jarosite (SCT, AM, CB, MC), 2 by celestine (AM), 1 by an assemblage of copiapite-pickeringite-tamarugite (CI), 1 by thenardite-eugsterite (AF), 1 by barite (MC), and 1 by baritina (MC) (Fig. 2). All samples were wrapped in tin capsules with V_2O_5 and converted into SO_2 in Thermo Fisher-EA 1112 coupled with a Thermo Fisher Delta V Isotope ratio mass spectrometer. Their distribution is reported in Figure 3.

3. Results and Discussion

Sulphur stable isotopic analyses of mineralogical samples (sulphur, gypsum, and Al-Fe-sulphates) collected in several SAS systems of Italy (Fig. 1) show distinctive distributions (Fig. 3) controlled by the interaction of hydrocarbon-related substances with deep-seated evaporites. These values can thus be compared with the end-member values of Triassic and Messinian evaporites, and bitumen deposits. Messinian gypsum (MG) from Bologna area shows a $\delta^{34}S$ value of 23.6‰, whereas the Triassic evaporites (TG) from Pietre Nere Formation in Apulia have a value of 15.1‰. Bitumen deposits (BIT) range between -18.9 and -17.2‰. The values of $\delta^{34}S$ in the various cave systems are listed below and range between: a) Monte Cucco -22.97 and 5.18‰; b) Acquasanta Terme -11.32 and -9.57‰; c) Cavallone-Bove -8.86 and 9.33‰; d) Capo Palinuro -25.85 and -17.28%; e) Monte Sellaro -10.46 and -9.32%; f) Cassano allo Ionio -28.15 and 15.77%; g) Santa Cesarea Terme -33.00 and -21.97‰; h) Acqua Mintina -14.18 and 1.31‰; Acqua Fitusa -2.53 and 23.57‰.

The most negative $\delta^{34}S$ values have been found in Santa Cesarea Terme, and are likely due to the mixing of hydrocarbon derived S-rich fluids with minor amounts of fluids deriving from the MSR of deep-seated Triassic gypsum. Monte Cucco and Cassano allo Ionio caves present a wide range of sulphur stable isotopes. As demonstrated by D'ANGELI *et al.* (2018), Monte Cucco showed phases of hypogene hydrothermal processes that probably influenced thermally the reduction of sulphates, as recorded in Cerna Valley (ONAC *et al.,* 2011).

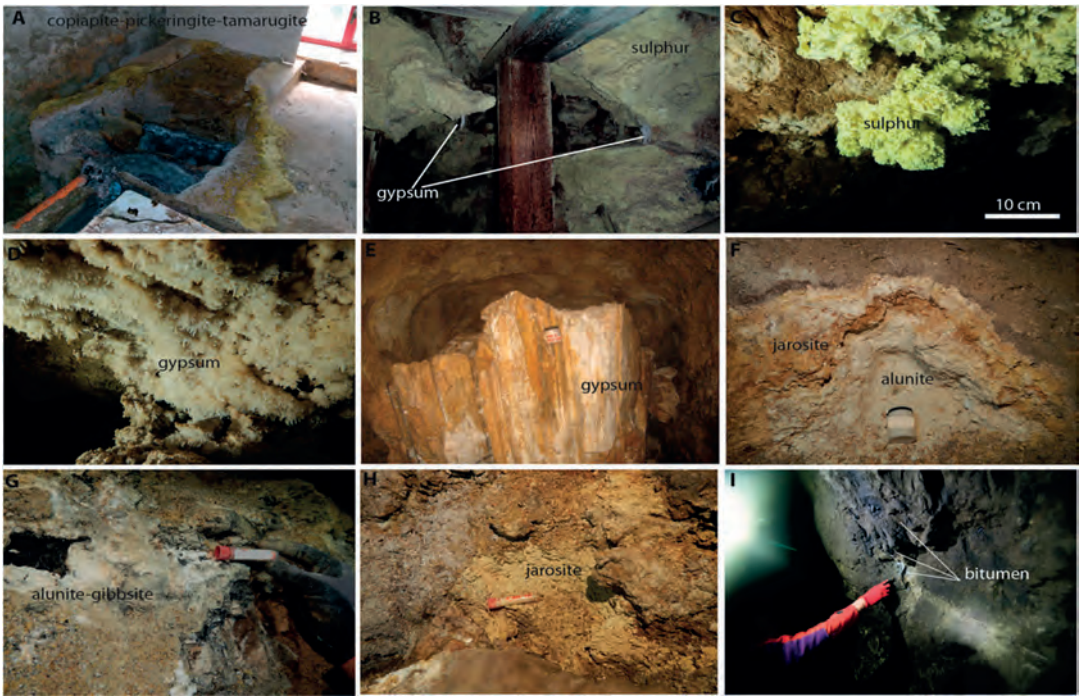

Figure 2: Some of the mineralogical deposits collected in sulphuric acid speleogenetic caves in Italy. A) copiapite-pickeringite-tamarugite from Terme Sibarite spa in Cassano allo Ionio (Calabria); B) Sulphur crusts covering the walls and gypsum stalactites from Gattulla Cave in Santa Cesarea Terme (Apulia); C) sulphur from Acqua Mintina cave (Sicily); D) gypsum from Acqua Mintina (Sicily); E massive gypsum deposits from "La Grotta" in Monte Cucco (Umbria); F-G-H) alunite and jarosite deposits in Cavallone Cave (Abruzzo); I) Bitumen in some mine caves in the Majella Massif. A photo by Soledad Cuezva, B by Mario Parise, C-D by Marco Vattano; E by Jo De Waele; F-G-H by Maria Nagostinis; I) by Jo De Waele

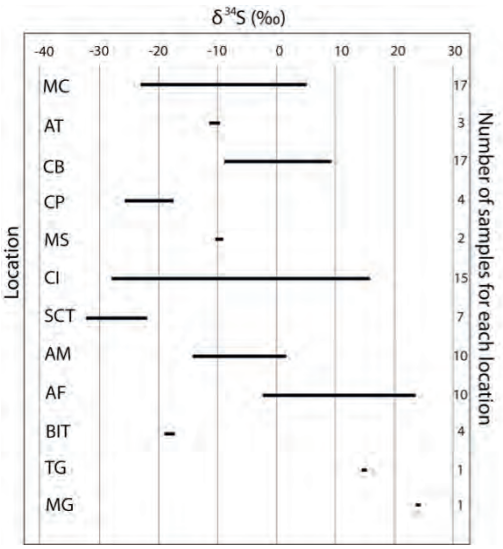

Figure 3: $\delta^{34}S$ values recorded in sulphur, gypsum and Al-Fe-sulphate deposits collected in several SAS systems of Italy. MC Monte Cucco (Umbria), AT Acquasanta Terme (Marche), CB Cavallone-Bove (Abruzzo), CP Capo Palinuro (Campania), MS Monte Sellaro (Calabria), CI Cassano allo Ionio (Calabria), SCT Santa Cesarea Terme (Apulia), AM Acqua Mintina (Sicily), AF Acqua Fitusa (Sicily), BIT bitumen collected in the Majella Massif area (Abruzzo), TG is the Triassic Gypsum from Pietre Nere in Apulia, and MG Messinian Gypsum from Sicily.

The samples collected in Cassano allo Ionio caves showed more or less the same distribution as those described by GALDENZI & MARUOKA (2019), and can be related to deep-seated Triassic evaporite reduction. Only one sample of gypsum collected in a recently discovered cave (called "Terme Sibarite Cave"), located close to the present sulphuric water table, recorded a positive value of 15.8‰.

4. Conclusions

Geochemical investigation using ^{34}S from Italian sulphuric acid speleogenetic cave systems shows wide variability in values of $\delta^{34}S$ ranging between -33 and +23.57‰. This great variability is the result of the geological and structural conditions of the investigated cave systems, characterized by an active Apennine chain with deep discontinuities well linked to deep-seated H_2S sources of sulphur (Triassic evaporites, sea water deep circulation, hydrocarbon tiers, volcanic activity, and the presence of sulphides). In addition, H_2S-enriched fluids might have undergone a different degree of microbial sulphate reduction (MSR) which was more efficient in the locations exhibiting negative values. The most negative values have been observed in the still-active Santa Cesarea Terme, a very peculiar system in which sea water mixes with rising sulphidic fluids producing characteristic geochemical patterns (D'ANGELI *et al.*, 2020). Nevertheless, our results are in agreement with those observed in Frasassi and Calabrian caves displaying a similar

tendency (ZERKLE *et al.,* 2016; GALDENZI & MARUOKA, 2019). This would demonstrate that the dominant source of H_2S are the Triassic evaporites located below the Apennine Chain, the privileged zone of sulphuric acid cave formation (D'ANGELI *et al.,* 2019). Despite that, the wide diversity might be explained by local interactions of fluids with other minor sources such as deep-seated hydrocarbon tiers, sedimentary sulphides (pyrite, marcasite, chalcopyrite), and volcanic activity (especially in Capo Palinuro).

Acknowledgments

Thanks to all the people who helped us during the field sampling. In particular, we thank Orlando Lacarbonara, Rosangela Addesso, Luca Poderini, Giuseppe Antonini, Paolo Forconi, and Maria Nagostinis. Thanks to the Circolo Speleologico Idrologico Friulano for the 4 samples from Capo Palinuro, a site which is difficult to access in the last years due to coastal landslides. Thanks to Sergio Pispico and to the Santa Cesarea Terme spa director, to Giuseppe Martire, Carlo Forace, and the "Associazione Speleologica Liocorno", and to the Terme Sibarite spa director. Thanks to Antonio Cesarini, to the whole caving group of "Serra del Gufo", and to the "Le Taddarite" cavers for the support during the fieldwork in Sicily.

References

BOTTRELL SH., CROWLEY S., SELF C., (2001). Invasion of a karst aquifer by hydrothermal fluids: evidence from stable isotopic compositions of cave mineralization. Geofluids, 1(2), 103-121.

BRUNNER, B., BERNASCONI, S.M., (2005). A revised isotope fractionation model for dissimilatory sulfate reduction in sulfate reducing bacteria. Geochim. Cosmochim. Acta 69, 4759-4771.

CANFIELD DE., (2001). Biogeochemistry of sulfur isotopes. Reviews in Mineralogy and Geochemistry, 43, 607-636.

CANFIELD DE., FARQUHAR J., ZERKLE AL., (2010). High isotope fractionations during sulfate reduction in a low sulfate euxinic ocean analog. Geology, 38, 415-418.

D'ANGELI IM., CARBONE C., NAGOSTINIS M., PARISE M., VATTANO M., MADONIA G., DE WAELE J., (2018). New insights on secondary minerals from Italian sulfuric acid caves. Int. Journal of Speleology, 47(3), 271-291.

D'ANGELI IM., PARISE M., VATTANO M., MADONIA G., GALDENZI S., DE WAELE J., (2019) Sulfuric acid caves of Italy: A review. Geomorphology, 333, 105-122.

D'ANGELI IM., DE WAELE J., FIORUCCI A., VIGNA B., BERNASCONI SM., FLOREA LJ., LISO IS., PARISE M., (2020). Hydrogeology and geochemistry of the sulfur karst spring at Santa Cesarea Terme (Apulia, southern Italy). Hydr. J., DOI: 10.1007/s10040-020-02275-y.

ECKARDT F., (2001). The origin of sulphates: an example of sulphur isotopic application. Progress in Physical Geography, 25(4), 512-519.

FRY B., RUF W., GEST H., HAYES JM., 1988. Sulfur isotopes effects associated with oxidation of sulfide by O2 in aqueous solution. Chemical Geology, 73, 205-210.

GALDENZI S., MENICHETTI M., (1995). Occurrence of hypogenic caves in a karst region: examples from central Italy. Environmental Geology, 26, 39-47.

GALDENZI S., MARUOKA T., (2003). Gypsum deposits in the Frasassi caves, Central Italy. J.Cav.Karst St., 65, 111-125.

GALDENZI S., MARUOKA T., (2019). Sulfuric acid caves in calabria (South Italy): Cave morphology and sulfate deposits. Geomorphology, 328, 211-221.

HILL CA., (1981). Speleogenesis of Carlsbad Caverns and other caves in the Guadalupe Mountains. In: BF. Beck, (Ed.) Proc. 8th Int. Congr. Spel., 1, 143-144.

HILL CA., (1987). Geology of Carlsbad Caverns and other caves in the Guadalupe Mountains, New Mexico and Texas. New Mex. Bur. Min. Min. Res. Bull., 117, 1-150.

HILL CA., (1990). Sulfuric acid speleogenesis of Carlsbad Caverns and its relationship to hydrocarbons, Delaware basin, New Mexico and Texas, AAPG Bull., 74, 1685-1694.

HOSE LD., PALMER AN., PALMER MV, NORTHUP DE., BOSTON PJ., DUCHENE HR., (2000). Microbiology and geochemistry in a hydrogen-sulphide-rich karst environment. Chemical Geology, 169, 399-423.

PICCINI L., DE WAELE J., GALLI E., POLYAK VJ., BERNASCONI SM., ASMERON Y., (2015). Sulphuric acid speleogenesis and landscape evolution: Montecchio cave, Albegna river valley (Southern Tuscany, Italy). Geomorphology, 229, 134-143.

PLAN L., TSCHEGG C., DE WAELE J., SPÖTL C., (2012). Corrosion morphology morphology and cave wall alteration in an Alpine sulfuric acid cave (Kraushöhle, Austria). Geomorphology, 169-170, 45-54.

PUCHELT H., BLUM N., 1989. Geochemische Aspekte der Bildung des Gipvorkommens der Kraushöhle/Steiermark Oberrh. Geol. Abh., 35, 87-99.

OHMOTO H., RYE RO., (1979). Isotopes of sulfur and carbon. In: HL. BARNES (Ed.), Geochemistry of Hydrothermal Ore Deposits, Wiley & Sons, 509-567.

ONAC BP., Wynn JG., SUMRALL JB., (2011). Tracing the source of cave sulfates: a unique case from Cerna Valley, Romania. Chemical Geology, 288, 105-114.

SEAL RR., (2006). Sulfur isotope geochemistry of sulfide minerals. Rev. Min. and Geochem., 61(1), 633-677.

SPIRAKIS CS., CUNNINGHAM KI., (1992) Genesis of sulfur deposits in Lechuguilla Cave, Carlsbad Caverns National Park, New Mexico. In: G. WESSEL, B. WIMBERLEY (Eds.), Native Sulphur-developments in geology and exploration. Am. Inst. Min. Metall. Petrol. Eng., 139-145.

STRAUSS H., (1997). The isotopic composition of sedimentary sulfur through time. Palaeo, 132, 97-118.

ZERKLE AL., KAMYSHNY A., KUMP LR., FARQUHAR J., ODURO H., ARTHUR MA., (2010). Sulfur cycling in a stratified euxinic lake with moderately high sulfate: constraints from quadruple S isotopes. Geochimica et Cosmochimica Acta, 74, 4953-4970.

ZERKLE AL., JONES DS., FARQUHAR J., MACALADY JL., (2016). Sulfur isotope values in sulfidic Frasassi cave system, central Italy: a case of a chemolithotrophic S-based ecosystem. Geochim. Cosmochim. Acta, 173, 373-386.

Some insight on hydrothermal speleogenesis based on conventional and clumped carbonate stable isotopes – preliminary results from the Mariovo hypogene karst system

Marjan TEMOVSKI[1,2], László RINYU[1], István FUTÓ[1] & László PALCSU[1]

(1) Isotope Climatology and Environmental Research Centre, Institute for Nuclear Research, Bem tér 18/c 4026 Debrecen, Hungary; temovski.marjan@atomki.hu
(2) SK Zlatovrv, 7500 Prilep, N. Macedonia

Abstract

$\delta^{13}C$, $\delta^{18}O$ and Δ_{47} were measured in calcites from fossil caves and cave remnants associated with the Mariovo hypogene karst system (N. Macedonia). The preliminary results show that the carbonate deposits have relatively high (above bedrock) $\delta^{13}C$ values, reflecting contribution of metamorphic CO_2. Δ_{47} values indicate low-temperature (<50°C) hydrothermal origin, confirming previous findings. Calcite marble core from Provalata Cave showed two isotope alteration trends: a dispersed $\delta^{18}O$ alteration in the inner part, and a narrow ~1 cm rim with alteration of both $\delta^{18}O$ values (lowered) and $\delta^{13}C$ values (increased). The lowered $\delta^{18}O$ values reflect bedrock interaction with thermal meteoric waters, and the increased $\delta^{13}C$ values are likely due to bedrock interaction with dissolved inorganic carbon mostly composed of high amounts of metamorphic CO_2. Δ_{47} values of the unaltered marble reflect higher (presumably blocking) temperatures from the last metamorphic event. The Δ_{47} values of the narrow altered rim reflect the lower temperature of the hydrothermal speleogenetic phase, suggesting that increased fluid-rock exchange rate of both oxygen and carbon isotopes in such high CO_2 conditions can sufficiently increase the rate of clumped isotope reordering to adjust to the lower temperature setting.

1. Introduction

Hydrothermal speleogenesis is one of the main hypogene speleogenetic mechanisms, where caves form as a result of dissolution of the carbonate bedrock by thermal waters that generally have higher CO_2 concentrations, resulting in characteristic suite of cave morphologies and deposits (DUBLYANSKY 2012). These thermal CO_2-rich waters cool down along the rising flow-path, thus increasing their aggressiveness due to the inverse relationship of calcite solubility and temperature. Pressure decrease towards the surface facilitates CO_2 degassing, leading to supersaturation and precipitation of calcite (DUBLYANSKY 2000).

Stable isotope composition of such deposits has been used to identify the sources of fluids as well as their formation temperature (e.g. BOTTRELL et *al.* 2001, PALMER & PALMER 2012, SPÖTL et *al.* 2009).

In addition to hydrothermal deposits, isotopic alterations of bedrock in hydrothermal systems, besides commonly recognized in ore-related studies, have also been studied in hypogene karst systems (e.g. BAKALOWICZ et *al.* 1987, BELLA et *al.* 2019, BOTTRELL et *al.* 2001, DUBLYANSKY et *al.* 2014, SPÖTL et *al.* 2009, 2016). Most commonly identified alteration is lowering of the bedrock $\delta^{18}O$ values, as a result of the interaction with low $\delta^{18}O$ meteoric waters, as well as lowering of bedrock $\delta^{13}C$ values due to interaction with dissolved inorganic carbon (DIC) with lower than bedrock $\delta^{13}C$ values.

Here we present some preliminary results of a stable isotope study of the carbonate deposits at Melnica locality in Mariovo (N. Macedonia), associated with CO_2-rich hydrothermal speleogenesis. We use conventional stable isotopes to study the CO_2 evolution in the hydrothermal system, as well as clumped isotopes to constrain formation temperatures. Furthermore, we study the conventional and clumped carbonate stable isotope composition of a profile from a drilled core including both the calcite coating and the underlying marble bedrock, where a narrow visible alteration can be found along the contact. To our knowledge, this is the first attempt to apply both conventional and clumped carbonate stable isotopes to identify bedrock isotope alteration halos connected to a hypogene karst system.

2. Materials and methods

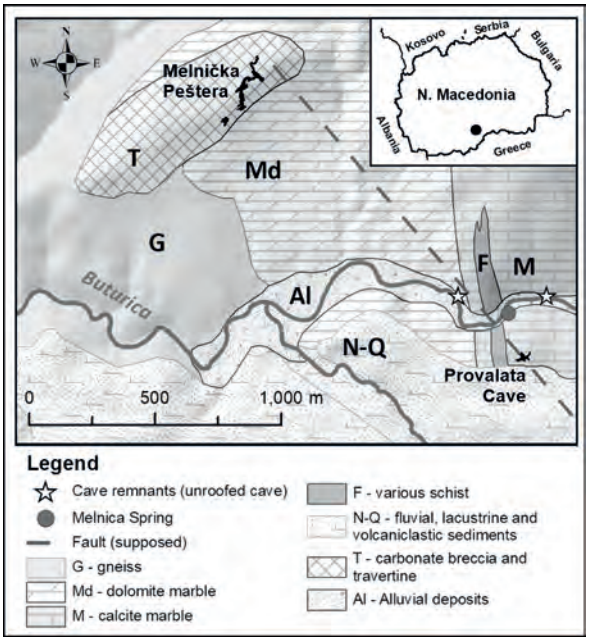

Figure 1: Location and geological setting of the hypogene karst at Melnica locality, Mariovo.

Hypogene karst in Mariovo (N. Macedonia) is found at several localities, at the intersection of low topography and major fault structures, developed mainly in calcite and dolomite marble part of a series of NNW-SSE oriented nappe structures (TEMOVSKI 2016). The main speleogenetic mechanism is hydrothermal speleogenesis, with increased geothermal gradient attributed to the Neogene-Quaternary Kožuf-Kozjak volcanism. At places, due to local geological or lithological control, this is coupled with other hypogene processes such as sulfuric acid speleogenesis (TEMOVSKI et *al.* 2013) or ghost-rock weathering (TEMOVSKI 2016). Melnica locality in Mariovo (Fig. 1) is one of the output zones of the hypogene karst system, where fossil caves (Provalata Cave, Melnichka Peshtera) and cave remnants (i.e. unroofed caves) can be found, developed in calcite marble, dolomite marble and carbonate breccia, as well as a small low-temperature thermal spring (Melnica Spring). Recent geochemical study of the karst groundwater in Mariovo (TEMOVSKI et *al.* in press) has identified that the springs associated with the hypogene karst localities, represent an output part of a regional groundwater system with a deep-circulating (~1 km), old (~15 ka), thermal (≥60 °C) water, where the old groundwater mixes with a small fraction of a young (<50 years), cold (<14 °C) and shallow epigene karst groundwater. Furthermore, presence of deep-seated gases was identified, having some contribution of mantle helium, but dominantly composed of CO_2 of metamorphic origin, with $\delta^{13}C$ of +4.5‰.

Various speleothem samples were collected from caves and cave remnants related to the hydrothermal speleogenesis at the Melnica locality in Mariovo. A core of calcite coating and underlying marble bedrock was drilled in Provalata Cave. Samples were also collected from calcite coatings covering cave passages in Melnichka Peshtera and from cave remnants found at several locations along Buturica Valley. The samples were cut, grinded and polished, and subsamples were drilled using handheld drill from each for conventional carbon ($\delta^{13}C$) and oxygen ($\delta^{18}O$) stable isotope analysis. At Provalata Cave, subsamples were collected also along the bedrock section of the core sample where a narrow visible alteration was observed. $\delta^{13}C$ and $\delta^{18}O$ measurements were done on an automated GASBENCH II sample preparation device attached to a Thermo Finnigan Delta^{PLUS} XP isotope ratio mass spectrometer (IRMS; VODILA et *al.* 2011). The results are expressed as per mill values (‰) relative to Vienna Pee-Dee Belemnite (VPDB). The precision of the measurements is better than ±0.1‰ for $\delta^{18}O$ and ±0.08‰ for $\delta^{13}C$.

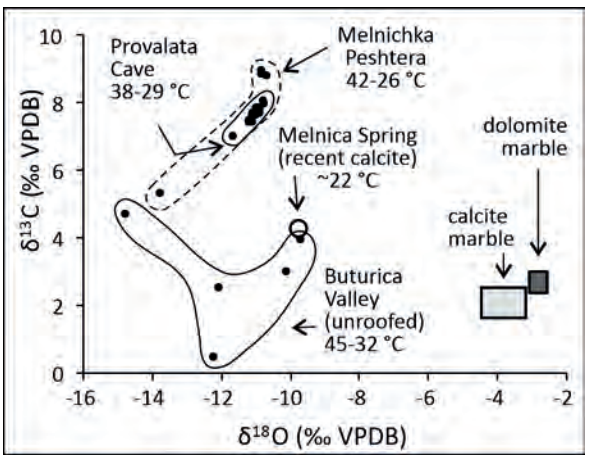

Figure 2: Stable isotope composition of studied calcite deposits. Δ_{47}-based apparent temperatures are given as averages for each sampled site. The range of $\delta^{18}O$ and $\delta^{13}C$ values for Melnica marble is also shown.

Additional subsamples were hand drilled from samples of each locality for clumped isotope (Δ_{47}) analysis, including subsamples of the visibly unaltered and altered sections of the marble bedrock at Provalata Cave. Clumped isotope analysis of the carbonate subsamples was done on a Thermo Scientific MAT-159 253 Plus IRMS, after phosphoric acid digestion at 70 °C using a Thermo Scientific Kiel IV automatic carbonate device. Each carbonate sample measurement consisted of ~10 replicate analyses of 100-120 µg aliquots that were measured alongside carbonate standard samples (ETH1. ETH2, ETH3, ETH4, and IAEA-C2) with assigned values (BERNASCONI et *al.* 2018). Data evaluation was done on the Easotope application, with the CO_2 clumped ETH PBL replicate analyses method and IUPAC parameters. A phosphoric acid correction factor ($\Delta^*_{25\text{-}70}$) of 0.066‰ (PETERESEN et *al.* 2019) was applied to represent the Δ_{47} results on the $CDES_{25°C}$ scale. Apparent temperatures in °C were calculated based on the Δ_{47}-temperature calibration of PETERESEN et *al.* (2019), with temperature uncertainties given as 1σ standard error (SE). All measurements were done at the Isotope Climatology and Environmental Research Centre of the Institute for Nuclear Research, Debrecen, Hungary.

3. Results

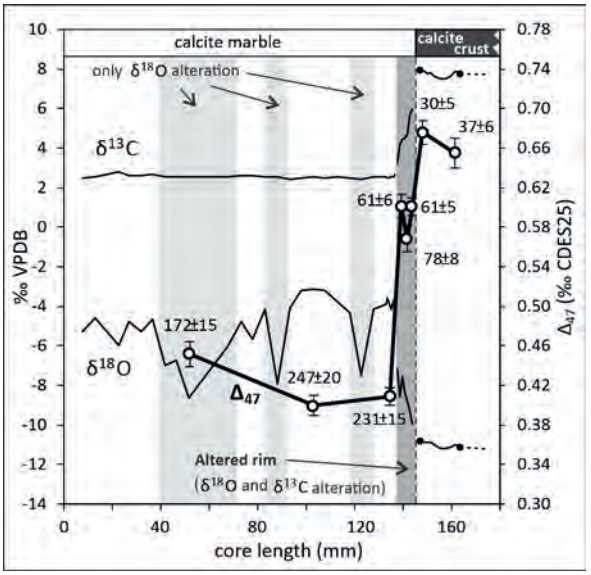

Figure 3: Clumped and conventional stable isotope profiles along the sampled core in Provalata Cave. Δ_{47}-based apparent temperatures in °C are also given.

$\delta^{13}C$ values of studied calcite samples range from +0.5‰ to +9.0‰, and $\delta^{18}O$ values from -14.8‰ to -9.7‰ (Fig. 2). Provalata Cave and Melnichka Peshtera had highest average $\delta^{13}C$ values, +7.5‰ and 8.1‰, respectively, with the calcite from the valley having lower and more varied values (+2.9‰). Provalata Cave and Melnichka Peshtera had similar $\delta^{18}O$ composition (-11.3‰), with the valley samples having slightly lower average values (-11.8‰). Δ_{47} values ranged from 0.637‰ to 0.687‰, giving apparent temperatures of 45 to 26 °C.

The core sample at Provalata Cave had visible color alteration in the marble section, with patches of dispersed whitish (pale grey) discoloration around the grey unaltered marble found in the inner part, and a narrow (~1 cm) rim at the contact with the overlying calcite coating with intense white discoloration. The grey unaltered marble had stable isotope composition of +2.5‰ $\delta^{13}C$ and -3.5‰ $\delta^{18}O$. The pale grey patches had similar $\delta^{13}C$ composition, with $\delta^{18}O$ values lowered as low as -8.6‰ (Fig. 3). The highest isotopic alteration was found in the narrow alteration rim, where $\delta^{13}C$ values were gradually increased up to a value of +6.0‰, and $\delta^{18}O$ values lowered to -9.9‰. The profile continues into the covering calcite coating that starts with $\delta^{13}C$ of 8.0‰ and $\delta^{18}O$ of -10.8‰. The unaltered marble section had Δ_{47} values of 0.399‰ and 0.409‰, that correspond to apparent temperatures of 239±18 °C. The pale grey section had slightly higher Δ_{47} composition (0.451‰), giving an apparent temperature of 172±15 °C. The narrow-altered rim had the highest measured Δ_{47} values in the marble section (0.568-0.601‰) giving apparent temperature of 67±6 °C.

4. Discussion

The stable isotope composition of the calcite deposits at Melnica locality is similar to the previously reported few values from Provalata Cave (TEMOVSKI et *al.* 2013). Their characteristically high $\delta^{13}C$ values likely reflect DIC mostly composed of high amounts of CO_2 of metamorphic origin. Recent modeling of the DIC composition at Melnica Spring indicates contribution of up to 54% of carbon from metamorphic CO_2 with $\delta^{13}C$ of +4.5‰ (TEMOVSKI et *al.* in press). The calculated apparent temperatures confirm the low-temperature (<50 °C) hydrothermal origin of the calcite, suggested also by fluid inclusions data (TEMOVSKI 2016).

The marble bedrock at Provalata Cave shows two alteration trends: a dispersed $\delta^{18}O$ alteration in the inner part, and a narrow ~1 cm rim below the contact with the calcite crust, where both $\delta^{18}O$ and $\delta^{13}C$ are altered. The narrow alteration rim corresponds to the thermal carbonic speleogenetic phase, with the values at the outer part shifting towards the ones of the subsequently deposited calcite. The dispersed section of only $\delta^{18}O$ alteration, likely reflects an older hydrothermal phase. While the lowering of $\delta^{18}O$ values is a common finding in other hypogene caves, as a result of bedrock interaction with meteoric waters (e.g., BAKALOWITZ *et al.* 1987, BOTRELL *et al.* 2001, SPÖTL *et al.* 2009), the increased $\delta^{13}C$ values in the alteration rim is not, and indicates interaction of the marble bedrock with groundwater DIC with high $\delta^{13}C$ values.

The clumped isotope composition of the marble section reflects the conventional stable isotope composition, such as the lowest Δ_{47} values are found at the unaltered grey marble, and highest at the narrow alteration rim, reflecting highest and lowest apparent temperatures, respectively. The highest temperatures at the unaltered marble (239±18 °C) probably reflect (blocking) temperatures from the last metamorphic event (RYB *et al.* 2017). The apparent temperatures of the pale grey marble (172±15 °C), combined with the altered $\delta^{18}O$ values, likely reflect an earlier hydrothermal alteration. The most interesting results come from the narrow-altered rim, where both $\delta^{13}C$ and $\delta^{18}O$ values are altered, and there is also increase in the Δ_{47} values, reflecting an apparent temperature of 67±6 °C. As the apparent temperature is below the blocking temperature for calcite marble, i.e., the temperature is too low to permit isotopic reordering (RYB *et al.* 2017), simple cooling cannot explain the high Δ_{47} values of the altered rim. Considering that also both $\delta^{13}C$ and $\delta^{18}O$ values are altered, increased fluid-rock exchange rate of both oxygen and carbon isotopes in such high CO_2 conditions might have sufficiently increased the rate of clumped isotope reordering to adjust to the lower temperature setting.

5. Conclusion

Clumped and conventional stable isotope composition of the calcite deposits at Melnica locality confirm their low-temperature (<50 °C) hydrothermal origin with high $\delta^{13}C$ related to metamorphic CO_2. Preliminary results of the isotopic composition of an altered marble bedrock profile in Provalata Cave show two alteration trends, of which a narrow alteration rim with increased $\delta^{13}C$ values and lowered $\delta^{18}O$ values indicates bedrock interactions with thermal groundwater rich in (high $\delta^{13}C$) CO_2, that corresponds to the thermal carbonic speleogenetic phase of this hypogene system. The isotopic alteration is also reflected in the clumped isotope composition, adjusting the Δ_{47} values to the lower temperatures of the hydrothermal speleogenetic system. This phase was followed by deposition of calcite coating with higher $\delta^{13}C$ and Δ_{47} values, indicating CO_2 degassing and lower depositional temperatures, likely reflecting shift to shallower conditions. The combined alteration of both conventional and clumped isotopes in the altered marble indicates that, in addition to $\delta^{13}C$ and $\delta^{18}O$ values, Δ_{47} values can also be used to identify wall bedrock alteration in hypogene karst settings.

Acknowledgments

We would like to thank the members of SK Zlatovrv – Prilep for assistance during sampling. Part of this research was supported by the MTA Postdoctoral Fellowship Programme, No. PP-030/2015, and was also supported by the European Union and the State of Hungary, co-financed by the European Regional Development Fund in the project of GINOP-2.3.2-15-2016-00009 'ICER'.

References

BAKALOWICZ M.J., FORD D.C., MILLER T.E., PALMER A.N. and PALMER M.V. (1987) Thermal genesis of dissolution caves in the Blach Hills, South Dakota. *Geological Society of America Bulletin*, 99 (6): 729-738.

BELLA P., BOSAK P., MIKYSEK P., LITTVA J., HERCMAN H. and PAWLAK J. (2019) Multi-phased hypogene speleogenesis in a marginal horst structure of the Malé Karpaty Mountains, Slovakia. *International Journal of Speleology*, 48, 203-220.

BOTTRELL S.H., CROWLEY S. and SELF C. (2001) Invasion of a karst aquifer by hydrothermal fluids: evidence from stable isotopic compositions of cave mineralization. *Geofluids* 1: 103–121

COPLEN T.B. (2007) Calibration of the calcite–water oxygen-isotope geothermometer at Devils Hole, Nevada, a natural laboratory. *Geochim. Cosmochim. Acta*, 71 (16), 3948-3957.

DUBLYANSKY Y. (2012) Hydrothermal caves, In: White,W.B., Culver,D.C. (Eds.) *Encyclopedia of Caves*, 2nd ed., Academic Press, 391–397.

DUBLYANSKY Y.V. (2000) Dissolution of carbonates by geothermal waters. In: Klimchouk A., Ford D.C., Palmer A.N. & Dreybrodt W. (Eds) *Speleogenesis: evolution of karst aquifers*. Huntsville: National Speleological Society, 158-159.

DUBLYANSKY Y.V., KLIMCHOUK A.B., SPÖTL C., TIMOKHINA E.I. and AMELICHEV G.N. (2014) Isotope wallrock alteration associated with hypogene karst of the Crimean piedmont. Ukraine. *Chem. Geol.* 377, 31–44.

PALMER M.V. and PALMER A.N. (2012) Petrographic and isotopic evidence for late-stage processes in sulfuric acid caves of the Guadalupe Mountains, New Mexico, USA. *International Journal of Speleology*, 41 (2), 231-250.

RYB U., LLOYD M.K., STOLPER D.A. and EILER J.M. (2017) The clumped-isotope geochemistry of exhumed marbles from Naxos, Greece. *Earth Planet. Sci. Lett.* 470, 1–12.

SPÖTL C., DUBLYANSKY Y., MEYER M. and MANGINI A. (2009) Identifying low-temperature hydrothermal karst and palaeowaters using stable isotopes: a case study from an alpine cave, Entrische Kirche. Austria. *Intern. J. Earth Sci.* 98, 665–676.

SPÖTL C., DESCH A., DUBLYANSKY Y., PLAN L. and MANGINI A. (2016) Hypogene speleogenesis in dolomite host rock by CO_2-rich fluids, Kozak Cave (southern Austria), *Geomorphology*, 255, 39-48,

TEMOVSKI M. (2016) *Evolution of karst in the lower part of Crna Reka river basin*. Springer International Publishing, Heildelberg, Springer Theses, 265 p.

TEMOVSKI M., AUDRA P., MIHEVC A., SPANGENBERG J., POLYAK V., MCINTOSH W. and BIGOT J.-Y. (2013) Hypogenic origin of Provalata Cave, Republic of Macedonia: a distinct case of successive thermal carbonic and sulfuric acid speleogenesis. *Int. J. Speleol.* 42 (3), 235–264.

TEMOVSKI M., TURI M., FUTO I., BRAUN M., MOLNAR M. and PALCSU L. (2020) *Multi-method geochemical characterization of groundwater from a hypogene karst system Hydrogeology Journal*, in press.

Hypogene karst associated with igneous intrusions and its influence on the subsequent karst evolution in high mountains (Central Andes, Peru)

Alexander KLIMCHOUK[(1)], Sasa MILANOVIC[(2)] & Cristian BITTENCOURT[(3)]

(1) Institute of Geological Sciences of NAS of Ukraine, Kiev, Ukraine. Email: klim@speleogenesis.info (corresponding author)
(2) University of Belgrade, Serbia, Email: sasa.milanovic@rgf.bg.ac.rs
(3) Hydrokarst Consulting, Minas Gerais, Brazil, Email: cbittencourt@hydrokarst.com.br

Abstract

Carbonate rocks of Cretaceous age are widespread in the Peruvian Andes. The studied area in the eastern part of the Cordillera Occidental, near a large igneous intrusion and a skarn deposit, exemplifies polygenetic and multi-phase karst development. Hypogene karstification is related to a hydrothermal activity associated with a magmatic event at ca. 11-9.7 Ma responsible for the emplacement of the nearby intrusion and related alteration of the carbonate rocks. It has resulted in deep-rooted, laterally isolated stair-case-rising shaft systems aligned to NE-trending sub-vertical fractures. These caves clearly exhibit a complete suite of remarkably well-preserved speleogens indicative of rising flow, standing as a foremost example of endogenous hypogene speleogenesis related to magmatic intrusions. Commencing in the Early Pleistocene, epigene karstification was strongly influenced by the presence of pre-formed hypogene caves that provided effective vertical drains across the vadose zone and defined hydraulic compartments. However, hypogene caves are largely isolated in the plan view, and lateral integration of the contemporary karst system by epigene karstification is incomplete, resulting in a complex flow system. The overprint of vadose features over hypogene morphologies is very distinct although local. Changes in the base-level position due to the landscape evolution and Pleistocene glaciations were further major factors that influenced epigene karst development.

1. Introduction and geological settings of the study area

In the Peruvian Andes, Cretaceous carbonate rocks cover about 13% of the total surface area and occur in two narrow, tectonized belts extending over 2,000 km long (EVANS, 2015; Fig. 1). Carbonate terrains, commonly karstified, host most of major metal ore deposits related to igneous intrusions and associated interactions between hydrothermal fluids and host rocks (LOVE, 2004; EVANS, 2015). Karst in the Andes is recognized in causing extreme hydrogeologic complexity and great challenges in mine dewatering and mine waste management (EVANS *et al.*, 2005; EVANS, 2015).

The orogeny that formed the Andes initiated in the Jurassic as crustal deformation due to a flat subduction of the oceanic Nazca Plate under the continental South American Plate. This caused crustal thickening of the overriding plate, the folding and faulting, uplift, volcanism, plutonism, hydrothermalism, and the formation of numerous mineral deposits in North Central Peru.

The study area lies ca. 30 km east of the crest of the Cordillera Blanca, within the belt of the Albian – Upper Cretaceous carbonates that stretches NW-SE in accordance with the regional framework. In the area, transverse (NE-trending) discontinuities are recognized at multiple scales, from regional basement structures (LOVE *et al.*, 2004) to faults and fractures cutting multiple rock packages. The latter are abundant in the study area (Fig. 2B).

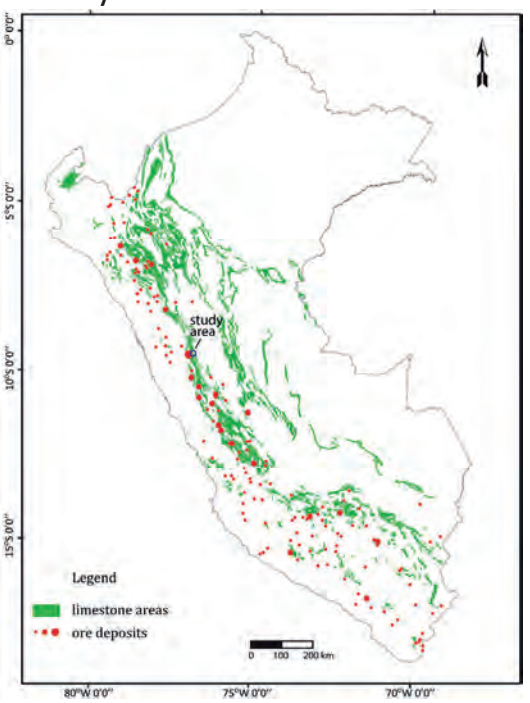

Figure 1: Carbonate terrain and operating mines in the Peruvian Andes (from EVANS, 2015).

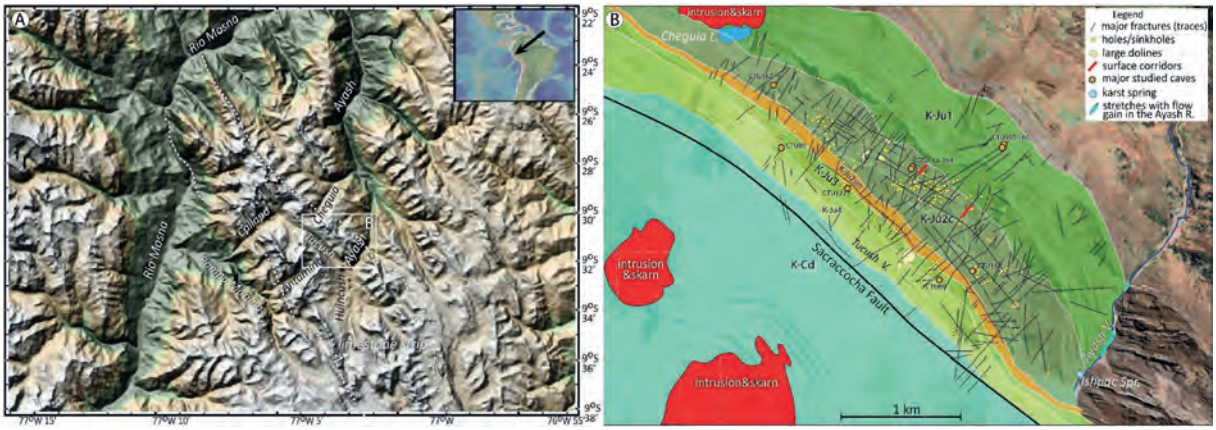

Figure 2: A - Digital elevation model showing the outer limits of the steeply inclined Jumasha limestone (white dotted lines) and the location of the Tucush area within the wider physiographic context. B - Shaded geological map of the Tucush area showing traces of major fractures, distribution of major surface karst features, and locations of studied caves.

The study area encompasses the NW-trending Tucush glacial valley and the adjacent ridge, cut by the NE-trending Ayash valley (Fig. 2A). The Jumasha Formation is intensely karstified and characterized by the rugged topography, with steep limestone slopes and peaks at altitudes ranging from 4,300 to over 5,000 m asl. The ridge is comprised by SW steeply dipping limestones (K-J1 to K-Ju4 units of Jumasha) bounded by marls and marly limestones of the Celendin Fm (Fig. 2B). The carbonate sequence is pierced by one large and two smaller intrusions in the study area.

2. Results and discussion: The Tucush karst system

The contemporary karst hydrogeological system is recharged through the Tucush ridge and drained by the Ishpac Spring and smaller springs along the Ayash valley. Phreatic flow is mainly strike-parallel, whereas vadose flow is chiefly controlled by transverse fractures and associated karst shafts. Discharge variations show strong seasonality and rapid reaction to rain events, indicating low regulating and storage capacity of phreatic and epikarstic zones.

Epikarst in the Tucush area is young and immature. Most surface karst features show strong control by transverse fractures and are out of genetic/functional adjustment with the landscape, being formed through exhumation and destruction by the denudational surface of various elements of the void/conduit system (shafts, passages, chambers, enlarged fractures, etc.).

Twelve caves up to 160 m deep were investigated in detail and over 100 karst openings were documented. Vertical caves of hypogene origin dominate, typically consisting of shafts developed along *en echelon* fractures at different intervals and connected by bedding-controlled passages (Fig. 3). In some cases, large hypogene chambers are cut by vadose shafts. Caves have abundant hypogene speleogens organized in easily recognizable, spatially and functionally related assemblages that are shown (KLIMCHOUK, 2019) to be strong evidence of hypogene karstification. Vadose dissolution overprints hypogene morphologies in places, particularly in vertical shafts (Fig. 3; Fig. 4 a, b).

Hypogene karstification in the area is associated with the same multiphase magmatic event that resulted in the emplacement of the nearby intrusions (11 to 9.7 Ma; MROZEK *et al.*, 2017). Acidic magmatic and metamorphic fluids escaping the intrusion zone and partly recirculating beneath the Celendín Fm are capable of causing extensive hypogene karstification. During the hypogene stage, deep-seated cave systems were formed, with stair-case-rising patterns controlled by transverse fractures. Exhumation of the region through erosional and tectonic processes started 5–6 Ma (GARVER *et al.*, 2005), with the Jumasha Fm exposure by the beginning of the Pleistocene.

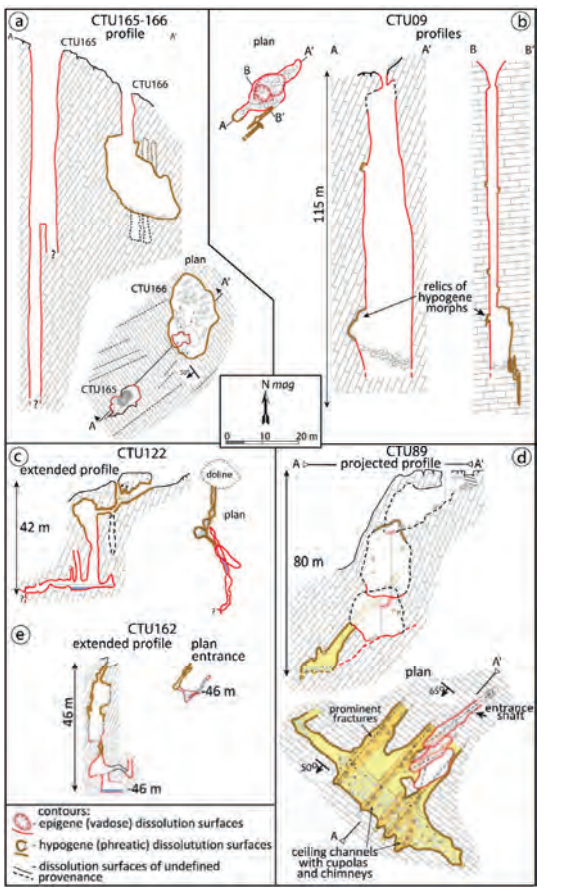

Figure 3: Profiles and plans of vertical caves showing sections with prevalent epigene and hypogene morphs.

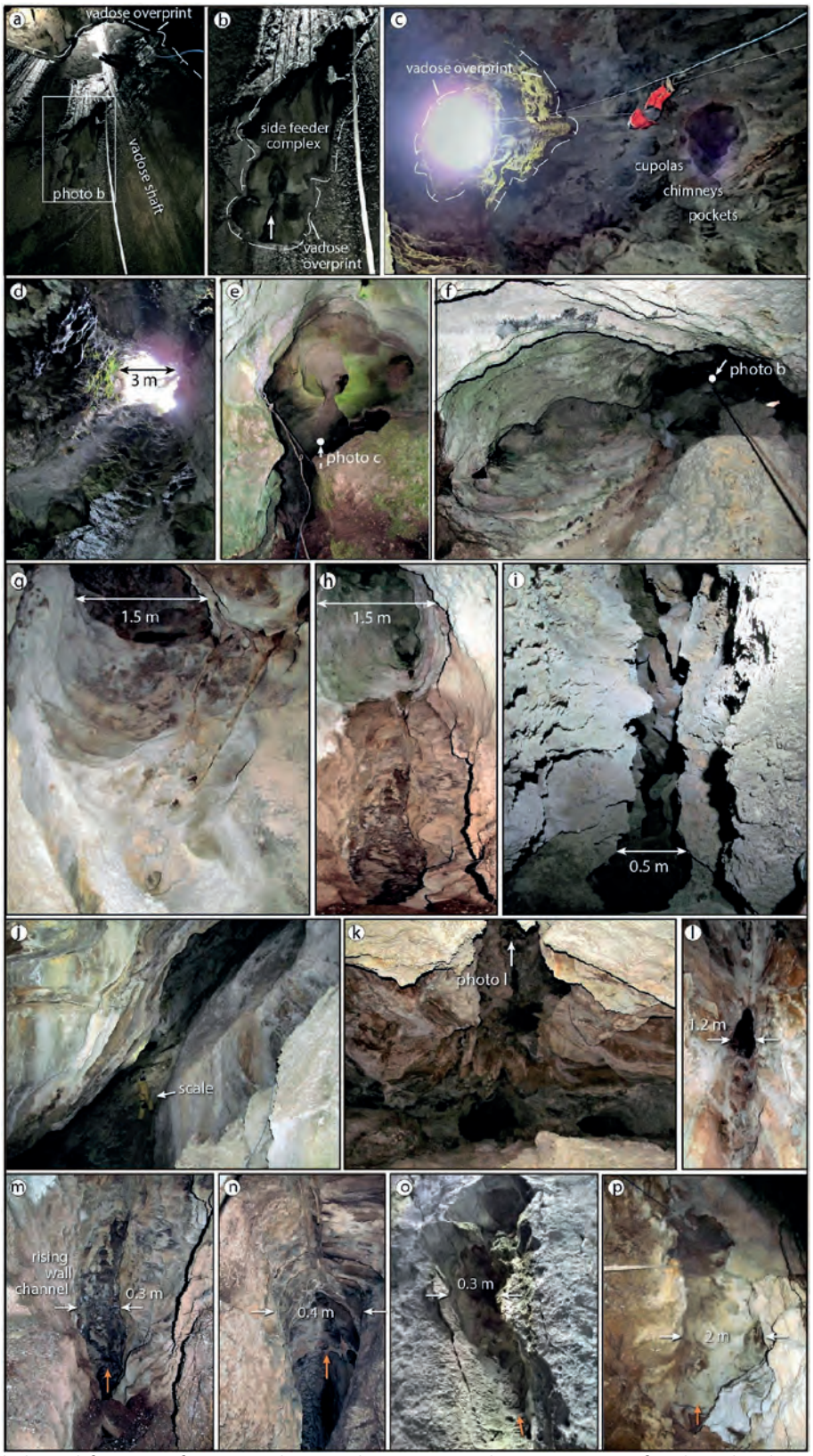

Figure 4: Morphological features of caves in the Tucush area. a-c – the overprinting of vadose dissolution surfaces onto hypogene morphs ; d – hypogene shaft open to the surface ; e – the top of the internal shaft viewed from above ; f and h – features at the tops of internal shafts, viewed from below (f is the same shaft shown in e); i – rift-like passage ; j-l – inclined, bedding-controlled chamber (j – strike-parallel view ; k – updip view where the arrow points to a rising chimney/shaft shown in photo l as viewed from below) ; m-p – side feeders in the shaft walls. Caves : a, b, i – CTU09 ; c – CTU165, g, h, m, n – CTU162 ; j, k, l – CTU89 ; o, p – CTU164.

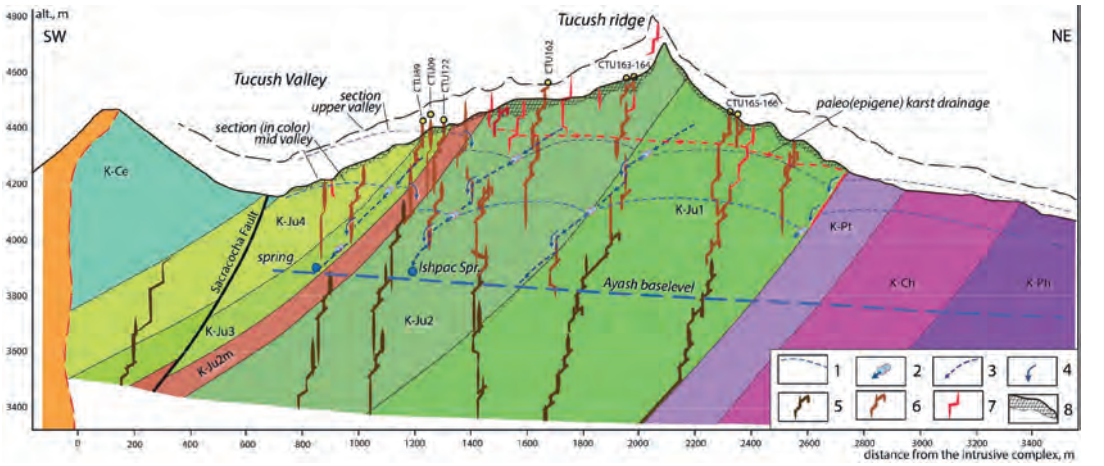

Figure 5: A quasi-3D conceptual model of the contemporary Tukush karst hydrogeological system.

Since then, epigene karst developed with varying intensity, depending on climate and neotectonic/geomorphological factors. Extensive karst landscape with conduit systems likely formed during the Early to Middle Pleistocene. The karst system was likely drained to the NE along transverse fractures and associated hypogene caves.

Glaciations during the LGM greatly contributed to the geomorphogenesis of the Tucush area and exerted considerable effects on karst development including hindering karstification during progressive phases, glacial scouring of epikarst and upper pre-formed shafts, and massive recharge during the regressive phases that facilitated the development of existing cave systems.

Epigene karstification was strongly influenced by the presence of hypogene shaft systems which provided effective drains across the vadose zone, and facilitated rapid deepening of the vadose zone - depending on the outflow conditions varying in space and time. The presence of laterally isolated hypogene shaft systems determined a complex pattern of associated hydraulic compartments and their complex interplay in the course of the initiation and development of lateral phreatic conduits. The development of phreatic conduits during the main epigene phase was strongly favored along the NE trends. Rapid incision of the upper Ayash canyon along the NE-trending karstified zone in the end of the LGM began re-orienting the flow to the southeast along strike, thus intergrating previously independent transverse karst systems.

3. Conclusions

At least three major phases of karstification are identified in the Tucush area: (1) hypogene; (2) major epigene; and (3) current (post-glacial) epigene.

Carbonic acid hypogene karstification by thermal fluids resulted in the formation of laterally isolated shaft systems aligned to transverse throughgoing fractures. These caves are a foremost example of endogenous hypogene speleogenesis related to magmatic intrusions. The polygenetic and multi-phase nature of the Tucush karst system defines the complexity of the hydrogeologic system. The inheritance of hypogene caves strongly influences subsequent epigene karstification, groundwater flow, and geomorphogenesis in the vicinity of igneous intrusions. Understanding of the origin and evolution of karst is crucial for development of conceptual groundwater flow models for karst terrains and assessment of karst-related hazards and risks.

References

EVANS D. (2015) Hydrogeological risks of mining in mountainous karstic terrain: lessons learned in the Peruvian Andes. In: Andreo B. *et al.* (eds.), Hydrogeological and Environmental Investigations in Karst Systems, Springer-Verlag Berlin, 465-475.

EVANS D., LETIENT H., ALEY T. (2005) Aquifer vulnerability mapping in karstic terrain—Antamina Mine, Peru. In: Proceedings from the Society of Mining Engineers Conference, Salt Lake City, USA, 1-13.

GARVER J.I., REINERS P.W., WALKER L.J., RAMAGE J.M., PERRYET S.E. (2005) Implications for timing of Andean Uplift from thermal resetting of radiation-damaged zircon in the Cordillera Huayhuash, Northern Peru. The Journal of Geology 113, 117–138.

KLIMCHOUK A.B. (2019) Speleogenesis – Hypogenic. In: White W., Culver D., Pipan T. (Eds.) Encyclopedia of Caves, 3rd edition, Elsevier, 974-988.

LOVE D.A., CLARK A.H., GLOVER J.K. (2004) The lithologic, stratigraphic, and structural setting of the giant Antamina copper–zinc skarn deposit, Ancash, Peru. Economic Geology 99, 887–916.

MROZEK S.A., CHANG Z., MEINERT L.D., CREASER R.A. (2017) The Antamina deposit, Peru: U-Pb and Re-Os age constraints on magmatic-hydrothermal activity. Conference Abstract FUTORES II, Townsville, Queensland, Australia.

Morfologías de origen hipogénico en la Cueva del Agua, Cartagena, España

José Luis LLAMUSI[(1)], Andrés ROS[(1)], José M. CALAFORRA[(2)], Ángel FERNANDEZ-CORTES[(2)], Fernando GÁZQUEZ[(2)], José SOTO[(1)] & Alejandro GETINO[(1)]

1) Centro de Estudios de la Naturaleza y el Mar – CENM, 30394 Cartagena, Spain, jl.llamusi@gmail.com, aros@blog56.com (corresponding author)
(2) Department of Biology and Geology, University of Almeria, 04120 Almeria, jmcalaforra@ual.es, f.gazquez@ual.es, acortes@ual.es

Resumen

La Cueva del Agua de Cartagena (Región de Murcia, SE España) es una cavidad inundada por aguas termales. Es una de las redes hidrotermales activas más largas de España, con más de 6.000m topografiados, y el nivel de sus aguas está marcado por la proximidad del Mar Mediterráneo. La cueva actúa como una surgencia submarina con una temperatura cercana a los 30°C. Las morfologías de la cueva son típicas de espeleogénesis hipogénica, aunque también se han identificado evidencias de periodos en los que la cavidad estuvo total o parcialmente emergida (p.ej. estalagmitas y estalactitas actualmente sumergidas, depósitos de calcita flotante, etc.). Las morfologías hipogénicas de la cueva varían dependiendo de la distancia a la línea de costa. En este trabajo presentamos el primer inventario de morfologías y espeleotemas de la Cueva del Agua que permitirá evaluar los procesos hipogénicos que determinaron su desarrollo.

Abstract

Hypogenic morphologies in Cueva del Agua, Cartagena, Spain. Cueva del Agua of Cartagena (Region of Murcia, SE Spain) is a subaqueous cavity flooded by thermal water. It is one of the longest active hydrothermal caves in Spain (>6.000 m). The water level in de cave is marked by proximity of the Mediterranean Sea. The cave acts a thermal outlet and the morphologies show clear sings of hypogene speleogenesis, although periods of subaerial conditions are evidenced by the presence of stalactites and stalagmites submerged at present and raft calcite deposits. The morphologies and cave features vary with distance to the shoreline. We present and inventory of cave morphologies and speleothems in Cueva del Agua that will permit us to evaluate the hypogene processes involved in its genesis.

1. Introducción

Cueva del Agua está situada en la Región, en el sudeste de España. Se trata de una cavidad de más de 6.000 m de recorrido que se encuentra cercana a las líneas de costa. La mayor parte de sus galerías se encuentran sumergidas por aguas termales, que fluyen en dirección NE-SO.

La cueva se desarrolla en calizas dolomíticas recristalizadas Triásicas con intercalaciones de yesos, que presentan una macroestructura de mantos de corrimiento y fallas de dirección NO-SE. La Cueva del Agua mantiene en su recorrido conocido la dirección NE-SO. La hidrogeología viene condicionada por la presencia de dos acuíferos: Vértice-Horno en el que se desarrolla la Cueva del Agua, y el acuífero Valdelentisco (LLAMUSI *et al*., 2020). Las aguas en la cueva mantienen una temperatura media de 29,6°C. La cueca actúa como un manantial submarino que vierte sus aguas al Mar Mediterráneo.

Durante las últimas décadas se vienen realizando exploraciones de espeleobuceo que han permitido elaborar una topografía detallada de la cavidad (Fig. 1). En las primeras inmersiones se localizaron espeleotemas epigénicos de origen aéreo bajo la plataforma de entrada a pocos metros de profundidad.

En el año 2002 se consigue avanzar hasta llegar a 860m en la zona Noroeste, donde se descubre una burbuja de aire (GARCIA *et al.,* 2019). Durante estas exploraciones en la distancia de 600m se encontraron espeleotemas de origen subaéreos, ahora sumergidos.

En el año 2013 se consiguió desobstruir un paso a 860m de distancia de la entrada (LLAMUSI *et al*., 2020). Este paso comunica con una extensa red de galerías y en muchas de ellas se han observado paredes y suelos colgados. La cavidad presenta una galería principal de recorrido lineal de más de 1.200m, que finalmente se ramifica para dar lugar a una red laberíntica de galerías.

En 2020 se descubrieron nuevas galerías y una pequeña sala con una burbuja de aire en la zona suroeste de la cavidad, a la que se le denominó Galería Soto (SOTO *et al.,* 2020). En ella se encuentran finas capas de calcita flotante tanto en superficie como bajo el agua (Fig. 2A) y cuyas paredes están cubiertas de costras de calcita subacuática tipo “nubes” (Fig. 3).

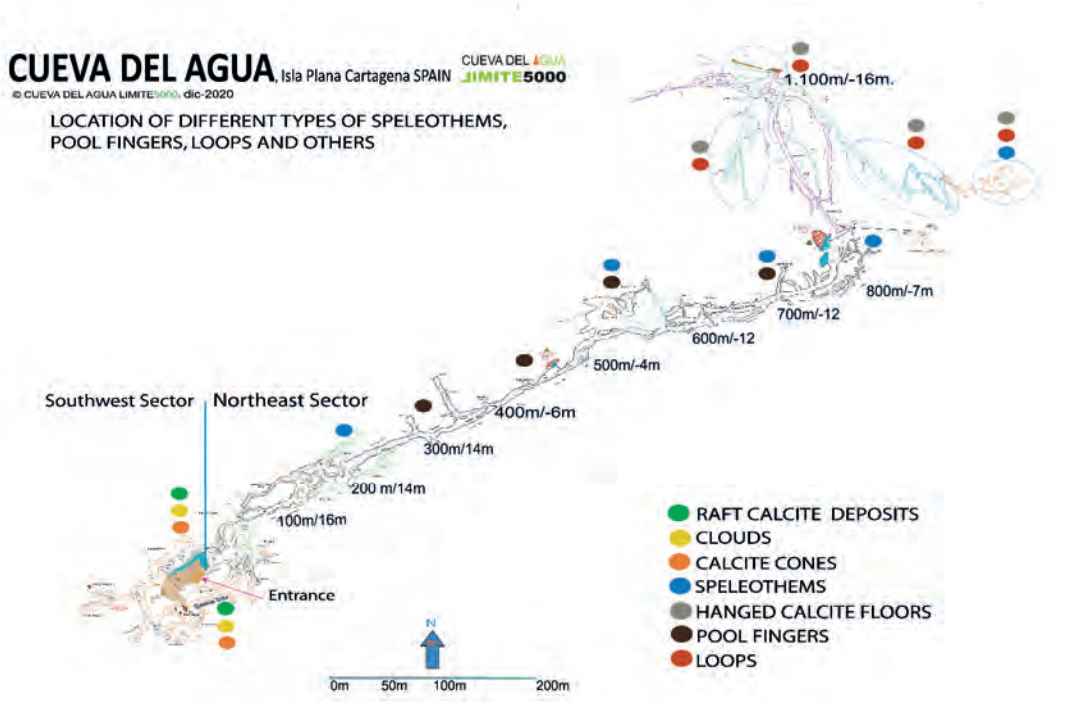

Figura 1, Cueva del Agua the locations of the speleothems are indicated © CUEVA DEL AGUA LIMITE5000

2. Materiales y métodos

Las investigaciones en Cueva del Agua se realizan bajo el agua por equipos de especialistas. Para la localización y situación de las morfologías y espeleotemas se ha utilizado plano topográfico de la Cueva del Agua desarrollado por el equipo de Cueva del Agua LIMITE5000. Para su realización se tomaron medidas manuales y de equipos de datos digitales ENC2 de Seacraft en recorridos lineales, las fotografías se realizaron con equipos Sony RX100 con carcasa submarina e iluminación led.
Los espeleotemas se han ido situando en plano junto con las profundidades y distancia desde la entrada, estos se midieron bajo el agua y se realizaron imágenes de conjuntos y fotografías de aproximación para identificar detalles.
Durante una de las inmersiones se llevó a cabo la medición del caudal del flujo de agua en la cavidad situando en uno de sus pasos más estrechos, a 860m de distancia desde la entrada, un equipo ENC2 con un sensor de velocidad del agua (m/min) que junto con las dimensiones aproximadas de la galería han permitido establecer el caudal en este punto.

3. Resultados y discusión

Morfologías y flujos de agua

La cavidad se encuentra sumergida casi en su totalidad por aguas termales 29,6°C (LLAMUSI et al., 2020 a, b) que fluye desde el acuífero hacia el mar con un promedio de 118,8 l/s, según mediciones correspondientes a noviembre 2020. Las morfologías de paredes y techos están erosionadas y presentan signos evidentes de corrosión, así como aristas, cantos afilados y particiones (Fig. 2 A-B-C-D). En los suelos aparecen importantes depósitos de sedimento procedente de la corrosión de la roca de caja, que en algunos lugares llega a tener un espesor de más de 3m (Fig. 2D). Existen numerosas fracturas que alcanzan más de 20m que se podrían relacionar con *feeders* cuando aparecen en suelos (foto 2D) y *outlets* cuando se encuentran en paredes y techos (Fig. 2B). Las galerías de las partes más alejadas a la entrada de la cueva, y por ello más distantes de la línea de costa, presentan una configuración laberíntica (SOTO et al 2020) (Fig. 1).

Espeleotemas

Los espeleotemas en Cueva del Agua no son muy abundantes. Se localizan principalmente en el sector noroeste. Se han encontrado espeleotemas aéreos epigénicos a 200m, 600m, 700 y 1.600m de la entrada en profundidades de entre 0 y -6m. En su conjunto son principalmente estalactitas, estalagmitas y bandera. A 600m del inicio del recorrido se han observado pavimento de calcita que ha quedado colgado (Fig. 3B). A partir del paso de 850m hay importantes zonas con suelos colgados, paredes y techos de calcita en profundidades entorno a los -20m.
En el sector sureste cerca del mar se han localizado espeleotemas de origen freático o epifreático como son los depósitos de calcita flotante (Fig. 3A), conos de calcita flotante (Fig. 3C) y nubes (Fig. 4). Algunas de las nubes

presentan pequeñas hendiduras a modo de canales de burbujas (Fig. 4B).

En toda la cavidad y más frecuentemente en el sector noroeste se han observado estructuras blandas y oscuras sobre paredes y techos que recuerdan a “pool fingers” (Fig. 3D, 5A), que en las zonas más profundas adquieren estructuras más complejas (Fig. 5B). Estudios preliminares de estas estructuras realizados por los autores (datos no publicados) indican concentraciones elevadas de hierro y manganeso en estos depósitos.

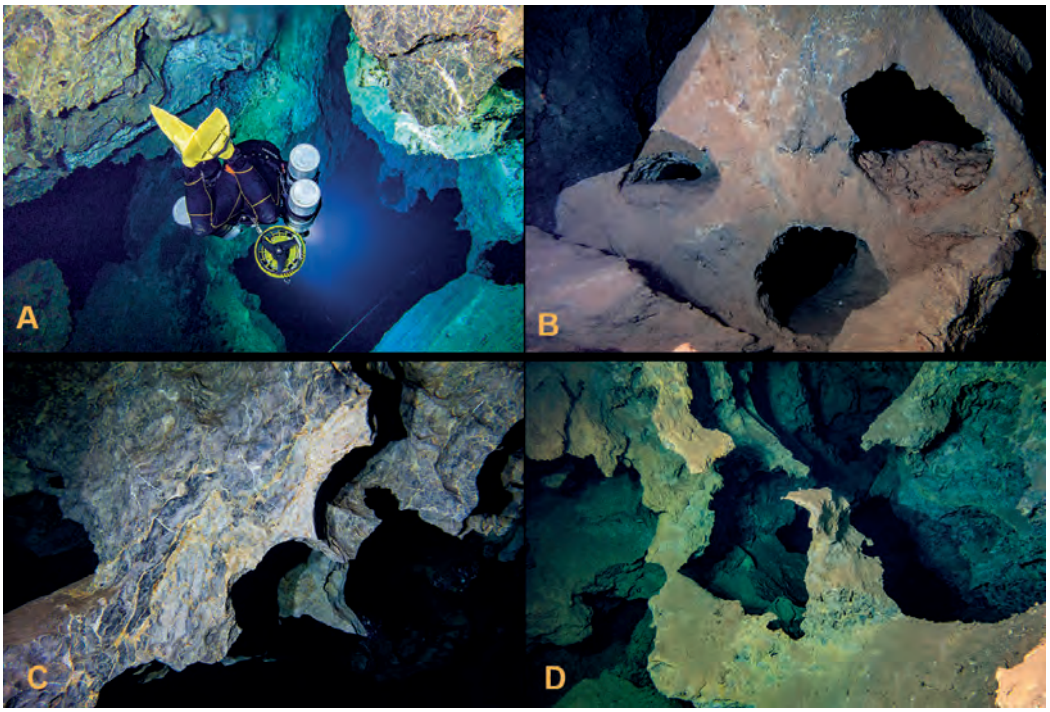

Figura 2. Morphologies in Cueva del Agua

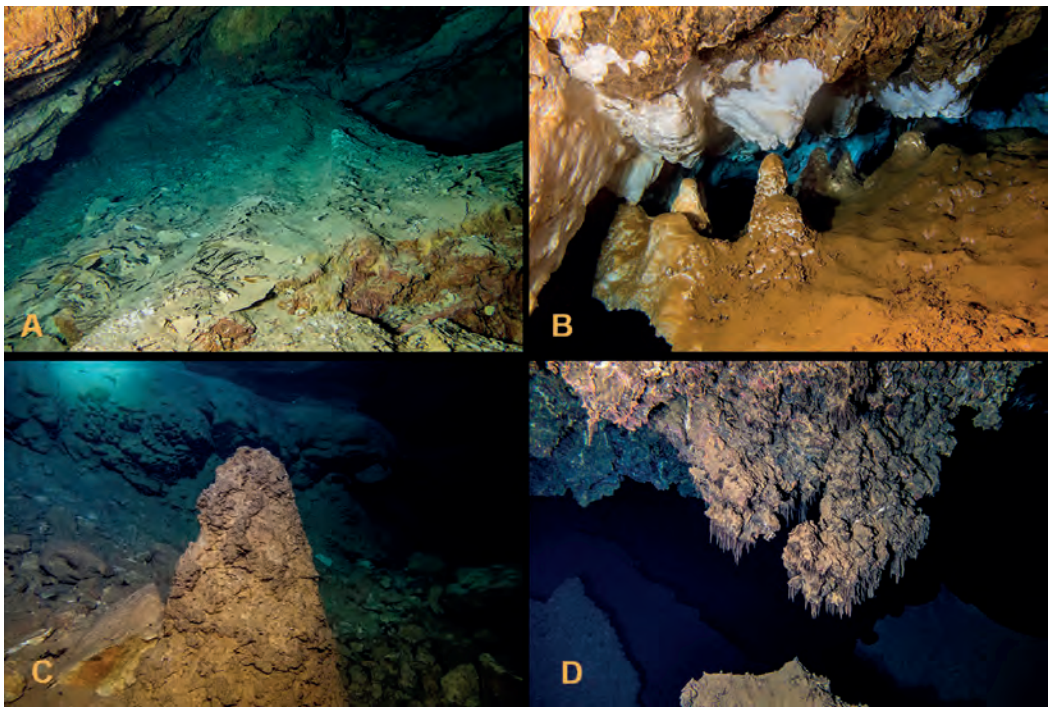

Figura 3. Speleothems, A. Raft calcite deposits, B. Submerged Subaerial speleothem, C. Raft calcite Cone, D. Structures similar to “Pool Fingers”.

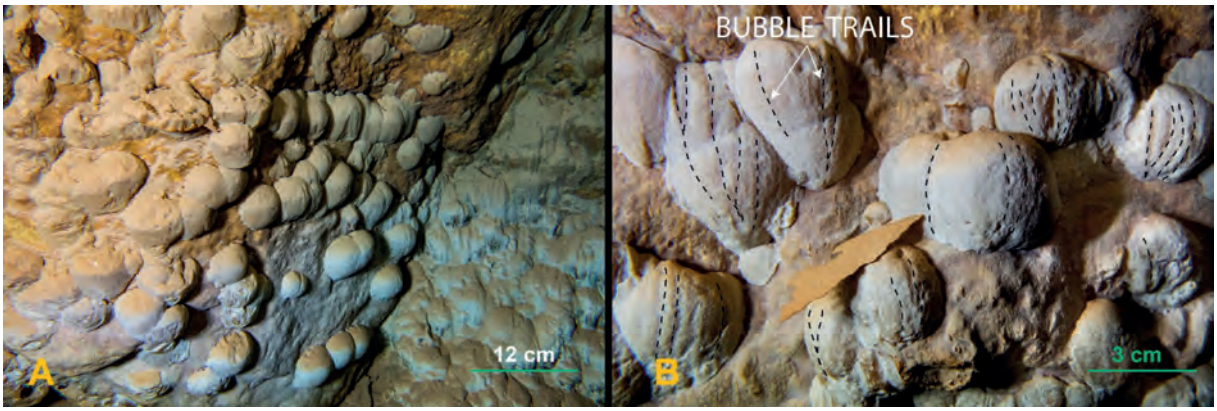

Figura 4. A. Cave clouds, B detail of cave clouds and bubble trails.

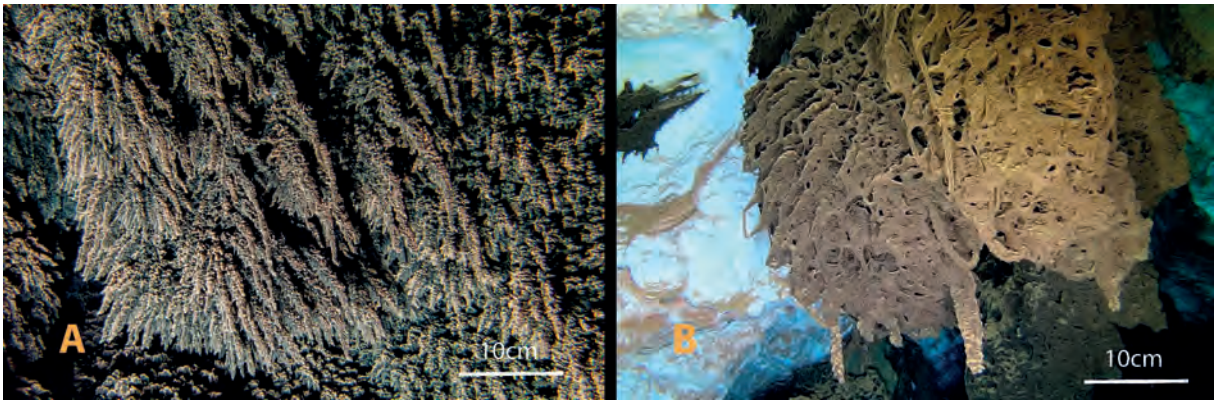

Figura 5: A, B. Deposits similar to pools fingers with high content of iron and manganese.

Conclusiones

Cueva del Agua es una cavidad hipogénica activa que actúa como manantial del acuífero Vértice-Horno y que vierte sus aguas al Mediterráneo. El agua termal con alto contenido en CO_2 ha dado lugar a la disolución de la roca de caja caliza y ha favorecido el desarrollo de morfologías típicamente hipogénicas. Además, se ha documentado la presencia de espeleotemas de origen subacuático, algunos de ellos formados típicamente (aunque no exclusivamente) en ambientes hidrotermales (p. ej. nubes de cuevas y calcita flotante). Sin embargo, también se han observado espeleotemas de origen subaéreo que hoy en día aparecen a varios metros de profundidad bajo el agua de la cueva. Esto sugiere que la cavidad ha tenido una historia ligada a los cambios en el nivel relativo del Mar Mediterráneo y que podrá ser estudiado en el futuro a través del análisis geocronológico de sus espeleotemas.

Agradecimientos

Javier Ruberte, Andrés Marín, Francisco M. Izquierdo Juan L. Ronda, José L. Carcelén, Ricardo Constantino, Belén de Andrés.

Referencias

GARCIA VICENTE, VARELA MARIA (2019) Historia de la exploración del tramo 200m - 860m de la Cueva del Agua en Isla Plana (Murcia). En Historia de las exploraciones, edición digital en www.cuevadelagua.es

LLAMUSI J.L., SANCHEZ, J., ROS A., GAZQUEZ F., RODRIGUEZ-ESTRELLA T., CALAFORRA J.M., FERNANDEZ A., CARCELEN J.L., TREMIÑO M., ALDEGUER M. (2020) Cueva del Agua – Sima Destapada cuevas hidrotermales de Isla Plana (Cartagena). Edit. Natursport, Murcia

LLAMUSI J.L., ROS A., FERNANDEZ-CORTES A., CALAFORRA J.M., GAZQUEZ F., SOTO J.A. (2020-A) Resultados preliminares de la monitorización termo-gaseosa en Cueva del Agua, Cartagena. En ediciones digitales CENM-naturaleza www.cenm.es

LLAMUSI J.L., ROS A., SOTO J.A., GAZQUEZ F., CALAFORRA J.M., FERNANDEZ-CORTES A. (2020-B) Caracterización ambiental del aire confinado en la zona epifreática de entornos hipogénicos: un ejemplo de Cueva del Agua (Cartagena, sur de España). pendiente publicación.

SOTO J.A., LLAMUSI J.L., ROS A., (2020) Memoria exploración galerías del Mar, sector Sureste Cueva del Agua 2020. Edita CENM-naturaleza en “Historia de las exploraciones”, edición digital www.cuevadelagua.es .

The first important thermal sulphuric caves of Albania (Holtas canyon, Central Albania)

Alessandro MARRAFFA[1,2], Ivano FABBRI[3], Katia POLETTI[3], Claudio PASTORE[1,3], Wainer VANDELLI[4], Michele SIVELLI[5] & Jo DE WAELE[1]

(1) Dipartimento di Scienze Biologiche, Geologiche e Ambientali, Università di Bologna, Bologna, Italy, jo.dewaele@unibo.it (corresponding author),
(2) Gruppo Speleologico Martinese, Martina Franca, Italy, alessandro.marraffa@studio.unibo.it, claudio.speleo@gmail.com
(3) Gruppo Speleologico Faentino, Faenza, Italy, ivanofabbri@alice.it, kapoletti@gmail.com
(4) Gruppo Speleologico Paletnologico G. Chierici, Reggio Emilia, Italy, wainwe.vandelli@cern.ch
(5) Società Speleologica Italiana, Bologna, Italy, michele.sivelli@gmail.com

Abstract

In 2018 the GS Faentino started cave exploration in the Holtas Canyon area, in central Albania. Several important cave systems were discovered, explored, and surveyed, among which Shpella Avulit (over 2 km long and around 500 metres deep), Shpella Kaceverrit-Baruttit (around 1 km long and 70 metres deep), Shpella e Kabashit (a 700 metres-long more or less horizontal cave), Sgardamene (around 200 metres long), and a couple of smaller caves. Along the Holtas river there are some thermal sulphuric springs, suggesting a possible hypogenic genesis of the caves in this area. The sampling campaign underlined the presence of sulphuric thermal water, and important secondary cave minerals such as gypsum and jarosite. All caves are characterised by morphologies such as replacement pockets, feeders, rising features. All these observations clearly demonstrate these caves to have formed in a sulphuric acid environment. The cave surveys show horizontal levels that reflect the prolonged stability of the aquifer level. The comparison of the altitudinal differences between the horizontal levels inside the cave with those of the river terraces has shown a clear relationship between landscape evolution and speleogenesis.

1. Introduction

Almost one quarter of Albania is characterised by the outcropping of carbonate rocks, with extensive development of both surface and underground karst features (EFTIMI & ZOJER, 2015). Earlier speleological explorations in this country were carried out only by local Albanian adventurers and researchers until 1989, and most caves were of rather easy access, of archaeological interest, or simply well known by local people. Albania is still a country with a poorly organized speleological structure, and most important discoveries since the gradual opening of its boundaries in the 90s have been achieved by foreign cavers. Most explorations were carried out by Italian and Bulgarian cavers, and to a less extent by caving groups of the Netherlands, Belgium, the UK, France, Croatia, Poland and the Slovak Republic (ZHALOV, 2015). The karst potential of this country is still enormous, and every year important cave systems are discovered and explored, with an increasing involvement of Albanian speleologists.

The strongly deformed inner and external Albanide regions of the country are also rich in geothermal resources, with a large number of thermal springs with temperatures as high as 65°C (Fig. 1). Some of these are also characterised by a Ca-SO_4 chemistry, with strong smell of rotten eggs testifying for the release of H_2S (FRASHERI, 2015). It is therefore strange no sulphuric acid speleogenesis (SAS) caves have yet been reported from Albania. This short paper describes an important SAS cave system in the Holtas canyon (Gramsh District, Central Albania).

Figure 1: Study area (Holtas canyon) and Gramsh district (inset) (from Google Earth).

2. Study area

Kanioni i Holtes (Holtas Canyon) is a natural reserve located in Central Albania, in the District of Gramsh (Elbasan Prefecture) (Fig. 1). This area is characterised by a gentle topography interrupted by some mountainous areas reaching heights of over 1300 m asl. The river Holtas, which is an eastern tributary of the Devoll River (which flows through the city of Gramsh) crosses a steeply inclined limestone ridge forming a spectacular E-W gorge. Two small villages (less than 50 inhabitants) overlook the valley: Kabash located northeast, and Tervol south.

On the western part of the gorge, where the river leaves the almost vertical limestone rocks, several sulphuric springs are in part used for tourist purposes. A little downstream from these springs there is a thermal swimming pool and a small restaurant, whereas more downstream along the river the construction of a dam is foreseen in the near future.

From a geological point of view the Holtas area is located in the Kruja tectonic zone (External Albanides) (VELAJ, 2012). The carbonate sequence outcropping in the area is of Upper Cretaceous-Eocene age and is characterised by many interruptions, erosional surfaces, and bauxitic levels. It can be divided in three main units: more or less dolomitic limestones with rudists (Upper Cretaceous), biomicritic limestones (Eocene), and biomicritic calcareous turbidites (Eocene). This carbonate succession is folded forming a NW-SE directed narrow anticline, forming the high portions of terrain surrounded by marly and easily erodible more recent deposits.

3.The caves

The area of Tervol and Kabash was first visited in 2018 by a team of Italian cavers, in an expedition organized by the Gruppo Speleologico Faentino, with the help of a local caver from Tirana (Etmond Cauli). During this first recognition, it became immediately clear that the area was very promising, and soon a series of interesting caves was discovered. Besides the well-known Shpella Kabashit, the most important newly explored caves are Shpella Barrutit-Kaceverrit, Shpella Avulit, and Shpella Sgardamene.

Barrutit-Kaceverrit is a complex system of caves with a total of 10 entrances, the biggest of which are situated at 367 and 318 m asl. It is the most important cave system in the southern flank of the canyon. The main passages are developed NW-SE, parallel to the flank of the mountain and to the steeply inclined Cretaceous limestone beds and develop on 8 more or less horizontal levels (370, 350, 310, 300, 280, 275, 269, and 255 m asl).
Shpella Kabashit (640 m asl) is known since a long time, and local guides sometimes bring visitors to this almost 700 m long cave. It is developed along a NNE-SSW fracture, has a rather small entrance followed by a wide and high more or less horizontal passage which floor is covered with large limestone blocks.

Shpella Sgardamene (632 m asl) is the shortest cave, a little over 100 metres long and composed of a unique large room opened to the surface by the collapse of the roof. Shpella Avulit is the most interesting cave, characterised by a predominantly vertical development and descending for over 500 m, with a development of almost 1.5 km. It is still in exploration in its deepest parts. The cave has a series of clearly horizontal levels at 510, 460, 410, 360, and 310 m asl.

4. Geomorphology, mineralogy, and geochemistry of waters

The two most important caves (Shpella Avulit and Shpella Barrutit-Kaceverrit) show evident signs of action of sulphuric fluids, still active today (in the deeper branches) (Fig. 2). These include typical morphologies such as replacement pockets, some of which (in intermediate and lower levels) still filled with gypsum crusts. Gypsum coralloid-lined feeders have also been found in the main level at 310 m asl in Barrutit-Kaceverrit, accompanied by rising wall and ceiling channels and megacusps. Other sulphates typical of SAS, such as jarosite, have also been sampled and analysed in small amounts. Replacement pockets are preserved in protected overhanging walls also in two smaller caves at 640 m asl and close to the upper entrances of Barrutit-Kaceverrit, and in a protected limestone wall in Sgardamene Cave.

Especially in Shpella Avulit, several feeding fissures have been recognised, and large gypsum deposits (gypsum “glaciers”) are present at 310 m asl. The smell of sulphuric waters and vapors is clearly present in the parts of Barrutit-Kaceverrit closer to the gorge, but has to be put in relation with rising warm air coming from the sulphuric springs located 10 meters lower in the river bed. The presence of large gypsum deposits in the deeper parts of the cave, far from the influence of incoming air from entrances, and their association with vertical fissures with replacement pockets and gypsum coralloid formations, allows to confirm the caves have formed by rising fluids and gases coming from deep inside the mountain, following deep-rooted fractures.

Three water samples have been taken in three springs occurring close to the exit of the Holtas river from the gorge: the most important is a thermal pool on the northern edge of the river (C2), approximately 100 meters inside the narrow gorge, occasionally used by local people. Closer to the exit of the gorge and on the opposite side there is another thermal sulphuric spring (C1). The last sample (C3) was taken at the foot of the close-to-vertical cliffs located

north of the exit of the Holtas canyon, the water of which is directed to the swimming pool 150 meters downstream.

C2 and C3 have temperatures of 24°C (measured in November 2019), whereas C1 is slightly less thermal (18.8°C) and is probably a mixture of fresh river water with the warm sulphuric fluids rising from below. The first two have sulphate concentrations of 1299 and 1312 mg/L respectively, with a conductivity of 2820 and 2830 microS/cm. C1, instead, contains only 580 mg/L SO_4^{2-} with an EC of 1612 microS/cm.

The two most important caves are developed along a well-defined series of horizontal cave levels, which are correlated to phases of relative stable position of the sulphuric water table (DE WAELE et al., 2016). These levels can be carved in a matter of thousand years or less, since the sulphuric acid speleogenetic mechanism is much faster (probably by two orders of magnitude) than the normal epigenic one. Two main levels at 350-360 and 310 m asl in both Baruttit-Kaceverrit and Avulit caves testify two stable periods separated by a 40-50 metres altitude difference, showing a rapid entrenchment of the Holtas river in a short period of time. Also, the higher levels in Shpella Avulit (at 410 and 460 m asl respectively) show a fast evolution of the caves and the correlated Holtas gorge. The altitudinal differences in the lower levels found in Baruttit-Kaceverrit cave (300, 280, 260 m asl) show minor values, which might be explained by a decreasing tectonic uplift rate (and related decreasing entrenchment of the gorge), or by an increased rise of sulphuric fluids (higher flowrates, or more aggressive chemistry). On the southern flank of the gorge, at 510 m asl, close to the ancient construction of a castle, a fluvial conglomerate has been found near a small cave. The ancient Holtas river appears to have flown here in the past, exiting the limestone ridge more to the South when the present canyon did not yet exist. Only when the river found a new path through the mountains, it started carving its 260-m deep canyon, with phases of rapid entrenchment and short stable intervals during which the sulphuric cave levels were carved. Dating of the different cave levels, and their comparison with river terraces and geomorphological evidences in the area, might shed light on the complex landscape evolution of this area.

5. Conclusions

Recent speleological explorations in the Holtas Canyon (Gramsh District, Central Albania) has allowed to discover a very interesting and extensive system of sulphuric acid caves. The two most important caves (Shpella Avulit and Shpella Barrutit-Kaceverrit) have developments of over 1 km, and the first is over 500 m deep. Both caves have extensive deposits of gypsum, many typical morphologies of sulphuric acid speleogenesis (replacement pockets, cupola, megacusps) and are arranged along different more or less horizontal cave levels. Geomorphological surveys carried out in the area have allowed to find alluvial sediments at 510 m asl, suggesting the Holtas River followed a different course in the past, sustaining the relatively young age of the Holtas Canyon and its caves. Chronological constraints would be needed to pin down the ages of the cave levels, with the aim of unraveling the interesting landscape evolution in this area of the external Albanides.

Acknowledgments

Many thanks to all the cavers that participated in the expeditions to Albania. Local people of both Kabash and Tervol villages are thanked for their hospitality. A special thanks to Etmond Cauli, our local interpret, who is gaining enthusiasm in caving and exploring the wonderful Albanian karst areas.

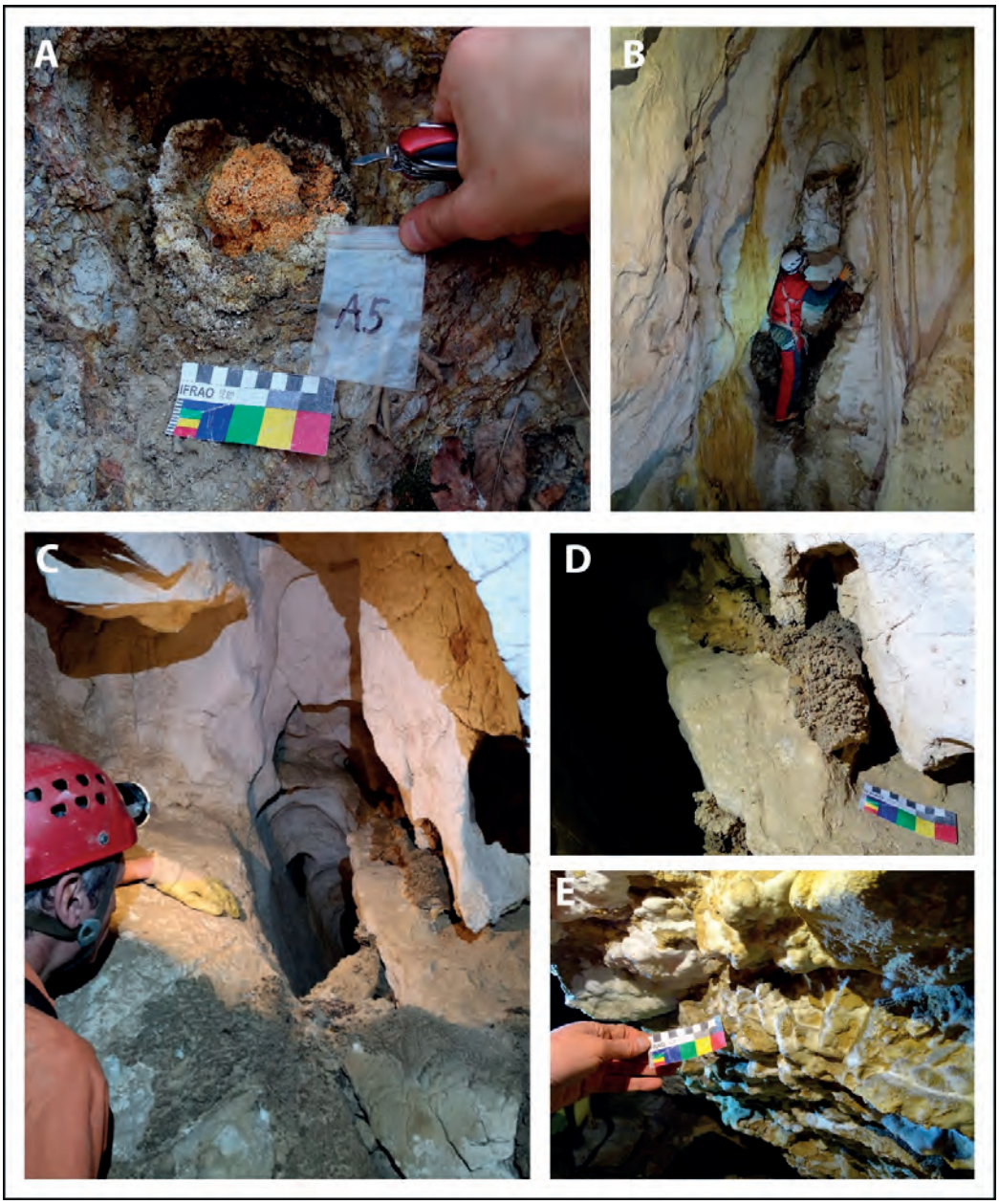

Figure 2: A. Pyrite nodule with secondary minerals; B. Replacement pockets with gypsum crust in Barrutit cave; C. Feeder inside Kaceverrit cave; D. Gypsum crust near feeder (Kaceverrit cave); E. Gypsum crust (Kaceverrit cave).

References

DE WAELE J., AUDRA P., MADONIA G., VATTANO M., PLAN L., D'ANGELI I. M., BIGOT J.Y. and NOBÉCOURT J.-C. (2016). Sulfuric acid speleogenesis (SAS) close to the water table: examples from southern France, Austria, and Sicily. *Geomorphology*, 253, 452-467.

EFTIMI R. and ZOJER H. (2015) Human impacts on karst aquifers of Albania. *Env. Earth Sciences*, 74(1), 57-70.

FRASHERI A. (2015) Geothermal Energy Resources in Albania-Country Update Paper. *Proceedings World Geothermal Congress*, 11 p.

VELAJ T. (2012). Tectonic style and hydrocarbon evaluation of duplex Kruja zone in Albania. *Nafta*, 63(7-8), 236-242.

ZHALOV A.K. (2015) Bulgarian speleological studies in Albania 1991–2013. *Berliner Höhlenkundliche Berichte*, 58, 1-91.

Hypogene karst in the External Albanides and its pronounced geomorphological effect

Alexander B. KLIMCHOUK[(1)], Romeo EFTIMI[(2)] & Viacheslav N. ANDREYCHOUK[(3)]

(1) Institute of Geological Sciences, National Academy of Sciences of Ukraine, Kiev, Ukraine, klimchouk.2020@gmail.com (corresponding author)
(2) Independent Researcher, Tirana, Albany, eftimiromeo@gmail.com
(3) Faculty of Geography and Regional Studies, Warsaw University, Warszaw, Poland, w.andrejczuk2@uw.edu.pl

Abstract

The structural fabric of Albania is defined by the NNE-SSE-trending tectonic zones. Besides longitudinal faults, the Albanides are broken by transversal faults at various scales. In the Kruja and Ionian zones of the External Albanides, carbonates of Cretaceous-Eocene age are widely spread although only locally exposed. Wells tap carbonate thermal aquifers and hydrocarbon reservoirs at depths up to 3,700 m. The deep aquifers/reservoirs have low matrix porosity but substantial and locally high fracture and karstic porosity. We investigated three sites of expressed hypogene karst (Holta, Lengarica, and Leskovik), scattered along the Kruja zone but possessing important common characteristics: (1) canyons crossing NE-SW the massifs of carbonates exhumed from beneath the flysh at the crests of anticlines; (2) rising thermal springs discharging H_2S-enriched waters, which are variable mixes of the deep flow with shallow groundwater; (3) abundant hypogene karst features, mainly associated with water-table-related SAS, although sub-vertical features controlling major canyon segments could have been formed in the deep setting by other processes. During uplift and denudation throughout Late Miocene – Pleistocene, discharge of deep groundwater focused upon the tops of emerging anticlines and caused intense hypogene karstification, which was the primary control in the formation of the antecedent canyons by karst piracy.

1. Introduction

Albania is part of the Dinaric-Hellenic range in the Mediterranean Alpine fold-thrust belt. This paper assesses the potential for hypogene karstification in the External Albanides and characterizes several areas where it is expressed at the surface. The potential is determined by the extent of carbonate rocks (including in the deep subsurface), tectonic structure, geodynamic and geomorphic evolution, and the fluid circulation regimes. It is accessed through the analysis of available geological and hydrogeological data, data from hydrocarbon reservoir studies and exploration (e.g., ALBPETROL, 1993), and studies on the geothermal field and thermomineral water resources (e.g., FRASHERI, 2013; EFTIMI & FRASHERI, 2016, 2018). We investigated three sites where hypogene karst is expressed at the surface and performed documentation of karst features, structural and geomorphological observations, geophotography using hand and drone cameras, water temperature and electrical conductivity measurements in springs, and spring- and well-water sampling for chemical analyses.

2. Geological conditions and the potential for hypogene karst

The geological structure of Albania comprises two major units, Internal Albanides to the east and External Albanides to the west (MEÇO & ALIAJ, 2000). The main structural fabric in the Albanides is defined by the NNW-SSE-trending fold-thrust belts, viewed as tectonic zones. The Korab, Mirdita, and Gashi zones form the Internal Albanides, dominated by metamorphic rocks and ophiolites. The Albanian Alps, Krasta-Cukali, Kruja, Ionian and Sazani zones belong to the External Albanides (Fig. 1A), a part of the S. Adriatic sedimentary basin highly affected by the westward thrusting in the Eocene and the late Oligocene-Miocene (WALL et al., 2006 and references therein). Besides a system of longitudinal faults, the Albanides are broken by a series of transversal (NE-SW) faults on many scales, of which the basement-related Scutari–Pec and the Vlora-Elbasan-Diber faults are the major ones (VAN GEET et al., 2002).

The extensive potential for hypogene karstification exists in the Kruja and Ionian zones, where platform and basinal carbonate formations of the Upper Cretaceous to Eocene are widely spread, although only locally exposed from beneath the capping Oligocene flysh sediments (siliciclastic). Carbonates are commonly exposed in the crests of characteristic anticlines associated with NNW-SSE-trending thrusts that define the fabric of the zones (Fig. 1 B). The flysh sediments form a low-permeability seal for aquifers/reservoirs hosted in carbonates. Along the dip, carbonates plunge down up to 10 km. A number of wells tap carbonate thermal aquifers and hydrocarbon reservoirs at depths up to 3,700 m. Deep groundwaters are commonly of Cl-Na-Ca or Cl-SO_4-Na-Ca type and rich in H_2S. The carbonate reservoirs are characterized by very low matrix porosity but substantial and locally high fracture and karstic porosity, particularly in the fault zones and the crests of anticlinal structures. Open and sediment-filled cavities up to dm size are reported from boreholes (VAN GEET et al., 2002). Diagenetic studies indicate that after an expulsion/over-pressurized regime with rock buffered (closed system) fluids, open system fluid advection became involved after

folding in the Late Oligocene–Aquitanian, reflecting large-scale fluxes of external CO_2-charged fluids derived from the basement or evaporitic décollement horizons (VAN GEET et al., 2002). This was enabled by the creation of vertical throughgoing discontinuities, of which those trending transversely (NE-SW) were the dominant pathways for carrying and storing fluids, based on widespread occurrence of open voids, calcite fill, and bitumen accumulation along them (WALL et al., 2006). During uplift and denudation of the flysh cover during the Late Miocene – Pleistocene, upward flow from deep aquifers focused upon anticlines, particularly in localities where carbonate formations were being brought to the shallow subsurface and locally exhumed.

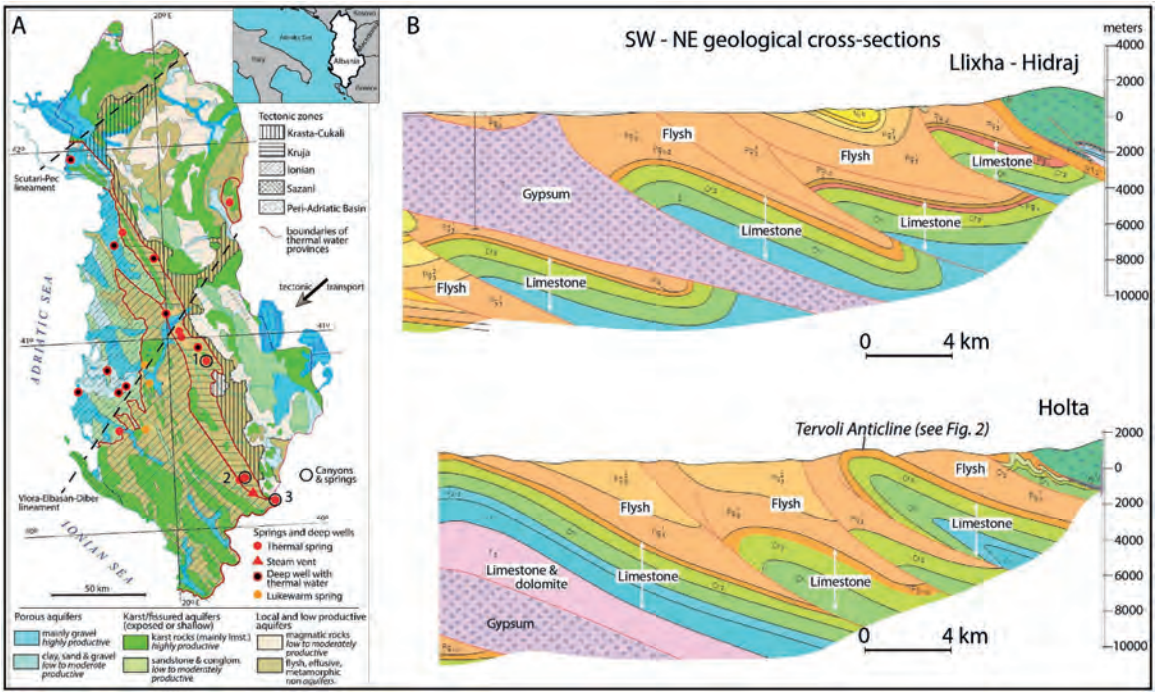

Figure 1: Tectono-hydrogeological map of Albania (A; modified after EFTIMI & FRASHERI, 2018) and typical SW-NE geological sections across the Kruja zone (B; modified after GEOLOGICAL MAP OF ALBANIA, 2002). The map shows tectonic zones, thermal water provinces, and important thermal springs and deep wells. Numbers on the map indicate sites described in this study: 1 – Holta, 2 – Lengarica, 3 – Leskovik.

3. Studied sites: Canyons with thermal springs

The Holta Canyon. The Holta River forms a canyon where it crosses the Tervoli Anticline (Fig. 1B, 2A-D). The lower stretch of the canyon displays numerous cavities in the walls, some of which are arranged at certain levels but many seem to randomly distribute at different heights. Caves are often vertically stacked along sub-vertical faults (Fig. 2F). In places, there are swarms of enlarged up to 30-40 cm vertical fractures. Karstified fault zones and fracture swarms have transverse (N to NE) trends. Caves at or close to the riverbed do not extend more than a few meters and display morphologies attesting rising flow. Some stretches of the canyon have overhanging walls, giving an impression of the formation along major conduits (Fig. 2E).

There are three rising springs in the lower stretch of the canyon and one outside it, at the flysh-limestone contact zone near the canyon exit (Fig. 2B). The canyon springs issue from caves or enlarged fractures. Discharges vary between 8-30 l/s and water temperatures vary between 22.9-24.1 °C. The waters are of SO_4-Ca-Mg type (TDS 2.363 - 2.437 mg/dm^3). H_2S is present in the spring waters albeit in small abundance (not measured).

Lengarica Canyon. The canyon is formed where the Lengarica River crosses the Benja Anticline (Fig. 3A&B). The main stretches of the canyon are defined by karstified segments of large vertical NE-NEE-trending fractures connected by a N-S-trending stretch, also structurally controlled (Fig. 3D&E). The walls display numerous cavities and solutionally enlarged fractures at various levels. There are eight springs of varying discharges (up to 70 l/sec) issuing thermal water (24.8 to 29.8 °C) of Cl-HCO_3-Na-Ca type (TDS 1.150 mg/dm^3), enriched in H_2S.

Leskovik Canyon. The canyon, located at the Albanian-Greek border, is formed where the Sarandaporo River crosses the anticline of the same name (Fig. 4A&B). The walls display numerous cavities aligned at various levels to solutionally enlarged N-NE-trending fractures (Fig. 4E). There are four thermal (27.6 °C) springs along the right bank of the river, with water of Cl-HCO_3-Na-Ca type (TDS 1.360 mg/dm^3), enriched in H_2S. The largest spring (around 16 l/sec) rises inside a sizable cave (Fig. 4D) and forms a lake overflowing to the river (Fig. 4C).

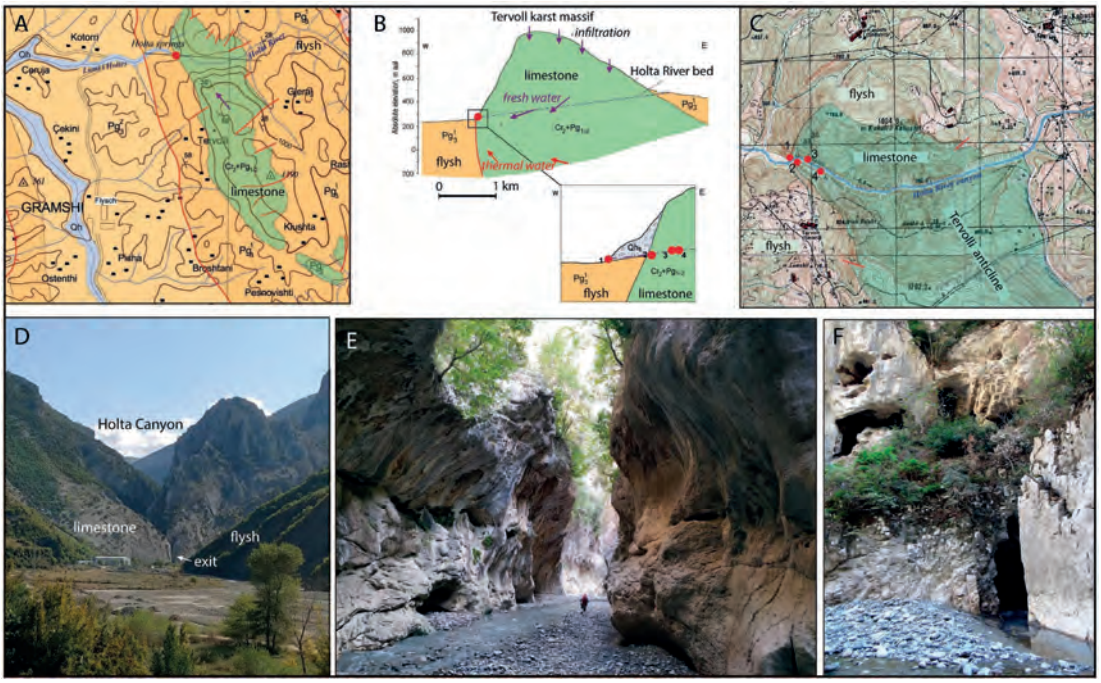

Figure 2: Holta Canyon and springs: A – geological map (Geological map of Albania, 2002); B – hydrogeological cross-section; C – topographic details with geology elements; D – the general view of the Holta Canyon; E – canyon morphology; F – karst caves in the canyon wall (the lower one with a spring).

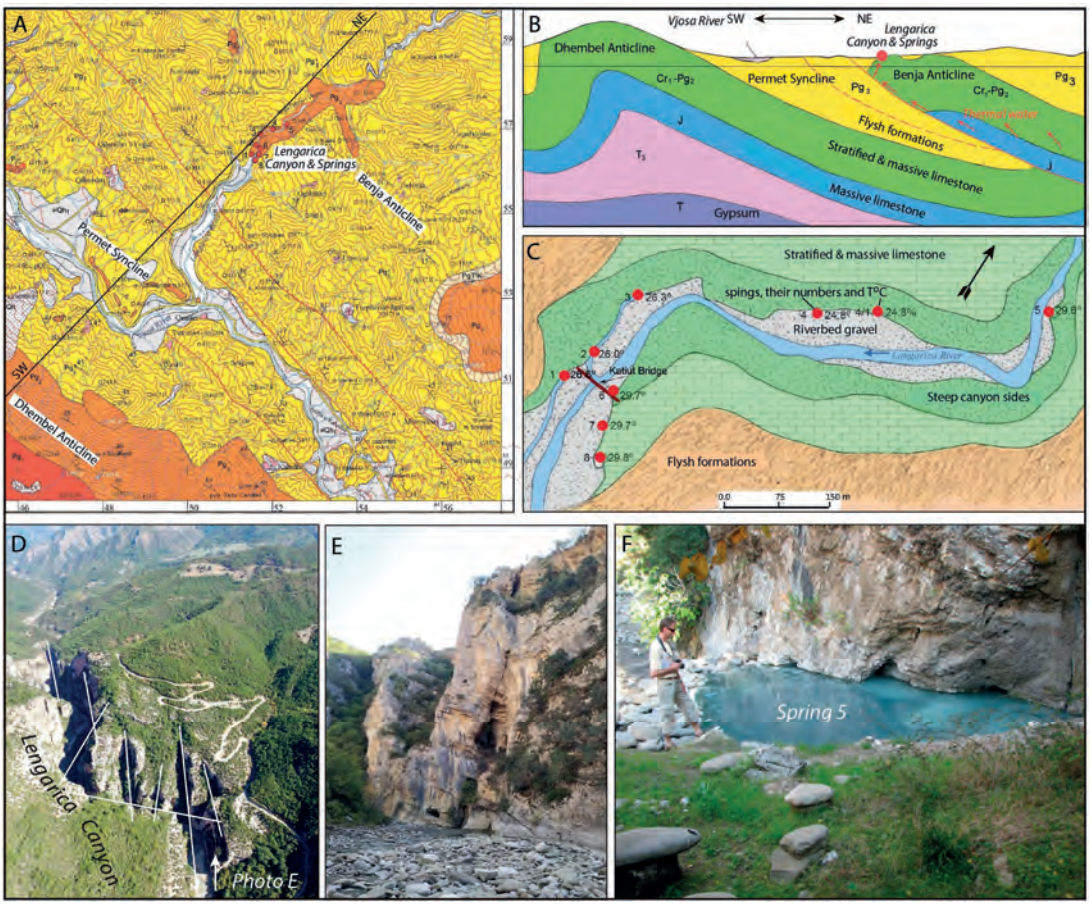

Figure 3: Lengarica Canyon and springs: A – geological map (Geological map of Albania, 2002); B – geological cross-section; C – location of springs (numbers to the right of symbols indicate T); D – the drone oblique view of the canyon (white lines indicate fractures that guide its segments); E – a large karstified fracture (see D for the photo position); F – Spring 5.

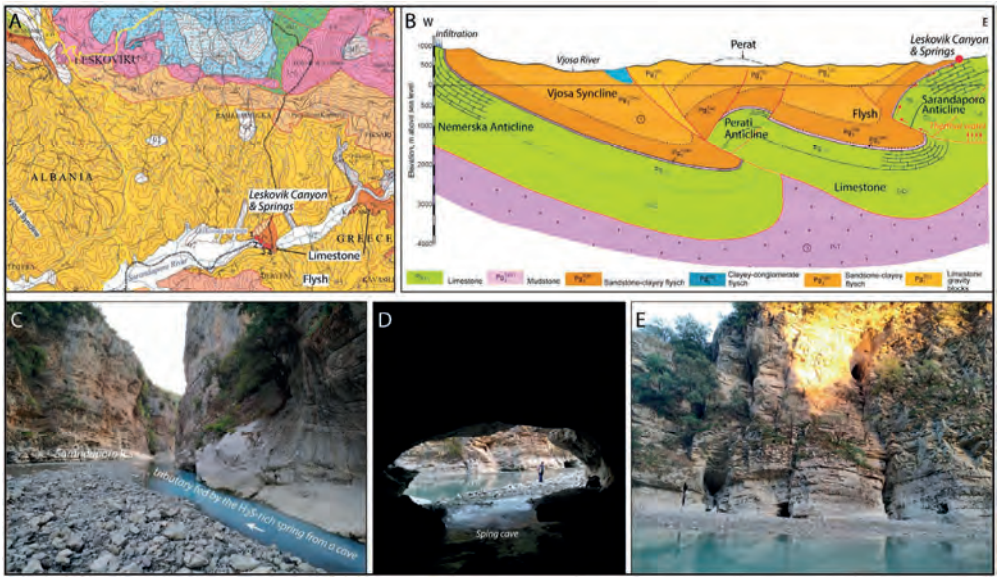

Figure 4: Leskovik Canyon and springs: A – geological map (from Bushati, 2005); B – geological cross-section; C – the general view of the canyon showing a confluence of the river water and the H_2S-rich water fed from a cave; D – cave with a H_2S-rich spring; E – karst features in the canyon wall.

4. Discussion and conclusions

The extensive potential for hypogene karst exists in the Kruja and Ionian zones, where Upper Cretaceous to Eocene carbonates are widespread although only locally exposed. In the Sazani zone, thick Cretaceous-Eocene carbonates are widespread beneath Burdigalian marls but data to access their hypogene karst potential are limited. Upward flow from deep aquifers follows vertical discontinuities of transverse trends and is focused upon anticlines, particularly in places where carbonates emerge from beneath the capping Oligocene flysh.

Three examined sites, scattered along the SSE stretch of the Kruja zone, are canyons formed where rivers cross the exposed carbonates at the crests of anticlines. Major segments of the canyons are controlled by large solution-enlarged fractures. There are numerous rising H_2S-rich thermal springs discharging SO_4-Ca-Mg (Holta) or Cl-HCO_3-Na-Ca (Lengarica and Sarandaporo) type waters, which are variable mixes of the deep flow with shallow meteoric groundwater. The canyons display abundant hypogene karst features (caves and enlarged fractures) mainly associated with water-table-related SAS, although some rift-like features could have been formed in the deep setting by other dominant processes.

Enhanced upwelling discharge of deep groundwater and associated hypogene karstification in the hinges of anticlines were the important, if not primary, controlling factors in the formation of the antecedent canyons through karst piracy.

References

ALBPETROL (1993) Petroleum Exploration Opportunities in Albania: First Onshore Licensing Round in Albania. Publicity Brochure. Western Geophysical, London, 35 pp.

BUSHATI S. (2005) Aplikimi teknikave gjeofizike në studimin e fushës gjeotermale në rajonin Sarandoporo-Konitza. ShGJSh, Qëndra e Kërkimeve Gjeofizike, 46, 24 p.

EFTIMI R., FRASHËRI A. (2016) Thermal and mineral waters of Albania. PRINT AL Tirana, 214 p. (in Albanian).

EFTIMI R., FRASHËRI A (2018) Regional hydrogeological characteristics of thermal waters of Albania. Acta Geographica Silesiana, 12/2 (30), 11–26.

FRASHËRI A. (ed.) (2013) Geothermal Atlas of Albania Academy of Science of Albania, Faculty of Geology and Mining, Polytechnic University of Tirana. Tirana. 122 p.

GEOLOGICAL MAP OF ALBANIA (2002) Sc. 1:200.000, Geological Service, Tirana.

MEÇO S., ALIAJ S. (2000) Geology of Albania: Beitraege zur Regionalen Geologie der Erde, v. 28, 256 p.

VAN GEET, SWENNEN R., DURMISHI C., ROURE F., MUCHEZ P.H. (2002) Paragenesis of Cretaceous to Eocene carbonate reservoirs in the Ionian fold and thrust belt (Albania): relation between tectonism and fluid flow. Sedimentology, 49, 697–718.

WALL B.R.G., GIRBACEA R., MESONJESI A., AYDIN A. (2006) Evolution of fracture and fault-controlled fluid pathways in carbonates of the Albanides fold-thrust belt. AAPG Bulletin, v. 90, no. 8, pp. 1227–1249.

Hypogenic karst inception and super-permeability zones in Neoproterozoic carbonates of Northeastern Brazil

Luca PISANI[(1)], Marco ANTONELLINI[(1)], Jo DE WAELE[(1)], Augusto AULER[(2)], Philippe AUDRA[(3)], Giovanni BERTOTTI[(4)], Cayo PONTES[(5)], Vincenzo LA BRUNA[(5)], Fabrizio BALSAMO[(6)] & Francisco Hilario BEZERRA[(5)]

(1) Department of Biological, Geological and Environmental Sciences University of Bologna, Italy, luca.pisani4@unibo.it (corresponding author), jo.dewaele@unibo.it, m.antonellini@unibo.it
(2) Instituto do Carste, Brazil, aauler@gmail.com
(3) University Cote d'Azur, Polytech'Lab EA7498, Nice, France, Philippe.AUDRA@univ-cotedazur.fr
(4) Department geoscience engineering TU Delft, Netherlands, G.Bertotti@tudelft.nl
(5) Department of Geology, Federal University of Rio Grande do Norte, Brazil, cayopontes@gmail.com, vincenzolabruna@gmail.com, bezerrafh@geologia.ufrn.br
(6) Natural and Experimental Tectonics research group, Università di Parma, Dipartimento Scienze Chimiche, della Vita e della Sostenibilità Ambientale, Italy, fabrizio.balsamo@unipr.it

Abstract

Hypogenic caves in carbonate reservoirs offer the opportunity to study exposed and accessible analogues of buried conduit systems. "Super-permeability zone" (here referred to as super-*k*) is a term adopted in petroleum geology literature to identify stratigraphic horizons characterized by exceptionally high permeability. In case of soluble rocks such as carbonates, super-*k* zones can focus fluid flow and facilitate the inception of an interconnected conduit system. In this contribution, we present the work performed in a hypogenic cave developed within a Neoproterozoic mixed carbonate-siliciclastic succession (*Calixto Cave*, Brazil). Detailed stratigraphic and structural characterization was complemented with 3D models acquired by terrestrial laser scanning techniques to highlight background geological features controlling the spatial and morphological organization of the conduit system. Furthermore, compositional analysis (XRD, XRF, SEM-EDX) of cave deposits and bedrock were performed to constrain its speleogenesis. We found that silicification, fractures properties, and lithostratigraphic variability determined the formation of super-*k* zones and seal units, which distribution was fundamental for the spatial and morphological organization of the hypogenic conduit system. This contribution may be of interest for both academic studies on fluid flow and karstification, and practical applications such as karst reservoir characterization for hydrocarbons, geothermal energy, and groundwater production.

1. Introduction

Hypogene caves form by dissolution of soluble minerals by rising aggressive solutions, whose origin is not directly connected to surface processes (KLIMCHOUK, 2009). The identification of efficient permeability pathways allowing fluid flow is critical for understanding the genesis and the spatial organization of karst systems, whose prediction is of broad interest for many applied fields (i.e., groundwater, hydrocarbons and geothermal reservoirs, geohazard, collapse dolines).

Structures like faults, joints, veins, stylolites and bedding interfaces have a fundamental role for fluid flow in rocks with low primary porosity and permeability. Opening-mode fractures usually represent conduits (FORD et WILLIAMS, 2007), whereas stylolites may form either barriers or conduits (ARAÚJO et *al.*, 2020). All these structures may be associated with fault damage zones or form in cluster into high-persistency and continuous domains of localized deformation (i.e., "fracture-corridors", "fracture-zones"). Bedding interfaces generally focus fluid flow due to their high lateral continuity and may compartmentalize volumes of rocks with different petrophysical properties (BALSAMO *et al.*, 2020). Other than tectonic structures, also sedimentary and stratigraphic features control fluid flow and can contribute to the resultant morphology of the conduit system. Continuous and sub-horizontal beds of insoluble or low-permeability lithologies may act as barriers for vertically rising fluids; on the other hand, specific units may represent super-permeability zones (super-*k*) due to their petrophysical properties and/or specific fracture patterns. Both these factors may control the formation of vast solutional networks developed at the same stratigraphic position (KLIMCHOUK et *al*., 2016).

In this contribution, we present the work conducted in a km-long cave (*Calixto Cave,* Brazil) formed in a mixed carbonate-siliciclastic succession. This sedimentary sequence is part of the Salitre Formation, of Neoproterozoic age (Fig.1). The aim of the work is to propose a conceptual speleogenetic model for *Calixto Cave*, highlighting the role of the super-*k* and seal layers in controlling hypogenic speleogenesis.

2. Materials and methods

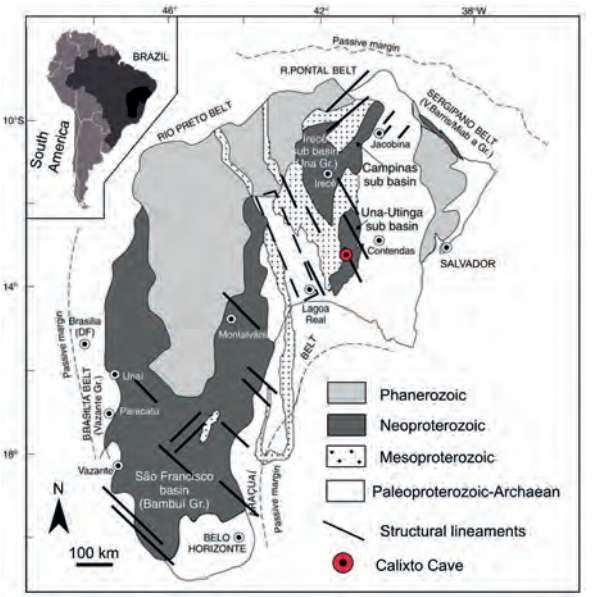

Figure 1: Schematic geologic map of the São Francisco Craton and localization of Calixto Cave (modified from MISI et al., 2011).

We performed a geomorphological, structural, and stratigraphic characterization of the sequence hosting the *Calixto Cave* conduit system. Structural measurements collected by scanline method were used to characterize fracture patterns and estimate fracture permeability of the main joint sets. Estimated fracture permeability for each individual fracture was derived from the computation of hydraulic aperture (*e*), calculated using the mechanical aperture (*E*) measured on the field and corrected for the Joint Roughness Coefficient (JRC), as expressed by the following equation (OLSSON and BARTON, 2001):

$$e = E^2 / \ JRC^{2.5}$$

The estimated fractures permeability was then calculated basing on the parallel-plate model of fractured media (PHILIPP *et al.*, 2013), and expressed in millidarcy (mD).

Terrestrial-laser-scanner (TLS) point clouds were processed with *CloudCompare* software to analyze conduit morphologies in the different levels of the cave system and put them in relation with the lithostratigraphic information collected by field and petrographic observations.

Cave deposits and bedrock were characterized by thin section observations at optical petrographic microscopy, XRD-XRF geochemical analyses and SEM-EDX.

3. Results

The *Calixto Cave* is a 3D multi-storey system that develops in 54 m of a sedimentary sequence dipping to NW at low-angle (5°-15°). The sequence was divided into three lithostratigraphic units (named A, B, and C, from bottom to top). Unit A consists of 19 m-thick cross-stratified dolostone layers (grainstone texture) rich in pyrite crystals. The lower part of unit B is a 1.8 m-thick dolostone pack, with ooidal wackestone or mudstone textures, characterized by intense silicification. Micro-crystalline silica (chert) is concentrated in nodules or discontinuous layers replacing the dolomite grains and is often associated with iron oxides. The upper part of unit B starts with a 0.9 m-thick interval characterized by heteroliths, marly dolostones and micritic dolostones with chert nodules. The unit is closed by 1.1 m-thick interval of sandy siltstones with cross-stratification and lenticular bodies of badly sorted sandstones/fine conglomerates composed of siliciclastic grains, intraclasts and dolomitized ooids. The upper unit C (ca. 31 m-thick) is entirely composed of thick dolostone layers (mudstone or wackestone textures) with frequent chert nodules and occasional layers of siltstones/shales (heterolithic texture).

The cave formed along three main speleogenetic levels controlled by the described lithostratigraphic variations. The lower level developed within unit A. This morphological unit is characterized by a phreatic sponge-work, large chambers, rift-like feeders, and rising channels (Fig.2). Calcite coralloids decorate the walls over much of the lower level. The middle level, within unit B, comprises sub-horizontal conduits organized in a maze-network pattern. In the highly silicified interval, SiO_2 crystals are intensely corroded (both at optical microscopy and SEM observations, Fig.3).

Ubiquitous macrocrystalline deposits of chalcedony and blocky euhedral quartz associated with inclusions of anhydrite, barite, Fe-Ti oxides, muscovite, k-feldspar, and minor amounts of phosphates occupy part of the solutional voids below the upper part of unit B (Fig.4).

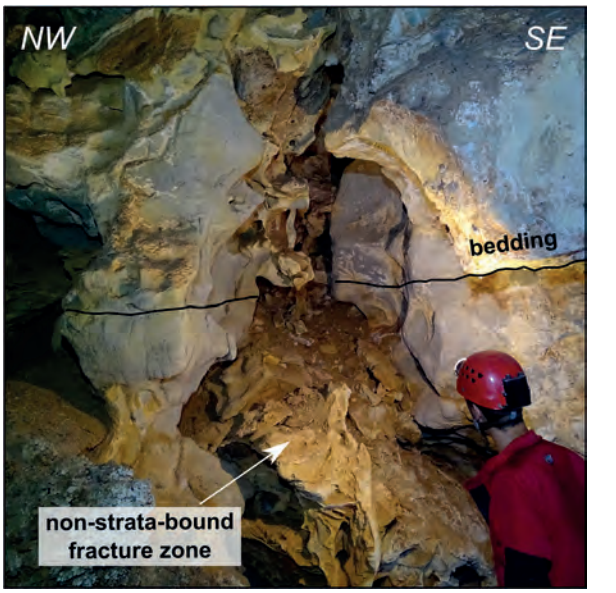

Figure 2: Lower level characterized by phreatic spongework and rising corrosional channels. Feeders and rising channels are generally developed along non-stratabound fracture clusters zones.

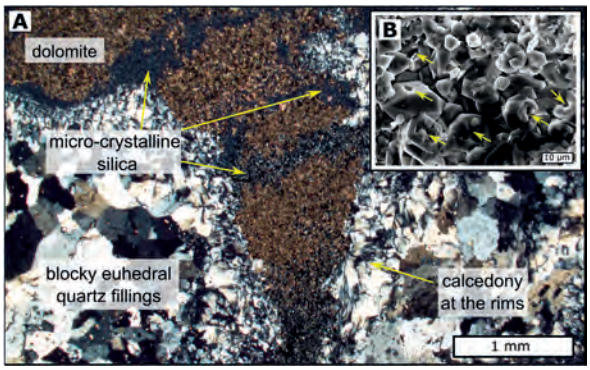

Figure 3: Different textures in the silicified dolostone layer at the base of unit B. A) microcrystalline SiO_2 replaces dolomite grains. Euhedral quartz associated with anhydrite and muscovite fills part of the secondary porosity (picture at cross-polarized-light); B) SEM image with evidence of SiO_2 grains' dissolution (shown by the yellow arrows).

The upper speleogenetic level is localized within unit C and is composed of small conduits with condensation-corrosion cusps, connected to the surface by a collapse doline. The cave shows no evidence of high energy groundwater flow and surface derived sedimentation, except for restricted mudflows associated with passages near its entrance. Most of the sediments in the whole cave are collapsed blocks, gypsum, and guano-related phosphates.

The sedimentary sequence is gently deformed by a few high-angle to sub-vertical structures. The most common structures are strata-bound joints or calcite veins with thin mechanical apertures (< 1 mm) and bedding-parallel stylolites. In unit A, veins may gather in non-strata-bound fracture clusters with apertures up to 0.5-1 cm, average linear intensity of around 18 m^{-1} and fracture permeability in the range of 10^3 – 10^5 mD. In units B and C, fractures are more widely spaced (average linear intensity of 8 m^{-1}), strata-bound and only rarely organized in clusters. The silicified layer at the base of unit B shows a significant increase in fracture intensity (up to 37 m^{-1}), and fracture permeability around 10^5 mD. The upper part of unit B shows fracture permeability with an average value around 10^3-10^4 mD; on the other hand, unit C has low fracture permeability and linear intensity, in the range of 1-10^1 mD and 11 m^{-1} respectively. Feeders and corrosional features in the lower level are controlled by fracture clusters zones and usually present bleaching of the surrounding bedrock.

4. Discussions and conclusions

The thick dolostone interval at the base of unit B was affected by intense silicification, which was later overprinted by dissolution. Fracture concentration is high in chert nodules whereas it is low in soft carbonates and siliciclastic lithologies such as those observed in the upper part of the sequence. In stiff chert, strain localization caused fracture clustering, providing a significant increase in intensity and connectivity (ANTONELLINI et *al.*, 2020). This deformation pattern significantly impacts fracture permeability in the whole sequence. A preliminary conceptual model is proposed to explain silica dissolution and the development of the resultant conduit system.

In the lower unit A, non-strata-bound fracture clusters zones controlled the vertical migration of rising aggressive fluids (Fig.2). The sub-horizontal highly silicified layer at the base of unit B, with dense fracture network and sealed at the top by less soluble and less fractured layers, represented a preferential permeability pathway for lateral fluid flow and dissolution. Evidence of silica dissolution and the paragenesis associated with crystalline euhedral quartz indicate that warm (probably > 200°C) and alkaline basic fluids, likely of hydrothermal origin, may have been the primary source for hypogene speleogenesis under deep-buried phreatic conditions. The seal layers halted vertical fluid flow, further boosting lateral dissolution, and producing a zone with high secondary permeability (super-*k* zone). When the solution pH or the water temperature decreased, dolomite dissolution started with the formation of the spongework in the lower level, and the dissolution of the dolomite-rich bedrock in unit B. During this speleogenetic stage, the solutional voids were partially filled by crystalline euhedral quartz reprecipitates (Fig.3 and Fig.4).

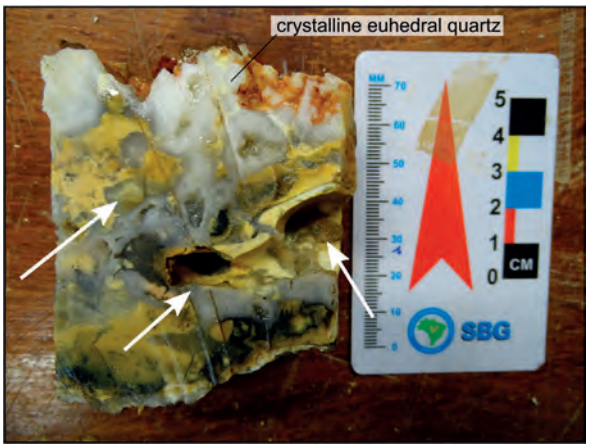

Figure 4: Sample with evidence of chert dissolution (pointed by the arrows) and partial filling of crystalline euhedral quartz.

The subsequent uplift of the area made fluids in the cave reach oxic conditions and sulfuric acid speleogenesis (SAS) occurred close to the paleo water-table, boosted by pyrite oxidation and H_2SO_4 formation (AULER and SMART, 2003). Through this SAS stage, dolostone layers of the seal unit were affected by dissolution as testified by their non-cohesive porous texture and replacement gypsum (Fig.5).

Progressive uplift caused the lowering of the water-table, deposition of calcite coralloids and collapse processes leading to the connection with the surface. After this stage, condensation-corrosion processes (still active) overprinted the solutional morphologies of the conduits system and further widened the passages in the upper and middle level. Our findings highlight that even unconventional karstified lithologies such as chert and silicified rocks may act as super-*k* zones and focus the inception of large dissolutional voids

in hypogenic (hydrothermal) settings. At the same time, sub-horizontal beds (even with thickness below seismic resolution) constituted by less soluble sediments with poor fracture development, may act as a seal and boost lateral dissolution in deeply-buried confined flow settings. In *Calixto Cave*, this dissolution pattern contributed to the formation of an extensive (more than 1 km long) horizontal network of conduits (Fig.6). We think that this contribution may be useful for many applied fields such as karst reservoir characterization for hydrocarbons, geothermal energy, and groundwater production.

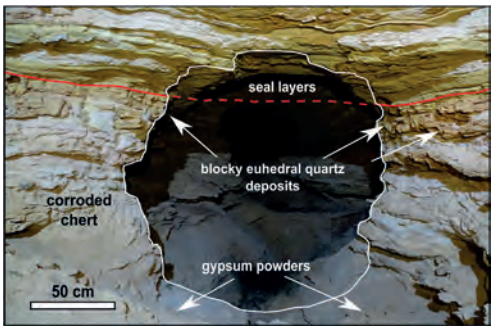

Figure 5: Typical morphology in the middle level (maze).

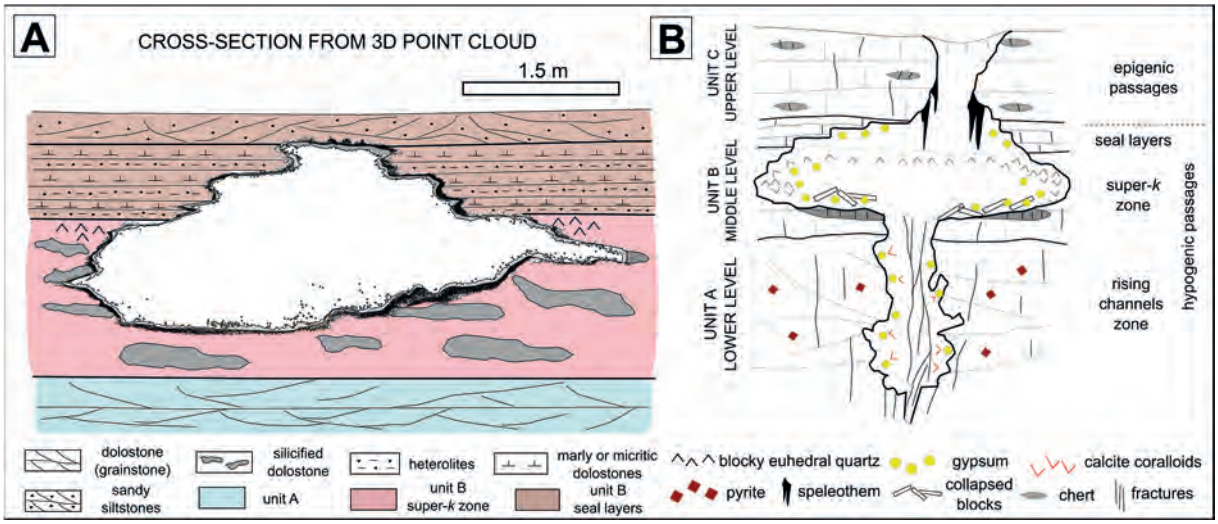

Figure 6: A) cross-section extracted from the TLS point cloud of a conduit in the middle level, associated with the bedrock lithostratigraphy; B) not-in-scale conceptual model of Calixto Cave spatial and morphological organization as observed at present time.

References

ANTONELLINI M., DEL SOLE L. and MOLLEMA P.N. (2020) Chert nodules in pelagic limestones as paleo-stress indicators: a 3D geomechanical analysis. *Journal of Structural Geology*, 132, 103979.

ARAÚJO R.E.B., LA BRUNA V., RUSTICHELLI A., BEZERRA F.H.R., XAVIER M.M., AUDRA P., BARBOSA J.A. and ANTONINO A.C.D. (2021) Structural and sedimentary discontinuities control the generation of karst dissolution cavities in a carbonate sequence, Potiguar Basin, Brazil. *Marine and Petroleum Geology*, 123, 104753.

AULER A.S. and SMART P.L. (2003) The influence of bedrock-derived acidity in the development of surface and underground karst: evidence from the Precambrian carbonates of semi-arid northeastern Brazil. *Earth Surface Processes and Landforms*, 28, 157–168.

BALSAMO F., BEZERRA F.H.R., KLIMCHOUK A.B., CAZARIN C.L., AULER A.S., NOGUEIRA F.C. and PONTES C. (2020) Influence of fracture stratigraphy on hypogene cave development and fluid flow anisotropy in layered carbonates, NE Brazil. *Marine and Petroleum Geology*, 114, 104207.

FORD D.C. and WILLIAMS P.W. (2007) *Karst Hydrogeology and Geomorphology*. John Wiley and sons, Chichester.

KLIMCHOUK A.B. (2009) Morphogenesis of hypogenic caves. *Geomorphology*, 106, 100–117.

KLIMCHOUK A.B., AULER A.S., BEZERRA F.H.R., CAZARIN C.L., BALSAMO F. and DUBLYANSKY Y. (2016). Hypogenic origin, geologic controls and functional organization of a giant cave system in Precambrian carbonates, Brazil. *Geomorphology*, 253, 385–405.

MISI A., KAUFMAN A.J., AZMY K., DARDENNE M.A., SIAL A.N. and DE OLIVEIRA, T.F. (2011) Neoproterozoic successions of the São Francisco Craton, Brazil: The Bambuí, Una, Vazante and Vaza Barris/Miaba groups and their glaciogenic deposits. *Geological Society of London*, Memoirs, 36, 509–522.

OLSSON R. and BARTON N. (2001) An improved model for hydromechanical coupling during shearing of rock joints. *Int. J. Rock Mech. Min. Sci.*, 38, 317–329.

PHILIPP S.L., AFŞAR F. and GUDMUNDSSON A. (2013) Effects of mechanical layering on hydrofracture emplacement and fluid transport in reservoirs. *Frontiers in Earth Science*, 1, Art.4.

Speleogenetic evolution of the Toirano cave system (Liguria, northern Italy)

Philippe AUDRA[(1)], Jo DE WAELE[(2)], Andrea COLUMBU[(2)], Ilenia Maria D'ANGELI[(2)], Fernando GÀZQUEZ[(3)], Jean-Yves BIGOT[(4)], Roberto CHIESA[(5)], Tsai-Luen YU[(6)], Chuan-Chou SHEN[(6)], Cristina CARBONE[(7)], Vasile HERESANU[(8)], Gabriella KOLTAI[(9)] & Jean-Claude NOBECOURT[(4)]

(1) University Côte d'Azur, Polytech'Lab, Nice, France, audra@unice.fr
(2) Dipartimento di Scienze Biologiche, Geologiche e Ambientali, Università di Bologna, jo.dewaele@unibo.it (corresponding author), andrea.columbu2@unibo.it, dangeli.ilenia89@gmail.com
(3) Department of Biology and Geology. University of Almeria, Spain, f.gazquez@ual.es
(4) French Association of Karstology, jeanbigot536@gmail.com, jcnobecourt@free.fr
(5) Gruppo Speleologico Cycnus, Toirano, bobchurch69@gmail.com
(6) Department of Geosciences, National Taiwan University, Taipei, Taiwan ROC, river@ntu.edu.tw
(7) DISTAV, Università degli Studi di Genova, Genova, Italy, cristina.carbone@unige.it
(8) CINaM, CNRS - Aix-Marseille University, Marseille, France, heresanu@cinam.univ-mrs.fr
(9) Institute of Geology, Innsbruck University, Innsbruck, Austria, gabriella.koltai@uibk.ac.at

Abstract

The Toirano karst system comprises different caves between altitudes of 340 m and 186 m asl. A detailed investigation of cave pattern, morphologies and of the sedimentary deposits attributes the origin of the caves to rising waters that followed the main vertical structural pathways. Many walls and roofs are sculpted with rising features (cupola and megacusps); in other areas, despite the presence of copious speleothem deposits, vertical feeders that brought the rising waters into the cave system have been localised. A series of geochronological analyses, including several U/Th dating and one cosmogenic burial date, alongside stable isotope and fluid inclusion analyses on some speleothems, have allowed to estimate the age of the highest lying cave (Ulivo) at 2.4 ± 0.40 and the lowest (Bàsura) at 1.45 ± 0.35 Ma ago. Many U/Th dates on speleothems have given ages beyond the limits of the method (>600 ka), confirming the system to be rather old. The stable isotope analyses indicate that the rising water was not peculiarly warm, with T values probably close to the current low-thermal spring in Toirano village, i.e. around 22-23 °C. The hypogenic evidences of the Toirano cave complex have been masked and modified by recent vadose infiltration, but especially by condensation-corrosion processes. Only a detailed multidisciplinary research has allowed to unravel the complex speleogenetic history of this cave system. The hypogenic origin of many ancient caves is probably hard to prove because of these late-stage processes, which erase the most obvious evidences, or hide the typical hypogene features.

1. Introduction

Most caves are epigene in origin, carved by infiltrating surface waters and often arranged in levels, which register the former base level stillstands (PALMER, 1987), helping in unravelling the landscape evolution of the areas in which they were carved. The common epigenic origin is usually supported by the current presence of infiltration waters in caves, the "rounded" tunnels interpreted as phreatic conduits, and the presence of typical evidences of fast-running water (e.g., scallops, fluvial sediments). The geomorphological and depositional evidences of early speleogenetical phases can be partially lost because of weathering, speleothem deposition, late-stage sedimentation, collapses, human activity, etc. There are also processes such as condensation-corrosion, boosted by the presence of guano and/or warm and moist air circulation in caves, which are greatly underestimated in the shaping of caves (CAILHOL *et al.*, 2019). These processes can be extremely important in the late speleogenetic stages, especially when cave passages become opened to the surface, erasing evidences of older events. Accordingly, the study of cave formation needs an accurate interpretation of underground morphologies and bedrock features, supported by geochemical and stratigraphic analyses of cave deposits, and the knowledge of geology of the area and surface dynamics related to climate and landscape evolution (AUDRA & PALMER, 2016; COLUMBU *et al.*, 2015, 2017; BALLESTEROS *et al.*, 2019; BELLA *et al.,* 2019). The Toirano karst system displays multiple cave levels and an impressive variety of underground morphologies, as much as probably making it the Italian show cave with the highest geodiversity. In-detail investigation of cave morphologies and stratigraphy, U-Th dating, stable isotope and fluid inclusion analyses of speleothems and cosmogenic burial dating of sediments, aimed at providing information on the evolution of this complex cave system in a changing climate, environment and landscape.

2. Study area and methods

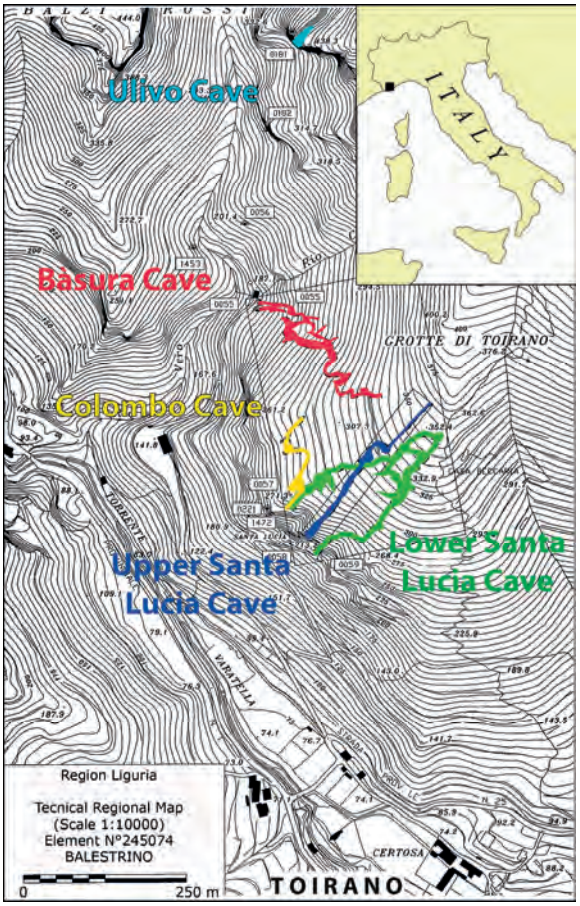

Figure 1: Study area displaying caves location. The thermal spring is placed some hundred metres south of the Certosa (just outside of this map) (Gruppo Speleologico Cycnus & Delegazione Speleologica Ligure, 2001).

The Toirano karst system develops along the lower slopes of Mt. Carmo di Loano (1389 m asl), half a kilometre north of the small village of the same name (Savona Province, Liguria, north-western Italy) (Figure 1).

The caves open at various altitudes along the slopes on the hydrographic left of the Varatella torrent, only 4.5 km away from the coast. They are carved in the lower calcareous part of the *San Pietro dei Monti Dolostones* (Middle Triassic). Toward the south, the carbonate rocks are interrupted by an important regional NE-SW fault with a vertical offset of at least 200 m, along which the thermal spring of Toirano is located (70 m asl). This spring (ca. 100 L/s) delivers slightly basic waters of 22-23 °C (ca. 600 µS/cm at 20 °C, hardness of 23 °F, 25-37 mg/L [SO_4^{2-}]) (CAVALLO, 1990; CALANDRI, 2001).

Climate in Toirano is mild Mediterranean and maritime, warm and temperate, with an average annual temperature of 14.3 °C (from a mean of 6.6 °C in January to 22.6 °C in July); annual rainfall is 830 mm with no pronounced wet season, whilst June and August are essentially dry. The caves of Toirano are known at least since the XV century and archaeological digging has shown they have been used by ancient human groups at least starting from the Lower Paleolithic (around 150 ka) (AROBBA *et al.*, 2008). Bàsura Cave became famous in the 50s when footprints of the Upper Paleolithic Man (12,000 years BP) were discovered. It is now connected with the Lower Santa Lucia Cave by an artificial tunnel, and equipped for tourist visits.

Toirano and its caves have been visited several times between 2015 and 2019 to carry out geomorphological observations in all passages. During these visits, sediments, speleothems (pieces found broken along the trails) and secondary minerals have been sampled in most of caves.

Minerals have been analysed with classical techniques (Diffractometry, Scanning electron microprobe analyses) at Genova University and at CINaM (CNRS and Aix-Marseille University). Some samples of quartz- and feldspar-containing sands have been sampled for Al-Be cosmogenic burial dating at the CEREGE-CNRS (Aix-Marseille University). Fragments of speleothems have been dated by the U-series method at the University of Taiwan, whereas stable isotopes were measured at the University of Cambridge (UK) and Almeria (Spain). A double-polished thin section has also been prepared to study a thick cm-sized calcite raft from Bàsura Cave for fluid inclusion petrography.

3. Results and discussion

A series of important speleogenetic indicators have allowed to reconstruct the evolution of the cave system (Fig. 2).

1. The caves develop along clearly distinguishable levels asl: Ulivo (340 m), Colombo (250 m), Upper Santa Lucia (215 m), Lower Santa Lucia (210-205-200 m), and Bàsura (185-175-165 m), respectively. These levels testify relative long-lasting stable phases in which the local base level and caves were at the same altitude.

2. Morphologies related to fast and turbulent flow (scallops) have not been detected. Clastic sediments are scarce, and range from coarse pebbles to gravels, sands and clays. Apart from angular clasts located in entrance areas (especially Bàsura), allogenic fluvial fine gravels are found only up to 100-200 metres into the caves, with an inward fining trend. These sediments were clearly introduced from outside, and in certain cases appear to have completely filled existing caves (e.g., Colombo Cave).

3. The caves are essentially characterised by morphologies of slowly flowing ascending fluids (rising channels, superposed cupola). Some rising conduits are almost certainly feeders. Except from limited seepage spots, no trace of significant active or inactive epigenic recharge, such as vadose shafts and meanders, have been detected.

4. The active thermal and slightly sulphidic spring in the village of Toirano, only 500 m south of the caves and ~100 m below the Bàsura Cave, indicates ongoing processes of deep fluid circulation today. Analogously, deep fluid circulation might have been active in the past.
5. No typical weathering by-products of sulphuric acid speleogenesis such as alunite and jarosite are present. The following minerals were detected: calcite, aragonite, huntite, and magnesite (minerals typical in dolostone-hosted caves), gypsum, ardealite, brushite, F- and OH-apatite, Leucophosphite/spheniscidite, and newberyite on the old guano deposits.

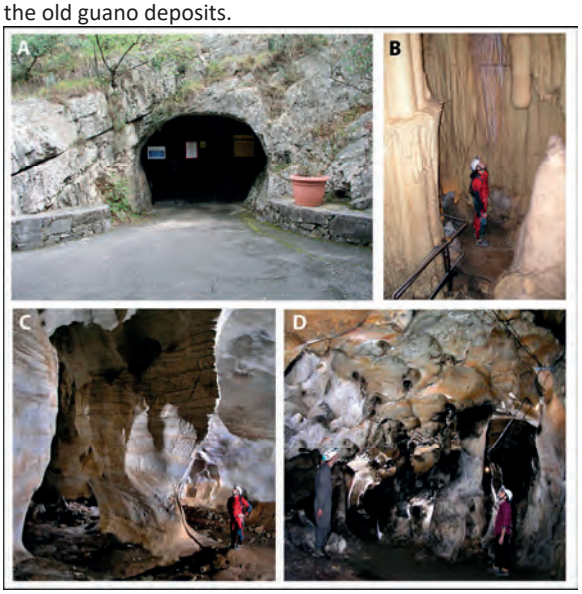

Figure 2: A. Entrance of Bàsura Cave (note stratification and the rounded cross-section); B. Poolfingers in the Cibele area, Bàsura Cave (note welt on the left with calcite rafts); C. The rock pillar isolated by condensation corrosion in Colombo Cave; D. Ceiling cupolas in the final part of Upper Santa Lucia Cave. All photos by Jean-Yves Bigot.

6. The cave-forming fluids were probably rich in CO_2, and might have been slightly thermal, whereas sulphate (and sulphuric acid), given the presence of the slightly sulphidic spring today, played only a very minor role (if at all).
7. Stable isotope analyses have pointed to paleo-temperatures in average of 13-14 °C confirmed also by the fluid inclusion observations on one sample of calcite raft. The $\delta^{13}C$ values (between -8 and -11‰) are consistent with a contribution from above lying soils, confirmed also by the $\delta^{18}O$ values which are typical of low temperature calcites precipitating from mid-latitude rain waters.
8. Most of the calcite speleothems (also in the lowest and youngest cave levels) reported ages beyond the U-Th method limit (ca. 600,000 years), older than 615 ka (POZZI *et al.*, 2019) and even 780 ka (reversed magnetic signal, BAHAIN, 1993), suggesting that the entire karst system is certainly older than 780 ka.
9. The allogenic sands sampled in Colombo Cave have delivered a burial age of approximatively 1.85 ± 0.35 Ma, which represents the minimum possible age of the voids these sands fill. This age and the mean global sea level during the Gelasian (-100/+10 m respect to today's sea level) allows to estimate a maximum uplift rate of 0.16 ± 0.03 mm/y, giving a rough idea of the age of all cave levels: Ulivo Cave (2.4 ± 0.4 Ma), Colombo Cave (1.85 ± 0.35 Ma), Upper Santa Lucia Cave (1.65 ± 0.35 Ma), Lower Santa Lucia (1.55 ± 0.35 Ma), and Bàsura Cave (1.45 ± 0.35 Ma).
10. Intense signs of condensation-corrosion are visible in the inner parts of the caves, where the cave atmosphere is close to moisture saturation. Warm moisture condenses on the cooler ceiling and the descending water film evaporates along the walls and floor. These processes probably started when low-thermal water was still present at depth, or at least the rock mass was still heated by the thermal fluids, producing rising warm and moist air flows.
11. Condensation-corrosion is particularly evident in the large passages of the entrance areas in Colombo, in both Upper and Lower Santa Lucia, and in Bàsura caves, which openings are located on a southwest facing cliff, where warm and wet air masses from the sea frequently rise along the valley. Cave voids significantly expanded by condensation-corrosion, probably for several metres, cancelling most of the original features and sediments.
12. The condensation-corrosion process is also boosted by bat colonies, which abundant presence in the past is testified by the large old guano mounds and phosphate minerals. Guano decay is an exothermic process releasing both water vapour and carbon dioxide, thus enhancing condensation above the guano heaps, and high CO_2 levels in the air. Other acids released by guano decay make the atmosphere particularly aggressive and corrosive (CAILHOL *et al.*, 2019). Based on our observations in Colombo Cave, the wall retreat by biocorrosion processes alone can here be estimated in at least 1 m on both sides of the passage, probably double on the roof.

4. Conclusions

On the basis of the geomorphological observations, geochemical analyses and U/Th dating, the Toirano caves formed by the action of rising hypogenic fluids that followed deeply-rooted subvertical fractures. In the lower passages (Bàsura and Lower Santa Lucia caves), the traces of ascending fluids are still well visible in many areas, with rising channels and superimposed cupolas.
Based on our data, the following speleogenetic scheme can be presented based on the burial date obtained in Colombo Cave:

A) The cave started forming at the water table level fed by a deep-rooted fracture, with thermal (possibly H_2S-rich) waters carving the cave in both phreatic, but mainly aerate conditions;
B) A marine ingression during the final phases of the Lower Pleistocene (Gelasian, ca. 2.6-1.8 Ma) caused the river valleys to aggrade, and the entrance parts of the cave were completely filled with gravels and sands (pockets on the roof of the cave are still filled with remnants of these sediments, whose burial age is around 1.85 ± 0.35 Ma);

C) successive Pleistocene mountain uplift caused the Varatella torrent to entrench, partially emptying the cave which, at least in the early stages, was probably still actively enlarging by rising hypogene fluids. The continuous uplift caused the intersection of the water table with the feeding fractures to shift laterally and to lower lying elevations, causing the formation of the lower levels of the cave system; D) in the final stages hypogenic waters abandoned the cave system: since then, the large cave entrances are subject to air circulation, bat roosting and frequentation, and condensation-corrosion processes started to remove most remnants of the older sediments and speleothems (several of which overcome the U/Th dating limit, i.e. > 600 ka). The lowest cave level, corresponding to Bàsura Cave, is certainly older than 780 ka, and might be older than 1 million years. E) The intense condensation-corrosion, still very active today, has erased many of the morphologies and deposits of the original hypogenic speleogenetic phase. Ancient guano deposits appear to have a strong influence on later vadose condensation-corrosion processes, playing an important role in shaping the voids they occupy. Wall retreat by sole condensation-corrosion can be estimated in over 1 metre in the highest caves (Colombo) because of their large entrance size, exposure to moving external air mass directions, and past presence of large bat colonies.

Acknowledgments

Many thanks to the staff of the Toirano Caves, and especially to Dr. Flavia Toso, local geologist interested in knowing more about the caves, to archaeologist Dr. Marta Zunino, Scientific Director of Toirano Caves, for her availability, enthusiasm and continuous support, to Dr. Elisabetta Starnini of the University of Pisa, and to the Archaeological Superintendency of Liguria, the Managing Authority of the show caves, and the Municipality of Toirano. Yves Krüger is thanked for the analyses on fluid inclusions in his laboratory in Bern University, and Régis Braucher of Aix Marseille University for cosmogenic burial dating.

References

AROBBA D., BOSCHIAN G., CARAMIELLO R., GIAMPIETRI A., NEGRINO F. e TOZZI C. (2008) La grotta del Colombo: indagini geoarcheologiche, palinologiche e sull'industria litica. Toirano e la Grotta della Bàsura. *Atti del Convegno*, Bordighera, 69-88.

AUDRA P. and PALMER A.N. (2016) Research frontiers in speleogenesis. Dominant processes, hydrogeological conditions and resulting cave patterns. *Acta Carsologica*, 44, 315-348.

BAHAIN J-J. (1993) *Datation par résonance de spin électronique (ESR) de carbonates et d'émail dentaire quaternaires - Potentiel et limites*. Thesis. Muséum National d'Histoire Naturelle, Paris, 114 p.

BALLESTEROS D., GIRALT S., GARCÍA-SANSEGUNDO J. and JIMÉNEZ-SÁNCHEZ M. (2019) Quaternary regional evolution based on karst cave geomorphology in Picos de Europa (Atlantic Margin of the Iberian Peninsula). *Geomorphology*, 336, 133-151.

BELLA P., BOSÁK P., BRAUCHER R., PRUNER P., HERCMAN H., MINÁR J., VESELSKY M., HOLEC J. and LÉANNI L. (2019) Multi-level Domica–Baradla cave system (Slovakia, Hungary): Middle Pliocene–Pleistocene evolution and implications for the denudation chronology of the Western Carpathians. *Geomorphology*, 327, 62-79.

CAILHOL D., AUDRA P., NEHME C., NADER F.H., GARAŠIĆ M., HERESANU V., GUCEL S., CHARALAMBIDOU I., SATTERFIELD L., CHENG H. and EDWARDS R.L. (2019) The contribution of condensation-corrosion in the morphological evolution of caves in semi-arid regions: preliminary investigations in the Kyrenia Range, Cyprus. *Acta Carsologica*, 48, 5-27.

CALANDRI G. (2001) L'evoluzione del carsismo nel Toiranese: nota preliminare. In *Atti V Convegno Speleologico Ligure "Toirano 2000"*, Italy; 117-120.

CAVALLO C. (1990). *Indagine idrogeologica su alcune sorgenti del Toiranese*. PhD thesis, Genova, 160 p.

COLUMBU A., DE WAELE J., FORTI P., MONTAGNA P., PICOTTI V., PONS-BRANCHU E., HELLSTROM J., BAJO P. and DRYSDALE R. (2015) Gypsum caves as indicators of climate-driven river incision and aggradation in a rapidly uplifting region. *Geology*, 43, 539-542.

COLUMBU A., CHIARINI V., DE WAELE J., DRYSDALE R., WOODHEAD J., HELLSTROM J. and FORTI P. (2017) Late quaternary speleogenesis and landscape evolution in the northern Apennine evaporite areas. *Earth Surface Processes and Landforms*, 42, 1447-1459.

GRUPPO SPELEOLOGICO CYCNUS & DELEGAZIONE SPELEOLOGICA LIGURE (2001) Speleologia e carsismo del Toiranese". *Atti V Convegno Speleologico Ligure "Toirano 2000"*. Toirano, Italy.

PALMER A.N. (1987) Cave levels and their interpretation. *National Speleological Society Bulletin*, 49, 50-66.

POZZI J.P., ROUSSEAU L., FALGUERES C. *et al.*, TOZZI C. (2019) U-Th dated speleothem recorded geomagnetic excursions in the Lower Brunhes. *Scientific Reports*, 9, Art. 1114: 1-8.

Karst terrain in the western upper Galilee, Israel

Amos FRUMKIN

Cave Research Center, Institute of Earth Sciences, The Hebrew University of Jerusalem, Jerusalem 91904, Israel. amos.frumkin@mail.huji.ac.il

Abstract

The Galilee is a transition zone between the highly developed karst of the northern Levant and the arid karst of the southern Levant. A karst survey of the western Upper Galilee in Israel shows that karst has been a dominant geomorphic factor throughout the Cenozoic. We discuss the geomorphic character of karst features of the region. Tens of caves distributed over the study area demonstrate that phreatic and hypogene isolated voids and conduit segments dominate over vadose shafts, sinking stream caves and spring caves, although all these types are present. Most caves belong to old stages of landform development, prior to Plio-Pleistocene uplift and stream entrenchment. Subaerial denudation and slope processes have opened some caves to the surface during the mid-late Pleistocene. The development of the caves in this region has not been studied. Here we use hydrogeologic and geomorphic observations of regional karst phenomena, to explain the regional karst and speleogenetic processes, as well as human cave choice. The present hydrogeologic system and the geologic and karst evolution of the region are examined in order to infer the possible hydrogeologic processes associated with the cave formation and development.

1. Introduction

The western Upper Galilee is a hilly region, descending along 30 km towards the Mediterranean Sea at the west. The groundwater divide is the structural and topographic high, ~1000 m a.s.l., where the lower Cretaceous aquiclude strata are at their highest structural elevation.

The region has a Mediterranean climate with cool wet winters (October–May) and dry hot summers (June–September). Annual precipitation is highly variable, commonly between 600–900 mm. Annual potential evaporation is ~1500 mm, but during the winter infiltration may amount to >30% of precipitation, while evapotranspiration may amount to >60%. The natural vegetation of the hilly region is Mediterranean forest and garrigue.

Being mostly under fluviokarst regime, the western Upper Galilee is dissected by channeled stream valleys draining the flow generally westward. Similar topography is observed towards the north, within SW Lebanon.

The outcrops of the western Upper Galilee consist of Early Cretaceous to Recent sedimentary rocks. Most of the section, excepting its basal and uppermost parts, is dominated by marine carbonates, of which the late Albian to Turonian strata constitute the Judea Group, reaching a total thickness of ~700 m. The karstified Judea Group is overlain by the hardly-permeable (aquifer) late Cretaceous to Paleocene Mount Scopus Group. These outcrops are restricted mainly to structural lows, where they evaded erosion. Mount Scopus Group is overlain by the Avedat Group chalks of Eocene age, which crop out only at a small area.

2. Materials and methods

The karst features in the western Upper Galilee, were recorded by surface and cave survey techniques over a 17x20 km area. Caves were mapped with Leica Disto laser range meter, inclinometer, and compass. Surveys were calculated using WinKarst cave mapping software and drafted by drawing applications.

The region around the cave was analyzed with ArcMap GIS software, with similar procedures as in other prehistoric caves of Galilee.

The caves' speleological features were recorded, analyzed and subdivided according to their morphology and functional role in the karst system. The studied features were then compared with the accumulated evidence of regional karst, hydrology and paleohydrology, in order to infer the hydrogeologic and geomorphic history of the caves (FRUMKIN *et al*., 2021).

3. Results

The most important paleokarst features of the western Upper Galilee are a system of paleo-dolines on the top of Judea Group, filled with Senonian chalk (BUCHBINDER *et al*. 1983). The Maalot doline (Long. 35.277228° Lat. 33.018704°) is cut into Santonian and Turonian bedrock. It is filled by chalky marine fill of Santonian and Campanian age. The Turonian, Santonian, and Campanian beds are all deformed, showing tilting, collapse and subsidence features. Most of the collapsed beds dip towards the center of the doline. In the Oshrat doline (Long. 35.173159° Lat.

33.014925°), chaotic blocks of Turonian limestones with Campanian to Eocene chalk matrix directly overlie Turonian limestones. Miocene calcarenites of the Ziqlag Formation were also found, dipping towards the center of the doline. The underlying Turonian bedrock is highly corroded, dipping also towards the center of the doline. Since the last marine retreat from the region during the Eocene and until today, the study area has been under continental regime, excluding short duration of limited marine transgressions in the west. The region has developed several karst-associated features, while others are missing.

Recent solution dolines, the most distinct features of surface karst topography, are notably undeveloped in the studied western Upper Galilee. Shallow solution dolines are better developed to the east of the study area, at Peqi'in and Meron karst plateaus of central Upper Galilee, commonly having karst drainage through vadose shafts. In western Upper Galilee, where steep slopes are more common than sub-horizontal plateaus, fluviokarst terrain dominates. On the other hand, karren rock features are common in the study area, controlled by fractured late-Cenomanian and Turonian carbonates. Karrens commonly reach a few meters in size, forming rough microtopography with rich oak-dominated forest and garigue, extracting water from the epikarst.

Three main groups of karst-related features are discussed below: recharge features, isolated voids, and discharge features, each of which can be further subdivided into two sub-groups. Of all these, the main karst features relevant for human habitation are isolated voids or caves, which are sparsely distributed over the entire western Upper Galilee.

3.1. *Focused recharge features*

Although precipitation recharge into the subsurface occurs across the entire karstic outcrops which occupy most of western Upper Galilee, two types of focused recharge features are observed, mainly in limited areas where karst depressions dominate over fluviokarst.

3.1.1. Stream sinks, where concentrated stream runoff is partly or totally swallowed into the subsurface. These active features, also termed swallow holes or ponors, are rare in the Galilee, unlike classic karst regions. Partial sinking is more common in the Galilee, and was used for tracer tests (MAGAL *et al*., 2013). Pollutants flowed occasionally down these stream sinks into the subsurface, underscoring their environmental importance. The only completely sinking stream is swallowed into Pa'ar Cave. This sub-horizontal ephemeral stream cave drains a ~1 km long closed depression at the central Upper Galilee, so it will not be discussed further here. The partial sinks, more common at the western Upper Galilee, are usually impenetrable to human exploration.

3.1.2. Vertical shafts, actively collecting local runoff and infiltration water from small areas, typically tens of meters in diameter. These shafts are very common at the karst plateaus of the central Upper Galilee which are not covered by the present paper, and become less common in western Upper Galilee. Their aperture at the surface is commonly few cm or more, increasing in diameter within the epikarst and reaching a diameter of a few meters in the bedrock. Their depth in the region reaches 187 m at Rahav Cave, the deepest cave in Israel. They drain meteoric water mainly during the wet season, flowing vertically through the vadose zone towards the water table.

3.2. *Isolated caves*

These caves have sub-horizontal dimensions larger than their vertical dimension. The term 'isolated cave' refers to an underground void which seems to lack genetic conduits connecting it to the input or output boundaries of the aquifer. Rather, isolated caves are originally connected to the surface only via tiny (~0.01-1 cm wide) flow routes, supporting diffuse, laminar flow. Ultimately, the caves became connected to the surface following subaerial denudation, cavity collapse, or anthropogenic breaching of the voids. The isolated caves in the Galilee are dominantly relict in terms of genetic water flow, and developed during previous morphotectonic regimes, probably of Neogene age. They commonly occur at high elevations, well above the present water table, high above the present water table. In some cases they are dissected by fault escarpments.

The isolated caves of Upper Galilee can be subdivided into two morphogenetic types:

3.2.1 Elongated caves, resembling conduit segments with few bifurcations or side passages. Examples are Sharakh, Dorbanim and Hanita caves. They commonly display 'phreatic' features, such as tube-like elliptical cross section of passages, smooth walls, cupolas, and solution pockets. These can be confused with condensation corrosion features, so caution in interpretation is needed. The side passages show slight resemblance to maze caves (FRUMKIN *et al*., 2017), possibly indicating speleogenesis under conditions of partial confinement.

3.2.2 Chamber isolated caves, whose original (prior to collapse) length and width are roughly similar. Examples are Tefen and Zawit caves. This type of caves is attributed to dissolution under unconfined conditions by hypogene water, possibly mixing with epigene water close to the water table. Commonly, the relatively large roof span renders them prone to collapse. In some cases, such as Yana cave, the gradual collapse has almost reached the surface. In others, such as Kisra and Qeshet caves, the chamber has reached the surface by ceiling collapse, forming collapse dolines. Original morphology is hard to detect in these caves, due to internal deposition, collapse and other deformations (FRUMKIN *et al*., 2015).

3.3. *Discharge features*

These occur at springs or nearby downstream areas, where water discharging from the aquifer resurges at the surface. Two types of features are discussed:

3.3.1. Active spring caves, best represented by Tamir Cave, consisting of an active sub-horizontal conduit which flows northward into Nahal Keziv stream channel. This entrenched canyon acts as a local base level for its surroundings, and was probably associated with local re-routing of the flow pattern during the Pleistocene. Tamir Cave morphology is dominated by fast flow features such as few-cm sized scallops. Dye tracing indicates that Tamir and Hardalit springs drain the areas south and north of Nahal Keziv respectively, rather than functioning as resurgences for infiltrating Ziv Spring water upstream (MAGAL *et al*., 2013).

3.3.2. Depositional subaerial tufa deposits of freshwater wetlands downstream from nearby springs. They are added to the discussed features due to their indirect but important evidence of major dissolution. The tufa deposits are represented by two Quaternary outcrops, Ga'aton tufa and Yehi'am tufa. The larger and better-exposed deposit, at Nahal Ga'aton streambed and banks, is ~12m m thick, covering an area 1.5 km^2. It represents mostly fossil deposition by freshwater arriving from the nearby Ga'aton springs and runoff, periodically dammed and breached downstream. At present, Nahal Ga'aton stream channel is incised into the older tufa layers, eroding them away. Additional tufa deposits, rich in plant remains, are deposited today by the Ga'aton spring water along the stream course of Nahal Ga'aton at the same location. The fossil tufa deposit consists of calcified stems, roots of plants, brown clays and lenses of small rounded pebbles. Its lower unit is composed of micritic mud containing ostracod remains, overlain by structureless micrite which contains an assemblage of well-preserved freshwater Melanopsis praemorsa gastropods, overlain by calcareous tufa with abundant calcified floral remnants and algae. Intercalated paleosols and pebbles also appear in the section. Although not well-dated, sedimentary and morphological constraints indicate early to mid-Pleistocene age for the fossil tufa (WEINBERGER & KRONFELD, 1992).

3.4. ***General remarks***

Within the western Upper Galilee discussed here, isolated chambers and elongated phreatic passages comprise most of the known caves. This contrasts with the central Upper Galilee where karst plateaus are common at Peqi'in and Meron regions, with a large majority of vadose shaft caves. The western Upper Galilee caves are mostly associated with old erosion surfaces, so today they are perched high above the water table, and commonly also above the modern stream channels which developed following recent uplift.

Considering all the discussed elements, the western Galilee is a dynamically-evolving karst region, with diversified karst features, both relict and active.

4. Discussion

Some researchers suggested that Upper Galilee meets the best criteria for karst development in Israel due to the high precipitation and mostly carbonate bedrock. The present study and others partly support this assumption in terms of vadose and phreatic caves such as vertical shafts and isolated voids which are abundant in Upper Galilee. The accumulated evidence also suggests that the western Upper Galilee underwent long-term intensive karst denudation (in the order of tens millions of years).

However, recent studies (e.g. FRUMKIN *et al*., 2017) show that large maze caves are better developed in the Judean Desert region of Israel, where they formed under prolonged periods of confined, hypogenic flow regime. These features are not observed in western Upper Galilee, where caves are an order of magnitude shorter than the Judean Desert caves, geometrically simpler in plan view, and smaller in volume.

In addition, underground conduits, such as active river caves are better developed in Mt. Lebanon north of Galilee, but they generally decrease southward in terms of size, discharge, and distribution. Upper Galilee has only slight development of river caves, with Tamir Spring Cave as the best example. This may be associated with (1) precipitation, which decreases southward; (2) outcrops of pure limestones, which also decrease southward through the southern Levant; (3) in the Galilee there are no Jurassic limestone outcrops, which, where exposed, form the best karstified outcrops in Lebanon and Mt. Hermon; (4) the dynamic tectonics of the Galilee, causing instability of aquifers and watertables over long periods.

In spite of these apparent unfavorable preconditions, hydrologic evidence (above), including dynamic springs, contamination events and groundwater velocities, all indicate that the western Upper Galilee karst is still highly active today. This activity may be associated with highly fractured carbonates with quasi-developed karst conduits.

Over the longest time scale, Senonian paleokarst of the western Upper Galilee presents clues for karstification through tens of millions of years. As noted above, BUCHBINDER *et al.* (1983) suggested that the paleo-dolines indicate subaerial exposure of the region and normal karst plateau development, associated with Santonian stratigraphic gaps in parts of the region. However, this is incompatible with the Santonian structural lows in which most paleo-dolines are located. These structural lows are inferred from the Santonian isopach map, showing maximal deposition of marine chalk in the lows. Another problem facing the subaerial exposure theory is the lack of other indications of subaerial exposure, such as lateritic paleosols and limonitic crusts.

The Oshrat doline (BUCHBINDER *et al*., 1983) is filled by chaotic blocks of Campanian, Eocene and Miocene marine sediments. Such long-term (tens millions of years) sedimentation can be explained in two ways: (1) long-term (millions of years) accumulation of horizontally stratified beds followed by collapse into a large underlying cavity, accompanied by erosional removal of correlative sediments from the surroundings; (2) multi-period development of the doline, which accumulated additional sediments at each stage. The small thickness of the various brecciated blocks in the dolines, compared with regional marine Campanian and Eocene rocks, indicate that option (1) is unlikely. Yet, the fragmentary condition of the various blocks within the dolines indicates that they were deformed during or after their deposition, which occurred over prolonged geological periods, as indicated by the faunal assemblages. The problem remains, however, how after being filled at each stage by relatively non-karstic sediments, the doline continued to develop, adding accommodation space for another period of deposition.

The option of normal epigenic runoff-infiltration subaerial dissolution would not favor the rejuvenation of a doline at the same point after being filled with hardly-soluble sediments. A more plausible scenario would be formation and rejuvenation by plumes of rising groundwater. Such hypogenic plume could remain in a hydrogeologically-preferred location for >70 Ma, as it follows a preconditioned

route determined by subsurface conditions, allowing better permeability structures and conductivity. This is compatible with the observed association of paleokarst dolines and faults at the western Upper Galilee. Other compatible observations include the sagging of the underlying Turonian bedrock which dips concentrically towards the doline center, and the extensive leaching zone under the Oshrat doline. These bedrock deformations are common in hypogenic dolines rather than epigenic ones (e.g. FRUMKIN *et al*., 2015).

The absence of subaerial paleosols remnants, as well as other exposure features, while marine sediments are dominant inside and outside of the dolines are important for deciphering their genesis. These features suggest that the paleo-dolines could develop under sub-marine regime, by artesian springs coupled with collapse into submarine karst voids.

Such a scenario is supported by modern submarine karst springs found in the eastern Mediterranean, west of Upper Galilee. Under present conditions, confined karst groundwater flows westward to the western edge of the western Galilee aquifers, where it emanates under sea water.

Within the present-day topography, formed long after Senonian palaeokarst development, many Senonian paleo-dolines are preserved on hilltops. The less karstified fill of the dolines seems to protect them from fast dissolution under modern conditions, while the surrounding karstic rocks are denuded faster.

The Ga'aton (and Yehi'am) tufa deposits may provide further indirect evidence for Quaternary karstification. Their importance for the present discussion stems from their source of Ca-carbonates. Few million tons of calcite deposited within the tufa units were derived from intensive dissolution within the associated watersheds, including subsurface catchments. The tufa deposits thus attests for some of the large volume of dissolved rock in the past. The tufa is more common than fluvial terraces along their stream valleys, providing an indication of the importance of karst in overall erosion, at least under Pleistocene erosional conditions.

This indicates that karst processes were intensive at least during the Pleistocene, including subaerial denudation and subsurface dissolution.

The topographic setting of spring features is of interest. Most springs are generally clustered close to stream channels or slightly higher. These Quaternary features demonstrate that the hydrologic-karstic system has dynamically adjusted to the new local base levels of the actively entrenching stream valleys. A relatively elevated spring, such as Ga'aton Spring (the westernmost large spring of its group), is active only during intensive rainy periods, acting as an overflow outlet. The Pleistocene tufa and spring features indicates that the springs were very active in the past.

The remains of the unroofed caves indicate the importance of karst in the denudation processes of the carbonate hilltops of the region. The estimated karst denudation rate is ~20 mm ka^{-1} under Mediterranean conditions in Israel.

Estimating the duration and age of karstification of the region is complex, due to the scarcity of chronological evidence.

Hayonim, a relict hypogenic cave yielded TL ages ranging from 230 to 140 ka for the lower part of its Mousterian sequence. Relict caves, such as the ones used by prehistoric hominins, have been attributed to speleogenesis from Neogene to early Pleistocene.

An interesting example of an unroofed cave is where the mid-Pleistocene (Early Toringian) remains of Bear's Cave were found on the surface. This unroofed cave, which was exhumed by natural subaerial denudation, included carnivore bones within stalagmitic breccia.

The evidence available today, in spite of the limited chronological constraints, indicates that the Pleistocene was an active karstification period. We argue that the speleogenesis of the unroofed and relict caves, such as Bear's cave, can be attributed at least to the Neogene, as shown in other parts of Israel.

References

BUCHBINDER B., MAGARITZ M. BUCHBINDER L.G. (1983) Turonian to Neogene palaeokarst in Israel. Palaeogeography, palaeoclimatology, palaeoecology, 43(3-4), 329-350.

FRUMKIN A. ZAIDNER Y., NA'AMAN I., TSATSKIN A., PORAT N., VULFSON L. (2015) Sagging and collapse sinkholes over hypogenic hydrothermal karst in a carbonate terrain. Geomorphology 229, 45-57.

FRUMKIN A., LANGFORD B., LISKER S., AMRANI A. (2017) Hypogenic karst at the Arabian platform margins: implications for far-field groundwater systems: Bulletin of the Geological Society of America 129 (11-12), 1636-1659.

FRUMKIN A., BARZILAI O., HERSHKOVITZ I., ULLMAN M., MARDER O. (2021) Karst terrain in the western upper Galilee, Israel: Speleogenesis, hydrogeology and human preference of Manot Cave, Journal of Human Evolution 160, p.102609.

MAGAL E., ARBEL Y., CASPI S., GLAZMAN H., GREENBAUM N., YECHIELI Y., 2013. Determination of pollution and recovery time of karst springs, an example from a carbonate aquifer in Israel. Journal of contaminant hydrology, 145, 26-36

Hypogene maze cave formation in confined carbonate aquifer by cooling geothermal flow

Roi RODED[(1)], Einat AHARONOV[(2)], Amos FRUMKIN[(2)],
Nurit WEBER[(3)], Boaz LAZAR[(2)] & Piotr SZYMCZAK[(4)]

(1) Hydrology and Water Resources, The Hebrew University, Jerusalem, Israel
(2) Institute of Earth Sciences, The Hebrew University, Jerusalem, Israel
(3) Department of Earth and Planetary Sciences, The Weizmann Institute of Science, Rehovot, Israel
(4) Institute of Theoretical Physics, Faculty of Physics, University of Warsaw, Warsaw, Poland

Abstract

Porous and fractured rocks in Earth's upper crust continuously undergo reactive flow, which alters their porosity and permeability. In carbonate aquifers, this process may produce extensive karst, with sizable cave systems (on the scale of kilometers). Of special interest are "hypogenic" karst and caves formed by upwelling deep-seated flow with no genetic connection to the surface. Despite its vast economic and environmental importance, the understanding of hypogenic karst formation remains elusive (AUDRA & PALMER, 2015; KLIMCHOUK, 2019). The present work combines geochemical and numerical analyses with field observations to demonstrate that cooling of CO_2-rich geothermal flows and upwelling into a confined permeable layer may induce aggressive karstification and cave-forming processes ("speleogenesis"). As the water cools, carbonate solubility increases, inducing undersaturation and forming caves on relatively short timescales (tens of thousands of years). This process explains the location of caves observed in a presented field case study (FRUMKIN, 2017) and captures the characteristics of cave morphology, particularly the formation of maze-like caves, which are typical of hypogenic karst. From a broad perspective, the results demonstrate that, in conjunction with deep-seated CO_2 fluxes, Earth's geothermal heat loss by upwelling of thermal fluids may extensively shape the upper crust, forming sizable cave systems.

AUDRA P., PALMER A. N. (2015), Acta Carsologica. 44(2), 315-348.

KLIMCHOUK A.B. (2019) In: White, W.B., Culver, D.C. Pipan, T. (Eds.), 3rd ed. Academic Press, New York, 974–789.

FRUMKIN A. et *al*. (2017) Geol. Soc. Am. Bull., 129(11-12), 1636-1659.

Symposium 04 – special session

Ghost-rock karstification

Ghost-rock karstification: principles, processes, perspectives

Grégory DANDURAND[(1)] & Laurent BRUXELLES[(2)]

(1) INRAP, UMR5608 - TRACES, CNRS - UT2J, Toulouse, France, gregory.dandurand@inrap.fr
(2) UMR 5608 TRACES - CNRS / Université Toulouse Jean Jaurès, INRAP et GAES, université du Witwatersrand, Johannesburg, laurent.bruxelles@inrap.fr

English

A slap in the face! A whole world has collapsed and must now be rebuilt when we learn that the water that flows through the mass of carbonate rocks does not systematically lead to the formation of caves. Fortunately, karstology recovered very quickly because it is a very dynamic discipline. Ghost-rock karstification, much more than a concept, is a "new" paradigm that challenges many things... mainly in the field of karstology and speleogenesis, but that could be extended, if given the means, to the fields of geomorphology and geology. Indeed, ghost-rock karstification, i.e. by isovolume alteration of carbonate rocks, challenges the classical theory of endokarst formation where water dissolves the limestone and exploits its weaknesses. Geological variability does not systematically lead to the creation of cavities, or at least not always in a synchronous manner. In ghost-rock karstification, water eats away at the massif from the inside, preparing it until the conditions are finally right to empty the alterite - transforming the porosity into networks of interconnected galleries.

Although alteration phenomena have been recognised for a long time in geomorphology and karstology studies, it is only recently that they have taken a central role in speleological models. Consideration of ghost rock-rock as a fundamental process is therefore a paradigm shift that has stimulated a review of the evolution of subterranean networks, particularly over long time scales.

Ghost-rock karstification is a process that takes place in the phreatic zone, whether deep or near the surface. Although the alteration phases need a long time, i.e. great geodynamic stability, they also require a renewed supply of acidity. These two conditions are mainly allowed in relatively flat lithospheric bulge zones. Several studies show that this alteration can occur from the surface as well as through deep circulations (bathyphreatic convection loops), or even through hypogene upwelling. Geological examples confirm the reality of ghost-rocks at great depths beneath the former continental surface.

After this long period of preparation of interconnected karstic discontinuities within the aquifer, subterranean voids of all sizes and lengths can form very quickly as soon as the hydraulic gradient conditions allow the establishment of drainage paths from an outlet by headward erosion. The first cavities can be formed by gradual compaction of the alterite when the ghost-rocks are above the base level by collapse of the alteration corridors, sometimes associated with the formation of chaotic boulders and breccias. Then, the removal of several weathered corridors organizes a real maze network corresponding to different hydrodynamic models.

The formation of caves, which occurs at a later stage, reflects a paleo-environmental destabilization that may be associated with variations in the base level, glacial and eustatic movements or an orogeny activity. The flooding of the subterranean networks and the evacuation of the alterites then allows the direct corrosion of the walls, ceilings and floors. Another history of speleogenesis then begins.

These past events still have implications for present-day human societies. In addition to the consequences for the evolution of landscapes, the rate of formation of caves, speleogenetic interpretation of "pseudo-infillings", dating, research and prospecting for archaeological remains, the impact on national and local infrastructure and their consideration in terms of geotechnics and civil engineering are all major issues of protection and risk prevention.

French

Une claque ! Dont la karstologie s'est remise fort heureusement très rapidement car c'est une discipline dynamique, qui sait se renouveler. La fantômisation, bien plus qu'un concept, est un "nouveau" paradigme qui remet beaucoup de choses en cause… principalement dans le domaine de la karstologie et de la spéléogenèse, mais que l'on pourrait étendre, en s'en donnant les moyens, à la géomorphologie et géologie *l.s*. Beaucoup de livres relégués aux bons souvenirs des historiens des sciences sont à réécrire. C'est tout un monde qui s'effondre et qu'il faut désormais reconstruire quand on apprend que finalement l'eau qui s'écoule dans la masse des roches carbonatées ne creuse pas systématiquement les grottes. En effet, la karstification par fantômisation, c'est-à-dire par altération isovolume des roches carbonatées, présente des différences majeures avec la théorie classique de formation de l'endokarst : l'eau qui dissout le calcaire et qui exploite les lignes de faiblesses et les contrastes géologiques n'aboutit pas toujours à la formation de vides, en tout cas pas toujours de manière synchrone. Elle ronge le massif de l'intérieur, le prépare sur le long terme jusqu'à ce que les conditions soient enfin réunies pour vidanger l'altérite, pour

transformer la porosité en des réseaux de galeries interconnectées.

Si les phénomènes d'altération sont reconnus et étudiés depuis longtemps en géomorphologie et en karstologie, ce n'est que récemment qu'ils ont pris toute leur place dans les modèles spéléogéniques, en considérant notamment que la karstification fait partie intégrante des phénomènes d'altération. C'est donc un changement de paradigme qui a permis de revoir l'évolution des réseaux souterrains, notamment sur le temps long.

La fantômisation est un processus qui s'exerce dans la zone saturée, qu'elle soit profonde ou superficielle. Si les phases d'altération requièrent le temps long, c'est-à-dire une grande stabilité géodynamique, elles demandent en même temps une source d'acidité renouvelée. Ces deux conditions sont permises principalement dans les zones de bombement lithosphérique relativement planes. Plusieurs études montrent que cette altération peut se produire aussi bien à partir de la surface que par des circulations profondes (boucles de convexion bathyphréatiques), voire par des remontées hypogènes. Les exemples géologiques prouvent la réalité de la présence de fantômes de roche à très grande profondeur sous l'ancienne surface continentale.

Après ce temps long de préparation de discontinuités karstiques interconnectées au sein du réservoir, des vides souterrains de toutes tailles et plus ou moins étendus peuvent se former de façon très rapide dès que les conditions de gradients hydrauliques permettent l'établissement de chemins de drainage depuis un exutoire par érosion régressive. Les premiers vides peuvent se former par tassement progressif de l'altérite, lorsque les fantômes se retrouvent au-dessus du niveau de base ou par effondrements des couloirs d'altération parfois associés à la formation de chaos de blocs et de brèches. Puis, le débourrage de plusieurs couloirs altérés organise un véritable réseau labyrinthique selon différentes modalités hydrodynamiques.

La formation des vides, qui se produit dans un second temps, traduit une déstabilisation paléo-environnementale qui peut être associée à des variations du niveau de base, des mouvements glacio-eustatiques ou bien une orogenèse ou une surrection relative. La mise en charge des réseaux et l'évacuation des altérites autorisent alors la corrosion directe des parois, des voûtes et des planchers. Une autre histoire de la spéléogenèse commence alors.

Mais ces histoires continuent d'avoir des implications pour les sociétés humaines actuelles. En effet, outre les conséquences sur l'évolution des paysages, la vitesse de formation des grottes, l'interprétation spéléogénétique des "pseudo-remplissages", les datations, la recherche et la prospection de vestiges archéologiques, l'impact sur les aménagements et leur prise en compte en terme géotechnique et de génie civil sont autant d'enjeux majeurs de protection et de prévention des risques.

Ghost-rock karstification

Yves QUINIF(1) & Sophie VERHEYDEN(2)

(1) Service de Géologie fondamentale et appliquée, Faculté Polytechnique, Université de Mons, Rue de Houdain, 9, 7000-Mons, Belgium, yves.quinif2@gmail.com
(2) Department of Earth History of Life, Royal Institute of Natural Sciences (RBINS), Brussels, Belgium (corresponding author) sverheyden@naturalsciences.be

Abstract

Ghost-rock karstification or karstification by alteration of limestones with removal of the altered rock (ghost-rock) in a later stage has important differences with the classical way of cave formation by water progressively dissolving limestone and widening secondary voids, i.e., total-removal karstification. It often enables us to explain observed morphologies more easily than with the classical theory. The formation of caves from a ghost-rock occurs in two steps linked with two completely different palaeogeographical and palaeotectonic contexts. In Belgium, a first step occurred during Cretaceous when a flat surface enabled very slow underground water movements with partial dissolution of the limestone and formation of the ghost rock. The slow water movements also include possible convection loops related to low to medium-temperature geothermal water. A second step occurred in Cenozoic times during continental phases and when continental uplift increased the hydrological potential. Higher energetic water movements, phreatic or vadose, erode the residual alterite and creates a “speleological” cave. An example of such cave formation was observed *in situ* in the Quentin cave in Carboniferous limestones in Belgium. The cave formed in only a few months.

Résumé

La karstification par fantômisation. La karstification par fantômisation, ou par altération des calcaires avec élimination de la roche altérée (fantôme) à un stade ultérieur, présente des différences importantes avec la théorie classique de formation de grottes, c’est-à-dire l’eau qui dissout le calcaire et qui agrandit progressivement les fissures ou encore la karstification par élimination totale. La karstification par fantômisation permet souvent d'expliquer plus facilement les morphologies observées que la théorie classique. La formation de grottes à partir d'un fantôme de roche se fait en deux étapes qui sont à mettre en relation avec deux contextes paléogéographiques et paléotectoniques distincts. En Belgique, une première étape s'est produite au Crétacé, lorsqu'une surface plane a permis des mouvements d'eau souterraines très lents avec dissolution partielle du calcaire et formation du fantôme. Ces mouvements de l'eau dans l’aquifère peuvent se faire par boucles de convection liées à du géothermalisme de basse ou moyenne température. Une deuxième étape s'est produite au Cénozoïque pendant les phases continentales et lorsque le soulèvement des continents a augmenté le potentiel hydrologique. Des mouvements d'eau plus énergétiques, phréatiques ou vadoses, érodent l'altérite résiduelle et créent une grotte "spéléologique". La formation d’une grotte par évacuation de l’altérite a été observée *in situ* dans la grotte Quentin dans les calcaires carbonifères. La grotte s'est formée en seulement quelques mois.

1. A new karst genesis paradigm

Ghost-rock karstification is a new way of explaining the formation of caves and karst. Instead of the usually accepted theory (*total removal karstification*) of water (meteoric or deep hydrothermal) progressively dissolving the limestone and widening passages, ghost-rock karstification first leads to huge amounts of altered limestones that are ‘washed away’ by flowing water several million years later, which leads to the creation of caves. Moreover, this theory has the advantage of explaining observed incoherent passage width in caves or caves in hard materials such as quartzites, more easily than the classical theory. The concept of ghost rock as a primary step of cave formation was developed by the *Laboratoire de Géologie of the Faculté Polytechnique de Mons*, now known as *Faculté polytechnique de l’Université de Mons* in Belgium.

2. A two-step cave formation in distinct palaeoenvironmental contexts

The ghost-rock paradigm takes into account that karstification is in the first place a weathering process, just similar as for alumino-silicates. For carbonates, this weathering process partially dissolves the carbonates, especially the micritic part, while it leaves *in situ* not only the insoluble phase (clay minerals, quartz, siliceous cherts…) but also mostly sparitic carbonates (fossils, veins…). The weathering often occurs along structural discontinuities (bedding planes, fractures, faults….). The weathering leaves behind an altered isovolumic (= with the same volume) bedrock but with a porosity which can exceed 50% (Fig. 1). In several cases the ghost rocks are rich in organic compounds that play a role in the bacterially mediated oxydo-reduction reactions, involving sulphides and leading

to the production of sulfuric acids that 'boost' the karstification (QUINIF, 2014). Ghost-rock based cave formation takes place in two steps:

Step 1: Ghost-rock weathering
In Belgium, ghost-rock formation took place in a specific environmental context: low relief, hot and humid climate, important vegetation. These conditions are in fact those of the so-called *biostasy* phase, as defined by ERHART in 1967 (QUINIF et *al* 2014). The weathering takes place in the phreatic zone. The low hydrological potential, related to the low relief, makes that water is flowing extremely slowly. In deeper parts, the water may even follow phreatic thermal cells. The porosity necessary to initiate the weathering process is in our case offered by joints opened during Cretaceous extensional tectonic phases.

Step 2: Ghost-rock removal and cave formation
The second phase of karst genesis (Fig. 2) starts with changing environmental conditions of tectonic uplift and subsequent water-level lowering. A change in vegetation may influence the process with a decrease in the protection of the soils. This is the so-called *rhexistasy* phase as defined by ERHART in 1967. The creation of a hydrodynamical potential will induce a compaction of the porous altered rock or ghost rock leading to the creation of larger voids. These voids may migrate to the surface, following weathered structures and create surface collapses. Surface run-off waters may follow easy-to-erode pre-formed weathered networks to create a complex speleological system with underground rivers, pits and mazes. The water will find its way and resurge into lower lying valleys, creating the cave systems like we know them today.

Figure 1. Ghost rock in the Gauthier-Wincqz Quarry in Soignies, Belgium. The limestone, a massive Tournaisian (Mississippian) 'encrinite' was partially dissolved, especially its micritic part. The larger remains of the crinoid fossils give a granular aspect to the 'ghost'. Inside the ghost-rock, remains of unaltered or less altered limestone are observed, e.g., behind the hammer.

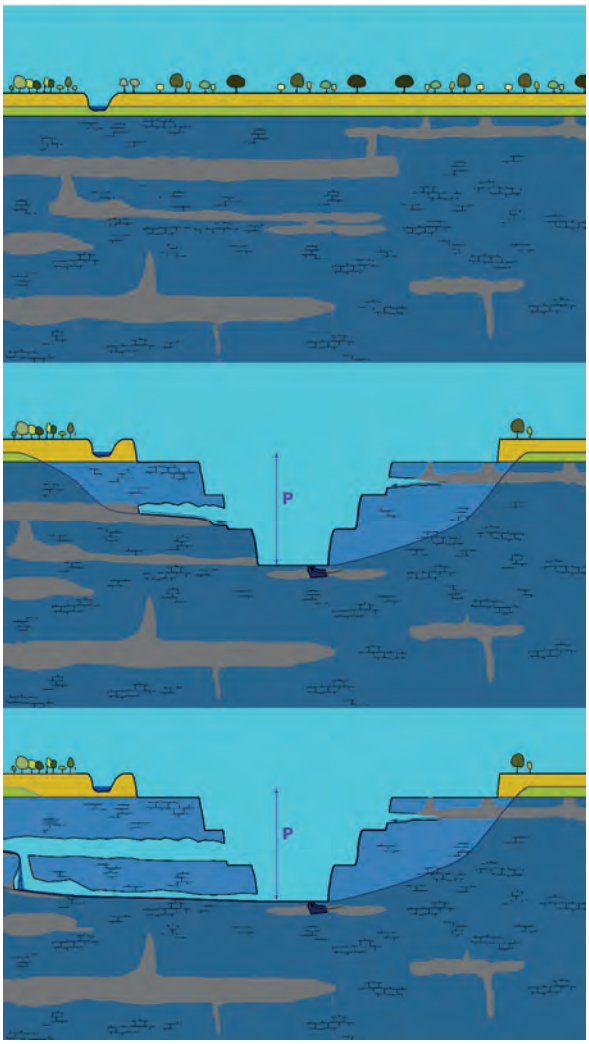

Figure 2. Evolution of a weathered or 'ghost-rock' karstified limestone as observed in the Nocarcentre Quarry (Ecaussinnes, Belgium). Above: Tertiary deposits cover in unconformity ghost-rock rich limestones that were karstified during Cretaceous. The residual ghost rock remained in place as long as the hydrodynamical potential was absent.
Middle: The digging of the quarry creates a hydrodynamical potential. Underground water flows from the surrounding aquifer into the quarry and 'washes away' the ghost rocks, creating 'speleological caves'.
Below: New underlying galleries form following the deepening of the quarry. This phenomenon mimics the natural process of deepening valleys.

The new concept has important consequences for several other aspects of karst and caves and even for cavers.

3. The consequences for caves (and cavers looking for new cave passages!)

Caves are older than previously thought…
In the classical karstification theory, Belgian caves were maximum ~10 Ma old, dating from Miocene age. Instead, the ghost-rock theory sets first karstification steps in Cretaceous times, when the weathering of the limestone pre-forms the future cave.

Looking for new caves? Better not digging into a ghost rock!

In contrast with the classical theory, the ghost-rock karstification does not enable to find an upstream or downstream part of a system, since it may be formed by irregular weathering of the limestone in any direction, depending on probably bacterial and chemical processes, and structural discontinuities. However, a river system may be organised afterwards by the water trying to find a passage and following successive altered levels. Of course, this means that digging into a ghost-rock will be probably less successful to find new open passages than digging in fluvial sediments, since the ghost rock indicates passages that were never emptied, while river sediments were deposited in already open passages. Best to be able to make the difference!

Relating cave levels with surface fluvial terrasses or erosion levels is hazardous

Since in the ghost-rock theory, flowing water tries to find a passage in the previously altered limestone, the opened passages were 'pre-figured' and are thus not progressively following the creation of the outside landscape as thought in the classical theory.

Key-holes and other roof channels are no proof of running water anymore.

Several macro and micro morphologies were observed inside ghost-rocks and are therefore no proof anymore for water flowing in open passages. Anastomosis and ceiling groves, key-hole galleries, ledges or terraces, ceiling channels or pockets are all morphologies that could have formed due to slow weathering and are no proof of running water in open passages (DUBOIS et *al*. 2014). Or said differently: Scallops and giant pothole patterns are the only 'sure' indication of flowing water.

Figure 3: Ghost rock in the quarry of Chansin (Namur Province, Belgium, DUBOIS & QUINIF, 2019). The ghost rock is surrounded by red lines. It seems be a gallery with a river deposit but this filling is in reality the residual alterite. The bedrock member affected by the weathering is a sandy limestone and the residual alterite is constituted essentially by sands with a great porosity.

4. Where is the ghost? A cave in a few months!

An important problem in proving the ghost-rock karstification in "nowadays" caves is that since these caves are open, it means that the alterite or weathered limestone or ghost-rock is gone. Most caves do not anymore contain the traces of the weathering and makes the ghost-rock karstification difficult to prove. However, some of them still do contain parts of weathered limestone such as Trabuc cave in Gard (BRUXELLES, 1997).

The best place to look for ghost-rock karstification is in quarries. In Belgium, 'ghost rocks' are observed in the quarries, such as in the Chansin quarry (Namur Province, Belgium) (Fig. 3) or in the quarries of the Hainaut region. The quarry of Nocarcentre (Soignies) in Belgium had several parts with altered limestones, so-called 'ghost rocks' (Fig 2). These parts were an important problem for the productivity of the quarries. Many springs were present, with water

flowing out of the altered limestones, as a typical consequence of the hydrological depression dome created by the pumping of the water by the quarry. After a few months, the water eroded the entire ghost rock and a classical–looking cave was born. We could enter the cave through a pit and navigate with a small boat on the river flowing on the compacted ghost rock residues. The water was coming from the not yet eroded ghost rock after several tens of meters (QUINIF, 2010). With the grotte Quentin, we witnessed the creation of a cave in a few months!

Nothing seems to be discriminating between a cave formed in the classical way and the cave formed from a ghost rock! Remaining questions are numerous and one of them is: 'are all the current known caves formed following the ghost-rock theory?' or is it a continuum between several possibilities in-between two extremes of ghost-rock (partial dissolution & sudden void creation) and total removal karstification (direct removal of matter and progressive widening of voids) depending on the regional topographical and tectonic situation?

5. Conclusions and perspectives

It is now well demonstrated that in specific environmental context, the karstification will not follow the classical theory of total removal of the carbonates by flowing water, dissolving the limestone to progressively enlarge initial crack. Instead, the limestone is, in a first step, weathered and remains *in situ* with a larger porosity, a situation that can last millions of years. In a second step, driven by changing environmental conditions related to tectonic uplift or lowering of the piezometric water-level, the weathered limestone or 'ghost rock' is washed away by flowing water and a cave is formed.
The ghost-rock theory often enables better explanations for observed hydrological dynamics, i.e., buffer zones, that are difficult to explain in highly karstified rocks or the absence of evidence for high energetic waterflow, i.e., pebbles or scallops in large galleries.

Further studies should probably focus on the universality and prerequisite of the process in the karstogenesis and the spatial and temporal (chronology) extension of ghost-rocks as primary karstification step. Another important question remains about the process of partial dissolution and the role of bacteria in the decarbonation processes.
The relation with other processes, such as deep karst formation, ore mineralisations and oil and gas reservoir formation should be also further clarified. Several ghost-rocks in the organic -rich limestones in Soignies delivered an oily residue suggesting a possible reservoir function. In Belgium several karstic voids are filled with lead and zinc ores, that are a mix of smithsonite, limonite and other oxides. Their deposition history should be investigated in the light of ghost-rock karstification processes to have a more precise idea on how exactly the ores filled up the cavities.

References

BRUXELLES L. (1997) Karsts et paléokarsts du bassin de Mialet. *Karstologia* 30(2) : 15-24.

DUBOIS C., QUINIF Y, BAELE JM, BARRIQUAND L, BINI A, BRUXELLES L, DANDURAND G., HAVRON C., KAUFMANN O., LANS B., MAIRE R., MARTIN J., RODET J., ROWBERRY M.D., TOGNINI P. and VERGARI A. (2014)-The process of ghost-rock karstification and its role in the formation of cave systems. *Earth-Science Reviews* 131, 116-148.

DUBOIS C. and QUINIF Y., (2019) - The ghost-rock of the Chansin quarry (Belgium) – A remarkable example of pseudogallery. *Geologica Belgica*, 22/3-4, 175-181.

ERHART H. (1967) *La genèse des sols en tant que phénomène géologique*. Masson Ed., Paris, coll. Evolution des sciences, 90 p.

QUINIF Y. (2010) *Fantômes de roche et fantômisation. Essai sur un nouveau paradigme en karstogenèse*. Karstologia Mémoires 18, 183p.

QUINIF Y. (2014) La fantômisation, une nouvelle façon de concevoir la formation des cavernes. *Regards* 79, 42-72.

QUINIF Y., BAELE J.-M., DUBOIS C., HAVRON C., KAUFMANN O. et VERGARI A. (2014) – Fantômisation : un nouveau paradigme entre la théorie des deux phases de Davis et la théorie de la biorhexistasie d'Erhard. *Geologica Belgica*, 17, 66-74

Cellules de convection géothermiques et fantômisation

Yves QUINIF[(1)], Alain RORIVE[(2)], Luciane LICOUR[(3)],
Grégory DANDURAND[(4)] & Laurent BRUXELLES[(5)]

(1) Service de Géologie fondamentale et appliquée, Université de Mons, rue de Houdain, 9, B-7000 Mons, Belgique, yves.quinif2@gmail.com
(2) Service de Géologie fondamentale et appliquée, Université de Mons, rue de Houdain, 9, B-7000 Mons, Belgique, alain.rorive@umons.ac.be
(3) Haute Ecole Provinciale de Hainaut-Condorcet, Dept d'Agronomie, rue Paul Pastur, 73, B-7500 Tournai) Tournai, Belgique. luciane.licour@condorcet.be.
(4) Inrap Nouvelle-Aquitaine (Poitiers) / UMR5608 TRACES (Toulouse). Gregory.Dandurand@Inrap.fr
(5) TRACES, UMR 5608 du CNRS, 5 allées Antonio Machado, 31058 Toulouse cedex 9. Laurent.bruxelles@inrap.fr

Résumé

L'initiation de la spéléogenèse a toujours constitué une énigme lorsqu'elle est considérée dans son contexte géologique. La découverte des fantômes de roche et surtout leur conception systémique dans le cadre de la karstogenèse conduit à reconsidérer cette initiation. La fantômisation est la division de la roche-mère en deux phases : une phase soluble exportée hors du système et une phase résiduelle constituant l'altérite. Les exemples des karsts de Lombardie et les paléokarsts du Hainaut ont montré que cette fantômisation se déroule plusieurs centaines de mètres sous la surface piézométrique. Le champ géothermique de Saint-Ghislain (Hainaut, Belgique) illustre une solution apportée à l'explication de l'initiation de la karstogenèse. Cet aquifère de calcaires et anhydrites carbonifères affleure au nord du Bassin de Mons et s'enfonce jusque 1700 à 4300 m de profondeur sous les formations houillères à la verticale de la ville de Saint-Ghislain, à l'ouest de Mons (Hainaut, Belgique). L'application de modèles thermo-hydrodynamiques à cet aquifère aveugle permet de considérer l'apparition de cellules de convection alimentées par le gradient géothermique. Ainsi, en fonction d'une perméabilité initiale et au-dessus d'une épaisseur limite, une circulation lente d'eau s'amorce et provoque la fantômisation que l'on peut alors rattacher à une spéléogenèse de type hypogène, l'énergie chimique étant ici apportée à la fois par les réactions bactériennes d'oxydo-réduction sur sulfures et la dissolution physique des sulfates. Le fantôme de roche se crée ainsi, l'altérite pouvant être érodée partiellement plus tard à la faveur de l'apparition d'un potentiel hydrodynamique, qu'il soit d'origine gravitaire ou, comme ici, d'origine géothermique.

Abstract

Geothermal convection cells and ghostrock karstification. The initiation of speleogenesis has always been an enigma when it is viewed in its geological context. The discovery of ghostrock and especially their systemic conception within the framework of karstogenesis leads to reconsider this initiation. "Ghosting" is the division of the bedrock into two phases: the weathering divides the bedrock in a soluble phase exported out of the system and a residual phase constituting the alterite. The examples of the karsts of Lombardy and the paleokarsts of Hainaut have shown that this ghosting takes place several hundred meters below the water table. The Saint-Ghislain geothermal field (Hainaut, Belgium) illustrates a solution to the explanation of the initiation of karstogenesis. This aquifer of limestone and carboniferous anhydrites outcrops north of the Mons Basin and sinks to a depth of 1,700 to 4,300 m under the coal formations vertically above the town of Saint-Ghislain, west of Mons (Hainaut, Belgium). The application of thermo-hydrodynamic models to this blind aquifer allows us to consider the appearance of convection cells fed by the geothermal gradient. Thus, depending on an initial permeability and above a limit thickness, a slow circulation of water begins and causes ghosting which can then be linked to a hypogenous type speleogenesis, chemical energy here being provided both by bacterial oxidation-reduction reactions on sulphides and the physical dissolution of sulphates. The phantom of rock is thus created, the alterite being able to be partially eroded later thanks to the appearance of a hydrodynamic potential, whether it is of gravity or, as here, of geothermal origin.

1. Introduction – Les fantômes de roche et les énergies mises en œuvre

La karstification par fantômisation se distingue de la karstification par enlèvement total (théorie « classique ») par le très faible potentiel hydrodynamique existant au départ de la karstogenèse. La formation des fantômes de roche se caractérise en effet par une attaque chimique séparant la roche mère en deux phases : une phase soluble exportée par les eaux souterraines et une phase résiduelle : l'altérite. La karstification classique, par enlèvement total, connaît quant à elle l'érosion à la fois des éléments solubilisés et les éléments solides détachés de la roche mère par la dissolution de la matrice. Un exemple type est la dissolution de la partie micritique du calcaire et le résidu sparitique. Dans le cas de la fantômisation, ce dernier reste sur place au moins temporairement en la compagnie des

insolubles et autres moins solubles : dolomite, minéraux argileux, silice. Le processus de fantômisation est bien connu dans le cas du granite où on l'appelle arénisation. La différence étant que les insolubles prennent largement la plus grande part dans l'altérite résiduelle : quartz, minéraux argileux secondaires, aluminosilicates résiduels. On a pensé longtemps que ce processus n'était pas de mise dans le cas des roches carbonatées. Or, les examens des paléokarsts en roches carbonatées dinantiennes de la province du Hainaut (Belgique) ont montré qu'il en est bien ainsi. Les formes souterraines gardent une altérite résiduelle formées de la partie moins soluble ; elle garde le volume initial, la perte de matière se manifestant par une augmentation de la porosité : c'est le fantôme de roche.

Figure 1 : Fantôme de roche (carrière du Clypot, Soignies, Belgique).

Cette distinction entre les deux types de karstogenèse se marque dans le concept thermodynamique de la karstification. La karstification, comme tout processus d'érosion, est le résultat d'une dissipation d'énergie. Parmi les types d'énergie concernée, l'énergie chimique est fondamentale car elle est la cause de la transformation de la roche mère. Elle tire sa source de réactions acide-base, l'acide pouvant être dû au CO_2 atmosphérique ou profond, aux sulfures qui s'oxydent en sulfates sous l'action de bactéries avec, comme corollaire, la présence d'acide sulfurique, en bref à la présence d'ions H_3O^+. Le second type d'énergie est l'énergie potentielle qui est la cause du mouvement de l'eau souterraine. Elle trouve sa source dans la gravité, le plus souvent invoquée, mais aussi dans le gradient géothermique, nous y reviendrons. Il manque encore un élément : la perméabilité initiale. En effet, les eaux souterraines doivent être capables de circuler au début du processus en l'absence d'érosion. Cette perméabilité initiale peut être due à une fracturation dont certaines familles directionnelles sont soumises à un régime tectonique en extension : c'est une troisième forme d'énergie de type mécanique. Il se peut que cette perméabilité initiale soit héritée d'une trop faible diagenèse, ou encore de la présence de cavités préexistantes.

Le gradient hydraulique joue le rôle fondamental dans le type de karstification. La fantômisation se satisfait d'un gradient hydraulique ΔH très faible puisque l'altérite résiduelle reste dans les formes souterraines sans être mécaniquement érodée dans cette première phase. Elle le sera lorsque le massif connaîtra l'augmentation de ce gradient (surrection, eustatisme, changement climatique). Son érosion mécanique aboutira alors à l'ouverture de cavités « spéléologiques ». Cette évolution qui part de l'altération chimique à l'érosion mécanique est une parfaite illustration de la théorie de la biorhexistasie d'ERHART (1967).

2. Le karst géothermique de Saint-Ghislain (Bassin de Mons, Belgique)

Un important aquifère constitué principalement de calcaires paléozoïques se situe dans le Bassin de Mons, structuré en fond de bateau comprenant des formations du Crétacé supérieur et du Paléogène incisées dans les formations paléozoïques du socle varisque (BOULVAIN & PINGOT, 2011). Sous les formations Houillères écaillées (Pennsylvanien et Serpukhovien), le Viséen et le Tournaisien regroupent des formations carbonatées (calcaires et dolomies) et sulfatées (anhydrite) d'une épaisseur avoisinant les 2.600 m d'épaisseur (Fig. 2). La karstification visible en affleurement au nord notamment grâce aux carrières des régions de Soignies et de Tournai se retrouve en profondeur, sans doute avec des différences morphologiques (dissolution des anhydrites, présence de brèches). Cet aquifère offre ainsi un modèle de karstification profonde dont les circulations ont été modélisées (LICOUR, 2012). En ce sens, il peut être considéré comme un holotype pour les circulations karstiques profondes.
En 1982, un sondage d'exploration géologique découvre de l'eau chaude artésienne au cœur du Bassin de Mons. Ce sondage recoupa vers 1.700 m de profondeur, dans les carbonates et sulfates viséens, des cavités et brèches très perméables contenant de l'eau à 70°C. Deux autres sondages (Douvrain et Ghlin) recoupèrent également les formations aquifères géothermiques. La configuration géologique visualisée par la figure 2 localise les zones d'infiltration au nord. Les eaux peuvent ainsi descendre au cœur de la structure où elles subissent le gradient géothermique normal (3°C/100 mètres). Il faut noter qu'aucune possibilité de sortie des eaux chaudes n'existe au sud, à l'est ou à l'ouest : l'aquifère s'ennoie profondément sous la nappe de charriage ardennaise sous la faille du midi. Les seules sources sont situées au nord de l'affleurement de l'aquifère et présentent des anomalies thermiques.
Ces constations ont conduit l'une d'entre nous (LICOUR, 2012) à concevoir un modèle de circulation des eaux dans l'aquifère suivant une ou plusieurs cellules de convection thermique dont le moteur est la différence de température suivant la profondeur (Fig. 3). La quantification de ce modèle par un logiciel adapté prouve la vraisemblance de ces circulations, les seules pouvant expliquer la karstification profonde nécessitant une évacuation des eaux minéralisées. Verticalement, le mouvement de l'eau se fait suivant une descente par le mur de l'aquifère et une remontée par le

toit. La modélisation dans une coupe verticale N-S indique l'initiation d'une cellule de convection dans un plan vertical (Fig. 3). Le mouvement peut être initié par le gradient géothermique à partir d'une épaisseur d'aquifère dont la valeur est fonction de la perméabilité initiale.

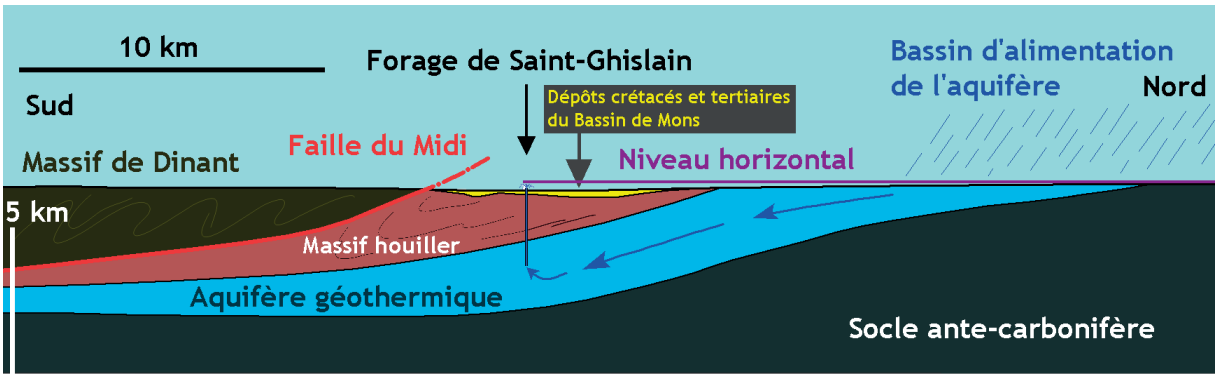

Figure 2 : L'aquifère géothermique du Hainaut. Cette figure est une coupe géologique interprétative orientée du nord vers le sud, à partir des données géologiques récoltées en affleurement, des forages et des investigations géophysiques. Les formations formant l'aquifère géothermique sont formées des calcaires, dolomies et anhydrites datant du Carbonifère inférieur. Elles reposent sur le socle primaire ante-carbonifère et sont surmontées par les formations du Carbonifère supérieur. Les eaux sont artésiennes au niveau des sondages forés dans le Bassin de Mons, étant à une altitude inférieure à la zone d'alimentation de l'aquifère.

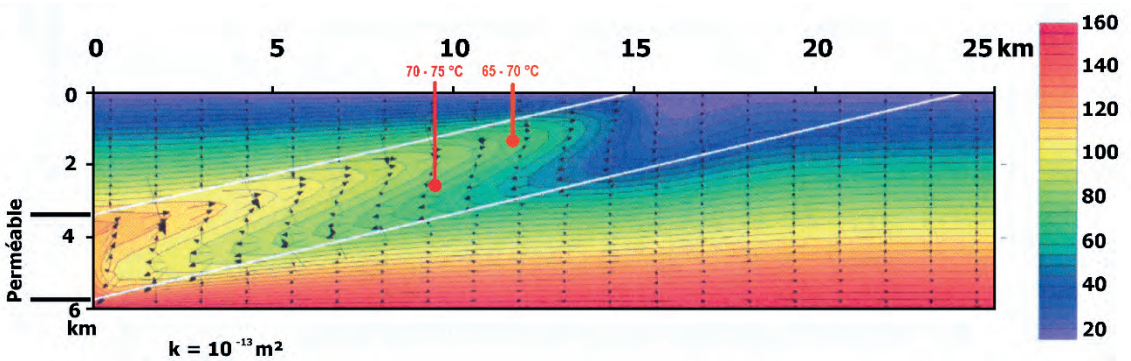

Figure 3 : Modèle de couche perméable inclinée à mur et toit imperméable et surface libre. A droite, l'échelle de température. Les deux lignes rouges verticales indiquent les positions des sondages de Saint-Ghislain et de Douvrain.

Les valeurs de discrétisation et des paramètres utilisés sont : 1. 25 km de long, soit 250 colonnes de 100 m, 6 km de profondeur, soit 60 rangées de 100 m ; gradient géothermique de 2,5 °C/100 m, soit 10 °C en surface et 157,5 °C au fond ; une porosité de 5 % et une perméabilité de 10^{-13} m² pour la couche perméable, une porosité de 2 % et une perméabilité de 10^{-20} m² pour les couches imperméables. La géométrie de l'aquifère a été calquée sur celle de l'aquifère du Carbonifère hennuyer. Les valeurs choisies sont adéquates pour l'initiation de la convection verticale. Le mouvement peut être initié par le gradient géothermique à partir d'une épaisseur d'aquifère dont la valeur est fonction de la perméabilité initiale.

3. La karstification de type fantôme de roche à moteur géothermal

Seule hypothèse expliquant la karstification profonde dans l'aquifère de Saint-Ghislain, le gradient géothermique génère ainsi des cellules de convection. Cette hypothèse résulte de la configuration géométrique de cet aquifère qui constitue un cul-de-sac au sud, en profondeur, avec des zones d'infiltrations et des exutoires limités aux régions d'affleurement septentrionales. Les mesures de température dans les sources et les sondages ainsi que leur distribution géographique conforte cette hypothèse. En outre, les grands « puits naturels du Houiller » apportent un argument supplémentaire à l'existence de cette karstification profonde (QUINIF, 1995 ; QUINIF & LICOUR, 2012). Ces formes géantes verticales, larges de plusieurs dizaines de mètres et profondes parfois de plus d'un kilomètre transpercent les terrains houillers et trouvent leur origine dans la karstification sous-jacente. On peut les considérer comme des fontis géants. Leurs remplissages, qui ont révélé les iguanodons de Bernissart, situent leur genèse au Crétacé.

La question de l'initiation de cette karstification se pose maintenant. Comme nous l'avons écrit ci-dessus, une perméabilité initiale et les deux types d'énergie sont nécessaires.

1. La perméabilité initiale est due dans ces roches compactes à une fracturation ayant joué en extension lors d'une phase de l'histoire géologique. Or, le Crétacé offre cette possibilité (QUINIF *et al.*, 1997). Cette chronologie est en parfait accord avec celle du fonctionnement des puits du Houiller daté par

la paléontologie. À cette profondeur, déjà acquise aux temps crétacés, seul le calcaire se fracture, l'anhydrite réagit de façon plastique.
2. L'énergie chimique est fournie, outre le CO_2 superficiel, par les réactions rédox affectant les sulfures (HAVRON *et al*., 2007). Les températures de l'aquifère ont favorisé en outre l'activité bactérienne.
3. Le gradient de potentiel est ici dû non pas à la gravité comme pour beaucoup de karsts mais à la chaleur, le gradient géothermique.

Lors de l'initiation, les vitesses de circulation de l'eau dans les cellules de convection étaient très faibles. Nous sommes donc amenés à penser que c'est une karstogenèse de type fantômisation qui a eu lieu. Ensuite, la formation des fantômes de roche touchant les évaporites, une dissolution physique simple s'est ajoutée à ce processus. La dissolution d'une partie de la roche mère a engendré par la suite des brèches d'affaissement, rencontrées par les forages.

4. Conclusion

L'aquifère de Saint-Ghislain, grâce à ses caractéristiques géologiques, fournit un modèle de karstification profonde. L'évolution en subsidence depuis les temps post-varisques nous le montre non affecté par l'érosion qui aurait suivi une surrection, effaçant les formes primitives de la karstification par fantômisation. Nous nous trouvons ici dans le cas de la karstification hypogène prouvée dans de nombreuses configurations géologiques (AUDRA et *al*., 2004 ; KLIMCHOUK, 2009). L'apport des considérations présentes est le concept d'initiation de la karstogenèse par fantômisation au sein de cellules de convection géothermiques. Pour cela, il faut une formation aquifère karstifiable dont l'épaisseur, la profondeur et la perméabilité initiale se situent dans la gamme de valeurs citées plus haut. Ainsi que nous l'avons déjà démontré dans une autre publication, ce mécanisme éclaire la genèse des résurgences vauclusiennes (DANDURAND et *al*., 2019).

Références

AUDRA P. et HOFMANN B. A. (2004) Les cavités hypogènes associées aux dépôts de sulfures métalliques (MVT). *Le Grotte d'Italia*, 5, 35-56.

AUDRA P., BIGOT J.-Y. & NOBÉCOURT J.-C. (2010) Hypogenic caves in France. Speleogenesis and morphology of the cave systems. *Bulletin de la Société géologique de France*, t. 181, 4, 327-335.

BOULVAIN F. et PINGOT J.-L. (2011) Genèse du sous-sol de la Wallonie. *Classe des Sciences, Académie royale de Belgique*, 190 p.

ERHART H. (1967) *La genèse des sols en tant que phénomène géologique*. Masson Ed., Paris, coll. Évolution des sciences, 90 p.

HAVRON C., BAELE J.-M. et QUINIF Y. (2007) Pétrographie d'une altérite résiduelle de type « fantôme de roche ». *Karstologia*, 49, 25-32.

DANDURAND G., QUINIF Y., GUENDON J.-L. et GRUNEISEN A. (2019) Sources vauclusiennes et fantômes de roche. *Karstologia*, 74 : 31-46.

KLIMCHOUK A. (2009) Morphogenesis of hypogenic caves. *Geomorphology*, 106, 1–2, 100-117.

LICOUR L. (2012) *Relations entre la géologie profonde et le comportement hydrogéologique du réservoir géothermique du Hainaut (Belgique)*. Thèse de doctorat, Université de Mons Ed. : 372 p.

QUINIF Y. (1995) Le Puits de Flénu (Belgique). La plus grande structure endokarstique au monde (1200 m) et la problématique des puits du Houiller. *Karstologia*, 24, 29-36.

QUINIF Y. and LICOUR L. (2012) The karstic phenomenon of Bernissart pit and the geomorphologic situation in the Mesozoic times. In: *Bernissart Dinosaurus*, Ed. Pascal Godefroit. Indiana University Press, 50-61.

QUINIF Y., VANDYCKE S. et VERGARI A. (1997) Chronologie et causalité entre tectonique et karstification - l'exemple des paléokarsts crétacés du Hainaut (Belgique). *Bull. Soc. Géol. Fr.*, 168, 4, 463-472.

Fantômisation et hydrogéologie

Yves QUINIF[(1)], Alain RORIVE[(2)] & Laurent BRUXELLES[(3)]

(1) Service de Géologie fondamentale et appliquée, Université de Mons, rue de Houdain, 9, B-7000 Mons, Belgique, yves.quinif2@gmail.com
(2) Service de Géologie fondamentale et appliquée, Université de Mons, rue de Houdain, 9, B-7000 Mons, Belgique, alain.rorive@umons.ac.be
(3) TRACES, UMR 5608 du CNRS, Maison de la Recherche, 5 allée Antonio Machado, 31058 Toulouse cedex 9 et GAES, université de Johannesburg, Afrique du Sud.

Résumé

L'hydrogéologie des calcaires karstifiés s'écarte de l'hydrogéologie en roches poreuses ou simplement fracturées par la non-linéarité des équations d'écoulement : la loi de Darcy ne s'y applique que dans le cas d'écoulements laminaires, c'est-à-dire lents, sous potentiel hydrodynamique faible. La découverte de la notion de fantômes de roche ainsi que de la karstogenèse qui s'ensuit change notre manière d'envisager ces écoulements. Dans les profondes carrières de la région de Soignies (Belgique) exploitant des calcaires tournaisiens, des pseudoendokarsts fossiles sont réactivés par le nouveau gradient hydrodynamique imposé par la profondeur de la carrière. Des afflux d'eau localisés et considérables (plusieurs centaines de m3/h) émergent au fond de ces carrières à la faveur de pseudoendokarsts dont l'altérite résiduelle est progressivement érodée. Contre toute attente, ces « rivières » sortent de cette altérite résiduelle parfois au fond de galeries, non seulement très poreuse (de 60 à 70% pour une altérite provenant d'une roche mère à porosité inférieure à 3 %) mais également assez perméable (jusqu'à 15.000 mD). Ces pseudoendokarsts peuvent ainsi jouer le rôle de premiers drains dans l'évolution d'un massif karstifié en fantômes de roche lors de l'activation par surrection de ceux-ci, mais également constituer des zones annexes capacitives s'ils ne sont pas reliés aux drains ou avant l'apparition d'un gradient hydrodynamique.

Abstract

Ghostrock karstification and hydrogeology. The hydrogeology of karstified limestones differs from hydrogeology in porous or simply fractured rocks by the non-linearity of the flow equations: Darcy's law only applies to the case of laminar flows, that is, i.e., slow, under low hydrodynamic potential. The discovery of the notion of rock ghosts as well as the karstogenesis that ensues changes the way we think about these flows. In the deep quarries of the Soignies region (Belgium) exploiting Tournaisian limestones, fossil pseudoendokarsts are reactivated by the new hydrodynamic gradient imposed by the depth of the quarry. Localized and considerable inflows of water (several hundred m3 / h) emerge at the bottom of these quarries thanks to pseudoendokarsts, the residual alterite of which is gradually eroded. Against all expectations, these "rivers" emerge from this residual alterite sometimes at the bottom of galleries, not only very porous (from 60 to 70% for an alterite coming from a bedrock with porosity of less than 3%) but also quite permeable (up to 15,000 mD). These pseudoendokarsts can thus play the role of first drains in the evolution of a karstified massif into rock ghosts during the activation by uplift of these ghostrock, but also constitute additional capacitive zones if they are not connected at drains or before the appearance of a hydrodynamic gradient.

1. Introduction – Les fantômes de roche

L'hydrogéologie des calcaires karstifiés s'écarte de l'hydrogéologie en roches poreuses ou simplement fracturées par la non-linéarité des équations d'écoulement : la loi de Darcy ne s'y applique que dans le cas d'écoulements lents, sous potentiel hydrodynamique faible. Ceci a conduit à mettre sur pied de nouvelles théories de l'hydrodynamique en système karstique (voir par exemple : BÖGLI, 1980 ; FORD & WILLIAMS, 2007 ; MANGIN, 1975). La découverte de la notion de fantômes de roche, ainsi que de la karstogenèse qui s'ensuit change notre manière d'envisager ces lois d'écoulement (DUBOIS et *al.*, 2014 ; QUINIF, 2010, 2014 ; QUINIF et *al.*, 2014). Les observations dans les calcaires carbonifères du Hainaut, au travers des profondes carrières qui les exploitent dans le Tournaisis et autour de la ville de Soignies, à l'origine de la notion de fantômes de roche et de fantômisation, permettent d'appréhender et de caractériser l'hydrogéologie particulière qui y règne. Ces observations sont à la base de cette nouvelle manière d'envisager la karstogenèse.

Les carrières de la région de Soignies exploitent les calcaires tournaisiens essentiellement pour la « pierre bleue », une encrinite compacte utilisée comme pierre ornementale et à bâtir. Le type d'exploitation par découpage du massif permet une observation fine des phénomènes karstiques qui les affectent. Ceux-ci sont des paléokarsts (Fig. 1), fossilisés par les transgressions paléogènes qui se sont mises en place sur la surface post-varisque.

Ces paléokarsts se regroupent en deux types de formes. Les premiers sont des couloirs verticaux partant au sommet de la surface post-varisque, larges de 1 à plusieurs mètres et hauts de plusieurs dizaines de mètres. Les seconds sont des formes totalement incluses dans le massif.

Figure 1 : Fantômes de roche (Carrière du Hainaut, Soignies). Ces cavités n'en sont en fait pas. La formation qui les colmate est constituée de l'altérite résiduelle, résultant de la dissolution partielle de la roche mère, ici une encrinite calcaire compacte du Tournaisien supérieur.

Elles renferment une altérite constituée des éléments insolubles et moins solubles de la roche mère : minéraux argileux, silice (cherts), calcite sparitique telle que les entroques, matière organique amorphe. Les uns et les autres sont regroupés sous le vocable de fantôme de roche. Ils doivent leur formation à une altération partielle de la roche mère, dans la zone phréatique, sous très faible potentiel hydrodynamique conditionnant des écoulements lents. Il a été prouvé que, dans le cas de l'apparition du potentiel hydrodynamique (surrection tectonique, régression, modification climatique, etc.), les circulations souterraines provoquent l'érosion mécanique de l'altérite résiduelle, créant ainsi des grottes « spéléologiques ». Cette karstogenèse se différentie de la spéléogenèse classique où les conduits se forment en une phase.

2. La réactivation hydrogéologique des paléokarsts fantômes dans les carrières

Ces carrières sont en creux dans un paysage de plaines. Elles constituent ainsi des puits dénoyés au sein de l'aquifère dont la surface piézométrique est affleurante au sommet des calcaires, sous la couverture transgressive tertiaire. L'exhaure indispensable à l'exploitation a remis ces karsts en activité hydrique par création d'un niveau de base artificiel de plusieurs dizaines de mètres à plus de 100 m sous la surface piézométrique. Des arrivées d'eau localisées surviennent parfois dans ces carrières. Une véritable rivière souterraine peut parfois être parcourue sur plusieurs mètres à plusieurs dizaines de mètres dans des galeries d'ordre métrique (Fig. 2).

Figure 2 : L'émergence de la grotte de l'Échelle (Carrière du Hainaut, Soignies). L'entrée de la grotte se trouve à droite, derrière le dernier spéléologue. La petite cascade donne une idée du débit qui en sort.

Les pseudoendokarsts peuvent se présenter sous la forme de formes horizontales, développées souvent le long de joints verticaux. Certaines familles directionnelles (N60°E, N150°E, N110°E) se sont trouvées en extension lors de phases tectoniques durant la fin du Jurassique et au Crétacé (QUINIF et *al*., 1997) et ont alors subi une karstification de type fantômisation. Hormis une activité hydrogéologique localisée au début du Paléocène qui a permis une érosion de l'altérite résiduelle de certains pseudoendokarsts et la sédimentation de séries fluviatiles (QUINIF et *al*., 2006), la plupart des fantômes de roche ont conservé leur altérite, le tout fut ensuite fossilisé par les transgressions du Thanétien et de l'Yprésien. Le seul potentiel hydrodynamique susceptible de provoquer l'apparition de courants érosifs dans les fantômes de roche est celui dû au creusement des carrières.

3. La grotte de l'Échelle

La grotte de l'Échelle, découverte en 1997 au fond de la carrière du Hainaut, fut la première à être interprétée correctement. Il s'agit d'une galerie d'une dizaine de mètres de long, large de 1,5 à 0,5 mètre, haute de quelques mètres. Elle était envahie par l'eau dont la profondeur est en moyenne de 1,3 mètre. Cet envahissement est dû à une obstruction de l'entrée par des blocs et un écoulement à l'amont pendage (Fig. 3). Les formes pariétales sont de type coupoles, arrondies mais peu profondes. En voûte, la galerie se termine sur des coupoles décimétriques allongées dans le sens de la longueur. À 9 mètres de l'entrée, il existe une petite arrivée d'eau par une cheminée elliptique large de 40 cm sur 20 cm.

Figure 3 : La grotte de l'Échelle (Carrière du Hainaut, Soignies). Il s'agit de la journée de la découverte. Le niveau atteint par la carrière ne permet pas encore à l'eau de s'écouler en rivière cascadante.

L'arrivée d'eau se produit au travers de l'altérite, ce qui suppose une porosité interconnectée assurant la perméabilité (fig. 4). Alors que la porosité de la roche mère ne dépasse pas 2%, elle atteint jusqu'à 46 % pour l'encrinite. Si la perméabilité de la roche mère se situe sous 0,5 mD (milliDarcy), elle atteint 15.000 mD dans le fantôme de roche, ce qui explique le débit observé à l'émergence. Il est important de souligner que ce courant d'eau sort de l'altérite elle-même et non d'un vide macroscopique. La suite de l'approfondissement permit d'apprécier le volume de la galerie (fig. 5).

Figure 4 : La terminaison de la grotte de l'Échelle (Carrière du Hainaut, Soignies). L'eau sort de l'altérite résiduelle du fantôme en place. La perméabilité est assurée par la porosité interconnectée de cette dernière, et non à partir de vides macroscopiques.

4. Conclusion - Hydrogéologie et spéléogenèse

Cette forme et son fonctionnement hydrogéologique permettent de jeter un nouveau regard sur la spéléogenèse. La grotte de l'Échelle considérée ici est le résultat de l'érosion de l'altérite résiduelle du fantôme de roche structuré en pseudoendokarst. Cette érosion est permise grâce au potentiel hydrodynamique créé par le creusement de la carrière.

Figure 5 : La galerie de la grotte de l'Échelle

Ce schéma évolutif est à rapprocher du creusement d'une vallée. Dans la même logique, c'est au fur et à mesure du creusement de la vallée que les fantômes de roche se mettent en activité hydrique, avec érosion mécanique de l'altérite résiduelle et spéléogenèse. Les altitudes des émergences sont alors déterminées par la position des fantômes de roche et non un niveau de base régional. Les calcaires carbonifères considérés ici, après une phase de fantômisation située au Crétacé inférieur (QUINIF et *al.*, 1997), seule une phase à plus haute énergie au début du Paléocène a provoqué une érosion très partielle de certains fantômes de roche, amenant à leur ouverture suivie d'une sédimentation fluviatile. Ensuite, deux transgressions, thanétienne et yprésienne, déposant sable et argiles, ont fossilisé ces fantômes de roche, la plupart ayant gardé leur altérite résiduelle en place. Une surrection suivie d'un enfoncement d'un réseau hydrographique aurait joué le rôle du creusement des carrières en ouvrant ces fantômes de roche pour en faire des réseaux spéléologiques.

Enfin, on conçoit ainsi que l'aquifère karstifié comprend plusieurs sous-systèmes. Si l'on se réfère au schéma conceptuel de Mangin (1975), le système karstique comprend deux types de sous-systèmes : les drains transmissifs mais peu capacitifs et les systèmes annexes, peu transmissifs, capacitifs, et connectés aux drains. Ce schéma ne fait aucune hypothèse quant à la forme de ces sous-systèmes, excepté les drains explorés par les spéléologues. Les fantômes de roche décrits ici se situeraient dans l'un ou l'autre type en fonction de leur position au sein de l'aquifère. Dans la zone phréatique, en l'absence d'un potentiel hydrodynamique appréciable, ils constituent des volumes remplis d'une formation poreuse : l'altérite résiduelle. Ils jouent le rôle de sous-système capacitifs. Lors de l'abaissement de la surface piézométrique et de l'apparition d'énergie cinétique pour les eaux souterraines, ils se transforment peu à peu en drains. Sans doute faut-il y voir l'expression géologique des systèmes annexes de Mangin, lorsque ces fantômes de roche se trouvent hydrogéologiquement isolés des drains transmissifs au sein de l'aquifère.

Références

BÖGLI A. (1980) Karst Hydrology and Physical Speleology. Springer-Verlag, New York: 284 p.

BONACCI O. (1987) Karst hydrology. Springer Series in Physical Environment: 184 p.

DUBOIS C., QUINIF Y., BAELE J.-M., BARRIQUAND L., BINI A., BRUXELLES L., DANDURAND G., HAVRON C., KAUFMANN O., LANS B., MAIRE R., MARTIN J., RODET J., ROWBERRY M.D., TOGNINI P. and VERGARI A. (2014) The process of ghost-rock karstification and its role in the formation of cave systems. Earth Science Reviews, 131: 116–148.

FORD D. and WILLIAMS P.W. (2007) Karst hydrogeology and geomorphology. John Wiley & Sons, Chichester, UK: 601p.

MANGIN A. (1975) Contribution à l'étude hydrodynamique des aquifères karstiques. Ann.Spéléol., 29 (3) : 283-332 ; 29 (4) : 495-601 ; 30 (1) : 21-214.

QUINIF Y. (2010) Fantômes de roche et fantômisation – Essai sur un nouveau paradigme en karstogenèse. Karstologia Mémoires, 18 : 196p.

QUINIF Y. (2014) La fantômisation, une nouvelle façon de concevoir la formation des cavernes. Regards, 79 : 42-72.

QUINIF Y., BAELE J.-M., DUBOIS C., HAVRON C., KAUFMANN O. et VERGARI A. (2014) Fantômisation : un nouveau paradigme entre la théorie des deux phases de Davis et la théorie de la biorhexistasie d'Erhart. Geologica Belgica, 17, 1 : 66-74.

QUINIF Y., VANDYCKE S. et VERGARI A. (1997) Chronologie et causalité entre tectonique et karstification - l'exemple des paléokarsts crétacés du Hainaut (Belgique). Bull.Soc.Géol.Fr., 168, 4 : 463-472.

QUINIF Y., MEON H. and YANS J. (2006) Nature and dating of karstic filling in the Hainaut Province (Belgium). Karstic, geodynamics and paleogeographic implications. Geodinamica Acta, 19/2: 73-85.

Regional karst network genesis due to removal of ghost rocks revealed by burial dating

Philippe VERNANT[(1)], Oswald MALCLES[(1)], David FINK[(2)] & Gaël CAZES[(1)]

(1) Géosciences Montpellier - UMR 5243 CNRS, Université de Montpellier, Place E. Bataillon, 34095 Montpellier, France, philippe.vernant@umontpellier.fr (corresponding author)
(2) Australian Nuclear Science and Technology Organisation, Lucas Heights, Australia

Abstract

We present a new burial age obtained from cosmogenic dating on quartz alluvium sampled in a cave of the Larzac plateau (France). The recent age obtained (0.28 ± 0.1Ma) for a cave located at more than 8km from the plateau edges and 250 to 400m above the regional base level show that the classical speleogenesis model of sub-horizontal galleries directly linked to transient steadiness of the regional base level is not relevant for the study area. We propose that the network geometry is inherited from a primokarst generated by ghost-rock karstification and subsequently emptied of its alterite by underground regressive erosion.

1. Introduction

Using burial ages of quartz alluvium in several caves of the Larzac plateau (France, Fig. 1), MALCLES et *al*. (2021) have shown that the classical approach linking sub-horizontal galleries to stability of the regional base level is not universal.

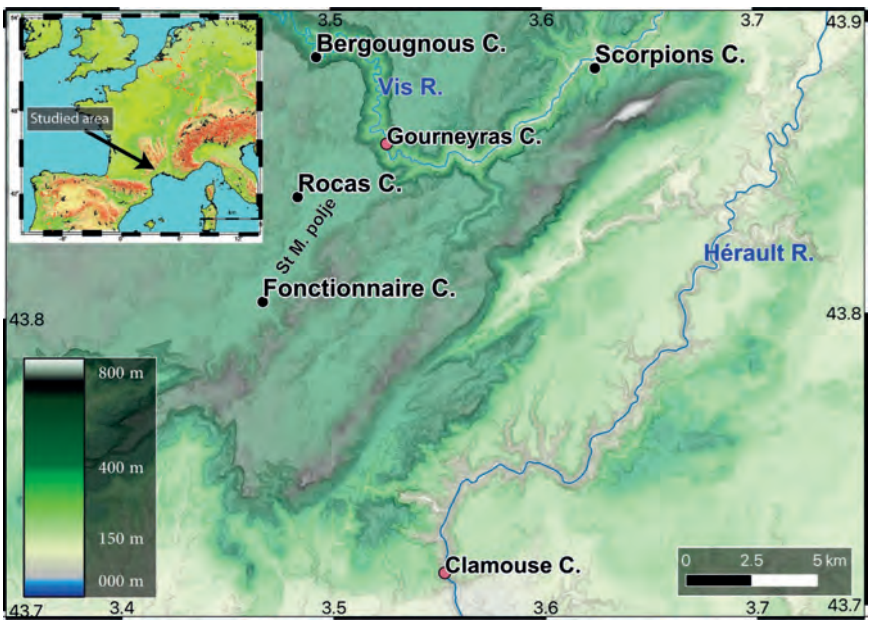

Figure 1: Location of the study. St M. polje is the Saint Maurice de Navacelles polje.

MALCLES et *al.* (2021) sampled buried quartz sediments in caves at different altitude. The goal was to estimate the Vis river downcutting rate since it started to carve a canyon in the Grands Causses plateau. Two caves about 100m above the river bed were found with entrances opening in the canyon walls (Scorpions and Bergougnous) and one about 30m above the surface of the Saint Maurice de Navacelles polje (Rocas). The height difference between these two sets of caves is on the order of 200m. Following GRANGER et *al*. (1997) approach, the quartz rich samples were analyzed to obtain the ^{26}Al and ^{10}Be concentrations in order to compute the burial age of the alluvium. This is possible since the upstream part of Vis watershed is located in the crystalline massif of the Cevennes. The theory postulates that once the quartz rich rocks come close to the surface due to erosion (approximately less than 30m depth) they start to be bombarded by cosmic rays and cosmogenic nuclides (^{26}Al and ^{10}Be in quartz) are produced. The concentrations will

build up during the surface exposure of the rocks. At some point the rocks are detached from outcrops and transported by the rivers. If the river flow into a cave and the alluvium are deposited deeply enough underground (i.e., depth greater than 30m), the concentrations will start to decrease since both ^{26}Al and ^{10}Be are radioactive. The half-lives of these two specific nuclides being different, the measured ^{26}Al/^{10}Be ratios can be used to estimate burial ages. Following this approach, MALCLES et *al*. (2021) obtained burial ages of 1.2 ± 0.3 Ma for the Bergougnous cave and an average value of 1.25 ± 0.35 for the four samples of the Scorpions cave. Given the elevation of the caves above the present-day riverbed, the derived incision rate is 83 ± 35 m/Ma, which is in agreement with the one obtained for the nearby valley of the Rieutord (MALCLES et *al*. 2020). The anomaly came from the Rocas sample located 200m above the two other caves. The burial age for the Rocas sediments is 0.9 ± 0.07 (MALCLES et *al*., 2021). Given the ~220m height difference between the Rocas samples and the others cave samples of the same age in the Vis valley it implies a steep gradient of ~6%. This slope excessively differs from the 0.4% gradient of the Vis riverbed. The Rocas can be divided in two parts, the upper one not deeper than 40m containing the quartz rich sediments, the lower one free of quartz alluvium but showing in some places limestone turning into powdery material typical of ghost rocks. Ghost rocks correspond to decalcified pockets or corridors still filled with undissolved elements of the original limestone, referred as residual or in-situ alterite (e.g., RODET, 1996; QUINIF, 2010; QUINIF & BRUXELLES, 2011). This weathering occurs when very low, if any, hydrodynamical potential is combined with chemical dissolution. The geometry of the cross section of the narrow horizontal segments is similar to the one described by DUBOIS et *al*. (2014) due to ghost-rock karstification. Hence MALCLES et *al*. (2021) suggest that the lower part of the Rocas was created when an underground connection was opened and allowed to empty the alterites (also known as ghost-rocks). Given the burial age of the Rocas sediments, we know that it occurred less than a million years ago. If MALCLES et *al*. (2021) postulate is true and that some regressive underground erosion is at play below the plateau and is emptying the alterite of the primokarst, the quartz rich alluvium should show younger ages as we move away from the plateau edges. In this study we present a new burial age estimate for a cave located below the same polje as the Rocas but further away from the canyon bordering the plateau and discuss the implications in term of spelogenesis.

2. Materials and methods

The sample (Fig. 2) was collected in the lower galleries of the Fonctionnaire cave at 75m below the surface, i.e., at an altitude of 520m. Therefore, the sediments are 50m in elevation below the Rocas ones and 150m above the sediments of the Bergougnous and Scorpions caves if we use the riverbed as the reference to compare the elevations of the samples.

The amalgamated centimetric quartz cobbles were first crushed and then purified using a sequential acid attack with aqua regia (HNO_3 + 3HCl) and diluted hydrofluoric acid (HF). We followed ANSTO's proto- col (CHILD et *al*., 2000) by adding ~300µg of a ^{9}Be carrier solution to the purified quartz powder before total dissolution. We used the 6MV SIRIUS AMS instrument at ANSTO for accelerator mass spectrometry (AMS) measurements (WILCKEN et *al*., 2017. The results were normalized to KN−5–4 (for Be, NISHIIZUMI et *al*., 2007) and KN−4–2 (for Al) standards.

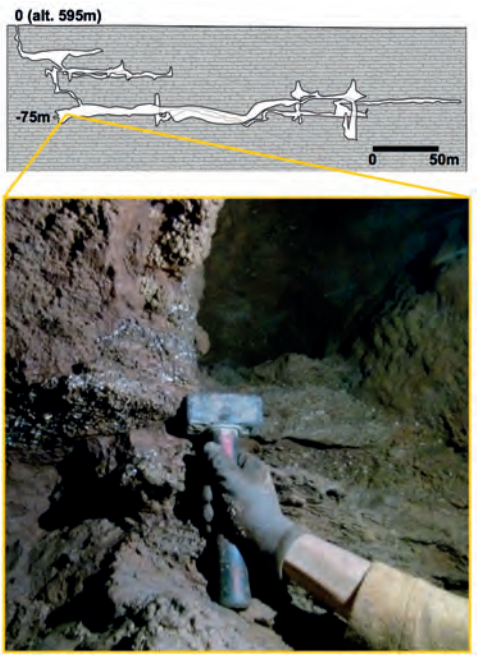

Figure 2: Top- cross-section of the Fonctionnaire cave and location of the sample. Bottom- picture of the sampling location.

3. Results

The obtained ^{26}Al and ^{10}Be concentrations, as well as the computed burial age are given in Figure 3. And reported on a two-nuclides diagram (Fig. 4). This burial age is significantly younger that the ones obtained by MALCLES et *al*. (2021) and ranging from 0.8 to 1.6 Ma. A dye tracing for the Fonctionnaire is reported in NURIT (1992). The dye was injected on July 2, 1972 and was reported at the Clamouse spring in the Herault valley 8 days later. This fairly high transfer of the dye at 75 m/h and the fact that the dye was injected at 21m depth since the lower part of the cave was unknown raise some questions on the real outlet of this cave, especially since a nearby cave outlet is located in the Vis valley according to another dye tracing. Nevertheless, the young burial age for the fonctionnaire sediments

hardened and later re-incised (Fig. 2) leads to slope gradients to the possible outlets of 3% to 4% which is 10 times mores that the 0.4% slope given by the river profiles.

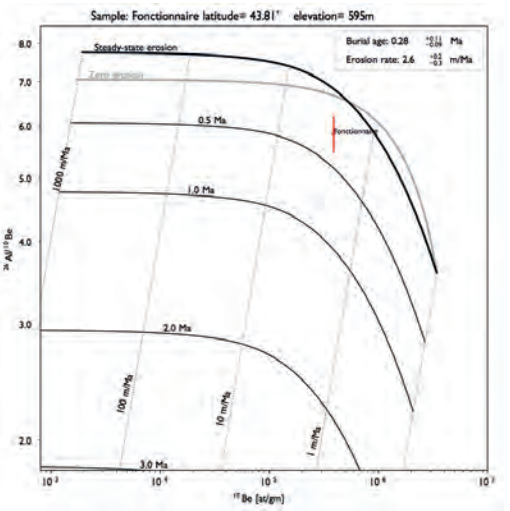

Figure 4: Scatter plot of isotope ratio $^{26}Al/^{10}Be$ versus ^{10}Be concentration for the Fonctionnaire sample commonly called "banana-plot".

Site	Lat. (°)	Lon. (°)	Alt. (m)	Depth (m)	^{10}Be (atm.g^{-1})	$\sigma^{10}Be$ (atm.g^{-1})	^{26}Al (atm.g^{-1})	$\sigma^{26}Al$ (atm.g^{-1})	Ratio $^{26}Al/^{10}Be$ (σ)	Burial age (Ma) (σ)
FONC	43.8054	3.4673	520	75	3.89E+05	9.80E+03	2.27E+06	8.79E+04	5.83 (0.37)	0.28 (0.1)

Figure 3: Concentrations and burial age of the Fonctionnaire sample. The altitude and the depth are given for the sample point of collection.

4. Discussions and conclusions

The results of this study confirm MALCLES et *al*. (2021) findings that the caves of the plateau are not directly linked with the regional base level and that sub-horizontal galleries of the area must be explained by other processes than the classical one linking cave horizontal level to the transient stability of the river beds. The burial ages of MACLES et *al*. (2021) combined with the new results presented in this study suggest that for the caves with entrances located on the plateau and sediments buried approximately at the same altitudes (555-570m for the Rocas and ~520m for the Fonctionnaire), the further away the cave is from the edge of the plateau the younger the burial ages are. This would mean that the speleogenesis of the plateau follows a regressive erosional pattern progressively opening shafts and galleries within the plateau. For the Rocas, clear evidences of ghost-rocks can be found. For the Fonctionnaire this has yet to be investigated but we will consider that the same processes are at play in our model. Based on the burial ages we can propose three steps (Fig. 4). The first one, the oldest, was before ~1 Ma, the lower part of the Rocas was not yet connected to the valley and still filled up with alterites. The surface drainage was active and burring quartz sediments from the St Maurice polje into the Rocas.

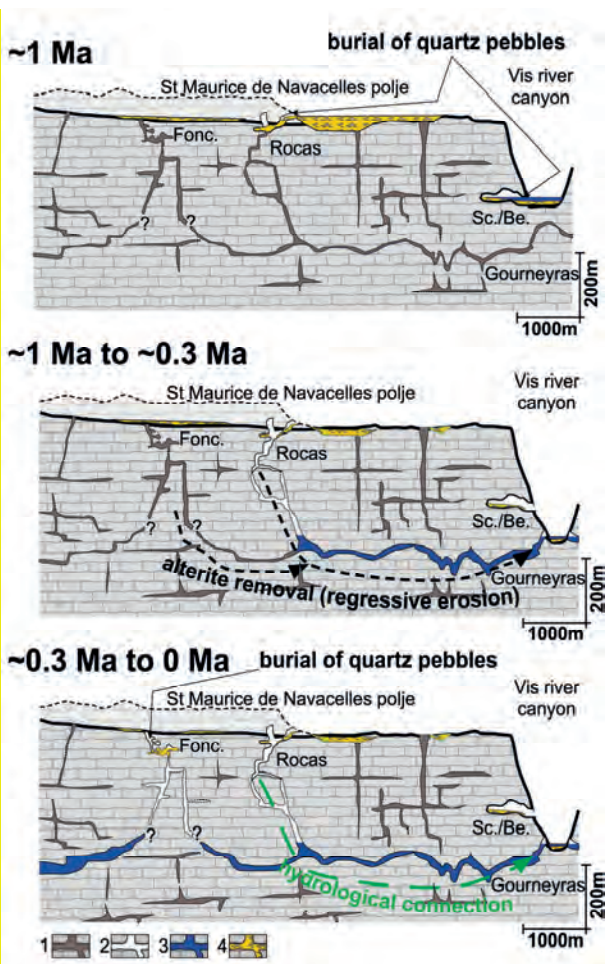

Figure 4: Speleogenesis model based on the burial ages obtained in the area of the St Maurice de Navacelles polje. The dashed ridge over the polje correspond to relief on the side of the polje. The speleogenesis of the area is related to alterite (ghost-rock) removal due to underground regressive erosion. 1. In-situ alterite, i.e. ghost-rock, indicating the primokarst; 2. Karstic network; 3. Active hydrological flow; 4. Allochtonous alluvial deposits. Fonc.: Fonctionnaire cave, Sc./Be.:Scorpions and Bergougnous caves.

Sometimes between 1Ma and 0.3Ma, the connection between the lower part of the Rocas and the Gourneyras karstic spring was established and the Rocas alterite was removed, the karstic network becoming active the surface drainages were fossilized. As the underground karstic erosion propagated further away from the plateau edges by regressive mechanical erosion of the alterite (see for example DUBOIS et *al*., 2014 for discussion of this process), new efficient karstic networks were formed and the surface sediments were transported in these networks. We propose that this is what occurred for the Fonctionnaire about 0.3Ma ago. When this occurred for the Fonctionnaire the drainage pattern around the cave must have been captured and mostly fossilized since the karstic network became efficient for underground water transport. One indicator of the efficiency of the underground water transfer is given by the occasional flooding events due to heavy rain. They occur in the areas located further away from the edges of the plateau where the younger karstic network is not well developed to transfer a large volume of water in a short time. More complex models could be proposed with captures of underground watershed between the Clamouse and the Gourneyras spring but with not enough constrains we choose to present the simplest model, knowing that new burial ages, dye tracing and underground observations will bring refinements to the overall understanding of the local speleogenesis.

Acknowledgments

We gratefully thank M. Magne for the access to the Rocas cave, Yann GUESSARD for the help in the underground sampling, Cyprien ASTOURY, Charles MIFSUD and Steve KOTEVSKI for the help during the sample processing.

References

CHILD D., ELLIOTT G., MIFSUD et *al*. (2000). Sample processing for earth science studies at ANTARES. *Nuclear Instruments and Methods in Physics Research, Section B: Beam Interactions with Materials and Atoms*, *172*(1–4), 856–860. https://doi.org/10.1016/S0168-583X(00)00198-1

DUBOIS C., QUINIF Y., BAELE J.-M. et *al*. (2014) - The process of ghost-rock karstification and its role in the formation of cave systems. *Earth Science Reviews*, 131, 116- 148. https://doi.org/10.1016/j.earscirev.2014.01.006

GRANGER D. E. KIRCHNER J.W. and FINKEL R.C. (1997) - Quaternary downcutting rate of the New River, Virginia, measured from differential decay of cosmogenic 26Al and 10Be in cave-deposited alluvium. *Geology*, 25, 107–110

MALCLES O., VERNANT P., CHERY J. et *al*. (2020) Determining the Plio-Quaternary uplift of the southern French Massif Central: a new insight for intraplate orogen dynamics. *Solid Earth*, 11(1), 241–258. https://doi.org/10.5194/se-11-241-2020

MALCLES O., VERNANT P., CHERY J. et *al*. (2020). Âges d'enfouissement, fantômes de roches et structuration karstique, cas de la vallée de la Vis (Sud de la France), *Géomorphologie : relief, processus, environnement*, 26(4), 255-264. https://doi.org/10.4000/geomorphologie.15043

NISHIIZUMI K., IMAMURA M., CAFFEE M.W. et *al*. (2007) Absolute calibration of 10Be AMS standards, *Nucl. Instrum. Meth*. B, 258, 403–413, 2007.

NURIT S. (1992) La montagne de la Séranne. Approche Spéléologique. *Explokarst* n°3. Bull. CLPA.

QUINIF Y. (2010). *Fantômes de Roche et Fantômisation — Essai sur un Nouveau Paradigme en Karstogenèse*. Karstol. Mém. 18.

QUINIF Y. et BRUXELLES L. (2011). L'altération de type « fantôme de roche » : processus, évolution et implications pour la karstification, *Géomorphologie : relief, processus, environnement*, 17(4), 349-358. https://doi.org/10.4000/geomorphologie.9555

RODET J. (1996). Une nouvelle organisation géométrique du drainage karstique des craies : le labyrinthe d'altération, l'exemple de la grotte de la Mansionnière (Bellou-sur- Huisne, Orne, France). *C. R. Acad. Sci*. III 322, 1039–1045.

WILCKEN K. M., FINK D., HOTCHKIS M. A. C. et *al*. (2017). Accelerator Mass Spectrometry on SIRIUS: New 6 MV spectrometer at ANSTO. *Nuclear Instruments and Methods in Physics Research*, Section B: Beam Interactions with Materials and Atoms, 406, 278–282. https://doi.org/10.1016/j.nimb.2017.01.003

Ghost-rock karstification in Gironde (France) Highlighting in quarries and drillings

Benjamin LANS[1,2], Richard MAIRE[3], Yves QUINIF[4] & Caroline DUBOIS[5]

(1) University of Pretoria – Depart. of Anthropology and Archaeology, Pretoria, South Africa, benjamin.lans@gmail.com
(2) Laboratoire TRACES, CNRS - Université Toulouse Jean Jaurès, Toulouse, France
(3) Laboratoire Passages, CNRS - Université Bordeaux Montaigne, France, richard.maire49@gmail.com
(4) Service de Géologie fondamentale et appliquée, Faculté Polytechnique de Mons, Belgium, yves.quinif2@gmail.com
(5) Haute Ecole Albert Jacquard, Namur, Belgium, caroline.dubois1987@gmail.com

Abstract

The alteration of the rupelian limestone in Gironde, by the process of ghost-rock karstification, was studied on the Entre-deux-Mers low plateau, into surface and underground quarries. Several types of morphologies were brought out: 1) *in situ* subhorizontal haloes; 2) subhorizontal recessing areas with vault pendants; 3) irregularly recessed weathered areas; 4) pseudoendokarst in the form of large multi-metric porches. Pleistocene palaeokarst exploiting ancient ghost-rock areas have also been identified. Some boreholes on the left bank of the Garonne River show a total loss during mud injection into the Rupelian limestone, between 15 and 35 m depth. Because of the induced decrease of the water table, pumping can lead to collapses. This highlighting of the phenomenon of ghost-rock karstification allows us to better understand the speleogenesis of the Gironde caves, either in non-phreatic zone (Entre-Deux-Mers) or in phreatic zone (porous reservoirs of the Graves area). Paleogeographic studies suggest that the alteration process first occurred during the platform's emersion at the end of the Rupelian, and probably in the Upper Miocene during the second emersion.

Résumé

Fantômisation des calcaires oligocènes en Gironde (SW France) - Mise en évidence dans les carrières et forages.
L'altération du calcaire rupélien de Gironde, de type « fantômisation », a été étudiée dans des carrières de surface et souterraines du bas-plateau de l'Entre-Deux-Mers. Plusieurs types de morphologies sont mis en évidence : 1) des auréoles subhorizontales en place ; 2) des zones subhorizontales en voie d'évidemment avec pendants de voûte ; 3) des zones altérées irrégulières ± évidées ; 4) des pseudoendokarsts en forme de grands porches plurimétriques. Des paléokarsts pléistocènes exploitant d'anciennes zones fantômisées ont aussi été identifiés. Certains forages en rive gauche de la Garonne montrent une perte d'injection dans le calcaire rupélien sur 15 à 35 m d'épaisseur. Cette mise en évidence du phénomène de fantômisation permet de mieux comprendre la spéléogenèse des cavités de la région, soit en zone dénoyée (Entre-Deux-Mers), soit en zone noyée (réservoirs poreux des Graves). A cause du rabattement de la nappe phréatique, les pompages peuvent induire des effondrements. L'étude paléogéographique suggère que la fantômisation s'est produite d'abord lors de l'émersion de la plate-forme à la fin du Rupélien et probablement au Miocène supérieur lors de la seconde émersion.

1. Introduction

Following discoveries made in Belgium (VERGARI, 1996; QUINIF, 2010), the phenomenon of ghost-rock in Gironde was first highlighted in an underground quarry of the Médoc (COURRÈGES, 1996; COURRÈGES & MAIRE, 2014). Other discoveries were subsequently made in the Entre-deux-Mers (LANS *et al.,* 2006; DUBOIS *et al.,* 2011). This phenomenon was better identified in the quarries of Frontenac and Jugazan. There are several types of morphologies: 1) the subhorizontal ghost-rock halo in place; 2) the subhorizontal altered areas being hollowed out, showing the weathered rock, an allogeneic laminated clay deposit, a summit void, and small arch pendants; 3) irregularly altered areas more or less hollowed out; 4) pseudo-endokarsts representing large multi-metric porches showing classical succession: ghost-rock, massive brown laminated clay, summit void and roof affected by domes and pendants. Moreover, Pleistocene palaeokarsts situated in ancient, altered areas have been identified in "Bernat" former quarry near Jugazan: some pockets of Pleistocene fauna and a gallery fossilized by sediments and speleothems, one of which was dated by U/Th.

2. Highlighting the ghost-rock alteration of Oligocene limestones in quarries

2.1 The phenomena of ghost-rock alteration in "Piquepoche" quarry (Frontenac)

The "Piquepoche" quarry is located in Frontenac, in the Entre-deux-Mers plateau. It was used to extract yellow and yellow-white limestone named locally "Calcaire à Astéries". This quarry shows several typical shapes.

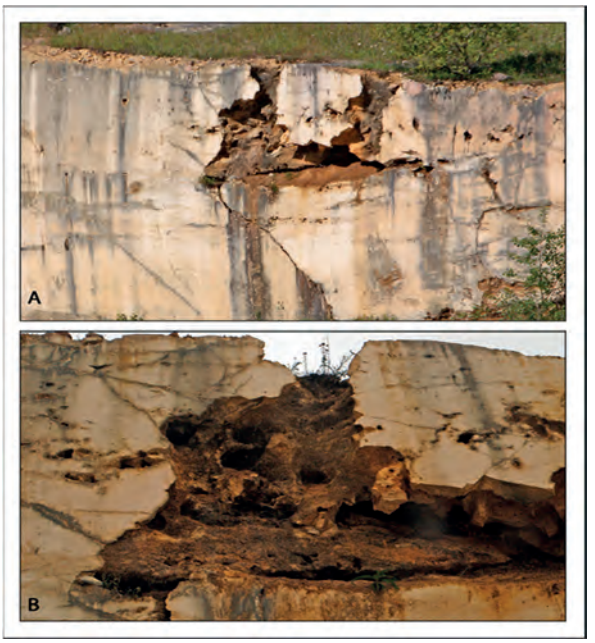

Figure 1: 3 m long cavity with very irregular morphology, related to the emptying of the alterite. A. Overview. B. Zoom on the cavity with typical vault pendants.

Subhorizontal ghost-rock not hollowed out

The faces show ghost-rock altered areas in the form of subhorizontal halos with irregular rounded contours. They are 10 to 30 m long by 1 to 2 m high and indicate an alteration without direct influence of lithology and joints. These morphologies can be observed in three dimensions thanks to the cuttings of the faces into perpendicular sections. We also observe vertical ghost-rocks, more or less hollowed out, sometimes intersecting the subhorizontal halos. The contours of the altered areas suggest that alteration ceased when the biochemical process stopped at the time of the uplift of the carbonated platform.

Subhorizontal or irregular ghost-rock hollowed out

There are many examples showing various forms of caves: irregular or rounded porches similar to classical caves.

Irregular caves with anastomosis

A typical example was observed in the form of an irregular cave; it is about 3 m wide by 2 m high and has a flared opening upwards. There are characteristic vault pendants related to the flushing of the alterite.

Corbelled levels

These are the most remarkable morphologies in terms of hollowing out of ghost-rock areas, which generally present, from bottom to top:

- a ghost-rock in place, infiltrated by green and brown clays
- a brown clay filling (20 - 30 cm thick) showing thin laminas attesting total decantation
- thin levels of reworked ghost-rock within brown clays
- a flat or corrugated roof.

This succession suggests a complex ancient evolution. Ghost-rock was partially evacuated and collapsed. Then the void was filled by green and brown clays.

Porches of pseudo-caves

These are major phenomena intersected by the exploitation of the quarry and similar to porches of classic caves. We observe here the presence of remarkable pseudo-endokarsts, in the form of galleries, whose interior is largely made up of rock altered in place, but whose top has been hollowed out and/or compacted.

The existence of green and brown clay deposits at the top of a compacted and/or partially emptied ghost-rock suggests a first stage of karstification with the existence of a cavity and a lacustrine type filling evoking two stages. The first supposes a frank emersion, the second evokes a return to submerged phreatic context with sedimentation of clay material from the external deposits. Examination of the sandy fraction makes it possible to specify the nature of the filling and its origin. Brown clay is of great interest because it is found in a generalized way in many clogged voids associated with ghosts-rocks. These are deposits of total settling corresponding to recurrent floods, carrying fine silts, clays, and a small sandy fraction. Locally we can observe coarser levels with micrograins of ghost-rock (calcite dust) transported by floods and/or the rise of the piezometric level.

2.2 The Middle Pleistocene palaeokarsts of "Bernat" quarry (Jugazan)

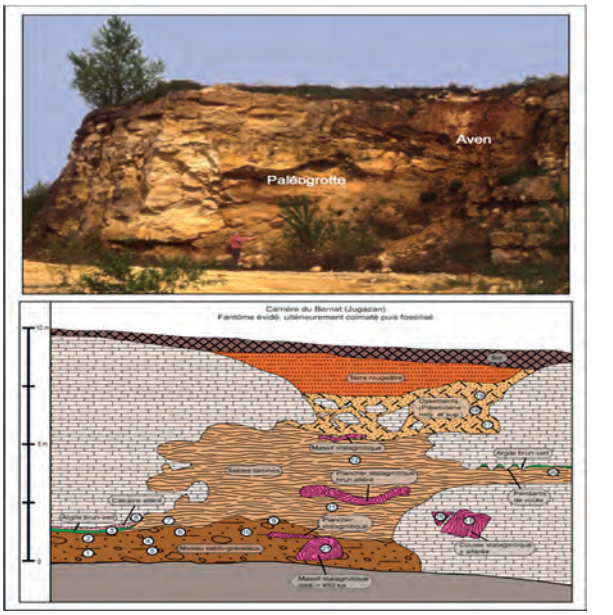

Figure 2: A. Fossilised palaeocave of the "Bernat" quarry (R. Maire). B. section with location of stratigraphic units and samples. The bottom is dated to more than 0.45 Ma per U/Th on a large stalagmitic massif.

The palaeokarst intersected by the ancient quarry of Jugazan is a fundamental milestone in the chronology of the caves of Gironde. It is indeed the only palaeocave, currently fossilised by sediments, which is dated at least to the Middle Pleistocene, first by the fauna studied in pockets located nearby (FERRIER and LEBLANC, 1990), then by U/Th dating. In addition, the analysis of surface states and parietal forms shows that it is an ancient ghost-rock later exploited by karstification. It is the incision of the adjacent valley

(Engranne) during the Pleistocene base-level rise that is responsible for the formation of the cave and its subsequent fossilisation by sediments. A stalagmitic sample was dated (B. Ghaleb, UQAM, Montréal). Micromorphological analysis shows a clean, not very porous calcite. Geochemical analyses in TIMS confirm the very low level of detrital thorium. As the U/Th ratio is at equilibrium, the calculation indicates an age greater than 450,000 years BP, which places the genesis of the cave probably at the beginning of the Middle Pleistocene or, even earlier.

3. Alteration of limestone on the Garonne left bank

3.1 Alteration observed in drillings

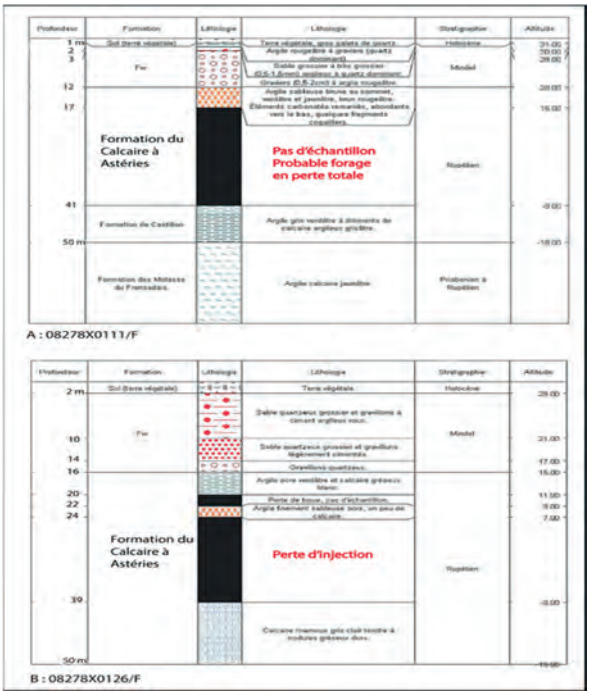

Figure 3: Drillings of Virelade area (BRGM - BSS, 2020). A: Arbanats, limestones altered significantly over 24 m thickness. B: Portets, very altered over 16 m thickness.

The drillings carried out on the left bank of the Garonne are of the utmost interest because they confirm field observations. The stratigraphic log of the Arbanats borehole (BRGM, log n°08278X0111/F) highlights a total drilling (BRGM, log n°08278X0126/F); the stratigraphic log loss of about 24 m thickness, attesting to the presence of a very porous limestone, with low mechanical cohesion and drowned by groundwater. The same applies to the Portets, indicating a loss of about 16 m thickness, still related to the very strong alteration of the "Calcaire à Astéries". Such mechanical fragility of these highly altered levels is favourable to the formation of large voids, 10 to 15 m high, such as that revealed by the Virelade collapse sinkhole. There is therefore an excellent concordance between field observations and drilling data.

3.2 Micromorphological analysis

Micromorphological analysis of altered limestone situated at the top of sinkholes reveals a high porosity. We thus observe many altered fossils and bioclasts presenting vacuoles at the level of round or elongated lodges. Inter-lodge micrite is also altered. Elsewhere, it is the sparitic calcite that is widely perforated. There is a strong contribution of the activity of sidero-bacteria, or even mangano-bacteria. There are also remarkable hematite microspherules (4 to 10 µm).

At the bottom of the sinkhole's level, micromorphological analysis of the altered limestone shows a bioclastic structure with many pores. The analysis highlights the importance and very irregular morphology of corrosion vacuoles in microsparite cement between bioclasts. The pores vary from 50-100 µm to 1 mm or more. The micritic calcite inside the microfossils is altered by the partial passage from ferrous iron to ferric iron.

4. Discussion

4.1 First dated signs of alteration: Rupelian

GAYET (1980) showed that an early emersion phase occurred before the end of the sedimentation of "Calcaire à Astéries". This period is attested by an altered carbonate layer that resembles a palaeokarst. It is only an alteration surface that does not penetrate the mass of the limestone due to too short a time to allow a first ghost-rock alteration. Then this karstified surface is sealed by a new carbonate sedimentation (thin layer).

4.2 Main phase of ghost-rock alteration: end of Rupelian

The study of the phenomenon of ghost-rock in surface and underground quarries makes it possible to propose a minimum age for the period of alteration of "Calcaire à Astéries". The condition for the ghost-rock process is the elevation of the water table: it must be located at a shallow depth so that there is no hydrodynamic potential, except for slow circulation of the aquifer linked to water loops essential to evacuate the dissolved $CaCO_3$. Stratigraphic and palaeogeographical studies make it possible to situate the main ghost-rock alteration phase at the period of emersion (end of Rupelian), thus before the detritic phase of the "Molasses de l'Agenais". It is a phase of slight emersion but long enough to erode-corrode the roof and penetrate the carbonate mass. The question of the role of the salt bevel is raised due to the proximity of the coastline and the stratiform altered morphologies.

4.3 Another phase of ghost-rock alteration: Miocene

The alteration of the limestones from the Lower Miocene of the Aquitanian is observed on residual mounds (Castelviel). The period of alteration is probably during the definitive emersion that occurred in the Late Miocene. Due to the long

duration of this period of low-altitude emersion (Mio-Pliocene), it is possible that the water table may have crossed the series of “Molasses de l’Agenais” to affect the underlying limestone during the Plio-Pleistocene uplift.

4.4 Genesis of the first caves: Early Pleistocene

The example of Bernat highlights an ancient caving phase related to the first base-level rise phase. The latter allows the appearance of a hydrodynamic potential and the emptying of the alterite and the genesis of the first caves. In addition to the U/Th dating, another chronological clue is provided by the origin of quartz gravel from the material of the high terrace of Sadirac dated from the Early Pleistocene The organisation of systems on the left bank of the Garonne allows the establishment of a first chronology. All the characteristics indicate a young karst system, without well-individualised conduits, but probably a network of voids in the form of "ancillary systems", separated by narrow stretches or very porous areas. The large collapse of Virelade shows there is a progression of karstification inwards. The presence of collapses around Virelade village shows that the downstream part is also subject to this type of karstification. There are two types of underground erosion: one from upstream to losses; the other coming from downstream by regressive erosion from a young outlet that may have changed due to the evolution of the base level.

4.5 Probable evolution since Late Pleistocene

The example of the Virelade system is more complex than the Entre-deux-Mers systems located in a free flow zone. The sinkhole-aven of Virelade shows the existence of large voids that can measure 20 to 30 m in diameter. This complexity of evolution must consider the evolution of the water-table level during the Pleistocene, especially since the Graves zone was raised allowing a flow of the aquifer to the north towards the Garonne.

It is also necessary to integrate the level of the water table during the last cold phases, especially during isotopic stages 6, 4 and 2. As seen on boreholes carried out in the axis of the Garonne, there is a clear ante-Holocene incision, with a deposit corresponding to the periods when the sea level was 100 m lower, causing a noticeable linear incision.

During the cold phases, it can be assumed that the underground flow emerged 10 m lower due to the lowering of the water table. Today these ancient emergences have been covered by Holocene alluvium. The karst formed at that time, in a cold context, functioned mainly during summer. In addition, it is possible that the pumping, responsible for a strong drop of the water table under the 0 NGF, drew the permanent reserves located in the partly karstified aquifer and generated during the cold phases.

5. Conclusion

The highlighting of the process of ghost-rock in the quarries of the Entre-deux-Mers is the essential condition for studying the speleogenesis of the actual caves of the region. The original and exceptional example of the fossilised palaeocave of Bernat has also made it possible to prove that cavities, probably equivalent to those we know today, were formed at least 500,000 years ago, or even well before. In the semi-karstic zone of Graves located on the left bank of the Garonne, the Virelade aquifer system is therefore like a karstic system in the process of formation in a drowned or even epiphreatic zone in the upstream part. These two examples differ in an opposite hydrodynamic context, one in the vadose phase, the other in the drowned phase, which supposes a theoretically faster evolution for the Entre-deux-Mers systems. However, the losses on the left bank compensate the weakness of the slope by a large volume absorbed during the floods. The lowering of the water table during the last glaciation is a direction of research to be explored further because this parameter played a more important role here than in the Entre-deux-Mers.

References

DUBOIS C. et al., 2011. Karstification de type fantômes de roche en Entre-deux-Mers (Gironde, France) : implications en karstogenèse et morphologie karstique. Karstologia 57, p. 19-27.

DUBOIS C. et al., 2014. The process of ghost-rock karstification and its role in the formation of cave systems. Earth-Science Reviews 131, pp. 116-148.

GAYET J., 1980. L’Ensemble des environnements oligocènes nord-aquitains : un modèle de plate-forme marine stable à sédimentation carbonatée. Thèse de Doctorat, Université Bordeaux 1, Talence, 571 p.

LANS B., 2014, Genèse des systèmes karstiques de Gironde (Entre-deux-mers et Graves) : rôle de la "fantômisation" et du potentiel hydrodynamique dans les calcaires oligocènes, crétacés et miocènes. Thèse de Doctorat, Université Bordeaux-Montaigne, Pessac, 346 p.

LEBLANC J.-C., FERRIER C., 1990. Le Bernat, un site paléontologique du Würm ancien en Gironde. Premiers résultats de l’étude géologique et karstique. Paléo 2 (2), p. 137-142.

QUINIF Y., 2010. Fantômes de roche et fantômisation - Essai sur un nouveau paradigme en karstogenèse, Karstologia-Mémoires 18, 196 p.

VERGARI A., 1998. Nouveau regard sur la spéléogenèse : le “pseudo-endokarst “ du Tournaisis (Hainaut, Belgique). Karstologia 31, p. 12-18.

Le karst de la région d'Orléans : quels processus et quels âges ?

Eglantine HUSSON, Gildas NOURY, Hélène TISSOUX, Alexis GUTIERREZ & Jérôme PERRIN

BRGM - 3 avenue Claude-Guillemin - BP 36009 - 45060 Orléans Cedex 2 - France
Corresponding author: e.husson@brgm.fr

Résumé

Le calcaire de Beauce est un calcaire lacustre d'âge aquitanien (Miocène inférieur), recouvert en grande partie de formations détritiques (sables plus ou moins argileux et lœss) et que l'on observe aujourd'hui localement à l'affleurement. Le calcaire de Beauce est karstifié, comme en attestent les circulations souterraines et les effondrements karstiques qui se produisent régulièrement dans le Val de Loire, mais l'origine de la karstification de l'Orléanais reste peu documentée. Les divers travaux effectués sur l'altération de ces calcaires en Beauce proposent une karstification en lien avec un contexte périglaciaire au cours des phases climatiques froides du Quaternaire. En effet de nombreuses formes de cryoclastie et de cryoturbation affectent le toit de ces carbonates, mais d'autres formes karstiques sont développées sous couverture perméable à semi-perméable, non karstifiable, constituée par les formations détritiques qui recouvrent le calcaire en Beauce. Ces morphologies témoignent du développement d'un karst sous couverture (cryptokarst). Nous proposons dans cet article d'illustrer ces morphologies développées sous couverture que nous tentons d'intégrer dans l'histoire de la karstification régionale, ainsi que de déterminer son rôle dans la structuration et le fonctionnement hydrogéologique du karst actuel.

Abstract

The Karst of Orléans region: which processes and which ages? The Beauce limestone is a lacustrine limestone of Aquitanian age (Lower Miocene), covered to a large extent by detrital formations (more or less clayey sands) that are now partially found at outcrop. The Beauce limestone is karstified as evidenced by rapid groundwater transit times and karst collapses that regularly occur in the Loire Valley, but the origin of the karstification of the Orléanais remains poorly documented. The various studies carried out on the weathering of these limestones in Beauce suggest karstification linked to periglacial context during cold climatic phases of the Quaternary. Indeed, many forms of cryoclasty and cryoturbation affect the roof of these carbonates. However, other karstic forms are developed under a permeable to semi-permeable non-karstifiable cover constituted by the detrital formations that cover the Beauce limestone. These morphologies indicate the development of an undercover karst (cryptokarst). We propose in this article to illustrate these morphologies developed under cover that we try to integrate into the history of regional karstification as well as to determine its role in the structuring and hydrogeological functioning of the present karst system.

1. Introduction

La région d'Orléans n'est pas réputée pour ses karsts. Pourtant il ne fait aucun doute que c'est une région karstique qui contient de nombreux exemples sous différentes formes. Les plus connues et les plus explicites se situent dans le Val de Loire en lien avec l'hydrodynamique du fleuve, comme les sources du Loiret (donnant accès à plusieurs km de conduits noyés) qui sont les résurgences de pertes situées dans la Loire. En revanche, sorti du Val, peu de sites sont reconnus comme présentant des évidences karstiques. On peut néanmoins citer la forêt d'Orléans qui abrite de nombreux gouffres (LORAIN, 1972 ; MOREAU, 2002) et des petites cavités (120 m de développement pour la plus grande) désobstruées par les spéléologues locaux. Le reste de la région est moins documenté, hormis par GIGOUT (1972) qui observe en Beauce et dans le Val, une forte altération du substratum calcaire de la région (par dissolution, par cryoclastie et par solifluxion) qu'il relie à une altération d'origine périglaciaire.

2. Contexte géologique

Le substratum rocheux régional est constitué par le calcaire de Beauce. Cette formation carbonatée s'est déposée au sein d'un environnement lacustre à dominance calcaire lors de l'Aquitanien, il y a 20 millions d'années environ. Il occupe une grande surface centrée sur Orléans (en jaune sur la Fig. 1). La cuvette formée par les formations lacustres est ensuite comblée progressivement par des apports détritiques fluviatiles provenant du Massif Central. Ces formations correspondent aux formations des sables et marnes de l'Orléanais, aux Sables et Argiles de Sologne (en violet sur la Fig. 1). Bien que très mal datée, un certain nombre de gisements de vertébrés permettent d'attribuer la base de la formation de l'Orléanais au Burdigalien (GINSBURG, 1990). Pour le reste des formations, elles sont attribuées à un âge « Burdigalien à plus récent » par défaut. À la fin du Miocène et au Pliocène, la compression alpine

entraîne une surrection à l'origine d'une période d'altération généralisée au sud du Bassin Parisien (WYNS, 2014). Au Quaternaire, les formations mio-pliocènes sont progressivement incisées lors de la mise en place des grands réseaux hydrographiques. Dans la région, le lit de la Loire atteint les calcaires de Beauce lors de l'avant dernier maximum glaciaire (GIGOUT et *al.*, 1972).

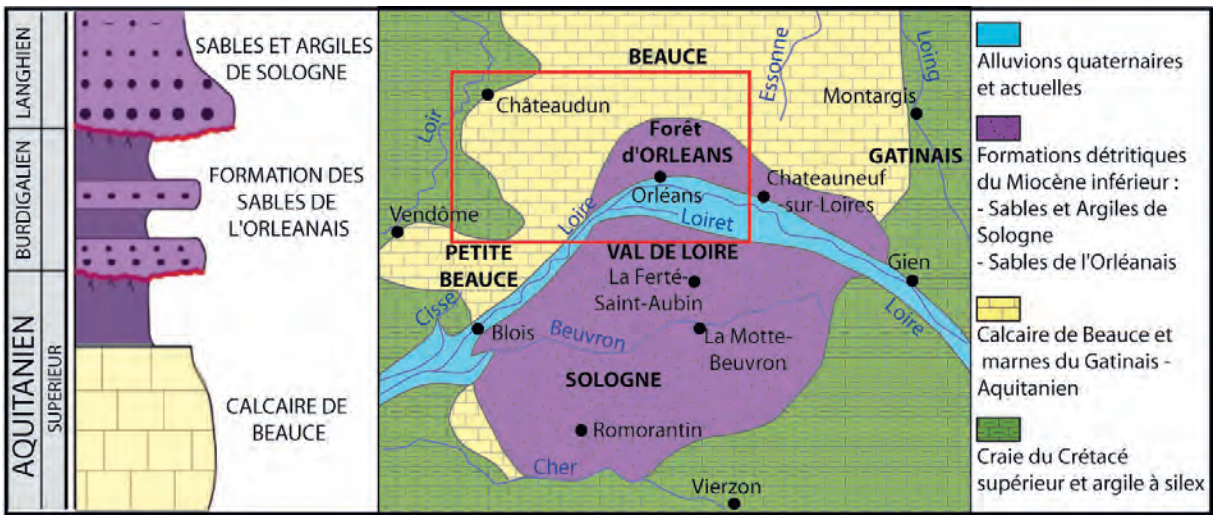

Figure 1 : Carte géologique simplifiée de la région du Val de Loire et log stratigraphique des formations miocènes affleurantes (modifié d'après Briais, 2015). Cadre rouge présentant la carte de la figure 2-A.

3. Les formes karstiques de la région d'Orléans

En Sologne - Le calcaire de Beauce se trouve recouvert par la Formation des Sables et Argiles de Sologne (SAS). Il est alors difficile d'observer le substratum calcaire sauf à l'occasion de travaux (routiers ou carrières) qui atteignent le toit, notamment dans la partie nord de la Sologne où l'épaisseur des SAS est encore relativement faible. On découvre alors une surface de contact très chaotique sous les sédiments détritiques qui le recouvrent (Fig. 2-G). Fréquemment, on trouve des argiles verdâtres ou brunâtres qui se développent au contact de l'encaissant carbonaté et des formations détritiques, qui sont des argiles de décalcification de l'encaissant calcaire (Fig. 2-G).

En Beauce - En Beauce le relief est très plat et les affleurements sont rares, les zones agricoles sont très importantes et les morphologies les plus visibles ont été modifiées ou rebouchées par l'Homme. Néanmoins, l'analyse du Modèle Numérique de Terrain (MNT) permet de déceler des indices de morphologies karstiques (Fig. 2-A). Tout d'abord, il montre parfaitement le tracé des vallons de la Conie amont, de la Retrève et du Nant, qui sont secs la majeure partie du temps, sauf en cas de très fortes pluies. Ces vallons sont des affluents du Loir qui s'écoule plus au nord-ouest (Fig. 2-A). Leur tracé est composé de nombreuses portions rectilignes qui relient des zones plus vastes déprimées, voire endoréiques (Fig. 2-A, C, D) et des dolines (Fig. 2-A, E). La confluence entre ces principaux vallons secs et leurs affluents se fait selon une géométrie orthogonale (Figure 2-A, B) et non par arborescence comme pour les cours d'eau classiques. Ces anomalies topographiques et hydrographiques se développent notamment dans la partie ouest, où le calcaire de Beauce est largement décapé de sa couverture détritique. Plus à l'est, lorsque le calcaire est sous recouvrement des sables de l'Orléanais, c'est au tour de cette couverture de se retrouver affectée par des dolines et soutirée dans les dépressions. Les exemples les plus flagrants se trouvent en forêt d'Orléans. Le couvert forestier et l'intervention modérée de l'Homme dans ce milieu permet de conserver et de préserver l'existence de ces formes de soutirage, dont certaines sont encore actives et jouent un rôle majeur dans l'absorption des eaux de ruissellement. En forêt d'Orléans, on trouve de nombreuses manifestations karstiques : des fontis, des « gouffres » (Fig. 2-A, F, H), quelques petites cavités en partie désobstruées par les spéléologues et des dolines qui poinçonnent le vallon de la Retrève et son bassin versant.

Dans le Val de Loire - Les circulations souterraines mises en évidence par traçages (Figure 2-A) ainsi que les nombreux effondrements associés qui s'y produisent (PERRIN et *al.*, 2017) attestent du caractère karstique du Val de Loire. La morphologie du Val de Loire tranche dans la topographie régionale. Les vallons affluents de la Loire sont mieux marqués qu'en Beauce en raison d'un dénivelé plus important et leur partie aval reste en eau toute l'année (Figure 2-A). Par endroits, la limite entre les bassins versants de la Loire et du Loir est estompée, affectée par des zones endoréiques de type ouvalas, créées par la coalescence de dolines (Figure 2-A, C).

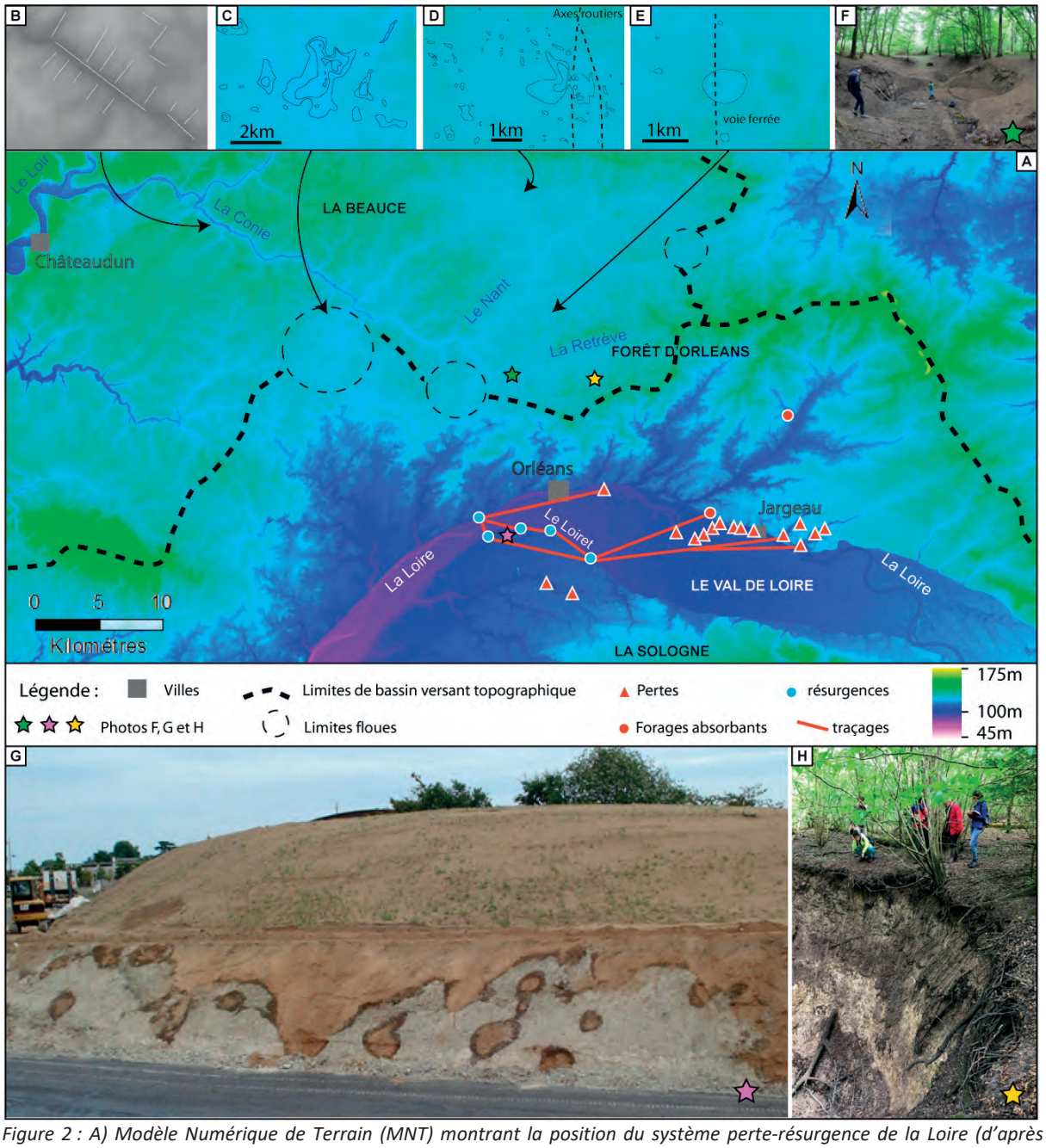

Figure 2 : A) Modèle Numérique de Terrain (MNT) montrant la position du système perte-résurgence de la Loire (d'après GUTIERREZ & BINET, 2010) au sein des bassins versants topographiques de la Loire (au sud), du Loir (au nord-ouest) et de l'Essonne (au nord-est ; affluent de la Seine). B) zoom sur le MNT et le tracé de la Conie montrant la morphologie des vallons secs en baïonnettes. C à E) zones endoréiques, dolines et mégadolines. F) Photo d'une doline sur un affluent de la Retrève en forêt d'Orléans. G) Photo d'une excavation à Olivet montrant la dissolution sous couverture du Calcaire de Beauce sous recouvrement des Sables et Argiles de Sologne (cliché : Ph. M. ISAMBER). H) Photo du gouffre « Jean Moreau » en forêt d'Orléans.

4. Discussion

Formes et processus. La karstification sous couverture, appelée aussi « cryptokarstification » est définie comme une dissolution du toit des calcaires sous une couverture sédimentaire perméable à semi-perméable (non karstifiable). L'interface présente des reliefs résiduels arrondis séparés de dépressions en entonnoir, et recouverts d'une frange superficielle de calcaire altéré et pulvérulent (GUENDON et *al.*, 1987). Les morphologies du toit des carbonates, décrites en Sologne (Fig 2-G) correspondent typiquement à cette définition. En Beauce, la karstification sous couverture est aussi à l'œuvre comme le montrent les nombreuses occurrences de dolines, ouvalas, fontis ou gouffres qui affectent la couverture détritique de surface. Dans les zones décapées de cette couverture (partie ouest

de la Beauce), la karstification se concentre le long de couloirs d'altération qui affectent le calcaire de Beauce. Ces axes rectilignes empruntés par les cours d'eau ainsi que les relations orthogonales avec leurs affluents sont caractéristiques de processus de dissolution qui pénètrent dans la masse du massif carbonaté.
Il convient de distinguer ces morphologies de karstification sous couverture des formes de cryoclastie, cryoturbation ou solifluxion produites par le gel/dégel. En effet, ces formes sous couverture ne sont pas nécessairement reliées à une altération d'origine périglaciaire (bien que cela ne soit pas exclu) mais la cryptokarstification est classiquement associée aux périodes d'altération, parfois même sous climat chaud.

Âge et mise en place du karst. Après le dépôt du calcaire de Beauce, celui-ci est enfoui sous les formations détritiques de l'Orléanais et de Sologne durant le début du Miocène. La karstification sous couverture pourrait commencer lors de l'altération provoquée par la surrection de la zone liée à la compression alpine au cours du Miocène supérieur (WYNS, 2014). La karstification sous couverture du calcaire de Beauce est en grande partie à l'origine de sa perméabilité qui permet aux eaux superficielles de s'infiltrer vers la nappe. Au cours du Pliocène et du Quaternaire, le potentiel hydraulique et la mise en place des premiers cours d'eau permettent d'éroder à leur aplomb la couverture détritique ; l'altération sous couverture se poursuit tant que le substratum calcaire n'est pas décapé. En parallèle, c'est la cryoclastie ou la solifluxion qui prend le relais dans les zones décapées ou sous faible recouvrement lors des périodes les plus froides. Lorsque l'incision de la Loire atteint les calcaires de Beauce lors de l'avant-dernier maximum glaciaire (GIGOUT, 1972), elle permet d'ouvrir une fenêtre hydrogéologique sur l'aquifère de Beauce. Depuis, la Loire est entrée en relation avec la nappe de Beauce qu'elle draine sur une partie de son cours. Dans les zones situées entre les plateaux et le val d'Orléans, l'incision a créé un gradient altitudinal et donc un potentiel hydraulique amont-aval. La Loire devient le nouveau niveau de base régional. Ce potentiel a permis de former les vallons et petits affluents en rive droite qui remontent en Beauce. Puis l'évacuation et la purge des couloirs d'altération ainsi que le soutirage de la couverture prend le relais avec la mise en place du drainage souterrain. Devenu prédominant, le soutirage karstique provoque le démantèlement du réseau hydrographique en surface. Actuellement, ce processus est visible au niveau de la ligne de partage des eaux et témoigne de la capture souterraine du bassin versant du Loir par la Loire.

5. Conclusions

Associée dans un premier temps aux morphologies périglaciaires, la karstification est souvent présentée dans la région comme un phénomène actif au Quaternaire. Or, la karstification régionale présente aussi des morphologies issues d'une altération sous couverture (cryptokarstification et fantômisation) qui ne sont pas nécessairement des morphologies typiques des périodes froides et dont la formation pourrait s'initier au Miocène supérieur, lors d'une première période d'altération. Cette karstification a été très peu étudiée et reste encore à explorer alors qu'elle semble conditionner, en grande partie, le fonctionnement karstique actuel.

Références

BRIAIS J. (2015) *Le Cénozoïque du bassin de Paris : un enregistrement sédimentaire haute résolution des déformations lithosphériques en régime de faible subsidence*. Thèse de doctorat, Rennes, 450 p.

GIGOUT M. (1972) L'altération périglaciaire du calcaire de Beauce. In : *Le calcaire de Beauce*. Compte rendu des journées d'études des 8 et 9 juin 1972 à Blois organisées par le Laboratoire central des Ponts et Chaussées et le Laboratoire régional de Blois, 54-59.

GIGOUT M., HOREMANS P. et RASPLUS L. (1972) Sur la géologie des environs d'Orléans. *Bull. BRGM*, section 1, n°1, 28 p.

GINSBURG L. (1990) The fauna and stratigraphical subdivisions of the Orleanian in the Loire Basin (France). In: Lindsay E., Fahlbusch V., Mein P. (eds), *European Mammal Neogene Chronology*, Plenum Press, New York, 157–176.

GUENDON J.-L., SALOMON J.-N. et NICOD J. (1987) Karstification sous couverture, comparaison entre karst tropical actuel et paléokarst. *Annales de géographie*, n°537, 557-563.

GUTIERREZ A. et BINET S. (2010) La Loire souterraine : circulations karstiques dans le Val d'Orléans. In : La Loire agent géologique, *Géosciences*, n°12, 42-53.

LORAIN J-M. (1972) Principe d'étude du réseau karstique de la forêt d'Orléans. In : *Le calcaire de Beauce*. Compte rendu des journées d'études des 8 et 9 juin 1972 à Blois organisées par le Laboratoire central des Ponts et Chaussées et le Laboratoire régional de Blois, 68-73.

MOREAU J. (2002). Les gouffres du nord d'Orléans. Groupe spéléologique orléanais, *Bulletin* n°7, 28 p.

PERRIN J., CARTANNAZ C., GILDAS N. and VANHOUDEUSDEN E. (2015). A multicriteria approach to karst subsidence hazard mapping supported by weights-of-evidence analysis. *Engineering Geology* 197, p 296–305.

WYNS R. (2014) Le Bassin parisien du Tertiaire à l'Actuel. In: Gély J.-P. & Hanot F. (Eds), *Le bassin de Paris, un nouveau regard sur la géologie*. AGBP, 85-93.

Le système karstique de la Touvre (Charente, France). Spéléogenèse par fantômisation

Grégory DANDURAND[(1)], Yves QUINIF[(2)], Richard MAIRE[(3)], Didier CAILHOL[(1)] & Laurent BRUXELLES[(4)]

(1) INRAP, UMR5608 - TRACES, CNRS - UT2J, Toulouse, France, gregory.dandurand@inrap.fr ; didier.cailhol@inrap.fr
(2) Université de Mons - Faculté Polytechnique - Service de Géologie Fondamentale et appliquée (UMONS - FPMS), yves.quinif2@gmail.com
(3) UMR5319 - Passages, CNRS - Université Bordeaux Montaigne, France, richard.maire49@gmail.com
(4) UMR5608 TRACES, CNRS - UT2J, Toulouse, France / School of Geography, Archaeology and Environmental Studies [Johannesburg, South Africa] laurent.bruxelles@inrap.fr

Résumé

Le système karstique de bas plateaux de La Rochefoucauld se caractérise par un fonctionnement en pertes/résurgences dont le principal exutoire est la Touvre, 2e émergence de France (débit moyen de 13 m^3/s). Les cavités, essentiellement développées subhorizontalement, forment des réseaux labyrinthiques. Malgré cela, les sources de la Touvre donnent accès à des puits noyés très profonds (>180m). Afin d'expliquer l'origine des cavités labyrinthiques associées à un unique exutoire de type vauclusien, plusieurs hypothèses ont été émises. Depuis 2010, des découvertes importantes en grottes et en carrières ont permis d'établir que la genèse des cavités du karst de La Rochefoucauld dépend de phénomènes de fantômisation épigènes dont de nombreux témoins ont été retrouvés. Mais les caractéristiques hydrogéologiques invitent ici à repenser le modèle de fantômisation à partir de la formation de boucles de convection thermo-hydrodynamique. Il faut alors aussi envisager une spéléogenèse de type fantômisation « hypogène » profonde dès l'origine, initiée par des boucles de convections bathyphréatiques au sein d'un puissant aquifère.

Abstract

The karstic system of La Rochefoucauld (Touvre, France): speleogenesis by phantomization (ghost-rock models). The "La Rochefoucauld" low plateau karstic system is characterized by a sinkhole/spring functioning whose main outlet is the Touvre springs, 2nd emergence in France (13 m^3/s). The caves, essentially developed sub-horizontally, form maze networks, but often presenting a little global development. In spite of this, the Touvre springs give access to very deep (>180m) submerged shafts. It must be insisted on the fact that, in this case, the ducts of the resurgence were formed in the deep karst. No marine regression can explain the phenomenon. In order to understand the origin of the maze caves associated with a single outlet constituted by a very deep shaft of emergence, various hypotheses have been put forward. Since 2010, important discoveries in caves and quarries have established that the genesis of the cavities of the La Rochefoucauld karst depends on epigenetic phantomization phenomena (ghost-rock) of which many witnesses have been found. But the hydrogeological characteristics here invite us to reconsider the ghost-rock model based on the formation of thermo-hydrodynamic convection loops. We must also consider a deep hypogenous ghostrock type speleogenesis from the beginning, initiated by bathyphreatic convection loops within a huge aquifer reservoir.

1. Introduction

L'origine des sources karstiques vauclusiennes est étudiée par de nombreux auteurs. Deux modèles explicatifs sont avancés : le karst barré et les oscillations eustatiques. Si pour le bassin méditerranéen, la régression marine messinienne avec un abaissement de l'ordre de 1 500 m est mise en avant pour expliquer la présence de conduits noyés profonds (≥150 m), il en est différemment pour le bassin atlantique dont le niveau marin n'a jamais connu une pareille chute (-125 m lors de dernière régression connue au pic du dernier âge glaciaire à - 20 000 ans). Un autre modèle de spéléogenèse est la formation de conduits profonds, de type thermo-hydrodynamique, issu de cellules de convection.

Afin d'expliquer la mise en place et les relations hydrauliques entre les cavités labyrinthiques de subsurface si particulières et l'unique exutoire constitué par un puits profond, plusieurs hypothèses sont émises : BIGOT (2009) évoque la possibilité d'une spéléogenèse épigène par engorgement des pertes, AUDRA *et al.* (2010) proposent une origine hypogène par remontée des eaux profondes, le long de grandes fractures qui s'enracinent dans le socle cristallin.

Depuis 2010, deux découvertes importantes permettent de montrer que d'autres phénomènes interviennent dans la genèse de ces cavités, comme la crypto-altération et la fantômisation. La vidange des fantômes par un processus hydraulique gravitaire (battement de nappe, perte) a été reconnue et analysée notamment dans la grotte de La Fuie (DANDURAND *et al.*, 2014). Par ailleurs, compte tenu d'un certain nombre de points communs entre l'aquifère du Hainaut et celui de la Touvre (épaisseur de la série

karstifiable, émergence profonde unique, vaste bassin d'alimentation, tectonique en distension), l'hypothèse d'une karstification profonde, générée sous forme de fantômisation grâce à l'établissement de circulations bathyphréatiques engendrées par cellules de convection thermique au sein de l'aquifère, pourrait expliquer l'origine et l'évolution de cet énorme puits noyé (DANDURAND *et al.*, 2019).

2. Matériels et méthodes

Les observations de terrain se sont concentrées sur l'étude de la relation entre altération de la masse carbonatée et formation des grottes. Trois carrières ont d'abord été étudiées : Combe Brune, Artenac, Peusec. Le choix des sites a été déterminé en fonction de leur répartition dans le bassin karstique de la Touvre (Fig. 1). L'étude systématique des forages réalisés par le BRGM et des carottages réalisés par le Centre d'étude Technique de Bordeaux nous a fourni une importante base de données. Une dizaine de cavités a été prospectée, dont deux ont fait l'objet de relevés morpho-sédimentaires et d'analyses pétrographiques et sédimentologiques plus précises : la grotte du Bois du Clos et celle de La Fuie, cette dernière étant prise comme exemple dans cet article. Ces observations ont été complétées par diverses analyses de laboratoire comprenant des analyses de densité, de minéralogie des éléments lourds et des argiles et de micromorphologie. Enfin, la découverte, l'exploration et le monitoring de la grotte de La Fuie ont permis l'étude des fluctuations de la nappe enregistrées par un « luirographe » (MOREL, 1996).

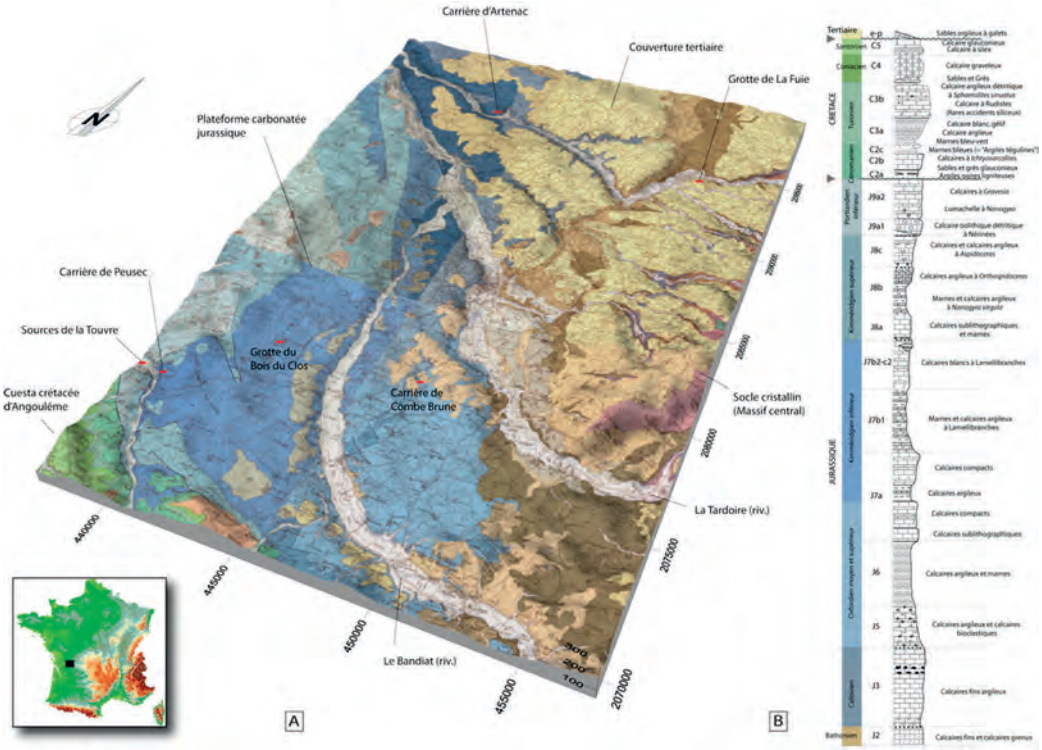

Figure 1 : (A) Diagramme 3D montrant les contextes géologique et géomorphologique du secteur karstique de La Rochefoucauld. (B) Colonne lithostratigraphique. Les deux flèches grises indiquent les principales discordances durant lesquelles la fantômisation a pu s'opérer.

3. Résultats

3.1 Les caractéristiques de l'altération

L'observation des fronts de taille révèle un profil d'altération qui progresse le long des joints stratigraphiques et des fractures et qui recoupe les différents faciès de dépôt jurassique. Le front d'altération se marque également par la formation d'anneaux de Liesegang qui sont généralement développés dans un contexte vadose avec les processus d'oxydoréduction. Nous remarquons aussi que les couloirs d'altération sont souvent associés à des brèches d'effondrement collatérales en lien avec la réactivation du fantôme de roche (Fig. 2). Les résultats des analyses de densité réalisées sur 12 échantillons prélevés en carrières donnent des pertes de 30 à 40 % (densité < 2 g/cm^3) par rapport à la roche-mère saine (densité 2,68 g/cm^3). Les résultats des échantillons prélevés en grottes donnent des pertes de 25 à 30 %. L'analyse pétrophysique montre un gradient depuis la roche complètement altérée au centre du phénomène à une roche très peu atteinte aux parois des galeries ou des épontes des couloirs (porosité 15 %). L'étude microscopique en lames minces d'échantillons prélevés dans les trois carrières et dans les cavités montre des similitudes micromorphologiques. La porosité résulte d'une attaque de structures microsparitiques inter-oolites qui progresse également dans les oolites micritiques. L'origine

de cette attaque est peut-être liée à des bactéries chimiolithotrophes, représentées par des amas de ferro-bactéries, qui utilisent les minéraux de la roche pour leur énergie.

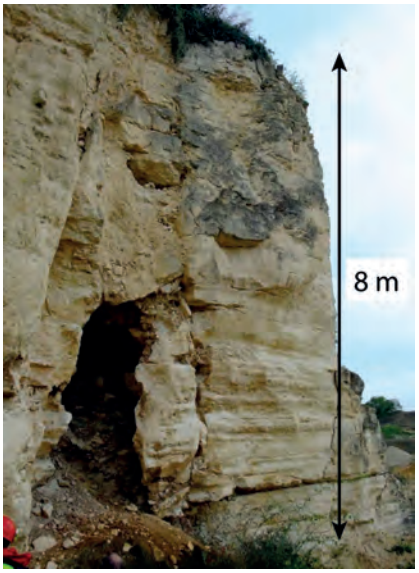

Figure 2 : Grotte recoupée par la carrière de Peusec. Notez le lien entre le fantôme à l'intérieur du couloir vertical, la fracture dans le calcaire jurassique et la brèche d'effondrement (photo : B. Losson, 18 septembre 2011).

Mais l'altérite n'est pas partout conservée. En effet, certains conduits karstiques reconnus à Peusec notamment ne contiennent plus de fantômes de roche. Ils sont remplis par des dépôts variés, attribués au Cénomanien inférieur (ROUILLER, 1987). Ces formations sont venues se substituer aux altérites résiduelles dès le début de la transgression du Crétacé supérieur.

3.2. Un fonctionnement karstique complexe

Les forages profonds révèlent l'existence de vides recoupés à -210 m NGF à Brie, à -282 m NGF à Chamarande, à -183 m NGF à Bouex et à -155 m NGF à La Rochefoucauld (BICHOT *et al.*, 2003). Ainsi, à l'instar des conduits explorés en plongée aux sources de la Touvre (>180 m), ils attestent de l'existence de drains qui indiquent une karstification en profondeur très évoluée.
Parallèlement, les résultats fournis par l'enregistrement continu du « luirographe » dans la grotte de La Fuie vont dans le sens d'un réservoir très capacitif. La dynamique hydrologique se caractérise par des battements saisonniers du niveau épinoyé de plusieurs mètres. Ces résultats confortent l'étude hydrogéologique des sources de la Touvre (LAROCQUE, 1997). Ainsi le développement de zones transmissives à grande profondeur n'interdit pas des circulations plus lentes probablement à travers les couloirs d'altérites poreuses. En effet, plusieurs de ces forages ont recoupé des conduits karstiques plus ou moins colmatés par des dépôts argilo-sableux. Les carottages réalisés sous la couverture tertiaire argileuse à cherts dans le secteur où s'ouvre la grotte de La Fuie, ont traversé des couloirs altérés entre 11 et 18 m de profondeur, niveau auquel la grotte de La Fuie a été recoupée.

L'essentiel de la porosité de l'aquifère serait constitué de fantômes de roche encore en place, l'altérite résiduelle étant suffisamment poreuse pour laisser circuler l'eau.

4. Discussions

Certaines grottes présentes dans le karst de La Rochefoucauld dériveraient de la vidange partielle de l'altérite résiduelle. La couverture tertiaire a joué un rôle important dans la crypto-corrosion et la conservation des fantômes de roche en place. Le recul de la couverture tertiaire par érosion régressive, qui a été provoquée par l'encaissement du réseau hydrographique durant le Quaternaire, expliquerait la formation de certaines cavités situées en bordure occidentale du bassin karstique. La grotte de La Fuie (Fig. 3), dans la partie amont du système, a permis de démontrer son origine et son évolution (DANDURAND *et al.*, 2014). À partir d'un pseudo-endokarst, situé à quelques dizaines de mètres sous la surface, certains corridors recoupés par le versant ou positionnés dans la zone épiphréatique se seraient vidés partiellement de leur altérite résiduelle par les battements de la nappe aquifère.
Mais la comparaison de l'aquifère de la Touvre avec d'autres aquifères géothermiques suggère que l'initiation de la karstogenèse pourrait être également due à la géothermie, comme le suggèrent AUDRA *et al.* (2010). La différence de température existant entre le mur et le toit de l'aquifère permettrait la formation de boucles de convection thermo-hydrodynamique. Cette circulation lente, durant plusieurs millions d'années (notamment durant l'émersion du Crétacé inférieur pendant 52 Ma), a pu karstifier l'aquifère lors de phases de tectonique en extension, permettant une circulation privilégiée par certaines familles de fissures, reconnues notamment au niveau de la Touvre.
Ainsi deux types de fantômisation sont distingués associés chacun à deux phases géologiques successives. Le premier type de fantômisation correspond à une fantômisation de type épigène, attesté à la grotte de La Fuie, dont l'origine est en lien avec des phénomènes de crypto-corrosion sous la couverture tertiaire et dont les produits d'altération ont été dégagés par recul de cette même couverture. Ce type d'altération suppose des conditions particulières biostasiques (faible potentiel hydrodynamique, peu de relief, abondante et dense couverture végétale).

Le second type de fantômisation correspond à un modèle « hypogène ». Ces circulations profondes peuvent être liées soit à des boucles de convections thermiques profondes dans l'aquifère, du même type que dans le Hainaut, ou bien des remontées de fluides le long des failles profondément enracinées dans le socle cristallin, ou encore des expulsions latérales des fluides en périphérie du bassin sédimentaire sous des contraintes de surcharge sédimentaire et tectoniques.

Figure 3 : Haut niveau de nappe dans la grotte de La Fuie (photo : D. Doucet, 23 mars 2007)

Si l'on replace ces deux types de spéléogenèse dans l'histoire géologique du Bassin aquitain, on identifie deux périodes. D'abord, entre la fin du Kimméridgien (152 Ma) et le début du Cénomanien (100 Ma), la plate-forme était faiblement émergée et le gradient hydraulique quasi inexistant. Ensuite, après l'émersion fini-crétacée, la plate-forme a évolué sous la formation d'une épaisse couverture détritique continentale.
Ces deux phases d'émersion sont à l'origine de divers phénomènes de fantômisation. La phase de transgression et de sédimentation des calcaires argileux du Crétacé supérieur pourrait avoir favorisé la mise en place de cellules de convection thermique profondes dans la zone saturée. La régression fini-crétacée et l'émersion au Tertiaire, quant à elles, laissent place à une longue période continentale, qui est marquée par la formation d'un épais manteau d'altérites. Compte tenu du contexte d'évolution biostasique sous climat tropical humide, les conditions sont alors réunies pour permettre une lente et profonde altération biochimique de la roche, depuis la surface, suivant les principales fractures en distension.
Enfin, la dernière étape de karstification se manifeste par l'érosion de cette couverture à partir de l'incision du réseau hydrographique, combinée à la surrection plio-quaternaire du Massif central. L'infiltration des eaux de surface, rendue possible par le décapage de cette couverture, a permis l'apparition d'un potentiel hydraulique et une augmentation des circulations, favorisant le tassement et/ou l'érosion mécanique des altérites souterraines. La spéléogenèse proprement dite (formation des grottes pénétrables) se produit par érosion mécanique de l'altérite. Les vastes conduits noyés de la Touvre résulteraient alors de l'érosion mécanique régressive de l'altérite résiduelle depuis les émergences - là où la concentration des écoulements conduit à une énergie hydrodynamique importante - vers les pertes en amont, situées principalement dans les vallées du Bandiat et de la Tardoire. Le tassement de l'altérite résiduelle se poursuit en périphérie du bassin karstique par les fluctuations de la surface piézométrique (modèle de la grotte de La Fuie).

5. Conclusion

Le rôle de deux types de fantômisation, épi- et hypogène, pendant deux longues phases d'émersion de la plateforme carbonatée jurassique du Bassin aquitain a été mis en évidence par l'étude de trois carrières, de forages et de la grotte de La Fuie. Les examens morphologiques de surface et les analyses microscopiques ont précisé les processus d'altération et leur relation avec la karstogenèse. Ces deux modèles de fantômisation expliquent à la fois la genèse de grottes labyrinthiques et aussi la complexité du fonctionnement de l'aquifère de la Touvre qui approvisionne la ville d'Angoulême. Le modèle de cellule de convection thermique invite à repenser le fonctionnement des réservoirs et l'évolution des puits noyés très profonds, lorsque leur origine ne trouve aucune autre explication tectonique ou eustatique satisfaisante.

Références

AUDRA P., NOBÉCOURT J.-C. and BIGOT J.-Y. (2010) Hypogenic caves in France. Speleogenesis and morphology of the cave systems. *Bull. de la Soc. Géol. de France*, 181(4), p. 327-335.

BIGOT J.-Y. (2009) Les grottes-labyrinthes du karst de La Rochefoucauld (Charente). *Actes de la 19e Rencontre d'Octobre*, Saint-Laurent-en-Royans, p. 29-34.

BICHOT F., KARNAY G. et LAVIE J. (2003) *Les sources de La Touvre – Synthèse des Connaissances*. Rapport BRGM RP-52738-FR, 54 p.

DANDURAND G., MAIRE R., DUBOIS C. and QUINIF Y. (2014) The Charente karst basin of the Touvre: alteration of the Jurassic series and speleogenesis by ghost-rock process. *Geologica Belgica*, 17, p. 27-32.

DANDURAND G., QUINIF Y., GUENDON J.-L. et GRUNEISEN A. (2019) Sources vauclusiennes et fantômes de roche. *Karstologia*, 74, p. 31-46.

LAROCQUE M. (1997) *Intégration d'approches quantitatives de caractérisation et de simulation des aquifères calcaires fissurés. Application à l'aquifère karstique de La Rochefoucauld (Charente, France)*. Thèse, Univ. Poitiers, 247 p.

MOREL L. (1996) Le Luirographe : étude de la crue du 22 avril 1995. *Karstologia*, 27, p. 20-26.

ROUILLER D. (1987) *Étude des systèmes karstiques de la Touvre et de la Lèche (Angoulême, Charente). Géologie, hydrodynamique, hydrochimie*. Thèse de 3e cycle, Fac. Sc. Avignon, 263 p.

Le primokarst de la Mansonnière (Perche, France)

Joël RODET[(1)], Anne-Véronique WALTER-SIMONNET[(2)] & Stéphane CHEDEVILLE[(3)]

(1) Centre Normand d'Etude du Karst (CNEK) & UMR 6143 M2C CNRS, Université de Rouen-Normandie, bât. Blondel, place Emile Blondel, 76821 Mont Saint Aignan, France, joel.rodet@univ-rouen.fr (corresponding author)
(2) UMR CNRS 6249 Chrono-environnement, Université de Bourgogne Franche-Comté, Besançon, France, Anne-Veronique.Walter@univ-fcomte.fr
(3) Centre Normand d'Etude du Karst (CNEK) & Communauté Urbaine Le Havre Seine Métropole, 630 Allée de la Ferme Debray,76133 Rolleville, France, stephane.chedeville@lehavremetro.fr

Résumé

La craie cénomanienne du Perche offre des développements spectaculaires des phases primokarstiques, révélés dans les années 1990. En particulier, le site de La Mansonnière, le premier décrit dans la littérature scientifique, a révélé près de 3 km linéaires d'axes altérés dans l'encaissant crayeux, dégageant un labyrinthe en mailles entièrement dépendant du réseau tectonique local. Plus de 1000 m de ces vides ont été parcourus spéléologiquement, grâce à un chantier spectaculaire de désobstruction. Les études sédimentologiques montrent une organisation subverticale des éléments meubles ou altérites et un apport de l'ancienne couverture. Les mesures de perméabilité révèlent l'état d'altération de l'encaissant. L'ensemble de ces mesures et observations permet de définir un processus de spéléogenèse original, illustrant plusieurs stades de pré-karstification depuis la fissure originelle jusqu'à l'introduction concentrée, regroupés sous le vocable de "primokarst". Largement observé depuis dans les cavités autour du monde, notamment dans les quartzites du Brésil, le concept a été diffusé comme paradigme de "squelette de roche" ou de "fantôme de roche". Malheureusement, par décision unilatérale des édiles locaux, ce site unique est interdit d'accès et, par conséquence, d'étude depuis 2018. Il est donc urgent d'obtenir un statut de protection au titre de site patrimonial exceptionnel.

Abstract

The Mansonnière Cave Primokarst (Perche, France). The Cenomanian chalk in the Perche region contains spectacular developments of prekarst stages, revealed in the 90s. In particular, the Mansonnière site, the first described in the scientific production, presents nearly 3 km long of weathered axis into the chalky substratum, showing a mesh network entirely dependent of the joint network. Over 1 km of theses voids was explored by speleologists thanks to a spectacular clearing work. Sedimentological studies show a subvertical distribution of the soft elements or regolith and a small contribution of the weathering cover. Permeability measurements reveal the state of alteration of the surrounding area. All of these measurements and observations allow us to define an original process of speleogenesis, illustrating several stages of pre-karstification from the original fissure to the concentrated introduction, grouped under the word of "primokarst". Since then, this concept has been widely observed in cavities around the world, especially in the quartzites of Brazil, and was disseminated as the paradigm of "rock skeleton" or "ghost-rock". Unfortunately, by unilateral decision of the local councilors in 2018, access and, consequently, study to this unique site have been prohibited. It is therefore urgent to obtain protection status as an exceptional heritage site.

1. Introduction

Dans la partie méridionale du Perche, région de rupture géomorphologique et géologique au sud de la Normandie, de nombreuses carrières souterraines ont été creusées dans les craies du Cénomanien inférieur et moyen, et constituent autant de sites d'observation de vides naturels recoupés, à l'image de la Mansonnière, à Bellou-sur-Huisne (Fig. 1). Ce site exploré spéléologiquement de 1993 à 1998, a livré plus de 1000 m de boyau naturel, humainement pénétrable après d'importants travaux de désobstruction. Le réseau se développe vers 143 m d'altitude, sous une épaisseur de craie de l'ordre de 5 à 8 m (RODET, 2004).

Ce qui frappe à l'examen du plan du réseau naturel est son aspect labyrinthique (Fig. 2). En effet le réseau de la Mansonnière est constitué d'axes orientés E-W, en fait des petits décrochements dextres inclinés, espacés de 3 à 5 m.

Figure 1 : Galeries du primokarst recoupées par la carrière souterraine de La Mansonnière.

Cette première orientation, la plus ancienne, est complétée par une fissuration secondaire, plus récente, généralement verticale, dont l'orientation varie de N-S à NW-SE. Son extension est limitée par les axes E-W qu'elle ne traverse jamais. C'est sur cette deuxième famille que s'organise la "galerie de la Cheminée", véritable colonne vertébrale du réseau spéléologique actuellement connu.

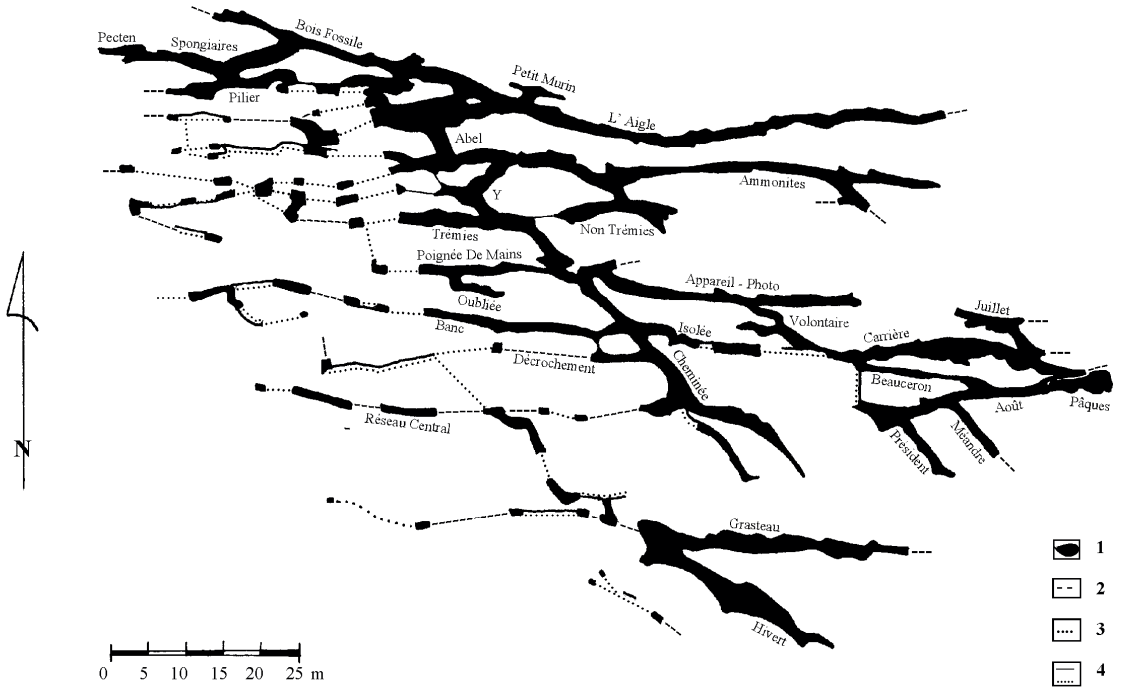

Figure 2 : Réseau principal de La Mansonnière, représentant plus d'un kilomètre de galeries. 1- galerie explorée, 2- galerie recoupée par la carrière, 3- galerie non explorée (étroite ou pleine), 4- paroi de galerie dans la carrière.

2. Définition du primokarst

Le réseau souterrain de la Mansonnière est surprenant à plus d'un titre. La première spécificité est illustrée par la densité exceptionnelle du réseau de conduits explorés (Fig. 2). Dans le secteur nord, l'emprise des vides peut atteindre 20 % de la surface concernée (RODET, 1999).

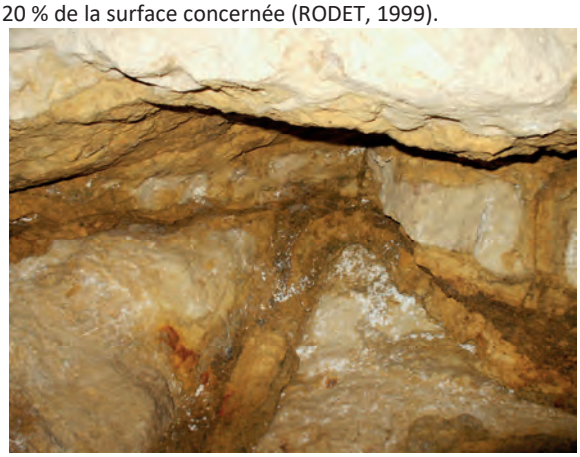

Figure 3 : Réseau tectonique altéré de La Mansonnière

Deuxième point, pas un mètre du millier exploré n'échappe à l'influence directe de la fissuration (Fig. 3).

La troisième surprise vient de l'extrême variabilité de section des conduits explorés qui peuvent passer sur une faible distance, de plusieurs mètres de largeur (jusqu'à 6 m dans la galerie Hivert), à quelques centimètres seulement.

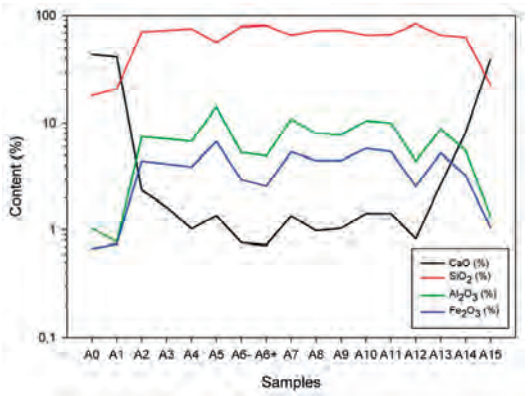

Figure 4 : Profils géochimiques d'une section de galerie, montrant la chute en % du CaO entre les deux parois (A0 et A15), et en conséquence l'augmentation des autres critères.

La quatrième interrogation vient de la stratigraphie sub-verticale des comblements, normalement sub-horizontale dans un conduit drainé (Fig. 4). Il s'agit donc, non pas de comblements karstiques apportés par un quelconque ruisseau souterrain, mais du produit de l'altération en place de l'encaissant le long des accidents tectoniques.

Des mesures de perméabilité ont été réalisées sur plusieurs sections du réseau primokarstique avec un appareil Tiny PermII de chez New England Research (NER). En particulier, sur le porche n° 8 (Fig. 5), les mesures font apparaître une perméabilité croissante depuis la roche encadrante jusque

vers le cœur de la veine où la perméabilité se réduit fortement dans les argiles noires.

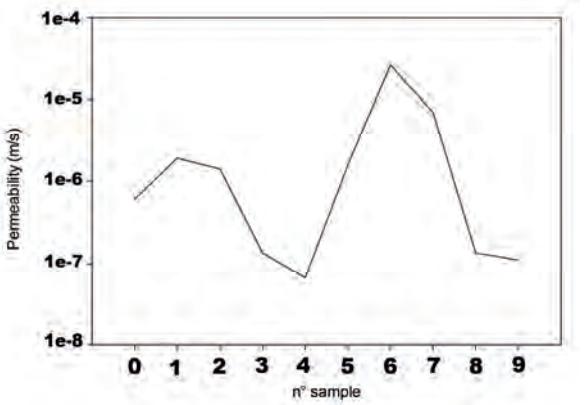

Figure 5 : Répartition des mesures de perméabilité réalisées dans le porche n° 8 de La Mansonnière. Les points 0 et 1, 8 et 9 sont dans l'encaissant, 4 dans les argiles noires (smectites), les autres points de mesure dans l'isaltérite.

Ces mesures montrent que ces argiles sont des allotérites compactées donc avec des vides très réduits, alors qu'entre celles-ci et l'encaissant, il s'agit d'isaltérites de la craie, plus ou moins évoluées et donc avec une croissance des vides allant jusqu'à la rupture mécanique et le tassement.

3. Schéma évolutif du primokarst

Tant les analyses géochimiques que les mesures de perméabilité démontrent la dimension altéritique des formations meubles. Dans les secteurs les plus évolués, des produits, eau ou éléments chimiques, ont été introduits depuis la surface, alors que dans les fissures les moins évoluées, on observe essentiellement des éléments autochtones. Cela permet de proposer un schéma évolutif en quatre temps, passant de l'altération initiale à l'ouverture d'une grotte spéléologique (RODET, 2014).

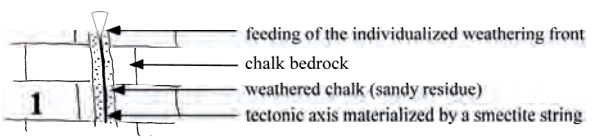

First stage : weathering of a (tectonic) axis

- stade 1 : Au travers de la couverture ou lors de son ablation, l'altération s'introduit dans le massif, en s'installant sur le maillage tectonique et rejoint un niveau de base qui peut être identifié comme un niveau induré ou le paléo-toit de la nappe de la craie.

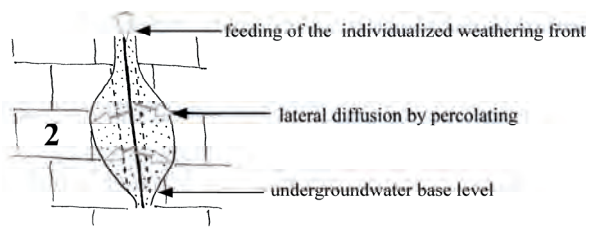

Second stage : local enlargement of the (tectonic) axis

- **stade 2** : À partir du niveau de base, l'altération se diffuse latéralement aux fissures, élargissant ces dernières. L'encaissant se transforme en altérites iso-volumétriques ou isaltérites.

En conséquence, les galeries souterraines pénétrables de la Mansonnière ne sont pas des conduits ou des drains dans le sens karstologique du terme, dans la mesure où ces développements n'ont jamais concentré d'écoulements d'eau. Il s'agit en fait d'axes tectoniques élargis par diffusion latérale dans une craie poreuse, à partir d'un accident au sommet d'un obstacle à la percolation verticale. Cet obstacle est le développement d'un aquifère dû soit à la fermeture des accidents par pression de la charge lithologique (épaisseur de roche au-dessus), soit à un niveau stratigraphique imperméable (hard-ground ou niveau induré), soit encore au niveau de base hydrologique régional illustrée par le réseau hydrographique. L'eau, ne pouvant plus descendre, s'épand latéralement en profitant des hétérogénéités de la roche encaissante. La vitesse est très réduite et le mélange intime entre l'eau et la roche autorise des échanges chimiques qui peu à peu vont dissoudre les bicarbonates. L'absence d'aval ouvert et de vitesse de l'écoulement n'autorise pas l'évacuation des éléments non dissous qui restent en place sous forme d'un squelette ou isaltérite, jusqu'à ce que le seuil de résistance mécanique soit dépassé, entraînant l'effondrement du squelette et la formation d'un vide (RODET, 2017). Ce squelette ou allotérite, est parfois appelé "fantôme de roche" (DUBOIS et *al*., 2014).

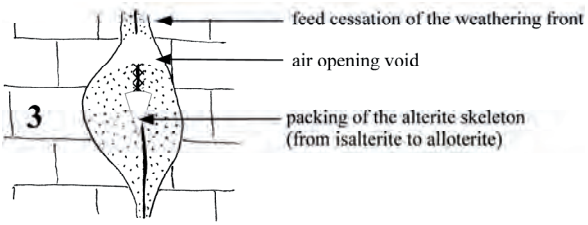

Third stage : breakdown of the weathering complex and air opening

- **stade 3** : L'altération se poursuit et entraîne la rupture mécanique de l'isaltérite qui se tasse par rupture mécanique du squelette de roche, libérant une lunule aérée au sommet de l'allotérite (fig. 6).

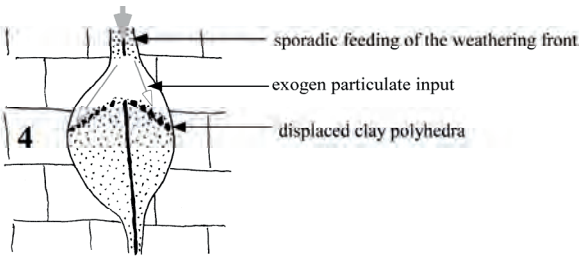

Fourth stage : first introduction of a karstic flow

- **stade 4** : L'évolution se poursuit et l'introduction possible d'eau de la surface, sous une forme concentrée, initie une potentielle évolution en drainage karstique. Des polyèdres argileux bousculés prouvent alors une circulation rapide tandis que des éléments de la surface peuvent être introduits. Les vides libérés peuvent être éventuellement pénétrables à l'homme.

4. Conclusions

Figure 6 : Galerie avec ses allotérites tassées dégageant une lunule aérée. Le crayon donne l'échelle.

Cet ensemble de données a permis de définir un cas spécifique de karst, que nous avons appelé "primokarst" (RODET, 1996 et 1997), à savoir une toute première phase de karstification, celle du cheminement ouvert chimiquement par l'eau au travers du massif carbonaté, permettant dans un second temps l'évacuation du cortège des éléments insolubles et donc le dégagement d'un conduit parcouru par l'eau, puis plus tard, "si morphodynamique lui prête vie", par le spéléologue. Le fait que ce type de conduit puisse être pénétrable par l'homme doit être considéré comme un fait exceptionnel. Normalement, le drainage karstique qui s'installe efface toutes les traces de ces premiers stades.

L'exploration de la grotte de la Mansonnière, sans présenter de difficultés majeures, se mérite, en raison de sa série d'étroitures et de ses longues reptations intégrales, parfois en marche arrière dans des boyaux sans issue. Cet aspect exploratoire ne doit pas masquer l'originalité karstologique des axes naturels pénétrables. Il s'agit assurément d'un modèle exceptionnel de par sa morphogenèse et du fait de sa pénétrabilité sur une aussi longue distance. Seul l'essoufflement de l'équipe de désobstrueurs a limité le développement connu à ce jour. Sans aucun doute, il reste plusieurs centaines de mètres à découvrir et à parcourir, nombril sur l'argile…

La Mansonnière est un site exceptionnel dans le sens qu'il présente un développement conséquent d'un type karstique quasiment inconnu par les spéléologues, sauf par ceux qui savent se transformer en terrassier. La variété des stades de développement, observée dans le kilomètre exploré, permet de dégager une évolution depuis la fissure initiale jusqu'à l'introduction concentrée d'un flux d'eau dans un vide. Cependant la solution de continuité entre l'introduction des eaux et leur restitution n'est pas établie, ce qui n'autorise ni le drainage des axes d'altération, ni le dégagement de leur résidu d'altération, ni leur calibrage par un flux concentré, ce qui donnerait une grotte classique comme les spéléologues aiment. En cela, on peut parler de premières phases de karstification, d'un "primokarst".
Spectaculaire à la Mansonnière, ce phénomène est observable dans l'ensemble du Perche méridional, autour et dans la dépression du cours supérieur de l'Huisne. En cela, on peut caractériser le karst du Perche comme étant essentiellement un "primokarst". Assurément, il s'agit d'un terrain de recherche prometteur pour les générations à venir, si les propriétaires ne laissent pas les accès disparaître... Depuis, nous avons porté notre attention dans d'autres sites, dans d'autres supports, sous d'autres climats, et nous y avons observé ces mêmes phénomènes, démontrant largement l'universalité de ces processus. Il ne tient qu'aux responsables politiques locaux que La Mansonnière conserve sa réputation internationale et que ce patrimoine ne soit pas détruit ou rendu inaccessible.

Références

DUBOIS C., QUINIF Y., BAELE J.-M., BARRIQUAND J., BARRIQUAND L., BINI A., BRUXELLES L., DANDURAND G., HAVRON C., KAUFMANN O., LANS B., MAIRE R., MARTIN J., RODET J., ROWBERRY M.D., TOGNINI P. and VERGARI A. (2014) The process of ghost-rock karstification and its role in the formation of cave systems. *Earth-Science Reviews*, 131, 116-148.

RODET J. (1996) Une nouvelle organisation géométrique du drainage karstique des craies : le labyrinthe d'altération, l'exemple de la grotte de la Mansonnière (Bellou sur Huisne, Orne, France). *Comptes Rendus de l'Académie des Sciences de Paris*, 322 (12), 1039-1045

RODET J. (1997) Typologie des karsts dans la craie du bassin de Paris. *Annales de la Société Géologique du Nord*, t. 5 (2ème série), 351-359.

RODET J. (1999) Le réseau de fracturation, facteur initial de la karstification des craies dans les collines du Perche : l'exemple du site de la Mansonnière (Bellou-sur-Huisne, Orne, France). *Geodinamica Acta*, 12 (2-3), 259-265.

RODET J. (2004) Karst et craie en Normandie : une approche géographique – Karst and chalk in Normandy : a geographical approach. *Actes des Journées Européennes de l'AFK 2003*, Rouen, 16-31.

RODET J. (2014) The primokarst, former stages of karstification, or how solution caves can born. *Geologica Belgica*, 17 (1), 58-65.

RODET J. (2017) La grotte, fruit d'une longue gestation appelée karstification. *Karstologia*, 69, 57-64.

Les effondrements karstiques du Tournaisis : un exemple révélateur du rôle des paléo-altérations dans le développement du karst

Olivier KAUFMANN & Yves QUINIF

Faculté Polytechnique de Mons, Service de Géologie Fondamentale et Appliquée, 9 rue de Houdain, B-7000 Mons, Belgique, olivier.kaufmann@umons.ac.be (corresponding author)

Résumé

Le Tournaisis est caractérisé par un relief peu accusé organisé autour de la vallée de l'Escaut et de ses affluents. Quelques buttes témoignent de l'épaisse sédimentation sablo-argileuse au Tertiaire. Le soubassement rocheux de la région est principalement constitué de calcaires et dolomies du Carbonifère, localement recouverts de marnes crétacées. C'est dans ce contexte que des effondrements soudains affectant les formations meubles de couverture ont été rapportés dès le début du XX^{ème} siècle. Ces phénomènes ont été associés dès les années 1960 à des manifestations d'un karst caché hérité du Jurassique. À la faveur des travaux de carrières, quelques courtes cavités ont d'ailleurs été explorées et décrites. Ce sont toutefois les observations de calcaires altérés en fantômes de roches sur les fronts de carrière et au fond de certains effondrements qui, avec l'examen des évolutions des niveaux piézométriques historiques, ont permis de comprendre l'origine des effondrements et ouvert la voie au développement d'un nouveau paradigme pour la création de cavités macroscopiques dans le karst. Le processus se passe en deux temps bien distincts : 1- développement d'une microporosité le long des joints aboutissant à la formation d'isaltérite ; 2- affaissement et transport des altérites laissant place à un vide macroscopique.

Abstract

The cover-collapse sinkholes of the Tournaisis: a revealing example of the role of paleo-alterations in the development of karst. The Tournaisis region is characterised by a gentle relief organised around the Escaut valley and its tributaries. A few mounds bear witness to the thick sandy-clay sedimentation in the Tertiary period. The bedrock of the region is mainly made up of limestone and dolomite from the Carboniferous period, locally covered with Cretaceous marls. It is in this context that sudden collapses affecting the drift formations have been reported as early as the beginning of the 20th century. These phenomena have been associated since the 1960s with manifestations of a hidden karst inherited from the Jurassic period. In the course of quarrying work, a few short cavities were also explored and described. However, it was the observations of limestone altered into "ghost rock" on the quarry faces and at the bottom of certain collapses which, together with the examination of the evolution of historical piezometric heads, made it possible to understand the origin of the collapses and paved the way for the development of a new paradigm for the creation of macroscopic cavities in karst. The process takes place in two distinct stages: 1- development of microporosity along the joints leading to the formation of isalterite; 2- collapse and transport of the alterite giving way to a macroscopic void.

Abstrakt

Die Karsteinbrüche des Tournaisis: ein aufschlussreiches Beispiel für die Rolle von Paläo-Alterationen bei der Entstehung von Karst. Die Tournaisis zeichnet sich durch ein nicht sehr ausgeprägtes Relief aus, das um das Tal der Schelde und ihrer Nebenflüsse herum organisiert ist. Einige Hügel zeugen von der dicken sandig-tonigen Sedimentation während des Tertiärs. Der felsige Untergrund der Region besteht hauptsächlich aus Kalkstein und Dolomit aus der Karbonzeit, örtlich bedeckt mit Mergeln aus der Kreidezeit. In diesem Zusammenhang wurde bereits zu Beginn des 20. Jahrhunderts von plötzlichen Einstürzen berichtet, die die lockeren Deckschichten betreffen. Ab den 1960er Jahren wurden diese Phänomene mit Manifestationen eines verborgenen Karsts aus der Jurazeit in Verbindung gebracht. Bei Abbauarbeiten wurden auch einige kurze Hohlräume erkundet und beschrieben. Es waren jedoch die Beobachtungen von zu "Gesteinsphantomen" alteriertem Kalkstein an den Abbauwänden und an der Sohle einiger Einstürze, die zusammen mit der Untersuchung der Entwicklung historischer piezometrischer Niveaus ein Verständnis für den Ursprung der Einstürze ermöglichten und den Weg für die Entwicklung eines neuen Paradigmas für die Entstehung makroskopischer Hohlräume im Karst ebneten. Der Prozess läuft in zwei verschiedenen Phasen ab: 1- Entwicklung von Mikroporosität entlang der Fugen, die zur Bildung von Isalterit führt; 2- Kollaps und Transport der Alteration, der zu einem makroskopischen Hohlraum führt.

1. Introduction

Le Tournaisis est une région située à l'extrémité occidentale de la province de Hainaut en Belgique.

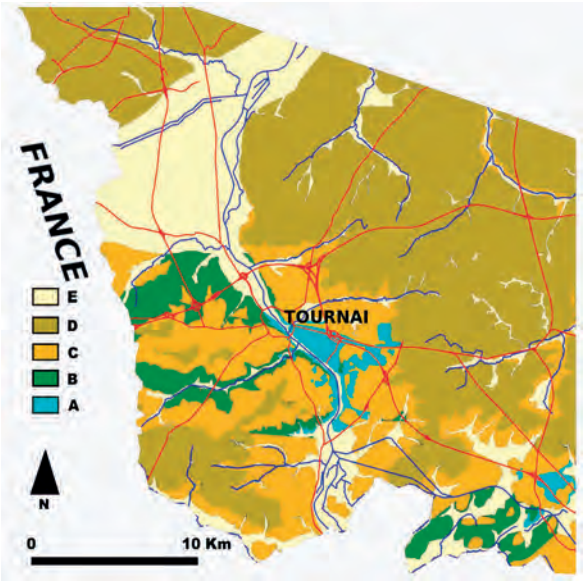

Figure 1 : Carte géologique simplifiée du Tournaisis. A – Socle paléozoïque; B – Crétacé; C – Thanétien; D – Yprésien; E – Alluvions quaternaires.

On peut y distinguer quatre zones géomorphologiques : (1) Au nord-est de Tournai, une région de collines dont l'altitude varie d'une trentaine de mètres à 150 m (Mont Saint-Aubert cf. Fig. 2). Il s'agit de buttes témoins qui renseignent sur l'épaisseur qu'avait jadis la couverture sédimentaire méso-cénozoïque dans la région ainsi que sur l'importance de l'érosion dont cette couverture a fait l'objet ; (2) Au nord-ouest de Tournai, la large plaine alluviale de l'Escaut où les altitudes sont comprises entre 10 et 25 m. Cette plaine s'étend principalement à l'ouest du cours actuel du fleuve et présente une très faible pente vers l'est ; (3) Au sud de Tournai, un relief de direction est-ouest. Il est franchi en une cluse étroite et encaissée par l'Escaut qui accuse plusieurs changements brusques de direction. Sur ce relief, la couverture sédimentaire a été plus ou moins intensément érodée et le socle paléozoïque affleure localement dans les vallées ; (4) À l'extrême sud du Tournaisis, une zone de larges plaines alluviales et de basses collines résulte du démantèlement de la couverture sédimentaire.

Le socle rocheux de la région est majoritairement constitué de calcaires et dolomies du Carbonifère (Tournaisien et Viséen). Ce socle est affecté de nombreuses failles dont les principales ont une direction essentiellement est-ouest et participent à une structure du type un anticlinal faillé (Hennebert, 1998).

Des marnes et craies du Crétacé surmontent le socle primaire au sud, à l'ouest et au nord de Tournai. Au sud-est de Tournai, les formations du primaire sont sub-affleurantes.

La Fig. 2 présente une coupe montrant l'anticlinal faillé du Mélantois-Tournaisis et sa couverture sédimentaire méso-cénozoïque. Les hauteurs sont y sont fortement exagérées.

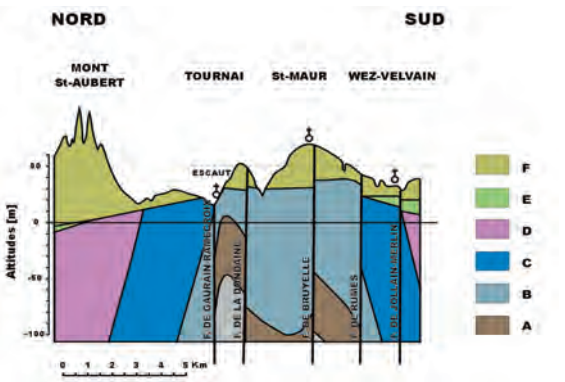

Figure 2 : coupe schématique nord-sud de l'Anticlinal faillé du Mélantois-Tournaisis à hauteur de Tournai. A – formation de l'Orient; B – formation de Tournai; C – formation d'Antoing; D – formation de Pecq; E et F couverture méso-cénozoïque.

La formation de l'Orient est constituée de shales calcaires. Elle est surmontée par les calcaires micritiques en bancs de 20 à 80 cm des formations de Tournai et d'Antoing. Ceux-ci présentent des teneurs en argile qui varient entre quelques pour-cent et une dizaine de pour-cent. Leur matrice renferme également de la silice sous forme cryptocristalline. La formation de Pecq comprend des dolomies et des calcaires dolomitiques massifs et grenus présentant divers niveaux riches en crinoïdes.

2. Manifestations karstiques et "fantômes de roches"

Des effondrements soudains tels que celui représenté à la Fig. 3 sont rapportés dans cette région depuis le début du XX^{ème} Siècle. Ces effondrements laissent voir en surface un vide dont la forme est habituellement cylindrique ou conique, d'axe vertical. Dans la plupart des cas, leurs parois ne montrent que des terrains meubles (limons, sables argileux ou argiles datant du quaternaire ou de l'ère tertiaire). Le fond de l'effondrement est généralement occupé par ces terrains meubles effondrés.

De courtes cavités ont également été découvertes et explorées, soit lors de travaux des carrières, soit suite à un effondrement des terrains meubles de couverture dans la cavité. Quelques-unes d'entre elles ont été décrites et certaines cartographiées (QUINIF et *al.*, 1985 ; QUINIF & RORIVE, 1990 ; VAN RENTERGEM et *al.*, 1993). Les cavités explorées dans les calcaires carbonifères de la région sont toutefois rares et de dimensions très modestes. Aucune de ces cavités ne reste accessible très longtemps du fait de l'activité des carrières ou du comblement des effondrements.

Figure 3 : Effondrement karstique affectant une prairie

Hormis ces quelques courtes cavités et les effondrements mentionnés plus haut, les autres manifestions classiques du modelé karstique sont rares dans le Tournaisis.

Les calcaires n'affleurant que sur une très petite partie du Tournaisis, c'est principalement à la faveur des travaux des carrières que le socle paléozoïque peut être observé. Ces carrières exploitant les roches calcaires pour l'industrie cimentière et la production de granulats entaillent le substratum rocheux jusqu'à plus de 100 m sous le niveau de la mer offrant ainsi point de vue unique sur le massif calcaire et le karst qui l'affecte.

De longue date, des phénomènes de dissolution appelés « poches » y ont été signalés dans la partie sommitale des calcaires carbonifères. Des altérations *in situ* de la roche calcaire y ont aussi été décrites. Ainsi, dès le début du XX^{ème} siècle, RUTOT (1903) observe et décrit une roche argileuse tendre de teinte gris foncé qu'il interprète comme une altération profonde, sur place, du calcaire carbonifère.

Quelques années plus tard, STAINIER (1921) complète et précise cette description, faisant aussi le lien avec des dépôts continentaux conservés au sommet des poches de dissolution : *« ...la stratification des bancs calcaires frais environnants pouvait se suivre dans la masse altérée ainsi que certains bancs insolubles de cherts. Mais, par suite de l'affaissement dû au départ du calcaire, les strates dans le calcaire altéré et la limite inférieure de la zone d'altération dessinaient des courbes concaves vers le haut. Ces poches d'altération étaient surtout fréquentes autour et au-dessous des poches de sables wealdiens... »*.

À la suite de Stainier, BAUDET (1939) signale également l'existence de « poches » aux formes particulières qui se développent au sommet du socle paléozoïque et s'allongent suivant les directions des diaclases. Ces « poches » présentent ainsi une forme en couloirs de largeur métrique. Sous des dépôts à faciès wealdien, une masse importante de roche primaire décalcifiée y est décrite.

CAMERMAN (1944) constate que la dissolution du calcaire compact du Tournaisis par un acide faible laisse un bloc cohérent de même forme que l'échantillon initial. Il décrit la matière résiduelle comme siliceuse, très légère et poreuse et remarque la ressemblance avec un matériau que l'on observe parfois dans les carrières, au toit du calcaire, principalement aux abords des diaclases.

Ces observations et descriptions correspondent de toute évidence aux « fantômes de roches » redécouverts et étudiés par VERGARI et *al.* (1997). Un examen approfondi des conditions du développement de telles altérites a été proposé par DUBOIS et *al*. (2014) sur la base de l'étude de plusieurs sites en Europe de l'Ouest.

Dans le Tournaisis, il s'agit vraisemblablement du résultat d'une phase d'altération qui survient lors de la continentalisation d'un orogène, lorsque la pénéplanation est presque achevée (QUINIF, 2018). Cette phase se termine avec la transgression cénomanienne.

KAUFMANN (2000) a montré que les effondrements karstiques rencontrés dans le Tournaisis se produisent au droit de zones altérées du substratum calcaire, en particulier à l'aplomb de couloirs d'altération développés de part et d'autre des diaclases. Ces couloirs peuvent se prolonger par des zones altérées, nommées pseudo-endokarsts (VERGARI, 1998), où un toit rocheux subsiste. Sous ce toit, des cavités peuvent se former par tassement des altérites. Ces cavités pourront alors accueillir les altérites et terrains meubles de couvertures transportés par des écoulements en zone non saturée.

3. Manifestations karstiques et contexte hydrogéologique régional

Un aquifère important se développe dans les calcaires et dolomies du Carbonifère inférieur du Parautochtone Brabançon depuis les environs de Namur jusqu'à la région de Lille. Il est limité au nord par les formations du Dévonien moyen et supérieur, il plonge au sud sous celles du Namurien et du Westphalien.

Dans le Tournaisis, une contribution importante à l'alimentation de la nappe portée par cet aquifère provient d'apports latéraux venant de l'est. Les conditions de réalimentation diffèrent néanmoins fortement entre la partie au nord de l'anticlinal du Mélantois-Tournaisis et celles au sud et au sud-est.

Au nord de Tournai, la réalimentation de l'aquifère est fortement limitée par la présence des marnes crétacées qui couvrent l'aquifère. De plus, cette zone est isolée de la partie sud par le relèvement des shales calcaires au centre de l'anticlinal faillé (RORIVE & HENNEBERT, 1997) alors que vers le nord-est, des anticlinaux transverses isolent encore un peu plus la partie nord de l'aquifère.

Avant la révolution industrielle, les niveaux piézométriques de la nappe des calcaires carbonifères devaient s'équilibrer avec celui des plaines alluviales des rivières dans l'ensemble du Tournaisis. À cette époque, l'écoulement de la nappe se faisait essentiellement vers l'Escaut le long duquel de nombreuses émergences existaient en aval de Tournai. Plus au nord, la nappe des calcaires carbonifères était captive sous les marnes crétacées.

Au XX^{ème} siècle, cette nappe a fait l'objet d'une intense exploitation dans le Tournaisis et la région de Lille-Roubaix. Alors qu'au sud de l'anticlinal du Mélantois-Tournaisis, les niveaux piézométriques restaient proches de l'équilibre naturel, au nord de Tournai, ils baissaient de manière importante. Dans la région de Mouscron, à la fin du XX^{ème} siècle, ils se situaient de l'ordre de 80 m sous leur niveau d'équilibre antérieur. Cette baisse substantielle des niveaux

piézométriques (de l'ordre de 1 à 2m par an entre 1946 et 1976) au cours du XX^{ème} siècle s'est accompagnée de la survenance de plus de 400 effondrements recensés. L'examen de leur localisation montre qu'ils se produisent là où le socle primaire a été dénoyé suite aux pompages (KAUFMANN, 2000).

Les infiltrations localisées constituent en outre un facteur déclencheur. Suite à ces travaux, une politique de limitation des prises d'eau dans la partie surexploitée de l'aquifère a été mise en place. Après une stabilisation puis une légère remontée des niveaux piézométriques, certains ouvrages indiquent à nouveau une tendance à la baisse.

4. Discussion et conclusion

Les effondrements du Tournaisis trouvent donc leur origine dans l'activation d'un paléokarst caractérisé par des formes de dissolution conservant une altération particulière de la roche calcaire : les fantômes de roche. Cette activation résulte des importantes modifications des équilibres hydrogéologiques dans la région au cours du XX^{ème} siècle.
Le processus de création des cavités à l'origine des effondrements se passe en deux temps bien distincts : 1- développement d'une importante microporosité le long des joints aboutissant à la formation d'isaltérite ; 2- affaissement et transport des altérites laissant place à un vide macroscopique (KAUFMANN, 2000 ; QUINIF, 2018) suite à l'abaissement des niveaux piézométriques.
Contrairement aux systèmes généralement considérés par l'hydrogéologie karstique, les cavités ainsi formées ne sont pas organisées en un réseau de drainage bien structuré. Les formes paléokarstiques restent pour la plupart pleines et l'organisation spatiale des formes altérées apparaît quasi exclusivement dictée par la fracturation et la lithologie.
Par contre, tout laisse à penser qu'une évolution au cours de laquelle un gradient hydraulique suffisant persiste et des exutoires deviennent possibles aboutira à une plus grande connectivité entre vides. En effet, en présence d'un gradient hydraulique, un phénomène de rétroaction positive aboutissant à la structuration de cette unité de drainage peut être proposé : les débits et les écoulements sont plus importants dans les zones où les altérites ont été évacuées alors que le transport des altérites est renforcé dans les zones où les débits sont importants et les écoulements rapides. Une illustration à petite échelle d'une telle évolution a pu être observée dans les carrières du Hainaut belge (QUINIF & MAIRE, 2009).

Références

BAUDET J. (1939) Quelques observations sur les morts-terrains du Tournaisis, *Bull. Soc. belge de Géol.*, T. XLIX, pp. 289-308.

CAMERMAN C. (1944) La pierre de Tournai, son gisement, sa structure et ses propriétés, son emploi actuel, *Mém. Soc. Belge de Géologie*, nouv. série in 4, n°1, pp. 1-86.

DUBOIS C., QUINIF Y., BAELE J.-M., BARRIQUAND L., BINI A., BRUXELLES L., DANDURAND G., HAVRON C., KAUFMANN O., LANS B., MAIRE R., MARTIN J., RODET J., ROWBERRY M.D., TOGNINI P. and VERGARI A. (2014) The process of ghost-rock karstification and its role in the formation of cave systems. *Earth Science Reviews*, 131, pp. 116-148.

H ENNEBERT M., 1998. L'anticlinal faillé du Melantois-Tournaisis fait partie d'une structure en fleur positive tardi-varisque, *Ann. Soc. Géol. du Nord*, T.6, pp. 65-78.

KAUFMANN O. (2000) Les effondrements karstiques du Tournaisis. Genèse, évolution, localisation, prévention, *Speleochronos*, Hors-Série, 350p.

QUINIF Y., BOUKO Ph., CANTILLANA R., DRUMEL P. et RORIVE A. (1985) Découverte d'un réseau karstique superficiel à Gaurain-Ramecroix (Hainaut occidental, Belgique) à la faveur de nouveaux puits naturels, *Bull. Soc. belge de Géol.*, T.94, fasc. 1, pp. 45-50.

QUINIF Y. et RORIVE A. (1990) Nouvelles données sur le karst du Tournaisis, *Bull. Soc. belge de Géol.*, T.99, fasc. 3-4, pp. 361-372.

QUINIF Y. et MAIRE R. (2009) La grotte Quentin (Hainaut, Belgique) : un modèle d'évolution des fantômes de roche. *Karstol. Mém*. 17, pp. 214–218.

QUINIF Y. (2018) Fantômisation et spéléogenèse : implications et questionnement, *Karstologia*, 69, 33-46.

RORIVE A. et HENNEBERT M., (1997) Nappe du calcaire carbonifère du Tournaisis : nouvelle interprétation du rôle de "barrière hydrogéologique" de la faille de Gaurain-Ramecroix, *Résumés du Colloque Artois-Brabant*, 9-11 avril 1997, Mons, Belgique, 1 p.

RUTOT A. (1903) Compte rendu des excursions de la séance extraordinaire de la Société belge de Géologie, de Paléontologie et d'Hydrologie, dans le Hainaut et dans les environs de Bruxelles du 23 au 27 août 1902, *Bull. Soc. belge de Géol.*,T. XVII, mémoires, pp. 463-466.

STAINIER X. (1921) Sur les formations résultant de l'altération du calcaire carbonifère, *Bull. Soc. belg. Géol.*, T. XXXI, pp. 123-133.

VAN RENTERGEM, BOUCKAERT P. et QUINIF Y. (1993) Une nouvelle grotte à Gaurain-Ramecroix, *Bull. Soc. belge Géol.*, T. 102, fasc. 3-4, pp. 395-399.

VERGARI A. et QUINIF Y. (1997) Les paléokarsts du Hainaut. *Geodinamica Acta*, 10, n°4, pp. 175-187.

VERGARI A. (1998) Nouveau regard sur la spéléogenèse : le pseudo-endokarst du Tournaisis (Hainaut, Belgique). *Karstologia* 31, pp. 12–18.

Apports de l'archéo-géomorphologie dans l'étude de *Cloggs cave* (Victoria - Australie)

Jean-Jacques DELANNOY[1,2], Bruno DAVID[2,3], Joanna FRESLOV[4], Russell MULLET[4], Glawac Gunaikurnai Land and Waters Aboriginal Corporation[4], Helen GREEN[5] & Johan BERTHET[1]

(1) Laboratoire EDYTEM (Environnements, Dynamiques et Territoires de la Montagne), *Campus scientifique Université Savoie Mont Blanc, 73376 Le Bourget du Lac cedex - France* – jean-jacques.delannoy@univ-smb.fr
(2) ARC Centre of Excellence for Australian Biodiversity and Heritage, *Canberra, ACT 2601, Australia*
(3) Monash Indigenous Studies Centre, *Monash University, Clayton Campus, VIC 3800, Australia* - bruno.david@monash.edu
(4) Gunaikurnai Land and Waters Aboriginal Corporation, *27 Scriveners Road (Forestec), Kalimna West, VIC 3909, Australia*
(5) School of Earth Sciences, University of Melbourne, Parkville, 3010 Victoria, Australia

Résumé

Cloggs cave (Australie) est connue pour ses vestiges de mégafaune et archéologiques. De nouvelles recherches ont été entreprises en 2019 pour mieux comprendre la stratigraphie des dépôts contenant ces vestiges. L'approche archéo-géomorphologique a été privilégiée pour reconstituer l'évolution de la grotte et préciser ses accès par la mégafaune puis par les communautés humaines. Les résultats obtenus indiquent une nette distinction entre les phases d'occupation de la mégafaune et des Hommes, remettant en cause des faits établis depuis près d'une cinquantaine d'années. L'étude fait ressortir qu'il y a 52 Ka la mégafaune accédait à la cavité par une entrée aujourd'hui fermée par un colmatage sédimentaire. C'est bien après que les Hommes (vers 20 puis 4 Ka) ont accédé par une autre entrée à la cavité. L'intégration des données archéologiques et géomorphologiques renouvelle les connaissances sur cette cavité considérée comme bien connue.

Abstract

Contributions of archaeo-geomorphology to the study of Cloggs cave (Victoria - Australia). Cloggs cave (Australia) is known for its megafauna and archaeological remains. New research was undertaken in 2019 to better understand the stratigraphy of the deposits containing these remains. The archaeo-geomorphological approach has been favoured to reconstruct the evolution of the cave and clarify its accesses by the megafauna and then by human communities. The results obtained indicate a clear distinction between the phases of occupation by the megafauna and by humans, calling into question facts that have been established for nearly fifty years. The study shows that 52 Ka ago the megafauna accessed the cavity through an entrance that is now closed by a sedimentary seal. It is well afterwards that humans (around 20 then 4 Ka) accessed the cavity through another entrance. The integration of archaeological and geomorphological data renews the knowledge of this cavity, which is considered to be well known.

1. Introduction

Cloggs Cave (État de Victoria-Australie) est connue dans la littérature archéologique suite aux travaux de J. Flood qui proposait une survie tardive de la mégafaune (22,9 ± 2 Ka) (FLOOD, 1980) et une coexistence de près de 25 Ka avec les premières communautés humaines arrivées sur le continent australien. Les causes de l'extinction de la mégafaune ont donné lieu à de nombreux débats dans lesquels le site de *Cloggs cave* apparaît comme un cas de plus en plus isolé. C'est dans ce contexte que l'étude de *Cloggs cave* a été reprise en 2019 à la demande de la *Gunaikurnai Land and Waters Aboriginal Corporation*, représentant les propriétaires traditionnels aborigènes. Les nouveaux travaux ont mobilisé les données géomorphologiques et archéologiques (DELANNOY *et al*., 2020) et un important cortège de datations (AMS ^{14}C, OSL et U/Th - DAVID *et al*., 2020) afin de préciser la stratigraphie des dépôts contenant les vestiges archéologiques et les conditions d'accès à la grotte par la mégafaune et par les *Old people*.

2. Contexte géologique et géomorphologique de *Cloggs cave*

La grotte s'ouvre à 72 m en rive droite de la *Buchan River* entre la localité de Buchan et sa confluence avec la *Snowy River*.

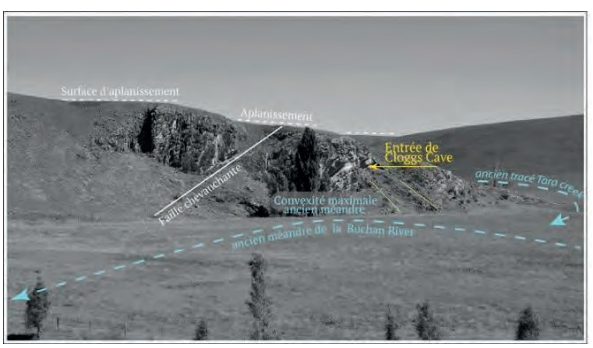

Figure 1 : Cloggs cave et son environnement extérieur- Cliff-line containing Cloggs Cave and fronting both a palaeo-channel of the Buchan River - Photo Bruno David

Dans ce secteur, la vallée méandriforme recoupe un bas plateau calcaire (200 m d'altitude) dont la planéité est associée à d'anciennes surfaces d'aplanissement qui tronquent les formations calcaires et volcaniques dévoniennes (Fig. 1). Expression d'une très longue phase d'érosion dans un contexte de faible énergie gravitaire, ces surfaces se sont agencées depuis la fin du Dévonien jusqu'à la première moitié du Cénozoïque. Au-dessus de la cavité, des dépôts littoraux oligo-miocènes ont été retrouvés en discordance angulaire sur les calcaires dévoniens. Le soulèvement qui a porté en altitude les dépôts miocènes (200 m) a été le moteur de l'incision de la *Buchan River*. Ces données permettent de poser un premier cadre de mise en place du karst qui nécessite un gradient hydraulique, ici lié à l'enfoncement du réseau hydrographique post-Miocène. La position perchée de la grotte par rapport au talweg souligne que sa genèse se rapporte à une ancienne phase d'enfoncement du cours d'eau. Par ailleurs, le recul ultérieur du versant engendré par l'ancien méandre a eu pour effet de décapiter le réseau souterrain. On retrouve à l'extérieur d'anciens édifices stalagmitiques en place soulignant un ancien prolongement du réseau souterrain vers le nord.

3. Caractéristiques morphologiques de *Cloggs Cave*

Bien que la grotte pénètre peu dans la masse calcaire, elle se caractérise par une diversité de paysages souterrains. Le porche (8m de haut) présente d'anciens dépôts stalagmitiques sur ses parois. Il se réduit fortement pour se raccorder à un conduit de dimension métrique (entrée actuelle). Sous celui-ci existe un conduit colmaté qui a été révélé par les anciennes fouilles archéologiques. Dès le franchissement de l'entrée (porte), la galerie s'élargit et descend vers la salle principale de la cavité (*Main Chamber*). Celle-ci est calquée sur la voussure d'un pli anticlinal (Fig. 2). Une fracture recoupe perpendiculairement l'axe du pli et guide le développement de la galerie principale : celle-ci est divisée de part et d'autre de la *Main Chamber* : l'*Upper et Lower Gallery*. Vers le NNW, la *Lower Gallery* se rétrécit rapidement pour passer à une fissure impénétrable. La géométrie de l'*Upper Gallery* retient également l'attention : (i) fermeture en sifflet du terminus au SSE : en quelques mètres, on passe d'une haute galerie (6m) à une fissure impénétrable ; (ii) la forte pente du talus en direction de la *Main Chamber* et sa nature limono-argileuse. La morphologie d'ensemble de la galerie et de la salle reflète une évolution par écroulements successifs des parois et du plafond. L'indigence des blocs écroulés au sol ainsi que dans l'excavation archéologique interroge.

L'*Upper Chamber*, en contre haut de *l'Upper Gallery* se différencie du reste de la cavité par sa position perchée et la sub-horizontalité de son sol. On retrouve ici aussi l'absence de blocs alors que la géométrie de la salle résulte indéniablement de processus gravitaires. Au sud-ouest de la *Upper Chamber*, un bas passage accède à l'*Upper Passage*, étroite galerie calquée sur une fracture et sur le pendage géologique (30°).

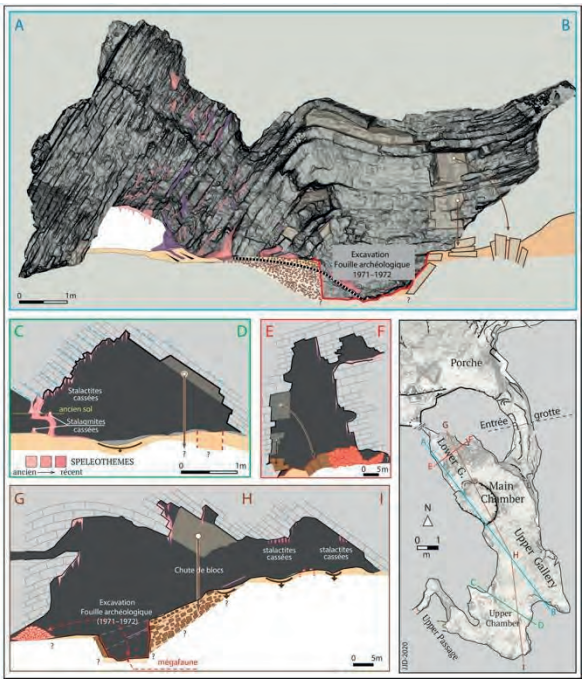

Figure 2 : Coupes synoptiques de Cloggs cave à partir du modèle 3D. Synoptic views across key sections of Cloggs Cave, as generated from the 3D model

Son terminus bute sur un colmatage chapeauté par un épais plancher stalagmitique. L'attention a été portée à ce secteur car il constitue un des rares conduits avec des morphologies et dépôts karstiques ; partout ailleurs les volumes souterrains ont connu d'importantes modifications ne permettant plus de reconstituer leur physionomie initiale.

4. Reconstitution morphogénique de *Cloggs cave*

L'*Upper Passage* présente les plus anciens témoins morphogéniques. Son terminus présente différentes natures de matériel (Fig. 3) : une formation argileuse inscrite dans la masse carbonatée ; un remplissage argilo-gréseux riche en quartz ; et un épais plancher stalagmitique. Cette séquence permet de différencier plusieurs phases. La formation argileuse inscrite dans l'encaissant calcaire s'apparente à un « fantôme de roche » (altération isovolumique des calcaires dans un contexte de faible énergie hydraulique ; QUINIF, 2010). Nous associons la fantômisation à la réalisation des surfaces d'aplanissement. L'enfoncement hydrographique post-miocène a favorisé la mise en place de circulations souterraines qui ont emprunté les conduits fantômisés et évacué l'altérite. Les eaux ont apporté sous terre les formations miocènes allochtones (sédiment riche en granules de quartz et quartzites). Ce remplissage a été ensuite déblayé par une lente érosion régressive. La datation du plancher stalagmitique indique que le début du décolmatage est antérieur à 285,6 ± 4,2 Ka. Pendant au moins 50 Ka, la galerie a été parcourue par des ruissellements incrustants. Ils ont localement induré le remplissage argilo-gréseux. Dans les zones non indurées, il a

pu être par la suite aisément évacué (vidange *Upper Passage*). Ces étapes peuvent être généralisées à l'ensemble de la cavité. En effet, l'organisation des réseaux dépendante de la fracturation, ainsi que la géométrie des terminus (passage rapide à des fissures impénétrables), sont des indices d'un agencement initial en conduits fantômisés. En dehors de l'*Upper Passage*, les autres volumes souterrains ne présentent plus de morphologies de dissolution ; elles ont été gommées par les processus gravitaires ultérieurs.

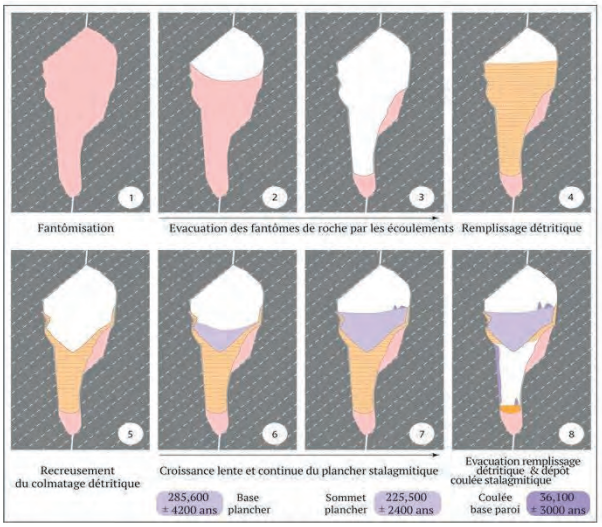

Figure 3 : Lecture et reconstitution spéléogénique du terminus de l'Upper Passage.
Diagrammatic interpretation of the geomorphological history of the terminus of the Upper Passage.

L'ouverture de vides souterrains par écroulements est ancienne si on se réfère à la datation d'un ancien plancher perché sur la paroi W de l'Upper Gallery (109,8 ± 12 Ka). Les vides créés par les phénomènes gravitaires sont compris entre le décolmatage des fantômes engagé dès la fin du Miocène et une période bien antérieure à 110 Ka ; durant cette longue période, les écroulements et l'érosion des blocs tombés ont rythmé l'agrandissement des vides souterrains. Le caractère perché de *Cloggs cave* est associé à un ancien stade d'enfoncement de la *Buchan River*. Dans les proches grottes de Buchan, l'étagement karstique (lié à l'évacuation progressive des altérites) a pu être relié aux différents stades d'enfoncement de la rivière dont les plus anciens remontent à la fin du Cénozoïque (WEBB *et al.*, 1992). Il est intéressant de relever que le fond des fouilles archéologiques de la *Main Chamber* se situe sous l'entrée actuelle. L'organisation des dépôts au fond de la fouille suggère un ancien soutirage et une évacuation des sédiments vers un réseau inférieur. Vu la proximité du versant, celui-ci devrait être visible à l'extérieur. Ce qui n'est pas le cas. Sous le porche, on relève la présence d'un éboulis de blocs jusqu'au pied du versant. Seuls des affleurements de coulées stalagmitiques en place permettent de suggérer un conduit sous *Cloggs cave*. Cet ancien réseau a été par la suite colmaté par les blocs provenant du porche d'entrée. Ceux-ci sont relativement anciens si on se réfère à la datation d'une coulée stalagmitique du porche (79 ± 6,2 Ka). L'architecture du porche et du talus de blocs est antérieure à cette date. L'étude des dépôts recoupés par les fouilles apporte des informations complémentaires. Trois grandes périodes morphogéniques ont été distinguées (Fig. 4) :

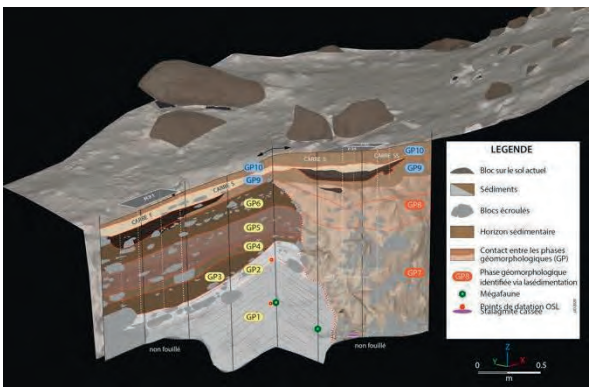

Figure 4 : Vue 3D synthétique des différentes phases morphogéniques (GP) du remplissage archéologique - Graphic synthesis of the Geomorphological Phases (GPs).

-1- Sédimentation dans un contexte de très faible énergie (GP1-GP6)**.** Le plus ancien dépôt est celui contenant les ossements de kangourou de très grande taille (> 3m). Les datations OSL et ^{14}C donnent un âge entre 51,8 ± 5,5 et 46,9 ± 4,1 Ka. Ce niveau se caractérise par un double pendage qui suggère un ancien soutirage vers lequel se mettent en place lentement les sédiments (1cm/1Ka). De GP3 à GP6 (45 à 6 Ka), la sédimentation s'accélère (1 cm/0,4 Ka) : elle est liée à un apport régulier d'éléments fins entrecoupés de niveaux de blocs effondrés. La géométrie du dépôt indique l'inefficience de l'ancien soutirage. C'est dans ce contexte de relative stabilité que la grotte est fréquentée par les Anciens (foyers, vestiges lithiques, artefacts datés entre 20,5-23,5 et 19,3-19,7 Ka.
-2- Événement catastrophique et lave torrentielle (GP7-GP8). Après 40 Ka d'accumulation, la cavité connaît un événement brutal. Une profonde entaille recoupe les précédents dépôts (GP1-GP6). Le caractère très localisé et les rebords abrupts de l'incision indiquent un phénomène de très forte énergie associée à une arrivée importante d'eau et à une réouverture du soutirage : celui-ci absorbe la totalité des sédiments évacués par l'incision torrentielle. Les dépôts (GP7) sont de type lave torrentielle. Les âges obtenus (OSL et AMS) confirment la soudaineté de ce phénomène : il s'est produit après 6,1 ± 1,1 et avant 6 Ka. Ce calage permet de le rapporter à une des phases humides du début de l'Holocène (Green *et al*., 2013). Suite à cet événement, la grotte retrouve des conditions de moindre énergie hydraulique comme l'indique la disposition des dépôts de GP8 (entre 6 et 4 Ka).
-3- Un contexte de faible énergie sédimentaire. En continuité avec le toit de GP8, la sédimentation limoneuse se propage dans l'ensemble de la *Main Chamber* (GP9). C'est durant cette période que l'ancien conduit sous la galerie d'entrée (porte) se remplit. De nombreux témoins d'activités à partir de 4,4 Ka ont été retrouvés dans ces niveaux (foyers, vestiges lithiques et structures anthropiques (DAVID *et al.,* 2020). Des sédiments fins (GP 10) ont ensuite recouvert les foyers et témoins d'occupation sans modifier l'allure des sols parcourus par les Anciens.

5. Conclusions : reconstitution de l'histoire de la grotte et de ses accès

Les relevés et datations menées dans la grotte permettent de restituer l'histoire de la cavité et les accès qu'en ont eu la mégafaune et les *Old People*.

1- Les témoins les plus anciens sont les surfaces d'aplanissement et la fantômisation qui répondent à une même morphogenèse : altération des calcaires dans un contexte de très faible énergie gravitaire et sur un temps très long. Cette dynamique engagée il y a 395 Ma, s'est prolongée jusqu'au Miocène (5 Ma).

2- La position altitudinale des formations littorales miocènes à plus de 200 m suppose un lent soulèvement régional évalué à 76m/Ma durant les 3,5 derniers Ma (ENGEL *et al*., sous presse). Il a pour incidence l'enfoncement du réseau hydrographique moteur de la karstification. Les écoulements souterrains empruntent les couloirs fantômisés de roche et évacuent les altérites avant de creuser les réseaux se raccordant au niveau de base karstique d'alors. A chacune des phases d'enfoncement hydrographique, un niveau de karstification a pu être identifié (WEBB *et al*., 1992).

3- S'en suit l'agrandissement des vides souterrains par réajustements mécaniques des parois et des plafonds : c'est à cette phase que nous attribuons la mise en place de la grande galerie et de la *Main Chamber*. L'indigence des blocs d'effondrement dans la cavité est attribuée à leur dissolution par les écoulements qui parcouraient la cavité.

4- L'accentuation du gradient hydraulique lié à l'enfoncement de la vallée se traduit par un nouveau drainage karstique. Dès lors, la grotte est parcourue par les eaux d'infiltration qui entraînent sous terre les formations superficielles et favorisent le colmatage des conduits. La datation du plancher stalagmitique de l'*Upper Passage* rapporte ce colmatage dans la seconde moitié du Pléistocène moyen (antérieur à 285 Ka). Le développement du plancher stalagmitique sur près de 50 Ka est contemporain du stade isotopique 7 (optimum climatique).

5- La grotte se vide ensuite partiellement de ses sédiments. Cette phase peut être rattachée à la péjoration climatique planétaire du stade isotopique 6 (cf. datations des surfaces repères de la grotte). C'est à cette période que nous rapportons l'agencement d'un premier talus vers la *Main Chamber.* La reconnaissance en paroi d'un plancher stalagmitique ayant scellé ce talus indique que la salle était alors fortement emplie de sédiments. En contrebas, il se raccordait à la zone d'entrée actuelle et à la base de la coulée stalagmitique du porche. Cette ancienne topographie des sols est antérieure à 110 Ka (datation plancher). Ce calage est important car il sous-tend que le conduit sous la galerie d'entrée était alors colmaté ; ce conduit étant une des hypothèses d'accès à la grotte pour la mégafaune.

6- Compte tenu de la position des ossements de la mégafaune (2 mètres sous le plancher daté à 110 Ka), la *Main Chamber* a connu entre l'étape 5 et sa fréquentation animale un important décolmatage associé à un soutirage au bas de la salle. A ce stade, les conduits sous *Cloggs cave* n'ont pu être retrouvés. Nous rapportons à cette phase, le décolmatage du conduit sous la galerie d'entrée actuelle.

7- De nouveaux dépôts se mettent en place, dans un premier temps, avec un fort pendage lié à la topographie du soutirage puis de plus en plus atténué. Les vestiges en place de la faune pléistocène indiquent que le soutirage était inactif et déjà en partie comblé. Le comblement progressif de la *Main Chamber* s'est ensuite poursuivi et enregistre les premières fréquentations humaines. La mégafaune a accédé à la grotte par le conduit sous l'entrée actuelle dont on sait par les sondages archéologiques dans le porche qu'elle était de plusieurs mètres de hauteur.

8- Vers 6 Ka, la grotte connaît un événement catastrophique rapporté à une grosse arrivée d'eau dans la cavité et à la réactivation conjointe du soutirage. Les âges du matériel entraîné par la lave torrentielle soulignent l'instantanéité de cet événement et le rapportent à une phase de l'Holocène connue pour ses instabilités climatiques dans un contexte chaud et très humide. Suite à cet événement, la cavité reprend un cycle de dépôt de faible énergie.

9- Cette nouvelle étape de dépôts fins marque la fin du colmatage de l'entaille torrentielle et la mise en place du talus de raccordement « actuel » entre *l'Upper Chamber* et la *Main Chamber*. Par son allure générale et la pente régulière des unités stratigraphiques du talus, il ressort que la galerie sous l'entrée actuelle était colmatée. La grotte est à ce stade régulièrement fréquentée par les *Old People* : nombreux foyers imbriqués, aménagement de l'accès à la grande salle, et prélèvements de concrétion. Les Hommes passaient alors par l'entrée actuelle.

Références

FLOOD J. (1980) The moth hunters: Aboriginal prehistory of the Australian Alps. Australian Institute of Aboriginal Studies, Canberra.

DAVID B. et *al*. (2020) 50 years and worlds apart: the Early Holocene abandonment of Cloggs Cave, East Gippsland, SE Australia. Australian Archaeologia.

DELANNOY J.-J. et *al*. (2020) Geomorphological context and formation history of Cloggs Cave: What was the cave like when people inhabited it? Journal of Archaelogical Sciences: Reports 33.

GREEN H., et *al*. (2013) Re-analysis of key evidence in the case for a hemispherically synchronous response to the YoungerDryas climatic event. J. Quat. Sci. 28, 8–12.

QUINIF Y. (2010). Fantômes de roche et fantômisation : Essai sur un nouveau paradigme de karstogénèse. Karstologia Mém., 18.

WEBB J.A. et *al*. (1992) Denudation chronology from cave and river terrace levels: the case of the Buchan Karst, southeastern Australia. Geol. Mag. 129, 307–31.

Les formes karstiques et le fantôme de roche dans les travaux BTP en Wallonie (Belgique) - Retours d'expérience

Cécile HAVRON

Département Géotechnique et Environnement Sol, Institut Interuniversitaire des Silicates, Sols et Matériaux (INISMa), 7000 Mons, Belgique, c.havron@bcrc.be

Résumé

Les roches carbonatées affleurent sur près d'un tiers du territoire wallon, et pourtant elles demeurent encore trop méconnues des ingénieurs du secteur du bâtiment et des travaux publics (BTP) en Belgique. Leur processus d'altération particulier, leur karstification et *a fortiori* leur fantômisation, sont encore largement méconnus, et donc rarement pris en compte dans les projets de construction. Les constructeurs non avertis vont dès lors souvent au-devant de déconvenues diverses : problèmes d'exécution, délais augmentés et surcoûts. Cette communication présente trois exemples de projet de construction (travaux d'infrastructure, bâtiments industriels et éoliennes) qui ont été confrontés aux phénomènes de karstification des roches carbonatées. L'ensemble fera état de la connaissance générale des domaines rocheux carbonatés dans le monde de la construction en Wallonie.

Abstract

Karst forms and the ghost-rock in Construction works in Wallonia (Belgium) - Feedback. Carbonate rocks outcrop over nearly a third of Walloon territory, and yet they are still too little known to construction engineers in Belgium. Their particular alteration process, their karstification and *a fortiori* their ghosting, are still largely unknown, and therefore rarely taken into account in construction projects. The uninformed builders therefore often face various disappointments: execution problems, increased deadlines and additional costs. This communication presents three examples of construction project (infrastructure works, industrial buildings and wind turbines) which have been confronted with the phenomena of karstification of carbonate rocks are presented. The whole will report on the general knowledge of carbonate rocky areas in the construction world in Wallonia.

1. Introduction

Le sous-sol de la Wallonie au sud de la Belgique (16 900 km² environ) est constitué pour environ un tiers de formations carbonatées, datant de différentes périodes. Peuvent être distingués les calcaires et dolomies dévoniens, les calcaires et dolomies carbonifères et le poudingue permien pour le Paléozoïque, les grès, siltites et argilites carbonatés jurassiques et les craies crétacées pour le Mésozoïque, et les sables carbonatés éocènes pour le Cénozoïque.
Toutes ces formations sont affectées de divers phénomènes générés par karstification. Toutes les formes karstiques classiques sont recensées : grottes, vallées sèches, pertes, sources, ainsi que dolines diverses, autres poches de dissolution et puits naturels, la récurrence des différentes formes pour chaque formation dépendant de sa compétence. La présence de « fantômes de roche » y est également confirmée (Dubois et *al*., 2014 ; Quinif, 2010).
En Wallonie, les aménageurs et autres opérateurs du secteur du bâtiment et des travaux publics (BTP) sont donc souvent confrontés tant aux formations carbonatées qu'aux phénomènes karstiques.

2. La reconnaissance géotechnique et ses outils

Pour les parcelles de terrain destinées aux projets BTP, le repérage et l'identification des phénomènes karstiques sont *a priori* l'objectif de la reconnaissance géotechnique préalable.
En Belgique, un laboratoire d'essais de sol en est chargé, qui déterminera pour l'essentiel la nature générale du terrain (roche, sol meuble), mesurera sa capacité portante et notifiera les anomalies éventuellement repérées (vide, couche de faible capacité). Ses principaux outils sont le

Figure 1 : Pointe de sondage de l'essai au pénétromètre

pénétromètre statique, le forage diagraphique et le forage avec prélèvement d'échantillons. L'emploi du pressiomètre, très prisé en France, est rare.
Le principe de l'essai au pénétromètre est simple : au moyen d'un engin lesté, un vérin enfonce une pointe à géométrie normée dans le sol, la force nécessaire à la pénétration de la pointe est mesurée en continu (Fig. 1). Deux résultats sont mis en diagrammes : la résistance à la pénétration de la pointe uniquement (**qc**) et la force nécessaire à l'enfoncement de tout le train de tiges (**Qst**) (Fig. 2). L'essai est normé sous la référence NF EN ISO 22476-12.
Les essais au pénétromètre et les forages sont des essais d'exécution simples et rapides. Ils sont donc aisément reproductibles, peuvent être multipliés et leurs résultats comparés ce qui explique qu'ils sont à la base de tout projet de construction en Belgique.

3. Le cas de Warchin

Warchin est une localité à l'ouest de la Wallonie. Dans le cadre d'un projet de future station d'épuration, une reconnaissance géotechnique préalable y a été menée.
À la lecture de la carte géologique de Wallonie, le site d'implantation était occupé d'une couche peu épaisse d'alluvions modernes quaternaires sur un éventuel reliquat de sables thanétiens (Formation de Grandglise), le tout directement établi sur le socle rocheux carbonaté tournaisien (Formation de Warchin).

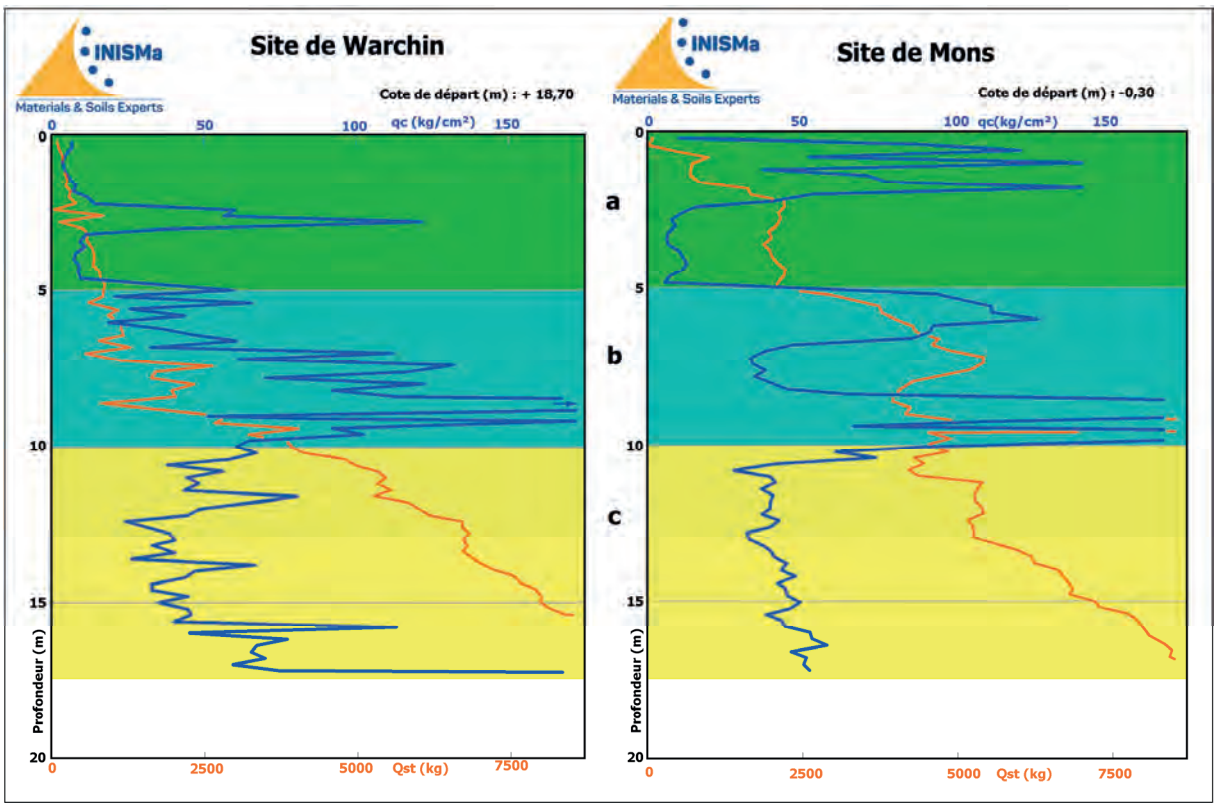

Figure 2 : Exemples de résultats pénétrométriques du site de Warchin sur socle carbonaté (partie gauche) et d'un site en plaine alluvionnaire à Mons (partie droite). Nature des couches : à Warchin, remblais et alluvions fines (couche a), fantôme de roche (couches b et c) ; à Mons, remblais et alluvions fines (couche a), alluvions sableuses et graveleuses (couche b), argiles yprésiennes (Formation d'Orchies) (couche c).

L'interprétation classique des diagrammes de résultats de la reconnaissance préalable du site de Warchin, dans un contexte de vallée à dépôts alluvionnaires, avait cependant conclu à la présence d'épaisses couches d'alluvions limoneuses, sableuses et argileuses, ainsi qu'à l'absence du socle rocheux, jusqu'à plus de 15 m de profondeur (Fig. 2-gauche). Ses diagrammes de résultats sont en effet très proches visuellement de ceux d'un site reconnu en plaine alluvionnaire comme il en existe à Mons par exemple (Fig. 2-droite). En outre, jusqu'à plus de 30 m de profondeur, les forages réalisés à Warchin ont averti de la présence d'un sol meuble de teinte noire, assimilé habituellement à de la tourbe.
L'ensemble de ces résultats relevaient un contexte géotechnique très défavorable au projet de construction : la tourbe étant un sol d'assise très compressible, des fondations de type pieux, fichés sous cette épaisse couche de teinte noire, à très grande profondeur, étaient envisagés. La viabilité du projet était menacée.
Dans un second temps toutefois, une nouvelle interprétation de ces résultats a eu lieu, qui intégrait la connaissance de la fantômisation des socles rocheux carbonatés. Sur ces nouvelles bases, le sol meuble de teinte

noire a pu être reconnu comme un vaste fantôme de roche. Celui-ci est en fait présent dès la base des alluvions limoneuses quaternaires à 5 m de profondeur.
La station d'épuration a été construite. Sa fondation sur pieux a été abandonnée afin de ne pas déstabiliser par les travaux de forage les équilibres existants au cœur de l'importante masse du fantôme de roche. La station d'épuration est fondée sur une épaisse dalle de béton armé « flottante » sur le fantôme de roche. À l'examen des diagrammes de résultats, celui-ci demeurait en effet suffisamment portant pour être considéré comme un sol d'assise satisfaisant, au moins à l'égal d'un sol meuble de fondation classique quaternaire ou cénozoïque.

4. Le cas de Peruwelz

Peruwelz est une autre localité de l'ouest de la Wallonie. Au cours des travaux de terrassement d'un vaste bâtiment industriel, un sol meuble de teinte noire a également été découvert jusqu'à plus de 4 m de profondeur (Fig. 4).
La carte géologique de Wallonie y mentionnait pourtant la présence du socle rocheux carbonaté viséen (Formation de Lens ou Formation de Basècle) quasiment affleurant.

Figure 3 : Fouille de reconnaissance du sol meuble de teinte noire lors de travaux de terrassement à Péruwelz.

En première approche, interprétée comme une hétérogénéité locale, la question de sa purge a été posée. Il pouvait s'agir d'une poche d'alluvions tourbeuses ou bien de « dépôts wealdiens » tels que décrits par les anciens auteurs (Marlière, 1934).
Un second examen visuel approfondi du sol meuble de teinte noire a toutefois permis de l'identifier comme le fantôme de roche au sommet du socle rocheux.
La purge a été évitée, qui aurait pu se poursuivre profondément sur la totalité de la zone de bâtisse et exiger une révision complète des moyens de fondation et d'exécution du futur bâtiment.

À la connaissance de l'auteur, au cours des travaux de reconnaissance géotechnique ou de terrassement, le fantôme de roche se présente essentiellement sous deux formes : un sol meuble argileux de teinte noire et huileux (tel un proto-pétrole) ou un sol meuble sableux de teinte grise et friables (Fig. 4 & 5).

Figure 4 : Fantôme de roche d'aspect argileux et huileux au pied du spéléologue. La photo est prise dans la galerie de la grotte Quentin (carrière de Nocarcentre, Ecaussinnes) (Quinif & Maire, 2009).

Figure 5 : Fantôme de roche d'aspect sableux et friable. La photo est prise dans une excavation pour assise d'éolienne (Beaumont).

On notera que depuis la nouvelle version de la carte géologique de Wallonie, la Formation du Hainaut, qui était destinée à remplacer l'ancienne dénomination des « dépôts wealdiens », a été élargie aux « argiles de décalcification témoins de la karstification » du sommet des calcaires carbonifères.

5. Le cas de Soignies

Dans le cadre de la construction d'éoliennes dans la région de Soignies, les essais au pénétromètre et forages de la reconnaissance géotechnique préalable ont montré la présence d'un socle carbonaté karstifié. Une campagne de forages diagraphiques complémentaires a été exécutée. Ceux-ci montrèrent la présence de nombreux niveaux karstifiés jusqu'à minimum 40 m de profondeur.
L'auteur attire dans ce cas l'attention sur l'inadéquation des moyens de forage mis en œuvre dans un contexte reconnu comme karstifié. S'agissant de forages instrumentés devant pénétrer de la roche jusqu'à grande profondeur, une machine de forage puissante a été employée couplée à un compresseur à air tout aussi puissant afin de chasser aisément à l'avancement les débris de roche hors des trous. La conséquence en a été des pertes de l'air injecté au sein du socle rocheux, qui remontaient localement en colonne jusqu'à 3 à 6 m de distance du trou en cours de forage (Figure 6). Les moyens trop énergétiques employés ont perturbé les équilibres des matériaux remplissant les niveaux karstifiés.
Après un épisode pluvieux intense, un effondrement s'est produit à l'aplomb d'un des forages. Et lors de l'exécution des pieux de fondation, d'importantes pertes de coulis de

Figure 6 : Remontées de l'air injecté en cours de forage.

béton ont été observées avec surconsommation de 100 % à 400 % pour certains pieux.

6. Discussions

En Wallonie, le secteur du BTP est confronté aux formations carbonatées et à leur karstification. Leur connaissance et les outils de leur auscultation leur manquent cependant. L'interprétation des essais au pénétromètre est incertaine dans les sols rocheux et/ou fortement hétérogènes wallons : « refus » précoces, faible représentativité des résultats. La connaissance de l'altération particulière par karstification des socles rocheux carbonatés, et d'autant plus par fantômisation, est encore trop parcellaire parmi la communauté belge des ingénieurs BTP.
Il en résulte souvent une inadaptation des moyens d'exécution et de fondation employés, et donc des difficultés d'exécution, des délais imprévus et finalement des surcoûts, qui s'emballent parfois jusqu'à menacer les projets de construction.

7. Conclusion

Afin que les projets de construction puissent mieux s'adapter aux spécificités des socles rocheux carbonatés, il est essentiel que la recherche progresse en ce domaine, mais aussi que les connaissances accumulées puissent se transmettre aux opérateurs, ingénieurs et aménageurs du secteur du bâtiment et des travaux publics.

Remerciements

L'auteur remercie le Prof. Yves Quinif pour ses recherches et ses efforts constants de vulgarisation envers ses élèves des sciences appliquées ainsi que pour son aide à la rédaction de cet article.

Références

DUBOIS C., QUINIF Y., BAELE J.-M., BARRIQUAND L., BINI A., BRUXELLES L., DANDURAND G., HAVRON C., KAUFMANN O., LANS B., MAIRE R., MARTIN J., RODET J., ROWBERRY M.D., TOGNINI P. and VERGARI A., 2014 - The process of ghost-rock karstification and its role in the formation of cave systems. *Earth Science Reviews*, 131 : 116–148.

MARLIERE R., 1934 - Argiles et sables wealdiens du Hainaut, *Bulletin de l'Association des Ingénieurs de Mons*, n°48, pp. 1-57.

QUINIF Y, 2010 – *Fantômes de roche et fantômisation – Essai sur un nouveau paradigme en karstogenèse*. Karstologia Mémoires, 18 : 196p.

QUINIF Y. et MAIRE R., 2009 – La grotte Quentin (Hainaut, Belgique) : un modèle d'évolution des fantômes de roche, in *Le karst, indicateur performant des environnements passés et actuels*, Karstologia Mémoires, 17 : 214-218.

From ghost rock to concretion: the formation of alterite crisps*

Lionel BARRIQUAND(1) & Vasile HERESANU(2)

(1) Université Savoie Mont Blanc, Laboratoire EDYTEM - UMR5204, Bâtiment « Pôle Montagne », 5 bd de la mer Caspienne, 73376 Le Bourget du Lac cedex, France, lionel.barriquand@wanadoo.fr
(2) Aix-Marseille Université-CNRS, CINaM, Campus de Luminy, case 913, 13009 Marseille, France.

** For speakers of North American English "crisps" = "chips"*

Abstract

The formation of the Balme Cave at Azé (France) is linked to the process of ghost-rock karstification. At several places in the cave, ghost-rock is still present. There are now very few flows of seepage water in the cave and these are localized at only four places over a length of 500 metres. The discovery in 2020 of one of these locations, the Salle du Palindrome, revealed the existence of a type of formation apparently hitherto unrecognized: alterite crisps. The altered rock has undergone cycles of hydration and dehydration which has led to the formation of mud-cracks on the walls and roof of the cave. As a result of these alternations, segments of alterite at the surface have shrunk, thus forming crisps which were then reinforced by a deposit of calcite. When the mass of these crisps became too great, gravity caused them to break off and fall to the floor of the cave. This led to the accumulation of crisps in a layer several decimetres thick which was observed on the floor of the Salle du Palindrome.

Résumé

Du fantôme de roche aux concrétions : la formation des chips d'altérite. La formation de la grotte de la Balme à Azé (France) est liée à un processus de fantomisation. En plusieurs points de la grotte le fantôme de roche est encore présent. Les écoulements d'eau d'infiltration dans la cavité sont rares et localisés (4 locus pour un développement de 500 m). La découverte d'un de ces locus, la salle du Palindrome, en 2020 a permis de confirmer l'existence d'une formation originale : les chips. La roche altérée a subi des cycles d'hydration-déshydration qui conduisent à la formation de *mud-cracks* sur les parois et la voûte. À la surface, la partie altérée se rétracte du fait de ces alternances. La chips d'altérite qui se forme alors est ensuite consolidée par un dépôt de calcite. Lorsque sa masse est trop importante, elle se détache par gravité et tombe au sol. Ainsi une accumulation de plusieurs décimètres d'épaisseur de chips a pu être observée sur le sol de la salle du Palindrome

1. Introduction

The Balme or Prehistoric Cave of Azé is situated near the village of Azé in Southern Burgundy (France). It has developed in limestones dating from the Upper Bajocian to the Lower Bathonian. Its length today is around 500 m. Most of its known network has been discovered as a result of continual removal of obstructions since 1963. Studies undertaken in the cave since the mid-2000s show that its speleogenesis is linked to fantomisation (DUBOIS et *al*, 2014). The cave contains few speleothems. These are grouped in three zones around 60, 130 and 160 m from the entrance and include two calcite blockages which have closed the cave at 60 and 160 m. In February 2020, the discovery of the Salle du Palindrome 340 m from the entrance proved to be not only novel for this network (an empty chamber) but also surprising for the original speleothems it contained: alterite crisps (Fig. 1).

Figure 1: Alterite crisps, speleothems on the wall of the Salle du Palindrome in the Balme Cave at Azé (photo S. Caillault).

2. Materials and methods

For this study we had at our disposal some bibliographic data:

- a detailed study of the nature of the surrounding rock (DESCHAMPS et *al*, 2014). In the course of this study, the strata were systematically sampled then analysed through examination of thin layers under the microscope.
- Studies on the ghost-rock and alteration of the surrounding limestone (BARRIQUAND et *al*, 2012, 2015).

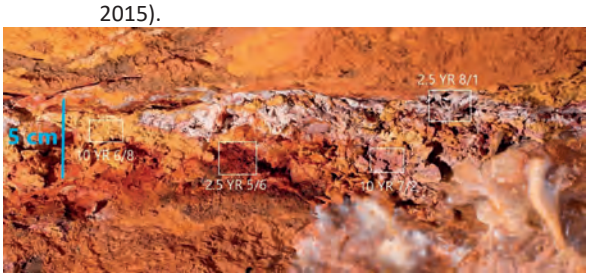

To complete these data, we used XRD to analyse samples taken from Upper Bajocian limestones:
- one of the crisps
- samples of alterite in a weathered zone of the Salle du Palindrome (Fig. 2)
- samples of alterite and of more or less altered limestones on the walls of the Baïonnette (about 200-220 m from the cave entrance).

The XRD measurements were taken using a theta-theta diffractometer, a Panalytical X'pert Pro equipped with a high-speed X'celerator detecter. The diffractograms were then analysed using X'Pert HighScore software: identification of the crystalline phases and semi-quantitative analysis (using the RIR from the PDF – ICDD files). The semi-quantitative results were considered only for phases with sufficiently intense peaks.

Figure. 2: Fantomised limestone in the Salle du Palindrome and sample positions for XRD analysis (photo S. Caillault).

3. Results

In terms of its geological context, the Salle du Palindrome lies in a stratigraphic unit more than 13.6 m thick. It is made up of pluri-decimetric layers which are quite uniform in their thickness and lithofacies. This is a sandy, clayey limestone which contains few faunal remains. Iron oxides are visible either in the form of coloured bands or pigment in the rock. In places this staining is absent because of leaching linked to the alteration of the limestone. These limestones have undergone the phenomena of dolomitisation and dedolomitisation.

The study dealing with the formation of the cave has shown that, in a part of this zone of the cave, the limestone is very altered and very often only alterite remains. In places it has been transformed into a sandy sediment, so much so that when cavers were removing obstructions, they had difficulty in distinguishing it from the sediments they were removing.

Granulometric analyses show that the alterite consists of clays (25% by mass), silts (45% by mass) and sands (30% by mass).

Mineralogical analysis by XRD (Fig. 3) shows that quartz and calcite are the principal constituents of the samples. However, two types of calcite can be distinguished: pure calcite, and magnesian calcite indicated by a shift of the calcite peaks towards greater 2theta angles. In certain cases, the shift of the peaks is too weak to affirm the presence of magnesium in the calcite. Muscovite is also omnipresent in the form of traces in all of the samples except for one where together with quartz it makes up the majority. These crystalline phases are also associated with iron oxides (haematite and goethite) and silicates (kaolinite and orthoclase).

Place		color (Munsell Chart)	Weathering	Calcite	Magnesian calcite	Quartz	Muscovite	Hematite	Goethite	Kaolinite	Microcline-orthoclase-potash feldspath
				(%, clear presence = X, possible presence = ?)							
La Baïonnette	Wall	10R 4/6	yes in surface		17	83	X	X	?		
		10R 3/4		6		94	X		X	X	X
		10YR 6/8			10	90	X		X	X	X
		10R 2,5/2				53	45	2			
		5Y 2,5/1		4		91	X		4		X
		5Y 7/2			21	79	X	1			
		10R 5/6		7		91	X	X			X
		10R 5/8	no	36		63	X	1		X	X
		10R 5/3			45	52	X	1	2		X
Palindrome	Wall	2,5YR 3/6	yes in depth	68		31	X	?	1		X
		10 YR 6/8		74		26	X	X		X	
		2,5YR 8/1		88		12	X				
		10YR 7/2		89		11	X				
	Crisps	10YR 5/8	/	70		30	X				X

Figure 3: Results of XRD analyses of altered and non-altered Upper Bajocian limestones in the Azé Caves as well as of one of the crisps. Percentages are given only for the phases where the quantity is sufficient (the peaks are large enough).

Most of the calcite in the samples from the Baïonnette is a magnesian calcite. For the others, with one exception, the analysis of the peaks of diffraction has shown a shift sufficient to distinguish magnesian calcite from pure calcite.

In contrast, all of the calcite in the samples from the Salle du Palindrome is pure calcite.

Regarding the calcite/quartz relationship, we can say that the samples from the Baïonnette are richer in quartz (52 – 94 %) than those from the Salle du Palindrome (11 – 31 %).

4. Discussion

The alteration of the Upper Bajocian limestones enabled the formation of the Balme Cave through a process of fantomisation. Part of the residual alterite is still in place as shown by studies of this limestone and its alteration.

At the Baïonnette, the limestone has been greatly altered. Despite the phenomena of dolomitisation and dedolomitisation, iron oxides and silicates are still more or less present in the limestone.

This is also the case for one of the samples from the Salle du Palindrome. For the two others hardly any of these elements are present. Only muscovite, which is a mica very resistant to hydrolysis, is still present.

The sample of one of the crisps contains only muscovite and microcline-orthoclase which is a potassium feldspar. It is therefore a product of very altered limestone where only the least soluble elements have remained.

At the Baïonnette, quartz is the major component of all the samples (between 52 and 94 %). This is not the case for the Salle du Palindrome where it makes up no more than 31% of a sample. This difference in composition has led to structural differences in the alterite. At the Baïonnette the alterite is in the form of a silty, sandy sediment because of the high proportion of quartz. In the Salle du Palindrome the alterite has a more plastic consistency because of its more clayey, silty composition.

The Salle du Palindrome contains speleothems which are a result of flows of seepage water in winter followed by dry periods in summer. The clay, a product of the alteration of feldspars, still present in the rock, in all likelihood undergoes phases of dehydration. At these times it shrinks but remains partially attached to the wall (Fig. 4). The deformation of the crips is linked to a differential desiccation between the faces exposed and not exposed to water.

Figure 4: Alterite crisps, centimetric in size, partially detached from the surface of the wall in the Salle du Palindrome (photo S. Caillault).

A new arrival of seepage water at the end of autumn causes a film of water rich in calcium carbonate to form on the surface of the wall which causes a deposit of calcite to form on the crisps, “fossilising” them on the surface of the wall.

The successive deposits of calcite little by little increase the weight of the crisps which finish by totally detaching from the wall and falling to the floor of the cavity. The repetition of these cycles leads to an accumulation of these speleothems on the cave floor. In the Salle du Palindrome, this has reached a thickness of about 30 cm (Fig. 5). The presence of pure calcite in the samples from the Salle du Palindrome is evidence that this has been formed on the crisps and does not come from the original limestone.

Figure 5: Accumulation of crisps on the floor of the Salle du Palindrome.

5. Conclusion

The discovery of the Salle du Palindrome led to the discovery of a new type of speleothem: crisps. These are a result of residual alterite from ghost rock, the phenomena of dehydration of feldspars, and finally their fossilisation by a deposit of calcite. With time they become increasingly heavy and finish by falling and forming an accumulation on the cave floor below the wall.

Acknowledgments

Thanks to Bob Norington for his translation.

References

BARRIQUAND L. and J., BAELE J.-M. and *al*. (2012) Les Grottes d'Azé (Saône-et-Loire, France) : de la roche altérée aux sédiments. *Karstologia*, n° 59, 19-32.

BARRIQUAND L., QUINIF Y., BAELLE J.-M., DECHAMPS S., GUILLOT L. et PAPIER S. (2015) La karstification par fantômisation : le cas du Mâconnais. *Actes des 24èmes Rencontres d'octobre*, Conseil Départemental de Saône-et-Loire, Spéléo-Club de Paris, 99-115.

DECHAMPS S., BOULVAIN F., BARRIQUAND L. and *al*. (2014) *Grottes d'Azé, Saône-et-Loire, France : contexte géologique et encaissant calcaire jurassique*, Imprimerie du Conseil Général de Saône-et-Loire, 85 p.

DUBOIS C., QUINIF Y., BAELE J.-M., BARRIQUAND L. and *al*. (2014) The process of ghost-rock karstification and its role in the formation of cave systems. *Earth-Science Reviews*, n°131, 116-148.

Ghost rocks and hypogene mineralization: Questions raised by the Grande Vernissière mine complex (Gard, France).

Laurent BRUXELLES[1,2] & Michel WIENIN[3]

(1) TRACES, UMR 5608 du CNRS, 5 Allées Antonio Machado 31058 Toulouse, France. Laurent.bruxelles@inrap.fr
(2) GAES, University of the Witwatersrand, Johannesburg, South Africa
(3) Parc National des Cévennes et Société cévenols de spéléologie et de Préhistoire, Grand'Rue, 30360 Vézénobres, France. michel@wienin.com

Abstract

In cavities inherited from ghost rock weathering networks, the alterite is rarely observed as most of it has been removed by erosion and the galleries are largely reshaped. So, we looked for old mines to search for *in situ* ghost rocks artificially recut. The Grande Vernissière mine complex was dug in the 19th and 20th centuries, in particular for the exploitation of lead and zinc. We found very clear examples of ghost rocks but also extensive hypogene mineralization (fluorite, barite). This assemblage is very interesting as it raises the question of the links between this case of ghost rock weathering and hypogene mineralization dating from the Eocene. Does this ghost rock have an hypogene origin or does it correspond to another stage of weathering, depending on hydrogeological, geological or geomorphological evolution?

Résumé

Roches fantômes et minéralisations hypogènes : Questions soulevées par le complexe minier de la Grande Vernissière (Gard, France). Il est très rare de retrouver l'altérite initiale dans les grottes que l'on suppose avoir initiées par un processus de fantômisation. La plupart du temps le fantôme, très fragile, a été entièrement emporté par la poursuite du processus de karstification qui a largement remodelé les conduits. La mine de la Grande Vernissière a été creusée durant le 19e et le 20e siècle pour l'exploitation du plomb et du zinc. Dans ces cavités artificielles, nous avons trouvé des exemples de fantômes très bien préservés ainsi que des indices de minéralisations d'origine hypogène (fluorite, barite). L'association entre les fantômes de roches et ces minéralisations incite à se poser la question de leurs liens génétiques. Est-ce que ces altérations se sont formées lors de la mise en place de ces minéralisations, à l'Eocène, ou est-ce qu'elles répondent de conditions plus tardives, en fonction d'un nouveau contexte géologique, géomorphologique et hydrogéologique ?

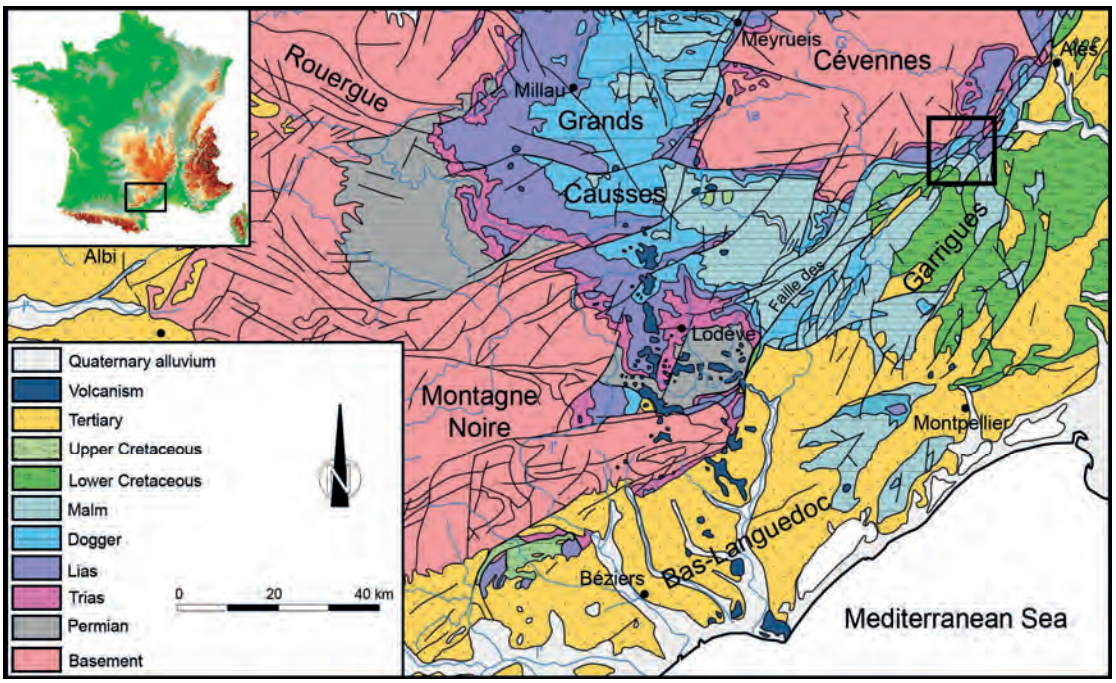

Figure 1: Geological map of the centre of the Southern part of France and localization of the studied area.

1. Introduction

Our work along the Cévennes border has shown that part of the caves originates from ghost rocks formation (BRUXELLES & BRUXELLES, 2002; BRUXELLES, 2010). That means that their formation was initiated by an isovolume alteration phenomenon developed in a context of low hydraulic gradient allowing the alterite to remain *in situ* (VERGARI, 1998; QUINIF, 1999, 2010; QUINIF & BRUXELLES, 2011; DUBOIS *et a*l., 2014). The extremely porous residual alterite is then evacuated by karstic water flows when a sufficient gradient appears. The voids are then reshaped by phreatic, epiphreatic and vadose evolution and thus, it is rare to find any remains of the initial ghost rock in these caves.

Like the Belgian quarries, where this phenomenon has been widely studied (e. g. VERGARI, 1998; QUINIF, 1999 and 2010), we looked for artificial structures likely to intersect nicely preserved ghost rocks. All along the Cévennes border, on the southern edge of the Massif Central, lead, zinc and silver mines have been exploited since at least Antiquity. They were dug in the limestone and dolomite of the Lias (early Jurassic). The idea was therefore to look for signs of ghost rocks in mines, as they have not undergone an evolution as complex as natural karst cavities, and thus, it should be possible to find residual alterite there.

2. Materials and methods

The Grande Vernissière mine, located in the town of Fressac (Gard, Occitanie, France) was exploited during Antiquity, Medieval times and then in the 19th and 20th century. It is several hundred meters long and formed in the same lithological context as the nearby 10 km Trabuc cave (BRUXELLES, 2003).

This mine is located in the Cévennes border (Fig. 1), a fairly tectonized strip located between the crystalline Cévennes and the Jurassic and Cretaceous limestones plateaus (*Garrigues*). It is part of a set of mineralized deposits that affects a quadrangular bulge located between the main sections of the Cévennes fault (PERISSOL, 1990). The mine galleries were dug in the limestones and dolomites of the Sinemurian, which are locally clayey and include frequent siliceous cherts.

Mineralization mainly affects these bedded limestones, creating various facies. They are Mississippi Valley type mineralizations, consisting mainly of calcite, dolomite, with fluorite including galena and sphalerite. Their origin has been debated for nearly fifty years, but recent studies has confirmed the role of hypogenic ascending flows (ROUVIER *et al*., 2001; JOST *et al*., 2004). The hypogene processes were dated from the Lower to Middle Eocene, and are believed to be due to gravity hydrogeological loops linked to the uplift of the Pyrenees. The mineralizing fluids were brought up along the Cévennes border, following the fractures and the most porous rocks.

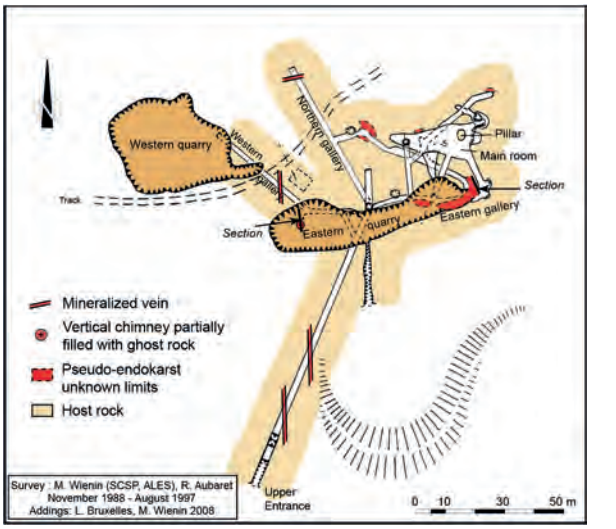

Figure 2: Map of La Grande Vernissière Mine showing the main ghost rocks occurrence.

3. Results

During the survey of the mine, more than thirty rock ghosts were identified and plotted on the map (Fig. 2). A typology of these ghost rocks can be proposed:

- Several mineralized veins are associated with a loose altered fringe. Vertical or inclined a few degrees, they do not exceed a few tens of cm in thickness. When these veins intersect the limestones, the weathered walls are clayey and orange. In contrast, in dolomite, the alterite is sandy and grey.
- Locally, vertical chimneys have been crossed by the mine galleries. Several meters wide, they are in the process of being emptied but mostly choked by the *in situ* alterite. They are more than 20 m in height and the process of collapse of the alterite is ongoing.
- Large amounts of ghost rocks also developed under a well-lithified limestone vault (Fig. 3). Mining works have sometimes cross them and we can easily recognize the pseudo-endokarsts therein (VERGARI, 1998; QUINIF, 1999). Here, the ghost rock developed horizontally, following the lithological contrasts exploited by the slow water flow. In the *in situ* alterite, one can recognize the continuous beds of cherts but we also the initial nature of the rock, depending on whether it consists of orange clay or dolomitic sand (Fig. 4 and 5).

Figure 3: Example of in situ ghost rock (light) preserved on a hard roof. Removed alterite is accumulating at the bottom of the wall.

Figure 4: Contact between the ghost rock and the limestone wall. Deformed cherts layers can be followed from the host rock to within the alterite, with the same tilt.

4. Discussion

It is interesting to note that whenever the galleries have intersected a ghost rock, it is associated with mineralization. On the other hand, not all mineralization is accompanied by ghost rocks. It is therefore difficult to genetically associate these two phenomena. In fact, some mineralization forms geodes or veins within the alterite (Fig 5). They are unlikely to have settled in the ghost rock without permeating it more diffusely due to its porosity. It is more logical to think that the ghost rock weathering occurred as a second step, not necessarily affecting all the mineralized zones.

Thus, two hypotheses can be proposed for ghost rock development:

- It occurs just after the mineralization period, while the hypogenic fluids still travel through the discontinuities. It could happen at the end of the mineralization process with probably a different chemistry although one still aggressive towards the carbonates.
- It occurs much later than mineralization and arises *per descensum* water flow. The hydrothermal feed is gone and the water, of epigenic origin, slowly flows into the carbonates, exploiting the discontinuities and parts of the mineralized veins that encompass the alterite.

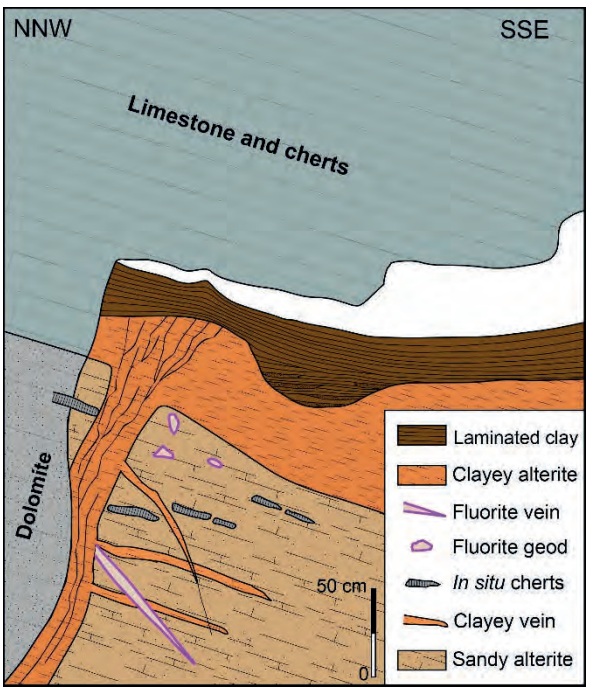

Figure 5: Section of the dead end of the northern gallery (see Fig. 2) where we can see the edge of a large ghost rock developed at the contact between dolomite and limestone.

5. Conclusion

At this stage, it is not possible to separate the two processes that gave rise to these ghost rocks, but other mines exist in this area, which may provide additional information to help discriminate the origin of the waters responsible for the formation of these ghost rocks.
A geochemical approach is also to be considered and could provide additional information.
In any case, the existence of hypogenic ghost rocks is theoretically quite possible. If the chemical conditions are met but the flow doesn't have sufficient competence to export the insoluble residues, this will lead, as for the *per descensum* ghost rocks, to the development of loose volume of alterite within the carbonates. Later, when the base level drops, these discontinuities will be exploited by more dynamic circulations and results in the formation of cavities. The beginning of this process can be observed at the top of the ghost rocks in this mine where bedded clays lie in a gully cut in the alterites (Fig. 5).

Since the cessation of mining, successive collapses have formed in weathered chimneys, contributing to the ghost emptying, a fast process. Furthermore, on a geological time

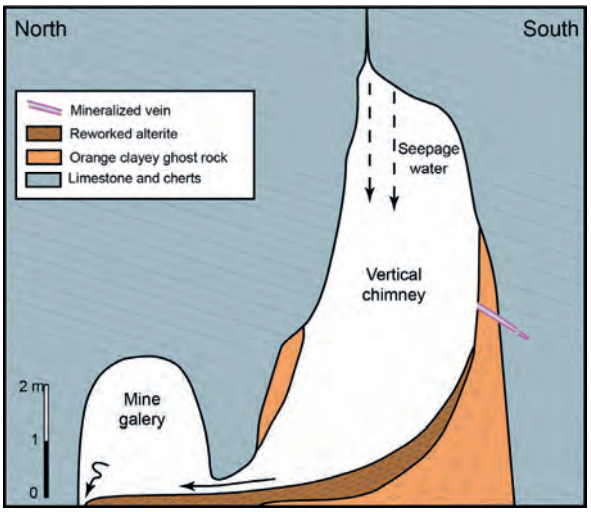

Figure 6: Vertical chimney created by the natural removal of the ghost rock after the abandonment of the mine.

scale, as large vertical chimneys were already emptied from the bottom after mine abandonment, only small amounts of seepage water come from the surface through cracks (Fig. 6).

In any case, the numerous ghost rocks found in this mine significantly show how these limestones are deeply weathered. It allows us to observe, for the first time, very demonstrative examples of pseudo-endokarst that are very rare (Fig. 7) and confirms the origin of maze caves like Trabuc cave in comparable contexts.

Figure 7: This dead-end of the northern gallery of the mine terminates on in situ pseudo-endokarst ghost rock. The section represented in Fig. 5 is located behind the caver.

References

BRUXELLES L. et BRUXELLES S. (2002) La chasse aux fantômes dans les Grands Causses. Utilisation d'un nouveau concept de spéléogenèse dans la recherche de cavités. Spelunca, 88, 2003, 14-20.

BRUXELLES L. (2010) La grotte de Trabuc : fantômisation et karst polyphasé. – In : Grottes et karsts de France. Karstologia Mémoires, n° 19, Association française de karstologie, 306-307.

BRUXELLES L. et WIENIN M. (2009) Les fantômes de roche de la mine de la Grande Vernissière (Fressac, Gard). Premières observations sur l'origine de certains karsts de la bordure cévenole. Karstologia Mém. n° 17, Actes du colloque AFK - Pierre Saint-Martin 2007, 192-200.

DUBOIS C., QUINIF Y., BAELE J.-M., BARRIQUAND L., BINI A., BRUXELLES L., DANDURAND G., HAVRON C., KAUFMANN O., LANS B., MAIRE R., MARTIN J., RODET J., ROWBERRY M.D., TOGNINI P., VERGARI A. (2014) The process of ghost-rock karstification and its role in the formation of cave systems. Earth Science Reviews, 131, 116–148.

JOST A., VIOLETTE S., MACQUAR J.-C. et DROMART G. (2004) Rôle potentiel des paléo-circulations de fluides engendrés par l'orogenèse pyrénéenne dans la genèse des minéralisations plomb-zinc péri-cévenoles : essai de modélisation. Bulletin de la Société géologique de France, vol. 175, 4, 317-329.

PERISSOL M. (1990) Sédimentologie et métallogénie du Trias et du Lias carbonaté de la bordure cévenole. Thèse, Université de Montpellier II, 2ème partie, chap. 9, p. 293-397 et 3ème partie, chap. 2, 417-487.

QUINIF Y. (1999) Fantômisation, cryptoaltération et altération sur roche nue, le triptyque de la karstification. Actes du colloque Karst 99, 159-164.

QUINIF Y. (2010) Fantômes de roche et fantômisation – Essai sur un nouveau paradigme en karstogenèse. Karstologia Mémoires, 18, 196p.

QUINIF Y. et Bruxelles L. (2011) L'altération de type « fantôme de roche » : processus, évolution et implications pour la karstification. Géomorphologie, 2011, 4, 349-358.

ROUVIER H., HENRY B., MACQUAR J.-C., LEACH D. L., Le GOFF M., THIBEROZ J. et LEWCHUK M.-T. (2001) Réaimantation régionale éocène, migration de fluides et minéralisations sur la bordure cévenole (France). Bulletin de la Société géologique de France, 172, 4, 503-516.

VERGARI A. (1998) Nouveau regard sur la spéléogenèse : le "pseudo-endokarst" du Tournaisis (Hainaut, Belgique). Karstologia, 31, 12-1.

Altération à volume constant et modelé karstique en Préalpes : Bauges, Chartreuse (France)

Dorota JAROMIN

France, dorota.jaromin@gmail.com

Résumé

Altération à volume constant et modelé karstique en Préalpes : Bauges, Chartreuse (France). Des traces géomorphologiques d'altération à volume constant sont recherchées dans les Préalpes françaises. L'étude porte sur des cavités en Bauges occidentales et en Chartreuse orientale, dans une séquence sédimentaire allant du Jurassique moyen au Crétacé supérieur. Les éléments relevés sont de simples indices macroscopiques de terrain mais semblent orienter le faisceau d'indices en faveur de l'existence présente ou passée de fantômes de roche. Les implications d'une telle présence sont brièvement discutées, particulièrement sous le volet de la karstogenèse. Les résultats restent à confirmer par des études complémentaires mais offrent potentiellement un regard différent sur ces karsts de moyenne montagne. En effet, le modelé observé semble être la résultante d'une succession d'étapes, alternant fantômisation et genèse « classique » par enlèvement total de matière.

Abstract

Isovolumic weathering and karstic shape in Prealps: Bauges, Chartreuse (France). Geomorphological traces of isovolumic weathering are sought in French Prealps. The study concerns Western Bauges and Easter Chartreuse caves, in a sedimentary sequence from the Middle Jurassic to the Upper Cretaceous. Field observations are only macroscopic field indicators but constitute a cluster of clues in favour of present or past ghost-rocks existence. Implications of such a presence are briefly discussed, particularly in the karstogenesis section. Results remain to be confirmed by further studies, but potentially offer a new point of view on these mid-mountain karsts. Indeed, the observed shape seems to be the result of a succession of stages, alternating ghost-rock genesis, and "classical" genesis by total removal of material.

1. Introduction

Une grotte est le fruit d'une longue histoire et naît sous plusieurs facteurs et processus, comme le conceptualise RODET (2018). Chacune est la résultante d'une évolution morphologique qui chemine à la jonction entre contraintes régionales géologiques, paléogéographiques, et conditions locales de site (DANDURAND & MAIRE, 2011).

L'image mentale de la formation « classique » d'une grotte correspond à deux actions simultanées : dissolution et enlèvement total de matière (QUINIF et *al*., 2014). Néanmoins, lorsque ce dernier est partiel, une altération à volume constant peut se produire. Il se forme alors une altérite résiduelle nommée le « fantôme de roche » (QUINIF, 2010). Bien plus poreux que la formation mère encaissante, il en garde toutefois d'abord l'aspect, puis peut évoluer vers un stade d'altération *In Situ* plus poussé (DUBOIS et *al*., 2019). Les vides se forment ensuite dans un temps disjoint, par déstabilisation mécanique tels un tassement et/ou un remaniement, voire une évacuation (DANDURAND et *al*., 2019). La convergence entre les formes issues d'une voie « classique » et d'une fantômisation (QUINIF, 2014, 2018), est prouvée par observations In vivo à la grotte Quentin en Belgique (QUINIF & MAIRE, 2009). Le karstotype de DUBOIS et *al*. (2014) ainsi que l'holotype de DUPONT et *al*. (2018), en précisent les contours. Depuis leur découverte, en fin de siècle dernier, de nombreux fantômes sont apparus dans le monde (QUINIF & BRUXELLES, 2011). En France, ils sont régulièrement invoqués ou aperçus sur de nouveaux sites (DANDURAND et *al*., 2014, 2019 ; PIERRE et *al.*, 2017). Leur présence réinterroge le modèle de structuration régionale du développement des réseaux karstiques (MALCLES et *al*., 2020). Peut-on en trouver trace dans les Préalpes françaises, en Bauges et en Chartreuse (Fig.1) ?

Le terrain de recherche d'indices d'altération à volume constant a deux chevauchements en limite ouest : le frontal des Bauges et celui de la Chartreuse orientale. Au nord, il inclut l'ouest des Bauges occidentales, entre Semnoz, Nivolet, Peney, et Margériaz. Au sud, c'est le nord-est de la Chartreuse orientale, avec Granier, Alpette, Alpe et Pinet. Il est constitué d'une séquence sédimentaire allant du Jurassique moyen au Crétacé supérieur. Les dépôts de l'océan alpin y alternent calcaires puissants et niveaux plus marneux. Les marques tectoniques, plis et failles, abondent dans ce substratum déformé et cassé, dont les roches ont été plissées, fracturées, soulevées, abrasées. Au Quaternaire, les glaciations ont fini de façonner ce paysage de moyenne montagne (Fig.1). Depuis des décennies, spéléologues et scientifiques y ont découvert et documenté de vastes réseaux spéléologiques.

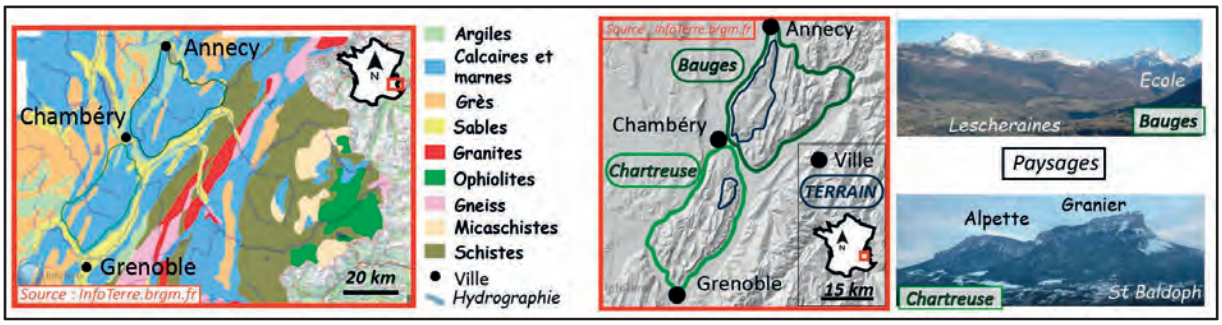

Figure 1 : Localisation, géologie et paysages.

2. Matériels et méthodes

Des indices géomorphologiques macroscopiques du paysage évoquant une altération à volume constant sont cherchés à partir de données issues du terrain. Pour en discriminer les formes, l'étude se réfère aux éléments décrits dans les processus de fantômisation par QUINIF (2010, 2014), DUBOIS et *al*. (2014), DUPONT et *al.* (2018), DUBOIS et *al.* (2019), DUBOIS & QUINIF (2019).

Pour cette étude, un recueil d'indices est d'abord mené dans la littérature : comptes-rendus d'activités de clubs, CDS 73 (1988, 1993, 2011), CDS 73 & SCS (2014, 2015), topoguides, FANTOLI (1996), magazines et revues, TESSANNE (2014, 2020), MANIGLIER & LESAULNIER (2015), ASAR et *al*. (2018), CHABOD (2020), publications scientifiques, HOBLÉA et *al*. (1996), REY (2016), JAILLET et *al*. (2018). Il recense des éléments de morphologie remarquables car compatibles avec un phénomène d'altération à volume constant. Textes, topographies, dessins et coupes, photographies évocatrices, sont les supports analysés.

Ce recueil indirect est non exhaustif. Il répertorie des sites potentiels. Ensuite, un examen direct du paysage karstique est dressé par quelques observations.

3. Résultats

En surface, sur les flancs des escarpements, une ligne paysagère peut être suivie. Elle se matérialise par une succession de porches métriques, bouchés, situés le long des strates. Sous terre, les réseaux s'organisent avec une grande verticalité, mais en concomitance avec de longues horizontalités. Les sites d'exsurgence ont des trop pleins actifs et des anciens exutoires délaissés. Certaines sources affleurent sous le niveau de base hydrologique actuel avec une sortie vauclusienne.

La lecture indirecte du modelé souterrain donne un paysage à galeries parallèles, avec étages horizontaux superposés, et parties de plan labyrinthique. Le réseau est ponctué de fossiles en relief dans la roche mère, surgissant de la surface, épinglés sur les banquettes et parois. Il est souvent orné d'anastomoses de voûte, quelquefois d'anneaux de Liesegang. Très hétéromorphe, il se lie aux faiblesses tectoniques et structurales, mais s'en détache aussi. De nombreux miroirs de failles sont décrits dans les salles. Le développement des galeries s'effectue en limite de strate, aux changements de faciès de la série sédimentaire. La grande salle, jusqu'à des longueurs hectométriques, à énormes blocs et tas de matériel fin quelques fois concrétionnés, avec murs d'argile métriques voire décamétriques, est décrite dans l'Hauterivien à son contact avec les calcaires à faciès urgonien. Dans ces derniers, elle est aussi citée dans les lentilles à orbitolines qu'ils incluent. Ceci contraste avec leur partie pure, à long méandre étroit pour des dizaines de mètres de haut. Il se dédouble ou plus, forme des voies parallèles et se réunifie, descend par boucles et baïonnettes à petite pente jusqu'à rejoindre une salle ou un autre réseau de tels méandres, mais d'altitude inférieure. La connexion entre méandres se fait par élargissements avec sol d'éboulis. Ce type de puits, pouvant atteindre des profondeurs impressionnantes, confère au réseau une forte part de sa verticalité. À la croisée des fins méandres pluridécamétriques, dans les évasements, une disposition qui interroge est la coexistence, à différents étages, de départs pour des salles volumineuses par des galeries dites fossiles, plus larges que hautes, à fond tapissé d'argile et avec de grands puits remontants.

Figure 2 : Indices sur terrain d'étude.

La toponymie des récits d'exploration et des topographies évoque la présence de matériel fin : efforts nécessaires pour équiper, progresser et désobstruer en conditions glaiseuses,

rivières et siphons de boue. La pratique de la spéléologie permet de confirmer cette présence récurrente et quantitative au sol et/ou sur les parois. De plus, des blocs de toutes tailles y sont inclus. Certains résistent en restant solides malgré la compression mécanique, d'autres sont détruits au toucher et perdent leur morphologie initiale d'encaissant, comme dans les salles des lentilles à orbitolines de Chartreuse. Les zones de paysage spéléologique fragile où la matière perd sa cohérence à chaque passage humain sont nombreuses. Du bloc au spéléothème, en passant par la varve et le sapin, les éléments déstructurés et déstructurables abondent. Sur de longues parties des parois à La Cavale sur la Feclaz, il y a une séquence varvée identique dans des niches différentes se situant au sein de la même section. À la grotte de Bange sur le Semnoz, de l'encaissant altéré est nettement visible.
D'autres éléments sont encore observés tels des blocs coincés en hauteur dans des méandres, des virages en baïonnette, des banquettes latérales perchées, des plafonds plats, des fossiles et silex en relief. L'ensemble des indices géomorphologiques (Fig.2) est relevé dans plus de quarante grottes au sein des unités géologiques du terrain.

4. Discussions

Cet inventaire se restreint à des éléments d'échelle macroscopique. Il est à poursuivre et à étendre à d'autres massif des Préalpes comme le Vercors.
Les indices connus indirectement ont des limites : peu d'échelles sur les photographies, pas de toucher ni de vue réelle, biais du ressenti des explorateurs sur l'interprétation. Mais ils sont la mémoire de paysages souvent remaniés et permettent de déterminer des zones à investiguer.
Les observations directes confirment qu'une partie du réseau karstique est comblé de matériel argileux, avec des blocs de différentes dimensions et de différentes textures. Des analyses de ce matériel et son encaissant préciseraient les lieux de présence d'altération à volume constant et ceux de comblement allochtone. Des datations des spéléothèmes scellant les remplissages pourraient permettre de poser des dates sur une chronologie relative.
Les indices semblent plaider pour l'existence d'épisodes de conditions favorables à une altération à volume constant, entrecoupés de genèse « classique » par enlèvement total. Reste à en chercher le nombre et les modalités d'inscription dans l'histoire de la karstogenèse. Ainsi, la zone à îlots de Liesegang sous l'anticlinal de Lachat pourrait être la relique d'une phase de saturation.
La cohérence entre la présence de fantôme, son état d'altération et son stade de mobilisation pourrait conduire à l'élaboration de scenarii de spéléogenèse à l'échelle de la grotte, du système karstique, du massif, et des Préalpes. Il y aurait là, alors, une archive paléogéographique inédite.

5. Conclusions

Après cette étude, deux constats morphologiques peuvent être faits concernant le modelé karstiques dans les Bauges et en Chartreuse. Le premier est géométrique : le modelé pariétal et la forme des réseaux semblent compatibles avec des processus de fantômisation. Le second est la présence de matériel de faible granulométrie à toute profondeur : dans les porches, méandres et salles, au sol et sur les parois. Or, l'altération à volume constant produit de la roche à grande porosité d'interstice et faible tenue mécanique, malléable et déstabilisée instantanément par un déséquilibre. Le paysage karstique pourrait donc porter la signature d'un ou de plusieurs temps de genèse des vides par altération des formations à volume constant. Ces temps seraient entrecoupés d'épisodes de formation « classique ». Dans ce cas, étudier les morphologies souterraines des Préalpes doit prendre en compte la convergence de formes, entre celles issues d'une karstogenèse « classique » et celles issues d'une fantômisation. De plus, l'existence d'une telle géodiversité potentielle serait à faire connaître car sa vulnérabilité est grande.

Enfin, si les indices trouvés révèlent des zones à fantômes, alors le spéléologue d'exploration y trouvera un nouvel angle de vue orientant ses prospections et désobstructions.

Remerciements

Merci à tous les spéléologues que j'ai eu l'honneur de rencontrer : CDS 38, CDS 73, ASAR, SGCAF, SCS, Ursus, Speleus.

Références

ASAR, BONVALLET O., CORMIER F.-E., DECKER Y., KLEINMANN S., LEGAT C., LEMAIRE L., VAJDA P. (2018) Le creux 222. Spelunca, n°149, 7-14.

CDS 73 (1988) Le Margériaz. Grottes de Savoie, n°14, 191 p.

CDS 73 (1993) L'aventure souterraine en Savoie. Ed. GAP La Ravoire, 302 p.

CDS 73 (2011) Explorations spéléologiques en Savoie et sur les massifs limitrophes. Grottes de Savoie, n°15, 120 p.

CDS 73, SCS (2014) Atlas du Granier souterrain. Grottes de Savoie, n°17, 240 p.

CDS 73, SCS (2015) Le réseau de la Doria. Grottes de Savoie, n°18, 258 p.

CHABOD P.-O. (2020) Trou souffleur n°5. Spéléo Magazine, n°112, 21-26.

DANDURAND G., MAIRE R. (2011) Essai de typologie des cavités du karst de la Rochefoucauld (Charente) : Rôle de la "fantômisation" crétacée Du battement de la

nappe et de l'effet de site. Dynamiques Environnementales, n°27, 101-118.

DANDURAND G., DUBOIS C., MAIRE R., QUINIF Y. (2014) The Charente karst basin of the Touvre: alteration of the Jurassic series and speleogenesis by ghost-rock process. Geologica Belgica, Vol. 17, 27-32.

DANDURAND G., QUINIF Y., GUENDON J.-L., GRUNEISEN A. (2019) Sources vauclusiennes et fantômes de roche. Karstologia, n°74, 31-46.

DUBOIS C., QUINIF Y. (2019). The ghost-rock of the Chansin quarry (Belgium) - A remarkable example of pseudogallery. Geologica Belgica, Vol. 22, 175-181.

DUBOIS C., QUINIF Y., BAELE J.-M., DAGRAIN F., DECEUSTER J., KAUFMANN O. (2014) The evolution of the mineralogical and petrophysical properties of a weathered limestone in southern Belgium. Geologica Belgica, Vol. 17, 1-8.

DUBOIS C., GODERNIAUX P., DECEUSTER J., POULAIN A., KAUFMANN O. (2019) Hydrogeological characterization and modelling of weathered karst aquifers. Applicability to dewatering operations in limestone quarries. Environmental Earth Sciences, Vol. 78 n°3, 78-99.

DUPONT N., QUINIF Y., DUBOIS C., CHENG H., KAUFMANN O. (2018) Le système karstique de Sprimont (Belgique). Holotype d'une spéléogenèse par fantômisation. BSGF Earth Sciences Bulletin, Vol. 189 n°1, 1-22.

FANTOLI J.-L. (1996) Les plus belles verticales, massifs Alpe, Alpette, Granier, spéléo guide Chartreuse. Ed. Arcanes project La Ravoire, 168 p.

HOBLEA F., DODELIN C., LASSERRE D., BOTTAZZI J., MANIEZ P. (1996) La tanne des Biolles : un axe de drainage majeur sous le massif du Margériaz (Bauges, Savoie, France). Karstologia, n°27, 41-56.

JAILLET S., PONS-BRANCHU E., HOBLEA F., BERTHET J., DELINE P., DUVILLARD P.-A., GENUITE K. (2018) La dépression glacio-karstique du Mariet (Bauges occidentales, France) : un marqueur de l'englacement würmien des Alpes françaises du Nord, Géomorphologie : relief, processus, environnement, vol. 24 n° 2, 107-120.

QUINIF Y. (2010) Fantômes de roche et fantômisation, essai sur un nouveau paradigme en karstogenèse. Karstologia mémoires, n°18, 196 p.

QUINIF Y. (2014) La fantômisation Une nouvelle manière de concevoir la formation des cavernes. Regards, n°79, 42-72.

QUINIF Y. (2018) Fantômisation et spéléogenèse : implications et questionnement. Karstologia, n°69, 33-46.

QUINIF Y., BAELE J.-M., DUBOIS C., HAVRON C., KAUFMANN O., VERGARI A. (2014) Fantômisation : un nouveau paradigme entre la théorie des deux phases de Davis et la théorie de la biorhexistasie d'Erhart. Geologica Belgica, Vol. 17, 66-74.

QUINIF Y., BRUXELLES L. (2011) L'altération de type «fantôme de roche» : processus, évolution et implications pour la karstification. Géomorphologie : Relief, Processus, Environnement, Vol. 17 n°4, 349-358.

QUINIF Y., MAIRE R. (2009) La Grotte Quentin (Hainaut, Belgique) : un modèle d'évolution des fantômes de roche. Karstologia Mémoires, n°17, 214-218.

MALCLES O., VERNANT P., CHERY J., RITZ J.-F., CAZES G., FINK D. (2020) Âges d'enfouissement, fantômes de roches et structuration karstique, cas de la vallée de la Vis (Sud de la France). Géomorphologie : relief, processus, environnement, Vol. 26 n°4, 255-264.

MANIGLIER S., LESAULNIER P. (2015) La lutte vaine des mineurs du Semnoz : le Germinal. Spéléo Magazine, n°92, 20-28.

PIERRE G., DEVOS A., BOLLOT N. (2017) Origin and influence of the superficial structure on the morphogenesis (Eocene plateaux of the eastern Paris Basin). GeoResJ, Vol. 13, 103-113.

REY P.-J. (2016) Archéologie du massif des Bauges du Néolithique à l'âge du Bronze. Les Dossiers du Musée Savoisien : Revue numérique, n° 01-2015, 102 p.

RODET J. (2018) La grotte, fruit d'une longue gestation appelée karstification. Karstologia, n°69, 57-64.

TESSANNE E. (2014) Savoie : grotte de Prérouge : au bout du reve. Grotte de Prérouge : l'explo au bout du parcours. Spéléo Magazine, n°86, 8-13.

TESSANNE E. (2020) Tanne à la Foire (-526m). Spéléo Magazine, n°109, 6-11.

The role of ghost rocks (phantomisation) in the formation of the Sterkfontein cave and the Gauteng karsts (South Africa)

Laurent BRUXELLES[(1)], Richard MAIRE[(2)] & Dominic STRATFORD[(3)]

(1) TRACES, UMR 5608 du CNRS, Université Jean Jaurès, 5 allées Antonio Machado, 31058 Toulouse, France, Inrap and GAES, University of Witwatersrand, WITS 2050, Johannesburg, South Africa. Email : laurent.bruxelles@inrap.fr
(2) PASSAGES, UMR 5319 du CNRS, Université Bordeaux-Montaigne, 12 Esplanade des Antilles, 33607 Pessac cedex, France. Email: richard.maire49@gmail.com
(3) School of Geography, Archaeology and Environmental Studies, University of Witwatersrand, WITS 2050, Johannesburg, South Africa. Email: Dominic.Stratford@wits.ac.za

Abstract

The Neoarchean dolomites of the Gauteng province, in South Africa, contain numerous cavities including the Sterkfontein Cave, famous for its Plio-Pleistocene fossil deposits. This network, measuring several kilometers in length, represents a true three-dimensional maze cave. This characteristic has been described as a manifestation of either hyperphreatic or hypogenic karstification processes. Our work in this cave over the last fifteen years has led us to discover large quantities of weathered dolomite remaining *in situ* (ghost rock), emulating the structure of the original rock. We suggest that this network was formed through phantomisation associated with a long period of alteration correlated with the development of the African Surface. Through the down cutting of the hydrographic network, the soft sandy alterite was easily evacuated, exposing the residual passages and chambers of the cave system, but leaving morphologies usually attributed to more classic karstification processes. In the contemporary Sterkfontein Cave, we can still witness the removal of the ghost rock and its association with the fluctuations of the karstic base level. The observations made here can be extrapolated to all the Gauteng karst, where occurrences of comparable alterites are widely represented and pose recurring geotechnical challenges.

Résumé

Le rôle de la fantômisation dans la formation de la grotte de Sterkfontein et des karsts du Gauteng (Afrique du Sud).

Les dolomies néoarchéennes de la province du Gauteng, en Afrique du Sud, contiennent de nombreuses cavités dont la grotte de Sterkfontein, célèbre pour ses gisements fossilifères plio-pléistocène. Ce réseau, de plusieurs kilomètres de développement, dessine un véritable labyrinthe en trois dimensions. Cette caractéristique a été expliquée successivement par différents modes de formations (hyperphréatique, hypogène). Les travaux que nous menons dans cette grotte depuis plus de quinze ans nous ont amenés à découvrir de grandes quantités de dolomie altérée encore en place, mimant la roche originelle. Il apparaît alors que c'est essentiellement par fantômisation que ce réseau a été formé, en lien avec une longue période d'altération corrélative de la formation de la Surface Africaine. Avec l'encaissement du réseau hydrographique, l'altérite sableuse a été évacuée, révélant le réseau d'altération initial mais aussi des morphologies habituellement attribuées à des modes de karstification plus classiques. L'intérêt de la grotte de Sterkfontein réside également dans le fait que l'on peut aujourd'hui encore assister à la vidange du fantôme au gré de la fluctuation du niveau de base karstique. Les observations réalisées ici peuvent être extrapolées à l'ensemble des karsts du Gauteng où des poches d'altérites comparables sont largement décrites et posent des problèmes géotechniques récurrents.

Symposium 04 – special session

Rock-living interaction

Introduction to Rock-living interaction

Lionel BARRIQUAND(1) & Laurent BRUXELLES(2)

(1) Université Savoie Mont Blanc, EDYTEM, 73376 Le Bourget du Lac cedex, France, lionel.barriquand@wanadoo.fr
(2) TRACES, UMR 5608 du CNRS, 5 Allées Antonio Machado 31058 Toulouse, France Laurent.bruxelles@inrap.fr

English

Karst morphologies have been considered for a long time as resulting only from interactions between rock and fluids, i.e. from physico-chemical processes only. Living organisms were then considered as opportunists who came to occupy the voids thus created. Nevertheless, in recent years, things are changing and the biogenic impacts and the resulting developments are highlighted, their contribution appearing more and more important.

The first approach concerns the formation of the cavity: studies show that microorganisms can intervene in the formation of the karst from its inception. Thus, bacteria can be at the origin of the gasses that will allow the formation of certain hypogene karsts. The role of microorganisms is also evoked in the context of ghost-rock processes and several research programs are devoted to them. Unfortunately, the means required for this type of study are enormous and the probability of success is very low, which greatly limits the development of research.

The second approach concerns the post-genetic evolution of karst. First of all, as far as they are concerned, microorganisms present on the rock surface have been known for a long time in the karst entrance zones. The democratization of DNA sequencing has made it possible to overcome the first hurdle of identifying the species present. Precursory studies were carried out for the preservation of prehistoric cave paintings. Today they are developing more and more for the preservation of tourist caves. Let us hope that the future will allow the generalization of this type of research in karst, to enrich the databases which remain poor and to highlight microforms resulting from the action of microorganisms on the karst walls.
Karst is home to many other living hosts, among whom bats are the most emblematic. In some countries the populations are still very important. In others, due to human pressure, they have become almost relict. The current impact of the presence of bat colonies on the morphology of cavities has been demonstrated in the past in tropical environments. But in recent years, the review of the forms present in many caves in the rest of the world shows that these impacts have also existed in all geographical areas that are climatically favorable to chiropterans. These impacts range from very localized forms to a real remodeling of the galleries, their section being able to double. It is therefore necessary today to review many caves where, due to a lack of reading keys, these traces were not seen and even led to erroneous speleological interpretations.

More modest are the traces left by numerous animals using the underground environment, whether on the walls, on the speleothems or on the fillings. For many years they have been systematically attributed to the bear. Here again a re-reading and the creation of references are necessary because they give information on the accessibility of the cave in the course of time and contribute to a better interpretation of the traces found on the archaeological sites for example.

The aim of this session is to make a first synthesis of these interactions and to provide new keys to readings which, hopefully, will become more and more numerous and complete in the future.

Français

Introduction aux Interactions roche-vivant

Les morphologies karstiques ont pendant longtemps été considérées comme résultant uniquement d'interactions entre la roche et des fluides, c'est-à-dire de processus uniquement physico-chimiques. Le vivant était alors considéré comme un opportuniste qui venait occuper les vides ainsi créés. Néanmoins, depuis quelques années, les choses évoluent et les impacts biogéniques ainsi que les évolutions qui en découlent sont mises en évidence, leur contribution apparaissant de plus en plus importante.

La première approche concerne la formation de la cavité : des études montrent que des micro-organismes peuvent intervenir sur la formation du karst dès son origine. Ainsi les bactéries peuvent être à l'origine des gaz qui permettront la formation de certains karsts hypogènes. Le rôle des micro-organismes est aussi évoqué dans le cadre des processus de fantômisation et plusieurs programmes de recherche leur sont consacrés. Malheureusement les moyens à mettre en œuvre pour ce type d'étude sont énormes et les probabilités de réussites très faibles, ce qui contraint énormément le développement des recherches.

La seconde approche concerne les évolutions post-génétiques du karst. Tout d'abord pour ce qui concerne les micro-organismes. Leur présence à la surface de la roche est connue depuis longtemps dans les zones d'entrée du karst. La démocratisation du séquençage ADN a permis de passer un premier écueil d'identification des espèces présentes. Les études précurseurs ont été réalisées pour la préservation des œuvres pariétales préhistoriques.

Aujourd'hui elles se développent de plus en plus pour la préservation des grottes touristiques. Gageons que le futur permettra de généraliser ce type de recherche dans le karst, d'enrichir les bases de données qui demeurent pauvres et de mettre en évidence des microformes résultant de l'action des micro-organismes sur les parois du karst.

Le karst abrite de nombreux autres hôtes vivants. Parmi eux, le plus emblématique est la chauve-souris. Dans certains pays, les populations sont aujourd'hui encore très importantes. Dans d'autres, du fait de la pression humaine, elles sont aujourd'hui devenues presque relictuelles. L'impact actuel de la présence de colonies de chauves-souris sur la morphologie des cavités a été démontré dans le passé dans les milieux tropicaux. Mais depuis quelques années, la relecture des formes présentes dans de nombreuses grottes dans le reste du monde montre que ces impacts ont également existé dans toutes les zones géographiques propices climatiquement aux chiroptères. Ces impacts vont de formes très localisées à un véritable remodelage des galeries, leur section pouvant aller jusqu'à doubler. Il est donc aujourd'hui nécessaire de revoir de nombreuses grottes où, faute de clé de lecture, ces traces n'avaient pas été vues et ont même conduit à des interprétations spéléogénétiques erronées.

Plus modestes sont les traces laissés par de nombreux animaux utilisateurs du milieu souterrain, que ce soit les parois, sur les spéléothèmes ou les remplissages. Pendant de nombreuses années elles ont été systématiquement attribuées à l'ours. Là encore une relecture et la création de référentiels sont nécessaires car elles donnent des informations sur l'accessibilité de la grotte au cours du temps et contribuent à une meilleure interprétation des traces trouvées sur les sites archéologiques par exemple.

Cette session a pour but de faire une première synthèse de ces interactions et de fournir de nouvelles clés de lecture qui, espérons-le, deviendront de plus en plus nombreuses et complètes dans les années futures.

Galerie des Tines, Orgnac, Ardèche

The karst: a mineral environment also shaped by the living

Lionel BARRIQUAND[(1)] & Laurent BRUXELLES[(2)]

(1) Université Savoie-Mont-Blanc, EDYTEM, UMR 5204, Bâtiment « Pôle Montagne », 5 bd de la mer Caspienne, F-73376 Le Bourget-du-Lac cedex lionel.barriquand@wanadoo.fr (corresponding author)
(2) TRACES, UMR 5608 du CNRS, 5 allées Antonio Machado, F-31058 Toulouse Cedex 9, Inrap et GAES, université du Witwatersrand, Johannesburg, Afrique du sud, laurent.bruxelles@inrap.fr

Abstract

Karst has long been seen as a mineral world shaped only by water and air. Recent research has shown this not to be true. Living things can also have an important role in the formation of karst right from the earliest stages. This leads to the development of numerous endokarstic features with specific biogenic characteristics. In all likelihood, microorganisms play a major role early in this evolutionary process (e.g., in ghost rock formation) and then later in more particular locations. Many animals use the karst during the course of their lives (bats, badgers, bears …) and, according to their ethology, modify it to a greater or lesser extent. Walls, speleothems, sedimentary fillings, nothing escapes their impact. Lastly, Man also plays a role in this evolution, whether through past occupations or current activities in caves. These different aspects are highlighted here through studies carried out in Southern Burgundy and in Occitania, in South-western France.

Résumé

Le karst, un environnement minéral qui est aussi façonné par le vivant. Le karst a longtemps été perçu comme un monde minéral uniquement façonné par les éléments que sont l'eau et l'air. Les recherches menées ces dernières années montrent qu'il n'en est rien. Le vivant peut aussi avoir un impact très important dès sa formation. Celui-ci entraînera également de nombreuses évolutions spécifiques à l'origine de morphologies endokarstiques originales. Les micro-organismes jouent vraisemblablement un rôle majeur dès sa formation (fantômisation par exemple). Ils interviennent ensuite plus localement dans son évolution. De nombreux animaux l'utilisent au cours de leur vie (chiroptères, blaireaux, ours…). Suivant leur éthologie ils entraîneront également des modifications plus ou moins importantes. Parois, spéléothèmes et remplissages sédimentaires, rien n'échappe à celles-ci. Enfin l'Homme joue également un rôle dans cette évolution, que ce soit au travers de ses occupations passées ou de ses activités actuelles dans les grottes. Ces différents aspects sont évoqués ici à travers des études réalisées dans le sud de la Bourgogne et en Occitanie.

1. Introduction

Since 1893, the date on which the word "karst" was introduced by Jovan Cvijić, it has been defined as a geomorphic structure resulting from the phenomena of erosion and corrosion of soluble bedrock, generally associated with the circulation of fluids. In recent decades, new paradigms have appeared to explain the formation and evolution of karst (fantomisation and hypogenic karst). More recently, the impact of bats on karst has been revealed. Today, this is probably one of the most studied and most impressive of the mineral-living interactions. But is it the only one? The studies carried out in Southern Burgundy and Occitania show that it is not.

2. Bacteria

It is clear that certain bacteria play a major role in karstification. It has been shown that the black ferro-manganic deposits visible in the Azé caves in all likelihood have a bacterial origin (PAPIER *et al*, 2011, 2012). To explain the formation of these structures, a chemolithotrophic metabolism has been suggested, similar to that responsible for the formation of stromatolites. This process directly impacts the karst wall leading to its alteration (CARMICHAEL & BRAUËR, 2015). Later flows of water enable the evacuation of the residual alterites cemented by the iron and manganese oxides (BARRIQUAND *et al*, 2012). The environmental conditions needed for the development of these microorganisms remain unknown.

Biofilms of actinomycetes also play an important role in creating a hydrophobic interface between the rock wall and its open surroundings (PFENDLER & BARRIQUAND, 2021). They perhaps have a dual effect in protecting the wall against the phenomena of condensation-corrosion but also in weakening it through their fixation.

The presence of cyanobacteria in zones of the karst subject to light leads to the formation of deposits of calcite (BARRIQUAND *et al*, 2021A). Lastly, the structure of the neo-formations of moonmilk in the Azé cave show that they have a bacterial origin (Fig. 2).

Figure 1: Underground River Cave at Azé, ferro-manganic deposits on the walls, and alterites cemented by these deposits in the sediments (photo S. Caillault).

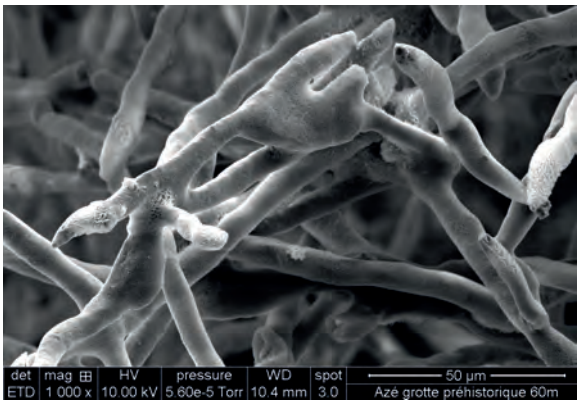

Figure 2: structure of neo-moonmilk in the Balme Cave at Azé showing its bacterial origin (photo from Centre des Microstructures, Uni. C. Bernard, Lyon 1).

3. Animals

Animals have inhabited the karst from the earliest times. Of these, bears and bats are undoubtedly the most well-known.

The presence of bears, as well as other mammals such as badgers and foxes, according to their ethology, brings about changes to the walls and sedimentary fillings of the karst. Repeated passage in the same places creates polished areas. Rock surfaces are abraded by animal claws (Fig. 3). The digging of wallows, passageways, grooming hollows and latrines have major impacts on sedimentary fillings. Lastly, their excreta can lead to the formation of phosphatic deposits causing alteration of the surrounding rock (BARRIQUAND *et al.,* 2021B).

Bats have a major role in the evolution of karst. This has been first of all demonstrated in tropical environments but today it is recognised that the same processes occur in Europe (AUDRA *et al.*, 2016; BRUXELLES *et al.*, 2016; BARRIQUAND *et al.*, 2021C). The heat emitted by large swarms and the gases exhaled during respiration lead to an alteration of ceilings and walls. Combined with the mechanical action of claws during repeated roostings, these have led to the formation of domes. The retreats of the walls are of the order of a few millimetres to a few tens of millimetres per thousand years. Such changes are clearly evident in the Balme Cave at Azé where the entrance has undergone considerable expansion which is not the case in the upstream part of the cave which was protected by a flowstone plug which closed the cave 60 m from its entrance (Fig. 4). Bat faeces have led to the formation of large phosphate deposits in caves. In a karstic environment, leachates from these phosphate deposits produce chemical reactions which bring about numerous forms of alteration (cupules, guano potholes …), directly on the underlying rock or on the speleothems which are exposed to them. Depending on the nature of the surrounding rock and on the cations present, these reactions will produce a diverse mineralogy (AUDRA *et al*., 2019).

Figure 3: wall in the Nabrigas Cave marked with grooves left by bear claws.

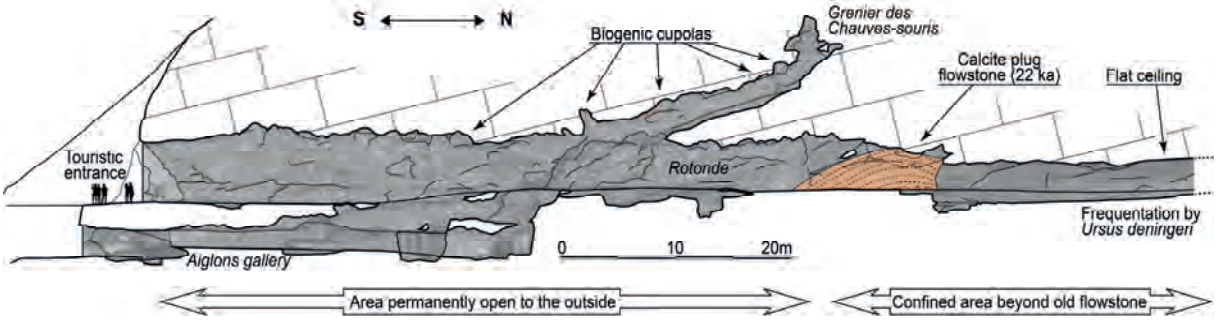

Figure 4: Balme Cave at Azé. The first 60 m of the cave have been occupied by bats since the Upper Palaeolithic whereas the upstream part was protected by a flowstone plug which closed the cave and divided it into two distinct compartments. The expansion of the entrance gallery is linked to biogenic corrosion (S. Jaillet).

4. Man

Man has long had an important relationship with the karst. From the Lower Palaeolithic he has frequented the entrance of the Balme Cave at Azé where he made opportunistic use of the cherts accessible in the cave walls (COMBIER *et al*., 2000; COMBIER, 2005). 176,000 years ago, in the Bruniquel Cave, men used speleothems to form circular structures in the deeper parts of the cave (VERHEYDEN *et al*., 2017). In the Upper Palaeolithic, his extensive frequentation of the underground environment led to its significant modification.

During the protohistoric period, more significant modifications were made through the construction of walls and alterations to cave floors (GALANT *et al*., 2012; BARRIQUAND & DUCREUX, 2021). Man was using caves to satisfy both domestic and spiritual needs. At times these modifications were quite substantial, even to the extent of closing cave entrances. Yet other modifications were more superficial - inscriptions on walls to mark his passage or to portray in graphic form aspects of his life.

With the arrival of underground tourism, of caving and sometimes large structural works, some caves experienced considerable upheaval linked to development projects and research. The digging of access galleries, enlargement of narrow passageways, removal of obstructions (BARRIQUAND, 2019) and even the construction of a roadway (Fig. 5) have had irreversible impacts.

Figure 5: Mas d'Azil Cave, tourist footbridge, building and even a roadway, profound modifications by man (D. Gliksman, Inrap).

5. Conclusion

Karst has long been considered as having evolved only through the actions of water and sometimes air.

Recent studies show that this is not the case. Microorganisms are present in the karst and in all likelihood have had a very significant impact on it over a long period of time. Microbiology is now evolving very rapidly and, in the years ahead, could well bring surprising new insights into the evolution of karst.

For a long time, the bear has had hegemony in relation to bioglyphs, but it is not the only animal to have frequented caves. Many other animals still frequent caves, leaving behind signs of their passage, according to their scale, in the modifications they make to cave walls. More systematic studies of these traces would be wise, and also likely to yield surprising new insights. This has been the case with recent studies on bats, mammals which have had very significant impacts on many caves in Europe and in the world.

Lastly, much too neglected, the role of man in modifying the karst has been underestimated. Whether from outside or directly within, man has intervened and continues to intervene in many caves, in ways that are irreparable. This implies a need for us to be well aware of the part played by human activities in the evolution of the karst, just as we need to be aware of it in the evolution of the planet as a whole.

Acknowledgments

We very warmly thank everyone who by their participation in all the studies carried out in the Mâconnais and Occitania have enabled a better understanding of the relationship which exists in caves between the living and the mineral. We also warmly thank Bob Norington for its translation.

References

AUDRA P., BARRIQUAND L., BIGOT J.-Y., CAILHOL D., CAILLAUD H. and VANARA N. (2016) L'impact méconnu des chauves-souris et du guano dans l'évolution morphologique tardive des cavernes. *Karstologia* n°68, 1-20.

AUDRA P., De WAELE J., BENTALEB I., CHRONAKOVA A., KRISTUFEK V., M. D'ANGELI I., CARBONE C., MADONIA G., VATTANO M., SCOPELLITI G., CAILHOL D., VANARA N., TEMOVSKI M., BIGOT J.-Y., NOBECOURT J.-C., GALLI E., RULL F. and Aurelio SANZ-ARRANZ A. (2018) Guano-related phosphate-rich minerals in European caves. *International Journal of Speleology*, n° 48, 75-105.

BARRIQUAND L., BARRIQUAND J., BAELE J.-M., DECHAMPS S., GUILLOT L., MAIRE R., NYKIEL C., PAPIER S. and QUINIF Y. (2012) Les Grottes d'Azé (Saône-et-Loire, France) : de la roche altérée aux sédiments. *Karstologia*, n° 59, 19-32.

BARRIQUAND L. (2019) La Grotte de la Rivière Souterraine d'Azé (Saône-et-Loire), les méthodes de désobstruction ayant menées à son exploration, les découvertes associées à celle-ci et les conséquences liées à la désobstruction. *Spelunca Mémoires*, n° 38, 114-138.

BARRIQUAND L., PFENDLER S., HERESANU V., DEMARIGNY Y. and RIGOBELLO V. (2021A) Modification by cyanobacteria of the wall of the entrance chamber of the Grotte de la Balme, Azé (Saône-et-Loire, France). *Actes du congrès UIS 2022*.

BARRIQUAND L., PHILIPPE M., CHEVALLIER J.-R., HERESANU V., ARIAGNO D., DEDIENNE G., DONZEY I. and GAILLARD C. (2021B). The multiple impacts of European badger (Meles meles) on the caves, Mâconnais cave example (Saône-et-Loire, France). *Actes du congrès UIS 2022*.

BARRIQUAND L., BIGOT J.-Y., AUDRA P., CAILHOL D., GAUCHON C., HERESANU V., JAILLET S. and VANARA N. (2021C) Caves and Bats: Morphological impacts and archaeological implications. The Azé Prehistoric Cave (Saône-et-Loire, France). *Geomorphology*, 388, 107785, 12p.

BARRIQUAND L. et DUCREUX F. (2021) - Les fouilles de la grotte de la Balme à Azé (Saône-et Loire). Reprise de la documentation et du mobilier archéologiques, de l'âge du Bronze, issu des fouilles anciennes. *Revue Archéologique de l'Est*, 70, 73-106

BRUXELLES L., JARRY M., BIGOT J.-Y., BON F., DANDURAND G. et PALLIER C. (2016) La biocorrosion, un nouveau paramètre à prendre en compte pour interpréter la répartition des oeuvres pariétales : l'exemple de la grotte du Mas d'Azil en Ariège. *Karstologia*, n° 59, 21-30.

CARMICHAEL S. K. and BRAUER S. L. (2015) Microbial Diversity and Manganese Cycling: A Review of Manganese-oxidizing Microbial Cave Communities. *Life in extreme environments, Microbial life of cave systems*, 137-160.

COMBIER J., GAILLARD C. et MONCEL M.-H. (2000) L'industrie du Paléolithique inférieur de la Grotte d'Azé (Saône-et-Loire) – Azé I-1. *Bulletin de la Société Préhistorique Française*, n° 97-3, 349-370.

COMBIER J. (2005) Quelle présence humaine dans l'espace rhodanien avant le stade 5 (135 kA) ?. Département du Rhône – Museum, Lyon, *Cahiers scientifiques*, HS n° 3, 71-99.

GALANT P., VILLEMÉJEANNE R., ÉTIENNE A., BRUXELLES L. et BOSCHI J.-Y. – 2012. - Une découverte majeure pour la connaissance de la fin du Néolithique sur les Grands Causses : le site de la Baumelle à Blandas (Gard). In : Dynamismes et rythmes évolutifs des sociétés de la Préhistoire récente. Actualité de la recherche, *Actes des 9èmes Rencontres Méridionales de Préhistoire Récente*, Saint-Georges-de-Didonne, 8 et 9 octobre 2010, 289-306.

PAPIER S., BAELE J.-M., GILLAN D., BARRIQUAND L. and BARRIQUAND J. (2011) Manganese geomicrobiology of the black deposits from the Azé cave, Saône-et-Loire, France. *Quaternaire*, Hors-série n°4, 297-305.

PAPIER S., BAELE J.-M., GILLAN D., BARRIQUAND L. and BARRIQUAND J. (2012) - Chemolithotrophic bacterial communities: a likely key factor in the formation of ghost rock. *Ghost- Rock Karst Symposium*. Abstracts book, Han-sur-Lesse, 7-11 octobre 2012, 28.

PFENDLER S. and BARRIQUAND L. (2021) Assessment of colored bacterial colonies on Azé and Blanot caves (France) limestone walls. *Actes du congrès UIS 2022*.

VERHEYDEN S., JAUBERT J., GENTY D., SOULIER M., BURLET C. *et al*. (2017) Grotte de Bruniquel (Tarn-et-Garonne, France) : éléments de datation complémentaires, *Karstologia* n° 70, p. 1-14. ⟨hal-01993163⟩

Assessment of colored bacterial colonies on Azé and Blanot caves limestone walls

Stéphane PFENDLER[1] & Lionel BARRIQUAND[2]

(1) Université de Bourgogne Franche-Comté, CNRS, Laboratoire Chrono-environnement, 4, place Tharradin, F-25250 Montbéliard (corresponding author)
(2) Université Savoie-Mont-Blanc, EDYTEM, UMR 5204, Bâtiment « Pôle Montagne », 5 bd de la mer Caspienne, F-73376 Le Bourget-du-Lac cedex lionel.barriquand@wanadoo.fr

Abstract

Coloured bacterial colonizations were observed in Azé and Blanot caves (France) in both touristic and non-touristic areas. These proliferations were observed on moist walls and ceilings. In this study, we have characterized the bacterial developments using high-throughput sequencing. The results have highlighted that app. 80% of all DNA strands belong to the Actinobacterial phylum, followed by 12.5% of Proteobacteria. Three operational taxonomic units were highly dominant, representing 79.9% of the DNA sequences.

1. Introduction

Microorganisms are able to colonize almost any habitat on Earth, especially Prokaryotes. In fact, bacteria play a critical role in biogeochemical processes. Several studies have recorded bacterial communities that are inhabiting caves. Some of them are distinguished by physical peculiarities like bright colours. This is the case in the Azé and Blanot caves (France) where several (e.g., blue, pink, white, green, yellow) colonies proliferate on the moistest cave walls. The aim of this study is to characterize these colonies using next generation sequencing (Illumina MiSeq).

2. Material and methods

The observed bacterial communities in Azé and in Blanot caves were photographed using an Olympus Tough 4.0. In order to distinguish photosynthetic communities from non-photosynthetic biofilms, quantum yield measurements, corresponding phototrophs metabolism, were carried out. Before each sampling, five measurements were taken on each biofilm, which were previously placed for 30 min in the dark. Quantum yield parameter (Fv/Fm) was monitored using the photosynthesis yield analyzer mini-PAM (WALZ, Germany). Eleven non-photosynthetic colonies were scraped from the limestone walls with a plastic sterile tube, and maintained at -80 °C until total DNA extraction, amplification steps and sequencing. PowerBiofilm DNA Isolation Kit was used by MicroSynth AG following the manufacturer's instructions (MoBio Laboratories, Inc., Carlsbad, CA, USA). The polymerase chain reaction (PCR) amplification followed a two-step PCR protocol using a state-of the-art high fidelity polymerase. PCR amplifications were performed with the primers p23SrV_f1 (5'-GGACAGAAA- GACCCTATGAA-3'), p23SrV_r1 (5'-TCAGCCTGT- TATCCCTAGAG-3') and 16S 799 f (5' -AACMGGATTAGATACCCKG- 3') and 16S 1115 r (5' -AGGGTTGCGCTCGTTG- 3').

3. Results

In both Aze and Blanot caves, we have observed several biofilms (Fig. 1 A, B, C and D) colours (pink, blue, white and yellow). The observations using magnifying glass have permitted to show that some bacterial proliferation may be a mix of communities (i.e., blue and yellow colonies, visible on Fig. 1 A). The colonies can invade large areas of the caves (Fig. 1 E) and are able to retain water drops conferring them a shiny gold or silver aspect (Fig. 1 C and E).

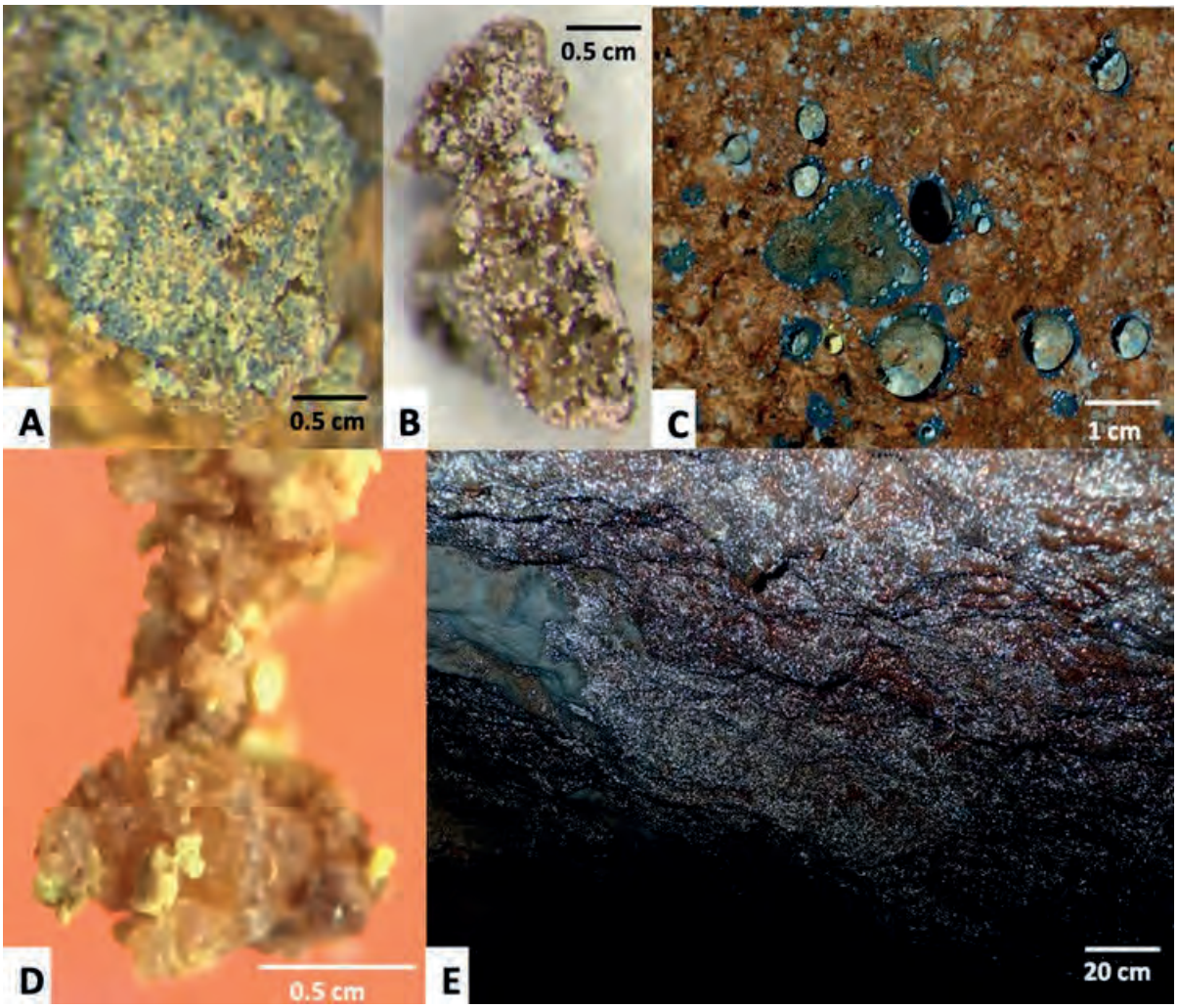

Figure 1: Bacterial colonies growing on limestone walls exhibited several colours (blue (A, C), pink (B), yellow (A, D)). The colonies are able to retain water drops (C) that are reflecting the light (E).

DNA sequencing (Fig. 2) has permitted to record 1056 Operation Taxonomic Units (OTU). However, 79.9% of the DNA sequences were gathered in 3 OTUs, while the other 20.1% corresponded to low abundant OTUs (<1%). The two most abundant OTUs belong to the actinobacteria phylum (Actinobacteria_unclassified (43.9%) and a gender belonging to the Euzebya (33.7%)). The third most abundant phylum is represented by the Gamma-proteobacteria (Nitrosococcus, 2.4%), known as an ammonia-oxidizing bacterium. The results permitted to link the colour to an OTU. In fact, pink-coloured colonies belong to the Euzebia while blue, yellow and white spots are linked with the unclassified Actinobacteria.

Only one sample of blue colony was linked with the Euzebia. The second most abundant phylum was represented by the Proteobacteria (12.5%). The results have also highlighted that touristic activities have no influence on these bacterial communities (Fig. 3). In fact, there is no significant difference between bacterial colonies developing in the touristic part in comparison to the non-touristic areas. Moreover, no difference has been observed between the coloured colonies in Azé and Blanot caves. However, significant differences have been detected between the samples regarding their colour (Fig. 4), especially the pink biofilms versus the other colored biofilms.

	Biofilm colour	Pink	White	Blue	Yellow	Pink	Blue	Yellow	Blue	Pink	Blue
	Samples	bla1	bla2	Bla3	Bla4	azeNT1	azeNT2	azeNT3	azeT1	azeT2	azeT3
Number of DNA sequences	OTU 1	321	4870	5671	8203	135	7147	5586	6454	110	8042
	OTU 2	8589	983	580	245	8098	332	398	60	9036	1
	OTU 3	6	82	524	24	406	246	811	345	138	10
	bla: Blanot cave; aze: Azé cave; NT: non touristic area; T: touristic area										
	OTU 1: Actinobacteria_unclassified; OTU 2: Euzebya; OTU 3: Nitrosococcus.										

Figure 2: Abundance of DNA sequences per sample depending on the biofilm color.

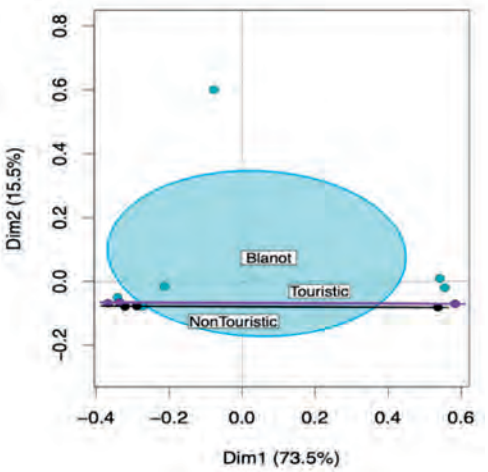

Figure 3: Principal coordinates analysis obtained using colonies that were sampled in both Azé (touristic and non-touristic areas) and Blanot caves (touristic area). A Bray-Curtis dissimilarity matrix was built and PERMANOVA was applied to this dissimilarity matrix. The result of PERMANOVA on the given Bray-Curtis dissimilarity matrix was shown under the Principal Coordinate Analysis (PCoA). The ellipses represent the area in which the centroid may be found (at 95% of probability).

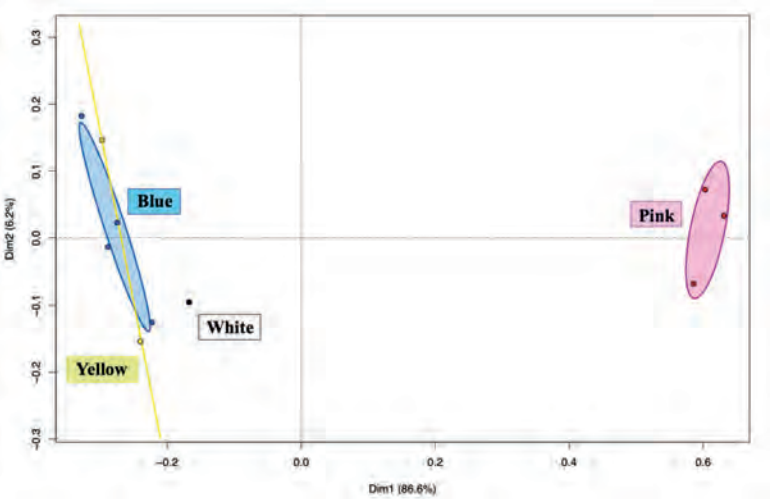

Figure 4: A principal coordinates analysis was performed depending on the colour of the sampled biofilms.

4. Discussion

Bacterial coloured biofilms developing in the Azé and Blanot caves were characterized as dominant Actinobacterial biofilm. This result is supported by the study of Porca et al. (2012). As well, Cuezva et al. (2009) reported high proportion of Actinobacteria but in a less extended proportion. However, Pašić et al. (2009) have reported that Proteobacteria were dominant. The variation in Actinobacteira proportion may be explain by the use of other molecular technics such as cloning or by the use of optical microscopy.

Cave microbial colonization is often related to touristic activities. However, this study has demonstrated that these communities may be considered as natural colony that grown independently of touristic tours.

Their expansion is probably conditioned by the physico-chemical parameters of the caves, in particular by high humidity conditions and the more or less regular presence of a water film. Thus the Balme Cave in Azé and the Cailleverdière Cave are instrumented to evaluate the environmental conditions conducive to the development of these biofilms. For a better understanding of these communities, a cultural approach (on Petri dishes) should be implemented. The definition of a model culture medium should make it possible to observe the growth mechanisms of these colonies and their impact on the cave walls. The latter can be significant and lead to an alteration of the casing and the anthropic traces that it may present (fig. 5). Thus, additional studies are needed to help understand the role of pigmented biofilms (Mulec et al., 2015).

Figure 5: Wall and graffiti dating from the end of the 19th century altered by biofilms in the Furtins cave (Berzé-la-Ville, France; picture by Serge Caillault).

5. Conclusion

Coloured bacterial colony developing on cave walls and ceilings is the consequence of bacterial biofilm proliferation, mainly composed by Actinobacteria and Proteobacteria. The two domain strains of Actinobacteria, representing more than 75% of the DNA strands sequenced, dominate all the biofilms. The unclassified actinobacteria gender is dominant for blue, yellow and white biofilm, while the Euzebia gender is dominant for pink coloured biofilm. These bacteria seem to be wild sprayed since no difference between the two caves was demonstrated.

Acknowledgments

First of all, we are grateful to the curators of the Azé and Blanot Cave, who kindly gave us permission to access the caves and to carry out all our field experiments. We also thank the Laboratory Chrono-Environment for their support and the association of the Azé cave for their financial contribution.

References

LEJLA PASIC, BARBARA KOVCE, BORIS SKET, BLAGAJANA HERZOG-VELIKONJA (2009). Diversity of microbial communities colonizing the walls of a Karstic cave in Slovenia. FEMS Microbiol Ecol, 71:50–60. DOI:10.1111/j.1574-6941.2009.00789.x.

SOLEDAD CUEZVA, SERGIO SANCHEZ-MORAL, CESAREO SAIZ-JIMENEZ, JUAN CARLOS CAÑAVERAS (2009). Microbial Communities and Associated Mineral Fabrics in Altamira Cave, Spain. International Journal of Speleology 38, 83-92.

JANEZ MULEC, ANDREEA OARGA-MULEC, ROK TOMAZIN, TADEJA MATOS (2015). Characterization and fluorescence of yellow biofilms in karst caves, southwest Slovenia. International Journal of Speleology, 44 (2), 107-114. DOI:10.5038/1827-806X.44.2.1.

Controlling lampenflora, the green disease of show caves

Rosangela ADDESSO[(1)], Daniela BALDANTONI[(1)], Jo DE WAELE[(2)] & Ana Z. MILLER[(3)]

(1) Department of Chemistry and Biology "Adolfo Zambelli", University of Salerno, Via Giovanni Paolo II, 132, 84084 Fisciano (SA), Italy, addros04@gmail.com (corresponding author), dbaldantoni@unisa.it
(2) Department of Biological, Geological and Environmental Sciences, University of Bologna, Via Zamboni, 67, 40126 Bologna, Italy, jo.dewaele@unibo.it
(3) Instituto de Recursos Naturales y Agrobiología de Sevilla, IRNAS-CSIC, Av. Reina Mercedes, 10, 41012 Sevilla, Spain, anamiller@irnas.csic.es

Abstract

Artificial lighting in show caves causes the growth of green photosynthetic biofilms, called lampenflora, on rock surfaces. This represents a worrisome ecological problem in caves as these biofilms cause aesthetical, physical and chemical damages on the rock substrates. Finding an efficient eco-friendly control method is now a priority to carry out a sustainable management of cave tourism. In this study we assessed the efficacy of three growth-control methods in Pertosa-Auletta limestone Cave (Italy). Reflectance spectra showed that the lampenflora is able to reflect only the near-infrared, absorbing all the visible light frequencies, likely due to its capability to produce secondary accessory pigments or to the mixotrophic metabolism of some cyanobacterial species. Filamentous organisms, knotted with minerals, promote rock corrosion and the precipitation of carbonate secondary minerals. Treatment of lampenflora with NaClO (commercial bleach) demonstrated its long-term efficacy in disinfection and cleaning of the surfaces, whereas the H_2O_2 (oxygenated water) revealed a recovery of the biofilms after three months and corrosive effects on the underlying carbonate bedrock. Both the chemical treatments eliminated the photoautotrophs, but not *Proteobacteria* and *Bacteroidetes* bacterial phyla, and, among the Eukaryotes, *Apicomplexa* and *Cercozoa*. UVC lighting showed no effects on lampenflora with the protocol used in such work.

1. Introduction

The frequentation of underground ecosystems by visitors requires artificial lighting systems, which can promote the growth of green biofilms, called lampenflora, on lithic substrates (Fig. 1). These green patinas, mainly composed of photoautotrophic organisms, implement aesthetical changes on the natural surfaces and biodeterioration processes through mechanical destruction activated by their appendages, as well as chemical corrosion due to their acid secretions. Moreover, they are responsible for an ecological disequilibrium, due to a considerable "alien" organic input in the cave oligotrophic environment (MULEC, 2019).

Currently, the most employed control technique is the commercial bleach for its low-price and efficiency in cleaning the colonized surfaces, but it results are detrimental from an environmental viewpoint. The H_2O_2 and the UVC radiation were recently proposed as "environmentally friendly" methods, not producing reaction by-products (BAQUEDANO ESTEVEZ *et al.*, 2019).

Yet, no definitive solutions exist to remove the lampenflora, and cave managers carry out chemical-physical techniques, based on few scientific studies, without understanding thoroughly their efficacy and effects on the substrates and overall underground ecosystem (BAQUEDANO ESTEVEZ *et al.*, 2019).

Figure1: Lampenflora from Pertosa-Auletta Cave

2. Materials and methods

To characterize the general behavior and the features of the lampenflora from Pertosa-Auletta Cave (southern Italy), reflectance analysis was performed using a Jaz System spectrometer (Ocean Optics), completed with a VIS-NIR module, whereas the PAR (photosynthetically active radiation) detection was based on an irradiance quantum meter (LI-250 Light meter, Li-COR). To control the biofilm photosynthetic activity, the maximal photosystem II (PSII) photochemical efficiency measures, given by Fv/Fm (variable fluorescence/maximal fluorescence), were carried out on 30 minutes dark-adapted surfaces, using a portable photosynthesis yield analyzer (MINI-PAM, WALTZ, Germany), equipped with a distance clip holder (Distance Clip 2010A, WALTZ, Germany). Oven-dried (50 °C) samples were analyzed by Field Emission Scanning Electron Microscopy (FESEM) using a FEI Teneo (ThermoFisher, MA, USA) microscope, with the secondary electron detection mode, and an acceleration voltage of 5 kV for ultra-high resolution images.

For assessing the efficacy of the most used lampenflora growth control methods, in the tourist trail section of Pertosa-Auletta Cave, 8 areas (50 x 50 cm) covered by lampenflora (4 bare rock surfaces and 4 rock surfaces with vermiculations, coated with 3-4 mm and 1-2 mm of lampenflora biofilms, respectively) were treated, once a growth-control methods. The NaClO was applied without any dilution; the 15% H_2O_2 solution was prepared from a 30% solution and diluted in distilled water in 1:2 ratio, as described in TRINH *at al.,* (2018); the germicidal UVC lamp was provided by Sa.Gest. srl (lamp type: INOLUX IN-C33DTDU13535 UVC LED; power max: 4 mW; power module max: 12 mV; spectrum wavelengths: 265-285nm; viewing angle: 130°; distance from surface: 40-50 cm). Two untreated areas (controls) were used for each surface typology. Before and after each treatment, we carried out measures of Fv/Fm. At the end of all treatments, lampenflora samples were collected, using disposable and sterile scalpel blades and Eppendorf tubes, for DNA-based analyses. DNeasy PowerSoil Kit was used to extract total DNA, according to the producer's protocol (Qiagen), and analyzed via next-generation sequencing (NGS) targeting the V3–V4 hypervariable region of the 16S rRNA gene for Prokaryotes and the 18S rRNA gene for Eukaryotes, using Illumina MiSeq 2 × 250 paired end, according to Macrogen (Seoul, Korea) library preparation protocol. RDP and NCBI were used, respectively, for Prokaryotes and Eukaryotes, as against reference databases for taxonomic identification of query sequences.

3. Results

The lampenflora samples from Pertosa-Auletta Cave absorbed the totality of the visible light (~ 400-700 nm), with a reflection of the near-infrared radiation only (~ 700-800 nm) (Fig. 2).

The analysis of chlorophyll fluorescence (Fv/Fm) showed values ranging from 0.62 to 0.72, whereas the PAR values ranged from 1.85 to 4.01 µmol m^{-2} sec^{-1}.

The microscopy surveys by FESEM (Fig. 3) showed the organization of the biofilms, mainly composed of filamentous bacteria and algae, as well as diatoms, knotted to the minerals and trapping them. There were also traces of corrosion processes and secondary minerals (calcite rods) from biologically mediated precipitation processes.

Concerning the experimental plan, set up for testing the efficiency of the most used lampenflora growth control methods, at time 0, all the surfaces (bare limestone and with vermiculations) showed Fv/Fm mean values equal to 0.71. After the two chemical treatments (H_2O_2 and NaClO), their biological activity stopped, decreasing to 0. After 3 months of cave closure, due to the Covid19 pandemic lockdown, there was a recovery of lampenflora on surfaces treated with H_2O_2. The 16S and 18S metagenomics analysis revealed that the most abundant bacterial phylum was *Cyanobacteria*, represented by *Brasilonema angustatum* species, whereas the *Streptophyta* phylum, represented by *Ephemerum spinulosum* species, was the most abundant within the Eukaryotes.

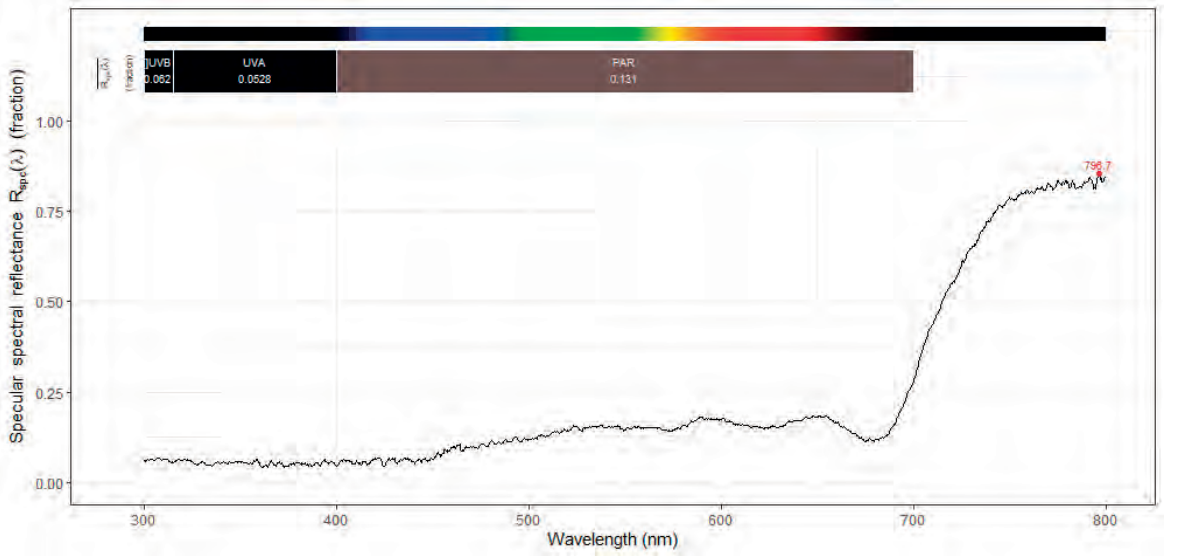

Figure 2: Example of a reflectance spectrum on lampenflora from Pertosa-Auletta Cave

After the chemical treatments on both surfaces, photosynthetic bacteria were removed, with the persistence of *Proteobacteria* and *Bacteroidetes*. The H_2O_2 revealed greater efficacy than NaClO in eliminating *Streptophyta* phylum, among the Eukaryotes, with a residual presence of *Apicomplexa* and *Cercozoa* phyla and several unclassified groups. The UVC lamp for both surfaces exhibited a similar tendency of the control areas, even after increasing the number of treatments (from 1 to 4 times in a month).

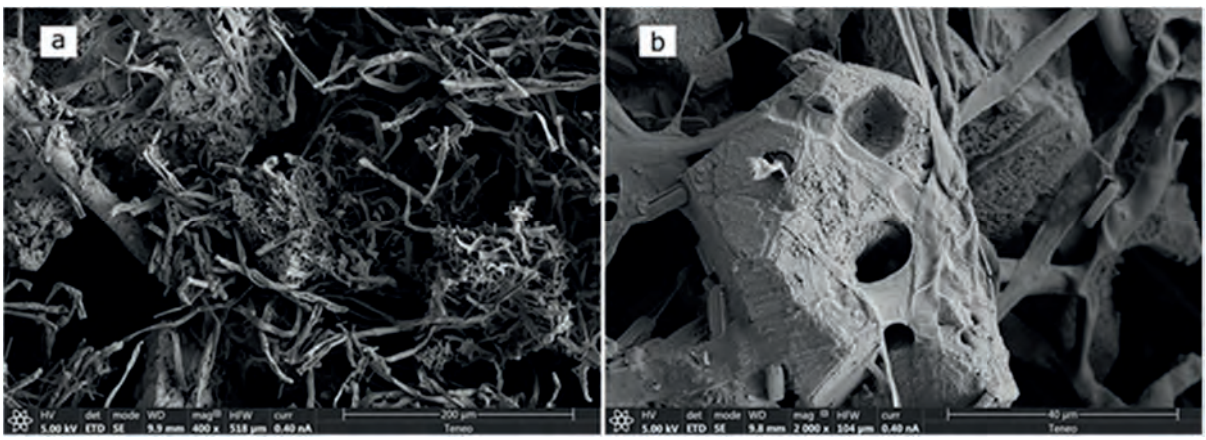

Figure 3: FE-SEM images of lampenflora from Pertosa-Auletta Cave. Filamentous organisms and biogenic calcite rods (a), diatoms, corrosion shapes and trapped minerals (b) are shown.

4. Discussions

The maximal PSII photochemical efficiency measures, representing a proxy of the photosynthetic activity, proved the good physiological activity of the microbial community of lampenflora from Pertosa-Auletta Cave, also at very low PAR intensities. Moreover, lampenflora showed its characteristic behavior regarding the reflectance spectra, i.e., not reflecting the green part of the spectrum, and absorbing the totality of visible light (~ 400-700 nm), except the near-infrared (~ 700-800 nm). Diverse organisms composing the lampenflora community, such as Cyanobacteria, are able to produce secondary accessory pigments enlarging their absorption spectrum. Moreover, they can use different metabolic pathways, such as mixotrophy and heterotrophy (MULEC, 2019). The microscopy observations highlighted the alterations activated by biofilms, through chemical-physical destructive and constructive processes, showing the serious damages implemented on the lithic substrates.

Concerning the efficacy and effects of the treatments for the removal and control of biofilm growth, commercial bleach seems to be the most efficient long-term removal technique for the surface disinfection and cleaning, but its toxicity

represents a drawback. The H_2O_2 displayed a recovery of lampenflora after three months without applications, with visible corrosion processes activated on the rock substrates. The germicidal UVC lamp did not solve the lampenflora problem, resulting ineffective.

5. Conclusion

Our results provided updated and important information concerning the understanding of lampenflora nature and the efficacy, as well as of the effects, of the most used methods for controlling this “green disease” in show caves. These photosynthetic-based biofilms showed peculiar optical features, with almost homogeneous absorbance of the entire visible spectrum, likely thanks to the capability of photoautotrophic organisms to produce a wide range of accessory pigments and to switch their metabolism regime in response to changing environmental conditions. These communities are mainly composed of filamentous organisms tangled with the mineral substrate, dominated by *Brasilonema angustatum* cyanobacterial species, and, among the Eukaryotes, by *Ephemerum spinulosum* and *Pseudostichococcus monallantoides*. Microscopy revealed the precipitation of $CaCO_3$ secondary minerals, and corrosion features, highlighting the irreversible damages of colonized substrates. The experimental trial to test the most used lampenflora removal techniques on the rock surfaces, revealed the good properties of NaClO in terms of biomass elimination, sterilization and integrity of surfaces, with the drawback regarding its toxicity. The UVC lamp showed null effectiveness in biofilm removal, whereas the H_2O_2 caused corrosion on the surfaces, especially if covered by vermiculations, and revealed a limited capability of oxidizing organic matter and removing lampenflora for long periods.

Acknowledgments

We gratefully thank the MIdA Foundation (Italy), manager of Pertosa-Auletta Cave, the speleo-guides Vincenzo Manisera, Umberto Del Vecchio e Giampaolo Pinto and all the MIdA staff, the Melandro, the Castel di Lepre, the CAI Napoli, and the Vespertilio Caving Groups, and the Sa.Gest. srl, for facilitating all the field activities with their technical and logistical support. This work received support from: a) the University of Salerno (Italy) under the research projects ORSA197159 and ORSA205530; b) the Spanish Ministry of Science and Innovation (MCIN) under the research project PID2019-108672RJ-I00 (TUBOLAN) funded by MCIN/AEI/10.13039/501100011033, and the Ramón y Cajal contract RYC2019-026885-I from the MCIN, and c) the Portuguese Foundation for Science and Technology (FCT) under the MICROCENO Project (PTDC/CTA-AMB/0608/2020).

References

MULEC J. (2019) Lampenflora. Encyclopedia of Caves. Elsevier, 635–641.

BAQUEDANO ESTÉVEZ C., MORENO MERINO L., DE LA LOSA ROMÁN A., DURÁN VALSERO J.J. (2019) The lampenflora in show caves and its treatment: an emerging ecological problem. International Journal of Speleology, 48 (3): 249-277.

TRINH D.A., TRINH Q.H., TRAN N., GUINEA J.G., MATTEY D. (2018) Eco-friendly Remediation of Lampenflora on Speleothems in Tropical Karst Caves. Journal of Cave and Karst Studies, 80(1):1-12.

Modification by cyanobacteria of the wall of the entrance chamber of the Grotte de la Balme, Azé (Saône-et-Loire, France)

Lionel BARRIQUAND[(1)], Stéphane PFENDLER[(2)], Vasile HERESANU[(3)], Yann DEMARIGNY[(4)] & Véronique RIGOBELLO[(4)]

(1) Université Savoie-Mont-Blanc, EDYTEM, UMR 5204, Bâtiment « Pôle Montagne », 5 bd de la mer Caspienne, F-73376 Le Bourget-du-Lac cedex lionel.barriquand@wanadoo.fr (corresponding author)
(2) Université de Bourgogne Franche-Comté, CNRS, Laboratoire Chrono-environnement, F-25250 Montbéliard
(3) Aix-Marseille Université-CNRS, CINaM, Campus de Luminy, case 913, F-13009 Marseille
(4) Laboratoire Bioingénierie et Dynamique Microbienne aux Interfaces Alimentaires, Equipe Mixte d'Accueil Université Lyon 1 - ISARA Lyon n°3733, 23 Rue Jean Baldassini, 69007 Lyon

Abstract

Since the time they were uncovered, the walls of the entrance chamber of the Balme Cave at Azé have undergone change. Macrophotographic observations revealed the presence of filaments on their surface. The analyses carried out showed that this layer of filaments was a biofilm, the product of biomineralization linked to the presence of cyanobacteria. The seasonal colour variations observed in all likelihood correspond to a period of hydric stress to which the biofilm is subjected during summer.

Résumé

Modification par les cyanobactéries de la paroi de la salle d'entrée de la Grotte de la Balme, Azé (Saône-et-Loire, France). Depuis leur dégagement, les parois de l'entrée de la grotte de la Balme à Azé ont changé. Des observations par macrophotographie ont montré la présence de filaments à leur surface. Les analyses effectuées montrent qu'il s'agit de bio-minéralisations au sein d'un biofilm liés à la présence de cyanobactéries. Les variations de couleurs saisonnières observées correspondent vraisemblablement à une période de stress hydrique que subit le biofilm en été.

1. Introduction, the Balme or Prehistoric Cave at Azé

The Balme Cave is situated in the Monts du Mâconnais (Saône-et-Loire, France). Its entrance is in the form of a large porch regularly used by humans and animals since the Middle Palaeolithic (Barriquand et *al*, 2011A). At the beginning of the 20th century part of the porch was filled in by sediments. During research activities beginning in the 1950s, then in the 1960s when work was done to open the site to the public, much of these sediments were removed thus exposing the walls as they are today (Barriquand et *al*, 2011B). However, since their uncovering, parts of the walls have evolved. Characteristic of this change is the seasonal variation of their colour, ranging from khaki in winter to grey-blue in summer (Fig. 1A). The aim of the study presented here is to understand what brought about this change and its variations.

2. Material and methods

The first observations carried out were photos taken of the wall using an Olympus Tough 4.0 camera (Fig. 1A).
Samples were also taken for:
- Observation in the laboratory using a standard optical microscope at a magnification of 1000x
- Observation using a scanning electron microscope. Before observation, the samples were dried for 2 hours at 105° C. The observations were done using the microscope at the Centre Technologique des Microstructures de l'Université Lyon 1
- Analysis using XRD. The measurements were carried out using a Rigaku RU-200BH X-ray generator equipped with a rotating anode, an Osmic multilayer optic and a mar345 2D detector. The wavelength used was that of Cu, λ = 0.15418 nm. The samples to be analysed were finely ground, the powder produced was well homogenised, then placed in a glass capillary 0.5 mm in diameter. The volume of powder exposed to the X-rays was around 0.1 µl. The diffractograms were analysed using X'Pert HighScore software.

The colonies were scraped from the limestone walls with a plastic sterile tube, and maintained at -80°C until total DNA extraction, amplification steps and sequencing. PowerBiofilm DNA Isolation Kit was used by MicroSynth AG following the manufacturer's instructions (MoBio Laboratories, Inc., Carlsbad, CA, USA). The polymerase chain reaction (PCR) amplification followed a two-step PCR

protocol using a state-of the-art high fidelity polymerase. PCR amplifications were performed with the primers p23SrV_f1 (5'-GGACAGAAA- GACCCTATGAA-3'), p23SrV_r1 (5'-TCAGCCTGT- TATCCCTAGAG-3') and 16S 799 f (5' - AACMGGATTAGATACCCKG- 3') and 16S 1115 r (5' - AGGGTTGCGCTCGTTG- 3').
The environmental conditions measured in this part of the cave were:
- Hygrometry: from November 2018 to December 2019 using an Omega OM-EL USB 2 data logger.
- Temperature: the temperature has been monitored a number of times since 2008, most recently using a ReefNet Sensus Ultra data logger.
- Luminosity: measured on 20 April 2018 using a LI-COR LI-250A lux meter.
- Level of carbon dioxide: measured using an Industrial Scientific portable gas detector, type MX6 iBrid, between 2013 and 2018.

3. Results

The macrophotographic images show that the wall is covered with a layer of green entangled filaments (Fig. 1B). This deposit is very porous.

Microscopic observation shows that these filaments consist of two distinct parts. The external envelope seems to be of mineral origin whereas the internal part appears to be of biological origin (Fig. 1C).

SEM images taken after drying confirm this structure of tubes made up of crystals (Fig. 1D). The crystals appear to be clustered together in a disorderly fashion. (Fig. 1E). The crystals have a rhombohedral form (Fig. 1F).

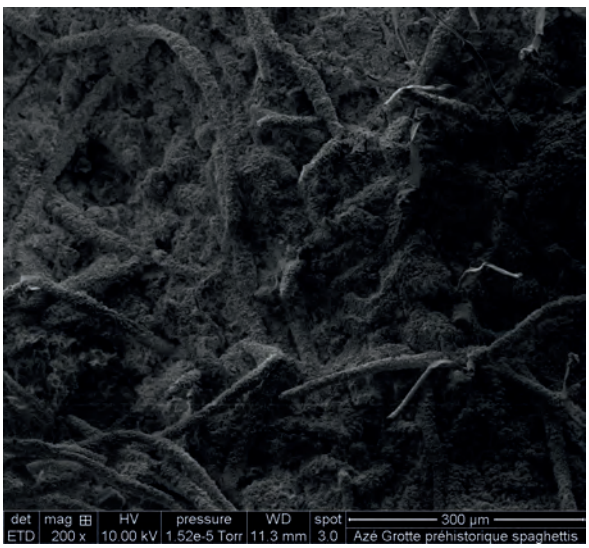

XRD analysis shows that the tubes of crystals consist essentially of calcite. In certain places the tubes appear crushed and stuck together. The porosity seems to have been lost (Fig. 2).

DNA sequencing shows that the photosynthetic biofilm consists of bacteria: cyanobacteria (93,5 %), proteobacteria (1,2 %) and eukaryota (3,4 %). The main phototrophic organisms present are cyanobacteria (Fig. 3). These have not been specifically identified with the exception of a small proportion of them which belongs to the order of Synechococcales.

Regarding the environmental conditions in the zone of the cave which is the subject of this study, the climatology of the exterior has an important influence. The temperature in this zone can be below zero in winter and as high as 20° C in summer. Humidity is very variable but rarely falls below 60%. The level of carbon dioxide is similar to that of the exterior. The intensity of light is reduced, in the order of 1 to 2 lumens on a sunny day. Periods of heavy rain can lead to water running down the walls.

Figure 2: zone where the porosity has been lost. The entanglement has been partly retained but the filaments are crushed.

Kingdom	Phylum	Class	Order	Familly	Gender	% dans échantillon 1	% dans échantillon 2
Bacteria(100)	Cyanobacteria(100)	Not_defined(100)	Not_defined_unclassified(100)	Not_defined_unclassified(100)		72,2	80,2
			Synechococcales(55)			21,3	13,5
Eukaryota(100)	Streptophyta(100)	Bryopsida(100)	Bryopsida_unclassified(70)	Bryopsida_unclassified(70)		2,0	0,4
	Chlorophyta(100)	Chlorophyceae(100)	Not_defined(100)	Not_defined(100)	Jenufa(100)	1,3	3,0

Figure 3: extract of results of DNA sequencing carried out on two samples taken from the wall studied.

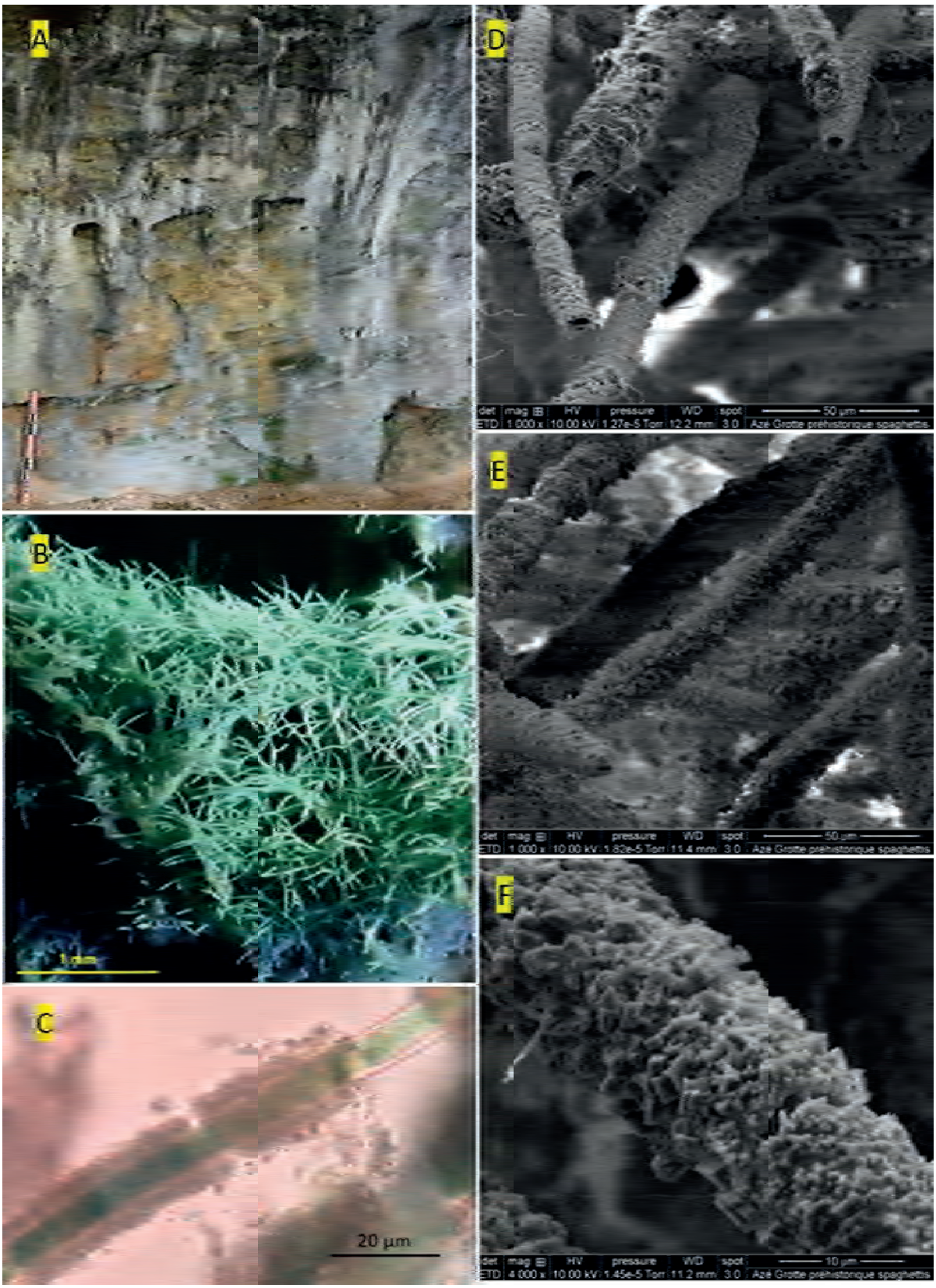

Figure 1: A: general view of the zone studied; B: macrophotographic image of the entangled filaments; C: under the microscope, two distinct parts of the filaments can be seen – a grey mineral component and a green biological component; D to F: MEB observations; D: after drying, the tube structure is retained; E: the external part of the tube consists of a jumbled mass of crystals; F: the crystals have a rhombohedral form.

4. Discussion

The results show that the parts of the wall studied are covered by a filamentous structure consisting of a mineral component and a biological component. DNA sequencing shows that the microorganisms are eukariota, proteobacteria and the mostly present in this milieu are cyanobacteria. Eukariota and proteobacteria can induce calcite precipitation but cyanobacteria have several particularities who can explain the wall modification in Azé cave:

a. They are phototrophs which explains their presence in this part of the cave still subject to natural light.

b. They are known for the biomineralization of calcite which they induce (Dupraz and *al*., 2009, Bundeleva, 2012), which in the majority of cases is produced at their surface. They therefore depend exclusively on prevailing environmental conditions which explains the disorderly nature of the crystal formations observed.

c. Cyanobacteria use carbon dioxide and water to produce oxygen. The carbonate comes from the water which is also the source of the calcium necessary for the production of calcite (Kammennaya et *al*, 2012).

Pigments frequently described and associated with photosynthetic microorganisms are chlorophyll a and b (quite green) and phycocyanin (quite blue). The variations in colour noticed in all likelihood correspond to climatic periods when photosynthesis is more or less active. Given that water is a key factor for the development of cyanobacteria (Barberousse, 2007; Roldan & Hernandez-Mariné, 2009), with its relative absence in summer it is possible that the cyanobacteria undergo a period of dormancy which would explain the disappearance of the blue-green tones from the wall. Nevertheless, the presence of this biofilm does not seem to be impacted by the significant climatic variations to which this part of the cave is subjected from season to season.

As the biofilm evolves, a deposit of calcite forms on the wall. The water which from time to time flows down the wall brings about changes in the structure of this deposit. The calcite loses part of its three-dimensional structure.

5. Conclusion

The modifications to the wall which have been observed since it was uncovered are linked to the formation of a biofilm which has developed through the process of biomineralization. This has occurred because of the presence of cyanobacteria. The variations in the colours observed in all likelihood correspond to a phase of hydric stress for the cyanobacteria. Over time, the biofilm evolves. After the microorganisms disappear, only the calcite remains which continues to evolve by losing its filamentous form linked to the presence of cyanobacteria. The result is a film of calcite which modifies the cave wall.

Acknowledgments

We thank for their support the Conseil Départemental de Saône-et-Loire, l'Association Cultuelle du Site d'Azé Bob Norington and the Laboratoire Chrono-Environnement de Besançon who have provided invaluable help for this study.

References

BARBEROUSSE H. (2007) Etude de la diversité des algues et des cyanobactéries colonisant les revêtements de façade en France et recherche des facteurs favorisant leur implantation. Thèse de doctorat, MNHN Paris, 186p. HAL Id : tel-00188566

BARRIQUAND J et L., ARGANT A., FLOSS H., GALLAY A., and al. (2011A) Le site des Grottes d'Azé. Quaternaire, Hors-série, n° 4, 15-25.

BARRIQUAND J et L., GUILLOT L., NYKIEL C. (2011B) Le site des grottes d'Azé Le fruit de 60 ans de recherches dans le karst du massif de Rochebin (Saône-et-Loire). Spelunca, n° 123, 7-16.

BUNDELEAVA I. (2012) Modélisation expérimentale de la précipitation des minéraux carbonatés lors de l'activité bactérienne. Thèse de doctorat, Université Paul Sabatier, Toulous III, 306p. HAL Id : tel-00671484

DUPRAZ C., REID P., BRAISSANT O., DECHO A., and al. (2009) Processes of carbonate precipitation in modern microbial mats. Earth-Science Review, n° 96, 141-162.

KAMENNAYA N., AJO-FRANKLIN C., NORTHERN T., JANSSON C. (2012) Cyanobacteria as biocatalysts for carbonate mineralization. Minerals, n° 2, 338-364.

ROLDAN M., HERNANDEZ-MARINE M. (2009) Exploring the secrets of the three-dimensional architecture of phototrophic biofilms in caves. International Journal of Speleology, n° 38, 41-53.

TABOROSI D., HIRAKAWA K. (2004) - « Stalactites extérieures » dans les karsts tropicaux humides : dépôts stalagmitiques de tufs calcaires. Karstologia, n°44, 43.

Origin of the asymmetry of certain fossil galleries: the major role of biocorrosion as exemplified in the Roquette cave (Gard, France)

Laurent BRUXELLES[1,2], Lionel BARRIQUAND[3], Jean-Yves BIGOT[4], Didier CAILHOL[1,5], Kim GENUITE[3] & Stéphane JAILLET[3]

(1) TRACES, UMR 5608 du CNRS, 5 Allées Antonio Machado 31058 Toulouse, France Laurent.bruxelles@inrap.fr (corresponding author)
(2) GAES, University of the Witwatersrand, Johannesburg, South Africa.
(3) Université Savoie-Mont-Blanc, EDYTEM, UMR 5204, Bâtiment « Pôle Montagne », 5 bd de la mer Caspienne, F-73376 Le Bourget-du-Lac cedex
(4) Association française de karstologie (AFK)
(5) Inrap, 13 Rue du Négoce, 31650 Saint-Orens-de-Gameville, France

Abstract

Some portions of fossil caves show asymmetrical gallery sections and these morphologies can be associated with biocorrosion. When the highest point of the gallery is not situated in the middle axis, we can observe, just below, an inclined to subvertical flat surface where the rock is strongly weathered and cut out by karrens and pots. At the foot of the opposite wall of the gallery, a well-marked basal notch is common. Above the notch, a succession of hollow shapes (conches) intersecting both limestone and calcite is present. The above features, as well as the presence of hydroxyapatite crusts, indicate significant occupation by bats and represent morphologies formed through ancient biocorrosive processes. The inclined wall, situated under the living areas of the bats, is transformed into a “biogenic lapiaz” formed under a layer of guano. The notches located at the base of the opposite wall correspond to the distal end of the guano heap, the acidity of which, released by mineralization, corrodes laterally. Above the notch, the hollow shapes, which we will call "biogenic conches", result from the upward circulation of gases and acid aerosols generated by the convection resulting from the degradation of guano. This process of differential alteration tends to increase the initial asymmetry of the gallery whose two walls have a very different morphology and texture.

1. Introduction

Geomorphological studies of caves in tropical areas have shown that the presence of large colonies of bats has an impact on the morphological evolution of galleries (MC FARLANE *et al*., 1995; LUNDBERG & MC FARLANE, 2012). Biocorrosion can result in occasional alterations, such as bell holes on the ceiling or pot holes on the ground. They develop around bat nesting areas or under piles of guano but it appears that biocorrosion can also be responsible for larger features manifested on the scale of the entire gallery (Fig. 1). These morphologies are often more difficult to identify, requiring consideration of a whole series of features that are still relatively unknown, the association of which reveals not only the different impacts of biocorrosion, but also the extent of biogenic reshaping. In certain cavities such as the Roquette cave (Gard, France), biocorrosion has erased the initial speleogenic features and radically modified the general section of the gallery.

Figure 1: Overview of an asymmetrical gallery marked by biocorrosion. The biogenic lapiaz on the right faces a smooth wall hollowed out with biogenic conches on the left that overlies a notch visible at the foot of the walls. The soil is made up of a thick layer of phosphates from guano mineralization (photo: P. Crochet).

2. Materials and methods

For the study of these forms, we have chosen to take the cave of La Roquette (Gard, France) as a case study where substantial evidence of biocorrosion has recently been identified (BRUXELLES *et al.*, 2022). Located about thirty meters above the Vidourle river, this cave consists of a large gallery almost 500 m long with two entrances, a 15 m sinkhole to the northwest and a prehistoric entrance, leading to the side of the valley, to the southeast (DU CAILAR & COUDERC, 1947). With the exception of the entrance sinkhole, the cavity is horizontal and corresponds to an old local base level linked to deepening of a large polje. Locally, abundant speleothem partially clogs the gallery. This cave is known since prehistory and has yielded archaeological material dating back to the Middle Palaeolithic (JEANJEAN, 1871; DE JOLY, 1938; MEIGNEN & COULAROU, 1981). Thus, it appears that this cavity has been connected to the surface at least since the Middle Pleistocene, meaning that it has therefore been able to shelter colonies of bats at least since this time.

The Roquette cave shows features of spectacular biocorrosion over almost its entire length (BRUXELLES *et al.*, 2022). It was necessary to characterize these features as carefully as possible in order to establish a typology of the different forms of evidence along the cavity. In addition to the photographs specifically dedicated to these features, we took photos and videos by drone in the cave. This allowed us to obtain novel perspectives and better highlight the particular morphologies caused by biocorrosion. Finally, two episodes of 3D scans utilising lasergrammetry were conducted using a Faro Focus 3D 360 short-range phase shift scanner (Edytem laboratory). The acquisitions were conducted with a density of about seven million points per scene, every 2-3 m. In total, 227 scan scenes were acquired over the entire network, making it possible to model the whole cave and then to generate numerous gallery sections in order to conduct morphometric analyses in particular sectors where the asymmetry is the most marked (Fig. 2).

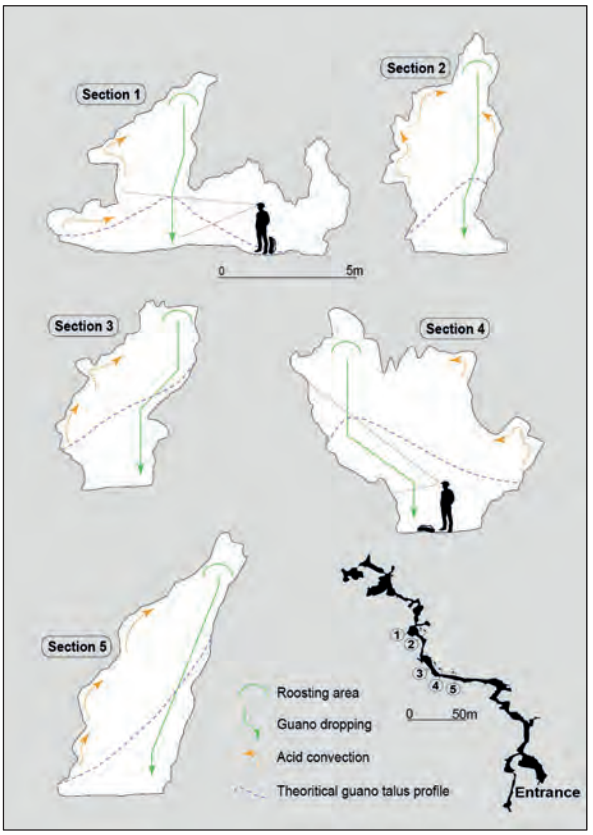

Figure 2: Some sections of galleries in the Roquette cave. The green arrow indicates the arrival of guano from the bat nesting area. The orange arrow materializes the convective phenomena responsible for the expansion of the gallery. The purple dotted lines give an idea of the geometry of the piles of guano, keeping in mind that their size is very variable over time (3D scan and drawing by S. Jaillet).

3. Results

Among all the biocorrosion features identified, some may be genetically associated. The most significant and the most characteristic feature is the asymmetrical galleries because it includes a whole suite of features deriving from several processes working together. This multifaceted feature represents a complex biogeochemical system (Fig. 2) that includes the following forms:

- ***At the vault***, bats occupy the highest part, often at the top of phreatic cupolas. Bell holes (biogenic cupolas) are superimposed in these forms. In these high parts, the rock is altered in a differential way by the condensation-corrosion enriched in CO_2 resulting from the respiration of bats. This results in a rough texture leaving the less soluble parts in relief and resulting in an "elephant skin" appearance (Fig. 3).

- ***When the high point of the gallery*** is not exactly in the center of the gallery but rather eccentric, the urine and the guano flows along a wall and a film of guano can persist if the wall is not too vertical. On contact with them, the surrounding rock is altered and the limestone is replaced by a layer of hydroxyapatite type phosphate. Here, the alteration of the rock takes place in a differential way and results in the formation of a biogenic lapiaz covered with a dark layer of phosphate (Fig. 4).

- ***On the ground***, the guano forms a heap leaning against one of the walls and flowing to the other wall (Fig. 2, sections 2-5). Its mineralization leads to the release of sulphuric and nitric acids and the formation of various types of phosphates.

Figure 3: "Elephant skin" appearance of the rock around the bat nesting areas. Here the rock is differentially altered by corrosion condensation made slightly more aggressive thanks to the CO_2 released by bats (photo: J.-Y. Bigot).

- ***At the base of the opposite wall***, the distal part of the pile of guano causes the formation of a notch, by the leaching of fermentation juices (whose pH can reach 2-3). This develops several decimetres to more than one meter into the limestone (Fig. 2, sections 1 to 5).

- ***Above the pile of guano***, fermentation causes a rise in temperature and convection processes raise acidic gases and aerosols. Above, at the contact with the cooler wall, which overhangs the guano, the gases condense and form a veil of acidic water that actively dissolves the limestone. Vertically organised dissolution features develop along these updrafts routes. These biogenic conches, similar in form to large wall cupolas, range in size from the decimetric to metric (left wall in Fig. 1). Here, the rock is perfectly smooth and these forms affect the limestone or calcite concretions equally, a sign of sufficient potency to overcome the difference in crystal size (micrite vs sparite) in particular.

Figure 4: Biogenic lapiaz formed by cryptocorrosion under a guano film. The dark parts (to the left of the personage) correspond to hydroxyapatite crusts (photo: P. Crochet).

Figure 5: Facing a biogenic lapiaz (on the back of the personage), the limestone wall shows the forms of successive upwelling waves. They cannot be attributed to paragenetic benches and correspond to a stage in the evolution of biogenic conches formed by the convection of acid gases resulting from the fermentation of guano (photo: J.-Y. Bigot).

4. Discussions

The association of features and the implied succession of processes are visible all along the cavity. Of course, the asymmetry changes axis depending on the initial position of the top point of the gallery, where the bats have settled (Fig. 2). The wall located under the droppings undergoes a direct alteration, but the guano film and the hydroxyapatite crusts protect it from the acid flows resulting from the fermentation of the main pile of guano (Fig. 4). On this wall, we therefore only observe forms of cryptocorrosion (biogenic lapiaz), sometimes pierced with pot holes and the retreat of the wall is moderate. The opposite wall, however, is constantly subjected to the action of acid fluxes resulting from the fermentation of guano. The development of notches at the foot of the opposing walls allows this phenomenon to extend laterally, altering the wall's morphology and accentuating the asymmetry of the gallery.

Above these notches, a series of biogenic conches are organized vertically and cause the progressive retreat of the wall (fig. 2 and 5).

They even sometimes result in a very particular morphology that resembles upwelling waves, illustrating the role of acid convection in their formation. Here the retreat of the wall is much more marked because it is constantly exposed to weathering, the limestone being always bare and exposed. This wall therefore moves back faster, increasing the initial asymmetry of the section (Fig. 1).
Of course, depending on the initial geometry of the gallery, all scenarios are possible and all of these manifestations are not always present. For example, if the high point of the gallery is located right in the center or if the walls are vertical or overlooking, we will not find any biogenic lapiaz. We will rather have a system with a double lateral notch overlain by facing biogenic conches (Fig. 2, section 1).

5. Conclusion

It is accepted that biocorrosion has an impact on the walls (i. e. LUNDBERG & MC FARLANE, 2012; AUDRA *et al*., 2016 & 2019) to such an extent that in some caves, the initial section of the conduit has sometimes been expanded by twice its original size (BARRIQUAND et al., 2021). This expansion is not homogeneous along the cavity but also on the scale of the section of the galleries. Depending on the initial geometry of the gallery, but also on the position of the bat nesting area and the density of the colonies, we observe a differential evolution of the walls, which can lead to the accentuation of the initial asymmetry of the conduit. This aspect is only one example of the many impacts of biocorrosion in caves, many forms of which have yet to be identified and described. It is important to know how to identify them because they testify to a post-speleogenic evolution, the impact of which on underground volumes and their organization constitutes a new perspective for karstologists and archaeologists. Indeed, this remodelling erases the initial speleogenic features of the cavity and the traces of art, if there were any before the arrival of the bats (BRUXELLES *et al*., 2016). This type of analysis, in decorated or partially decorated cavities, therefore becomes essential to the study of the integrity and preservation of the cave rock art.

Acknowledgments

We gratefully thank the French Ministry of Culture, the CNRS PEPS & the MSHS-T APEX programs and Dominic Stratford.

References

AUDRA P., BARRIQUAND L., BIGOT J.-Y., CAILHOL D., CAILLAUD H., VANARA N., NOBECOURT J.-C., MADONIA G., VATTANO M et RENDA M. (2016) L'impact méconnu des chauves-souris et du guano dans l'évolution morphologique tardive des cavernes. *Karstologia* n° 68, 2016, p. 1-20

AUDRA P., DE WAELE J., BENTALEB I., CHRONAKOVA A., KRISTUFEK V., D'ANGELI I.M., CARBONE C., MADONIA G., VATTANO M., SCOPELLITI G., CAILHOL D., VANARA N., TEMOVSKI M., BIGOT J.-Y., NOBECOURT J.-C., GALLI E., RULL F., SANZ-ARRANZ A. (2019) Guano-related phosphate-rich minerals in European caves. *International Journal of Speleology*, 48 (1), 75-105.

BARRIQUAND, L., BIGOT, J.-Y., AUDRA, P., CAILHOL, D., GAUCHON, C., HERESANU, V., JAILLET, S., VANARA, N. (2021) Caves and bats: Morphological impacts and archaeological implications. The Azé Prehistoric Cave (Saône-et-Loire, France). *Geomorphology* 388, 107785

BRUXELLES L., BEAUVILLIERS M., BARRIQUAND L., CAILHOL D., FROUIN M., GALANT P., GENUITE K., LE GUILLOU Y., HOELLINGER S., JAILLET S., KANIEWSKI D., LARTIGES B., LEROUX G., OTTO T., PALLIER C., PFENDLER S., PONS-Branchu E., TOURON S., et VANARA N. (2022) *Impact de la biocorrosion sur les grottes ornées et les monuments historiques*. Rapport de 1ère année de Programme Collectif de la Recherche, Ministère de la Culture, 336 p.

BRUXELLES L., JARRY M., BIGOT J.-Y, BON F., CAILHOL D., DANDURAND G. et PALLIER C. (2018) La biocorrosion, un nouveau paramètre à prendre en compte pour interpréter la répartition des œuvres pariétales. L'exemple de la grotte du Mas d'Azil en Ariège. *Karstologia*, n°68, p. 21-30.

DU CAILAR, J., COUDERC J. (1947) – Recherches spéléologiques dans le Languedoc Méditerranéen. Explorations dans le Gard du groupe Cévenol de Spéléologie (Saint Hippolyte du Fort) et de la section du Languedoc Méditerranéen du C.A.F. (Montpellier). Annales de Spéléologie (*Spelunca 3ème série*), 2, 205-222

GIMON L. (1907) Mode d'emploi des rabots ou grattoirs verticaux. *Bulletin de la Société préhistorique française*, 4-3, 183-186

JEANJEAN, A. (1871) *L'homme et les animaux des cavernes des Basses-Cévennes*. Imprimerie Clavel-Ballivet.

DE JOLY, R. (1938) Compte rendu sommaire des explorations de 1938. *Spelunca*, 9, 19-34.

LUNDBERG J. et MC FARLANE D.A. (2012) Post-speleogenetic biogenic modification of Gomantong Caves, Sabah, Borneo. *Geomorphology*, p. 153-168

MC FARLANE D.A., KEELER R.-C. and MIZUTANI H. (1995) Ammonia volatilization in a Mexican bat cave ecosystem. *Biogeochemistry*, n° 30, p. 1-8.

MEIGNEN, L., COULAROU, J. (1981) Le gisement paléolithique moyen - La Roquette (Conqueyrac, Gard). *Étude archéologique, Valbonne*. Notes internes 26.

The guano holes and guano pots: two new climate-controlled biogenic corrosion forms in Puerto Princesa karst area (Palawan, Philippines)

José Maria CALAFORRA[1,2], Jo DE WAELE[1,3], Paolo FORTI[1,4], Fernando GÁZQUEZ[5], Tommaso SANTAGATA[1] & Marco VATTANO[1,6]

(1) La Venta Esplorazioni Geografiche, Italy
(2) Water resources and Environmental Geology, University of Almeria, Spain
(3) BIGEA Dept., University of Bologna, Italy
(4) Istituto Italiano di Speleologia, University of Bologna, Italy, paolo.FORTI@unibo.it
(5) Department of Biology and Geology. University of Almería, Spain
(6) Earth and marine Sciences Dept., University of Palermo, Italy

Abstract

New biogenic forms were recently observed inside the caves of Palawan. They consist of perfectly rounded holes, developed over any kind of limestone surface interested by bat droppings. Their genesis is controlled by the peculiar Palawan climate, which is characterized by short but strong rainfalls followed by rather long dry periods. Keyword: Corrosion form, climatic control, genetic mechanism, cave minerals

1. Introduction

Guano is a very strong agent of limestone corrosion in caves. Its digestion processes produce large quantities of CO_2 and several strong acids. For this reason, corrosion forms and plenty of cave minerals are normally related to guano deposits (ONAC & FORTI 2011).

Recent investigations in the karst area around the Puerto Princesa Underground River (Palawan, Philippines) (DE VIVO & FORTI 2017; AGNELLI et al. 2018) have allowed to discover two new limestone corrosion forms: the guano holes and guano pots (Fig. 1). They consist of perfectly rounded vertical holes, from 3 cm up to over 50 cm wide and from 5 to 80 cm deep and with a slightly concave bottom, developed over any kind of limestone surface interested by bat droppings. Their development is clearly related to the strong acids produced by the decay of guano deposits.

The genetic mechanism of the guano holes has already been discussed in detail (CALAFORRA et al. 2019) and it was proven that the local climate is the fundamental factor controlling the development of these forms.

2. The cave climate

The climate of Palawan is “tropical wet and dry”; the average rainfall is relatively high (close to 2,000 mm/yr, 95% of which occurs during the wet period from May to November) concentrated in a few, short but heavy rainstorms (BADINO 2017).

As a consequence of this special climate cave dripping is scarce, or totally absent, for long periods of time, while condensation may be high or very high in some places, especially in areas close to and directly linked to the outside. Speleothems are thus inactive or even being corroded for most of the time, while during and immediately after the heavy rains intense and widespread dripping (coming both from stalactites and fractures characterizes) large areas, thus allowing the development of some peculiar forms (CALAFORRA et al. 2019).

The very high external relative humidity, together with the extremely low daily temperature fluctuations within the caves inhibit the evaporation processes which are limited to branches where relatively strong air currents occur. Anyway, within the PPUR, it is sometimes possible to see active condensation processes with the development of large subterranean clouds and consequent light rains (BADINO 2017).

3. The shape and evolution of guano holes

Guano holes were observed in several caves of the area, but the most important actually known site is within PPUR where guano holes have been observed in different areas (Navigator Chamber, Australian Inlet, Gaia Branch).
Some of the largest guano-hole fields within PPUR have been mapped by means of 3D photogrammetry (AGNELLI et al. 2018). The guano holes are vertical cylinders, or very elongated upside-down cones with an average diameter between 3 and 6 cm, while their depth ranges between 10 and 15 cm.
Many of the holes are empty but some have the bottom covered by a thin layer of guano. Their inner surface is smooth, but sometimes it is covered by a layered speleothem, partially detached from the limestone surface. This occurs when the energy of dripping water is not able to totally remove the secondary minerals formed as a consequence of acid aggression (CALAFORRA et al. 2019).
The characteristics of the sites in which guano-holes develop are always the same: holes are grouped in clusters of tens or hundreds of elements, developed over rather flat, or only gently inclined, limestone surfaces, which are covered by a relatively thin guano deposit (just up to a couple of cm thick) so that it can be totally removed from the impact area by dripping.
Most of the evolution of the guano holes occurs during intense rainstorms or in the immediately following days.
In conclusion, in order to allow guano-holes to develop, three boundary conditions must be fulfilled (CALAFORRA et al 2019):

1. *The surface of the limestone needs to be close-to-horizontal*
2. *The thickness of the guano deposit should not exceed a couple of centimeters*
3. *The area has to be under intense dripping for short periods of time, interrupted by long periods of drought (no dripping) and guano deposition*

In many caves of the PPUR karst area the condensation is scarce, therefore most, if not all, of the development of guano holes occurs during the rainstorms and the few days after them. In fact, their evolution stops when no more water is available on their bottom.
At present the single known cave in which their development seems to be active also during the dry periods is the Hundred Cave where, thanks to the high number of multilevel entrances, condensation is strongly active all year round thus allowing a fast evolution of guano holes.
Finally, if condensation corrosion is active in areas where dripping is locally decreased, guano holes are rapidly dismantled with the evolution of a rather flat limestone surface almost totally buried by a guano layer from which only few, small sharp remnants of the former guano holes protrude.

4. The shape and evolution of guano-pots

Guano-pots were firstly observed in PPUR (DE VIVO & FORTI 2017) but they are present in many other caves of the area. The most important actually known site for guano pots is the Hundred Cave (a relatively small epidermic multilevel cave located some 20 km far from PPUR). Its structure, characterized by tens of entrances, induces strong condensation in most of its galleries where practically all speleothems are deeply corroded.
Guano-pots exhibit a larger dimensional variability (ranging from 10 to 80 cm in diameter and reaching a depth of 80 cm or even more), they develop on any kind of surface with an even steep slope and the thickness of guano deposit seems to have no role in their development.

Therefore, the single boundary condition for guano-holes which, at least in some circumstances, is valid also for guano-pots is the third one: the presence of intense dripping for short periods of time.

Yet the most important factor in driving guano-pot evolution lies elsewhere: the condensation-corrosion, which normally hinders the evolution of guano-holes by causing diffuse corrosion of the limestone surface below the guano deposit. Condensation is extremely important in the development of any kind of guano-pot, being often the main driving factor

for the genesis of these forms, as testified by the presence of plenty of them within the Hundred Cave, where condensation is by far the most important source of aggressive water.

Three different types of guano-pots exist (Fig.1): two of which develop over flat or gently inclined limestone surface, while a third one also forms over relatively steep slopes. The first type of guano-pot is directly related to the presence of guano-hole fields (Fig. 1.4,.5): it develops thanks to the coalescence of several guano-holes, when a slight excess of guano and/or of dripping density may enhance the corrosion of the thin crests dividing the different holes.
At any rate, the deepest and largest ones develop on close-to-horizontal limestone surfaces over which guano is randomly distributed, being localized in few huge (conical) deposits, the diameter of which controls that of the related pot. The thickness of the deposit inhibits the guano from being entirely washed away by dripping. Drip water, during rainstorms, penetrates into the porous guano deposit reaching its bottom where it comes in contact with the limestone surface underlying the guano.

Therefore, a pot develops with the diameter of the overlying guano deposit, while phosphate crusts cannot develop because the small mineral grains are dispersed within the guano and are probably washed away, when the excess of dripping during rainstorms causes the spilling over of the water from the developing guano-pot.

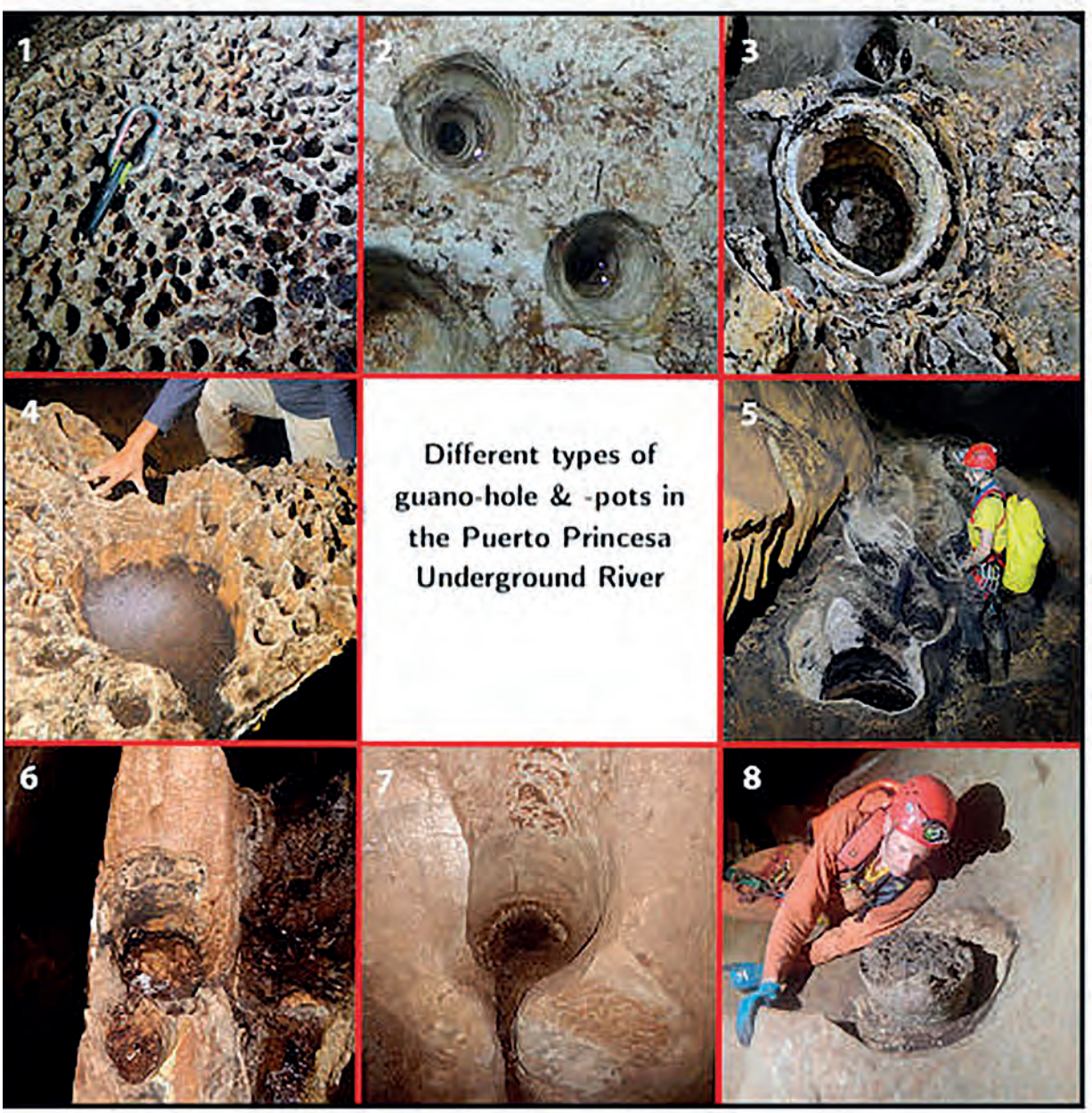

Figure 1: Types of guano-holes & -pots in the PPUR area: PPUR-Navigator chamber: 1- Cluster of guano-holes; 2- Two perfectly rounded guano-holes; PPUR-Australian inlet: 3- Layered phosphate ring developed inside a guano-hole; PPUR Gaia Branch: 4 - A guano-pot developed over a guano holes field; 5- A series of giant guano-pots; Hundred cave: 6- Guano-pots developed on a steep surface; 7- Guano-pot with a deep carved discharge channel; 8- PPUR Gaia Branch: phosphate deposit within a former pot now completely destroyed.

The third type of guano-pot forms over relatively steep surfaces. It occurs starting from selected points corresponding to a local smoothing of the slope, which in turn allow thin guano deposits to accumulate there (Fig. 1.6). During strong rain storms the spill-over phenomenon may occur to any kind of pots, but is more common for those developed over steep slopes. The temporary presence of aggressive water in contact with the limestone surface downstream the pot, causes the development of a discharge channel, morphologically and genetically very similar to those already well known for “kamenitzas” (Fig. 1.6).

5. Guano pots and guano holes "old age"

Finally, when dripping decreases or even definitively stops, condensation-corrosion becomes the main, or even the single factor controlling the evolution of the already well-developed guano-pots and -holes.
Due to the decrease in water energy, dripping is no longer able to wash away the guano, thus rapidly covering the whole site formerly affected by guano-hole and guano-pot development. The corrosion starts acting over the whole limestone surface.
The area is rapidly transformed into a sub-horizontal surface completely covered by a thin guano layer, from which just small and sharp limestone pinnacles protrude, which are the remnant of the former guano-hole and guano-pot vertical walls. (Fig. 1.8)

6. Conclusion

The Palawan climate, characterized by strong and short rainstorms followed by long dry periods, together with widespread guano deposits allow the development of some totally new corrosion-depositional forms. Among them the most characteristic ones are the guano-holes and -pots.
The guano-pots differ from guano-holes not only for their larger dimensions but also for the mechanism of their development which is mainly controlled by condensation waters and not by infiltration dripping.

Therefore guano-pot evolution is faster than that of guano-holes because they can theoretically grow all year round while the guano-hole evolution occurs only during rainstorms and a few days thereafter.

Acknowledgements

The research was performed in the framework of the "Philippines-Italy Debt for Development Swap Program". The Authors thank the Local Authorities, the Managers and all the staff of the Puerto Princesa Underground River Park and the cavers of the Gaia Club of Manila and of the La Karst Club of Sabang for the help given during the research

References

AGNELLI P., DE VIVO A., DE WAELE J., FORTI P., PICCINI L., VANNI S. (2018) Preserving an astonishing ecosystem while improving tourism: the case of Natuturingam Cave (Palawan, Philippines). NSS News, 76(6), pp.4-10.

BADINO G. (2017) Driving pressure of subterranean airflows: an analysis. Proceedings 17th International Speleological Congress, Sydney, 2, pp. 205-208.

CALAFORRA J. M., DE WAELE J., FORTI P., SANTAGATA T., VATTANO M. (2019) The guano holes: a new corrosion form from Natuturingam Cave (Palawan, Philippines). Travaux of the Institute of Speologie Emil Racovitza, 47, pp. 35–47.

DE VIVO A., FORTI P. (Eds.) (2017) Support for Sustainable Eco-Tourism in the Puerto Princesa Underground River Area, Palawan, Philippine. Report on the first expedition to Palawan. Tintoretto, Treviso, 110 p.

ONAC B., FORTI P. (2011) State of the art and challenges in cave minerals studies. Studia UBB Geologia 56 (1), pp. 33-42.

Are reshaped speleothems reliable indicators of former rises of the karstic base level? Some criteria for distinguishing between flooding, hydrodynamic reuse and biocorrosion

Laurent BRUXELLES[1,2], Jean-Yves BIGOT[3], Didier CAILHOL[1,4], Grégory DANDURAND[1,4], Jean-Louis GALERA[3], Frédéric SWIERCZYNSKI[5], Nathalie VANARA[4,6] & Franck VASSEUR[7]

(1) TRACES, UMR 5608 du CNRS, 5 Allées Antonio Machado 31058 Toulouse, France Laurent.bruxelles@inrap.fr (corresponding author)
(2) GAES, University of the Witwatersrand, Johannesburg, South Africa.
(3) Association Française de Karstologie (AFK)
(4) Inrap, 13 Rue du Négoce, 31650 Saint-Orens-de-Gameville, France
(5) *Underwater Experience* (*UWX*), 13740 Le Rove, France - https://uwx.fr/
(6) Université Paris 1 – Panthéon-Sorbonne, France
(7) Celadon, France - http://celadons.free.fr/

Abstract

Classical speleothems (stalactites, stalagmites, pillars and flowstones) form in the vadose parts of karst cavities. Their presence therefore represents the total or partial, sometimes temporary, dewatering of associated parts of the karstic network. Conversely, the hydrogeological reuse of an old gallery, for example in connection with the rise of the base level, limits or even stops the development of these concretions. When cavities are flooded, corrosion of the speleothem surface or mechanical erosion (abrasion by sand, pebbles impacts) can alter their morphology. Many highly altered concretions, recognized in fossil networks across the world, have been interpreted as indicators of previous base level rises. The resultant hydrodynamic interpretations sometimes require the development of complex supporting geodynamic hypotheses. But it appears that in many cases speleothems are instead affected by biocorrosion linked to the ancient presence of bat colonies. Guano fermentation and convection of acidic gases combined to deeply reshape nearby calcite deposits – meaning that these altered speleothems were never submerged after their formation. We will present some examples of this process and some criteria that allow us to distinguish submerged concretions from those that were affected by biocorrosion.

1. Introduction

Apart from a few special cases, percolation concretions such as stalactites, stalagmites, pillars or stalagmitic flows have formed in the vadose zone of the karst. Indeed, it is the combination of the outgassing of CO_2 in the cave atmosphere and the dripping or flow of a film of water guided by gravity that are at the origin of these common speleothems. However, they are characteristic of a very specific area of the karst located between the epikarst and the submerged zone. These concretions, some of which can date back several million years, therefore characterize the ancient and present condition of this environment. In fact, when cave divers observe this type of concretion underwater, it undoubtedly indicates that the hydrogeological context has changed.

But can we necessarily assume that the presence of altered or eroded speleothems is only indicative of reflooding of the cavity? Are there other phenomena capable of significantly reshaping these concretions? If so, what are the criteria that make it possible to distinguish them to avoid the interpretative implications of a rise in the base level and complication of the local geodynamic or geomorphological evolution each time an eroded concretion is observed? Here, we will demonstrate that biocorrosion may represent an important contributor to the erosion of concretions and that there are distinctive criteria that allow it to be identified.

2. Materials and methods

As part of our work on biocorrosion since 2020 (BRUXELLES *et al*., 2021), we have studied more than 200 cavities in the south of France, allowing us to compile a substantial corpus of biocorrosion evidence. Each exploration was documented by a photo session and observations were all recorded in dedicated reports. To document the processes, samples were taken, both for geochemical analyses, petrographic observations, or for dating. In some cavities, we carried out

3D scans to quantify these shapes as well as photogrammetry, for example for the pillar of the Isturitz cave (Fig. 1).
While the impact of biocorrosion on speleothems has been clearly demonstrated (AUDRA *et al.*, 2016; BRUXELLES *et al.* 2021), particularly using geochemistry, it was important to review, for comparison, those subjected to more classic karstic processes to be able to distinguish their forms. Thus, several cave studies were devoted to active or semi-active caves without traces of biocorrosion. We were then able to document the impact of floods and erosion on the speleothems. Similarly, it was important to take into account examples of flooded galleries in our repository. We have therefore integrated observations of cave divers carried out on concretions from different karstic areas.

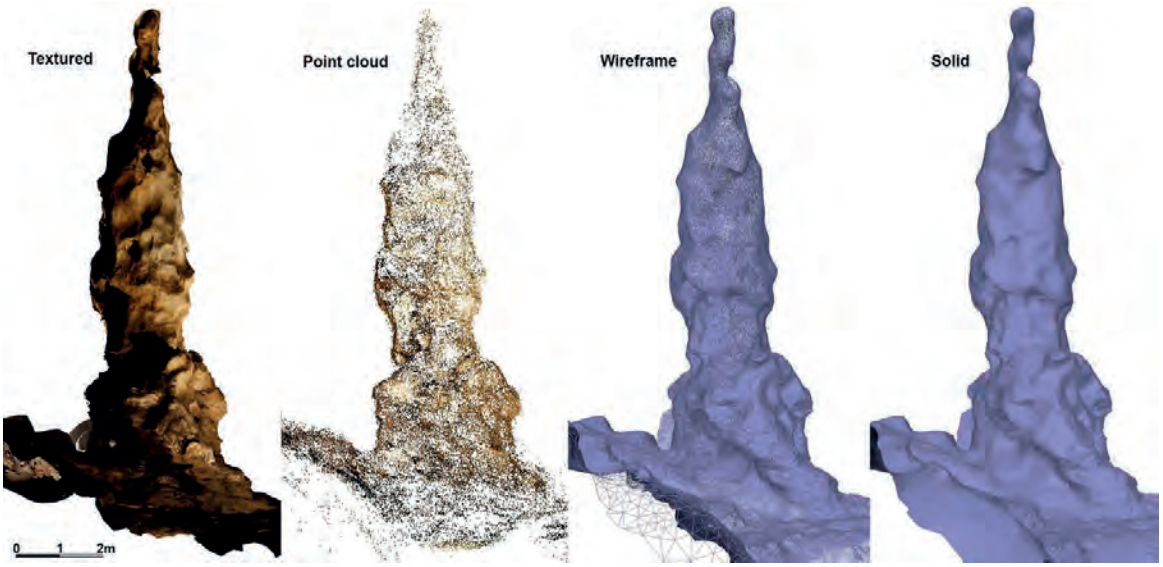

Figure 1: Photogrammetric model of the biocorroded pillar from Isturitz cave (France). We can clearly see the curious morphology of this concretion, hollowed out by numerous large scallops, generally interpreted as proof of the reflooding of the cave. But here, these forms correspond to biogenic conches which are typical signs of intense biocorrosion (photogrammetry: L. Bruxelles).

3. Results

It is not possible to present an exhaustive analysis in the context of this article, so only some results will be presented here, but it is already possible to propose distinctive criteria.

First of all, the reflooding of a fossil and concretionary gallery is not necessarily accompanied by a dissolution of the calcite. In some cases, they are not altered (Fig. 2) or even serve as foundations for new kind of concretions. However, if the water is under-saturated in calcite or even slightly aggressive, the submerged concretions are subject to dissolution. Dissolution operates in a differential manner, the finest forms or the smallest crystals being altered first, resulting in an irregular, jagged appearance. Centimeter to multi-centimeter spoon-shaped scallops affect their surface, oriented in the direction where the water is flowing. When the flow is powerful enough, the concretions decorated with scallops are also profiled. In all the cases, the eroded calcite forms and limestone walls are significantly rough. Due to the different size of the crystals between calcite and limestone, for example, a differential response between the walls and the concretions is perceptible. The micritical rock (like limestone) is much less resistant than concretions made up of larger calcite crystals: it is dependent on contact surface structure. The result is that the retreat by dissolution is therefore less for calcite than for limestone.

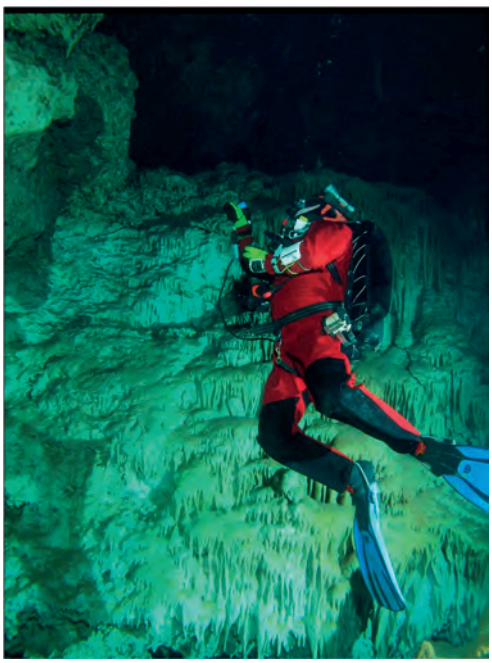

Figure 2: Calcite flow and small stalactites minimally affected by the flooding of the gallery (Cova del Drac de Santany, Spain; photo: F. Vasseur).

If the flows carry a coarse detrital load (as often in the epiphreatic zone or in temporarily active karsts), mechanical abrasion locally affects the speleothems in addition to dissolution. The upstream face, sandblasted and impacted by pebbles, develop erosion facets and spoon-shaped scallops (Fig. 3). Here, one no longer recognizes initial details of the speleothem surface that are still preserved on the other side of the concretion protected from abrasion. The stalagmites even sometimes give the impression of curving upstream, their base being systematically eroded by the saltation of the grains. In the case of coarser sediments, calcite shows greater sensitivity to the impact of pebbles. Indeed, the large crystals are more easily exposed by the percussion of the pebbles, and we observe a greater retreat for the calcite surfaces than for the limestone (Fig. 4).

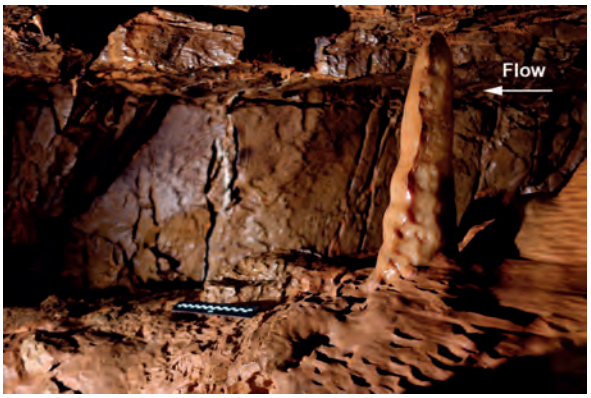

Figure 3: Stalagmite subjected to dissolution and sandblasting during floods. The part exposed facing the current (on the right) is faceted and affected by spoon-shaped scallops, while the other part is almost intact (Grotte du Sergent, France; photo J.-Y. Bigot).

Figure 4: Calcite flow eroded by the impact of gravels and pebbles. The retreat of the orange calcite is greater than that of the limestone (Grotte du Sergent, France; photo: J.-Y. Bigot).

Biogenic corrosion results from the occupation of a gallery by colonies of bats (MC FARLANE *et al*., 1995; LUNDBERG and MC FARLANE, 2012; AUDRA *et al*., 2016; BARRIQUAND *et al*., 2021). The release of CO_2 from their breathing, but above all, the acidic gases and aerosols released by the fermentation of the guano, radically change the conditions of the environment and affect both on the limestone walls and calcite concretions. One of the characteristics of biocorrosion is the smoothing of shapes. The speleothems take on a "ghostly" appearance (Fig. 1, 5, 6 and 7) revealing internal calcite laminae.

They can develop guano pot holes or biogenic lapiaz (see BRUXELLES *et al*, this volume). Sometimes, concretions may appear streamlined. This is due to the circulation of acid gases and aerosols in the cavity, either by convection above the piles of guano or due to the general aerology of the cavity. In all cases, biocorroded concretions do not show spoon-shaped scallops pattern and are smooth with very soft general shapes (Fig. 6). This is very different from the sharpness due to water dissolution.

Another distinctive criterion is that biocorrosion allows calcite and limestone to intersect on the same plane (Fig. 6). This phenomenon involves such strong acids (sulphuric, nitric) that no differential dissolution is observed: biogenic domes or conches develop between these two materials indistinctly, which is in contrast to the observations cited above concerning dissolution or abrasion. Stalagmites, pillars and stalagmitic flows are often marked at the base by a guano pile notch. It is then surmounted by cupolas of multi-decimetric order, smooth, organised vertically (Fig. 1 and 6). These are biogenic conches, formed by the condensation of acidic gases that rise by convection from the guano talus. The small draperies are the most sensitive to this phenomenon and can be the starting point of these conches.

Figure 5: Biocorroded "ghostly" column. We recognize the internal laminae of the initial stalagmite which constituted the core of the column and therefore illustrate the importance of erosion (Gcwihaba cave, Botswana; photo: L. Bruxelles).

Finally, biocorrosion is accompanied by a large quantity of by-products, particularly phosphatic minerals. These are a

result of the mineralization of the guano or the reaction of the guano fluids with the host rock. In the latter case, they form crusts that are found on the speleothems (Fig. 7) or residually in the crevices. If doubt still persisted solely on the basis of the forms of alteration of the concretions, the presence of these phosphates is an unmistakable sign of the action of biocorrosion and makes it possible to attribute the alteration of the concretions to corrosion of biogenic origin.

Figure 7: Grey light phosphate crust formed by the epigeny of limestone and calcite concretions, the truncated forms of which are recognized by biocorrosion (Grotte de la Roquette, France; photo: J.-Y. Bigot).

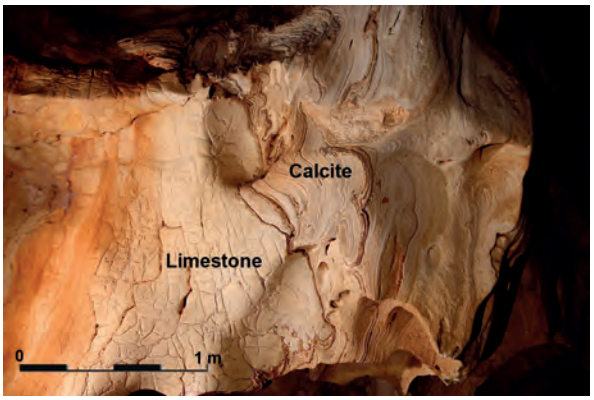

Figure 6: Biocorrosion forms are expressed in a comparable and continuous manner from the limestone wall (left) and over the entire calcite flow (Grotte des Fées, France; photo: J.-Y. Bigot).

4. Conclusion

Many caves around the world show altered or deeply eroded concretions. It is not always possible or relevant to interpret these as indicative of a reflooding of the system, a process that often carries important geomorphological implications. It is therefore important to ensure that the morphologies are not due to biocorrosion, which simplifies hydrogeological interpretations. A few distinctive criteria, resulting from extensive fieldwork, have been presented here and are sufficient in many cases to provide an initial diagnosis. The general smoothing of the detailed forms, the truncation of the bedrock and the concretions on the same plane, the presence of other forms of biocorrosion or the persistence of phosphate encrustation are all evidence that allow us to rule out the likelihood of reflooding.

Of course, the answer is not always binary. For example, in the Mescla cave (France), biocorroded concretions, covered with a layer of phosphate, were observed at a depth of more than 10m under water. They thus testify to the fact that the network was re-flooded after a phase of concretion and a period of occupation of the cave by bats. This shows the complexity of the karst, but also the wealth of information it contains if you have the right reading criteria.

Acknowledgments

We gratefully thank the French Ministry of Culture, the CNRS PEPS & the MSHS-T APEX programs and Dominic Stratford.

References

AUDRA P., BARRIQUAND L., BIGOT J.-Y., CAILHOL D., CAILLAUD H., VANARA N., NOBECOURT J.-C., MADONIA G., VATTANO M et RENDA M. (2016) L'impact méconnu des chauves-souris et du guano dans l'évolution morphologique tardive des cavernes. *Karstologia* n° 68, 2016, p. 1-20

BARRIQUAND L., BIGOT J.-Y., AUDRA P., CAILHOL D., GAUCHON C., HERESANU V., JAILLET S. & VANARA N. (2021) Caves and bats: Morphological impacts and archaeological implications. The Azé Prehistoric Cave (Saône-et-Loire, France). *Geomorphology* 388, 107785

BRUXELLES L., BEAUVILLIERS M., BARRIQUAND L., CAILHOL D., FROUIN M., GALANT P., GENUITE K., LE GUILLOU Y., HOELLINGER S., JAILLET S., KANIEWSKI D., LARTIGES B., LEROUX G., OTTO T., PALLIER C., PFENDLER S., PONS-BRANCHU E., TOURON S. et VANARA N. (2022) *Impact de la biocorrosion sur les grottes ornées et les monuments historiques*. Rapport de 1ère année de Programme Collectif de la Recherche, ministère de la Culture, 336 p.

LUNDBERG J. et MC FARLANE D.A. (2012) Post-speleogenetic biogenic modification of Gomantong Caves, Sabah, Borneo. *Geomorphology*, p. 153-168

MC FARLANE D.A., KEELER R.-C. and MIZUTANI H. (1995) Ammonia volatilization in a Mexican bat cave ecosystem. *Biogeochemistry*, n° 30, p. 1-8.

Biogenic origin of sulfuric acid and its corrosive action in speleogenesis in the karst of the Irecê Basin, Una Group, Bahia state, Brazil

Tom Dias Motta MORITA[(1)], Ivo KARMANN[(1)], Renato Gamba ROMANO[(2)], Lucas Padoan de Sá GODINHO[(1)] & Vivian PELLIZARI[(2)]

(1) Instituto de Geociências da Universidade de São Paulo, 562 Lago Street São Paulo, SP, 05508-080, Brazil, tomdmmorita@gmail.com
(2) Instituto Oceanográfico da Universidade de São Paulo, 191 Oceanográfico Square, São Paulo, SP, 05508-120, Brazil

Abstract

Sulfuric acid speleogenesis research in Brazil is still restricted to a few regions and there is a lack of studies about the microbial induced origin of sulfuric acid, a hypothesis that still needs to be proven in Brazilian karst. This research, under development, aims to characterize the groundwater hydrochemistry and microbiome and identify the origin of sulfur in the karst system of the Irecê Basin, Northeast Brazil (BA), hosted by neoproterozoic limestones of the Salitre Formation, Una Group. Water samples were collected from wells, springs and caves for hydrochemical, sulfur isotope ($\delta^{34}S$) and microbiological (sequenced DNA by metagenomic technique) analyses. Physicochemical parameters were determined in the field. Previous microbiological results (rRNA 16S sequencing) indicate significant relative abundance of sulfur cycle bacteria in groundwater, in sites where hydrogeochemical analysis presents high sulfate concentrations. Preliminary results demonstrate a wide variation in the contents of sulfates and a higher R^2 value of $SO4^2$ X(Ca^{2+}+Mg^{2+}) in comparison to HCO^{3-}X(Ca^{2+}+Mg^{2+}), suggesting that H_2SO_4 is the main acid in the limestone corrosion. It is intended to demonstrate the biogenic production of sulfuric acid as a corrosive agent and contribute to the speleogenesis model of the conduit network of the Irecê Basin karst aquifer.

1. Introduction

Sulfuric acid speleogenesis (SAS) of karst aquifers, compared to epigenic karst systems, comprise a more complex hydrochemical model in which a known sulfur source is needed to be complete. In Brazil, SAS researches are still restricted to a few regions in which the main sulfur source is assigned to the oxidation of sulfides, mainly pyrite, once there are not many indicatives of evaporites or hydrocarbons deposits in the host rock of these caves or bellow. The main hypothesis is that the sulfuric acid origin through sulfide oxidation is induced and catalyzed by microbiological activity. The present study aims to improve the knowledge about the microbiological influence in speleogenesis, approaching the karst system of the Una Group, southern region of the Irecê Basin, central portion of Bahia State, Northeastern Brazil. This area is notable for the high concentrations of sulfates in groundwater, published over decades (*e.g*. GUERRA, 1986; VALLE, 2004) and for the diversity and volume of gypsum speleothems in caves in the county of Iraquara.

SAS is suggested for these caves by AULER (1999) as a possible hypogenic initiation prior to epigenic and paragenetic processes. VALLE (2004) sought to establish relationships between major cations and anions in which the high correlation between SO_4^{2-} and (Ca^{2+} + Mg^{2+}), suggested that the chemical system should have an additional corrosive agent beyond epigenic carbonic acid, the sulfuric acid. VALLE (2004), based on the identification of sulfur cycle bacteria, such as *Thiobacillus* genus proposed its origin to be biogenic.

The studied karst is inserted in neoproterozoic limestones of the Salitre Formation which covers the mesoproterozoic pelites and conglomerates of the Bebedouro Formation, both belonging to the Una Group. Due to a general syncline structure with north-south axis, the limestones are bordered (east, west and south) by quartzite and conglomerates hills of Chapada Diamantina Group (Fig. 1), stratigraphically situated below the Una Group (MAGALHAES et *al.*, 2016). The limestones of the Salitre Formation, host occurrences of sulfides, such as galena, pyrite and chalcopyrite (MISI & SOUTO, 1975).

The geomorphological setting provides variations in the type of water recharge in the karst system. In the southern region, whose rainfall is higher, the allogeneic recharge from the hills is predominant. Meanwhile, the northern region of the study area, delimited by the Jacaré River, in addition to having lower rainfall, also consists in extensive carbonate areas, with a mostly autochthonous recharge in farther regions from the hills.

2. Materials and methods

Field works were carried out in the southern region of the Irecê Basin in January/February 2021 (rainy season) and August and October 2021 (dry season) enabling seasonal comparison. It was dedicated for water sampling from wells and caves for hydro-chemical and microbiological analysis and rock and speleothem sampling to chemical, mineralogical and isotope analysis.
Physicochemical parameters were determined *in situ* using multiparameter probes while ion contents were obtained by various analytical techniques as shown in figure 1. The hydrochemical data was then statistically processed using the *Aquachem*, *Origin* and *PHREEQC* softwares.

Analysed elements	Analytical methods
Ba, Ca, Sr, Fe, Mg, Mn, K, Na	SMEWW, 23rd Ed. 2017, Method 3120 B / USEPA 6010C - 03:2007, SMEWW 23rd Ed. 2017 Method 3030E
Cl, F, PO_4, NO_3, NO_2, SO_4	EPA SW - 846 - 300.1 - 1999
H_2S	SMEWW, 23rd Ed. 2017, Method 4500-S2-, H / G
N-NH_3	SMEWW, 23rd Ed. 2017, Method 4500-NH3, B e F

Figure 1: Hydrochemical analytical methods.

3. Results

The distribution of wells with sulfate concentration data (extracted from the SIAGAS platform CPRM 2020) along the study area is shown on figure 2. The boreholes were compared by its depth, sulfate content and geographical location, indicating an increase of sulfate content heading to the northern portion of the karst aquifer.
The analytical results show a wide range of contents in major cations and anions, and based on the piper diagram plot a predominance of calcium bicarbonated and calcium sulfated waters were identified. Both display calcium as the major cation, provided by the host rock, meanwhile the anions, HCO_3^- or SO_4^{2-}, could be provided by the corrosive agent of the system, carbonic or sulfuric acid, respectively. Sulfate concentrations, if generally observed, covering all samples, vary between 2 and 1542 mg/L, with an average of 391 mg/L, median of 131 mg/L and a non-normal distribution

Comparing both of these anions individually with the sum of the Ca^{2+} and Mg^{2+} (Fig. 3), we identified that, within a wide overview of all the samples collected, that sulfate presents a correlation R^2=0.91 while bicarbonate presents a much lower value of R^2= 0.17. Furthermore, the plot of Figure 3, shows that there are different groups of samples that must be identified and studied separately.
The possible hydro-chemical groupings were analyzed according to following parameters: Geographically, the study region is divided into north and south; seasonality was divided into two field campaigns (Jan/Feb – rainy season and Aug/Oct – dry season) and hydro-chemical facies were divided into samples from phreatic cave lakes, boreholes (deep-seated aquifer), karst springs, and vadose cave water (Fig. 5).

SIAGAS database (CPRM, 2020), known caves and previous research conducted by VALLE (2004) and MORITA (2018) were used as a base for choosing the sampling sites (Fig. 2) for new and accurate hydrogeochemical microbiological data.

The genetic material extracted from the collected samples has still to be analyzed by metagenomic techniques for the characterization of the microbial community structure. The results on microbial diversity presented here were collected in 2018 by sampling and filtering 5 liters of water through Sterivex (0.22 um) filters, storing it in RNA-Latter preserved solution, and keeping it at temperatures below 20 degrees Celsius. After DNA extraction by standard kits and protocols, the 16S rRNA gene was sequenced using the *Illumina MiSeq 2500* platform. The computational processing of the data from the sequencing, and statistical inferences, were performed using next-generation bioinformatics platforms and the programming language R.

All cave samples are authorized by ICMBio nº 76989-1.

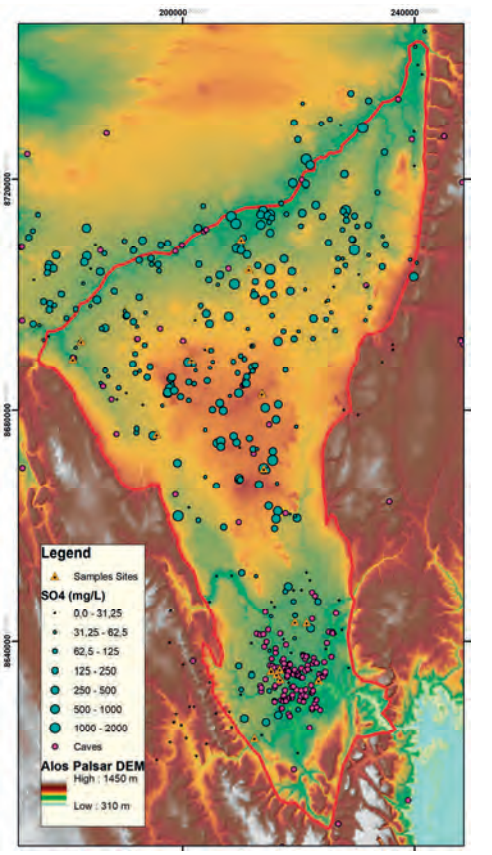

Figure 2: Irecê Basin DEM. Red line delimits the study area. Pink dots indicate known caves, the green dots SO_4^{2-} content of CPRM (2020) boreholes database. Orange triangles represent sampling sites of this study.

Geographic – From the Schoeller-Berkaloff diagram, it is possible to observe that samples collected in the northern region of the study area tend to present higher concentrations of HCO_3^-, SO_4^{2-}, Mg^{2+} and Ca^{2+}.

Seasonality: It was not possible to identify significant changes in the concentrations of the major ions by comparing the same samples. In this case, it is important to point out that the sampling carried out in the first field campaign, scheduled for the rainy season, took place in an atypical meteorological year with an extensive drought period from November 2020 to February 2021. This factor may have led to a reduction in seasonal hydro-chemical variation.

Hydro-chemical facies – With a distribution similar to the geographic one, it was observed that the deep-seated aquifer water samples collected from boreholes tend to present higher concentrations of ions related to the dissolution of the rock. This factor may also be related to the geographic location, since not many cavities are known in the northern region, thus the northern region samples were collected from boreholes, with the exception of a vadose cave sample in Lapa do Sumidouro.

The samples collected for microbiological analysis through the metagenome method have not yet been analyzed. However, previous results (MORITA et *al*., 2019) have already demonstrated through 16S RNA sequencing that bacteria whose metabolism is linked to the biogeochemical cycle of sulfur are found in significant relative abundances in locations that have high levels of sulfates (Fig. 3).
Samples IR5 and IR6 show (Fig. 4), respectively, great abundances of bacteria of the genus *Thiotrix* and *Thiobacillus*, which can act in the oxidation and reduction of metallic sulfides. These points correspond to samples carried out from wells, in the county of Souto Soares in a locality that historically presents remarkable hydrochemical data with average sulfate content of 746 mg/L (VALLE, 2004) and 1348 mg/L in the present study.

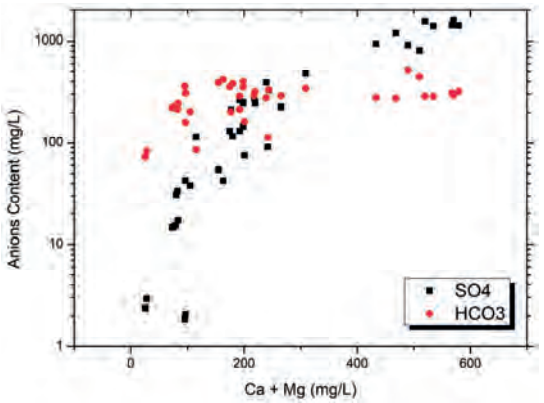

Figure 3: Scatter plot comparing HCO_3^- and SO_4^{2-} with Mg^{2+} and Ca^{2+} sum.

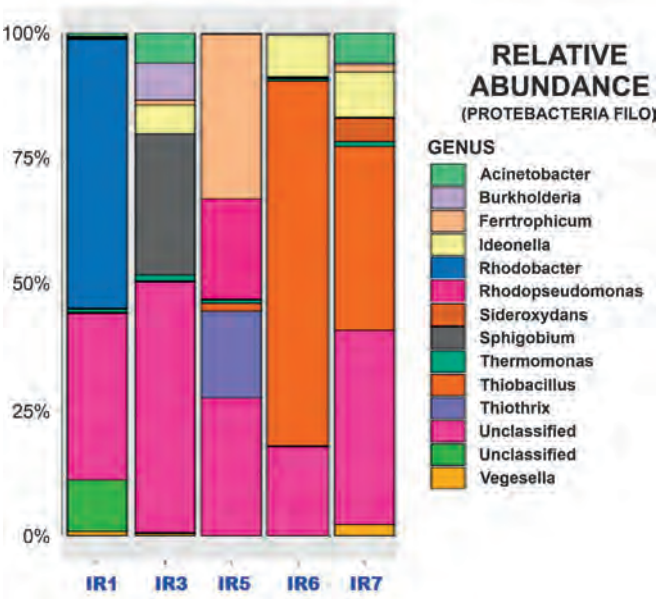

Figure 4: Relative abundance, at the taxonomic level of genus, of microorganisms sequenced per sample. Each color in the bars represents a different genus. The sampled points are represented on the x-axis. On the y-axis, the scale of percentages of relative abundance. Figure from Morita et al. (2019).

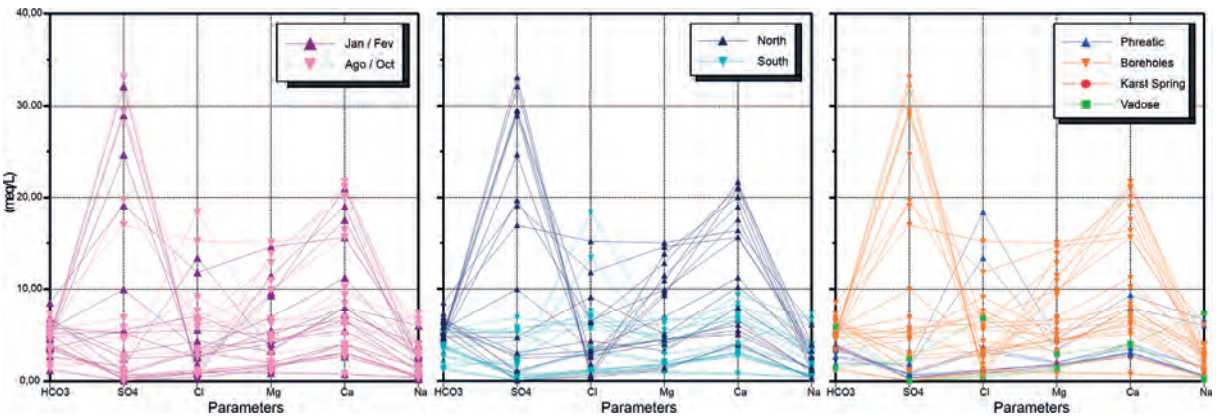

Figure 5: Schoeller-Berkaloff diagrams grouping samples by seasonality, geographic region and hydrochemical facies.

4. Discussion

The hydrochemical results indicate that the northern region of the study area tends to exhibit the highest levels of sulfates in groundwater when compared to the southern region. These values when compared to the HCO_3^- contents, in which no correlations were found, is an indication that, under the SAS hypothesis for the Irecê Basin, the bicarbonate present in the water does not come exclusively as a product of H_2CO_3 carbonate rock dissolution. Southward, the sulfate content decreases, indicating greater epigenic activity, as evidenced by greater cave density (Fig. 1) as well as morphological and sedimentological characteristics of the caves. Considering the speleogenetic model suggested by AULER (1999) and the predominance of epigenic karst over hypogenic according to the denudation rate and annual rainfall (AULER & SMART, 2003), it is understood that the hypogenic features, responsible for the initial stage of speleogenesis, are superimposed by epigenetic features.

The southern region of the Irecê Basin has higher rainfall and higher allogenic recharge, which enables the exposure and development of caves closer to the surface and less sulfated groundwater. On the other hand, the northern region represents an earlier stage of karst development at greater depth and a more significant performance of H_2SO_4 as a corrosive agent, originating in the host rock itself.

The association of previous 16S rRNA sequencing data with hydro-chemical analyses from previous and current research demonstrate the presence of sulfur oxidizing bacteria predominantly in places with high SO_4^{2-} contents. This supports the hypothesis that microbial activity is responsible for the production of the corrosive agent in the karst system.

5. Conclusion

Although important data are still lacking for the consolidation of the SAS hypothesis in the karst system of the Irecê Basin and mainly for the biogenic production of this acid, the sulfates present in groundwater are in notable concentrations among Brazilian karst.

Correlations found between SO_4^{2-} and the major cations, geographic location and relative abundance of Thiothrix and Thiobacillus genus bacteria corroborate to the understanding that sulfur has an effective participation in the local speleogenesis.

Ongoing analysis are intended to complement the research developed so far with additional microbiological sequencing. Analyses of $\delta^{34}S$ will also be carried out in order to trace the isotopic signature of sulfur in groundwater, speleothems and metallic sulfides in the host rock.

Acknowledgments

We thank Lívia Rocha, Aghata Zarelli and Gabriela Duarte for helping in our field works, the LECOM-IO and Karst System Lab – Igc teams for the contributions throughout the research and ICMBio-CECAV/Ferro Puro (TCCE 01/2020) for the research funding We would also like to thank Laurent Bruxelles and Lionel Barriquand for the support.

References

AULER A. (1999) *S. Karst evolution and paleoclimate of eastern Brazil*. 264 p. PhD, University of Bristol.

AULER A. and SMART P. L. (2003) The influence of bedrock-derived acidity in the development of surface and underground karst: evidence from the Precambrian carbonates of semi-arid northeastern Brazil. *Earth surface processes and landforms*, 28, 157-168.

COMPANHIA DE PESQUISA DE RECURSOS MINERAIS. CPRM. (2020) *Sistema de Informações de Águas Subterrâneas*. SIAGAS. Brasília: CPRM. Avaiable on: <http://siagasweb.cprm.gov.br/layout/index.php>

MAGALHÃES A. G. C., G. P., RAJA GABAGLIA C. M. S., SCHERER M. B., B´ALLICO F., GUADAGNIN E., BENTO FREIRE L. R., SILVA BORN O. and CATUNEANU (2016) *Sequence hierarchy in a Mesoproterozoic interior sag basin: From basin fill to reservoir scale, the Tombador Formation, Chapada Diamantina Basin*, Brazil: Basin Research, v. 28, no. 3, 393–432.

MISI A. & SOUTO P. (1975) Controle estratigráfico das mineralizações de chumbo, zinco, flúor e bário no Grupo Bambuí–parte leste da Chapada de Irecê (BA). *Brazilian Journal of Geology*, v.5, n.1, 30-45.

MORITA T.D.M., KARMANN I., ROMANO R. G., PELIZZARI V., VALLE M. A. & GODINHO L. P. de S. (2019) *Ácido sulfúrico como agente corrosivo no sistema cárstico de Iraquara* (Grupo Una, BA). In: ZAMPAULO, R. A. (org.) CONGRESSO BRASILEIRO DE ESPELEOLOGIA, 35, Bonito. Anais: SBE, Campinas, 45-51.

GUERRA A. M. (1986) *Processos de carstificação e hidrogeologia do Grupo Bambuí na região de Irecê-Bahia*. PhD. Instituto de Geociências, Universidade de São Paulo.

VALLE M. A. (2004) *Hidrogeoquímica do Grupo Una (Bacias de Irecê e Salitre): um exemplo da ação de ácido sulfúrico no sistema cárstico*. 122 p. PhD. Universidade de São Paulo.

The multiple impacts on caves of the European badger (Meles meles), the case study of the Mâconnais (France)

Lionel BARRIQUAND[1,2], Michel PHILIPPE[3], Jean-René CHEVALLIER[2], Vasile HERESANU[4], Daniel ARIAGNO[5], Georges DEDIENNE[2], Isabelle DONZEY[2] & Claire GAILLARD[6]

(1) Université Savoie Mont Blanc, Laboratoire EDYTEM - UMR5204, Bâtiment « Pôle Montagne », 5 bd de la mer Caspienne, F-73376 Le Bourget du Lac cedex, lionel.barriquand@wanadoo.fr
(2) Association Culturelle du Site d'Azé, Grottes d'Azé, 135 route de Donzy, F-71260 Azé.
(3) Spéléo-club de Villeurbanne, Rhône et Conservateur honoraire du Muséum d'Histoire naturelle de Lyon.
(4) Aix-Marseille Université-CNRS, CINaM, Campus de Luminy, case 913, F-13009 Marseille.
(5) Groupe spéléo Vulcain, Lyon et France Nature Environnement- Rhône
(6) Museum National d'Histoire Naturelle, UMR 7194 HNHP "Histoire naturelle de l'Homme préhistorique" MNHN-CNRS-UPVD, 1, rue René Panhard, F-75013 Paris.

Abstract

The European badger (Meles meles) occupy a large part of the Palaearctic region since the Middle Pleistocene. It exhibits a particular preference for natural cavities because of the protection offered by their solid structure and their pre-existing empty spaces which can be enlarged into voluminous burrows. Its bones have been found in numerous caves but its role in the evolution of these caves is largely unknown. In the Mâconnais (Southern Burgundy, France), given that humans no longer use caves for shelter, that cavers tend not to frequent the smaller caves, and that many of the dry limestone pastures have been allowed to return to fallow, badgers have reinhabited many of these caves. As a result, their impacts can be observed and characterised. Polished areas and claw marks can be seen on walls and archways, as well as changes to the floors of cavities caused by badger excrement, the introduction of vegetable matter and even rubbish generated by humans such as plastic wrappings. The badgers' need to dig burrows and therefore remove obstructions has led to the reworking of large quantities of karstic fillings. Lastly, they have been responsible for a number of other features which have changed the shape of cave floors: sleeping hollows, dung pits and slides.

Résumé

Les impacts multiples sur les grottes du blaireau européen (Meles meles), le cas du Mâconnais (France). Le blaireau européen (Meles meles) occupe une grande partie de la zone paléarctique depuis le Pléistocène moyen. Il affectionne particulièrement les cavités naturelles, qui lui offrent une voûte solide et des volumes vides déjà existant pour y creuser ses volumineux terriers. Ses ossements ont été trouvés dans de nombreuses grottes mais son rôle sur l'évolution de ces grottes est méconnu. Dans le Mâconnais (Sud Bourgogne, France), du fait que l'homme n'utilise plus les abris qu'offrent les zones karstiques, que les spéléologues fréquentent peu ces petites grottes et du retour en friche des anciennes pelouses calcaires, le blaireau a reconquis de nombreuses cavités. Ainsi ses impacts ont pu être observés et caractérisés. Sur les parois et les voûtes il est à l'origine de polis et de griffades. Il modifie également la nature du sol par l'apport de matière végétale, par ses déjections ainsi que par l'apport des déchets générés par l'homme tels que des films plastiques. Son besoin de creuser des terriers et donc de désobstruer entraîne le remaniement de volumes importants des remplissages karstiques. Enfin il est à l'origine de nombreux aménagements : bauges, tines, toboggans… qui façonnent le sol des grottes.

1. Introduction

The badger is a member of the *Melinae* subfamily of Mustelidae and is widely distributed over the palaearctic region. In France it has been known since the Villafranchian and has been found in numerous palaeontological deposits. In the Mâconnais-Clunisois, remains dating from the Middle Pleistocene have been found in Château breccia (ARGANT & MALLYE, 2005). The European badger is ubiquitous and wherever it finds a favourable environment in terms of habitat and food it will become established there. In the Mâconnais, the abandonment of many less productive pastures and the revival of woodlands has allowed the species to flourish and to reinhabit many cavities.

Numerous bioglyphs have been found in caves (polished surfaces, claw marks, sleeping hollows), generally attributed to bears. However, because of their repeated occupation, badgers may also be responsible. Consistent with their ethology, badgers bring plant matter into caves and defecate there. What impacts could this have on cave sediments and walls? Our aim is to study contemporary use of caves by badgers and to define these impacts.

2. Materials and methods

We identified 11 cavities currently occupied by badgers: the Mère Lafayette, Verchizeuil and Follatière Caves (Fig. 1) at Verzé; the Beurne aux Griffures Cave at Martailly-les-Brancion; the Charmes Cave at Mancey; the N°2 Préty, Lacrost and Cachettes Caves at Igé; the Carrière Cave at Bray; the Blaireau Cave at Bissy-la-Mâconnaise; and the Dacotet Cave at Berzé-la-Ville (GUILLOT et al, 2005).
An infrared video camera was positioned for few days (e.g. less than one week each time) in a number of these caves in order to record badger behaviour.
In each cave measurements were taken of the sleeping hollows, claw marks, polished areas, dung pits and slides.
In the Follatière Cave we were able to collect a range of samples from a cross section of sediments which had been impacted by the badgers. After drying for 2 hr at 105°C, the samples were subjected to the following analyses:

- pH, after formation of a suspension with a sediment to demineralised water by weight ratio of 1/3 and agitation for 2 hr
- proportion of organic matter (MO): by the calculation, MO=1.72 x (Ctotal – 12/100*carbonates total), with Ctotal measured according to the Dumas dry combustion method ISO 10694 1995 and total carbonates according to NF EN ISO 10693.
- total nitrogen (NT) Dumas dry combustion method NF ISO 13878
- total phosphorus (P) and sulphur (S) according to NF ISO 11466, NF ISO 11466 and determined by ICP AES: NF EN ISO 11885.

Lastly, we collected samples from the Verchizeuil and Follatière Caves for XRD analysis (Fig. 1C). The measurements were done using a Rigaku RU-200BH X-ray generator equipped with a rotating anode, an Osmic multilayer optic and a mar345 2D detector. The wavelength used was that of Cu, λ = 0.15418 nm. The samples to be analysed were finely ground, the powder produced was well homogenised, then placed in a glass capillary 0.5 mm in diameter. The volume of powder exposed to the X-rays was around 0.1 µl. The diffractograms were analysed using X'Pert HighScore software.

Figure 1: general view inside the Follatière. Cave showing the impacts of badgers: sedimentary deposit (A); polished area and passageway used (B); encrustation of gypsum on the sedimentary filling (C); lumps of clay removed (D); sleeping hollow (E); dung pit as confirmed by the presence of fruit pits (F).

3. Results

The anatomy of badgers is characteristic of fossorial animals. When living in caves they make a number of changes to adapt them to their needs or which are a result of their behaviours (Mallye, 2009). We have identified four main types of modifications: sleeping hollows (Fig. 1E), dung pits (Fig. 1F), slides (Fig.2) and access holes. We have characterised their dimensions in Fig. 3. Their rear paws are slightly longer (10%) and less flat on the ground than their front paws which facilitates the removal of excavated earth. Material evacuated typically consists of lumps of clay and chunks of limestone (Fig. 1D). Their mass has been measured (Fig. 4) and is dependent on the nature of the

filling. As on the outside, digging an access passage in an elevated position leads to the formation of a talus or spoil heap in front of the entrance to the sett (Fig. 5).

Figure 2: slide and blackened walls in the Verchizeuil Cave.

Type		Sleeping hollows			Dung pits			Slides		
Quantity		9			15			14		
Characteristic		min	max	med	min	max	med	min	max	med
Length	cm	70	136	100	12	43	24	80	322	132
Width		70	103	93	12	30	22	32	46	40
Depth		18	36	25	4	19	8	5	21	9

Figure 3: Characteristics of the sleeping hollows, dung pits and slides.

		Lumps of clay	*Chunks of limestone*
Quantity		69	31
Min	g	28	869
Max		1943	4818
Med		186	2005

Figure 4: mass of the lumps of clay and pieces of limestone removed during digging.

After watching 57 video recordings, we could see that a badger nearly always takes the same path inside a cave (Figs 1B and 5). This is often marked on the ground by the presence of dropped litter to the side. It will repeatedly brush against the same parts of the wall. The brushing by its fur, the clay present on the wall or its fur, and the wall itself make up the trilogy necessary for the tribological phenomenon which produces polished areas (Fig. 1B).

These are visible up to around 40 cm above the cave floor as well as on the ceilings of low galleries, and can be several metres in length. To provide its sleeping hollow with suitable bedding material, a badger will bring into the cave large quantities of dry grass, hay, moss, but also rubbish from humans such as plastic (Fig. 6).

Figure 5: talus produced from digging the sett in the Préty Cave.

Figure 6: sleeping hollow covered by a layer of dry grass in the Charmes Cave.

Badgers also leave numerous claw marks on cave walls (Fig. 7) which can be as much as 1 m above the floor. While badgers have 5 claws, of the 40 examples recorded, 10% have one groove, 43% two, 40% three and 7% four. The maximum length of a groove was 14.2 cm and the median distance between two grooves was 1.0 cm (min = 0.5 cm and max = 1.8 cm.

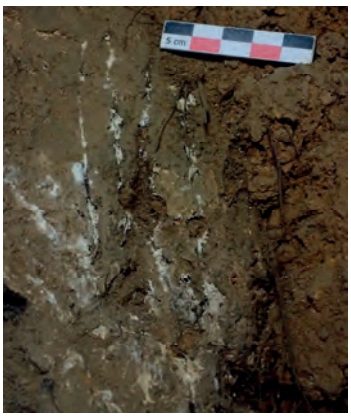

Figure 7: Badger claw marks in the Charmes Cave.

The analyses carried out on the sediments (Fig. 1A) are given in Figure 8.

Sample	Position/floor (cm)	Comments	Colour after drying and 2mm sieving	pH	MO	Ctotal	Total carbonates	NT	C/N	P	S
					g/Kg	g/Kg	g/Kg	g/Kg	/	g/Kg	g/Kg
1	0 to 19	edge of sleeping hollow	7,5 YR 5/6 strong brown	4,84	57,7	33,6	10	6,6	5,1	9,9	2,3
2	19 to 32	old dung pits	10YR 3/3 dark brown	4,53	137,7	80,0	9	15,8	5,1	9,8	5,4
3	62 to 65	presence of fruit pits	7,5YR 5/4 brown	4,22	44,7	26,0	9	5,6	4,7	13,1	1,7
4	100 to 110		7,5YR 5/4 brown	4,73	29,2	17,0	7	2,7	6,2	13,9	0,4
5	> 110	karstic filling of cherts	7,5 6/6 reddish yellow	4,62	4,9	2,8	7	0,7	3,9	5,6	0,4

Figure 8: characteristics of the sediments from the Follatière Cave. Sample 5 = base of the filling not impacted by badgers, Samples 2 to 4 = adjacent to old dung pits, Sample 1 = edge of an old sleeping hollow.

The XRD analyses performed on the walls (Fig. 2), polished and non-polished, of the Verchizeuil Cave show the presence of elements from the surrounding rock but also a proportion of 32 to 34 % hydroxylapatite. The sample taken from the sediments in the Follatière Cave, before preparation of the cross section, consists of 51 % gypsum.

4. Discussion

In using a cave for habitation, badgers modify and use it for different functions. This adaption of the cave habitat requires considerable modification of the karstic fillings through digging and relocating them, as well as through the introduction of organic matter (even anthropic rubbish).
When an access passage is excavated in an elevated position in a cave, the talus created beneath it can have a volume of hundreds of litres. More modest in size are the slides.
According to the measurements taken, the largest sleeping hollow required the removal of 260 L of sediment. The badger then placed into it a layer of dry grass bedding which enriched the surroundings in organic matter.
Less voluminous are the dung pits, only around 1 L in size. On the other hand, the quantity of excrement is considerable. This requires regular relocation of dung pit sites, after 2 or 3 uses, another significant way in which organic matter is introduced to the karst.
The analyses carried out on the sediments from the Follatière Cave show considerable enrichment in organic carbon, nitrogen, phosphorus and sulphur by comparison with the levels of the control base.
The presence of sulphur leads to the formation of gypsum.
The presence of phosphorus leads to the formation of acidic liquids which will react with the calcium carbonate of the surrounding limestone to form hydroxylapatite, as is also the case with bat guano (AUDRA et *al*, 2016). This reaction causes alterations to the cave walls.
The cave walls are also affected by the claw marks of badgers as well as by the polished areas produced by their repeated passage in the same places.

5. Conclusion

The badger is an unobtrusive mammal which has been present in most of the Palaearctic region throughout the Quaternary. The present-day representative of this line, the European badger is still present. Its opportunism has enabled it to recolonise many areas abandoned or neglected by humans, as is the case in the Mâconnais. In a habitat of limestone terrain, it takes advantage of the secure lodgings offered by the cavities of the karst. Given its immutable behaviours and innate propensity for digging, it has the ability to profoundly alter the caves it inhabits and leave behind long-lasting imprints.
It is therefore possible that many ancient bioglyphs have been attributed a little too systematically to bears in cases where badgers may have been their cause.

References

ARGANT A, MALLYE J.-B. (2005) Badger remains from the Breccia of Château (Burgundy, France). Remarks on Middle Pleistocene Badgers. In Nagel D. dir., Festschrift für Prof. Gernot Rabeder, Vienne, Verlag der Osterreichischen Akademie der Wissenschaffen, Mittelungen der Kommission für Quatärforschung der Osterreichischen Akademie der Wissenschaffen, n°14, 1-12.

AUDRA P., BARRIQUAND L., BIGOT J.-Y., CAILHOL D., CAILLAUD H., VANARA N., NOBÉCOURT J.-C., MADONIA G., VATTANO M., RENDA M (2016) L'impact méconnu des chauves-souris et du guano dans l'évolution morphologique tardive des cavernes. Karstologia, n° 68, 1-20.

GUILLOT L., MOREL J., SIMONNOT G. (2005) Gouffres et cavernes des Monts du Mâconnais. Sous le plancher, Ligues spéléologiques de Bourgogne et Franche-Comté, Dijon, 196p.

MALLYE J.-B. (2009) Les restes de blaireau en contexte archéologique : taphonomie, archéozoologie et éléments de discussion des séquences préhistoriques. HAL Id : tel-00394204

Symposium 12

Glacier, firn and ice caves

Why continue deep glacier exploration? Pourquoi continuer l'exploration des glaciers en profondeur ?

Luc MOREAU

Laboratoire EDYTEM, CNRS, Université Savoie Mont Blanc, F-73376 Le Bourget du Lac, moreauluc@chx.fr

English

In this context of global warming, rising sea levels due to the acceleration of polar glaciers at the velocity front, but also renewable energy such as hydroelectricity, it is crucial to continue to explore the intra- and subglacial spaces of our Alpine glaciers. They are natural laboratories, easily accessible and the recently discovered hydraulic processes are motivating, as we will see in this Symposium 12. We can also easily test new techniques.

Moreover, the invisible interior of glaciers and the way they flow, rub the rocky bed and evolve in this context of climate change has always provided scientists with questions. Today, technology allows us to identify invisible cavities from the surface of the glacier, but this remains far too approximate, especially when it comes to locating the flow of melt for hydroelectric purposes. Glacio-speleological exploration is always welcome for the help it brings, especially in terms of topography. But how to penetrate the ice mass, what are the potential openings offered by the glaciers? Have these penetrations evolved with the current exponential retreat of the glaciers?

Numerous points of access are possible, ranging from glacial porches and rimayes, to crevasses and rotures (space between the flank of the glacier and the mountain), sub-glacial hemispherical channels dug by air currents and torrential flows or geothermal energy, decollement cavities under the glacier, sometimes filled with water. But the glacial mills are a good solution to follow the course of the water, source of our rivers and clean hydroelectric energy; to measure the parameters in situ of the internal deformation of the glacier, and especially to see the interior of the glaciers visually in live.

Français

Dans ce contexte de réchauffement climatique, de remontée du niveau des mers suite aux accélérations des glaciers polaires à front de vêlage, mais aussi d'énergie renouvelable comme l'hydroélectricité, il est crucial de continuer d'explorer les espaces intra- et sous-glaciaire de nos glaciers Alpins. Ce sont nos glaciers "laboratoire", facilement accessibles et les processus hydrauliques découverts récemment sont motivants, nous le verrons dans ce Symposium 12. On peut également et facilement y tester aussi de nouvelles technologies.

De plus, l'intérieur invisible des glaciers et la façon dont ils s'écoulent, frottent le lit rocheux et évoluent dans ce contexte de changement climatique attisent toujours la curiosité du scientifique explorateur. Aujourd'hui la technologie nous permet d'identifier depuis la surface du glacier des cavités invisibles mais cela reste trop approximatif surtout lorsqu'il s'agit de localiser les circulations de fonte à des fins hydroélectriques. L'exploration glacio-spéléologique est toujours la bienvenue pour l'aide qu'elle apporte notamment en matière de topographie. Mais comment pénétrer la masse de glace, quelles sont les ouvertures potentielles que nous offrent les glaciers ? Ces pénétrations ont-elles évolué avec le recul exponentiel actuel des glaciers ?

De nombreux accès sont toujours possibles, comme les porches glaciaires, les rimayes, les crevasses, les rotures (espace entre le flanc du glacier et la montagne), les chenaux hémisphériques sous-glaciaires creusés par les courants d'air et les écoulements torrentiels ou l'énergie géothermique, ou les cavités de décollement sous le glacier, parfois remplies d'eau. Mais le principal accès au monde intra-glaciaire reste les moulins glaciaires. C'est souvent la meilleure solution pour suivre le parcours des eaux, source de nos rivières et d'énergie hydroélectrique, pour mesurer les paramètres in situ de la déformation interne du glacier, et surtout pour voir l'intérieur des glaciers en direct.

Glacier Tempanos (Chile), photo B. Tourte / Centre Terre

Instrumentation and exploration of moulins in the Paakitsoq region of the Greenland Ice Sheet

Matthew COVINGTON[(1)], Jason GULLEY[(2)], William GADD[(3)], Vickie SIEGEL[(4)], David OCHEL[(5)], Celia TRUNZ[(1)] & Jessica MEJIA[(2)]

(1) University of Arkansas, Fayetteville, AR, USA, mcoving@uark.edu (corresponding author)
(2) University of South Florida, Tampa, FL, USA
(3) Will Gadd Consulting, LLC, Canmore, Alberta, Canada
(4) Sisu Field Solutions, LLC, Del Valle, TX, USA
(5) UT Grotto, Austin, TX, USA

Abstract

For three years we have conducted scientific expeditions to the Paakitsoq region of western Greenland. We instrumented moulins and supraglacial streams for continuous water level measurements and deployed GPS units in the study area to measure ice motion. The central goal of our work is to improve understanding of the interactions between meltwater delivery to moulins and the rates of ice sliding. In the fall of 2018 and 2019, we explored and mapped two moulins in the study area, which is much further inland than previous moulin exploration in Greenland. We found that moulin volumes can be substantially larger than previously assumed, with cross-sectional areas of the shafts reaching at least up to 500 m^2. The large measured volumes explain the relatively limited daily water level variation that we observed at our sites. Together, our exploration, moulin water level records, and a simple hydrological model suggest that moulins volumes can be an important regulator of subglacial water pressure. Currently, we know relatively little about how these volumes vary from one location to another or what controls those variations.

1. Introduction

The Greenland Ice Sheet (GrIS) is a primary contributor to ongoing sea-level rise, contributing around 0.5 mm/yr in recent decades (VAN DEN BROEKE et al., 2016). While much of the mass loss from Greenland has occurred from marine terminating glaciers, recent observations suggest that land-terminating glaciers within SW Greenland will be a major contributor to future mass loss (BEVIS et *al*., 2019). Most of the meltwater from the surface of the GrIS is routed to moulins, which deliver the water to a subglacial drainage system that flows ultimately to the margin (SMITH et *al*., 2015).

It has long been observed on mountain glaciers that spring meltwater accelerates ice sliding (IKEN and BINDSCHADLER, 1986). Early observations on the GrIS suggested that similar positive feedback between meltwater and sliding might lead to runaway ice loss (ZWALLY et *al*. 2002). However, subsequent modelling (SCHOOF, 2010) and observations (SUNDAL et *al*., 2011, TEDSTONE et *al*., 2015) suggest that spring speedup may be offset by later slowdown after development of an efficient subglacial drainage system. Other observations (ANDREWS et *al*., 2014) and models (HOFFMAN et *al*., 2016) demonstrate that sliding velocity of the GrIS may be more strongly regulated by portions of the glaicer bed that are hydrologically weakly connected. Observations of sliding velocities far inland (~50 km) exhibit persistent acceleration under increased melt (DOYLE et *al*. 2014).

Direct observations of subglacial hydrological conditions on the GrIS are limited, and model structures and parameters are largely based on observations from mountain glaciers. Here we report on a 3-year field campaign on the GrIS to instrument and explore moulins and provide needed constraints on models of subglacial hydrology on the GrIS. The data presented here are described in more detail and compared against modelling results in COVINGTON et al. (2020).

2. Methods

During summer field campaigns in 2017 and 2018, we instrumented moulins in the Paakitsoq region of the GrIS to conduct continuous measurements of moulin water level over seasonal timescales. Moulins were instrumented from two camps, referred to here as Low Camp and High Camp, located at approximately 765 and 950 m. a.s.l., respectively.

Water levels were measured by lowering pressure transducers (Geokon 4500HD-7.5MPa) into moulins on 1.3 cm armored cables that were marked by length. Water levels were recorded on Campbell CR1000 data loggers that were installed on the ice surface. Ice thicknesses were estimated from BedMachine v3 (MORLIGHEM et *al*., 2017).

During the fall of 2018 and 2019, we explored and mapped two moulins, one near High Camp and one near the location of a previous moulin study, FOXX Camp (ANDREWS et *al*., 2014). The focus of the expedition in 2018 was filming a documentary, and there were limited time and resources available for mapping the moulin. Consequently, the Phobos Moulin, which was explored in 2018 was mapped using estimations of dimensions from known rope lengths, photos, and an in-cave sketch. In fall of 2019, we mapped the FOXX Moulin using standard cave survey techniques using a DistoX and Topodroid running on a Samsung Active Tab2. Splay shots were taken from survey stations to enable accurate estimation of cross-sectional dimensions.

3. Results

During the summer of 2017, moulins at Low and High Camp were instrumented beginning in July. Moulin water levels exhibit daily oscillations that are driven by diurnal cycles in meltwater production at the ice surface (Figure 1). The range of diurnal water level oscillation at the Low Camp moulin was around 50 m, or about 10% of floatation. At High Camp, diurnal oscillations were only about 20 m, or 3% of floatation. The ranges observed at both moulins were much less than in any of the other few studies of moulin water levels on the GrIS (ANDREWS et *al*., 2014; COWTON et al., 2016). Modelling results suggest that these low water level oscillation amplitudes are most likely a result of substantial englacial storage (COVINGTON et *al*., 2020), larger than what would be expected within moulins given prior assumptions about the magnitudes of moulin cross-sectional areas.

Moulin exploration demonstrated that moulin cross-sectional areas can be much larger than previously assumed (Figures 2-3), with cross-sectional areas near water level for Phobos and FOXX moulins equal to about 500 m² and 50 m², respectively. Models typically have assumed that moulin cross-sectional areas are around 1-10 m² (e.g., WERDER et *al*., 2013; BANWELL et *al*., 2013; BARTHOLOMEW et *al*. 2012).

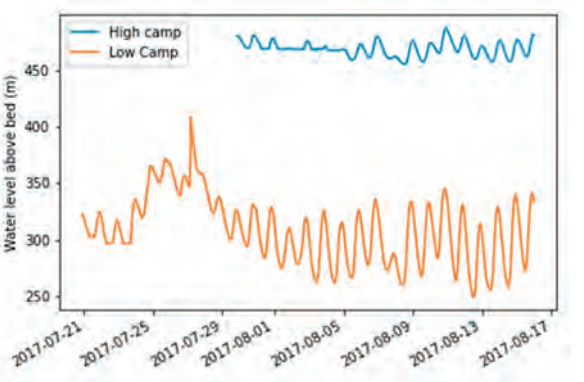

Figure 1: Observed moulin water levels in meters above the bed.

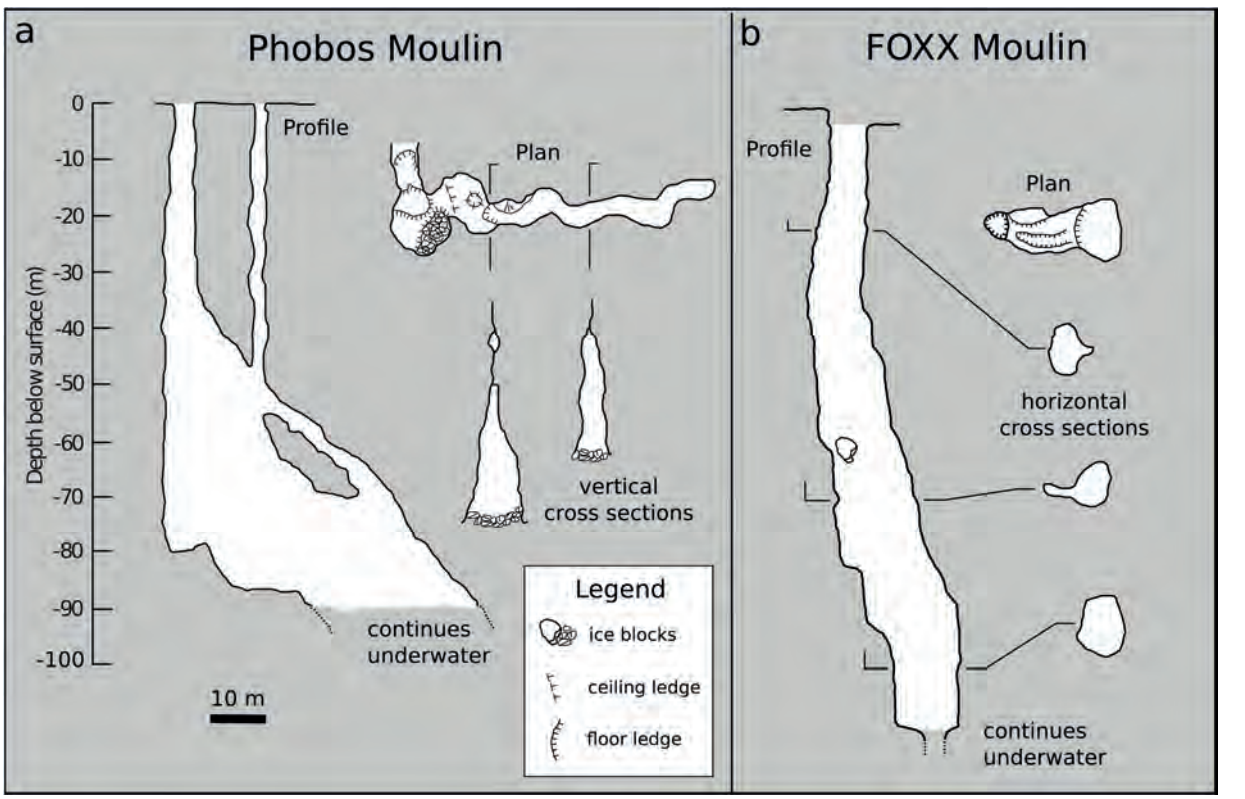

Figure 2: Maps of the two explored moulins near High Camp (a) and FOXX Camp (b). Moulin cross-sectional areas were much larger than previously assumed in models.

Figure 3: Moulin morphology in Phobos Moulin (left) and FOXX Moulin (right).

4. Discussion and Conclusions

Historically, science and exploration have often gone hand in hand. However, nowadays it is less common for the frontiers in science and the frontiers in physical exploration to coincide. Here we report on discoveries from a series of expeditions that made important scientific discoveries while conducting original geographic exploration within moulins on the GrIS.

Our summer observations of moulin water level demonstrated surprisingly low water level variability in comparison to prior studies. Modelling results suggested that this reduced variability is produced by large storage volumes (COVINGTON et *al*., 2020). Our subsequent exploration demonstrated that much larger storage volumes exist within moulins in this region of the ice sheet than previously assumed. Similarly, we found a larger moulin volume in a region where moulins displayed very low variation in water level and a smaller moulin volume within a region that previously displayed larger variability. Together, these results suggest that moulin volume is an important control on subglacial water level variation.

These discoveries cast uncertainty on our understanding of the coupling between glacial hydrology and ice sliding and illustrate crucial unknowns about the extent to which moulin volumes vary across the ice sheet. Daily water level variation is an important driver for evolution of subglacial hydrological connectivity (HOFFMAN et *al*. 2016), and therefore systematic trends in moulin volumes could influence the response of ice sliding to future changes in meltwater production, particularly as summer melt and the development of moulins shift further inward onto the ice sheet. Very few prior studies have explored moulins on the GrIS, and most prior studies have explored moulins near the ice sheet margin (e.g., REYNAUD AND MOREAU, 1994). Future, systematic exploration of moulins would enhance understanding of the controls of moulin volume and enable models to incorporate any resulting systematic changes in englacial storage across the ice sheet.

Acknowledgments

We acknowledge Charles Breithaupt, Jonathan Carlson, Brandon Conlon, and Ronald Knoll for assistance in the field. This material is based on work supported by the National Science Foundation under Grant Nos. 1604022 and 1603835. The exploration of Phobos moulin was supported by Red Bull. Any opinions, findings, and conclusions or recommendations

expressed in this material are those of the authors and do not necessarily reflect the views of the National Science Foundation or Red Bull.

References

ANDREWS L. C., CATANIA G. A., HOFFMAN M. J., GULLEY J. D., LÜTHI M. P., RYSER C., HAWLEY R.L. and NEUMANN T. A. (2014). Direct observations of evolving subglacial drainage beneath the Greenland Ice Sheet. *Nature*, 514 (7520), pp. 80-83.

BANWELL A.F., WILLIS I.C. and ARNOLD N.S., 2013. Modeling subglacial water routing at Paakitsoq, W Greenland. *Journal of Geophysical Research: Earth Surface*, *118*(3), pp.1282-1295.

BARTHOLOMEW I., NIENOW P., SOLE A., MAIR D., COWTON T. and KING M.A., 2012. Short-term variability in Greenland Ice Sheet motion forced by time-varying meltwater drainage: Implications for the relationship between subglacial drainage system behavior and ice velocity. *Journal of Geophysical Research: Earth Surface*, *117*(F3).

BEVIS M., HARIG C., KHAN S.A., BROWN A., SIMONS F.J., WILLIS M., FETTWEIS X., VAN DEN BROEKE M.R., MADSEN F.B., KENDRICK E., CACCAMISE D.J., VAN DAM T., KNUDSEN P. and NYLEN T. (2019). Accelerating changes in ice mass within Greenland and the ice sheet's sensitivity to atmospheric forcing. *Proceedings of the National Academy of Sciences*, 166 (6), pp. 1934-1939.

COVINGTON M.D., GULLEY J.D., TRUNZ C., MEJIA J. and GADD W., 2020. Moulin Volumes Regulate Subglacial Water Pressure on the Greenland Ice Sheet. *Geophysical Research Letters*, *47*(20), p.e2020GL088901.

COWTON T., SOLE A., NIENOW P., SLATER D., WILTON D. and HANNA E., 2016. Controls on the transport of oceanic heat to Kangerdlugssuaq Glacier, East Greenland. *Journal of Glaciology*, *62*(236), pp.1167-1180.

DOYLE S.H., HUBBARD A., FITZPATRICK A.A., VAN AS D., MIKKELSEN A.B., PETTERSSON R. and HUBBARD B., 2014. Persistent flow acceleration within the interior of the Greenland ice sheet. *Geophysical Research Letters*, *41*(3), pp.899-905.

HOFFMAN M.J., ANDREWS L.C., PRICE S.F., CATANIA G.A., NEUMANN T.A., LÜTHI M.P., GULLEY J., RYSER C., HAWLEY R.L. and MORRISS B., 2016. Greenland subglacial drainage evolution regulated by weakly connected regions of the bed. *Nature communications*, *7*(1), pp.1-12.

IKEN A. and BINDSCHADLER R.A., 1986. Combined measurements of subglacial water pressure and surface velocity of Findelengletscher, Switzerland: conclusions about drainage system and sliding mechanism. *Journal of Glaciology*, *32* (110), pp.101-119.

MORLIGHEM M., WILLIAMS C.N., RIGNOT E., AN L., ARNDT J.E., BAMBER J.L., CATANIA G., CHAUCHÉ N., DOWDESWELL J.A., DORSCHEL B. and FENTY I., 2017. BedMachine v3: Complete bed topography and ocean bathymetry mapping of Greenland from multibeam echo sounding combined with mass conservation. *Geophysical research letters*, *44*(21), pp.11-051.

REYNAUD L. et MOREAU L. (1994). Moulins glaciaires des glaciers tempérés et froids de 1986 à 1994 (Mer de Glace et Groenland) : morphologie et techniques de mesures de la déformation de la glace. *Cahiers de géographie de Besançon (Les), 34, pp.109-113.*

SCHOOF C., 2010. Ice-sheet acceleration driven by melt supply variability. *Nature*, *468*(7325), pp.803-806.

SMITH L.C., CHU V.W., YANG K., GLEASON C.J., PITCHER L.H., RENNERMALM A.K., LEGLEITER C.J., BEHAR A.E., OVERSTREET B.T., MOUSTAGA S.E., TEDESCO M., FORSTER R.R., LEWINER A.L., FINNEGAN D.C., SHENG Y. and BALOG J. (2015). Efficient meltwater drainage through supraglacial streams and rivers on the southwest, Greenland ice sheet. *Proceedings of the National Academy of Science*, 112 (4), pp. 1001-1006.

SUNDAL A.V., SHEPHERD A., NIENOW P., HANNA E., PALMER S. and HUYBRECHTS P., 2011. Melt-induced speed-up of Greenland ice sheet offset by efficient subglacial drainage. *Nature*, *469*(7331), pp.521-524.

TEDSTONE A.J., NIENOW P.W., GOURMELEN N., DEHECQ A., GOLDBERG D. and HANNA E., 2015. Decadal slowdown of a land-terminating sector of the Greenland Ice Sheet despite warming. *Nature*, *526*(7575), pp.692-695.

WERDER M.A., HEWITT I.J., SCHOOF C.G. and FLOWERS G.E., 2013. Modelling channelized and distributed subglacial drainage in two dimensions. *Journal of Geophysical Research: Earth Surface*, *118*(4), pp.2140-2158.

ZWALLY H.J., ABDALATI W., HERRING T., LARSON K., SABA J. and STEFFEN K., 2002. Surface melt-induced acceleration of Greenland ice-sheet flow. *Science*, *297*(5579), pp.218-222.

VAN DEN BROEKE M.R., ENDERLIN E.M., HOWAT I.M., KUIPERS P., NOËL B.P.Y., VAN DE BERG W.J., VAN MEIJGAARD E. and WOUTERS B. (2016). On the recent contribution of the Greenland ice sheet to sea level change. *The Cryosphere*, 10 (5), pp. 1933-1946.

Englacial conduits & crevasses in the artificial tunnel inside Langjökull glacier, Iceland

Trevor FAULKNER

GEES, University of Birmingham, Edgbaston, Birmingham, B15 2TT, UK. e-mail: trevor@marblecaves.org.uk

Abstract

A 500m-long artificial tunnel into Langjökull glacier, NE of Reykjavik, Iceland, was constructed as a tourist attraction in 2015 and visited one month after its opening. The 3 m-tall and 3.5 m-wide horizontal tunnel provides an opportunity to view the inside of a glacier, from the entrance snowpack to solid ice, at depths increasing to 25 m below the surface, where bedrock is 200 m below. The tunnel remains well above the Plastic Behaviour Limit, so that the containing ice creeps downhill as a brittle material that exhibits a large natural englacial crevasse and narrower vertical fractures. The crevasse forms a glacier cave that is >20 m high and >20 m deep relative to the tunnel, with fine ice speleothems. Some open fractures are offset by a horizontal or vertical movement along a bedding plane or closed vertical joint. Several fractures have been enlarged by meltwater in conduits that continue on the opposite side of the tunnel. The meltwater was presumably supplied from moulins or supraglacial lakes that form in summer. This demonstrates that similar englacial conduits could form as outlets to any ice-dammed lakes that submerged karst caves and fractures during major deglaciations, and supports the concept that some such caves were initiated phreatically during deglaciation.

1. Introduction

Karst caves in the northern parts of the planet primarily developed to their present extent during the Quaternary period. It is therefore important to understand their relationships to the c. 50 glaciations that have occurred during the last 2.5 million years. Apart from 'young' caves developed only in the Holocene, some 'older' caves were eroded and therefore shortened by overriding ice sheets and glaciers. These were subsequently lengthened and deepened, and others were initiated, phreatically during deglaciation, and then developed in vadose conditions in the lowered topography of the next interglacial (FAULKNER, 2008; 2022). During deglaciation, glacial and karst hydrology became integrated systems, when water from submerging glacial lakes flowed via underlying fractures and pre-existing caves into lake outlets at supraglacial streams, englacial Röthlisberger channels and subglacial waterways along Nye channels, typically in valleys at the base of the icesheet. Studying englacial conduits in present glaciers can aid the understanding of glaciokarst hydrological relationships. In June 2015, the opportunity was taken to observe englacial conduits in a new artificial tunnel near the Equilibrium Line Altitude (ELA) at 1270m a.s.l. in the southwest part of Langjökull glacier in Iceland.

2. The artificial tunnel inside Langjökull glacier

The tunnel was constructed over a period of fourteen months by a commercial consortium and opened for public visits in early June 2015. A large machine designed for cutting sandstone excavated 5500 m^3 of ice, with some delays when 8m of winter snowfalls blocked the entrance (Figure 1) and spring meltwater widened crevasses. The tunnel, including a looping end passage, is c. 500m long, 3m tall and 3.5m wide, with three artificial side chambers (Figure 2). At its far end, the overlying ice is 25m thick, above 200m of solid ice to bedrock. Regular maintenance is required to protect the integrity of the tunnel as the glacier slowly creeps down the mountain. The author visited the tunnel on 30 June 2015 as part of a tourist group brought to Langjökull from Reykjavik by minibus and transported on to the glacier in a specially adapted vehicle.

Figure 1: The entrance to the Langjökull tunnel.

3. Observations inside the tunnel

The soft snowpack at the entrance became compressed and turned to ice with distinctive horizontal bedding planes c. 10 m inside the tunnel (Figure 3), some ice being blue without air bubbles, where liquid water has refrozen. Several relict englacial open fractures and conduits were observed, commonly with a phreatic-above-vadose keyhole morphology (Figure 4). The open fractures were commonly vertical and were rarely inclined. Some fractures were 2–3 m tall and only c. 20 cm wide (Figure 5), of which one had clearly been offset later in its lower part by a movement of c. 10 cm along a horizontal bedding plane (Figure 6). There was only one recorded horizontal conduit, which in this case

had been offset vertically by later movement along a vertical joint (Figure 7). This example suggests initiation along a bedding plane fracture that is analogous to an inception horizon in sedimentary limestones (LOWE and GUNN, 1997). Although all these narrow conduits have previously carried meltwater, they appear to have initiated tectonically by movements and tension within the ice. In several cases, aligned conduits continued in the opposite wall of the tunnel, showing that they predate it.

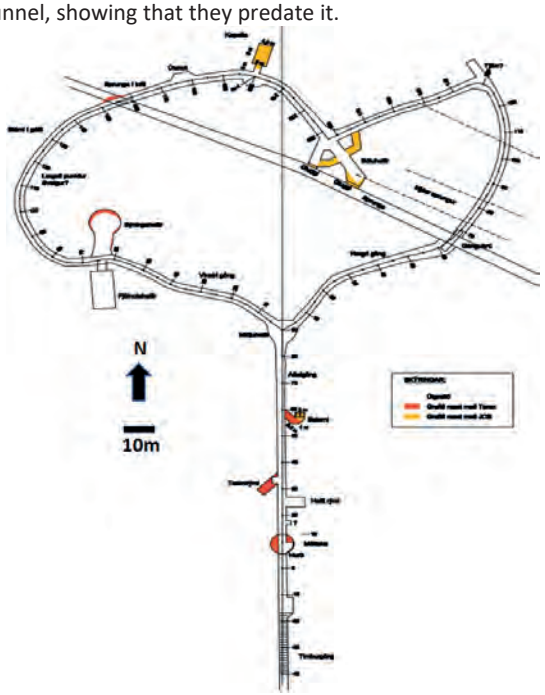

Figure 2: Langjökull tunnel (Helgadottir, 2015)

Figure 3: Inside the Langjökull tunnel, showing compressed ice with bedding planes

Two tunnels from the looping passage terminate in the side of a crevasse with ice speleothems (Figure 8). The crevasse is >20m deep below the tunnel level and is blocked to daylight by firn. No flowing, static or dripping water was seen in the tunnel, conduits, crevasses or on speleothems, suggesting that liquid water only occurs during the springmelt or after rainfall in this tunnel.

Figure 4: Keyhole-shaped englacial conduit

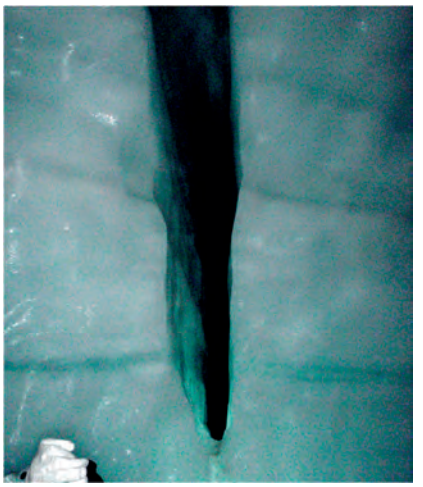

Figure 5: Tall relict vadose conduit. Gloved hand for scale.

Figure 6: The offset lower part of a tall englacial conduit

4. Discussions

The main properties that determine the local internal hydrology of a glacier or ice sheet are temperature, pressure and the availability of flowing water. Surface water supply ceases in winter, when englacial conduits tend to drain away or freeze. In summer, the water supply is greater in the ablation zone below the ELA. than in the accumulation zone, because the temperature is higher at lower altitudes. Cold ice has a temperature below its pressure melting point.

Warm (temperate) ice is at the pressure melting point and contains dispersed liquid water. Cold ice at low pressure behaves like a brittle rock and can retain much of its internal structure of open fractures, conduits and crevasses over several years, as it moves forward down-slope. Sustained warm ice at low pressure is probably undergoing deglaciation. Cold or warm ice at high pressure moves by plastic flow, which closes any air spaces within the ice, so that deep relict conduits cannot exist. The boundary between the two pressure regimes at which air-filled openings close within one year during winter aridity is called the Plastic Behaviour Limit (PBL: BADINO, 2001), which is commonly 100–200m below the ice surface. Isenko *et al*. (2005: Fig. 1) showed that the radius of an empty conduit reduces to zero more slowly at lower temperatures. Englacial channels supplied with phreatic water, especially from the ablation zone, can survive deeper, as modelled by Röthlisberger (1972), and perhaps to 300m depth (FOUNTAIN AND WALDER, 1998: 305–307). Such channels can also survive to greater depths at lower ice temperatures (ISENKO *et al*., 2005: Fig. 5).

Fountain *et al*. (2005) found that interconnected non-tubular fracture systems with widths 0.3–20cm account for >80% of the englacial cavities to a depth of 131m in the 250m-thick temperate valley glacier Storglaciären in Sweden. Some carried laminar water flow at 0.5–4cms^{-1}. Church *et al.* (2019) showed, by using several combined geophysical methods, that a network of englacial conduits exists below the ablation area in the warm-based Rhone glacier. Fountain and Walder (1998) also reported that half the boreholes drilled in glaciers drain before bedrock is reached, indicating intersection with englacial conduits, most being horizontal. Video evidence showed that these are commonly proximal to bands of blue ice, suggesting that such bands can act as inception horizons.

Ice temperature can vary downwards at several different timescales, to create a cold- or warm-base, being dependent on the surface air temperature, the geothermal heat flux from the bedrock, and the hysteresis of the state of the ice, which is determined by its glacial inheritance. In contrast, pressure commonly increases with depth, especially below the PBL, being dependent on the weight of ice above.

It is clear from the observed absence of liquid water that the ice in the shallow Langjökull tunnel is below 0°C and well above the PBL, so that it can retain its internal openings for many years. By comparison with the Rhone glacier, Langjökull probably also has an interconnected conduit network that operates hydraulically during the spring melt at least. The vertical open fractures correspond with similar fractures seen in boreholes in other glaciers. In those, water can fill the cracks and freeze to form super-clear ice, but such fractures are also the places along which englacial channels are likely to be initiated by the melting of side walls (Andrew Fountain, pers, comm., 2015). The sources of the meltwater that fed the conduits in the Langjökull tunnel are unknown but could be from a nearby moulin that terminates a supraglacial stream (e.g., Figure 9) or a supraglacial lake (e.g., Figure 10) or an ice-dammed lake, where ice melts against warm bedrock at the rear of the glacier in spring and summer. It will be interesting to learn how this artificial tunnel behaves over time. This is an important research site for studying ice temperature, pressure, composition (HELGADOTTIR, 2015) and movement, fracture generation, crevasses, meltwater flow, and conduit enlargement.

Figure 7: Offset horizontal opening.

Figure 8: Crevasse with ice speleothems, lit internally.

Figure 9: Moulin on Langjökull. Photo from the internet.

Figure 10: Supraglacial lakes on Langjökull. Internet photo

Although Iceland is not a karst area, the presence of the conduits created by fracturing and enlarged by meltwater demonstrates how glacial hydrology can operate in a glaciokarst environment. Of interest to karst speleologists is the way in which evolving glacial conditions create a varying mosaic of cold- and warm-based ice and bodies of meltwater in mountainous and northern areas during the stages of glaciation, deglaciation and interglaciation. These can cause erosion and sedimentation to remove and block conduits, and dissolution to enlarge them (FAULKNER, 2006). Figure 11 represents deglaciation of a N–S aligned ridge (e.g., LUNDQVIST, 1972) that has a karst area on its west side. It gives an example of how an ice-dammed lake above a subglacial reservoir at the rear of a glacier can transmit aggressive water through karst fractures and cave passages en route to flowing away as a supraglacial stream or into an englacial conduit. This dissolutional flow thereby promotes the next generation of cave passages in the following interglacial (FAULKNER, 2008).

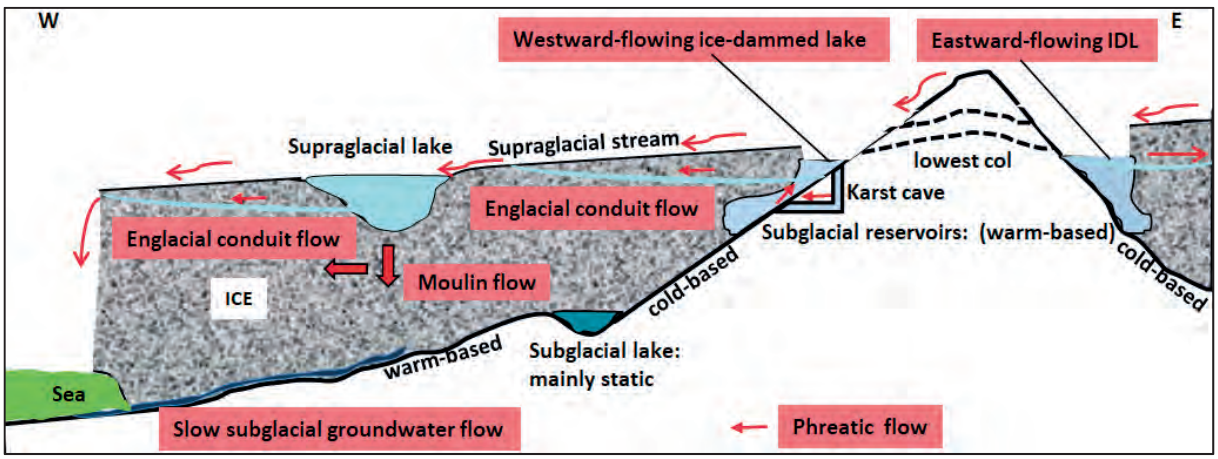

Figure 11: Integrated glacial and karst hydrology during deglaciation.

Acknowledgments

The International Society for Glaciology is thanked for organising the International Symposium on hydrology of glaciers and ice sheets, from 21–26 June 2015 at Höfn, on the SE coast of Iceland, and a subsequent field trip return to Reykjavik. This generated the opportunity to visit Langjökull.

References

BADINO G. (2001) Glacial karst phenomenology. *13th International Speleological Congress, Brasilia*, 15–22 July 2001. Proceedings Paper no. 179. 5 pp.

CHURCH G., BAUDER A., GRAB M., RABENSTEIN L., SINGH S. and MAURER H. (2019) Detecting and characterising an englacial conduit network within a temperate Swiss glacier using active seismic, ground penetrating radar and borehole analysis. *Annals of Glaciology* 60 (79) 193-205.

FAULKNER T. (2006) Limestone dissolution in phreatic conditions at maximum rates and in pure, cold, water. *Cave and Karst Science* 33 (1) 11–20.

FAULKNER T. (2008) The top-down, middle-outwards, model of cave development in Central Scandinavian marbles. *Cave and Karst Science* 34 (1) 3-16.

FAULKNER T. (2022) The high-flow low-storage extreme in marble aquifers. *18th International Speleological Congress Proceedings*.

FOUNTAIN A.G. and WALDER J.S. (1998) Water flow through temperate glaciers. *Reviews of Geophysics* 36 (3), 299–328.

FOUNTAIN A.G., JACOBEL R.W., SCHLICHTING R. and JANSSON P. (2005) Fractures as the main pathways of water flow in temperate glaciers. *Nature* 433, 618–620.

Horizon Hypothesis. *Acta Carsologica* 26/2 38, 457–488.

HELGADOTTIR H.R. (2015) Densification of firn on Langjökull Glacier, Iceland. Thesis. University of Iceland. 37pp.

ISENKO E., MAVLYUDOV B. and NARUSE R. (2005) Survival of developed intraglacial water channels in cold and temperate glaciers. In Mavlyudov B., ed. *7th International Symposium on glacier caves and glacial karst in high mountains and polar regions*. Institute of geography of the Russian Academy of Sciences, Moscow. Proceedings 49–53.

LOWE D.J. and GUNN J. (1997) Carbonate Speleogenesis: An Inception LUNDQVIST J. (1972) Ice-lake types and deglaciation pattern along the Scandinavian mountain range. *Boreas* 1 27–54.

RÖTHLISBERGER H. (1972) Water pressure in intra- and subglacial channels. *Journal of Glaciology* 11 (62), 177–203.

La rivière « chaude » supérieure de Kverkfjöll (Vatnajökull, Islande) : le plus profond réseau sous-glaciaire connu

Gérald FAVRE

Route de Crassier 16, 1277 Borex, Suisse, geologos@bluewin.ch - +41 22 367 22 59

« Ce qui est curieux dans cette terre d'Islande n'est pas au-dessus, mais dessous ! »
(Jules Verne, voyage au centre de la Terre)

Résumé

Réalisant que l'énergie thermique représentait le vecteur le plus important en ce qui concerne le creusement des cavités sous-glaciaires et intra-glaciaires, nous avons, dès le début des années 1980, dirigé nos recherches en Islande ou l'énergie géothermique est omniprésente et ceci, même sous les glaciers. Depuis cette époque, nous suivons régulièrement l'évolution de la rivière sous glaciaire du glacier de Kverkfjöll qui s'écoule dans de spectaculaires galeries sur plus de 2,5 km de développement et 500 m de profondeur. Le réchauffement climatique va-t-il influencer l'évolution de cette cavité si particulière ?

Abstract

The Upper Kverkfjöll "Hot" River (Vatnajökull, Iceland): the deepest known sub-glacial system. Realizing that thermal energy represented the most important vector for the digging of subglacial and intraglacial cavities, we have, since the beginning of the 80s, directed our research in Iceland where geothermal energy is omnipresent and this, even under glaciers. Since that time, we have regularly followed the evolution of the subglacial river of the Kverkfjöll glacier which flows through spectacular galleries over 2.5 km of development and 500 m of depth. Will global warming influence the development of this very special cave?

1. Terminologie

Si la glaciospéléologie est depuis longtemps déjà une discipline à part entière, nous avons proposé au début des années 1980 que ce genre de recherches particulières, lorsqu'elles mettent en relation la glace et un substratum libérant de l'énergie géothermique, fassent partie d'une discipline que l'on peut appeler **« volcanoglaciospéléologie ».**

Mis à part l'Islande, ce type d'investigations peut se mener aux États-Unis, en Alaska, au Kamtschatka, en Antarctique ou ailleurs (?), lorsque volcans et glaciers se côtoient, ce qui n'est pas si fréquent sur notre planète.

2. Descriptif

Visible depuis la base du Kverkjökull (partie nord de la calotte du Vatnajökull), une grande pente de glace recouverte de neige occupe le flanc extérieur occidental de la caldeira d'un volcan important d'Islande. Au sommet sud-ouest de cette dernière s'ouvrent plusieurs « chaudron » dans la glace, en relation avec un important réseau sous glaciaire. Dans cette zone, le glacier ne recouvre pas entièrement le substratum rocheux et les tufs volcaniques apparaissent par endroits selon une légère crête ou par pointements rocheux au travers du glacier déchiqueté. Les entrées du réseau, dont le nombre peut varier selon les années entre une et six, changent continuellement de physionomie en fonction de l'enneigement et de l'activité géothermique, mais leurs emplacements demeurent les mêmes, car elles coïncident avec des zones chaudes fixes sur le flanc extérieur du volcan (Fig. 1). Globalement, nous avons constaté un léger retrait de la calotte glaciaire entre 1982 et 1984. Par la suite, et jusqu'en 2006, les variations ont été peu importantes, mais, dans l'ensemble, on assiste à une diminution d'épaisseur généralisée de la glace sur le flanc du volcan et à l'apparition de nouvelles entrées, surtout dans la partie supérieure du réseau.

En 2005, il a même été possible, suite à une coloration, de trouver une entrée inférieure au réseau, tout en bas de la pente. Depuis toutes ces années, l'accès le plus commode à la galerie principale se fait par l'entrée II (Fig. 1), sauf lorsque toute la coupole d'entrée est effondrée ! À cet emplacement, nous pouvons observer une importante marmite bouillonnante. Cette dernière s'écoule en direction de la rivière sous-glaciaire par une courte galerie. C'était toujours le cas en 2014, lors de notre dernière visite. L'amont de la rivière principale a pu être parcouru sur 200m

jusqu'à une étroiture infranchissable d'où émerge l'eau entre la glace et la moraine. Sur ce parcours, la galerie se divise en plusieurs bras et une salle latérale est taillée presque exclusivement dans la glace. Une galerie remontante aboutit à l'extérieur (entrée I). Dans ce secteur, et selon les années, plusieurs galeries supérieures se développent entièrement dans la glace vive avec de très belles formes de creusement et des parois alvéolées. Nous sommes ici en présence de la tête du réseau accessible à l'homme, même si la rivière active prend naissance quelques centaines de mètres en amont, dans une zone où le glacier est très tourmenté.

Figure 1 : Kverkfjöll, zone géothermique, flanc ouest de la caldeira. Contact entre le glacier et le volcan.

En direction de l'aval, la cavité devient de plus en plus intéressante : sitôt le ressaut Axel passé au moyen d'une petite corde ou une échelle d'électron fixée à une broche à glace, on atteint une première bifurcation d'où part une galerie aboutissant à un siphon. Sur les côtés de la galerie principale on note la présence de plusieurs talus morainiques formés par la partie inférieure des parois de glace qui, dans leur mouvement, agissent comme le socle d'une charrue. Tout au long de l'axe principal, plusieurs stades de poussée et de retrait sont visibles. Ces dépôts ont une composition mixte de roches à éléments volcaniques. À l'emplacement des solfatares Turleson, la galerie prend des allures de salle, car à de tels endroits, le volume excavé est directement en relation avec l'activité géothermique. Comme l'émission de calories est quasiment ponctuelle et occupe une surface de quelques mètres carrés, il se forme une coupole dont la hauteur a pu être estimée à 20 ou 30 m au travers d'une atmosphère très nébuleuse. Résultat d'une activité beaucoup plus faible, un bombement rocheux au sol, aux coloris divers, a donné naissance à « l'Igloo », simple alvéole montrant un équilibre permanent entre l'activité géothermique et la glace. Autour de certains solfatares se forme des micro-gours de couleur orange-ocre, sans squelettes rigides et comparables à de la gélatine. Présence insolite en ces lieux de colonies de bactéries thermophiles. Vers –80, une galerie se détache en rive gauche à la hauteur du plafond. Après avoir passé « Le Col », on aboutit 60 m plus loin à une autre zone chaude. Comme la pente du substratum est fortement inclinée en direction du nord, l'écoulement ne rejoint pas la rivière principale et forme ainsi un système indépendant : le « Diffluent ». Rapidement, l'aval du Diffluent devient impénétrable, car l'énergie émise par ce solfatare et véhiculée par le cours d'eau est très rapidement dissipée dans les premiers 100 m.

Toutefois, certaines années, comme en 2004 et 2005, des salles et des galeries peuvent se former et rejoindre la suite du réseau dans la partie supérieure de la salle des solfatares d'Odin. En continuant à l'aval de la rivière principale, la galerie change d'aspect, car la glace ne forme que son plafond tandis que le sol et les parois sont constitués de tuf volcanique et de dépôt morainiques. L'actif coule au fond d'une gorge où l'on progresse de bassin en bassin avec la technique de l'opposition. À ce point, on atteint le dernier groupe de solfatares actifs (Odin), puis la galerie continue sur 200 m avec une section importante (galerie Björnsson). La glace forme à nouveau le plafond et les parois latérales.

À la profondeur de –122 m, la galerie plonge brutalement à 45° par une série de plans inclinés de ressauts et de puits. L'axe général de la cavité change également et prend une direction nord, selon la pente. Plusieurs particularités sont à noter ici : la section de la galerie présente la forme en « trou de serrure » typique, avec un plafond de glace et un canyon entièrement taillé dans le substratum de roche volcanique.

En rive droite, une galerie ornée de stalactites de glace aboutit à un siphon. En rive Gauche, une lucarne accessible avec les crampons et le piolet conduit à une galerie parallèle (Ali Baba caverne) qui diffère complètement du reste de la cavité. Elle ne semble pas subir l'influence des solfatares et ressemble davantage à un fond de crevasse des Alpes avec une cristallisation abondante sous la forme de glace hexagonale dont les cristaux peuvent atteindre 15 cm de côté. C'est en 2005 que nous comprendrons la raison d'être de ce piège à froid : à cet emplacement la surface n'est pas très loin et c'est l'air froid de l'extérieur qui est responsable de ces formations. Une nouvelle entrée s'est même formée et l'un d'entre nous a pu rejoindre l'extérieur. Actuellement la galerie est beaucoup plus large, la lumière du jour bien visible, et les formations glacées ont entièrement disparu.

Figure 2 : Galerie « géothermique » développée en pleine glace

Pour descendre dans le canyon, il faut tout d'abord progresser en rive droite, horizontalement ou obliquement, et fixer une grande main courante avant de pouvoir descendre verticalement. Ce passage est très esthétique et a représenté l'un des grands moments de notre exploration. La progression se poursuit ensuite sur rive gauche, dans la « galerie du Canyon » jusqu'au puits Lindenbrock. Ce dernier est le premier obstacle réellement vertical de la cavité et son

passage nécessite un fractionnement dans la paroi de glace en rive gauche. Le canyon atteint dans cette zone une profondeur de 6 m par endroits. Mis à part un ressaut de 5 m, la galerie aval se parcourt aisément sur 400m jusqu'à la verticale suivante, le puits Saknussem. Par endroits, la galerie se divise en plusieurs branches et présente des sections elliptiques très esthétiques (1982). En rive droite, nous pensons avoir reconnu une petite zone de solfatares d'où diverge un écoulement parallèle. Le puits Saknussem, d'une verticale de 35 m (40 m avec les ressauts à la base) est sans conteste l'endroit le plus impressionnant de la cavité. C'est ici que la jonction historique s'est effectuée en 2005 entre les équipes qui venaient du haut et du bas. Le départ se fait en main courante, en rive droite ou gauche, selon les circonstances, dans le plafond avec trois fractionnements dans des lames de glace… Malgré toutes les précautions, il est impossible d'éviter les frottements sur les protubérances rocheuses ; les protège-corde se révèlent ici très utiles. À mi-puits, des dalles très instables menacent de s'écrouler au moindre frottement. À partir de cet endroit, la vue est spectaculaire, avec une immense voûte glacée. L'actif principal tombe en cataractes et un affluent surgit en cascade de la paroi opposée. À la base du puits, un lac et les embruns des cascades nous accueillent. Encore un ressaut et la progression se poursuit, parmi les blocs rocheux plus ou moins horizontalement. L'influence des solfatares se fait de moins en moins de sentir et dans les années 1980, nous avons observé une diminution des sections. Par la suite, en 2005, l'important courant d'air qui parcourait la cavité a permis le développement de galerie de taille respectable (6 m de hauteur pour 15 m de largeur ou plus). Certains dépôts dans la galerie sont formés non pas par de la glace vive mais par de la neige tassée.
En 2005 nous avons observé le même type d'accumulation au niveau du puits Saknussem.

Figure 3 : Galerie géothermique dans la partie aval du réseau

Il s'agit, en réalité, d'intrusion de neige soufflée depuis la surface. Comme ce phénomène est de plus en plus fréquent dans la cavité, nous en déduisons que l'épaisseur de glace a diminué et que les entrées se multiplient. En 1984, un peu plus en aval nous avons observé une étrange lumière bleutée à travers la glace, mais malgré nos vigoureux coups de piolet, nous ne sommes pas parvenus à ouvrir un passage cette année-là.
Par contre, en 2005, la nature avait fait le travail pour nous ; entrer ou ressortir à cet emplacement n'était vraiment plus un problème. Alors que nous pensions, en 1984 avoir touché le terminus, l'un de nous (Maurice Chiron) força l'étroiture aval (impassable en crue) et trouva la suite sous la forme d'une grande galerie (galerie Maurice) taillée dans la glace, au sol caillouteux, et qui nous conduisit quelque 200 m plus loin à une étroiture terminale cette fois-ci à la cote mesurée de -525 m. En 1982 déjà, nous pensions nous trouver sous l'extrémité de la pente glacée qui recouvre les flancs nord-ouest de la caldeira et que, selon les conditions, la traversée intégrale devait être possible. De l'extérieur, nous avions repéré un fort courant d'air qui sortait d'une fente de 2 cm entre l'eau et la glace. En 2014, nous sommes retournés dans cette cavité, pour constater son évolution et réaliser des prises de vues complémentaires destinées à un film futur. Constatation : peu de changements à signaler, si ce n'est un volume des salles de plus en plus important. Les deux topographies réalisées en 1984 et 2006 (Fig. 4) ne sont pas identiques, car entre ces deux époques, le glacier s'est modifié dans les zones aval et amont (fonte). En conclusion, un phénomène à avoir « à l'œil » dans le futur, et ceci, comme ailleurs sur Terre en relation aussi avec le réchauffement climatique.

3. Remarques

De ces découvertes, plusieurs constatations d'ordre local et général peuvent être tirées : la rivière supérieure de Kverkfjöll, sans être certainement un cas unique au monde, reste un lieu d'étude privilégié pour l'observation des interactions entre un volcan est un glacier. Il convient de raisonner en fonction du dynamisme des phénomènes en cause et de tenir compte aussi bien de l'activité variable des solfatares que des mouvements du glacier et des circulations des masses d'air. La pérennité dans la position des solfatares, va par contre créer un réseau sous-glaciaire qui va conserver durant de très longues périodes une orientation identique, déterminée en grande partie par le contexte topographique et morphologique local. Les variations de section des conduits seront quant à elles, directement en relation avec l'activité géothermique pour une période donnée. Elles sont également liées à la présence de courants d'air et d'eau parcourant la cavité. De plus, il faut tenir compte du déplacement de la masse de glace sus-jacente par rapport aux « points chauds ». De la valeur de chacune de ces différentes variables va dépendre la physionomie du réseau à un instant précis. Dans le cas de la rivière supérieure de Kverkfjöll, le creusement de la cavité s'effectue en premier lieu grâce à l'activité solfatarienne de la partie amont du réseau.
Dans cette partie, les énormes volumes excavés résultent de la chaleur directe émise sous forme de vapeur à partir des points chauds. L'aval du réseau est davantage lié au courant d'eau en provenance de l'amont, qui progressivement libère ses calories. Un rôle très important est joué dans cette cavité par le courant d'air qui lui aussi véhicule des calories et est responsable de la formation des cupules dans les parois du glacier et les plafonds. Sans cette circulation d'air, la cavité se refermerait certainement à partir de -300 m. Une observation très importante, concernant l'âge de la cavité a été effectué dans la partie amont : l'actif principal ne suit pas ici la ligne de plus forte pente, ce qui pourrait paraître aberrant dans un contexte « normal ». Sa direction vers le

nord-est, jusqu'aux rampes inclinées, à –122 m s'oriente ensuite vers le nord jusqu'au point le plus bas. Mis à part le solfatare du Diffluent, tous les autres points chauds sont situés sur le même axe en amont du point –122 m. Afin d'expliquer cet écoulement, diagonalement à la pente, peu respectueux de la gravité, nous proposons l'explication suivante : dans une première phase, alors qu'une calotte glaciaire recouvrait la zone, les solfatares sont apparus selon l'axe actuel nord-est / sud-ouest. À la verticale de chaque point chaud, la cavitation s'est développée et les différentes alvéoles ont rapidement jonctionné. L'eau de fusion s'écoula de l'une à l'autre en direction du nord-est, selon « l'axe thermique ». L'écoulement, selon le plus fort gradient, ne fut pas possible à cause de la pression de la glace au nord qui forma une sorte de barrage naturel. Vers le point –122 m, les solfatares disparaissent et l'écoulement a alors trouvé un passage parallèle à la pente. Dans un deuxième temps, selon le même tracé la rivière a creusé un vallon diagonalement à la pente en s'enfonçant de plus en plus (profond canyon taillé dans le tuf) Cette morphologie est visible à plusieurs endroits et spécialement au « Col » où il faut remonter avant d'atteindre le Diffluent. Cette évolution morphologique tend à prouver la pérennité du réseau à cet emplacement depuis plusieurs centaines, voire plusieurs milliers d'années.

La rivière supérieure de Kverkfjöll est donc une cavité sous-glaciaire qui n'est pas près de disparaître, à moins que ne cesse l'activité géothermique ou encore que le glacier se retire.

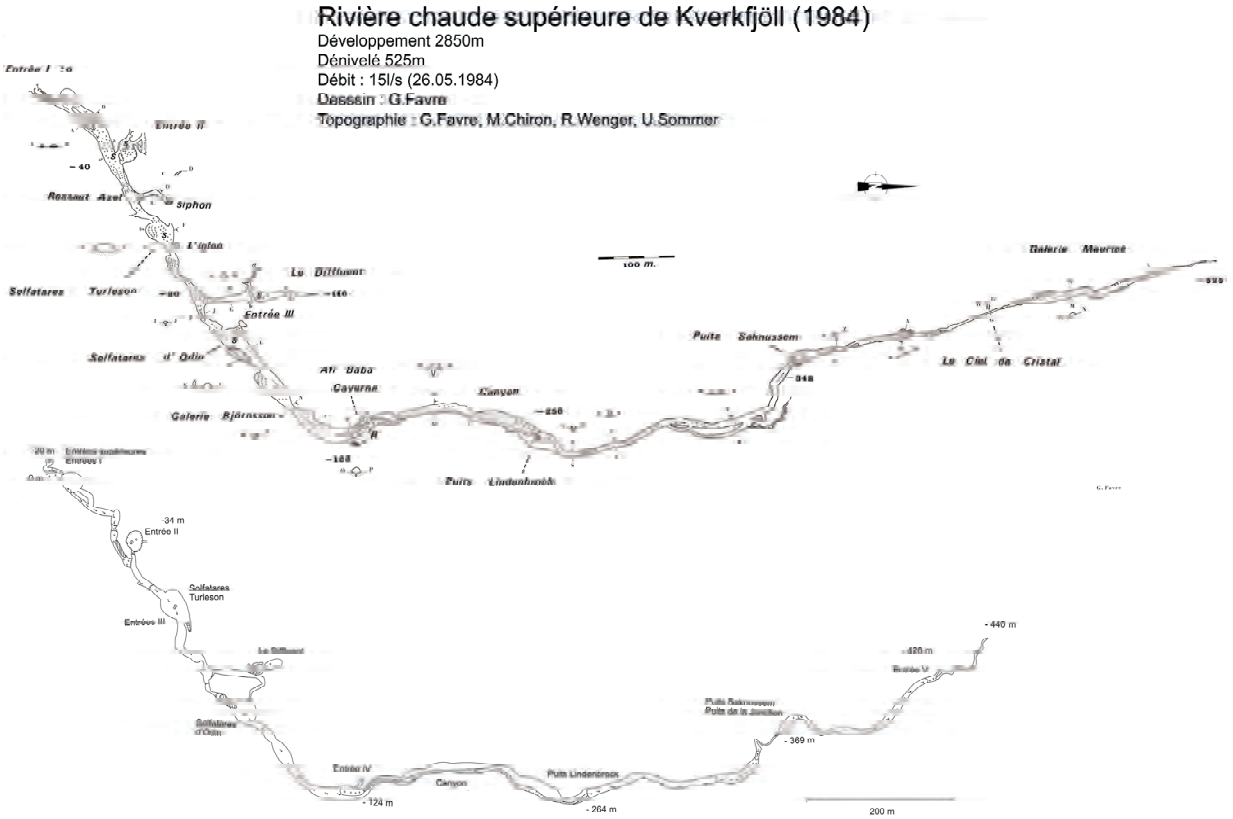

Rivière chaude supérieure de Kverkfjöll (2005)
Développement 2225m
Dénivelé 440m
Desssin : p.Marti
Topographie : P.Marti, F.Monney, A et M. Pahud, L.et C. Savoy, V.Berclaz

Remerciements

À tous les membres et amis de la Société Spéléologique Genevoise et autres spéléologues qui ont participé à ces explorations depuis 1980.

Glaciospéléologie dans les Alpes suisses : plus de 40 années de recherche et d'exploration (résumé des types de cavités)

Gérald FAVRE

Route de Crassier 16, 1277 Borex, Suisse, geologos@bluewin.ch - +41 22 367 22 59

Résumé

Zermatt, Aletsch, Arolla, Chamonix ; que de régions mythiques des Alpes qui, dès 1977, ont aiguisé notre curiosité pour une forme d'exploration spéléologique assez « exotique ». Au début, ce fut pour notre part dans des buts à la fois exploratoires et filmographiques destinés à réaliser le film « Spélé-ice », présenté au festival international du film de spéléologie de la Chapelle-en-Vercors en 1982. Puis, jusqu'à ce jour, nous avons essayé de comprendre et de suivre l'évolution de ces phénomènes particuliers liés à une hydrologie intra et sous-glaciaire. Cet article présente quelques exemples de cavités symboliques qui se développent dans cet environnement naturel particulier pour les spéléologues que nous sommes. Un « univers » fascinant, mais à appréhender avec prudence et respect par rapport à certains risques qui lui sont propres…

Abstract

Glaciospeleology in the Swiss Alps: more than 40 years of research and exploration (summary of cave types). Zermatt, Aletsch, Arolla, Chamonix; only mythical regions of the Alps which, since 1977 have sharpened our curiosity for a rather "exotic" form of speleological exploration. At the beginning, for our part, it was for both exploratory and filmographic purposes intended to make the film "Spele-ice", presented at the international festival of speleology film of La Chapelle-en-Vercors in 1982. Then, until day, we tried to understand and follow the evolution of these particular phenomena linked to an intra and subglacial hydrology. This article presents some examples of symbolic cavities that develop in this particular natural environment for speleologists like us. A fascinating "universe", but to be understood with caution and respect in relation to certain risks that are specific to it...

1. Cadre

Il existe principalement **deux types d'exploration sous glaciaires** qui, chacune, demandent du matériel spécifique et adapté. Dans le premier cas, il s'agit d'exploration **intra-glaciaire**. L'action consiste à progresser dans les bédières ou rivières supra-glaciaires ou de descendre dans les moulins glaciaires. Ces derniers se poursuivent parfois par des méandres taillés dans la glace vive ainsi que par des puits successifs jusqu'à une profondeur qui peut dépasser 120 m dans les Alpes. La profondeur maximale atteinte à ce jour, à notre connaissance, est de -203 m au Groenland (Lamberton et *al*.). Dans ce type d'exploration verticale, il semble difficile de pénétrer dans la masse glaciaire plus profondément, à cause du comportement mécanique de cette dernière et des forces physiques de compression. Mais ceci reste à démontrer et l'espoir subsiste de pouvoir descendre plus en profondeur. Pour cela, les moulins du Groenland sont de bons candidats, et ceci aussi depuis quelques années à cause du réchauffement climatique… Les crevasses d'origine tectonique représentent aussi un sujet d'exploration et d'investigation particulier, avec des informations intéressantes à collecter. Dans le deuxième cas, il s'agit d'exploration **sous-glaciaire**, avec des cavernes et des galeries qui se forment entre la surface latérale ou inférieure du glacier et la roche en place ou les alluvions déposés. C'est le domaine des galeries-tunnels et des porches, des pertes et des résurgences glaciaires. Afin d'appréhender les différents types de cavités pouvant se développer dans et sous un glacier le lecteur aura grand intérêt à lire l'article synthétique écrit à ce sujet par J. Schroeder, M.Pulina et J.Rehak publié dans *Karstologia* n° 42 (2003). Sans reprendre ce descriptif détaillé, nous décrivons ici quelques exemples qui nous sont propres et qui concernent les divers types de cavités intra et sous-glaciaires les plus répandues.

2. Types de cavités

Lacs de confluences et lacs latéraux avec pertes :

Lorsque deux glaciers se rencontrent à partir de deux vallées confluentes, ils peuvent former un barrage naturel avec une dépression en amont qui va recueillir les eaux de ruissellement locales et ainsi former un véritable lac-réservoir de parfois plusieurs millions de m^3. En été, avec l'élévation des températures, le volume accumulé augmente fortement et, la pression hydrostatique aidant, l'appareil glaciaire subit une sustentation, ce qui permet à l'eau de transiter à la base du glacier, tout d'abord en petite quantité, puis rapidement sous la forme d'une crue sous-glaciaire importante qui peut durer de quelques heures à quelques jours et occasionner d'importants dégâts à l'aval. L'exemple le plus significatif que nous avons suivi durant de nombreuses années est celui du Gornersee à Zermatt, à la confluence des glaciers Gorner et Grenzer (Mt Rose) dont le lac de 6 M° de m^3, dans les années 1960, se vidait en 3 jours.

C'est ici que les explorations spéléologiques ont été les plus instructives, avec de grandes galeries sous glaciaire qui se développaient jusqu'à 100 m de profondeur pour 300 m de longueur, à la base du glacier.
En bordure des glaciers, des lacs temporaires peuvent aussi se former et se vidanger en période estivale principalement. L'un des cas les plus célèbres dans les Alpes est celui du Märjelensee, en rive droite du glacier d'Aletsch en Valais, où il a été possible de pénétrer sous le glacier sur une distance de 200 m, avant que la pression due à la masse de glace comprime les galeries. Des contextes de cavitations intéressants pour les spéléologues, mais avec un environnement très instable…

Bédières et moulins :

Sur le plan de l'esthétisme, ce type d'exploration est certainement le plus motivant, avec tout d'abord des progressions mi-jour mi intra-glaciaires dans des bédières (canyons en méandres) sur plusieurs centaines de mètres, puis une plongée (avec ou sans bouteilles…) dans des gouffres et des galeries en méandres (moulins) entièrement taillés dans la glace vive. Dans le glacier du Gorner, il nous a été possible de descendre jusqu'à 115 m de profondeur dans le moulin du Congélateur (Fig. 1 et 2). À ce sujet, depuis une dizaine d'années, plusieurs équipes de spéléologues français ont exploré en détail ce type de formations sur les glaciers du Gorner et d'Aletsch (cf. biblio existante). À ce jour, aucun moulin n'a permis d'établir une connexion avec le torrent principal qui s'écoule à la base du glacier, rêve des spéléologues (mais la glace n'est pas le calcaire…).

Figure 1 : Méandre intra-glaciaire du Glacier du Gorner.

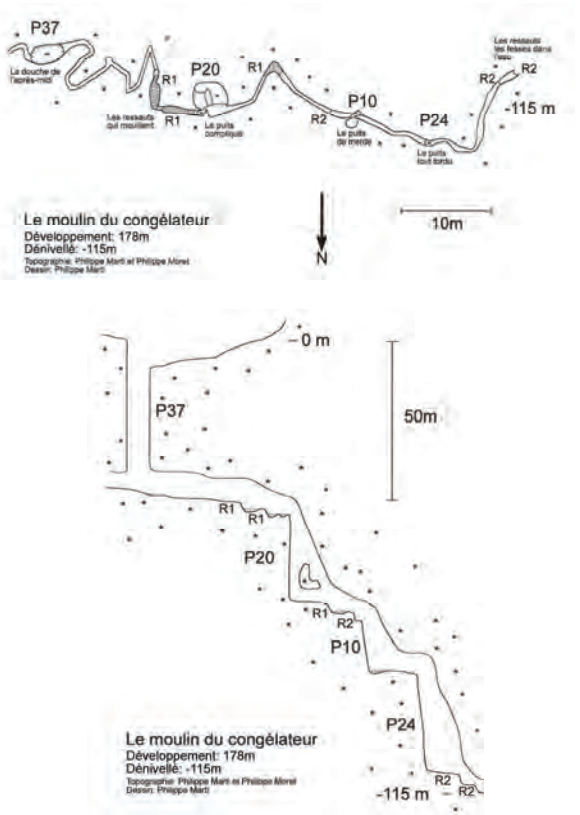

Figure 2 : Plan et coupe du moulin du congélateur.

Cavités de décollement :
Selon la morphologie du bed-rock, il arrive que le glacier décolle à l'aval des ressauts rocheux. Des cavités de grandes dimensions peuvent alors se former, comme dans le cas du glacier d'Argentière qui a été étudié en détails depuis 40 ans par le glaciologue Luc Moreau (cf. article dans les actes congrès). Si le phénomène est purement mécanique pour ce type de cavités, des élargissements dus aux énergies hydraulique ou thermique sont aussi possibles. Dans ce type de cavités, il est possible d'observer les traces de glissement du glacier par en-dessous, sur son lit rocheux, comme vu aussi sous le glacier de Tsanfleuron qui décolle de petites falaises dues aux bancs massifs des calcaires urgoniens (Fig. 3).

Figure 3 : Cavité de décollement sous le glacier de Tsanfleuron.

Portails glaciaires :

Au front de la plupart des glaciers, on observe que l'eau sous-glaciaire collectée en amont et qui transite sous les glaciers apparaît de façon laminaire entre la glace et le substratum rocheux ou alluvionnaire. Parfois, un porche avec une grotte sous-glaciaire peu profonde se développe à cet emplacement. On parle ici de portail glaciaire. Ces cavités ne conduisent pas à des conduites développées en amont et sont le résultat d'un « écaillage » de la glace au front du glacier. Comme constaté au front des glaciers islandais ou au Groenland (lac Centrum), et ceci malgré les grands volumes d'eau concernés (dizaines de m^3/s) aucune galerie ne se développe. L'eau s'écoule de façon laminaire entre le glacier et le substratum. Vu sa température trop basse, elle n'a pas la possibilité de former des galeries spacieuses dans la glace. L'agent principal du creusement de galeries spacieuses et pénétrables à l'homme (hormis les cavités de décollement ou tectoniques) est bien la température et non les volumes d'eau. Ce sont les calories véhiculées dans l'eau ou dans l'air qui sont responsables du creusement des cavités, comme cela est bien illustré par les exemples suivants.

Figure 4 : Galerie sous-glaciaire, glacier d'Arolla (C. Bernhard).

Systèmes pertes-résurgences et galeries-tunnels :

Nos récentes explorations (2018-2019) ont été possible grâce aux conditions climatiques actuelles et au retrait rapide des glaciers qui dans plusieurs cas se sont segmentés dans leur parties aval. Si en Islande, les cavités sous-glaciaires sont principalement dues à **l'énergie géothermique**, par contre, dans les Alpes, les calories nécessaires à la fusion de la glace sont dues à **l'énergie solaire**. Dans un premier temps, l'eau qui cascade à l'air libre sur les roches à l'extérieur se réchauffe légèrement et est à l'origine du creusement d'une première « galerie », souvent impénétrable à l'homme, entre une perte située à l'amont d'une masse glaciaire et sa résurgence à l'aval. Cette première conduite naturelle va ensuite être élargie et ceci de façon parfois spectaculaire par les courants d'air qui parcourent la cavité. Ces derniers peuvent parfois avoir en été une température d'entrée sous l'appareil glaciaire de plus de 20°. Cette **énergie thermique** permet alors à la galerie de s'agrandir de façon parfois spectaculaire et d'atteindre des dimensions qui peuvent aller de 20 m de largeur pour 8 m de hauteur. Ces courants d'air tempéré sont à l'origine des spectaculaires alvéoles formées dans la glace et qui peuvent dépasser 1 m de diamètre. Durant toutes nos investigations, nous avions rarement eu l'opportunité d'explorer en Suisse ce type de cavités, car, dans les années 1980 le réchauffement climatique n'était pas aussi spectaculaire qu'aujourd'hui. Les périodes chaudes qui se succèdent depuis plus de 20 ans, ont un impact spectaculaire sur nos glaciers et leurs zones frontales principalement. Depuis quelques années paraissent dans les revues spécialisées (Spéléo magazine, Spelunca) des comptes rendus d'explorations sous-glaciaires de ce type, qui sont possibles grâce au retrait des glaciers et surtout à cause de leur morcellement dans leur partie inférieure. En 2017 déjà, nous suspections qu'une importante galerie sous-glaciaire devait exister à l'aval du glacier du Gorner (Zermatt) formée qu'elle devait être par le torrent de surface issu de l'Unterertheodulgletscher, situé sous le petit Cervin.

Figure 5 : Perte dans le glacier du Gorner (G. Favre).

En 2018, nous avons repris plus systématiquement nos investigations en trois emplacements différents des Alpes helvétiques propices au développement de ce genre de cavités. À Zermatt, la galerie supposée existait bien lors de notre visite de 2019 et son mode de formation correspondait bien à ce qui est décrit ci-dessus. Une topographie a pu être réalisée (Fig. 7) et des photographies prises (Fig. 5 et 8). Vu la rapidité avec laquelle le glacier fond à cette altitude, il est très probable que ce système « perte-résurgence » n'existe plus d'ici deux à trois ans. À Arolla, nous avons pu parcourir, aussi en 2019, un tunnel sous-glaciaire de plus de 400 m de longueur sous le Bas glacier d'Arolla, qui est actuellement détaché de sa zone nourricière du Haut glacier d'Arolla (Fig. 6). Lors de nos différentes visites, nous avons pu progresser dans cette galerie spectaculaire sans prendre trop de risques, vu son profil proche de l'équilibre (Fig. 4). Dans la même vallée d'Hérens, plus à l'est, ce sont les glaciers de Ferpècle et du Mont Miné qui ont retenu notre attention. Pour le premier, ce sont des spéléologues français qui ont suivi son retrait et exploré d'impressionnantes cavités (Spéléo Magazine n° 101, mars 2018). Quant au deuxième, il va très certainement présenter un intérêt certain ces prochaines années, lorsque le torrent qui ruisselle sur les parois de rocher plus de 2 km en amont va disparaître sous le glacier. Toutefois, son parcours à l'air libre est trop court pour l'instant pour que des calories d'origine solaire puissent « réchauffer » l'eau et amorcent une cavitation dans laquelle l'air tempéré pourra circuler.

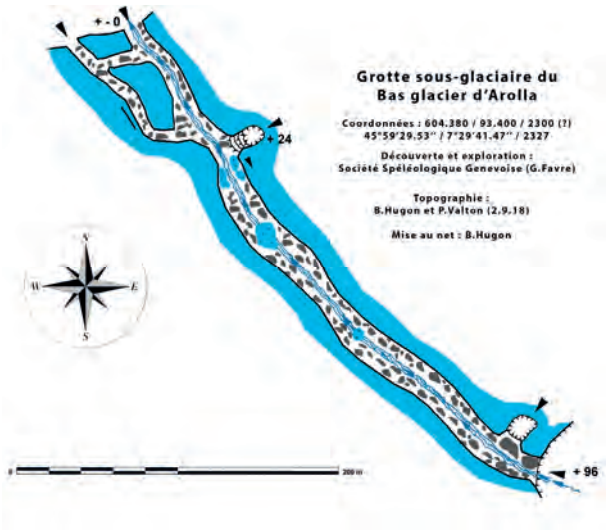

Figure 6 : Plan du système perte-résurgence, Bas glacier d'Arolla.

Figure 7 : Plan du système perte-résurgence, au front du Gornergletscher.

Figure 8 : Résurgence du torrent de l'Unterertheodulgletcher au front du glacier du Gorner.

Remerciements

À tous les membres et amis de la Société Spéléologique Genevoise qui ont participé à ces explorations depuis 1977.

Fumarole-ice dynamics in cryo-speleology on volcanic edifices—Mount Rainier, Washington, USA

Lee FLOREA[(1)], Andreas PFLITSCH[(2)] Eduardo CARTAYA[(3)] & Christian STENNER[(4)]

(1) Indiana Geological and Water Survey, Indiana University, Bloomington, Indiana, USA, lflorea@indiana.edu
(2) Ruhr-University Bochum, Bochum, Germany, andreas.pflitsch@gmx.de
(3) Glacier Cave Explorers, Redmond, Oregon, USA, glaciercaveeddy@gmail.com
(4) Alberta Speleological Society, Calgary, Alberta, Canada, cstenner@telus.net

Abstract

The persistent fumarole ice caves nearly circumnavigating the East Crater of Mount Rainier in the Cascade Volcanic Arc in Washington, USA, are a natural laboratory to study the dynamic equilibrium between thermal flux and glacial ice. The large circum-crater passage connects to entrances on the crater rim by steep transverse passages, and fumarole gas convection and advection maintains the cave passage distribution and morphology. Between August 2016 and August 2017, we collected hourly data using remote sondes that include temperatures at three fumarole, cave air temperature and pressure, water temperature and depth in an in-cave meltwater lake, and the outside temperature and snow depth at Paradise Visitors Center. Correlation and wavelet analyses of these data reveal complex associations between patterns of weather, fumarole activity, and lake level. At longer scales, fumarole temperatures behave largely independently and connected to spatial and temporal changes in volcanic heat flux and glacial melt circulation. At the scale of individual storm-events, major snowfalls seal the cave entrances, increasing cave air temperature and pressure from fumarole output and causing rising lake levels from increased melt until entrances reopen. Repeating freeze-thaw cycles observed in the cave monitoring data are a primary cause of crater mass-wasting.

1. Introduction

The volcanic edifice of Mount Rainier, at 4392 m (elevation datum above mean sea level), dominates the viewscape of western Washington, USA (Figure 1). Although an active volcano, listed as a Decade Volcano by the International Association of Volcanology (NEWHALL, 1996), eruptive activity has been quiescent since 1895 and throughout the growth of urban centers in the Pacific Northwest. The major eruption of nearby Mount Saint Helens in 1980, with associated ash fall, lahars, and loss of life, was a wakeup call for hazard planning and mapping.

Today, over 1.5 million people live within the shadow of Mt. Rainier, ranking it as the most dangerous volcano in the Cascade Range. Glacier outbursts and small serac falls are common on Rainier, which, while dangerous, are not cataclysmic. However, melting glaciers and minor eruptions could send debris flows, pyroclastic flows, and lahars toward Puget Sound and the Seattle/Tacoma metropolitan area (GRAHAM, 2005). A broader understanding of the thermal regime of Mount Rainier, estimated by FRANK (1985) at 10.3 MW, and short term changes to that thermal flux are a critical component to models of hazard prediction.

2. Fumarole Ice Caves

In the summit craters of Mount Rainier (East and West, with most recent eruptive activity in East) fumaroles exist under the ice plugs (FRANK, 1995; ZIMBLEMAN *et al.*, 2000). Heat flux and the cycling of glacial melt have produced the world's most extensive fumarole ice cave system in the East Crater, developed primarily along the contact between the ice and the crater floor (FLOREA *et al.*, 2020; STENNER *et al.*, in review). The East crater cave is currently mapped to 3,593 m in length by expeditions in 2015-2017 led by Cartaya and managed by Glacier Cave Explorers of the Oregon High Desert Grotto (an internal organization of the National Speleological Society) (Fig. 1). Passages almost encircle the east crater and span 134 m in depth, with larger rooms in fumarole areas and rising passages that connect the cave to entrances along the crater rim (Fig. 2). The highest of the 14 primary entries to the East Crater system, at 4,373 m, is located 19 m below Columbia Crest. The highest entrance to the West Crater system is at 4,382 m and is the highest known cave entrance in North America.

Continuity of position and scale of cave passages in recent expeditions (STENNER *et al.*, in review), and similitude with earlier survey efforts described in KIVER & STEELE (1975) and ZIMBLEMAN *et al.* (2000), suggest an inter-annual dynamic equilibrium between thermal flux, cave ventilation, and ice accumulation. Cave expansion around the west margin of the East Crater and extensive changes in the West Crater may be related to changes to volcanic heat flux in these areas.

Glacial melt and fumarole condensate flow down the cave walls and floor and into heated bedrock, where they are recycled as fumarole steam. Occasionally, melt and condensate water accumulate as lakes in places where the ice-rock contact, and underlying bedrock, have low permeability. During the 1970s exploration, Bill Lokey and team discovered Lake Muriel below the ice in the West crater (KIVER & STEELE, 1975). During pre-expedition reconnaissance in 2014, Lake Muriel had disappeared, and a new lake (Lake Adélie) was discovered in the East crater cave. Currently, Lake Adélie is the highest persistent body of water in the United States. The perched nature of this lake provides a unique opportunity for expeditions to collect water monitoring data to add to larger studies of the cave environment and how it responds to the driving forces of thermal flux and external climate. A comprehensive description of the methods of data collection and the interpretation of these data are published in FLOREA *et al.* (2020) and explore the synoptic and seasonal-scale microclimates of the cave with an emphasis on Lake Adélie. Concentrations of volcanic gases (e.g., CO_2, SO_2, and H_2S) and hazards of those to exploration are described in Stenner et al. (in review). This extended abstract presents a synopsis of these data for the international cave science community.

3. Research Challenges

The summit of Mount Rainier layers a harsh environment upon the normal challenges of mountain climbing, cave exploration, and science. In addition to the technical equipment, skills, and training required for navigating seracs and crevasses en-route (Fig. 1), the effective oxygen concentrations at summit air pressures are approximately 12.1%, reducing the pace of exertion and creating the real possibility of altitude sickness and immediate evacuation. Rapid changes of summit weather can lead to snow blindness and sunburn at one extreme, and whiteout conditions and hurricane force winds at the other. At the cave entrances, the uncertainty of firn strength can lead to punch throughs and collapse. Inside the caves, slope instability can cause rock (or person) fall. Additionally, near-freezing temperatures and high humidity increase the possibility of hypothermia. Finally, and particular to these fumarole ice caves, volcanic gases that are more dense than air (CO_2, SO_2, and H_2S) accumulate in low-elevation pockets with limited airflow. Exploration in these sections of the cave requires SCBA equipment and training.

As a designated Wilderness Area of the U.S. National Park System, restrictions at Mount Rainier additionally constrain the capacity of team members to transport equipment and supplies to the summit, and return samples and waste products from scientific study. Wilderness permits limit the number of people at the summit, and the required support for extended summit stays on Mount Rainier is extensive; scientific gear is bulky and heavy, personal gear must be highly specialized, and caloric and hydration needs can be excessive. So, teams of porters transported approximately 400 kg of shared gear and food up the mountain for each expedition in packs that regularly exceeded 30 kg (Fig. 1). Expedition planning starts at the beginning of the year and includes permit applications, safety planning, identifying porters, and ongoing training. Mobilization begins during June, and equipment arrives at Mount Rainier several days before the expedition starts. Full expeditions spanned 12 days, including three days to ascend, acclimatize, and stage gear at base camp, five workdays in the crater base camp to complete all objectives, two days to descend and demobilize base camp, and two contingency days for weather. Expeditions included wilderness medics and experts in mountain and cave rescue.

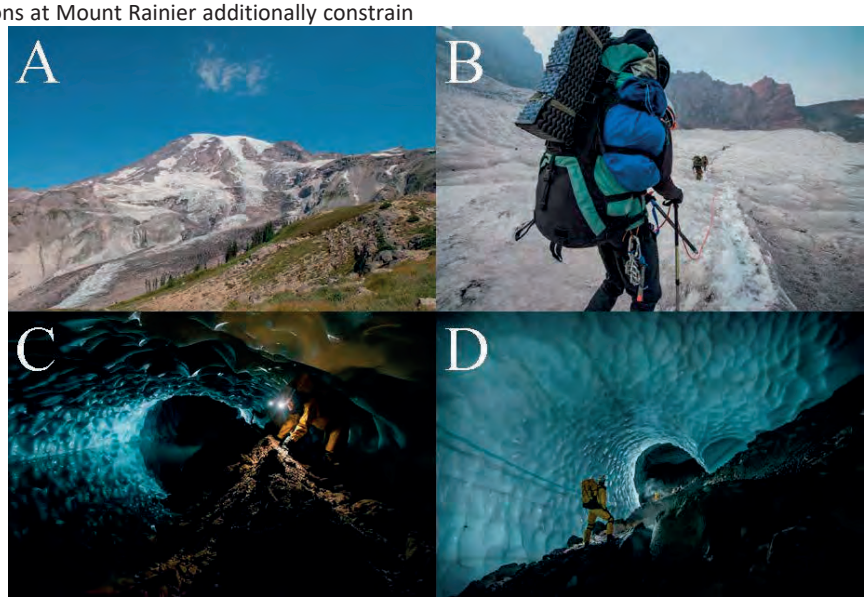

Figure 1: Photos from Mount Rainier expeditions (courtesy of Francois-Xavier De Ruydts). A) Mount Rainier as viewed from Paradise Visitors Center. B) Expedition porters, laden with supplies and equipment, traverse the Cowlitz Glacier after Camp Muir en-route to Ingrahm Flats. C) Expedition members Lee Florea and Tabbatha Cavendish pass around the side of Lake Adélie. D) The main circum-crater borehole between Lake Adélie and The Coliseum.

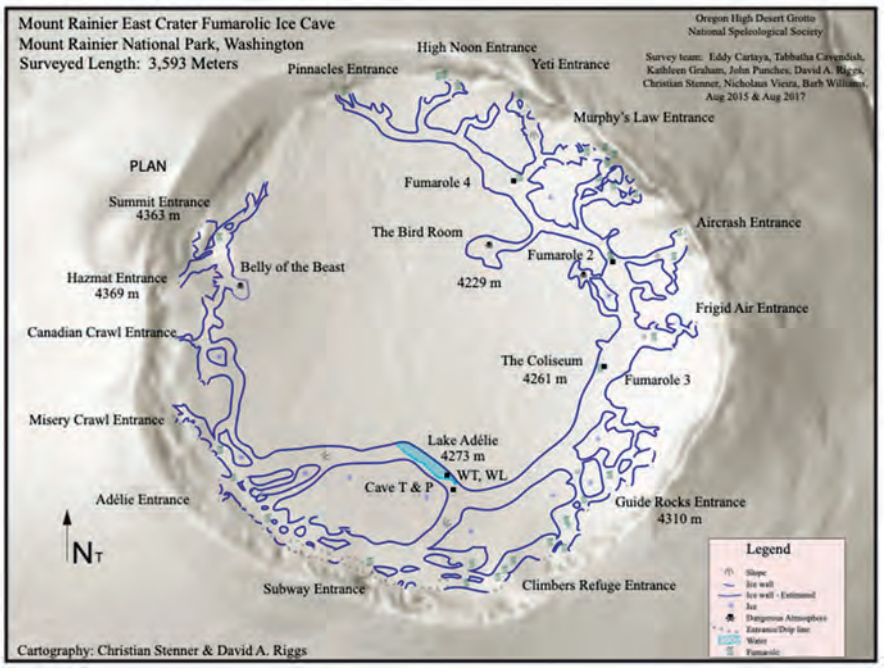

Figure 2: Map of fumarole ice caves in the East Crater of the summit of Mount Rainier—map legend lists a key to features. Figure originally published in FLOREA *et al. (2020) and reproduced with permission. Base map is a shaded digital elevation model of elevation. Monitoring locations shown for fumarole temperature, cave-air temperature and pressure, and lake temperature and depth. Outside temperature and snow depth measurements are from the Paradise Visitors Center not visible on this map.*

4. The data

Time-series data considered herein were collected in an hourly manner between August 2016 and August 2017 from Lake Adélie and the passage and fumaroles in the large rooms to the east of the lake (Fig. 2). Those data include monitoring water depth, temperature, and specific conductance using a non-vented In-Situ Aqua TROLL 200 and corrected using a paired In-Situ Baro TROLL for air temperature and pressure. GeoPrecision M-Log5W-CABLE temperature sensors provided temperature for three fumaroles in the southeast quadrant of the cave (Fig. 3). Available online for comparison were temperature and snowpack depth data collected at the Paradise Visitors Center (Fig. 3).

Both In-Situ sondes were anchored to a massive boulder that moved over the year-long instrument deployment. The resulting data include an observed increase in water level, with variable rates of change guided by shifts in cave climate, and punctuated by rapid fluctuations in instrument depth from a moving anchor—including periods when the instrument was entirely out of the water (Fig. 3). Ordinarily, a moving datum overprinted on water-level changes would be a significant challenge to interpretation; however, FLOREA *et al.* (2020), through detailed observation and analysis, deconvolved the components of water depth contributed by anchor rotation (reducing instrument depth) and translation (increasing instrument depth) from downslope movement, and the realized changes to lake level. In summary, the lake level increased by about 2 m, and the vertical projection of slope movement was on the order of 2.2 m (Fig. 3).

5. Key findings

The original purpose for deploying instruments in Lake Adélie in the summit fumarole ice caves of Mount Rainier was to see if a year of time series data would record changes in temperature and specific conductance due to minor shifts in volcanic activity, similar to other lakes in active volcanic craters. However, neither the lake sondes nor the fumarole sensors recorded events attributable to changes in magmatic heat flux or volcanic gas. In fact, the chemistry of Lake Adélie showed that it is virtually all glacial melt and fumarole condensate recycled from this melt.

Despite this first look, the fumaroles have independent long-term temperature trajectories (Fig. 3). Broadly the trend is toward cooler temperatures, which follows from decadal shifts compared to data by FRANK (1985) and ZIMBLEMAN *et al.* (2000). Temperatures are also higher closer to Columbia Crest and the West Crater, consistent with a shift in the locus of activity. There is also an annual pattern to some of the fumaroles, with lower temperatures during the summer when greater overall melt channels thermal flux into water with high heat capacity. To better understand these and other patterns, the data were analyzed in

MATLAB® software using cross correlograms and wavelet coherence scalograms and compared to cave air temperature and pressure, external temperature and snow depth, and the temperature and the water level at Lake Adélie corrected for datum shifts.

These analyses revealed microclimate behaviors of cave air pressure and temperature connected to wintertime storm events that bring freezing cave temperatures and snow pack accumulation sealing the cave entrances, freezing Lake Adélie, and limiting cave ventilation and advection of fumarole heat and steam to the outside. During these times, the cave becomes a more closed system, causing a positive feedback cycle of increased cave temperature leading to increased melt and fumarole output followed by greater thermal convection in the caves until the cave entrances reopen. The repeated freeze-thaw cycles in the cave during and after these storm events are a major contributor to down-slope movement of talus. This cyclicity also translates into annual changes in cave volume and interannual variability in the position, scale, and morphology of entrances.

With this study, and nearby ongoing investigations at Mount Saint Helens, there is growing evidence that the dynamics of climate and heat flux on active volcanoes with glacial mantles greatly influences fumarole activity, and thus, the size and morphology of fumarole ice caves. These fumarole ice caves, as also seen at Mount Erebus in Antarctica (CURTIS & KYLE, 2011) are persistent on decadal or longer scales. Changes to the climate and volcanic heat, leading to alterations in glacial volume and rates of mass wasting, introduce imbalances in the systems and may shed further light into the life cycle of volcanic edifices and the resulting natural hazards from their deterioration.

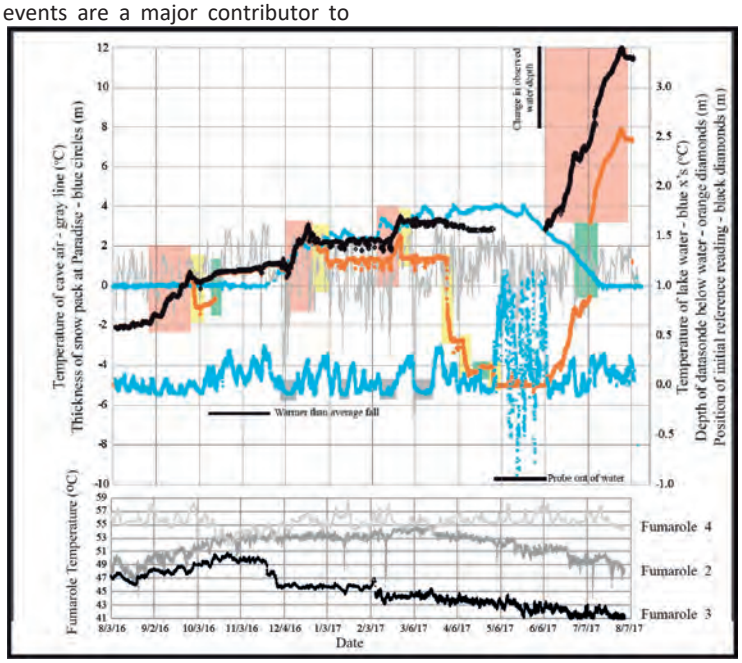

Figure 3: Time-series monitoring data from sondes in and near Lake Adélie, selected fumaroles in the East Crater, and weather data available from Mount Rainier National Park. A full analysis of these data are available in FLOREA et al. *(2020).*

References

CURTIS A. and KYLE P. (2011). Geothermal point sources identified in a fumarolic ice cave on Erebus volcano, Antarctica using fiber optic distributed temperature sensing. Geophysical Research Letters, 38(16).

FLOREA L.J., PFLITSCH A., CARTAYA E. and STENNER C. (2020). Microclimates in fumarole ice caves on volcanic edifices—Mount Rainier, Washington, USA. Journal of Geophysical Research—Atmospheres.

FRANK D.G. (1985). Hydrothermal processes at Mount Rainier, Washington. PhD thesis, University of Washington.

GRAHAM J. (2005). Mount Rainier National Park Geologic Resource Evaluation Report: Natural Resource Report NPS/NRPC/GRD/NRR—2005/007, 38 p.

KIVER E.P. and Steele W.K. (1975). Firn caves in the volcanic craters of Mt Rainier, Washington. National Speleological Society Bulletin, 37(3), 45–55.

NEWHALL C.G. (1996). IAVCEI/International Council of Scientific Unions' Decade Volcano Projects: Reducing Volcanic Disaster, Status Report. United States Geological Survey, Washington, D.C.

STENNER C., PLITSCH A. FLOREA L.J., GRAHAM K. and CARTAYA E. (In Review). The development and persistence of hazardous atmospheres within a glaciovolcanic cave system – Mt. Rainier, Washington, USA. Journal of Cave and Karst Studies.

ZIMBLEMAN D.R., RYE R.O. and LANDIS G.P. (2000). Fumaroles in ice caves on the summit of Mt Rainier–Preliminary stable isotope, gas, and geochemical studies: Journal of Volcanology and Geothermal Research, 97, 457–473.

How melting of the alpine glaciers impact development of glacio karst?

Barnabé FOURGOUS[(1)], Alain MAURICE[(2)], Pierre-Bernard LAUSSAC[(2)], Tristan GODET[(1)], Benoit MAGRINA[(1)], Alexandre FAUCHEUX[(1)] & all team members Mille et un pas sous la glace

(1) Association Spéléologique Vercors et collectif mille et un pas sous la glace - barnabe.fourgous@gmail.com
(2) Groupe Spéléologie Montagne et collectif mille et un pas sous la glace

Abstract

A look at the glacial receding through 15 years of exploration of the intra- and sub-glacial cavities of in the Swiss and French Alps glacier such as Aletsch and Mer de Glace, Arolla, Ferpecle and Langgegletscher, Zinal, Moiry and Allalin, Mer de glace, Pilatte and Bonnepierre. At the margins, under or at the heart of the glacier, we were able to observe the evolution of surface and intra-glacial drainage of some glaciers. Decreases in thickness or length, or modifications of crevasses system seems to have modified the configurations of these moulins, natural "losses" which become more numerous. They are subsequently less deep but not always. The slowing down of the glaciers no longer allows the renewal of new wells. The moulins sometimes dig down to the rocky bed, especially when they are close to the banks. On the other hand, real networks develop, arranged in sub-glacial channels in contact with the rocky bed. These contact cavities seem to grow strongly with the recession.

Résumé

Comment la fonte des glaciers alpins impacte le développement du glaciokarst ? Une observation spéléologique de la décrue glaciaire au travers de 15 ans d'exploration des Moulins des glaciers alpins français et suisses : Aletsch, Mer de Glace, Arolla, Langgegletscher, Zinal, Moiry, Allalin, Pilatte et Bonnepierre. Nous avons ainsi pu observer l'évolution des drainages intra glaciaires par l'exploration des systèmes marginaux et des moulins alpins. La diminution en épaisseur et en longueur des glaciers semble associée à une multiplication des pertes que sont les moulins ; des cavités qui souvent ne sont plus aussi profondes qu'auparavant. Ralentissement de l'écoulement des glaciers et développement de véritables systèmes intra- et sous-glaciaires paraissent liés. Ces réseaux commencent ainsi à s'ouvrir au contact du lit rocheux, aux marges ainsi qu'au centre du glacier.

1. Introduction

We will try to improve the understanding more widely of the functioning and evolution of these intra or sub-glacial cavities by placing them in a wider context (size of the glacier and surface morphology, layering and altitudinal distribution, sub-glacial geomorphology and climatology)

We have based our study on the glaciers of the Alpine Arc which are quite specific, and which have been monitored by us over our 15 years of exploration; Aletsch and Mer de Glace, Arolla, Ferpecle and Langgegletscher, Zinal, Moiry and Allalin, Mer de glace, Pilatte and Bonnepierre.

2. Cryokarst speleologists are field topographers by necessity!

Our collective is essentially coming from the speleological environment. Views and methods of investigation are thus largely influenced by this original identity. We find ourselves in the safest in a cryokarstic approach.

Topography:

the first stage of our approach consists in surveying the explored cave.

In the event, that it is not possible to carry out a survey using accurate measuring tools, we make a sketch of it.

In the end, whatever the type of rendering, we use it to report all the observations made during the exploration:

-hydrological or aerological digging forms/excavation profile;

-Presence of sedimentation or other exogenous elements brought by the glacial basin/layering of layers of sediment imprisoned posteriori in the glacier;

-fracturing passing through the cave or decompression planes within the cavity.

We therefore use a Leica laser meter for measurements. Where the ice is too wet, the laser gives erroneous values. Laser can't catch the relief of the cave. Moreover, in the entrance, we have to deal with the over brightness of the glacier under sun compared to the laser. We reduce length of measure or do it by night

However, in 80% of the cases, relative darkness and low humidity ice does not disturb the sighting.

Finally, compass errors due to the presence of magnetised rocks trapped in the ice are rare.

Coupled with a topodroid-type smartphone application, we favour this technical combination for various reasons. It remains the most efficient solution for moving forward quickly to face with in a cold, humid environment and

exposed to flooding or wall breakage depending on the period.
Furthermore, if the entry point has been georeferenced, as soon as the exploration is completed, it is possible to position the underground system under the surface relief. These twin tools are interesting to have a better image of the terrain once at the surface. For example, by observing directly in the field how a network is built on or escapes from crevasse.
Finally, laser readings allow the geometric rendering of the cave to be densified in a simple way during the speleological The accuracy of the measurements is less than 5% error on length, orientation and slope. On an average mapping process, checking loops or sizing way and back will give this % of error

We rework the topographic minutes afterwards. Given the limited development of the cave, we do not use complex topography software capable of superimposing large networks. If networks begin to open under certain glaciers in contact with the rocky bed, these are still rare and do not justify the use of complex topography software.
These plans or sections are redrawn using drawing software to enhance the path of field observations.

Cartography:
Commonly, the second part of the documentation consists of the cartographic formatting of the data collected in the field.

Input surveys are carried out using outdoor GPS none DGPS. By convention and technicality, we only retain values less than 5 m in accuracy. However, we need to be able to take into account the movements of the glacier. In the case of almost highly mobile glaciers, we try to multiply the measurements with different GPS to average the coordinates.

All these elements are compiled under GIS in order to be able to characterize each cave and help to a better view and understanding of its place, organization and functioning. We do not use any particular GIS as the data analysis we do is quite standard.
Beyond these aspects, we will have for the following years prospecting maps taking into account the depths, volumetry and other specific characteristics of each cavity.

3. Monitoring of intra- and sub-glacial landscapes in alpine temperate glaciers.

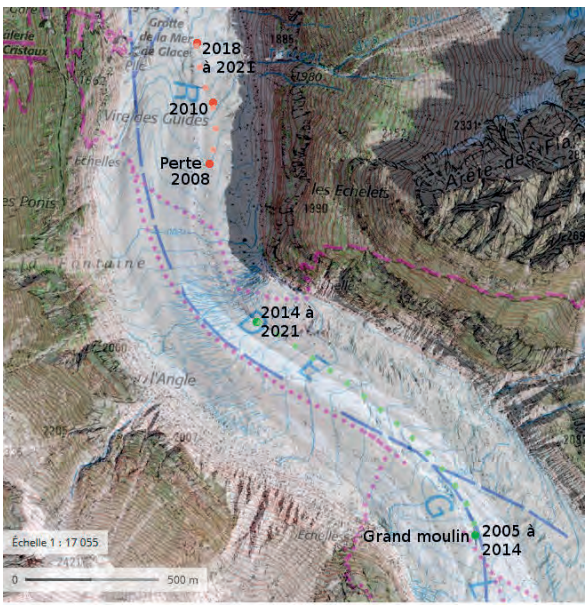

Figure 1: Downstream cave drift, Mer de Glace

Through the explorations made, we will try here to draw up a catalogue of the intra- and sub-glacial phenomena observed.

A/ Brutal drift downstream of cavities.
The Mer de Glace presents two obvious cases of drift downstream (Fig. 1). From Vallot (Vallot 1898) to beginning of millenium, the Grand Moulin was located upstream on the Lechaux and Mer de Glace confluence (Reynaud, 1987). We have no precisely location only description. Between 2005 and 2014, we were able to observe a gentle downstream drift of the grand Moulin on the right bank. This is the historic Moulin, the one that gave its name to this place of the Mer de Glace. According to GPS readings, it slipped 120 m downstream over this period. In the following years, in parallel with the gradual disappearance of the dense system of crevasses in the left bend under the ladders and the general flattening of the glacier, this Moulin water basin was suddenly lost almost a kilometre downstream. In total this mill will have gone down 1.2 kilometres.

In the first years it opened in a deep vertical of about a hundred metres before finding a meandriform profile (Fig. 2). Since then, it has reached 80 m deep each year and has developed over 200 m in a succession of small rises, with a maximum of 6m in a similar morphology each year, becoming flatter every year. From 2008, even further downstream, a water basin in the centre of the glacier developed, feeding a moulin some twenty metres deep.

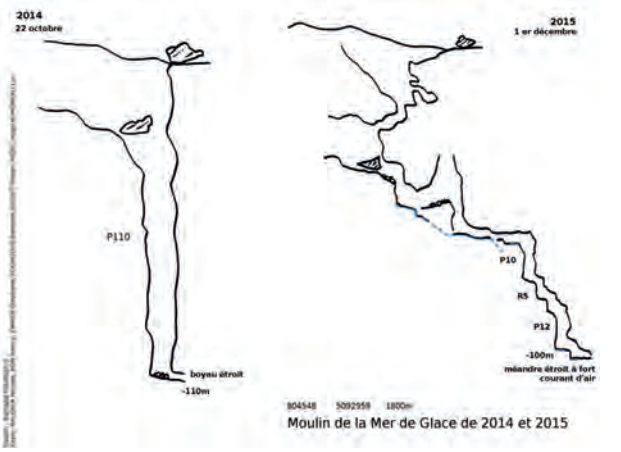

Figure 2: Deep pitch to meander cave, Mer de Glace

Although this mill was only slightly displaced until 2010, it made a total leap of almost 618m downstream until now.
Very vertical at its origins, it has become meandriform. 80 cm wide, it meanders in short two-metre long climbs before getting lost in a narrowing after a final 8-metre shaft.
We could observe other case as on Aletsch glacier of downstream drift with a 51m moving betweenn 2011 and 2016. From a 5m diameter pure vertical pitch, it starts to get a wide oval pitch (320 to 30 m diameter).

B/Glaciers with different characteristics of altitude, sun sensitivity, climatology or morphology, seem to have experienced a multiplication of surface drainage systems. From the micro-bay to secondary bays capturing basins of a small square kilometre, these glaciers seem to experience a densification of surface and intra-glacial drainage. The common point is a low slope and a low-tension zone. Observed on the Mer de Glace, a moulin appear on the left flank of the glacier and on the center, same altitude than the Grand Moulin. The center one still constant in position and shape, a vertical 30 m deep pitch. The left one start on a small meander in 2015 to a straight 90 m pitch until now. A total of three drainage systems appear during the studied period. The Grosser Alestchfirn perfectly illustrates this phenomenon between 2900 and 2700 m altitude. On the right bank, on the surface of the glacier, an extremely dense cover of micro-drainage has appeared. During the day, a thin layer of ice gorge itself with water over 5 cm. There is no marked structuring before this water ends up being captured by the bédière along the east side of the central moraine. The Moulin capturing these waters opens much further down the slope upstream of the next break in the slope. On the left bank, i.e., on the inside of the bend taken by the Grosser, two then three small berries have started to share the surface flow and are captured by moulins located upstream of the original hole. In spite of the small size of the bidets, the Moulins retain penetrable dimensions; vertical 20 m long, which follow on from short horizontal drains, in the form of forced conduits stopped on pinching.

C/Although it was common to explore cavities within or under the glaciers, sometimes more than 100m deep but always poorly developed, explorations are now revealing increasingly larger systems. Sometimes more than a kilometre long, these cavities can be arranged in real networks with collectors and tributaries as on Ferpecle (Fig. 3). Two major networks have been explored on this glacier - see gealti coco. They large networks are arranged under areas with an average slope of between 20 and 40°. As soon as the slope reaches 0°, these networks are pinched. The rare galleries explored under the horizontal parts do not have more than 20 m of ice on the ceiling. We are then on the front of glaciers such as the Arolla or Langgletscher where mega-resurgent tunnels (20 m high by 50 m wide) open up.

4. Discussions

A/ Could the drift of the Moulins be a corollary to the morphological modification of the glacier surface, identifiable by the settling of the relief ?
Last part of the Mer de glace turn on flattening during those year with a regular 19%slope. Even the massive crack system on the right flank under Les Echelles almost disappear during that period. The relief downstream the 2005-2014 moulin doesn't exist anymore. The bediere extend is range, breaking through and push is way to the next point: les Echelles crack system where a moulin could take form.
This idea is less obvious on the Aletsch one, maybe even insignificant. We could not measure relief change, just observe that glacier get more regular slope on that part where the previous cave was. Not being catch, the bediere could reach a lower part of the glacier where it will encounter the formation condition of a moulin (ERASO A et PULINA M, 1992). On the other side, the shape moulin change is interesting too: from deep shaft to a continuous short waterfall for the Mer de Glace, Gorner or Bonnepierre. Is there a consequence of the increase of the glacier slope, decrease of thickness or slowing down of glacier?
Less obvious is the shape that took the main moulin on Aletsch. From a straight shaft, it moves to an oval one. Meander shape start to appear slowly. Could the crack field on which the main moulin is slowly push year after year explain this particular shape? On the satellite picture, we can clearly see how the cave is sealed into the crack system.

Figure 3: Gelati coco cave, longest system, Ferpecle Glacier

B/ Might it be that the loss of ice height on some glaciers seems to be related to the appearance of labyrinthine and long sub-glacial cavities in contact with the rocky bed.
No cave was found on the horizontal front part of glacier. Thus, the slope is also a function of the cavities?
Usually, the losses at the edge that collect streams or rushes on the mountainside form large entrance tunnels that stop after about ten metres on a rock-ice pinch. The increase in surface drained water flows due to global warming seems to have only a slight impact on the size and length of these conduits. However, in the case of a thin glacier, these losses can develop over long distances, of the order of one kilometre, as was the case under the Ferpecle glacier in particular. This type of gallery exists under ice thicknesses ranging from 5 m to 20 m, where the pressure of the glacier is low.
In these same conditions of thickness, some moulins can flow into the collectors located in the middle of the glacier. The deep presence of these collectors fed by marginal or central losses also seems to be favoured by the presence of an uneven rocky substratum. Favouring sub-glacial detachments, these voids, if they connect to a network or to galleries leading to the outside, even throughout tiny passages, are preserved from year to year and grow rapidly under the effect of aerological circulation. This growth can be expressed in metres per year.
At the front of these thin glaciers, resurgences deepen. If, over short distances and with difficulty, the resurgences manage to form under the effect of the melting of the ice by the water which is little constrained by the low-pressure effect, in this case, large tunnels appear. They are about ten metres high, up to 50 m wide and 200 m long (Arolla, Langglegetscher).
In addition to the low ice thickness and the slope, a final factor is the loss of speed of the glacier. As the glacier no longer advances, the Mill remains in its place and thus continues to grow year after year, growing under the effect of the aerology, as shown by the parietal waves. The Mill will only disappear by the erosion of the glacier front or will collapse under its own weight.
In the case of a combination of high speed and thickness, its thinness and marked retreat have led to the junction of loss and resurgence on the Pilatte glacier in the Ecrins massif in France. A system is thus fully highlighted. Does this mean that it can be used as a model to explain the hydrological circulations within and under the glaciers?
Here we have taken a great deal of interest in the fusion-pressure couple. It seems to be a reading element for interpreting the changes in landscapes within and under glaciers.
We have only looked a little further into aspects relating to the field of aerology and the effects of sublimation which seem to play a role in the deepening of these networks, especially under glaciers and a little less intra-glacial. Although accustomed to the underground circulations in karst, our transfer of knowledge to cryokarst remains a simple supposition or attempts at explanation by field observation or even an intuition.
Can the highlighting of hydrological circulations by the appearance of complete systems from loss (marginal or central) to resurgence be used as a model to understand and model the transfer of water in and under the glacier?
Unless the conditions of low thickness or glacial retreat make it a model in its own right with its own characteristics. Wouldn't our speleological representation of the hydrological circulations in the heart of the karst influence too much our interpretation of glacial hydrological circulations?

5. Conclusion

Although 15 years represents only a tiny amount of geological and glacial time, we can clearly feel how quickly these alpine intra- and sub-glacial landscapes have evolved. In a context of glacial retreat, the multiplication of drainage networks is apparent and makes the structuring of these networks more complex. Conversely, these changes allow a deeper penetration of these networks by the cavers, making visible phenomena that were previously only accessible through acoustics, resonance and other interpretation tools.
In some cases, the glacier receded so abruptly that the surface of the glacier seemed to conceal the work of undermining it. A form of bottom-dragging, where the sublimating action of sub-glacial aerology often appears denser and more scattered than the melting action.
It would thus be interesting to push this aspect further and to see to quantify the part of this one in the digging of the cryokarst. These effects of the aerology in the melting from below could be related to the hydrological action under the glacier but also and especially on the surface.

Acknowledgments

A very friendly thought and a big thank you to Jeannot Lamberton for sharing this passion which he opened and more widely to all those we had the pleasure and the chance to meet, to exchange, to follow or to embark with us, the crampons at the foot or the head never far from the heart of the glaciers.

References

ERASO A y PULINA M. (1992) *Cuevas en hielo y rios bajo los glaciaires*. Mc Graw-Hill, Madrid, 242 p.

REYNAUD L. (1987) The November 1986 survey of the Grand Moulin on the Mer de Glace, Mont Blanc Massif, France, *Joumal of Glaciology*, 113.

J. VALLOT (1898) *Exploration des moulins de la Mer de Glace*, Edition de glaciologie

Le pseudo-karst du glacier Tempanos (Patagonie, Chili) – Indicateurs de fonte rapide

Richard MAIRE[1,4], Marius SCHAEFER[2], Masahiro MINOWA[2], Shuntaro HATA[3], Bernard TOURTE[4], Arnauld MALARD[4], Natalia MORATA[4] & toute l'équipe de Centre Terre

(1) Laboratoire Passages, CNRS-Université Bordeaux-Montaigne (richard.maire49@gmail.com, auteur correspondant)
(2) Universidad Austral de Chile Valdivia
(3) Hokkaido University
(4) Association Centre-Terre (www.centre-terre.fr)

Résumé

Le glacier Tempanos est situé dans le Champ de glace Sud de Patagonie, le 3ème plus vaste ensemble glaciaire de montagne de la planète. Le recul du glacier est de 4 km depuis 1945 et la perte d'épaisseur de 149 m en 19 ans sur la partie frontale. Durant l'expédition, plusieurs pertes juxta-glaciaires (au contact roche/glace) et pertes supra-glaciaires (moulins) ont été explorées. Celles-ci montrent une activité hydrologique importante liée aux conditions humides (fortes pluies) et à une température positive toute l'année. Les vitesses d'avancement du front du glacier ont été mesurées et montrent des valeurs comprises entre 0,5 et 1,1 m/jour. Le glacier avance par « cran » en fonction de l'intensité des épisodes pluvieux. Les eaux infiltrées sous la glace soulèvent et font ripper le glacier. Ces phénomènes s'accompagnent de forts mouvements d'eau (vidange de lacs subglaciaires, intraglaciaires et/ou supraglaciaires), vibrations, etc.

Abstract

The pseudo-karst of Tempanos glacier (Patagonia, Chile) – Indicators of rapid melting. During the UP2019 expedition of Centre-Terre, a team studied the frontal part (altitude 0-400 m) of the Tempanos glacier located in the Southern Icefield of Patagonia, the third largest mountain glacial complex on the planet. The glacier has retreated by 4 km since 1945 and the loss of thickness of 149 m in 19 years on the frontal part. During the expedition, several juxta-glacial losses (at rock / ice contact) and supra-glacial losses were explored. These show significant hydrological activity linked to wet conditions (heavy rains) and positive temperature all year. The forward speeds of the glacier front have been measured and show values between 0.5 and 1.1 m / day. The glacier advances by "notch" depending on the intensity of the rainy episodes. Water infiltrated under the ice lifts and rips the glacier. These phenomena are accompanied by strong water movements (draining of subglacial, intraglacial and / or supraglacial lakes), vibrations, etc.

1. Introduction

Le glacier Témpanos est situé dans la partie nord-ouest de la grande calotte glaciaire du Champ de glace Sud de Patagonie ou « Campo de Hielo Sur », la plus vaste du globe en zone de montagne, après le Groenland et l'Antarctique (Fig. 1-A). Elle mesure 350 km de long entre 48°20' et 51°30' pour une superficie de plus de 12 000 km^2. Nos recherches se sont orientées particulièrement sur la zone frontale de débordement ouest (lat. 48°40') entre le niveau de la mer et 400 m d'altitude (Fig. 1-B). Le mot « tempanos » signifie icebergs en raison de la zone de vêlage du glacier. Le but était d'explorer les types de cavités pseudo-karstiques (HALLIDAY, 2004) creusées dans la glace et d'examiner les indicateurs d'une fusion rapide : écoulements, faciès de la glace, recristallisation, formes associées. Dans le même temps, c'était aussi une opportunité d'observer les conséquences du réchauffement climatique en zone australe, réchauffement qui a débuté dès la fin du Petit Âge glaciaire dans la seconde moitié du XIX°S, et qui s'est s'accéléré durant les dernières décennies.

2. Historique des recherches et recul global

Le glacier Tempanos appartient à un ensemble glaciaire regroupant les glaciers Occidental-Tempanos-Greve d'une superficie totale de 842 km^2 et d'une altitude moyenne de 950 m pour un flux de glace annuel de 3,27 ± 0,4 gigatonnes (GOURLET et *al.*, 2016). Les épaisseurs maxima de glace peuvent atteindre 1500 m dans le glacier Occidental. Les importantes précipitations peuvent atteindre 6000 à 8000 m/an, principalement entre 1500 et 2500-3000 m d'altitude, correspondant au minimum à 20 m de neige. Depuis les recherches pionnières de L. Lliboutry (1956), de multiples mesures, cartographies et observations ont montré un fort recul des glaciers de Patagonie depuis 75 ans. Pour le Campo de Hielo Sur, Andrés Rivera (2019) indique que la superficie englacée est passée de 13 883 km^2 en

1944-45 à 13 070 km^2 en 1986, à 12 787 km^2 en 2000 et à 12 133 km^2 en 2018, soit une baisse de 1 750 km^2 (12,6 %). La zone frontale du glacier Tempanos connaît des températures positives toute l'année, d'où des formes de fusion très nombreuses et une diagenèse de la glace importante. Sur la rive droite, à l'altitude de 81 m, le glacier s'est abaissé de presque 149 m en 19 ans, soit une altitude de 230 m en 2000 (SCHAEFER et *al*., 2019). La baisse annuelle moyenne est donc de l'ordre de 7 à 8 m. Sur le versant argentin, le grand glacier Upsala (vêlage sur le Lago Argentino) s'est abaissé en moyenne de 14 ± 2 m/an entre les années 1965-95 (NARUSE et *al*., 1996). À titre de comparaison, dans les Alpes, la baisse est actuellement de 4 m/an en moyenne à la Mer de Glace entre 1986 et 2016 dans sa partie aval, avec même une baisse de 8 m/an ces dernières années (MOUREY et RAVANEL, 2017).
Un levé photographique aérien (TRIMETROGON) a été réalisé par l'AAF (Force Aérienne des Etats-Unis), notamment sur le Campo de Hielo Sur en janvier-février 1945, donc pendant l'été austral. L'une des photos aériennes obliques montre un recul du glacier Tempanos de 3,5 à 4 km environ au niveau du fjord Tempanos et surtout une réduction spectaculaire de l'épaisseur du glacier. Des mesures plus récentes à partir des images satellitaires montrent que le recul annuel a été de 55 m ± 8 m de 1984 à 2000 et de 41 m ± 13 m entre 2000 et 2010 (SAKAKIBARA et SUGIYAMA, 2014).

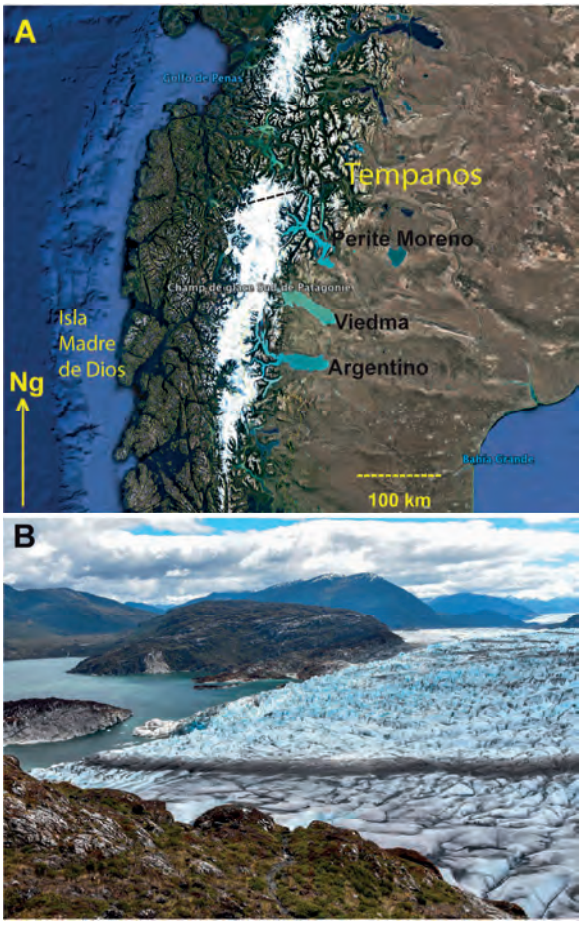

Figure 1 : A. Physionomie du Champ de glace Sud (Patagonie), d'après une image Google Earth. B. Partie frontale du glacier Tempanos (photo Centre-Terre).

3. Les dirt-cones (cônes débris/glace)

Le glacier Tempanos présente, dans sa partie basse, de remarquables et nombreux « dirt cones ». Ce sont des morphologies d'ablation différentielle de forme conique de 20-30 cm à 2-3 m de haut associant une couverture de débris sombres et un noyau de glace conique (Fig. 2-A). L'examen microscopique des fins débris montre qu'une partie importante est constituée par des cendres volcaniques (tephra) composées notamment de verres, d'échardes de quartz, de micas etc. Ces cendres proviennent du grand strato-volcan Lautaro (3 607 m) situé 45 km au sud-est et dont la dernière éruption remonte à 1979. Lors des retombées de cendres, les cinérites forment des couches horizontales, mais peuvent aussi colmater des fentes et des crevasses. Suite à la fusion de la glace, notamment dans la partie inférieure des glaciers, les cendres protègent la glace et finissent par former des cônes résiduels de glace masqués par les fins débris. Rappelons que les dirt-cones sont présents aussi bien sur les glaciers des zones tempérées que dans les régions polaires L'explication par ablation différentielle a été donnée à propos des dirt cones du Vatnajokull en Islande par Charles Swithinbank (1950).

4. Types de cavités dans la glace

Les cavités dans les grands glaciers de Patagonie (Perite Moreno, Tyndall, Grey) ont fait l'objet de plusieurs expéditions depuis 1995, notamment par les spéléologues italiens du groupe La Venta. Les types principalement reconnus sont les moulins (pertes) et les grottes de marge glaciaire (BADINO et *al*., 2001)
En 2019, sur le Tempanos, les zones explorées en rive droite et gauche se situent entre zéro et 300 m d'altitude. Les cavités liées à la fonte rapide de la glace présentent des convergences de forme avec les cavités karstiques. Les cavités de la zone supraglaciaire/intraglaciaire sont constituées en amont par des bédières (ruisseaux de fonte) et en aval par des moulins. Ce sont des puits-pertes donnant accès à des cavités composées d'une succession de puits et de galeries en méandres. Ces réseaux subverticaux rejoignent le lit imperméable sous-glaciaire. Les cavités juxtaglaciaires sont des pertes localisées au contact roche / glace (Fig. 2-B). Ces ruisseaux sont issus de la zone granitique imperméable et correspondent aux exutoires de petits lacs perchés ou de vallées adjacentes. Ces cavités sont formées

parfois par de grands porches se poursuivant par des conduits bas devenant impraticables, voire par un large conduit à plafond plat emprunté par un torrent à fort débit. En raison du fort recul du glacier, le lit rocheux est devenu accessible dans la zone frontale. Un autre type de cavités a donc pu être exploré. Il s'agit des cavités proglaciaires qui se situent au niveau de la sortie des torrents sous-glaciaires que l'on peut assimiler à des résurgences. En raison des forts débits (plusieurs m^3/s), la progression sous-glaciaire devient rapidement impossible. Remarquons l'instabilité du toit de certaines cavités juxta- et proglaciaires matérialisée par des lucarnes liées à l'amincissement du glacier.

Figure 2 : Indicateurs de la fonte accélérée de la partie frontale du glacier. A. Dirt cone typique avec cendre volcanique protégeant le cône de glace sous-jacent. B. Glace amorphe bleue dans la grotte juxtaglaciaire « Rêve de Blue ». C. Grotte sous-glaciaire avec écoulements et nombreux panaches de microbulles. D. Zoom sur des chapelets de micro-bulles au sein de la glace amorphe (photos Centre-Terre).

5. Diagenèse et comportement de la glace

On observe une glace translucide bleue très plastique au contact du plancher granitique. La glace épouse la surface irrégulière et bosselée de la roche. De nombreux petits écoulements sont situés au contact roche-glace. En raison de la fusion rapide, on observe de petites circulations dans la zone de bordure avec des exutoires en forme de robinet au sein de la glace (Fig. 2-B). L'état de la glace dépend de deux paramètres : la pression et la température. La faible pression de la glace joue ici un rôle quasi nul dans la partie frontale peu épaisse du glacier. Par contre, en raison de la température de la glace voisine de 0°C, on observe une diagenèse typique de transitions de phase dans le solide. Cela se traduit par une recristallisation avec une disparition des couches annuelles correspondant au passage d'une glace cristalline à structure hexagonale à une glace amorphe translucide à transparente. Cette transition se traduit par la remontée de chapelets de microbulles d'air et de canalicules (air-eau) (Fig. 2-C et 2-D). Des stries de Forel sont également observées à la surface des parois de glace bleue sous la forme de rides liées à des micro-circulations sur le pourtour des grains de glace. Sur les parois des cavités, on observe des « vagues » de sublimation ressemblant aux vagues pariétales dans les conduits karstiques ou les cavités dans les cônes d'avalanches (rôle de la circulation de l'air à température positive). Cette morphologie est typique dans la grotte "Rêve de Blue" (Fig. 2-B). Cette diagenèse de la glace à une température légèrement supérieure à 0°C est identique à celle observée dans la fusion rapide du glacier souterrain de Scarasson dans les Alpes du Sud franco-italiennes (MOREL et *al.*, 2017).

6. Biologie supraglaciaire

Des algues vertes d'eau douce du genre *Chlamydonas*, contenant un pigment rouge de type caroténoïde, ont été observées régulièrement sur le glacier. Selon les conditions environnementales avoisinantes, cette algue, aussi surnommé « le sang des glaciers » peut être observée sous deux formes : enkystée (spores immobiles de 20 µm de diamètre) ou flagellée (cellule mobile grâce à ces deux flagelles). Leur observation au microscope a permis de mettre en évidence la présence de la forme flagellée. En diminuant le pouvoir réfléchissant de la glace (le couleur rouge absorbe plus de chaleur que le blanc), la prolifération de cette algue entraîne une augmentation de la fonte de la glace. En Arctique, des études ont montré que ce « sang des glaciers », peut contribuer à une diminution de 13 % de l'albédo et donc accélérer la fonte des glaciers. En outre, la diminution de l'albedo par temps nuageux contribue aussi à l'augmentation de la fusion.

7. Conclusion

Rappelons que les glaciers occidentaux du Campo Hielo Sur, sur le versant pacifique, sont les moins connus car les moins accessibles contrairement à ceux du versant argentin. Ils feront donc l'objet d'une autre étude de reconnaissance en 2022. D'ores et déjà des mesures précises GPS ont permis de montrer le rôle fondamental des écoulements de fonte à la base du glacier à la fois dans son avancement et léger soulèvement (SCHAEFER et *al*., 2020). Cette dynamique s'inscrit dans le cadre d'un recul global du Champ de glace Sud, malgré certaines exceptions, et de l'abondance des cavités dans la partie avale des glaciers permettant ainsi de mieux comprendre la physique de la glace à proximité du niveau du point-triple glace/eau/vapeur.

Remerciements

Nous remercions la CONAF (Corporacion Nacional Forestal) et le Parc National Bernardo O'Higgins pour la mise à disposition d'un de ses refuges, situé à proximité du glacier Tempanos.

Références

BADINO G., DE VIVO A. et PICCINI L. (2001). Preliminary results of the glacios-speleological expedition on Tyndall glacier. *Proc. of 13Th Int. Congr. Spel. Congress*, Brasilia, 2001, vol. 1, p. 184-187.

GOURLET P., RIGNOT E., RIVERA A. et CASASSA G. (2016). Ice thickness of the northern half of the Patagonia Ice Fields of South America from high–resolution airborne gravity surveys. *Geophysical Research Letters,* 10.1002 / 2015GL066728 (American Geophysical Union).

HALLIDAY W.R. (2004). Pseudokarst. In *Encyclopedia of Caves and Karst Science*, John Gunn ed., p. 604-608.

LLIBOUTRY L. (1956). Nieves y glaciares de Chile. Fundamentos de Glaciologia. *Ed. de la Universidad de Chile, Santiago de Chile,* 471 p., 103 phot., 62 fig.

MAIRE R., SCHAEFER M., TOURTE B., MORATA N., RUIZ L., MALARD A., BOUDOUX d'HAUTEFEUILLE L., MORALES D., MAIFRET S., CHENU F., JAC C. et CAILLAULT S. (2019). Le glacier Tempanos: contexte et indicateurs de fonte rapide. *Rapport d'expédition, Ultima Patagonia 2019*, p. 130-135.

MOREL L., MAIRE R., VALLA F., DECKER J., SIFFRE M., J. BOSCART, S. CAILLAULT, C. LAMBOGLIA, J. LAMBOGLIA, J.-R. PETIT et M. OGAND (2017). Fonte du glacier souterrain de Scarasson (Marguareis, Italie). Coll. Edytem, Cahiers de géographie, n° 19, *Monitoring en milieux naturels*, p. 101-108.

MOUREY J. et RAVANEL L. (2017). Évolution des itinéraires d'accès aux refuges du bassin de la Mer de Glace (massif du Mont Blanc, France). *Journal of alpine resarch, Revue de géographie alpine*, 105-4, varia 2017, 17 p. (http://journals.openedition.org/rga/3780)

NARUSE R., SKVARCA P. and TAKEUCHI Y. (1996). Thinning and retreat of Glaciar Upsala, and an estimate of annual ablation changes in Southern Patagonia. *Annals of Glaciology,* 24, january 1996.

RIVERA A. (2019). Desafios glaciologicos del Campo de Hielo Sur. In *En las huellas de Lliboutry*, p. 224-227.

SAKAKIBARA D. and SUGIYAMA S. (2014). Ice-front variations and speed changes of calving glaciers in the Southern Patagonia icefield from 1984 to 2011, *J. Geophys. Res. Earth Surf.*, 119, 2541–2554.

SCHAEFER M., MINOWA M. et HATA S. (2020). Retrait et dynamique du glacier Témpanos/Retroceso y dinamica del glaciar Témpanos. *Rapport d'expédition Ultima Patagonia 2019*, Centre-Terre, p. 126-129.

SWITHINBANK C. (1950). The origin of dirt cones on glaciers. *Journal of Glaciology,* vol. 1, 8, p. 461-465.

Possible huge cave system of Southern Inyltchek Glacier, Kyrgyzstan

Bulat MAVLYUDOV

Glaciolab, Chamonix, France

Abstract

Since 1980th cave explorers of the former USSR try to penetrate into cave system of Southern Inylchek Glacier (Kyrgyzstan). The glacier has length more than 60 km and width of 2-2.5 km. Drainage channel with possible length about 14 km once per year used by water of glacier-dammed Mertsbacher Lake for outbursts with discharge about 1000 m^3s^{-1}. The first group who begin to study caverns of glacier was speleologist of Moscow State University in summer 1991. Second expedition happened in April of 1992 when cave with length about 100 m at glacier tongue and some moulins closely to Lake were investigated. Since 1992 different Soviet, Russian and international speleo-groups try to penetrate into glacier drainage system. As in the summer all cavities in a glacier strongly watered all expeditions to glacial caves were spent in autumn, winter or spring when there is not or not enough quantity of current water on glacier. In November, 2019 the international speleological group (France, Italy, Canada, Russia and Indonesia) spent expedition to Southern Inyltchek Glacier. There were studied some cavities and moulins but penetration into the general drainage system of glacier did not happen.

1. Introduction

Drainage systems of large glaciers from speleological positions practically are not studied. It is connected mainly with difficulties of carrying out of researches, especially because they are possible only during the periods when melting on glaciers is absent, i.e. during winter time. Here there are also difficulties with logistics because of problems with transport and snowfalls. Southern Inylchek Glacier in Kyrgyzstan is one of objects of research where these problems can be shown to a minimum. The glacier has rather simple transport availability during winter time, and also favorable climatic conditions with practically absence of a snow cover in Inyltchek valley and at least in lower 14 km part of glacier. For this reason, the glacier Southern Inylchek Glacier is one of the most interesting objects where studying of cave systems of large glaciers is possible.

2. History

The Kyrghyz cave explorers have paid attention for a long time to Southern Inyltchek Glacier because of existence in 14 km from glacier tongue of glacier-dammed Mertsbacher Lake which waters one time per year outburst through ice thickness forming the drainage channel. For the first time, I have received this information in 1981 at karstological meeting in Urals Mountains. In 1991, I participated in glaciological expeditions on Southern Inylchek Glacier where there are many features of glacial karst and possibility to penetrate into drainage system of a glacier. There were many speleological expeditions on this glacier from this time. However, expeditions 1992, 1994, 1997, 2003, 2010 have not allowed to penetrate into internal drainage system of glacier though serious attempts were undertaken. During this time, it was possible to survey a cave in glacier tongue, small marginal caves and some moulins. But penetration into drainage system of the lake and a glacier was not happen. There are some data that in glacier tongue one of caver group has passed in englacial channel in different years on 300 and 800 m, but absence topographic survey and publications allows doubting in these results. Last speleological expedition on Southern Inylchek Glacier has taken place in November, 2019. In article we will spend some common results of researches during different expeditions.

3. Place of researches

Southern Inylchek Glacier is located in southeast part of Kyrgyzstan at boundary with China (Fig. 1). The main trunk of glacier has length more than 60 km at width to 2.5 km. The Lower 14 km of a glacier is covered by layer of surface moraine and ice move very slowly (from 0 to 20 m/year) BORMUDOI *et al.* (2012). In a lateral valley at the right side of Southern Inyltchek Glacier connected with Northern Inyltchek Glacier there is Mertsbacher Lake which at the maximum volume has the sizes 4×1 km and depth near to an ice dam by different sources from 80 to 130 m MAVLYUDOV (1997). The right half of Southern Inylchek Glacier flows not down to glacier tongue as it is done by the left part of glacier but turns on the north and unloads in the form of icebergs into Mertzbacher Lake. Velocity of ice movement here reaches 120 m per year. Metzbacher Lake after filling by water at the end of summer or in autumn annually outburst water through glacier thickness with discharge about 1000 $m^3 \cdot s^{-1}$. This channel arising at lake outburst attract attention of cave explorers. Thus, the part of ice of Southern Inylchek Glacier closely to lake (an ice dam), float and the lake is drained. After outburst the floated part of a glacier go down and as a rule blocking the channel.

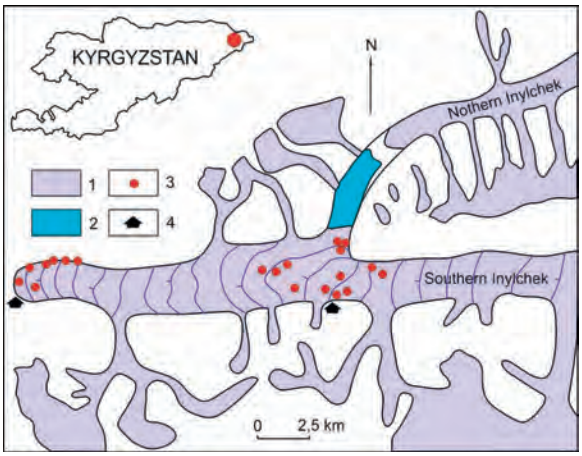

Figure 1: Southern Inylchek Glacier with tributaries and its position in Kyrgyzstan (red circle). 1 - glaciers (horizontals are given only for the main trunk of a glacier), 2 - Mertsbacher Lake, 3 - glacial caves and moulins (investigated and found out in 2019), 4 - camps.

4. Results of researches

Because of availability of researches from camps which situated or at glacier tongue, or on Mertsbacher Glade only lower part of a glacier and area closely to Mertsbacher Lake as a rule were visited. The place between these camps practically is not visited.

There were different situations in winter on glacier tongue in different years from water outflow from one or several places or to its complete absence. The largest cavity at glacier tongue was observed in April, 1992, MAVLYUDOV (1995b). At width of entrance about 24 m and height about 6 m it was possible to penetrate into channel approximately on 100 m inside of glacier. The sunken arch of the channel was a barrier for movement. There are no other documentary data about penetration into the central channel of water outflow though attempts to get into it were undertaken.

At the same time some fragments of caves along edge of a glacier at its both boards (marginal channel systems) were revealed MAVLYUDOV (1995b). These channels as a rule did not unite in uniform drainage system and have been broken into the separate fragments by impassable places because of channel narrowness, ice collapses or siphons. In dry depressions traces of former lakes which filled them were visible. Even in the absence of water it was visible by presence of scallops on the ice walls caused by thermocirculation in water thickness or by dry or liquid clay on ice walls. It is interesting that even neighbor lake depressions can be differently connected with an internal drainage network. Sometimes water from lake depression with weak connection with drainage system flows along ice surface to the neighbor depression with better connection. Thus, on an overflow on the base of vertical crack sometimes subhorizontal cave channel origin that connected two depressions.

There were some attempts to penetrate into system of drainage channels in area of Mertsbacher Lake but all attempts were not successful. The main researches in this part of a glacier were accented on studying of moulins absorbing superficial water streams as they could open way into central drainage system of the glacier. The maximum depth of the surveyed moulins reached 100 m at common ice thickness about 100-150 m, MACHERET *et al.* (1993). In most cases moulins finished by siphons which sometimes represented lakes in them. A part of observed moulins received water from superficial water streams and other part were died and not receive water as stream has been intercepted by a crevasse upstream. In the right part of a glacier which turns to Mertsbacher Lake moulins were formed on many cross-section crevasses crossing water streams. But moulins depth here usually changes from 20 to 40-50 m. The abundance of moulins did not allow their complete inspection.

In the autumn and in the spring many of depressions filled in the summer by lakes appeared empty. Their depth also did not usually exceed 100 m.

Marginal system of channels around Mertsbacher Lake does not exist. Below Mertsbacher Glade marginal system was replaced by a chain of lakes along a lateral moraine.

5. Expedition of 2019

In November, 2019 the international speleological expedition has been organized by the known Kirghiz geologist and cave explorer Alexey Dudashvili (Fund of preservation and research of caves of Kyrgyzstan). The expedition purpose was traditional: to carry out dream of several generations of cave explorers - to try to penetrate into internal drainage system of Southern Inylchek Glacier.

To penetrate into this channel from side of Mertsbacher Lake was never possible as if this channel exist it blocked by ice fragments and blocks and to move among them is too dangerous. Nevertheless, according to space images there were some periods when this channel can not be blocked completely and river from Northern Inylchek Glacier flows in it and during some time not filling a lake basin.

Climate of this part of Tian-Shan is sharply continental with hot summer and very cold winter. Feature of a microclimate of Inylchek Valley is a few precipitations and in winter almost no snow cover at negative air temperature in the majority of years. It happens also at lower part of Southern Inylchek Glacier where snow sometimes drops out, but very quickly evaporates and melts. Intensive solar radiation results melting of snow and ice on a glacier surface in winter what results in formation of the small water streams which are flowing into cavities in ice in the afternoon even in the winter.

As the lower part of the glacier moves very slowly, glacial karst forms intensively develop with the numerous closed depressions which part is filled by lakes, and a part drains through moulins.

24 persons have taken part in expedition: 19 Frenchmen, 2 Italians, one Polish from Canada, Indonesian and Russian, MAVLYUDOV (2019). During expedition it was possible to find out a huge cavity near the glacier tongue named "Metro" (Fig. 2), some quantity of small marginal caves at the right board of a glacier, some caves and moulins around Mertsbacher Lake.

Figure 2: Entrance of «Metro» Cave, a view from within. The figure of the person for scale is visible.

Many caves and moulins were finished by siphons. To go down to bottom of Mertsbacher Lake was not possible because of an abundance of crevasses (Fig. 3). The maximum depth of observed moulins has not exceeded 100 m. Internal drainage system of the glacier again to get was not possible.

Figure 3: A view on empty Mertsbacher Lake with numerous icebergs at the bottom, 11.11.2019.

6. Discussion

Approximately identical maximum depth of the moulins and depressions on the glacier around Mertsbacher Lake give to assume that for this part of a glacier uniform level of ground water exist. This ground water level can locate closely to sliding plane located closely to bottom of glacier as it is supposed in MAVLYUDOV (2017). That such sliding plane can exists it is possible to judge on a place on the right branch of a glacier before Mertsbacher Lake. By georadar data the ice thickness before lake is about 300 m, MACHERET *et al*. (1993), and depth of lake at an ice dam is about 80-130 m. We do not see rising of glacier edge at lake boundary after ice movement over bed overdippening. It means that the glacier here does not move along the bed, and dead ice exists in the bottom part of overdippenning under moving ice. The upper part of a glacier with thickness about 100 m moves only. Probably, it can be promoted also by a step on glacial bed to south from Mertsbacher Lake edge which indirect reflexion is practically invariable position of edge of an ice dam in different years, MAVLYUDOV (1997). In that case glacier movement occurs along englacial sliding plane which is probably that basis on which drainage channel annually formed. If it so, drainage channel from lake can have the slot-hole form, and this channel is formed only at uplift of ice dam edge. After outburst ice move down and the channel should be closed and become inaccessible.

On the other hand, the continuous water drainage from glacier tongue with discharge about 11 $m^3 \cdot s^{-1}$ in the summer assumes presence of the central drainage system which operates on a glacier at least during all summer. And water from Mertsbacher Lake at outburst moves through this central drainage system. There is a probability that this central drainage channel of all Southern Inylchek Glacier was generated on the sliding plane located in the lower part of ice thickness. If it so, the sliding plane touch to tops of all ledges on a glacier bed, and dead ice remains between ledges.

As the upper part of ice on Southern Inylchek Glacier is cold the crevasses arising on a glacier in some cases can penetrate on depth about 100 m directly to a sliding plane. Melt water from a surface along crevasse (or along systems of the interconnected crevasses) reaching directly or by steps to sliding planes and spreads on it moving in a direction of glacier tongue. When in the spring time water penetrates on a sliding plane it spreads on plane in the form of a film forming inefficient drainage system. Further during a summer season along a sliding plane, the arborescent system of channels is formed and the drainage system becomes effective. In autumn and in winter with the termination of water inflow from a surface channels of drainage system can be compressed under the influence of ice plastic deformation. In this case in the spring all drainage system revives again, and the remained fragments of former channels can participate in its formation.

Often in last time in publications there is a statement that at a sufficient water feeding on glaciers hydrofractures can be formed which are capable to reach glacier bed even in very cold glaciers, such as Greenland, DAS *et al*. (2008), KRAWCZYNSKY *et al.* (2009). Unfortunately, it is an error. On Southern Inylchek Glacier it was repeatedly observed how water inflow in a new crevasse arising across water stream. And through time necessary for filling of empty space of this crevasse water outflow from it and further simply flows over crevasse filled by water not paying on it of attention. There was such episode in one of summer expeditions on Southern Inylchek Glacier. Nearby to Mertsbacher Lake the large moulin that receive water stream with discharge about 1.5 $m^3 \cdot s^{-1}$ has been found. It happened before lake outburst. After the flood water level in the lake has strongly gone down, after that on surface of glacier set of new cross-section crevasses origin. As a result of it the stream was intercepted by crevasses and water in a moulin not move completely. We have gone down in moulin and study its upper part and lower part have decided to study in next day. However, having returned to moulin next day we have found out that stream of former the size again flows in it. It was need approximately one day for the stream to fill all again arisen crevasses on the way and has returned to a former

moulin. And no one among filled by water crevasses did not become a hydrofracture. And it occurred in not so cold ice of Southern Inylchek Glacier. In Greenland where ice temperature inside glacial sheet reaches up to -29°C formation of hydrofractures is completely impossible. Calculations show that the limit ice temperature where the crevasses filled by water not freeze is about -8°C, MAVLYUDOV (1995a). As a result, it is possible to assert that formation of hydrofractures hardly plays an essential role on Southern Inylchek Glacier as well as on other glaciers.

7. Prospects

In spite of the fact that neither expedition of 2019 nor expedition of previous years have not allowed to penetrate into the main central drainage system of Southern Inylchek Glacier, the hope to get into it is not lost. Except already visited areas which should be studied once again because of the serious annual changes, one of perspective directions of the further researches is studying of an average part of a area between glacier tongue and Mertsbacher Glade where research were not spent before.

One more possibility - studying of places of absorption of water inflows from the glaciers-tributaries located on the left glacier board. Next possibility - study of the flooded areas of moulins by cave divers. Probably it will allow to understand a structure of moulins in their bottom flooded parts and to find out (or not to find out) connection of moulins and channels of glacier internal drainage system. However, it is not simple logistically.

8. Conclusion

The possible structure of internal drainage system of Southern Inylchek Glacier attempts of which of studying were undertaken by many expeditions including expedition of 2019 is considered. It is possible that the system of glacier drainage is dated for the sliding plane located in the lower part of glacier thickness on depth about 100 m from a surface. Such sliding plane is touched for the top parts of ledges on the bed and under it an inactive or dead ice is situated. Melt water on crevasses or systems of crevasses penetrates on sliding plane and forms drainage system. Penetration of water from Mertsbacher Lake on opened at lake filling of sliding plane allows to water from lake to outburst. How much this assumption is correct the future speleological researches will shows.

Acknowledgments

Work is executed within the limits of the state task 0148-2019-0004 (AAAA-A19-119022190172-5) «Glaciation and accompanying natural processes at climate change».

References

BORMUDOI A., SHABUNIN A., HAZARIKA M.K., ZAGINAEV V. and SAMARAKOON L. (2012) Studying the outburst of the Merzbacher Lake of Inylchek Glacier, Kyrgyzstan with remote sensing and field data. *Proceedings 33rd Asian Conference on Remote Sensing* (ACRS 2012), Pattaya, 26-30.

DAS S.B., JOUGHIN I., BEHN M.D., HOWAT I.M., KING M.A., LIZARRALDE D. and BHATIA M.P. (2008) Fracture propagation to the base of the Greenland ice sheet during supraglacial lake drainage. *Science*, 320, 778–781.

KRAWCZYNSKY M.J., BEHM M.D., DAS S.B. and JOUGHIN I. (2009) Constraints on the lake volume required for hydro-fracture through ice sheets. *Geophysical Reasearch Letters*, 36(10). L10501. doi.10.1029/2008GL036765

MACHERET Yu.Ya., NIKITIN S.A., BABENKO A.N., VESNIN A.V., BOBROVA L.I. and SANKINA L.V. (1993) Thickness and structure of the Yuzhniy Inylchek Glacier from the data of radio echo sounding. *Materialy Glyatsiol. Issledovaniy/Data Glaciol. Stud.,* 77, 86-97 (in Russian).

MAVLYUDOV B.R. (1995a) Problems of en- and subglacial drainage origin. *Actes du 3 Symposium International "Cavites glaciaires et cryokarst en regions polaires et de haute montagne"*, Chamonix-France, 1-6.XI.1994. Annales litteraires de l'universite de Besancon, N 561, serie Geographie, n 34, ed. M. Griselin, Besancon, 77-82.

MAVLYUDOV B.R. (1995b) Caves Investigations at South Iniltchek Glacier, Central Tian-Shan. *Actes du 3 Symposium International "Cavites glaciaires et cryokarst en regions polaires et de haute montagne"*, Chamonix-France, 1-6.XI.1994. Annales litteraires de l'universite de Besancon, N 561, serie Geographie, n 34, ed. M. Griselin, Besancon, 101-104.

MAVLYUDOV B.R. (1997) Drainage of the ice-dammed Mertzbacher Lake, Tien Shan. Mater. *Glyatsiol. Issled./Data Glaciol. Stud.* V. 81. P. 61–65.

MAVLYUDOV B.R. (2017) Origin of caves in glaciers and glacial sheets. *Proceedings of the 17th International Congress of Speleology*. Eds. K. Moore and S. White, v 2, 160-164.

MAVLYUDOV B.R. (2019) Expedition «Inylchek-2019». *Peshery* (Caves), v 42, 137-141. (in Russian).

Origin and evolution of moulins in the Grey Glacier, Patagonia

Marco MECCHIA & Alessio ROMEO

La Venta Esplorazioni Geografiche, Italy, alessioromeo71@gmail.com

Abstract

Moulins in the east tongue of Grey Glacier were located and explored in the falls of 2004 and 2016. Their origin and evolution were studied with the aid of four satellite images taken from January 2013 to March 2016 that allowed identifying moulin positions and tracking their movement downslope; average glacier velocities in the range 0.53-0.61 m d^{-1} were measured. In the twelve years between the two visits, the glacier surface had been thinning 70-100 m and the calving front retreating ~1 km, but the positions of the main active moulins were found to be retreating only 150-200 m. Two zones suitable for generation of moulins, where streams disappear, are observed: before entering the highly crevassed terminal section of the glacier at the downstream end of the near-impermeable ice surface area on which the supraglacial streams flow, and ~1 km upstream where an arcuate fracture system cyclically develops. Downstream of each active moulin, a sequence of abandoned, dry moulins is found. Moulin approximate birth dates can be calculated from the average glacier flow velocity.

Résumé

Origine et évolution des moulins du glacier Grey (Patagonie). Les moulins de la langue orientale du glacier Grey ont été localisés et explorés au cours des automnes 2004 et 2016. Leur origine et leur évolution ont été étudiées à l'aide de quatre images satellites prises de janvier 2013 à mars 2016 qui ont permis d'identifier les positions des moulins et de suivre leur mouvement vers l'aval ; des vitesses moyennes du glacier de l'ordre de 0,53-0,61 m/j ont été mesurées. Au cours des douze années séparant les deux visites, la surface du glacier s'est amincie de 70 à 100 m et le front de vêlage a reculé de ~1 km, mais les positions des principaux moulins actifs n'ont reculé que de 150 à 200 m. Deux zones propices à la génération de moulins, où les ruisseaux disparaissent, sont observées : avant d'entrer dans la section terminale fortement crevassée du glacier, à l'extrémité aval de la zone de surface de glace presque imperméable sur laquelle les ruisseaux supraglaciaires s'écoulent ; et ~1 km en amont où un système de fractures arquées se développe cycliquement. En aval de chaque moulin actif, on trouve une séquence de moulins abandonnés et secs. Les dates d'apparition approximatives des moulins peuvent être calculées à partir de la vitesse moyenne d'écoulement du glacier.

1. Introduction

Since the 19th century, it has been observed that moulins form in specific places in a glacier, and form again in the same locations year after year. These places correspond to zones where the ice is subjected to tensile stress, generally near highly crevassed area (BADINO, 2002). However, the mechanisms of moulins formation are still far from been fully understood.

Moulins drift with ice, so they have short lifespans, lasting up to a few years. For example, SCHROEDER (1998) described the evolution of Gouffre Félix in the Hans Glacier, Svalbard, discovered in September 1988 that still existed in May 1992, though inactive. In the Gorner Glacier, Switzerland, the lifetime of the major moulins were observed to range from three to five years, depending on the local glacier movement rate (PICCINI *et al.*, 2002). In the Matanuska Glacier, Alaska, GULLEY (2009) documented the evolution of conduits that remained open over 3 years. In the western margin of the Greenland ice sheet, moulin lifetimes of about 11 years were suggested by CATANIA & NEUMANN (2010) based on the regional ice velocity and moulins spacing. In this study, the origin and evolution of moulins in the Grey Glacier, their relationships with the fracture systems, and their ages and persistence on the glacier surface are discussed.

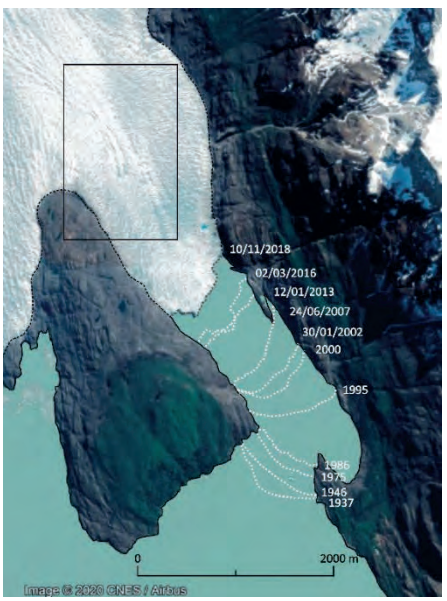

Figure 1: The eastern tongue of Grey Glacier. The retreat of the calving front is shown: 1937 to 2000 from RIVERA & CASASSA (2004), and 2002 to 2018 from Google Earth imagery. The square indicates the study area location.

2. Study site and methods

The Grey Glacier is located in the Patagonian Andes Mountains, Chile. This temperate glacier terminates with three tongues into Grey Lake, and our study area is included in its eastern tongue (Fig. 1). The ice thickness at the glacier front, i.e., the lake depth, is approximately 300 m (SUGIYAMA *et al.*, 2019).

As most calving glaciers in Patagonia, Grey Glacier has been retreating during the past century (Fig. 1), with a retreat of around ~1 km from 2004 to 2016. Large ice surface lowering, up to -6/-8 m a^{-1}, has been observed in the study area between 2000 and 2015/16 (MALZ *et al.*, 2018). According to the model of WEIDEMANN *et al.* (2018), the ice loss by surface ablation in this lateral tongue exceeded the ice loss by its frontal ablation. However, the climatic mass balance showed a high year-to-year variability.

Speleological reconnaissance of englacial conduits in the study area were conducted by La Venta teams in the autumns of 2004 (BADINO *et al.*, 2007) and 2016, at the end of ablation seasons.

Between 20 and 24 April 2004, 37 moulins were found (Fig. 2a), and 15 of them explored and surveyed to a maximum ice depth of 65 m. Entrances coordinates and elevations were measured by GPS and barometric altimeter. Directions of their guiding fractures, major and minor axes of shaft entrances, and approximate discharges of the meltwater runoff entering each moulin were also assessed.

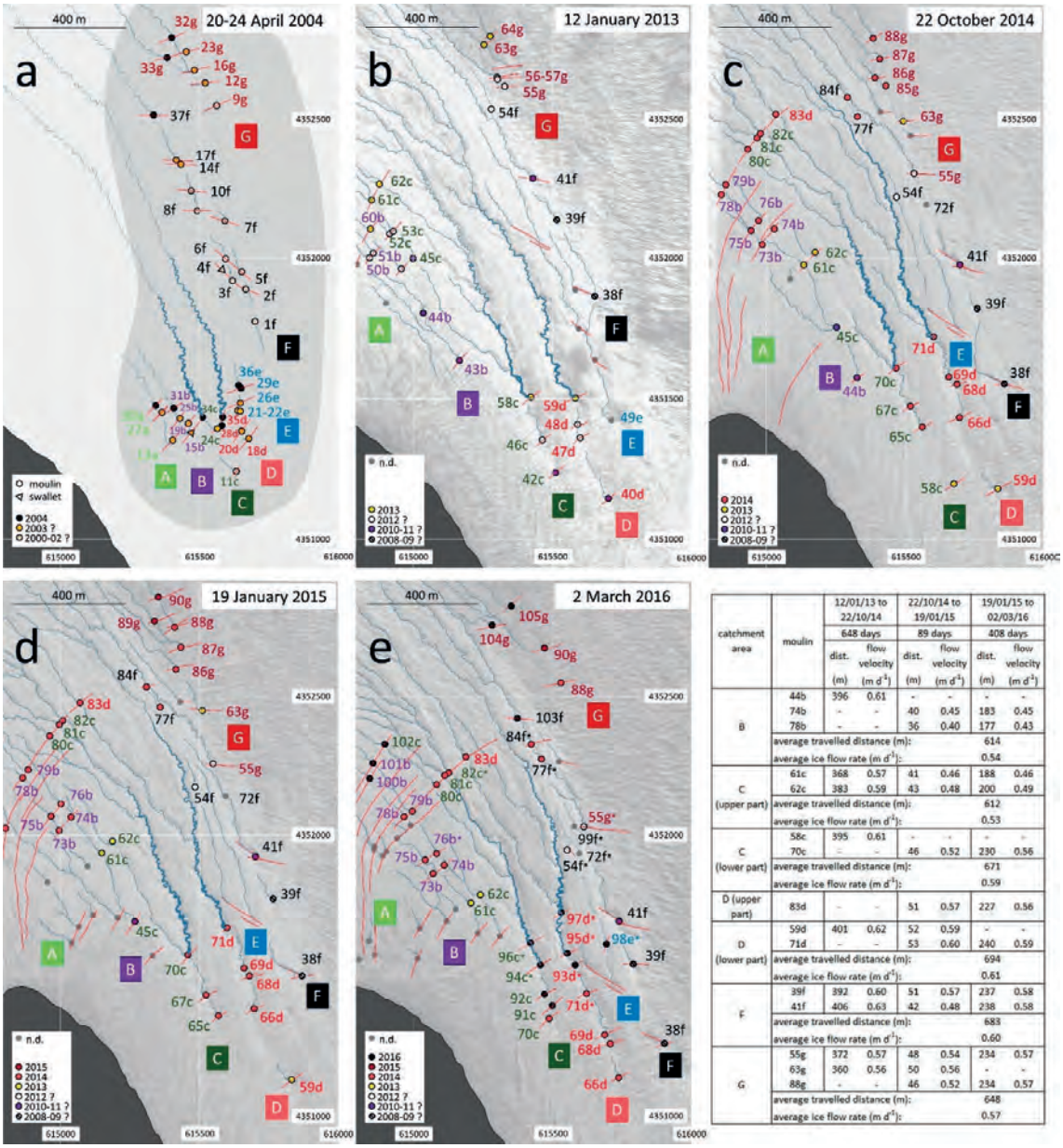

catchment area	moulin	12/01/13 to 22/10/14 (648 days) dist. (m)	flow velocity ($m\ d^{-1}$)	22/10/14 to 19/01/15 (89 days) dist. (m)	flow velocity ($m\ d^{-1}$)	19/01/15 to 02/03/16 (408 days) dist. (m)	flow velocity ($m\ d^{-1}$)
B	44b	396	0.61	-	-	-	-
	74b	-	-	40	0.45	183	0.45
	78b	-	-	36	0.40	177	0.43
	average travelled distance (m):					614	
	average ice flow rate ($m\ d^{-1}$):					0.54	
C (upper part)	61c	368	0.57	41	0.46	188	0.46
	62c	383	0.59	43	0.48	200	0.49
	average travelled distance (m):					612	
	average ice flow rate ($m\ d^{-1}$):					0.53	
C (lower part)	58c	395	0.61	-	-	-	-
	70c	-	-	46	0.52	230	0.56
	average travelled distance (m):					671	
	average ice flow rate ($m\ d^{-1}$):					0.59	
D (upper part)	83d	-	-	51	0.57	227	0.56
D (lower part)	59d	401	0.62	52	0.59	-	-
	71d	-	-	53	0.60	240	0.59
	average travelled distance (m):					694	
	average ice flow rate ($m\ d^{-1}$):					0.61	
F	39f	392	0.60	51	0.57	237	0.58
	41f	406	0.63	42	0.48	238	0.58
	average travelled distance (m):					683	
	average ice flow rate ($m\ d^{-1}$):					0.60	
G	55g	372	0.57	48	0.54	234	0.57
	63g	360	0.56	50	0.56	-	-
	88g	-	-	46	0.52	234	0.57
	average travelled distance (m):					648	
	average ice flow rate ($m\ d^{-1}$):					0.57	

*Figure 2: Moulin locations (circles) in the study area. Colors in the circles refer to their year of birth. a) Moulins measured in the field in April 2004. b-e) Moulins observed in 2013 to 2016 satellite images. Moulins identified in the field in April 2016 are marked with an * in the March 2016 map. A to G represent catchment areas of supraglacial streams. The table shows the average flow velocities, using the data of some well identifiable moulins. The coordinates are in UTM zone 18S in meters.*

Twelve years later (11-14 April 2016) a second investigation was carried out in the same area of the glacier. Fourteen moulins were located, and five of them explored reaching a maximum depth of 90 m. The entrances of two of the main moulins were also mapped in 3D using photogrammetry techniques.
The described fieldwork has been integrated with the interpretation of the free-available satellite image data displayed in the historical imagery of Google Earth (GE).

We used four high-resolution images: 12 January 2013, 22 October 2014, and 19 January 2015 provided by Maxar Technologies through GE, and 2 March 2016 provided by CNES/Airbus.
The error in relative position was calculated for each image by measuring the coordinates of well-identified stable features (solid rock) surrounding the glacier and comparing them with those measured for the same features on the image taken in March 2016. Results give relative accuracies of 53 m (January 2013 image), 50 m (October 2014 image), and 38 m (January 2015 image) with a 90% confidence level (CE90).
A large active moulin is generally easily identifiable on a high-resolution satellite image as a dark feature where a stream abruptly disappears with no apparent outlet (Fig. 2). Abandoned or minor moulins can be identified with less certainty, so field reconnaissance becomes valuable. In any case, it was certainly not possible to identify all the moulins on the images. Nonetheless, images interpretation allowed assessing the general pattern of moulins evolution, to draw maps with their distribution and calculate their downhill movement along the glacier (Table in Fig. 2). Fractures and crevasses distribution was also assessed on the satellite images.
The second field investigation was carried out just one month after the last satellite image was taken. Moulin positions measured by GPS were generally slightly downslope from their positions in the satellite image, although their positional accuracy was not good enough to allow a reliable comparison. In Fig. 2e, an asterisk highlights the moulins found on both the field and the image.

3. Results and discussion

Seven main catchment areas (denominated as A to G in Fig. 2) were identified in the field and on satellite images. Their whole area represents a near-impermeable ice surface that sustains the flow of supraglacial streams.
The downstream end of this area, where the great active moulins of C e D central watersheds are found, was located ~2.7 km from the glacier front in April 2004, and ~1.8 km in April 2016. However, in this 12 years period, the position of the active moulins retreated of only 150-200 m. According with the MALZ *et al.* (2018), the average glacier surface elevation decreased between 2004 and 2016 has reached up to 70-100 m. This estimate is consistent with our altimeter measurements taken at moulin entrances.
The near-impermeable ice surface extends 2.0-2.3 km upstream of the active moulins of central C and D streams. A highly crevassed ice surface surrounds this area. When a new moulin opens (e.g., 71d in Fig. 2c) swallowing the entire surface water flow, it leaves a dry valley downstream, and an abandoned moulin at its end (69d in Fig 2c). More dry valleys and moulins are often recognizable further downstream along the old stream path (68d and 66d in Fig 2c). However, as long as water no longer flows into a moulin the shaft tends to collapse; at a depth of 50 m the conduit is supposed to have an average life span of about one season, and the collapse time is even shorter as depth increases (BADINO, 2002). However, sometimes the depression representing the remains of an old moulin entrance persists to the next years (moulin 59d in Fig 2c) before merging with crevasses and disappearing into the mass of fluid ice.
A second zone of moulin generation is active in the near-impermeable ice surface area, represented by an arcuate fracture system observed between 0.8 and 1.2 km upstream of C-D active moulins. Fractures are open in the western side of the glacier (areas A, B, C), fade in its central part (area D) and are again open on its east side (area G). For example, moulins 61c and 62c are detectable in January 2013 as small new active moulins (Fig. 3).

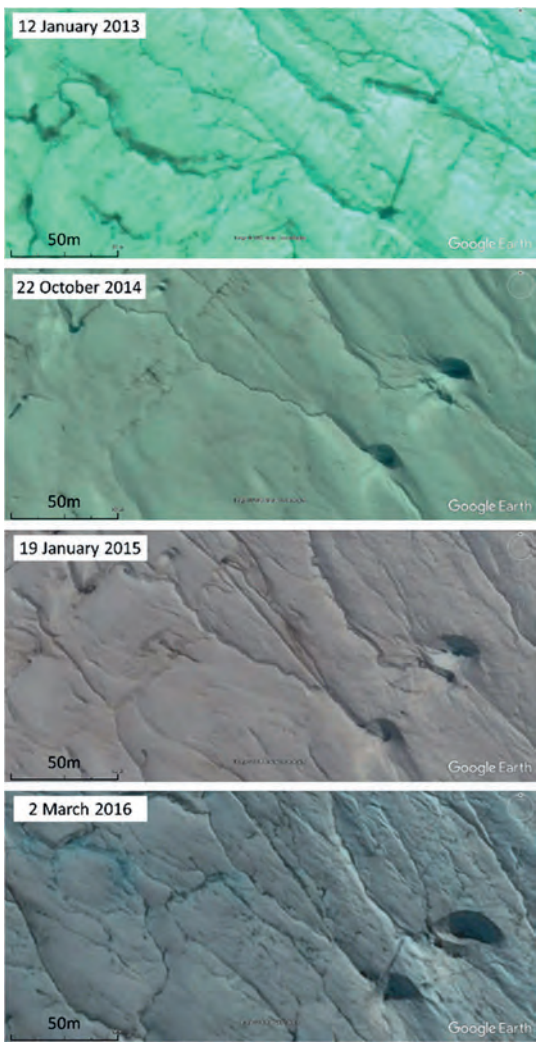

Figure 3: Moulins 61c and 62c in GE imagery from January 2013 to March 2016.

They are then observed 370-380 m downstream in October 2014 as large moulins (61c is active, 62c has already been abandoned), and at the same time a new generation of moulins (80-81-82c) form near their previous positions. In January 2015, 61c and 62c moulins are ~40 m still downstream.
In March 2016, their entrances are observed 190-200 m furthermore towards the terminus, but they are dry and probably collapsed, while small active moulins are visible ~20 m upstream, and at the same time a new moulin (102c) appears upstream along a new fracture.
Drifting downstream at the glacier surface velocity, the moulins generated in the upper part of the near-impermeable ice surface area tend to disappear, or to merge with those originated a few years later at the supraglacial stream ends.
The downstream movement of the glacier surface over the 1145-day total observed time was found to be between 612 m and 694 m (table in Fig. 2) with a margin of error less than 9%. Therefore, the average glacier velocity varied in the range 0.53-0.61 m d^{-1}. Much greater velocities, up to 2.8 m d^{-1}, were measured by SCHWALBE *et al.* (2017) for the central tongue of Grey Glacier close to the front.
The average velocity increases from the western catchment area B (0.54 m d^{-1}) to the central part D (0.61 m d^{-1}). Slightly lower ice velocities were found for the upper part of the study area. Glacier velocity in the warm season from October 2014 to January 2015 did not accelerate with respect to the long-term average velocity (table in Fig. 2).
Glacier flow velocity can be used to estimate the age of dry moulins. For example, assuming that the active moulin 34c was born at the beginning of April 2004, and according to the results of our evaluation, moulin 24c should be born at the beginning of November 2003 and moulin 11c in December 2002 (Fig. 2a).

4. Conclusion

The moulin distribution pattern on the eastern tongue of Grey Glacier has been outlined.
Although the calving front in this area retreated ~1 km between 2004 and 2016, and the glacier surface lowered of 70-100 m, the hydrologic network and the moulin positions did not change much (150-200 m retreat for the active moulins of C and D streams).
This study shows the existence of two zones on this glacier tongue suitable for the generation of new moulins:

- a main zone at the downstream end of the near-impermeable ice surface, where the great active moulins of streams C and D are generated, before entering the intensely crevassed area;
- an arcuate fracture zone that cyclically forms ~1 km upstream of the main zone, absorbing part of the stream flow.

References

BADINO G. (2002) The glacial karst. Proc. V Int. Symp. on Glacier Caves and Cryokarst, 2000. *Nimbus*, 23/24, VII: pp. 82-93.

BADINO G., MECCHIA M., LO MASTRO F. and ROMEO A. (2007) Hielo Continental Sur: l'altro carsismo. *Speleologia*, 56, pp. 64-77.

CATANIA G.A. and NEUMANN T.A. (2010) Persistent englacial drainage features in the Greenland Ice Sheet. *Geophys. Res. Lett.*, 37, 5 p.

GULLEY J. (2009) Structural control of englacial conduits in the temperate Matanuska Glacier, Alaska, *USA. J. Glaciol*., 53, pp. 681–690.

MALZ P., MEIER W., CASASSA G., JAÑA R., SKVARCA P. and BRAUN M.H. (2018) *Elevation and mass changes of the Southern Patagonia icefield derived from TanDEM-X and SRTM data*. Rem. Sens., 10:188, 17 p.

PICCINI L., ROMEO A. and BADINO G. (2002) Moulins and marginal contact caves in the Gornergletscher, Switzerland. Proc. V Int. Symp. on Glacier Caves and Cryokarst, 2000. *Nimbus*, 23/24, VII, pp. 94-99.

RIVERA A. and CASASSA G. (2004) Ice elevation, areal, and frontal changes of glaciers from National Park Torres del Paine, Southern Patagonia Icefield. *Arct. Antarct. Alp. Res.*, 36, pp. 379-389.

SCHROEDER J. (1998) Hans Glacier moulins observed from 1988 to 1992, Svalbard. *Norsk Geogr. Tidsskr.*, 52, pp. 79-88.

SCHWALBE E., KRÖHNERT M., KOSCHITZKI R., E. JOHNSON E., CÁRDENAS C. and MAAS H-G. (2017). Determination of spatio-temporal velocity fields at Grey Glacier using terrestrial image sequences and optical satellite imagery. In *LFirst IEEE Int. Symp.f Geosc. and Rem. Sens. (GRSS-CHILE)* (Valdivia), 6 p.

SUGIYAMA S., MINOWA M. and SCHAEFER M. (2019) Underwater ice terrace observed at the front of Glacier Grey, a freshwater calving glacier in *Patagonia. Geophys. Res. Lett.*, 46, pp. 2602–2609.

WEIDEMANN S.S., SAUTER T., MALZ P., JAÑA R., ARIGONY-NETO J., CASASSA G. and SCHNEIDER C. (2018) Glacier mass changes of lake-terminating Grey and Tyndall Glaciers at the Southern Patagonia Icefield derived from geodetic observations and energy and mass balance modeling. *Front. Earth Sci.*, 6:81, 16 p.

30 years of sliding velocities continuous measurements under the Argentière glacier (Mt-Blanc): 77% of speed loss!

Luc MOREAU[1] & Luc PIARD[2]

(1) Laboratoire EDYTEM, CNRS, Université Savoie Mont Blanc, F-73376 Le Bourget du Lac, moreauluc@chx.fr (corr. author)
(2) Institut des Géosciences de l'Environnement, F-38400 St Martin d'Hères luc.piard@univ-grenoble-alpes.fr

Abstract

The ice-rock interface, the contact area between the glacier and its rocky bed, is a crucial place to understand glacier dynamics: sliding, friction, deformation, water circulation and pressure, and glacier erosion. Yet these areas are very unknown because very difficult to access. The sub-glacial catchment site of the Franco-Swiss hydroelectric company Emosson S.A. provides access under the Argentière glacier and allows this interface to be studied all year round. Thanks to a long series of measurements, the correlation between the decrease in the volume of ice and the sliding speeds divided by four over the last 30 years is highlighted. On the other hand, hydrology is proving to be of prime importance to explain the increase in summer velocities and punctual accelerations due to water pressure. A better resolution of the records revealed daily variations in sliding velocities as a function of melt flow rates. Topographic rock bar appears as thresholds that regulate the variations of ice masses from upstream and amplify these variations downstream. Following the generalised receding of the glaciers, it's very visible that slope breaks are the most sensitive areas where ice retreats very quickly.

Résumé

30 ans de mesures du glissement sous le glacier d'Argentière (Mont-Blanc) : 77% de perte de vitesse ! L'interface glace-roche, zone de contact entre le glacier et son lit rocheux est un lieu capital pour comprendre la dynamique glaciaire : glissement, frottement, déformation, circulation et pression d'eau, érosion du glacier. Pourtant ces espaces sont très méconnus car très difficile d'accès. Le site de captage sous-glaciaires de la société hydroélectrique franco-suisse Emosson S.A. permet d'accéder sous le glacier d'Argentière et d'étudier cette interface toute l'année. Grâce à une longue série de mesures, on met en évidence la corrélation entre la diminution du volume de glace et les vitesses de glissement qui ont été divisées par quatre au cours des 30 dernières années. D'autre part, l'hydrologie se révèle primordiale pour expliquer l'augmentation des vitesses estivales et les accélérations ponctuelles suite aux pressions d'eau. Une meilleure résolution des enregistrements a permis de révéler des variations quotidiennes des vitesses de glissement en fonction des débits de fonte. Les verrous glaciaires topographiques apparaissent comme des seuils qui régulent les variations de masses de glace de l'amont et amplifient ces variations vers l'aval. Suite à la décrue généralisée des glaciers, il est notable que les ruptures de pente sont les secteurs les plus sensibles qui se déglacent très vite.

1. Introduction: A bicycle wheel to measure the sliding speeds!

Under the Argentière glacier (Mont-Blanc, Fig.1), and thanks to the network of catchment galleries of Emosson S.A. (ESA), a franco-swiss hydroelectric company, a subglacial cavity was equipped with a "cavitometer" (BOCQUET 1973), a wheel fixed at the end of an arm (Fig.1c, VIVIAN 1975). Since 1990 we have recorded with this instrument more than 30 years of almost continuous measurements of the sliding velocity of the temperate glacier on its bed. The initial objective was, thanks to this unique site, to measure the way the glacier is sliding on its bed (VIVIAN 1973; LLIBOUTRY 1968), according to the seasons, the variations in the mass of the glacier and the circulation of water. Today, with the pronounced retreat of the glaciers and the volumes of melting, but also the acceleration phenomena of the polar glaciers towards the sea (LÜTHIE 2016), these recordings are precious. It can be noted that over the long multi-year period, the sliding speeds depend on the mass (VINCENT 2016, Fig. 2). but that over the year and the seasons the correlations with hydrology are primordial (MOREAU 1991, 1995, 1999; VINCENT 2016).

Figure 1: Lognan Ice Fall. Subglacial cavity and cavitometer, 2019, cl. L.M.

Daily variations and punctual accelerations during stormy rains have been noted each year, and always in relation to flows. The long series of measurements since the 1990s also underlines the role of slope failures which finally govern the ice mass variations, by draining the overflow of ice from the upstream part to the downstream part. Conversely, speeds decrease in the event of a glacial recession, as they have for the last 30 years (Fig. 2)!

2. Methods and results: Sliding velocity records, a unique data set of 30 years!

In 1972, Robert Vivian with the EDF/Emosson installed a bicycle wheel in a natural subglacial cavity discover at the ice-rock interface, called cavitometer (BOCQUET 1973). The temperate glacier was sliding at the time at a rate of almost one meter per day under the effect of its weight, i.e., more than 300 m per year. Today, 40 years later, the thinning of the glacier allows it to slide by barely 0.15 m per day, or barely 50 m per year (Fig.2). We notice an important decrease in sliding speed since 1990 of 77%, from 207m in 1990 to 49m.y in 2019, the slowest speed ever recorded since 30 years! This demonstrates the link between volume variation and sliding speeds on a multi-year scale. In figure 3, a correlation between summer melt flows and mass sliding is clearly visible. The meltwater fills the interface and the voids created by the disbonding on the humps of the rocky bed. Slide velocities are multiplied by 1.5 to 1.8 in summer.

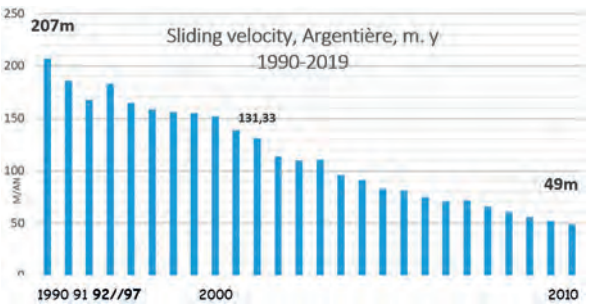

Figure 2: Annual velocity of the Argentière glacier on its bed (meters/year; the years 1993-1996 are missing because not continuous).

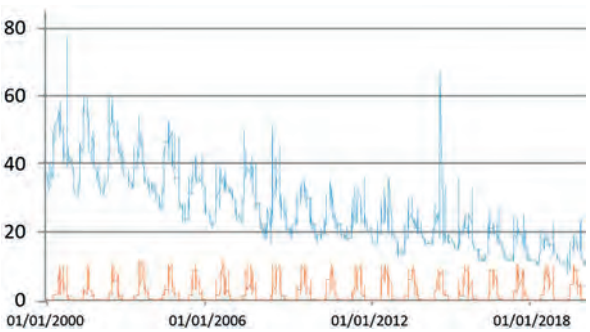

Figure 3: Sliding (blue) and water runoff in m3 (datas ESA).

The glacier slows down, noticeably in winter. It frees itself from disturbance by melt water, so it is only due to the sliding of the ice mass! These measurements have been carried out continuously for more than thirty years (3 cm of resolution).

A simple correlation method allows us to capture the links between measured parameters, flows (Emosson datas) and climate data by GlacioClim (D. Six, IGE). The 2018 and 2019 records (above Fig. 4) show a strong correlation between the collected flow (in red) and the sliding (blue). The sliding reacts as early as spring, following the increase in snow and ice melt flows (May and June). The ice-rock interface opens with the water and creates the channels evacuating it downstream. Enlargement of the channels reduces pressure and increases friction (RÖTHLISBERGER, 1972), sliding velocities decrease slowly.

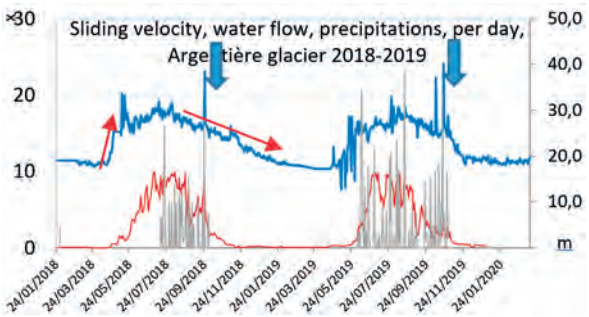

Figure 4: Variation of slip in cm/day, precipitation (in gray, GlacioClim D. Six) and water flow in m3 (ESA).

In the autumn, the decrease in melting is again favourable, as in the spring, to the pressurization of the subglacial channels during major inflows (Fig. 6). The channels are no longer suitable for evacuating volumes (IKEN 1986). On 24.09.2018, a spontaneous increase in velocities due to an increase in flow rates and pressures due to precipitation (gray curve, right-hand scale) can be observed, as well as in autumn 2019 (23.10 and 10.10.2019).

Hydrology appears paramount in these events! In 2017, a multidisciplinary mission (named RESOLVE) on the surface of the glacier and under the glacier allowed to collect good correlations between seismic events, water pressure, glacier sliding on its bed, and circulating flows under the glacier (ROUX, 2008). We note (Fig. 5, NANNI 2020) that these four factors are all perfectly correlated for the three glacier acceleration events, with water pressures at the source of the event measured under the glacier. It should be noted that seismic had already proven its ability to collect events of this type from the glacier surface (Greenland) (HELSMETTER, 2014). Thanks to this new resolution provided by a 5000-points encoder installed on the wheel axis (L. Piard and L. Moreau), accelerations are recorded every day during the summer evening peak flows (Fig.5 and Fig.7).

The schematic (Fig.6) explains the pressurization process of the ice-rock interface and cavities. Pressure channels at the ice-rock interface reduce glacier friction. The glacier rises slightly (SUGIYAMA 2004) and opens the cavities and accelerates. In this case, the cavities become larger, and the water or torrent may change its route under the glacier.

From the point of view of applied research on catchment, the torrent may, during these events, change its path and pass by a catchment well. It would then be visible from the outside in the serac fall on the rock bar by our time lapse camera.

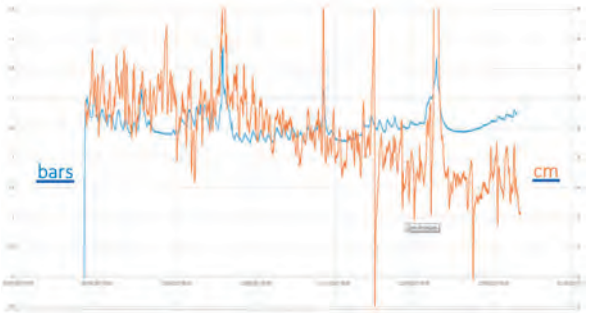

Figure 5: Daily pressure oscillations (in blue) and sliding of the Argentière glacier (in orange) (L.Piard, 2017).

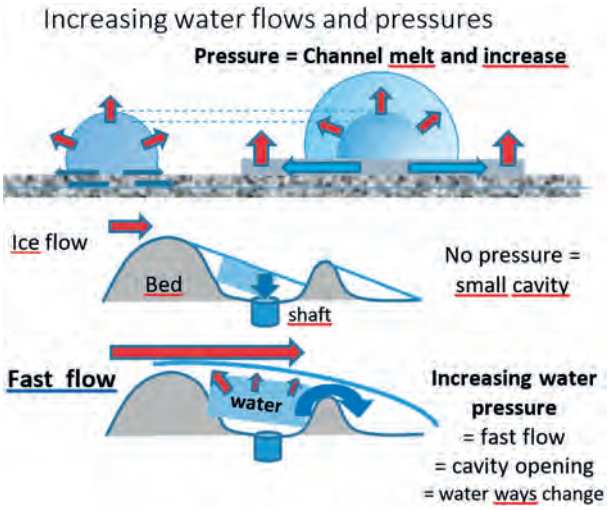

Figure 6: loading process of sub-glacial channels or conduits when large volumes of water arrive at the interface.

3. Discussion: daily speed variations but no stick slip recorded.

In view of the stick slip that are often mentioned in the literature and measured from the surface of glaciers or ice caps (ROEOESLI 2016), we have improved the resolution of the wheel.

The sensors of vertical variations are very important because they allow us to specify the nature of the acceleration of the glacier.

However, no 'stick slip' has been recorded so far. In this quest for information on the fine sliding of the glacier, one must also record the vertical variations of the arm that can compensate for acceleration or deceleration (Fig.8).

Indeed, an acceleration can be due either to a raising of the arm, by the passage of a stone for example, or to the pressurization of the ice-rock interface (precipitations, or a momentary sub-glacial water pocket, emptying of a crevasse or a supra lake or a moulin).

Finally, thanks to all these measurements, we realize that there is never any acceleration of the glacier if there is no water involved. The role of hydrology is crucial. In accordance with these facts, we never record any acceleration of the glacier in winter. Winter sliding is the true sliding of the ice mass only, undisturbed by the water and its pressures. This Argentière glacier is a "laboratory" temperate glacier measured for more than 40 years from above (IGE mass balance) and from below for more than 30 years. Its accessibility has allowed long series of measurements which continue today especially in this very changing climatic context!

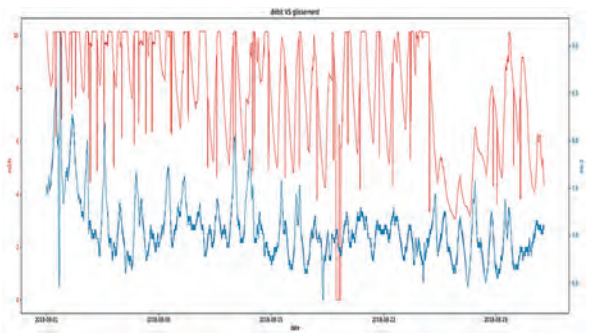

Fig. 7: Sliding daily variations (blue) and water flow (red), 08.2018

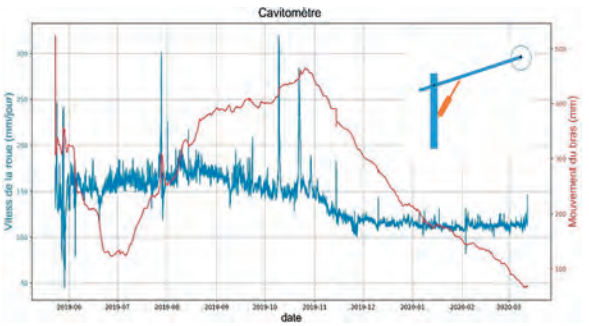

Fig. 8: Vertical variation 2019 of the arm and wheel.

4. Conclusions: No acceleration without water pressure!

At the Argentière glacier, the subglacial accesses of the Emosson company have allowed great discoveries to be made about the knowledge of the base of the glaciers. The installation of a unique instrument, the cavitometer, well thought out for the sub-glacial cavity, has made it possible to record more than thirty years of continuous measurements of the glacier's sliding on its bed. With the loss of mass of the glacier sliding velocities decrease, divided by four in 30 years. There are significant variations in the arrival of meltwater in spring and autumn when the sub-

glacial spaces (ice-rock interface and sub-glacial cavities) are reduced. Spontaneous accelerations of a few half hours are recorded in direct relation with hydrology (water pressures). Its improvement in high resolution (0.07 mm) records daily accelerations in the summer in phase with the high end-of-day flows.
No stick slip has been recorded so far. It can be seen that there is never any acceleration of the slip without taking into account the circulating water. Glacier sliding speeds are never the same throughout the year and adapt to water pressure conditions. Variations in sliding velocities are amplified in slope breaks (or serac falls) following variations in the mass of the glacier.
This glacier is currently the subject of a multidisciplinary research program (ANR "SAUSSURE" 2019-2023). The objective is to improve the laws of flow and friction in order to better understand the reaction of the large ice caps to climate and their acceleration towards the sea in the context of rising sea levels.

Acknowledgments

We would like to thank all the staff of the Électricité d'Emosson company, A. Bozon, B. G. des Combes and R. Vivian, L. Reynaud, A. Pahud, E. Moreau, D. Six, C. Vincent, L. Piard and F. Kadded.

References

HELMSTETTER A., MOREAU L., NICOLAS B., COMON P. & GAY M. (2014) Intermediate-depth icequakes and harmonic tremor in an Alpine glacier (Glacier d'Argentière, France): Evidence for hydraulic fracturing? *Journal of Geophysiqual Research*, Earth Surface, 120, 2014JF003289 (2015).

IKEN A. & BINDSCHADLER R. A. (1986) Combined measurements of subglacial water pressure and surface velocity of Findelengletscher, Switzerland: conclusions about drainage system and sliding mechanism. *J. Glaciol*. 32, 101–119.

LLIBOUTRY L. (1968) General theory of subglacial cavitation and sliding of temperate glaciers, *J. Glaciol.*, *7*, 21–58.

LÜTHI P. M., VIELI A., MOREAU L., JOUGHIN I., REISSER M., SMALL D. and STOBER M. (2016) A century of geometry and velocity evolution at Eqip Sermia, West Greenland. *Journal of Glaciology*, Available on CJO 2016 doi:10.1017/jog.2016.38.

MOREAU L. (1995) *Comportement d'un glacier tempéré sur son lit rocheux, glacier d'Argentière, Mont-blanc, France*. Étude effectuée au sein du site de la société d'Electricité d'Emosson S.A. Thèse de doctorat de géographie alpine, 311 p., Université Joseph Fourier, Grenoble I.

MOREAU L. (1999) Synthèse des variations de l'hydrographie sous-glaciaire du glacier d'Argentière de 1970 à 1999. *La Houille blanche*, Revue Générale de l'électricité, 5-99, p 40-46.

MOREAU L., RIGNOT E. and FRIEDT J.M. (2008) Study on time Lapse photography of Ilulissat glacier, west Greenland. Poster, *Alpine Glaciological Meeting*, Chamonix.

NANNI U., GIMBERT F., VINCENT C., GRÄFF D., WALTER F., PIARD L. and MOREAU L. (2020) DATA of Quantification seasonal and diurnal dynamics of subglacial channels using seismic observations on an Alpine Glacier, *Zenodo*, https://doi.org/10.5281/zenodo.3701520.

ROEOESLI C., A. HELMSTTER A., WALTER F. and KISSLING E. (2016) Meltwater influences on deep stick-slip icequakes near the base of the Greenland Ice Sheet, *J. Geophys. Res. Earth Surf.*, *121*, doi:10.1002/2015JF003601.

RÖTHLISBERGER H. (1972) Water pressure in intra-and subglacial channels, *J. Glaciol.*, 11, 177–203.

ROUX P-F, MARSAN D. METAXIAN J-P, O'BRIEN G. and MOREAU L. (2008) Microseismic activity within a serac zone in in an alpine glacier (Glacier d'Argentiere, Mont Blanc, France), *Journal of Glaciology*, 54, 157–168.

SUGIYAMA S. & GUDMUNDSSON H. G. Short-term variations in glacier flow controlled by subglacial water pressure at Lauteraargletscher, Bernese Alps, Switzerland. *J. Glaciol*. 50, 353–362 (2004).

VINCENT C. and MOREAU L. (2016) Sliding velocity fluctuations and subglacial hydrology over the last two decades on Argentière glacier, Mont Blanc area. *Journal of Glaciology*, Available on CJO 2016 doi:10.1017/jog.2016.35.

VIVIAN R. (1975) *Les glaciers des Alpes occidentales*, Ed. Allier.

VIVIAN R. and BOCQUET G. (1973) Subglacial cavitation phenomena under the glacier d'Argentière, Mt-Blanc, France, *J. Glaciol*., 12, 439–451.

VIVIAN R. A. and ZUMSTEIN J (1973) Hydrologie sous-glaciaire au glacier d'Argentière (Mont-Blanc, France), *IAHS-AISH P.*, 95, 53–64.

Moulins of the Mer de glace, from Vallot (1897) to today: filling, emptying and 3D measurements of the deformation in depth

Luc MOREAU[(1)], Farouk KADDED[(2)], Barnabé FOURGOUS[(3)] & Tristan GODET[(3)]

(1) EDYTEM Laboratory, CNRS, Université Savoie Mont Blanc, 73376 Le Bourget du Lac, moreauluc@chx.fr (corresp. author)
(2) Leica Geosystems SAS, 35 avenue de l'Île Saint-Martin, 92000 Nanterre, farouk.kadded@leica-geosystems.fr
(3) « Mille et un pas sous la glace » Collectif.

Abstract

The current retreat of the Mont-Blanc glaciers is slowing down the flow of the terminal tongue of the Mer de Glace. The crevasses are disappearing, and the rivers are getting longer. The moulins are positioned further downstream, remain active for longer and dig deeper. With the melting of the ice, there has been a multiplication of melt rivers and moulins on the Mer de Glace since the 2000s. Previously, given the dense network of crevasses, a single large moulin, sometimes as deep as 110m, drained the melting network further upstream at the place known as 'les moulins' from the confluence of the Tacul and Leschaux glaciers. In 2020 the vertical 'Kira' moulin was explored to -94m this autumn (1796m altitude). It was found to be completely filled and emptied, a hydraulic phenomenon that is crucial in the processes that challenge glaciologists but also hydro-electric engineers! The process is not exceptional as Joseph Vallot had already noted it in his 1897 exploration. We took advantage of this natural vertical section to calculate the volume of the moulin and the potential water storage (mobile Scan Leica) and to measure the internal deformation with the help of a few fixed markers inserted in the ice walls.

1. Introduction

Figure 1: Le Grand Moulin, Vallot sketch, 1898.

The hydraulic systems of glaciers are today at the heart of our concerns to better understand the flow of ice masses and their sudden accelerations, from alpine glaciers to ice sheet. On this theme, our Alpine glaciers offer us great opportunities for exploration and observation. We have been focused for 30 years on exploring the famous "Grand Moulin" of the Mer de Glace (REYNAUD 1987). Why? Because these alpine moulin are easily accessible, some times very deep (-110 m, LAMBERTON J. and BOIVIN J. M.) close to us and historic too! We have a topographical sketch (Figure 1) of this historical exploration by J. Vallot and Fontaine in 1897 (VALLOT 1898). This is the origin of the name "moulin", adopted in glaciology. These shaft dug by the torrents reminded Vallot of the waterfall system of the old flour moulins. Of course, for more than a century, this largest French glacier has been shrinking in mass, losing more than 150m in thickness at the site of the Vallot moulin under the Charpoua refuge (MOREAU et *al.* 2019). There has been a clear change in surface area with a decrease in fracturing, especially over the last twenty years or so. As glacier speeds decrease, crevasses disappear and the share of deformation increases in the general movement of the glacier. The melting river can therefore lengthen its path, and the moulin of this main bédière has been located much further downstream since 2005, but still on the right bank (Figure 2).

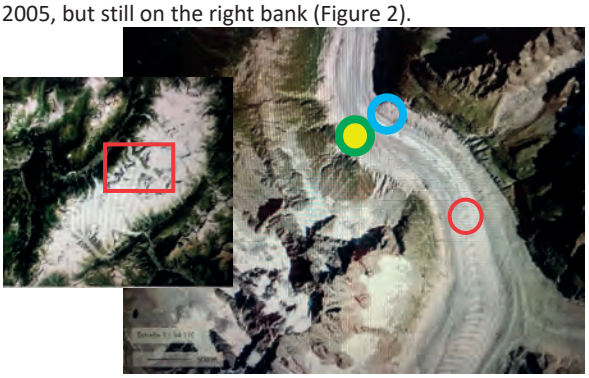

Figure 2: Location of the Gd Moulin Mer de Glace in 1897 in red and 2020 in blue, Moulin Kira in yellow-green, Map géoportail.

It is therefore a notable change, but it is very meandering even though it goes down to -85m (Nov. 2020, measured at the Leica disto). Then, if J. Vallot was thinking of measuring the thickness of the glacier there in 1897 (he explored 60 meters deep, VALLOT 1898), today we take the opportunity to see the intra-glacial water paths with our own eyes, an interesting observation especially when a Hydroelectric company like EdF (Electricité de France) captures the water under this glacier downstream! But it is also, when the well is vertical and deep like this moulin 'Kira' (-94m), a chance to measure the deformation of the ice at depth.
And when we noticed that the moulin filled up twice in a month, and that a nearby surface lake emptied completely

in the meantime, it seemed interesting to observe the phases of emptying and filling of this local hydraulic system (place called Les Angles, left side, 1796m altitude, 45°55'11.78N and 6°55'36.53E)

2. Materials and methods of observation of the moulin 'Kira' (-94m, 2020)

The 'Kira' has therefore been equipped with a time lapse camera to record any fill-ups and empties, at the rate of one photo per hour. Due to its almost vertical topography, deformation measurements at different depths were carried out. Bamboo buoys, according to a tested procedure (REYNAUD 1995) were inserted every 10 to 15 metres deep into the opposite walls of the shaft on seven levels (from 17m to -93m). The distances between them were measured manually every ten days with a distance meter (Fig. 7, disto Leica).

Figure 3: the time lapse camera on the surface.

The well was then precisely surveyed on the surface for the first time on 23.11.20 with a Leica GPS with integrated photos (topography of the 3 axes x, y, z, coloured by its photos, (Figure 5).

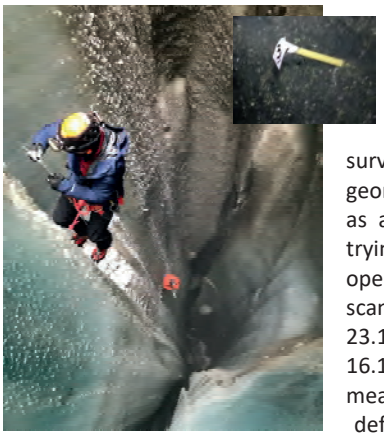

Figure 4: Installation of fixed markers in the moulin Kira, -95m

The operation then consisted of lowering a portable scanner (Leica) to survey the entire geometry of the moulin as a first reference and trying to repeat this operation later. A first scan was carried out on 23.11 and a second on 16.12. The idea is to measure the deformation speed (tightening of the shaft) at different depths over time, but also to calculate the volume of the moulin and therefore the storage of the water that has filled it almost completely twice, with a complete emptying in the meantime, which allowed us to carry out the two 3D scan operations.

3. First results of the deformation in depth and volume of the moulin

The two GPS measurements taken at 22-day intervals (23.11 and 16.12.20) recorded 0.98m of glacier displacement with the time lapse camera (photo above), which allows us to estimate the annual displacement of the glacier at almost 17m. This speed of the glacier is a function of the mass, which has been decreasing very rapidly over the last 30 years. The speed is probably ten to twenty times less than in Vallot's time, when the glacier had to move more than one metre per day (not measured), i.e. almost 400m per year with thicknesses of the same order (400m under the Charpoua), but this is precisely what Vallot wanted to measure . In spite of this slight displacement, the marginal fractures are created by the tensions of the left bank, faults which run upstream to the center of the glacier at 45° to the banks (red arrows Fig. 9), at the origin of the moulin.

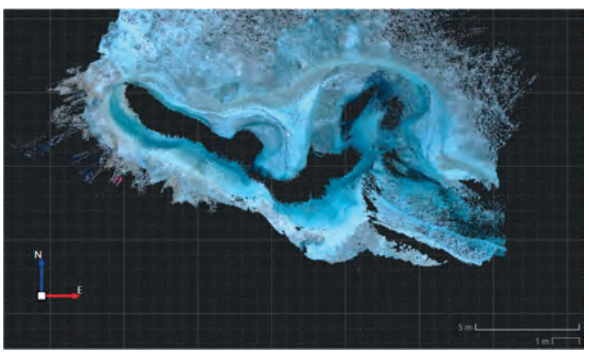

Figure 5: Moulin 'Kira', -95m, plan view, topo and photos with GPS Leica GS18i on 23.11.20 (photo on the left), F.Kadded.

Figure 6: Lowering of the Leica BLK2GO dynamic scanner in the middle of the shaft and below with the adapted lighting (Méandre Technologie / Focale fixe), cl. M. Dalmasso

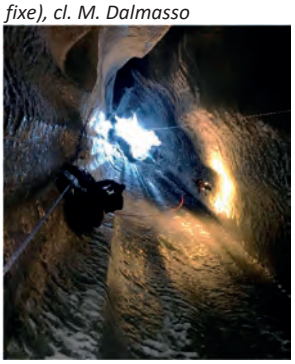

In a second step, the dynamic Leica BLK2GO scanner (400 000 points per second) was lowered to the bottom of the moulin for a 3D laser topography (Fig.6). The moulin was 95m deep on 23.11.20, but 11m shallower on 16.12 (water and snow filling). We lost the bottom marks but some results were recovered (Fig. 7). We can see the progression of the tightening rate of the moulin to more than 0.51m in 25 days at 82m depth. This process of ice deformation is natural and takes place in temperate ice above 30 m depth (i.e., 3 bars of pressure). This is the origin of the closure of the moulin and their eventual filling. The shaft was then filled with water over 11 metres from the bottom (seepage observed in the walls on the left bank side).

Déformation Moulin 'KIRA'	Manual measurement	Manual measurement	Manual measurement	**alt. 1796 m**
Deep (m)	Date **21.11**	Date 01.12	Date **16.12**	**= 25 days**
alt. 1796 m				
-17m	2,84		-	-
-31m	2,9	-	-	-
-45m	**2,23**	2,18	**2,05**	**-18 cm**
-61m	**3,41**	3,28	**3,12**	**-29 cm**
-71m	**3,03**	2,85	**2,63**	**-40 cm**
-82m	**2,68**	2,44	**2,17**	**-51 cm**
-93m	0,83	Under water	Under water	-

Figure 7: Results of deformation measurements at the marker (L.Moreau) and 3D topography of the moulin Kira (F.Kadded)

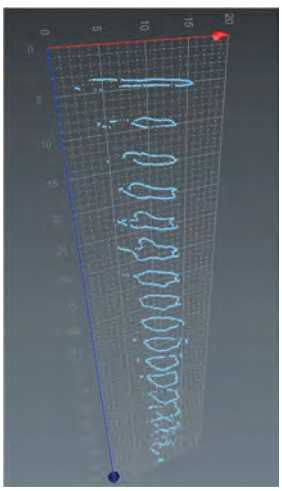

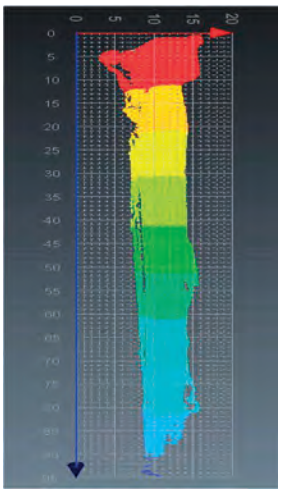

4. Discussions: Moulins are balance chimneys!

Experience from observations and explorations has shown that the moulins do not only allow surface melt water to continue its journey downstream through the glacier to reach the rocky bed and feed the glacial river, they also act as pressure "valves" where necessary. In fact, while the torrent is already dry, there are fillings proving inflows of water within or under the glacier. This was the case for this moulin 'Kira' this autumn (Fig. 9), but this is not so new: Vallot had already noticed it (VALLOT, 1898, Fig. 8) by observing ice floors above the void (Fig.8). We had also noticed these ice ledges in 1994 (MOREAU 1995), when the Gd moulin was still under the Charpoua, as is also often seen in Greenland (BOURSEILLER et LAMBERTON 2002; COVINGTON 2020). At this Kira moulin at an interval of one month the moulin filled twice and emptied once, at the same time a lake further downstream emptied (Fig.9). If these events are frequent in these moulins, precisely because they are part of the hydrographic network of the glacier and of the water flows, it is more difficult to know where the source of these waters comes from. It can be said that moulins behave like a sort of "balance chimney" (hydroelectricity) which compensates for the excessive water pressure at the base by storing inputs that are too large for the evacuation capacities of the sub-glacial channels at this time. It is moreover during these events that the mass may skid more strongly on the rocky bed, as we record every year under the Argentière glacier this kind of acceleration of the glacier (VINCENT and MOREAU 2016).

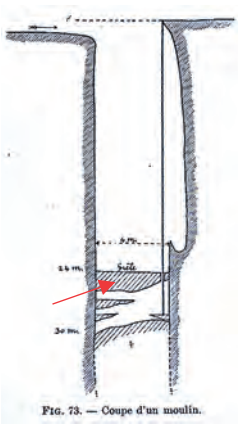

Figure 8: Floes showing filling and emptying, Vallot 1898

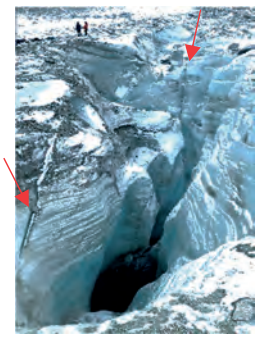

Figure 9: Moulin -94m, filling up to -35m after the 23.11 (info P.B Laussac) and observe empty the 01.12, then observe completely full the 27.12. (cl. J. Mercier). The red arrows show the fractures at the origin of the moulin.

5. Conclusions

Following the significant loss of mass of the Mer de Glace since the 1990s, the glacier is only sliding 25m per year. Crevasses are rare below 1800m and the moulins are no longer renewing themselves. They are situated well downstream today from those of the last century explored by Vallot, or even of the 1990s. If the glacier has lost a lot of thickness, beautiful depths are still encountered as they remain active for longer. Two moulins of more than 90 metres were explored this year 2020 with one almost vertical moulin down to -94 metres. The filling of the moulin and its emptying a few days later, as well as the emptying of a supra-glacial lake nearby, called us to a hydraulic network interesting to understand in the area. The moulin was equipped with a time lapse camera for possible future fillings which took place on 27.12.20. The mission to measure the volume of the shaft with a portable laser scan evaluates the volume of the 'Kira' moulin at the value of an Olympic swimming pool (3000 m^3). The topography renewed twice with this equipment from inside the shaft but also manually from our markers (17 fixed markers were inserted in the walls) shows the deformation and tightening of the shaft losing 10% of volume and -0.50m of tightening in 25 days at -82m depth, in temperate ice). These measurements are interesting to carry out because the moulin allows them to be carried out manually and visually. Then it is possible to observe the changes that take place in the moulin, walls, aspect, at each visit, what an ice borehole instrumented for deformation (an inclinometer for example) could not bring. The objective this winter will be to continue the deformation measurements with the laser scan and to better understand the hydraulic filling-emptying process, a non-exceptional phenomenon that Vallot had already noticed in his time. These measurements allow us to argue that the moulins tighten up quickly as soon as they are empty, close up again and become retention vessels that fill and empty at the slightest fracture with also the thrust of the weight of the stored water. These moulins behave like balancing chimneys which have the function in hydroelectricity of absorbing the overflow of water pressure from the collectors and conveyance galleries.
All this science is also practised in very aesthetic intra-glacial settings which motivate our commitment.

Acknowledgements

We would like to thank the caving team for their help (Kira, Emilie, Katherine, Benoît, P. Bernard, Baptiste, Alain, Philippe, Clément, F. Eric, Laurent, Bruno, Gaëtan). Special thanks to the Lamberton Family, L. Reynaud, A. Tazieff, J.-M. Boivin O. Halin and O. Renard (PGHM 1994, 2020†, exploration -90m)! Monica Dalmasso, Jeff Mercier, the Montenvers team of the Cie Mt Blanc, Jeremy and Loïc from Hotel du Montenvers. The special Light for the BLK2GO Leica and soft 3D is developped by Meandre Technologie and Focale fixe S.A. (Philippe Sage and Gaëtan Curt). All the 3D sketches are from F. Kadded, Leica, and photos without name from L. Moreau.

Références

BOURSEILLER P., LAMBERTON J., COUTE A. et MOREAU L. (2002). *Voyage dans les glaces*. La Martinière, Paris, 195 p.

COVINGTON M. D., GULLEY J. D., TRUNZ C., MEJIA J. & GADD W. (2020). Moulin volumes regulate subglacial water pressure on the Greenland Ice Sheet. *Geophysical, Research Letters*, 47.

MOREAU L. et REYNAUD L. (1995). Moulins glaciaires des glaciers tempérés et froids de 1986 à 1994 (Mer de Glace et Groenland). Morphologie et techniques de mesure de la déformation de la glace, *Actes du 3e Symposium international Cavités glaciaires et cryokarst en régions polaires et de haute montagne*, Chamonix, novembre 1994, 109-113.

MOREAU L., REYNAUD L., SIX D. et VINCENT C. (2019). *Dans les secrets de la Mer de Glace*, 2e édition Esope Chamonix, 144 p.

MOREAU L. (2009). L'exploration du cryokarst glaciaire et son intérêt scientifique pour l'étude du drainage des eaux de fonte : porches, cavités, crevasses, bédières et moulins. *Neige et glace de montagne : Reconstitution, dynamique, pratiques*, Collection EDYTEM --- Cahiers de Géographie, n°8, pp. 163-17.

REYNAUD L. (1987). The November 86 survey of the Grand Moulin on the Mer de Glace, Mont-Blanc. *Journal of Glaciology*, 33, 113, 130-131.

VALLOT J. (1898). Explorations des moulins de la mer de glace. *Annales de l'Observatoire du Mont-Blanc*, 3, 183-190.

VINCENT C. and MOREAU L. (2016). Sliding velocity fluctuations and subglacial hydrology over the last two decades on Argentière glacier, Mont Blanc area, *Journal of Glaciology*, 1-11.

35 years of glacio-speleological investigation on Gorner Glacier, Switzerland

Alessio ROMEO[(1)] & Leonardo PICCINI[(1,2)]

(1) La Venta Esplorazioni Geografiche, Treviso, Italy, alessioromeo71@gmail.com
(2) Department of Earth Science, Università di Firenze, Italy, leonardo.piccini@unifi.it

Abstract

The Gorner Glacier is in southern Switzerland and is one of the most studied glaciers in the World regarding englacial caves. The first research, by Italian speleologists, date back to 1985 and since then investigations have been performed almost annually. Several sinking shafts (moulins), deep up to 135 m, and numerous contact cavities were surveyed confirming a high development of englacial drainage structures. Repeated investigations during the same year allowed us to follow the seasonal evolution of some active absorbing shafts. Supraglacial water flow has a relatively stable pattern and the moulins fed by the major streams usually are formed year after year in a similar position. In more recent years, we have recorded a trend of major drainage structures and sinking shafts to migrate downstream, probably because of changed dynamic flow conditions, due to the strong thinning that the glacier has suffered in recent decades, and to different feeding conditions. The same dynamics probably is the cause of a general reduction of the maximum explorable depth inside the moulins, an indication that also the internal drainage network is affected by the consequences of the global warming.

Résumé

35 années de recherches glaciospéléologiques dans le glacier du Gorner (Suisse). Le glacier du Gorner est l'un des glaciers les plus étudiés au monde en ce qui concerne les grottes glaciaires. Les premières recherches des spéléologues italiens remontent à 1985 et depuis, des investigations ont été effectuées presque chaque année. Plusieurs puits (moulins), profonds jusqu'à 135 m, et de nombreuses cavités de contact ont été étudiés confirmant un fort développement des structures de drainage intra-glaciaires. Des investigations répétées au cours de la même année nous ont permis de suivre l'évolution saisonnière de certains puits absorbants actifs. Le débit d'eau épi-glaciaire est relativement stable et les moulins alimentés par les grandes bédières se forment généralement année après année dans une position similaire. Au cours des dernières années, nous avons enregistré une tendance des principales structures de drainage et des moulins à migrer vers l'aval, probablement en raison des changements des conditions d'écoulement dynamique, en raison du fort abaissement d'épaisseur que le glacier a subi au cours des dernières décennies, et des différentes conditions d'alimentation. La même dynamique est probablement à l'origine d'une réduction générale de la profondeur explorable à l'intérieur des moulins, ce qui indique que le réseau de drainage interne est affecté par les conséquences du réchauffement climatique.

1. Introduction and historical outline

The Gorner is one of the most investigated mountain glaciers in the World, and particularly by speleologists because of its exceptional development of sink shafts (also called “moulins”) and contact caves. For this reason, Gorner is a relevant site for studying the evolution of the glacier caves and their hydrological behavior.

After a first survey by Swiss cavers at the beginning of ’80 (G. FAVRE, pers. com.), in 1985 and 1986 a group of Italian speleologists performed the descents of deep moulins up to the depth of 135 m (PICCINI, 2001). In 1988 and 1989 Italian and Swiss speleologists conducted further explorations of moulins and marginal contact caves. In 1993 and 1994, French cavers descended some moulins up to 55 m of depth (WENGER, 1994).

Since 1998, researchers coming from the Dipartimento di Fisica Generale of Torino, Dipartimento di Scienze della Terra of Firenze and from the Association “La Venta” have performed a new campaign of investigation that is still in progress. The aim is the physical and morphological characterization of moulins and the monitoring of their short and long-term evolution. In 1999 and 2000 a detailed study concerned the seasonal evolution of moulins. For the first time the development of a sink shaft was followed from the beginning of summer to late dawn (PICCINI et *al*., 2002). In the autumn of 2003, two sink shafts about 100 m deep were descended along with a large subglacial cavity, formed during the sudden emptying of the glacier dammed lake (Gornersee) that develops at the confluence of the Gorner (s.s.) and Grenz ice tongues, which was surveyed for over 100 m.

In the following years, quick expeditions surveyed several moulins in the upper and in the central part of the northern and major ice stream (in 2005, 2006, 2007, 2009 and 2010 missions). From 2013, several investigations were made by Italian speleologists coming from different towns. In 2014, the central part of the glacier was mapped and explored during an International Camp of 10 days by more than 40 cavers coming from different European countries. The same area was surveyed in the next years studying the morphological change of moulins and their position also using a portable laser-scanner device and a drone. In 2020 two different expeditions (in August and October) revealed

a further and strong reduction of the thickness of ice in the Gorner/Grenz confluence sector, where we were able to explore a contact cave created by external river coming from the residual tongue of the Gorner branch.

This paper summarizes the most relevant results and field observations of the investigation performed from 2000 to present day.

2. Geographical framework

The Gorner Glacier is in the Swiss Alps. Its catchment area encloses the northwestern side of M. Rosa (4554 m) and the northern slopes of Lyskamm-Breithorn (4479-4159 m) ridge. Presently, the entire Gorner and its tributaries cover a total extension of about 50 km^2 and it is the second largest glacier of the Alps, after the Aletsch Glacier. Only 20 years ago, the total extension was about 65 km^2, testifying for a recent dramatic reduction (PICCINI et *al*., 2002).

The ablation zone, between the altitude of 2400 and 2600 m, has a mean steepness of 5 %. This morphologic setting allows the development of an exceptionally structured drainage system, which exhibits longitudinal streams (bédières) and several pools (Fig. 1). Two major medial moraines act as longitudinal watersheds dividing the glacier into three different sectors, hydrologically shared; the central one, the widest, is incised by canyons, up to 40 meters deep, which feed supraglacial lakes. The zone where a well-channeled runoff occurs has a surface of about 5.5 km^2, whereas the total length of the main supraglacial channels (those having a significant morphological expression) is about 20 km. The main streams flow in the left side of the glacier draining most of the supraglacial meltwater that feed the englacial drainage through the moulins.

The Gorner lays in a wide E-W oriented valley; although the elevation of the watershed which borders the glacier on the S is more than 4000 m, the shape of the valley results in a high insulation, all year. For this reason, the surface melting is very high, probably more than 3 m per year. According to our measurements, performed in different years (1985-1999), we can assume a maximum daily surface melting of 30 mm in the months July and August. In this period, the mean meltwater discharge usually ranges from 230 to 350 l/s on a surface of 1 km^2 (PICCINI et *al*., 2002).

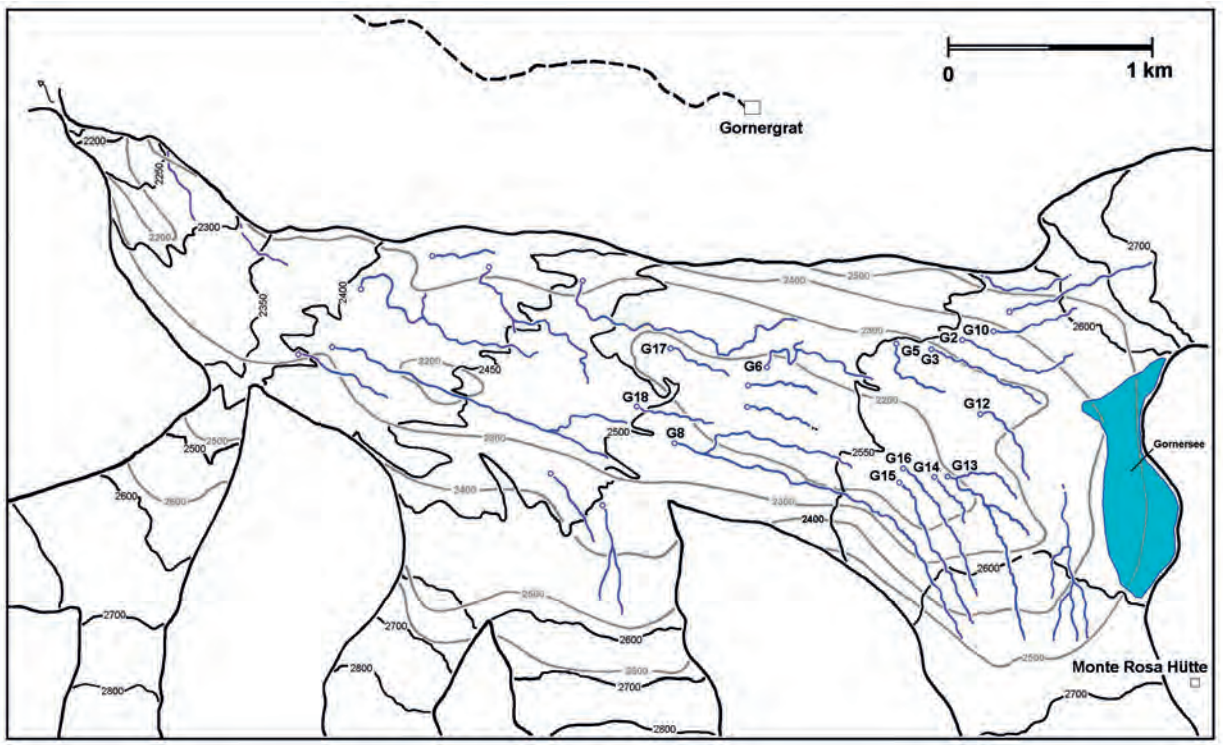

Figure 1: Sketch map of the ablation zone of Gorner Glacier showing the supraglacial network and the location of the major moulins surveyed in 1999-2000. Black contour lines refer to 1995 (1:25.000 Swiss map), grey contour lines show the topography of bedrock (from BEZINGE, 1970).

3. Supraglacial streams and sink shafts evolution since 1999 to 2020

A dense network of supraglacial streams occurs on the Gorner's surface, thanks to the high melting ablation and to the low gradient, which allows for the development of a well-incised rills network. Since 1999, we observed an amplification of surface run-off with the formation of deep and meandering canyon-like incisions. Most of the major supraglacial channels survive during the winter, thus at the end spring the drainage network is reactivated with only

small differences from the previous year. It has been observed that melting runoff reactivates the previous year swallow holes only if a new sinking crevasse does not develop upstream capturing the water. In 1999-2000 several sink shafts were found. Most of them were located downstream the Gorner/Grenz confluence zone. The position of the major moulins was along the main extension zones controlled by the morphology of the glacier bed, as suggested by the fact that almost all the moulins open on transversal fracture (PICCINI, 2001). Another group of active moulins was surveyed in the lowermost part of the glacier. Some of these have wide feed basins (up to 1 km^2), and experience large in-flowing discharges.

In the final seasonal evolution stage, major moulins are usually shaped like a first vertical shaft, the dept of which mainly depends on the inflow discharge, followed by a high and narrow canyon (Fig. 2). At a greater depth, the form of passages tends to change from almost vertical drops to gently-dipping canyons. Canyons-like caves with a horizontal pattern also occur, but often they are epidermal caves which develop from meandering supraglacial channels covered by firn or refreezing ice.

The shape of a moulins changes year after year. During our surveys we have followed the evolution of a large moulin (G6) which forms almost every year in the central part of the glacier at about 2500 m a.s.l. (elevation in 1999-2000). This sink shaft is fed by an important supraglacial stream that is visible also on 1:25.000 maps since the beginning of Eighties. First descend was performed in 1988 (Fig. 3). In 1985, in the same area there was a large supraglacial lake, whereas in 1986 the lake was empty. The same shaft has been surveyed in 1999, 2003, 2005, 2014, 2015 and 2020 showing different morphological features. In 1988 and 1999, it was possible to reach the englacial water table, while in the following years the first pit was followed by a steep canyon that was followed until it became too narrow to be accessed. In 2015, we reached the deepest development at -110 m from glacier surface.

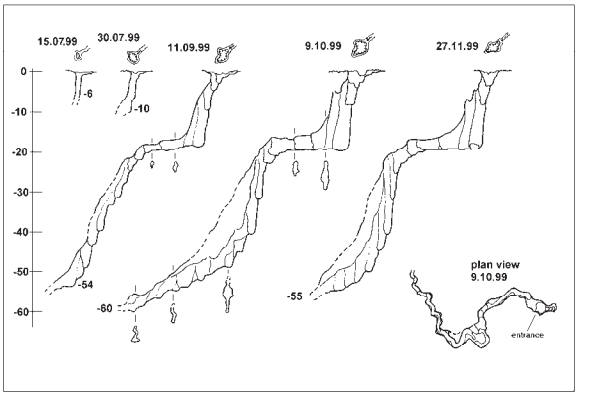

Figure 2: Seasonal evolution stages of the moulin G10 from summer to late dawn 1999.

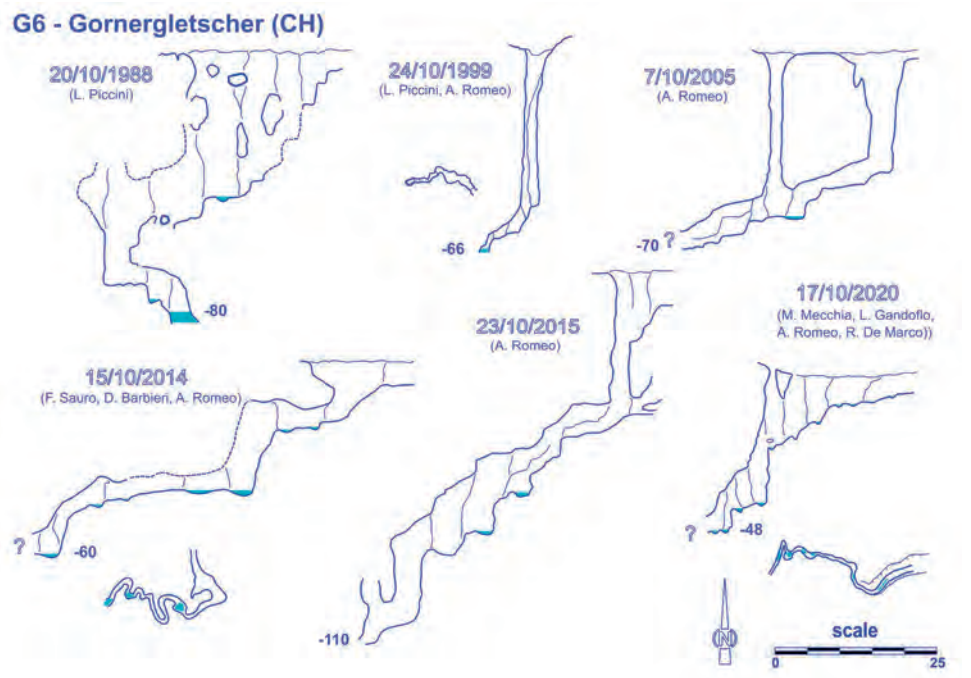

Figure 3: Evolution of the moulin G6 since 1988 to 2000.

4. Discussions

According to our observations, the life of the largest moulins ranges from 3 to 5 years and it depends on the local glacier movement rate: the faster the movement, the shorter the active period. The depth of the surficial crevasse, the hydrodynamic of the in-flowing stream and the temperature of the ice, influence the internal pattern of moulins. Position depends on the distribution of stress inside the glacier and the effect of this on the surface topography. Several Authors

have testified that spatial distribution of moulins remains almost the same year after year (e.g., MONTERIN, 1930; PICCINI, 2001). In recent years we have conversely observed a relevant movement downstream. Two of the major sink shafts surveyed on the Gorner, G6 and G13, have migrated downstream of about 350 and 200 m respectively from 1999 to 2020 (Fig. 4).

Probably, the stability of the location of a moulins was documented in a period when glaciers were in an almost steady-state equilibrium, and their feeding was uniform.

In recent years, the Gorner Glacier have experienced a dramatic change of its dynamic. The northern tongue, descending from M. Rosa, do not join anymore with the main ice-stream coming from the northern sides of Lyskamm (Grenzgletscher), which furthermore does not receive the supply from left tongues anymore. The lack of a lateral constraint probably produced the transversal extension of the Grenz tongue and therefore its reduction in thickness. This also could have provoked a reduction of flow velocity and a different distribution of internal stress which could justify the downstream migration of sink points of major supraglacial streams.

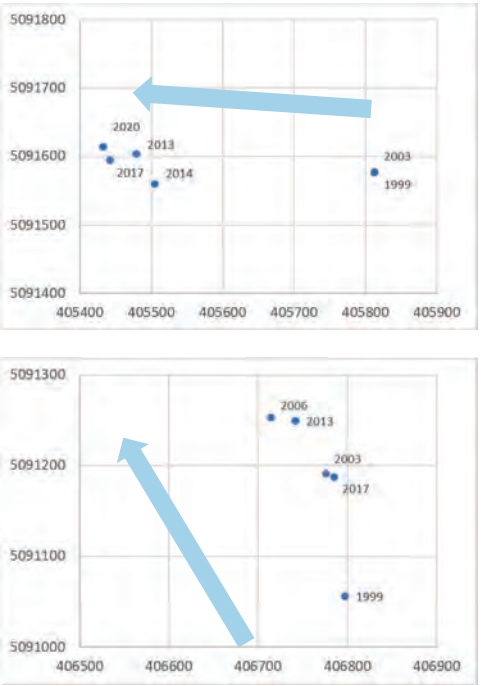

Figure 4: Migration of the position of moulins G6 (a) and G13 (b) since 1999 to 2020. Arrows indicate the glacier movement direction.

5. Conclusion

35 years of repetitive investigations on Gorner Glacier allowed us to verify that moulins and subglacial marginal caves act an important role on the dynamic of glaciers. Their cyclic life is strictly correlated with the ice-flow velocity and with the trend (positive or negative) of the mass-balance. Most of the supraglacial channels survive during the wintertime, thus every spring the drainage network is reactivated with only small differences from the previous year.

Our observations seem to indicate that in the last decades the number of moulins and their period of life has been decreasing. From 2010 we do not have news about the Gornersee lake, and the morphology of glacier's surface change a lot. As most of the alpine glaciers, the Gorner tongue is dramatically retreating year by years and most of the melting water flows now along lateral moraines, reducing the supraglacial run-off and the possibility for the formation of large and accessible moulins.

Acknowledgments

We gratefully wish to thank our friend and ice-caving companion Giovanni Badino, disappeared in 2017, who worldwide join with us discovering the fascinating world of the internal side of glaciers.

References

BEZINGE A. (1970). *Études sur le lac glaciaire du Gorner. Société hydrotechnique de France*, Étude destinée à la section de glaciologie.

MONTERIN U. (1930). Sulla costanza di posizione dei pozzi glaciali. *Boll. Com. Glac. It.*, 10, 211-227.

PICCINI L. (2001). The Glacier caves of Gornergletscher (Switzerland): preliminary notes on their morphology and hydrology. Atti Convegno "Risposta dei ghiacciai alpine ai cambiamenti climatici", Bormio (TO), 9-12 settembre 1999. *Geografia Fisica e Dinamica Quaternaria*, Suppl. 5, 151-156.

PICCINI L. ROMEO A. and BADINO G. (2002) Morphology and hydrology of the Gornergletscher's moulins. 5th International Symposium on Glacier Caves and Cryokarts in *Polar and High Mountain Regions*, Courmayeur (AO), April 14-18, 2000. *Nimbus*, 23-24, 94-99.

WENGER R. (1994) Explorations dans les moulins glaciaires de la Mer de Glace (Chamonix-France) et du Gornergletscher (Zermat - Suisse). *3e Symp. Intern. Cavités Glaciaires et Cryokarst en Régions Polaires et de Haute Montagne*, Chamonix – France, 105-10.

"Inside the glaciers" expeditions 2017-2018: hydrological and microbiological investigation of the Greenland icecap subsurface

Francesco SAURO[1,2,3], Alessio ROMEO[2], Joseph COOK[3,4], Alun HUBBARD[5] & Arwyn EDWARDS[4]

(1) University of Bologna (BIGEA & FABIT), Via Zamboni, 33, Bologna, Italia francesco.sauro2@unibo.it (corr. author)
(2) Inside the Glaciers, Italy
(3) Ice Alive, United Kingdom
(4) Aberystwyth University, United Kingdom
(5) The Artic University, Norway

Abstract

In the last decade, the accelerated melting of the glaciers is an evidence that anyone can see. Despite the urgency to understand the dynamics of mass loss in the most important glaciers on the planet, modern glaciology still struggles to understand the importance in this balance of two invisible factors: the intra-sub-glacial drainage cavities and microbiology. The project "Inside the glaciers" performed two expeditions (2017-2018) to the Greenland icecap with the aim of investigating these topics through the exploration of moulins right after the melting season. The team included speleologists, glacial hydrology specialists, microbiologists, robotic engineers and professional photographers. This effort allowed to monitor for two subsequent years a series of giant moulins reaching up to 130 meters of depth. The microbial analysis showed the presence of bacterial activity in buried cryoconites along the moulin walls and the accumulation of organic matter derived by algal activity in the waters at the bottom of the caves. Direct exploration and GPR surveys showed the presence of voluminous deep sub-glacial lakes that could be preserved as liquid water through the winter. This process allows a faster reactivation of the hydrologic network and an efficient heat transfer to the interior of the icecap.

1. Introduction

The Greenland ice sheet represents the Eldorado of glaciospeleology because of its gigantic moulins fed by rivers that can exceed 50 km in length and tens of cubic meters per second of discharge during the summer melting peak. Since the late Eighties, this area has been explored by French expeditions led by Janot Lamberton, pioneering the exploration and study of subglacial hydrology and microbiology (BOURSEILLER *et al.*, 2002; MOREAU, 2009).

In 2014, during an international glacio-speleological camp on the Gorner Glacier (Switzerland), supported by La Venta Association and the European Federation of Speleology, a new project called "Inside the Glacier" has born with the objective of exploring and monitoring glacial caves in different areas of the world. After several expeditions to Alpine glaciers (Gorner, Mer de Glace, Aletsch) and Patagonia (Moreno, Grey and Tyndall), in 2017 and 2018 the team has organized a new series of expeditions to the Greenland icecap. The first two missions aimed returning to the area of the Russel Glacier on the west coast, where the French expeditions had reached a depth of -173 meters in 1993. The main objective was to understand if the depth of the flooded zone has remained unchanged compared to twenty-five years ago or if the accelerate melting of the icecap could have modified the subglacial hydrology in the last years. Satellite images from the last decades show that a very long bédière (superficial stream) forms every year feeding one of the largest and highest discharge moulin system in the world. The position of the main sink points changes from year to year of only a couple of kilometres, often leaving open the accesses to no longer active moulins from the previous season. The expeditions were composed of a multidisciplinary team of scientists, performing interconnected research on the same area. This included 3D mapping of the cavities (also using a novel type of UAVs), geophysical surveys of subglacial melt-water flows, microbiology of the cryoconites on the surface and within the moulins. The project is on-going and aims to continue the monitoring of moulins in this area for the next years.

2. Explorations and mapping of moulins during "Inside Greenland 2017-2018"

In 2017 the expedition focused on the same area explored in 1993 by the French team of Serge Aviotte, Luc Moreau and Janot Lamberton (BOURSEILLER *et al.*, 2002). A preliminary survey flight in June showed the presence of a long river divided in branches sinking in two different moulins. The expedition took place in the end of September with the installation of a base camp close to the two moulins. Since June, one of the river branches was fully captured by the other leaving one of the cavities inactive. This was the first moulin explored, called "Northern Lights".

It consisted of a gigantic shaft 120 meters deep. The bottom of the moulin was occupied by a large lake (60x35 m) of unknown depth. Along the walls of the shaft we sampled a sequence of ice layers for isotopic analysis and an ancient cryoconite at a depth of about 50 meters. Waiting a few days with temperatures below zero, also the main river froze allowing the descent of the second large active moulin, reached similar depth as in 1993 or if it was also filled by water at higher levels.

After these preliminary results, a second expedition was organized for October 2018. This time the exploration and survey were strengthened by the presence of the Swiss company Flyability using a novel type of Collision Tolerant Drones. These UAVs allowed reaching the maximum depths, even when direct exploration by speleologists would have been not possible due to safety reasons. In total, the team consisted of 15 people, including the logistical support, two videographers and one photographer. The mission was also enriched with several scientific experiments, including: 1) in situ DNA sequencing of cryoconites collected on the surface and within the moulins 2) transects with Ground Penetrating Radar for the identification of underground water basins or flooded conduits connected to the moulins.

In summer 2018 the moulin system explored the previous year formed approximately in the same location, but a second system opened 2.3 km downstream, exactly where the 173m-deep moulin was explored in 1993. The expedition targeted first this new moulin, called “Kraken”. While direct exploration by speleologists reached 70 meters of depth, the drones were able to reach the bottom on a wide lake surface at 130 m of depth. GPR measurements called “Living Ice”. The shaft was rigged up to a depth of about 60 m where a precarious and fractured ledge was posing risk of collapses, making the descent too dangerous. From this point the shaft was measured with laser finders for at least other 70 m, indicating a minimum depth of this moulin of 130 m. The expedition ended without the possibility of knowing if this second moulin

showed that the flooded channel belonging to this moulin can be detected up to 200 meters of depth and for several hundred meters of distance, representing an important storage of meltwater within the icecap.

The second part of the expedition was dedicated to the exploration of the newly formed system in the same location as in 2017. Similarly, also in this case the moulin were two, the first downstream and a second capturing the main river few tens of meters upstream. The inactive moulin (“Pantagruel”) was explored to a depth of 115 m ending in a small lake full of green algal material concentrated by percolating waters from the surface. The most recent active moulin, called “Gargantua” was descended to a gigantic lake (70 m of diameter) also at a depth of 115 m.

In the same location, in September 2019 a following Danish-British exploration descended a new moulin in the same location of Gargantua, also leading to a big frozen lake at approximately 175 meters of depth estimated only measuring the rope length.

The most recent Italian-Danish-British expedition in October 2021 has descended again a moulin in the same area to 165 m of depth (instrumental survey), also with a big frozen lake at the bottom.

3. Scientific research

During the expedition "Inside Greenland” the team performed scientific research mainly focused on glacial microbiology and subglacial hydrology (SAURO *et al.*, 2019). In 2017, cryoconite microbial samples were removed from the upper surface of the ice and returned to the UK for genomic analysis. These were the first microbial samples ever to be removed from the Greenland Ice Sheet at this time of year, and therefore represent an important datapoint for understanding the year-round contribution of glacier microbes to carbon cycling and the processes that enable these microbes to exist year-round. The samples confirm the existence of an autumn-winter microbial community on the Greenland Ice Sheet and studies are on-going to compare how these microbes operate in summer and winter thanks to previous sampling in July of 2017 during another expedition in the same area.

The team was also able to collect cryoconite sample along the moulin walls. To our knowledge, microbiological samples have never been extracted from inside a moulin anywhere before on the Greenland Ice Sheet. These cold, dark, icy environments are the closest analog for deep extraterrestrial ice on Europa or Enceladus, and the existence of a viable microbial community in deep ice sites could provide interesting insights to potential niches favourable to life in extra-terrestrial ice caps. At the same time, it is possible that the microbial samples extracted from the moulin walls could be thousand of years old, being isolated from the environment for that time. This would allow to explore how the genomes of microbes that have diverged since they were buried in the ice thousands of years ago, potentially providing important ecological information about life on ice.

In 2018 the sampling was extended to other moulins and the base camp was equipped with a laboratory tent where analysis with third generation sequencing devices were performed just few hours after sampling. Nanopore sequencing using MinION from Oxford Nanopore Technologies allowed a rapid analysis of crude extracts of nucleic acid through shotgun metagenomics performing amplicon-based analyses (e.g., 16S rRNA gene sequencing) on a USB-based device. This was the first application ever of these techniques directly in a remote field camp on the Greenland Ice Sheet during the Arctic autumn (EDWARDS *et al.,* 2020). The team of microbiologist from Aberysrwith University were able to extract nucleic acids and sequence them in ambient temperatures of circa −20°C by using freeze-dried reagents and adapted protocols for nanopore sequencing. In situ data processing and analysis permitted a refined experimental strategy for genome-centred metagenomic comparison of glacial habitats.

Additional samples collected during the expeditions are under analysed at several UK institutions. The ice collected from the moulin has been oxygen-isotope dated at the British Geological Survey in Keyworth (UK). Additional

microbial samples are on-going at Aberystwyth University. Linked with the moulin mapping undertaken, this project will provide the first microbiological assessment of Greenlandic moulins.

In addition to microbiology, studies on hydrology of the moulins were performed in 2018 through a GPR survey. The discovery of big lakes at the bottom of the moulins at depths between 110 and 140 meters is an important observation to evaluate the existence of a store of water inside the Greenland Ice Sheet. It is important because it means water is not always transferred directly from the surface to the bed, with implications for our understanding of ice-melt contributions to sea level rise. The existence of a liquid melt water lake inside the ice sheet while the surface is frozen solid suggests that there could be year-round microbial activity that has never been quantified before. Conforming that the ice sheet remains microbiologically active in its interiors over winter would be a very important information. The discovery of englacial lakes is a novelty compared to the observations performed by the French team in the nineties. This suggests that the meltwater volume in the hydrological subglacial network is increasing in the last years, causing also a higher level of the flooded zone compare to twenty years ago. Analysing data from previous expedition and future monitoring could allow to understand the evolution of the subglacial hydrological network in this area of the icecap (LINDBÄCK *et al.,* 2015).

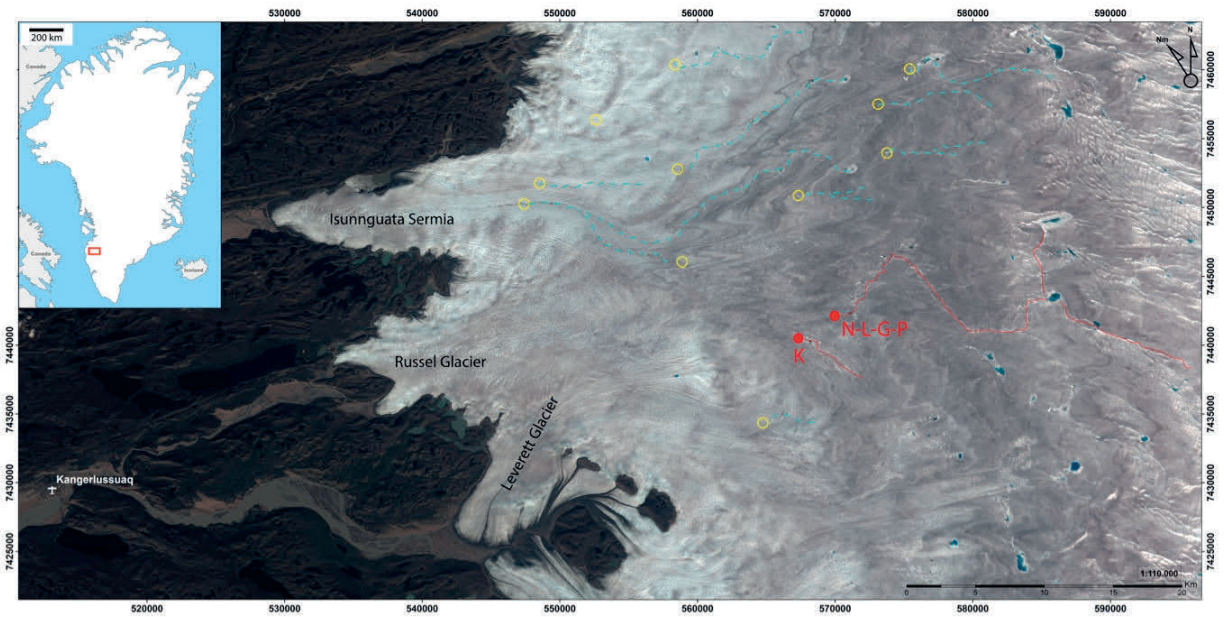

Figure 1: Map of the area of investigation during the expeditions 2017-2018. In red the moulin system explored: N) Northern Lights 2017; L) Living Ice 2017; G) Gargantua 2018; P) Pantagruel 2018; K) Kraken 2018.

4. Conclusions

Although the "Inside Greenland 2017-2018" expeditions confirmed that the exploration potential of moulins is now limited to about 100-140 meters of depth compared to the French expeditions of the 1990s, such explorations have shown that the ice cap is characterized by a system of flooded conduits and interconnected intraglacial basins. The implications of these discoveries could have an impact on hydrological models of the Greenland icecap. However, it is important to consider that our research, like those of the French expeditions, were limited to a small area. It would be important to investigate other moulins located about 20-30 km further inland and at higher altitudes. Here the potential for in-depth exploration may be greater. The use of new technologies, such as Flyability drones, would allow a fast and safe exploration of dozens of moulins in a single season, verifying the structure and connections of the subglacial water table. There is no doubt that glacio-speleological explorations in Greenland will continue in the coming decades, because there are still too many unanswered questions.

Acknowledgments

We thank Moncler for supporting the project as main sponsor. Also we thank the Greenland Expedition Office for the permits granted. Oxford Nanopore provided support and equipment for the metagenomic in situ analysis. Other technical sponsors supporting the expedition were Malachowsky, Gaibana and Crioproject.

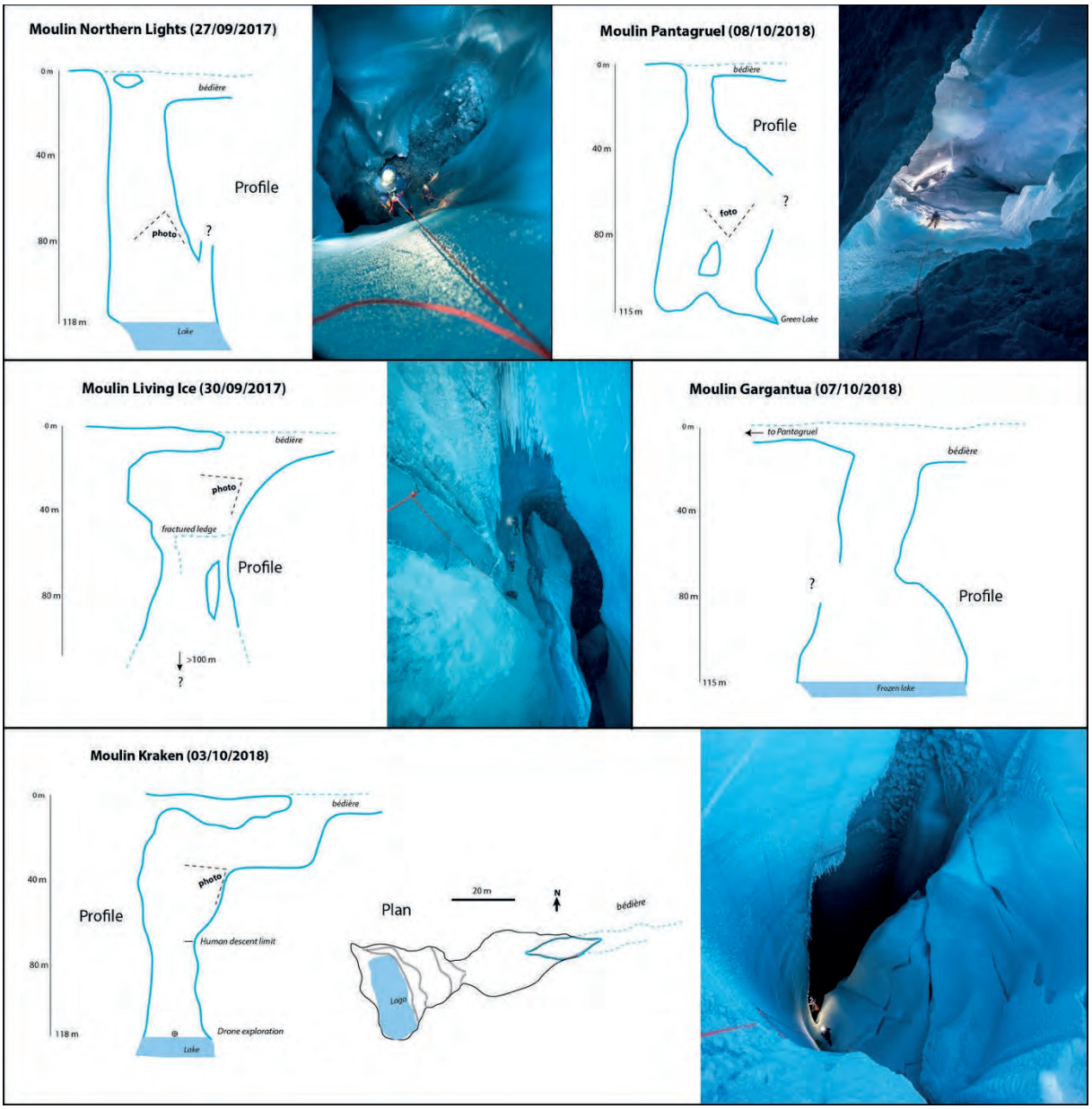

Figure 2: Topographic profiles of the moulins explored during the expeditions "Inside Greenland" 2017-2018.

References

BOURSEILLER P., LAMBERTON J., COUTÉ A. et MOREAU L. (2002) *Voyage dans les glaces*. La Martinière, Paris, 195 p.

EDWARDS A., CAMERON K. A., COOK J. M., DEBBONAIRE A. R., FURNESS E., HAY M. C. and RASSNER S. M. (2020) Microbial genomics amidst the Arctic crisis. *Microbial Genomics*, mgen000375.

LINDBÄCK K., PETTERSSON R., HUBBARD A.L., DOYLE S.H., VAN AS D., MIKKELSEN A.B. and FITZPATRICK A.A. (2015) Subglacial water drainage, storage, and piracy beneath the Greenland ice sheet. *Geophysical Research Letters*, 42(18), 7606-7614.

SAURO F., ROMEO A. e COOK J.M. (2020) La frontiera del ghiaccio profondo: le spedizioni del progetto "Inside the Glaciers" in Groenlandia. *Speleologia*, 82, 42-48.

MOREAU L. (2009) L'exploration du cryokarst glaciaire et son intérêt scientifique pour l'étude du drainage des eaux de fonte : porches, cavités, crevasses, bédières et moulins. In *Neige et glace de montagne : Reconstitution, dynamique, pratiques*, Collection EDYTEM, Cahiers de Géographie, n°8, pp.163- 170.

Volume IV

Géomorphologie / *Geomorphology*

Table des Matières / *Contents*

Symposium 04 : Géomorphologie et spéléogenèse / *Geomorphology and speleogenesis*

Session spéciale : Les karsts hypogènes / *Hypogene karst*

Special session : La fantômisation / *Ghost-rock karstification*

Special session : Interaction roche vivant / *Rock-living interaction*

Symposium 12 : Spéléologie glaciaire / *Glacier, firn and ice caves*

ISBN : 978 - 2 - 7417 - 0694 - 6
Imprimé par Gap éditions en juillet 2022
Dépôt légal 3e trimestre 2022




20 €

9 782741 706946